

# Hereditary pancreatitis

Richard M Charnley

**Richard M Charnley**, Consultant Surgeon, Freeman Hospital, Newcastle upon Tyne, NE7 7DN, UK

**Correspondence to:** Richard M Charnley, DM FRCS, Consultant Surgeon, Freeman Hospital, Newcastle upon Tyne, NE7 7DN, UK. richard.charnley@nuth.northy.nhs.uk

**Received:** 2002-11-30 **Accepted:** 2002-12-08

## Abstract

Hereditary pancreatitis is an autosomal dominant condition, which results in recurrent attacks of acute pancreatitis, progressing to chronic pancreatitis often at a young age. The majority of patients with hereditary pancreatitis express one of two mutations (R122H or N29I) in the cationic trypsinogen gene (PRSS1 gene). It has been hypothesised that one of these mutations, the R122H mutation causes pancreatitis by altering a trypsin recognition site so preventing deactivation of trypsin within the pancreas and prolonging its action, resulting in autodigestion. Families with these two mutations have been identified in many countries and there are also other rarer mutations, which have also been linked to hereditary pancreatitis.

Patients with hereditary pancreatitis present in the same way as those with sporadic pancreatitis but at an earlier age. It is common for patients to remain undiagnosed for many years, particularly if they present with non-specific symptoms. Hereditary pancreatitis should always be considered in patients who present with recurrent pancreatitis with a family history of pancreatic disease. If patients with the 2 common mutations are compared, those with the R122H mutation are more likely to present at a younger age and are more likely to require surgical intervention than those with N29I. Hereditary pancreatitis carries a 40 % lifetime risk of pancreatic cancer with those patients aged between 50 to 70 being most at risk in whom screening tests may become important.

Charnley RM. Hereditary pancreatitis. *World J Gastroenterol* 2003; 9(1): 1-4  
<http://www.wjgnet.com/1007-9327/9/1.htm>

## INTRODUCTION

Hereditary pancreatitis (HP) is an autosomal dominant condition characterised by recurrent attacks of acute pancreatitis and progressing to the development of chronic pancreatitis over a variable period of time. Symptoms usually begin in childhood or adolescence and with time, exocrine and/or endocrine insufficiency may develop. The clinical spectrum of hereditary pancreatitis was first reported in 1952<sup>[1]</sup>. Mutations causing HP have been identified in the PRSS1 gene which encodes cationic trypsinogen<sup>[2-4]</sup>. This article discusses the genetics of HP, its pathophysiology and clinical spectrum.

## THE GENETICS OF HEREDITARY PANCREATITIS

HP is an autosomal dominant condition with 80 % penetrance. The specific mutations responsible for HP were identified in 1996 when it was confirmed that the hereditary pancreatitis

gene could be mapped to chromosome 7q35<sup>[5,6]</sup>. Whitcomb *et al* demonstrated that a mutation in these patients existed in the third exon of the cationic trypsinogen gene (PRSS1)<sup>[7]</sup>. This mutation, a guanine (G) to adenine (A) transition, alters arganine (CGC) to histidine (CAC) at codon 117 (using the chymotrypsin numbering system) and was originally known as R117H. This first mutation is easily identified because it creates a novel recognition site for the restriction endonuclease *Af*/III. More recently, it has been shown that a neutral polymorphism within this enzyme recognition site may produce a false negative result<sup>[8]</sup>. A second mutation in the cationic trypsinogen gene was subsequently discovered, which was found to be a single A to thiamine (T) transversion mutation in exon 2 resulting in an asparagine (ACC) to isoleucine (ATC) substitution at amino acid 21<sup>[3]</sup>. These two mutations (R117H and N21I) have now been identified in families with hereditary pancreatitis from many countries including France<sup>[4]</sup>, Germany<sup>[9]</sup>, United Kingdom<sup>[10]</sup>, Japan<sup>[11]</sup> and the USA<sup>[3,7]</sup>. A further mutation, which appears to be much less common, is the A16V mutation, which was originally identified in three patients with idiopathic pancreatitis and in one patient with HP<sup>[12]</sup>. There is also evidence that mutations in genes other than the cationic trypsinogen gene might be associated with HP<sup>[13]</sup>. Since the discovery of the cationic trypsinogen gene mutations, a new nomenclature system for human gene mutations has been devised and accepted. This has changed the names of the common mutations from R117H to R122H and N21I to N29I<sup>[14]</sup>.

## PATHOPHYSIOLOGY

The mechanism by which mutations of the cationic trypsinogen gene cause hereditary pancreatitis is important for several reasons. Firstly, the cellular mechanisms of acute pancreatitis and progression to chronic pancreatitis are poorly understood. Secondly it is not known why the pancreas of one individual is susceptible to alcohol whilst the pancreas of another is not. Thirdly, focusing on the link between genetics and pancreatitis might provide a clue to the etiology of pancreatic cancer which can occur as a complication in sporadic and hereditary pancreatitis.

Trypsinogen is secreted by the pancreatic acinar cell<sup>[15]</sup>. It is activated to trypsin within the duodenum by enterokinase, which cleaves an 8-aminoacid N-terminal peptide. Trypsin then activates a cascade of digestive enzyme precursors. A number of mechanisms exist to prevent inappropriate activation of trypsin within the pancreas before its secretion into the duodenum. It is hypothesised that the R122H mutation alters a trypsin recognition site, which would prevent deactivation of trypsin within the pancreas, thus prolonging its action<sup>[2]</sup>. The mechanism whereby the N29I mutation causes pancreatitis is unclear. It has been speculated, however, that the N29I mutation would enhance autoactivation of trypsinogen, altering the binding of pancreatic secretory trypsin inhibitor (PSTI)<sup>[3]</sup> or impairing trypsin inactivation by altering the accessibility of the initial hydrolysis site to trypsin. Predicted molecular conformational changes in the structure of trypsin support this<sup>[16]</sup>. The pathogenic mechanism whereby the A16V mutation causes pancreatitis is speculative but it is thought to alter the cleavage site of the signal peptide<sup>[12]</sup>. Because the two common mutations, R122H and N29I produce such a similar

clinical picture, it has been speculated that these mutations, rather than being the cause of hereditary pancreatitis, simply represent markers for a number of linked pancreatic defects. There appears no doubt, however, that inappropriate prevention of the deactivation of trypsin within the pancreas is responsible for HP in the majority of cases.

The penetrance of cationic trypsinogen gene mutations remains at approximately 80 % in the majority of studies. To investigate factors contributing to this, a study of monozygotic twins with HP was carried out<sup>[17]</sup>. Of 11 sets of twins, seven were suitable for this study. Whereas four of these seven sets were concordant for pancreatitis, three of the seven sets of twins (43 %) were discordant for phenotypic expression of pancreatitis. The overall penetrance in the seven pairs of twins was 78 %. The conclusion from this study was that genetic and/or environmental factors contribute to the expression and age of onset of HP. As yet the mechanism of non-penetrance remains unclear.

### CLINICAL PRESENTATION IN HEREDITARY PANCREATITIS

The initial presentation of a patient with HP is usually indistinguishable from a case of sporadic pancreatitis. The clinical presentation is variable but typical patients present with recurrent attacks of acute pancreatitis in childhood, progressing to chronic pancreatitis with time<sup>[1,18]</sup>. The presentation during an acute attack is identical to an attack of gallstone-induced, alcoholic or idiopathic, acute pancreatitis. The presentation of chronic pancreatitis in these patients is likewise indistinguishable from alcoholic, idiopathic or other forms of chronic pancreatitis<sup>[18-20]</sup>. Pediatric patients with HP have a similar presentation to idiopathic juvenile chronic pancreatitis<sup>[21]</sup>. It is however very common for these patients to remain undiagnosed for many years having often suffered from chronic symptoms since childhood. We have found that recognition of the disease within a family often results in several relatives being newly diagnosed with pancreatitis whereas previously they had been labelled as "peptic ulcer" or "chronic abdominal pain". In Newcastle upon Tyne, UK, the pancreatic clinic now has individuals belonging to thirteen families with hereditary pancreatitis. Data on nine of these families has been previously published<sup>[10]</sup>. The R122H (R117H) mutation was identified in three families and the N29I (N21I) mutation was demonstrated in a further five families. In a remaining family, no mutations were demonstrated in any of the five exons of the PRSS1 gene. The families and patients belonging to the R122H group were compared with those belonging to the N29I group. Comparison of clinical details including complications of pancreatitis was carried out. The mean age at onset of symptoms of pancreatitis was lower in the R122H group at 8.4 vs 6.5 years, ( $P=0.007$ ) and more patients with the R122H mutation had developed symptoms by the age of 20 years (89 vs 64 %). More patients with the R122H mutation required surgical intervention (8 of 12 vs 4 of 17,  $P=0.029$ ) and this occurred at an earlier age. There was also a tendency for more patients with the R122H mutation to develop exocrine failure but the incidence and age of onset of endocrine failure (as measured by the development of insulin dependent diabetes mellitus) was similar in both groups. Patients in both groups identified alcohol as a provoking factor for the symptoms. These observations were also noted in the original description of the N21I mutation in 1997<sup>[3]</sup> and have also been noted by the European Registry of Hereditary Pancreatitis and Pancreatic Cancer (EUROPAC)<sup>[22]</sup>. It is also clear that as well as hereditary pancreatitis being identical to other forms of pancreatitis in terms of the mode of clinical presentation, radiological and histopathological features are also identical<sup>[23]</sup>. Apart from earlier onset and delay in diagnosis, hereditary pancreatitis has been found to have a

natural history similar to that of chronic alcoholic pancreatitis in terms of a similar prevalence of pancreatic calcification, a similar amount of pancreatic insufficiency both endocrine and exocrine but a higher prevalence of pseudocysts<sup>[24]</sup>.

### CATIONIC TRYPSINOGEN GENE MUTATIONS IN NON-HEREDITARY PANCREATITIS

Taking a family history is very important in all patients with pancreatitis because the majority of patients with cationic trypsinogen gene mutations have a clear cut family history of pancreatitis. It is, however, common for patients to be referred to a pancreatic specialist with so-called idiopathic pancreatitis without a reliable family history having been obtained<sup>[25]</sup>. It has also been considered whether idiopathic chronic pancreatitis might be due to PRSS1 gene mutations. An investigation of patients with chronic alcoholic pancreatitis showed no evidence of the R122H or N29I mutation in 21 patients<sup>[26]</sup> but a much larger and important study investigated 221 patients with idiopathic chronic pancreatitis and no family history. The entire PRSS1 gene was sequenced in these patients. Only three patients had mutations, one with R122H and two patients with A16V<sup>[27]</sup>. A genetic background has also been investigated in patients with idiopathic juvenile chronic pancreatitis, a disease which closely mimics the clinical pattern of hereditary pancreatitis<sup>[28]</sup>. The R122H mutation was detected in one patient with idiopathic juvenile chronic pancreatitis and the A16V mutation was also found in one patient. It is clear from these studies that new mutations do occur and that screening of individuals with idiopathic pancreatitis for cationic trypsinogen gene mutations is worthwhile. It is, therefore, our policy in patients with idiopathic pancreatitis, after exclusion of other causes, to perform genetic counselling and genetic testing. We have found that patients are keen to know their genetic status in relation to this disease.

### RISK OF CANCER IN HEREDITARY PANCREATITIS

Sporadic chronic pancreatitis carries a significantly increased risk of pancreatic cancer. This has been clearly demonstrated by a multi-centre historical cohort study of over 2000 patients<sup>[29]</sup>. The standardized incidence ratio, i.e. the ratio of observed to expected pancreatic cancers was 16.5. This study may have been subject to detection bias in that increased surveillance of chronic pancreatitis patients may have increased the number of cancers diagnosed compared with the general population. A study of Swedish patients, however, confirmed an increased risk of pancreatic cancer in sporadic chronic pancreatitis but with a standardised incidence ratio of 3.8<sup>[30]</sup>. Patients with HP have not been included in either of these studies but have since been examined for the risk of developing pancreatic cancer by the International Hereditary Pancreatitis Study Group. A cohort of 246 patients with hereditary pancreatitis was identified from ten countries with a mean follow-up period of over 14 years<sup>[31]</sup>. Eight patients with pancreatic adenocarcinoma were identified yielding a standardized incidence ratio of 53.3. The estimated cumulative risk of pancreatic cancer developing in these patients was nearly 40 % and was greater for patients with a paternal inheritance pattern. These figures have been confirmed by the Midwest Multicentre Pancreatic Study Group<sup>[32]</sup>. The conclusions from these cancer studies are that, firstly chronic pancreatitis is a risk factor for pancreatic cancer and secondly hereditary pancreatitis puts patients at an even higher risk of developing cancer than the sporadic disease. Although it is not absolutely clear whether the risk of cancer is due to prolonged inflammatory change or whether it is related to the presence of a cationic trypsinogen mutation per se, the evidence available at present indicates that those patients with HP who

develop cancer, are those with a prolonged history of chronic pancreatitis<sup>[32]</sup>. The number of cancers, which have developed in HP patients have so far not allowed an investigation into which mutation (s) might predispose to cancer more than another. This data, however, will be available with time. A study of pancreatic tissue from 34 patients with sporadic ductal adenocarcinoma has shown no specific relationship between the R122H mutation and pancreatic cancer<sup>[33]</sup>. Further such studies are expected as tissue from patients with hereditary pancreatitis becomes available for analysis.

## MANAGEMENT DILEMMAS IN HEREDITARY PANCREATITIS

When faced with a patient or a family with a possible diagnosis of HP, three questions are commonly asked. Firstly, what can be done about the patient with pancreatitis? Secondly, are other relatives likely to be affected? Thirdly, what can be done to reduce the risk of cancer?

### Management of the pancreatitis

There are no specific medical therapies recommended in patients with HP. The management of acute attacks of pancreatitis are the same as for the sporadic disease that is, rehydration, analgesia and careful monitoring. Severe necrotising pancreatitis is rare in HP but pseudocysts seem to be relatively common. It has been suggested that antioxidant therapy may be helpful to prevent acute attacks but there is no evidence to support this and it is not recommended. Chronic pancreatitis should be treated as for any other patients. Enzyme supplements are likely to be required and analgesics as necessary. If diabetes mellitus occurs it is likely to require insulin therapy. Surgical treatment is for complications such as pseudocyst, biliary obstruction or duodenal obstruction. In older patients requiring surgery, a total pancreatectomy should be considered in order to abolish the cancer risk (see below).

### Genetic counselling of relatives

Relatives should be told that although the majority of HP cases are revealed by the age of 18, the disease may not manifest itself until the age of 30 or older. In these unaffected individuals, genetic testing confers no advantage and should be discouraged. Since unaffected (non-carrier) individuals and unaffected carriers do not have pancreatitis, they carry no increased risk of developing cancer.

### Screening of hereditary pancreatitis patients for cancer

Since patients with this disease exhibit a 53-fold increased risk of pancreatic cancer with a cumulative risk of 40 % by the age of 70, an attempt at screening would appear to be essential. Unfortunately, no adequate screening test exists. The measurement of tumor markers, endoscopic techniques and radiological imaging lack the sensitivity and specificity for early diagnosis. Tumors are particularly difficult to detect on a background of chronic pancreatitis. It is thought therefore that molecular based strategies are likely to offer the best opportunities for the screening of these high risk patients for pancreatic ductal adenocarcinoma<sup>[34]</sup>. It has been suggested that the banking of blood and pancreatic juice samples should be mandatory in any screening protocol and that imaging of the pancreas should be carried out by endoscopic ultrasound<sup>[35]</sup>. One such protocol for the secondary screening of patients with HP has been established by EUROPAC (European Registry of Hereditary Pancreatitis and Pancreatic Cancer). As part of a research programme only, affected individuals over the age of 30 are offered imaging by CT and endoscopic ultrasound (EUS), followed after genetic counselling, by genetic analysis of pancreatic juice obtained at ERCP for K-ras mutations. Patients negative for K-ras continue with repeat screening at

3 yearly intervals by CT, EUS and K-ras analysis of pancreatic juice. Patients who are K-ras positive undergo further genetic analysis in the form of p53, p16 and aberrant methylation. If positive, these patients may be at risk of pancreatic ductal carcinoma and an attempt should be made to obtain cells for cytology by ERCP brushing of the pancreatic duct. The ultimate preventative measure in these patients would be a total pancreatectomy but this is a relatively high morbidity operation with the certainty of becoming diabetic. Certainly any patient with HP aged 30 or over, who requires surgery for relief of symptoms should undergo a total pancreatectomy in order to abolish the cancer risk rather than a lesser procedure. This is not, however, appropriate in patients who are well unless there is clear evidence that they possess cellular atypia or a focal abnormality suspicious of cancer.

## CONCLUSIONS

Hereditary pancreatitis is a fascinating condition which has provided new insights into the pathophysiology of pancreatitis. There are however many unanswered questions particularly in relation to the ways in which these mutations relate to pancreatitis and cancer. Management of these patients should be carried out by a team of experienced pancreatic specialists who are also able to provide genetic counselling. Registration of patients with one of the large Hereditary Pancreatitis Registries is essential if management strategies are to be improved and genetic research to be continued.

## REFERENCES

- 1 **Comfort MW**, Steinberg AG. Pedigree of a family with hereditary chronic relapsing pancreatitis. *Gastroenterology* 1952; **21**: 54-63
- 2 **Whitcomb DC**. Hereditary pancreatitis: new insights into acute and chronic pancreatitis. *Gut* 1999; **45**: 317-322
- 3 **Gorry MC**, Gabbazadeh D, Furey W, Gates LK Jr, Preston RA, Aston CE, Zhang Y, Ulrich C, Ehrlich GD, Whitcomb DC. Mutations in the cationic trypsinogen gene are associated with recurrent acute and chronic pancreatitis. *Gastroenterology* 1997; **113**: 1063-1068
- 4 **Ferec C**, Raguene O, Salomon R, Roche C, Bernard JP, Guillot M, Quere I, Faure C, Mercier B, Audrezet MP, Guillausseau PJ, Dupont C, Munnich A, Bignon JD, Le Bodic L. Mutations in the cationic trypsinogen gene and evidence for heterogeneity in hereditary pancreatitis. *J Med Genet* 1999; **36**: 228-232
- 5 **Whitcomb DC**, Preston RA, Aston CE, Sossenheimer MJ, Barua PS, Zhang Y, Wong-Chong A, White GJ, Wood PG, Gates LK Jr, Ulrich C, Martin SP, Post JC, Ehrlich GD. A gene for hereditary pancreatitis maps to chromosome 7q35. *Gastroenterology* 1996; **110**: 1975-1980
- 6 **Pandya A**, Blanton SH, Landa B, Javaheri R, Melvin E, Nance WE, Markello T. Linkage studies in a large kindred with hereditary pancreatitis confirms mapping of the gene to a 16-cM region on 7Q. *Genomics* 1996; **38**: 227-230
- 7 **Whitcomb DC**, Gorry MC, Preston RA, Furey W, Sossenheimer MJ, Ulrich CD, Martin SP, Gates LK Jr, Amann ST, Toskes PP, Liddle R, McGrath K, Uomo G, Post JC, Ehrlich GD. Hereditary pancreatitis is caused by a mutation in the cationic trypsinogen gene. *Nat Genet* 1996; **14**: 141-145
- 8 **Howes N**, Greenhalf W, Rutherford S, O'Donnell M, Mountford R, Ellis I, Whitcomb D, Imrie C, Drumm B, Neoptolemos JP. A New polymorphism for the R122H mutation in hereditary pancreatitis. *Gut* 2001; **48**: 247-250
- 9 **Teich N**, Mossner J, Keim V. Mutations of the cationic trypsinogen in hereditary pancreatitis. *Hum Mutat* 1998; **12**: 39-43
- 10 **Creighton JE**, Lyall R, Wilson DI, Curtis A, Charnley RM. Mutations of the cationic trypsinogen gene in patients with hereditary pancreatitis. *Br J Surgery* 2000; **87**: 170-175
- 11 **Nishimori I**, Kamakura M, Fujikawa-Adachi K, Morita M, Onishi S, Yokoyama K, Makino I, Ishida H, Yamamoto M, Watanabe S, Ogawa M. Mutations in exons 2 and 3 of the cationic trypsinogen gene in Japanese families with hereditary pancreatitis. *Gut*

- 1999; **44**: 259-263
- 12 **Witt H**, Luck W, Becker M. A signal peptide cleavage site mutation in the cationic trypsinogen gene is strongly associated with chronic pancreatitis. *Gastroenterology* 1999; **117**: 7-10
- 13 **Bartness MA**, Duerr RH, Ford MA, Zhang L, Aston CE, Barmada M. Potential linkage of a pancreatitis associated gene to chromosome 12. *Pancreas* 1998; **17**: 426
- 14 **Antonarakis SE**. Recommendations for a nomenclature system for human gene mutations. Nomenclature Working Group. *Hum Mutat* 1998; **11**: 1-3
- 15 **Scheele G**, Kern H. The exocrine pancreas. In: Desnuelle P, Sjöström H, Norén O, eds. *Molecular and Cellular Basis of Digestion*. Amsterdam: Elsevier 1986: 173-194
- 16 **Whitcomb DC**. Hereditary pancreatitis: new insights into acute and chronic pancreatitis. *Gut* 1999; **45**: 317-322
- 17 **Amann ST**, Gates LK, Aston CE, Pandya A, Whitcomb DC. Expression and penetrance of the hereditary pancreatitis phenotype in monozygotic twins. *Gut* 2001; **48**: 542-547
- 18 **Perrault J**. Hereditary pancreatitis. *Gastroenterol Clin North Am* 1994; **23**: 743-752
- 19 **Konzen KM**, Perrault J, Moir C, Zinsmeister AR. Long-term follow-up of young patients with chronic hereditary or idiopathic pancreatitis. *Mayo Clinic Proc* 1993; **68**: 1993
- 20 **Kattwinkel J**, Lapey A, Di Sant' Agnese PA, Edwards WA. Hereditary pancreatitis: three new kindreds and a critical review of the literature. *Paediatrics* 1973; **51**: 55-69
- 21 **DuBay D**, Sandler A, Kimura K, Bishop W, Eimen M, Soper R. The modified Puestow procedure for complicated hereditary pancreatitis in children. *Journal of Paediatric Surgery* 2000; **35**: 343-348
- 22 **Howes N**, Rutherford S, McDonald F, Ellis I, Whitcomb D, Mountford R, Neoptolemos JP. For the UK and Ireland Consortium of EUROPAC. Trypsinogen mutations in families with Hereditary Pancreatitis in the UK and Ireland. *Int J Pancreatol* 1999; **25**: 237
- 23 **Sossenheimer MJ**, Aston CE, Preston RA, Gates LK Jr, Ulrich CD, Martin SP, Zhang Y, Gorry MC, Ehrlich GD, Whitcomb DC. Clinical characteristics of hereditary pancreatitis in a large family, based on high-risk haplotype. The Midwest Multi-Centre Pancreatic Study Group (MMPCG). *Am J Gastroenterol* 1997; **92**: 1113-1116
- 24 **Paolini O**, Hastier P, Buckley M, Maes B, Demarquay JF, Staccini P, Bellon S, Caroli-Bosc FX, Dumas R, Delmont J. The natural history of hereditary chronic pancreatitis: a study of 12 cases compared to chronic alcoholic pancreatitis. *Pancreas* 1998; **17**: 226-271
- 25 **Creighton J**, Lyall R, Wilson DI, Curtis A, Charnley R. Mutations of the cationic trypsinogen gene in patients with chronic pancreatitis. *Lancet* 1999; **354**: 42-43
- 26 **Teich N**, Mossner J, Keim V. Screening for mutations of the cationic trypsinogen gene: are they of relevance in chronic alcoholic pancreatitis? *Gut* 1999; **44**: 413-416
- 27 **Chen JM**, Piepoli Bis A, Le Bodic L, Ruzsniowski P, Robaszekiewicz M, Deprez PH, Raguene O, Quere I, Andriulli A, Ferec C. Mutational screening of the cationic trypsinogen gene in a large cohort of subjects with idiopathic chronic pancreatitis. *Clinical Genetics* 2001; **59**: 189-193
- 28 **Truninger K**, Kock J, Wirth HP, Muellhaupt B, Arnold C, von Weizsacker F, Seifert B, Ammann RW, Blum HE. Trypsinogen gene mutations in patients with chronic or recurrent acute pancreatitis. *Pancreas* 2001; **22**: 18-23
- 29 **Lowenfels AB**, Maisonneuve P, Cavallini G, Ammann RW, Lankisch PG, Andersen JR, Dimagno EP, Andren-Sandberg A, Domellof L. Pancreatitis and the risk of pancreatic cancer. International Pancreatitis Study Group. *N Engl J Med* 1993; **328**: 1433-1437
- 30 **Ekbom A**, McLaughlin JK, Karlsson BM, Nyren O, Gridley G, Adami HO, Fraumeni JF Jr. Pancreatitis and pancreatic cancer: a population-based study. *J Natl Cancer Ins* 1994; **86**: 625-627
- 31 **Lowenfels AB**, Maisonneuve P, DiMagno EP, Elitsur Y, Gates LK Jr, Perrault J, Whitcomb DC. Hereditary pancreatitis and the risk of pancreatic cancer. International Hereditary Pancreatitis Study Group. *J Natl Cancer Ins* 1997; **89**: 442-446
- 32 **Whitcomb DC**, Applebaum S, Martin SP. Hereditary pancreatitis and pancreatic carcinoma. *Ann NY Acad Sci* 1999; **880**: 201-209
- 33 **Hengstler JG**, Bauer A, Wolf HK, Bulitta CJ, Tanner B, Oesch F, Gebhard S, Boettger T. Mutation analysis of the cationic trypsinogen gene in patients with pancreatic cancer. *Anticancer Research* 2000; **20**: 2967-2974
- 34 **Howes N**, Greenhalf W, Neoptolemos J. Screening for early pancreatic ductal adenocarcinoma in hereditary pancreatitis. *Medical Clinics North Am* 2000; **84**: 719-738
- 35 **Martin SP**, Ulrich CD 2nd. Pancreatic cancer surveillance in a high-risk cohort. Is it worth the cost? *Medical Clinics North Am* 2000; **84**: 739-747

Edited by Ma JY

# Design of a ribozyme targeting human telomerase reverse transcriptase and cloning of it's gene

Zhi-Ming Hao, Jin-Yan Luo, Jin Cheng, Quan-Yin Wang, Guang-Xiao Yang

**Zhi-Ming Hao**, Department of Gastroenterology, 1st Hospital, Xi'an Jiaotong University, Xi'an 710061, Shaanxi Province, China

**Jin-Yan Luo, Jin Cheng**, Department of Gastroenterology, 2nd Hospital, Xi'an Jiaotong University, Xi'an 710061, Shaanxi Province, China

**Supported by** the National Natural Science Foundation, No. 39800061. (Reversal of malignant proliferation of a telomerase-specific ribozyme on colonic carcinoma cells)

**Correspondence to:** Dr. Zhi-Ming Hao, Department of Gastroenterology, 1st Hospital, Xi'an Jiaotong University, 1 Jiankanglu, Xi'an 710061, Shaanxi Province, China. haozhm@public.xa.sn.cn

**Telephone:** +86-029-5265523

**Received:** 2002-04-13 **Accepted:** 2002-04-27

## Abstract

**AIM:** To design a hammerhead ribozyme targeting human telomerase reverse transcriptase (hTERT) and clone it's gene for future use in the study of tumor gene therapy.

**METHODS:** Using the software RNAstructure, the secondary structure of hTERT mRNA was predicted and the cleavage site of ribozyme was selected. A hammerhead ribozyme targeting this site was designed and bimolecular fold between the ribozyme and hTERT was predicted. The DNA encoding the ribozyme was synthesized and cloned into pGEMEX-1 and the sequence of the ribozyme gene was confirmed by DNA sequencing.

**RESULTS:** Triplet GUC at 1742 of hTERT mRNA was chosen as the cleavage site of the ribozyme. The designed ribozyme was comprised of 22nt catalytic core and 17nt flanking sequence. Computer-aided prediction suggested that the ribozyme and hTERT mRNA could cofold into a proper conformation. Endonuclease restriction and DNA sequencing confirmed the correct insertion of the ribozyme gene into the vector pGEMEX-1.

**CONCLUSION:** This fundamental work of successful designing and cloning of an anti-hTERT hammerhead ribozyme has paved the way for further study of inhibiting tumor cell growth by cleaving hTERT mRNA with ribozyme.

Hao ZM, Luo JY, Cheng J, Wang QY, Yang GX. Design of a ribozyme targeting human telomerase reverse transcriptase and cloning of it's gene. *World J Gastroenterol* 2003; 9(1): 104-107  
<http://www.wjgnet.com/1007-9327/9/104.htm>

## INTRODUCTION

Telomeres form the ends of eukaryotic chromosomes consisting of an array of tandem repeats of the hexanucleotide 5'-TTAGGG-3'. Their functions are protecting the ends of chromosomes against exonucleases and ligase, preventing the activation of DNA-damage checkpoints, and countering the loss of terminal DNA segments that occur during linear DNA is replicated<sup>[1,2]</sup>. Telomerase, a ribonucleoprotein enzyme, add

the hexanucleotides to the ends of replicating chromosomes<sup>[3]</sup>. It is believed that telomerase plays a crucial role in cellular senescence and immortalization<sup>[3-5]</sup>. Telomerase is strongly repressed in most human somatic cells, and telomeres shorten progressively with each cell division<sup>[6]</sup>. Most cancer cells express telomerase activity<sup>[3,6-9]</sup>. The restoration of telomerase activity is considered to immortalize cells and to be an important step in carcinogenesis. Inhibition of telomerase can lead to telomere shorting and tumor cell death. Thus, specific inhibition of human telomerase is suggested to be an efficient means of tumor therapy. Nowadays, a limited number of means can be used experimentally to inhibit the activity of human telomerase including chemical agents<sup>[10]</sup>, antisense oligonucleotide<sup>[11,12]</sup>, peptide nucleic acid<sup>[13]</sup>, and ribozyme<sup>[14-16]</sup>. Telomerase is composed of at least three subunits<sup>[17]</sup>. The RNA subunit and the catalytic subunit are the essential components for telomerase activity<sup>[18]</sup>. The RNA subunit of telomerase serves as the template for addition of short sequence repeats to the chromosome 3' ends<sup>[19]</sup>. And the catalytic subunit, telomerase reverse transcriptase (TERT), is the most important component in telomerase complex which is responsible of catalytic activity of telomerase. The expression of TERT correlates with the presence of telomerase activity<sup>[20]</sup>. These studies suggest that hTERT is a good target for cancer gene therapy.

Ribozymes are *sis*- or *trans*-acting, sequence-specific catalytic RNA molecules. Based on the studies about natural ribozymes, we can design site-specific *trans*-acting ribozymes to suppress the expression of genes by recognize and splice the mRNA. Hammerhead ribozyme and hairpin ribozyme are intensively studied because of their simple structures and dual activity of splicing as well as blocking<sup>[21]</sup>. Ribozymes may surpass the efficiency of the antisense oligonucleotide and are considered a promising means of gene therapy<sup>[22,23]</sup>. In this study, we designed a hammerhead ribozyme targeting hTERT and cloned the gene encoding the ribozyme for future study of this ribozyme in the treatment of malignancies.

## MATERIALS AND METHODS

### Materials

Plasmid vector pGEMEX-1, X-gal and IPTG were Promega products. T4 DNA ligase, Klenow fragment and restriction endonucleases used in this study were purchased from Sino-America Biotechnology Co.

### Design of the hammerhead ribozyme

Using the software RNAstructure 3.6 (mFOLD for windows version), the full-length telomerase mRNA (GenBank NM003219) was analyzed and the second structure of telomerase mRNA was predicted. Since *trans*-acting hammerhead ribozymes preferentially recognize and cleave the GUC sequence, all the fragments containing GUC were candidate target sequences for ribozyme binding and cleavage. Considering the predicted local conformation near the GUC triplets and the nucleotide sequences flanking the GUCs, triplet GUC located at 1 742 of the hTERT mRNA was chosen as the target site of ribozyme. According to the rules of hammerhead ribozyme design suggested by Haseloff *et al*<sup>[24]</sup>, the ribozyme

was primarily designed. Then, bimolecular fold between the ribozyme and substrate RNA was predicted and modification of the ribozyme sequence was made according to the prediction to improve the binding between the ribozyme and the substrate. The hammerhead ribozyme designed was comprised of 39 nucleotides, including 22nt catalytic core and 17nt (5' 7nt and 3' 10nt) flanking antisense sequence. The sequence is 5' - TCTCCGTCTGATGAGTCCGTGAGGACGAAACATAAAAGA - 3' (The underlined are nucleotides complementary to the substrate).

### Synthesis of the ribozyme gene

DNA synthesis was carried out by Shanghai Sangon Biotechnology Co. LTD. with 3 900 DNA autosynthesis instrument. The primers used for the ribozyme were as follows: 5' - CCCAAGCTTCTCCGTCTGATGAGTC - CGTGAGGACGAAAC - 3' (strand A) and 5' - GGAATTCATCGATAGATCTTTTATGTTTCGTCTCA - 3' (strand B). Twelve nucleotides from the 3' ends of the two strands were complementary to each other. A *Hind*III restriction site was introduced into the 5' end of strand A. And restriction sites of *Bgl*II, *Cla*I and *Eco*RI were introduced into the 5' end of strand B. Equal molecule of the two strands were mixed and annealed to form a hemiduplex. The hemiduplex was extended with Klenow fragment to form full duplexes. The reaction mixture contained 50 mM Tris-HCl (pH 7.2), 10 mM MgSO<sub>4</sub>, 0.1 mM DTT, 0.4 mM dNTP mixture, 4 µg each of the two single strand oligonucleotides, 20 U Klenow fragment in a final volume of 50 µl. The reaction was carried out at 37 °C for an hour. The reaction mixture was extracted with phenol-chloroform and precipitated with sodium acetate ethanol (The methods referred to Sambrook *et al*<sup>[25]</sup>).

### Cloning of ribozyme gene

The double strand DNA was digested with *Hind*III and *Eco*RI. The product was electrophoresed in 2 % agarose for purification followed by electroelution in a dialysis bag for DNA recovery. The recovered fragment was inserted into the *Hind*III/*Eco*RI site of plasmid vector pGEMEX-1 with T4 DNA ligase. *E. coli* JM109 was transformed with the recombinant plasmid and cultured on a solid medium containing ampicillin, X-gal and IPTG. Six white colonies were picked and plasmid was extracted by alkaline lysis. The plasmid was digested by *Hind*III, *Not*I, *Eco*RI, *Bgl*II, respectively. Endonuclease digests of plasmid DNA were analyzed on 1 % agarose. DNA sequencing was carried out to further confirm the inserted sequence of ribozyme gene (The methods referred to Sambrook *et al*<sup>[25]</sup>).

## RESULTS

### Selection of cleavage site and design of the ribozyme

Aided by computer prediction of RNA secondary structure, we selected the triplex GUC situated at 1 742 of the hTERT mRNA as the cleavage site (Figure 1). The ribozyme could co-fold with the substrate RNA to form a desired conformation in computer-aided prediction (Figure 2).

### Analysis of the transformants

Six white colonies were picked. All the plasmids were cleaved into two fragments (1.0kb+3.0kb) by *Bgl*II. The plasmid from colony number 6 was digested with *Hind*III, *Not*I and *Eco*RI respectively. The plasmid DNA was linearized by *Hind*III or *Eco*RI but not by *Not*I. This result suggested plasmid from colony number 6 was a correct recombinant (Figure 3,4).

### DNA sequencing

The DNA sequencing of the plasmid DNA from colony number

6 confirmed that the ribozyme gene was correctly inserted into the vector pGEMEX-1. This recombinant was named pGEMEX-1-RZ. The diagram of DNA sequencing is shown in Figure 5.

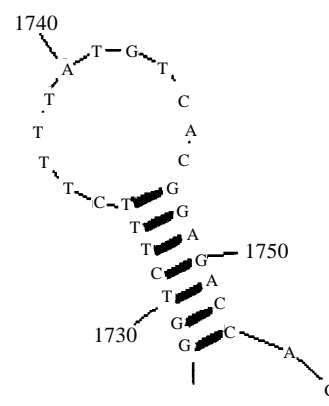


**Figure 1** Predicted second structure of the substrate RNA surrounding the selected cleavage site

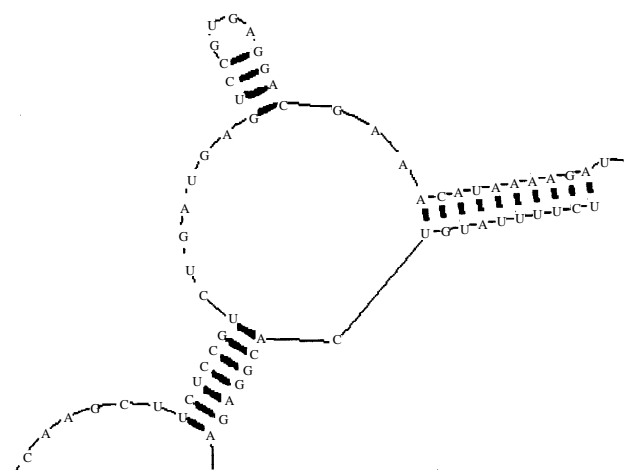


**Figure 2** Predicted bimolecular co-fold between the hammerhead ribozyme and the substrate RNA

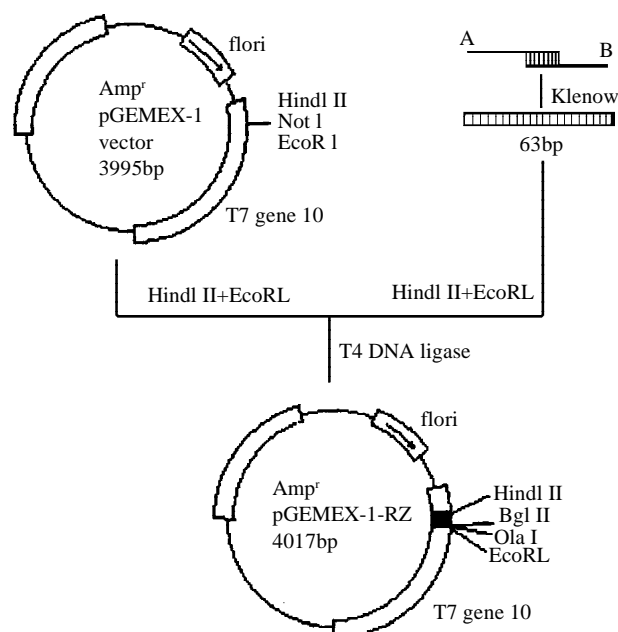


**Figure 3** Diagram of the cloning of the hammerhead ribozyme

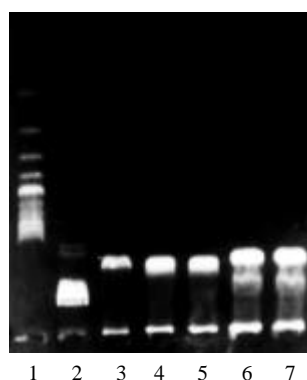


**Figure 4** Gel analysis of the plasmid containing the ribozyme gene. Lane 1: 200 bp DNA ladder; lane 2:  $\lambda$ DNA/*Hind*III marker; lane 3: pGEMEX-1-RZ/*Bgl*II; lane 4: pGEMEX-1-RZ/*Hind*III; lane 5: pGEMEX-1-RZ/*Eco*RI; lane 6: pGEMEX-1-RZ/*Not*I; lane 7: pGEMEX-1-RZ

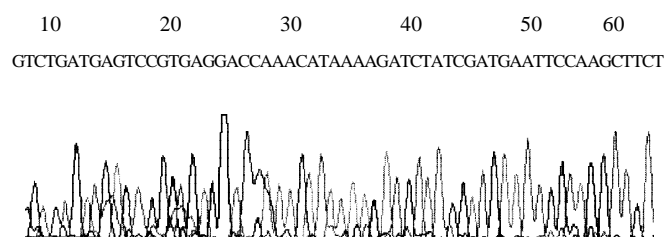


**Figure 5** DNA sequencing of ribozyme gene

## DISCUSSION

A hammerhead ribozyme is composed of a 22nt or 23nt catalytic core and the flanking complementary sequences. The catalytic core determines the cleavage activity of the ribozyme. And the nucleotide sequence of the catalytic core is conserved. Whereas the flanking sequences determine the recognition specificity of the ribozyme<sup>[24]</sup>. The catalytic mechanisms of hammerhead ribozyme and related factors have been intensively studied<sup>[26]</sup>. Hammerhead ribozyme can cleave the triplet sequence NUH (N is anyone of A, U, C or G, and H could be C, U or A), but the triplet GUC is most efficiently cleaved<sup>[27]</sup>. The length of complementary sequence also influences the catalytic activity. Short complementary sequence will decrease the recognition specificity of the ribozyme and the annealing between ribozyme and substrate. In contrary, long complementary sequence will influence the dissociation of ribozyme from the substrate and hence the turnover of the ribozyme. Commonly, the proper length of each of the flanking sequence is 6-8nt<sup>[28,29]</sup> although some studies suggested that longer antisense flanking arms have higher intracellular cleavage efficacy<sup>[30,31]</sup>. This opinion is also supported by the estimation that stretches of 11-15 nucleotides define unique sequences for cellular RNA<sup>[32]</sup>. It was reported that asymmetric ribozymes (longer helixIII, shorter helixI) have higher cleavage activity than symmetric ribozyme<sup>[33]</sup>. In this study, we designed a asymmetric hammerhead ribozyme which had 7nt helixI and 10nt helixIII.

The premise of ribozyme cleavage is the base pairing between flanking sequence of the ribozyme and the substrate mRNA<sup>[34]</sup>. This step is akin to the antisense oligodeoxyribonucleotides used for the same purpose. And the base pairing is determined by the secondary structure of the target site, Triplet NUH situated in a loop, protruding or linker of the substrate is advantageous to the annealing between

ribozyme and substrate and then the cleavage of the substrate RNA by the ribozyme<sup>[35]</sup>. The selection of the cleavage sites is most important in the design of ribozymes. Nowadays, two approaches are available in the selection of the cleavage sites of ribozymes. One approach is to use *in vitro* accessibility assays. The other is to use theoretical prediction, that is, computer-aided prediction. A number studies aimed to compare the two approaches in their consistency have suggested that theoretical prediction is positively correlate with the intracellular accessibility of the target sites in mRNA<sup>[35-37]</sup>. So we performed computer-aided analysis of the secondary structure of the substrate RNA. mFOLD is a commonly used software for RNA secondary structure<sup>[38]</sup>, so we used mFOLD to predict the secondary structure of hTERT mRNA previous to designing the ribozyme. We choose 1742 GUC as the cleavage site of ribozyme in total 57 triplet GUC in hTERT mRNA. The reasons included: (1) 1 744 triplet RNA is located in coding region of an essential motif of telomerase activity-T motif, and T motif is unique to telomerase in all kinds of reverse transcriptase<sup>[39]</sup>. (2) 1 742 triplet GUC is situated in a rather large loop of the predicted secondary structure of telomerase RNA where comparatively more unpaired bases are present near the cleavage triplet. It was reported this kind of structure was correlated with the hybridization accessibility for hammerhead ribozymes<sup>[35]</sup>. (3) The sequence surrounding 1742 triplet GUC is rich of adenosine and uridine. It is reported that for efficient catalytic turnover, the free energy of the ribozyme-substrate duplex should be less than -16 kal/mol, that is, higher ratio of A+U will be advantageous to the annealing between ribozyme and substrate<sup>[28]</sup>. Next, we performed a computer-aided bimolecular fold prediction between the ribozyme and the substrate and modified the complementary sequences until the ribozyme and the substrate can co-fold into a correct conformation in computer-aided prediction.

Commonly, cloning of short double-strand DNA is carried out by synthesizing the full-length sense strand and antisense strand, annealing and then inserting into a cloning vector. In this study, both the sense strand and antisense strand synthesized were partial of the ribozyme gene which were 12 nucleotides complementary to each other on the 3' ends. After annealing to form a hemiduplex, the hemiduplex was extended with Klenow fragment to obtain full-length double-strand DNA. The reliability of this method is proven by the present study. The advantages of this method including comparative simplicity, higher precision and lower cost to synthesize shorter single-strand DNA.

Since the hammerhead ribozyme gene is only about 50 bps in length, primary analysis of the recombinant relies on PAGE conventionally. Because PAGE is comparatively complex, in this study, we introduced *Bgl*II and *Cl*aI restriction sites to the 3' end of the ribozyme gene for the convenience of restriction analysis. As shown in figure, correct recombinants can be linearized by *Cl*aI as well as cleaved into two fragments (1.0kb+3.0kb) by *Bgl*II. Also, because *Not*I restriction site in pGEMEX-1 had been removed, correct recombinant could not be cleaved by *Not*I. Then agarose electrophoresis can be used to analyze the recombinants. One of the six recombinants selected by this strategy was sequenced, and the sequence of the inserted ribozyme gene was confirmed. The result suggests that this strategy is applicable. The recombinant plasmid pGEMEX-1-RZ also would be used as an *in vitro* transcription vector to test the *in vitro* cleavage activity of the ribozyme. The recovered 2.0 kb fragment after *Bgl*II restriction would be used as the transcription template. The transcribed product would have two additional nucleotides on the 3' end of the ribozyme, but these two additional nucleotides have no influence on the secondary structure of the ribozyme predicted by computer.

Design and cloning of a ribozymes are the essential work of

studies about ribozymes. In this study, we designed and cloned the anti-hTERT ribozyme successfully. Next, we will test the *in vitro* cleavage activity of the ribozyme and will investigate the growth inhibition effect of this ribozyme on colonic tumor cell lines.

## REFERENCES

- 1 **Greider CW.** Chromosome first aid. *Cell* 1991; **6**: 645-647
- 2 **Levy MZ, Allsopp RC, Futcher AB, Greider CW, Harley CB.** Telomere end-replication problem and cell aging. *J Mol Biol* 1992; **225**: 951-960
- 3 **de Lange T.** Activation of telomerase in a human tumor. *Proc Natl Acad Sci USA* 1994; **91**: 2882-2885
- 4 **Rhyu MS.** Telomeres, telomerase, and immortality. *J Natl Cancer Inst* 1995; **87**: 884-893
- 5 **Shen ZY, Xu LY, Li EM, Cai WJ, Chen MH, Shen J, Zeng Y.** Telomere and telomerase in the initial stage of immortalization of esophageal epithelial cell. *World J Gastroenterol* 2002; **8**: 357-362
- 6 **Bodnar AG, Ouellette M, Frolkis M, Holt SE, Chiu CP, Morin GB, Harley CB, Shay JW, Lichtsteiner S, Wright WE.** Extension of life-span by introduction of telomerase into normal human cells. *Science* 1998; **279**: 349-352
- 7 **Harley CB.** Telomerase loss: Mitotic clock or genetic time bomb? *Mutat Res* 1991; **256**: 271-282
- 8 **Dhaene K, van Marck E, Parwaresch R.** Telomeres, telomerase, and cancer: an up-date. *Virchows Arch* 2000; **437**: 1-16
- 9 **Zhan WH, Ma JP, Peng JS, Gao JS, Cai SR, Wang JP, Zheng ZQ, Wang L.** Telomerase activity in gastric cancer and its clinical implications. *World J Gastroenterol* 1999; **5**: 316-319
- 10 **Yakoob J, Hu GL, Fan XG, Zhang Z.** Telomere, telomerase and digestive cancer. *World J Gastroenterol* 1999; **5**: 334-337
- 11 **Xu D, Gruber A, Peterson C, Pisa P.** Suppression of telomerase activity in HL60 cells after treatment with differentiating agents. *Leukemia* 1996; **10**: 1354-1357
- 12 **Herbert BS, Pitts AE, Backer SI, Hamilton SE, Wright WE, Shay JW, Corey DR.** Inhibition of human telomerase in immortal human cells lead to progressive telomere shortening and cell death. *Proc Natl Acad Sci USA* 1999; **96**: 14276-14281
- 13 **Zhang FX, Zhang XY, Fan DM, Deng ZY, Yan Y, Wu HP, Fan JJ.** Antisense telomerase RNA induced human gastric cancer cell apoptosis. *World J Gastroenterol* 2000; **6**: 430-432
- 14 **Shammas MA, Simmons CG, Corey DR, Shmookler-Reis RJ.** Telomerase inhibition by peptide nucleic acids reverse "immortality" of transformed human cells. *Oncogene* 1999; **8**: 6191-6200
- 15 **Yokoyama Y, Takahashi Y, Shinohara A, Lian Zenglin, Wan Xiaoyun, Niwa K, Tamaya T.** Attenuation of telomerase activity by a hammerhead ribozyme targeting the template region of telomerase RNA in endometrial carcinoma cells. *Cancer Res* 1998; **58**: 5406-5410
- 16 **Ludwig A, Saretzki G, Holm PS, Tiemann F, Lorenz M, Emrich T, Harley CB, von Zglinick T.** Ribozyme cleavage of telomerase mRNA sensitizes breast epithelial cells to inhibitors of topoisomerase. *Cancer Res* 2001; **61**: 3053-3061
- 17 **Yokoyama Y, Takahashi Y, Shinohara A, Wan X, Takahashi S, Niwa K, Tamaya T.** The 5' -end of hTERT mRNA is a good target for hammerhead ribozyme to suppress telomerase activity. *Biochem Biophys Res Commun* 2001; **273**: 316-321
- 18 **Ramakrishnan S, Sharma HW, Farris AD, Kaufman KM, Harley JB, Collins K, Prujin GJ, van Venrooij WJ, Martin ML, Narayanan R.** Characterization of human telomerase complex. *Proc Natl Acad Sci USA* 1997; **94**: 10075-10079
- 19 **Masutomi K, Kaneko S, Hayashi N, Yamashita T, Shiota Y, Kobayashi K, Murakami S.** Telomerase activity reconstituted *in vitro* with purified human telomerase reverse transcriptase and human telomerase RNA component. *J Bio Chem* 2000; **275**: 22568-22573
- 20 **Feng J, Funk WD, Wang SS, Weinrich SL, Avilion AA, Chiu CP, Adams RR, Chang E, Allsopp RC, Yu J, Le S, West MD, Harley CB, Andrews WH, Greider CW, Villeponteau.** The RNA component of human telomerase. *Science* 1995; **269**: 1236-1241
- 21 **Martin-Rivera L, Herrera E, Albar JP, Blasco MA.** Expression of mouse telomerase catalytic subunit in embryos and adult tissues. *Proc Natl Acad Sci USA* 1998; **95**: 10471-10476
- 22 **Cristoffersen RE, Marr JJ.** Ribozymes as human therapeutic agents. *J Med Chem* 1995; **38**: 2023-2037
- 23 **Jen KY, Gewirtz AM.** Suppression of gene expression by targeted disruption of messenger RNA: Available options and current strategies. *Stem Cell* 2000; **18**: 307-319
- 24 **Haseloff J, Gerlach WL.** Simple RNA enzymes with new and highly specific endoribonuclease activity. *Nature* 1988; **334**: 585-591
- 25 **Sambrook J, Fritsch EF, Maniatis T, eds.** Molecular cloning A laboratory manual, 2<sup>nd</sup> ed. Cold spring harbor laboratory press, 1989
- 26 **Vaish NK, Kore AR, Eckstein F.** Recent development in the hammerhead ribozyme field. *Nucleic Acid Res* 1998; **26**: 5237-5242
- 27 **Kore AR, Vaish NK, Kutzke U, Eckstein F.** Sequence specificity of the hammerhead ribozyme revisited; the NHH rule. *Nucleic Acids Res* 1998; **26**: 4116-4120
- 28 **Herschlag D.** Implications of ribozyme kinetics for targeting the cleavage of specific RNA molecules *in vivo*: More isn't always better. *Proc Natl Acad Sci USA* 1991; **88**: 6921-6925
- 29 **Hertel KJ, Herschlag D, Uhlenbeck OC.** A kinetic and thermodynamic framework for the hammerhead ribozyme reaction. *Biochemistry* 1994; **33**: 3374-3385
- 30 **Hormes R, Homann M, Oelze I, Marschall P, Tabler M, Eckstein F, Sczakiel G.** The subcellular localization and length of hammerhead ribozyme determine efficacy in human cells. *Nucleic Acids Res* 1997; **25**: 769-775
- 31 **Sloud M.** Effects of variations in length of hammerhead ribozyme antisense arms upon the cleavage of longer RNA substrates. *Nucleic Acids Res* 1997; **25**: 333-338
- 32 **Helene C, Toulme JJ.** Specific regulation of gene expression by antisense, sense and antigene nucleic acids. *Biochim Biophys Acta* 1990; **1049**: 99-125
- 33 **Tabler M, Homann M, Tzortzakaki S, Sczakiel G.** A three nucleotide helix I is sufficient for full activity of a hammerhead ribozyme: Advantages of an asymmetric design. *Nucleic Acid Res* 1994; **22**: 395
- 34 **Campbell TB, McDonald CK, Hagen M.** The effect of structure in a long target RNA on ribozyme cleavage efficiency. *Nucleic Acids Res* 1997; **25**: 4985-4993
- 35 **Amarzguioui M, Brede G, Babaie E, Grotli M, Sproat B, Prydz H.** Secondary structure prediction and *in vitro* accessibility of mRNA as tools in the selection of target sites for ribozyme. *Nucleic Acids Res* 2000; **28**: 413-4124
- 36 **Patzel V, Steidl U, Kronenwett R.** A theoretical approach to select effective antisense oligodeoxyribonucleotides at high statistical probability. *Nucleic Acid Research* 1999; **27**: 4328-4334
- 37 **Scherr M, Ross JJ, Sczakiel G, Patzel V.** RNA accessibility prediction: a theoretical approach is consistent with experimental studies in cell extracts. *Nucleic Acids Res* 2000; **28**: 2455-2461
- 38 **Mathews DH, Sabina J, Zuker M, Turner DH.** Expanded sequence dependence of thermodynamic parameters improves prediction of RNA secondary structure. *J Mol Biol* 1999; **288**: 911-940
- 39 **Nakamura TM, Morin GB, Chapman KB, Weinrich SL, Andrews WH, Lingner J, Harley CB, Cech TR.** Telomerase catalytic subunit homologs from fission yeast and human. *Science* 1997; **277**: 955-959



# HBV DNA vaccine with adjuvant cytokines induced specific immune responses against HBV infection

De-Wei Du, Zhan-Sheng Jia, Guang-Yu Li, Yong-Ying Zhou

**De-Wei Du, Zhan-Sheng Jia, Guang-Yu Li, Yong-Ying Zhou,**  
Department of Infectious Diseases, Tangdu Hospital, Fourth Military Medical University, Xi'an 710038, Shaanxi Province, China  
**Supported by** the National Natural Science Foundation of China, No. 39770665

**Correspondence to:** Dr. De-Wei Du, Department of Infectious Diseases, Tangdu Hospital, the Fourth Military Medical University, Xi'an 710038, Shaanxi Province, China. ddw0715@yahoo.com.cn  
**Received:** 2002-05-02 **Accepted:** 2002-07-30

## Abstract

**AIM:** To seek for an effective method to improve the immune responses induced by DNA vaccine expressing HBV surface antigen (pCR3.1-S) in Balb/c mice (H-2<sup>d</sup>).

**METHODS:** The pCR3.1-S plasmid and the eukaryotic expression vectors expressing murine IL-2 (pDOR-IL-2) or IL-12 (pWRG3169) were injected into mice subcutaneously. The immune responses to pCR3.1-S and the adjuvant effect of the cytokines plasmid were studied. Meanwhile the effect of pCR3.1-S on anti-translated subcutaneous tumor of P815 mastocytoma cells stably expressing HBsAg (P815-HBV-S) was also studied. Anti-HBs in serum was detected by enzyme-linked immunosorbent assay (ELISA) and HBsAg specific cytotoxic T lymphocytes (CTLs) activity was measured by <sup>51</sup>Cr release assay. After three weeks of DNA immunization, the cells of P815-HBV-S were inoculated into mice subcutaneously and the tumor growth was measured every five days. The survival rate and living periods of mice were also calculated.

**RESULTS:** After 8 wk DNA immunization, the A 450 nm values of sera in mice immunized with pCR3.1, pCR3.1-S and pCR3.1-S codelivered with IL-2 or IL-12 plasmids were 0.03±0.01, 1.24±0.10, 1.98±0.17 and 1.67±0.12 respectively. Data in mice codelivered pCR3.1-S with IL-2 or IL-12 plasmids were significantly higher than that of mice injected pCR3.1 or pCR3.1-S only. The HBsAg specific CTL activities in mice coinjected with pCR3.1-S and IL-2 or IL-12 eukaryotic expression vectors were (61.9±7.1) % and (73.3±8.8) %, which were significantly higher than that of mice injected with pCR3.1 (10.1±2.1) % or pCR3.1-S (50.5±6.4) %. The HBsAg specific CTL activities in mice injected with pCR3.1, pCR3.1-S, pCR3.1-S combined with IL-2 or IL-12 eukaryotic expression vectors decreased significantly to (3.2±0.8) %, (10.6±1.4) %, (13.6±1.3) % and (16.9±2.3) % respectively after the spleen cells were treated by anti-CD8<sup>+</sup> monoclonal antibody, but presented no significant change to anti-CD4<sup>+</sup> monoclonal antibody or unrelated to monoclonal antibody. The HBV-S DNA vaccine (pCR3.1-S) could evidently inhibit the tumor growth, prolong the survival period of mice and improve the survival rate of mice and these effects could be improved by IL-12 gene codelivered.

**CONCLUSION:** HBV DNA vaccine has a strong antigenicity in humoral and cellular immunities, which can be promoted by plasmid expressing IL-2 or IL-12. CD8<sup>+</sup> cells executed

the CTL activities. DNA vaccine may be useful for both prophylaxis and treatment of HBV infection.

Du DW, Jia ZS, Li GY, Zhou YY. HBV DNA vaccine with adjuvant cytokines induced specific immune responses against HBV infection. *World J Gastroenterol* 2003; 9(1): 108-111

<http://www.wjgnet.com/1007-9327/9/108.htm>

## INTRODUCTION

Many animal models of infectious diseases have been reported<sup>[1-3]</sup> which shows DNA vaccine induced broad range of protective immunities, including antibodies, CD8<sup>+</sup>CTL, CD4<sup>+</sup>Th cells against challenge with the pathogens, such as plasmodium<sup>[4]</sup>, influenza virus<sup>[5]</sup> simplex virus<sup>[6]</sup> and HIV-1<sup>[7]</sup>. Application of this genetic vaccination approach has been extended to the treatment of cancers<sup>[8,9]</sup> as well as allergic diseases<sup>[10,11]</sup> and autoimmune disease<sup>[12]</sup>. Because DNA vaccines can induce weak and short-lived immune responses in large out-bred animal<sup>[13]</sup>, seeking for an effective way to promote the immune responses of DNA immunization is an urgent case. Relying on the knowledge above, we constructed a recombination vector expressing HBV S protein, pCR3.1-S, to study the possibility of DNA vaccine in controlling and preventing the HBV infection. In addition, the eukaryotic expression vectors expressing murine IL-2 or IL-12 were coimmunized to mice with pCR3.1-S and their effects as adjuvants for immune responses were also studied. Meanwhile, we established the HBV-infectious animal model through the inoculating of the P815-HBV-S and observed the treatment and preventive effect of pCR3.1-S to HBV infection *in vivo*.

## MATERIALS AND METHODS

### Plasmids, cell lines and mice

Plasmid expressing hepatitis B virus surface antigen (pCR3.1-S)<sup>[14]</sup> was constructed by Prof. Yao ZHQ (in this Department). Plasmids expressing murine IL-2 (pDOR-IL-2) and IL-12 (pRW1369)<sup>[15]</sup> were generous gift from Dr. Feng ZHH (in this Department). P815 mastocytoma cells were generous gift from Dr. Zhao (Department of Pathology, the Fourth Military Medical University). Female Balb/c (H-2<sup>d</sup>) mice were obtained from the Center for Experimental Animals of the Fourth Military Medical University and used at the age of 5-8 weeks.

### Transfection and expression of pCR3.1-S in P815

P815 cells were maintained in RPMI 1640 (Sigma) with 10 mL·L<sup>-1</sup> fetal bovine serum in a six-well tissue culture plate at 37 °C in 5 % CO<sub>2</sub> humidified atmosphere and then transfected with the pCR3.1-S or the pCR3.1 alone by using lipofectamine (GIBCO). For each transfection 20 µg of plasmid and 15 µL of lipofectamine in 0.2 mL of serum free medium were mixed in tube for 30 minutes. After 0.8 mL of serum-free medium were added to the tube, the DNA-lipofectamine complexes were overlaid onto the cells. After incubated 12 hours, the cells were washed two times with the complete culture medium and

the medium was replaced with 2 mL of the complete culture medium. After another 24–48-hour incubation, the cells were transferred from the culture medium, which was then replaced by medium contained  $300 \text{ mg} \cdot \text{L}^{-1}$   $\text{G}_{418}$  (Promega). Two weeks later, the  $\text{G}_{418}$ -resistant clones were selected and the expression of HBsAg was detected by using of indirect immunofluorescence (IIF). The HBsAg-expressed cells were designated as P815-HBV-S and used as the target cells for CTL assay.

### DNA immunization in mice

Four groups of mice were used, each consisting of 5 mice which were immunized with one of the following regimens in 100  $\mu\text{L}$  of sterile saline: (1) 100  $\mu\text{g}$  of pCR3.1-S; (2) mixture of 100  $\mu\text{g}$  of pCR3.1-S and 100  $\mu\text{g}$  of pDOR-IL-2 (IL-2); (3) mixture of 100  $\mu\text{g}$  of pCR3.1-S and 100  $\mu\text{g}$  of pRW1369 (IL-12); (4) 100  $\mu\text{g}$  of pCR3.1 vector. The mice in the last group served as negative control. All injections were done intramuscularly into the left thigh quadriceps muscle of mice at 0, 2, 4, 6 and 8 weeks.

### HBsAg-specific antibody assay

Sera samples were collected by tail bleeding at different times, beginning at 1 wk after immunization, and the presence of HBsAg-specific antibody was analyzed by ELISA. The ELISA kits for the HBsAg-specific antibody detection were purchased from Huamei Co. and performed according to the manufacturer's instructions.

### CTL assay

Spleen cells of mice were segregated 8 weeks after immunization and the CTL activities were measured by  $^{51}\text{Cr}$  releases assay.  $\text{Na}^{51}\text{CrO}_4$  was purchased from Dubang Co. Target cells ( $1 \times 10^6$ ) were labeled with 3.7 MBq radiolabeled sodium chromate. The assays were performed in triplicate with  $1 \times 10^5$  targets/well at various effector cell/target cell (E:T) ratios of 100:1. Results were expressed according to the formula: % specific lysis = (experimental release - spontaneous release) / (maximum release - spontaneous release). Experimental release represents the mean count per-minute released by target cells in the presence of effector cells. Maximum release represents the radioactivity released after lysis of target cells with 50  $\text{g} \cdot \text{L}^{-1}$  Triton X-100. Spontaneous release represents the radioactivity present in medium derived from target cells alone.

### Blocking of CTL response by monoclonal antibodies

At the effector cell/target cell ratio of 100:1, CTL assays were performed in the presence of 10  $\text{mg} \cdot \text{L}^{-1}$  of anti- $\text{CD}_4^+$  or anti- $\text{CD}_8^+$  monoclonal antibody added to the spleen cells in 96-well plates. As a control an unrelated antibody was added to the spleen cells. The monoclonal antibodies to mouse  $\text{CD}_4^+$  or  $\text{CD}_8^+$  cell were purchased from Sigma Chemical Co.

### DNA vaccine against subcutaneous translated tumor

Four groups of mice were used, each consisting of 5 mice immunized with one of the following regimens in 100  $\mu\text{L}$  of sterile saline: (1) 100  $\mu\text{g}$  of pCR3.1-S; (2) mixture of 100  $\mu\text{g}$  of pCR3.1-S and 100  $\mu\text{g}$  of pRW1369 (IL-12). (3) 100  $\mu\text{g}$  of pCR3.1; one group of mice without immunization. Three weeks after DNA immunization, cells of P815-HBV-S were inoculated into mice by subcutaneous injection in abdomen. The growing tumors were measured every five days with a calipers using average diameter. The survival period of mice was observed and the survival rate of mice was calculated.

### Statistical analysis

Data were reported as  $\bar{x} \pm s$  and were analyzed by professional statistical computer software SPSS. Significance was set at  $P < 0.05$ .

## RESULTS

### Codelivery of cytokines gene augmented the titer of antibody induced by pCR3.1-S

The pCR3.1-S showed a strong antigenicity in humoral immunity and the anti-HBsAg could be detected in sera of mice after pCR3.1-S vaccination. The serum titres of anti-HBsAg in mice increased with the times of immunization in a period of time. The titres of anti-HBsAg in sera of mice were significantly promoted by genes expressed murine IL-2 or IL-12, especially by IL-2 gene (Figure 1).

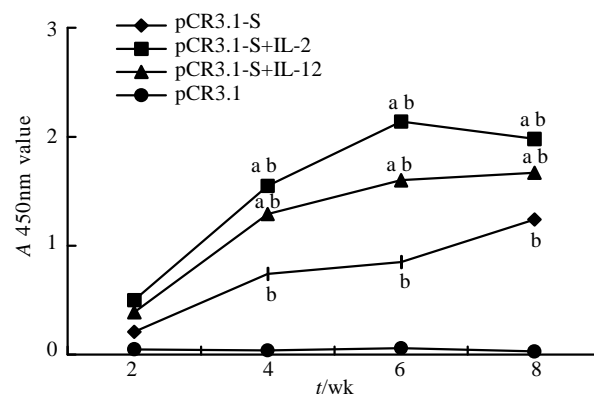


**Figure 1** Serum anti-HBsAg level of Balb/c mice.  $^bP < 0.01$  vs pCR3.1;  $^aP < 0.05$  vs pCR3.1-S

### Cytokines gene effected on the CTL activity induced by pCR3.1-S

The HBsAg specific CTL activities were developed in the mice after pCR3.1-S immunization. The CTL activities were augmented by coimmunized with IL-2 or IL-12 gene. The mice immunized with pCR3.1 alone did not elicited detectable HBsAg specific CTL activities. IL-12 was more effective than IL-2 in promoting the HBsAg specific CTL activities. The CTL activity was blocked by anti- $\text{CD}_8^+$  monoclonal antibody but not by anti- $\text{CD}_4^+$  monoclonal antibody or unrelated antibody (Table 1). Taken together, these results indicated that the CTL activity induced by pCR3.1-S *in vivo* was executed by cells expressing  $\text{CD}_8^+/\text{CD}_4^-$  surface phenotype and the CTL activity could be enhanced or suppressed depending on the cytokines gene expressed.

**Table 1** The effect of cytokines gene on CTL activity induced by pCR3.1-S ( $n=5$ ;  $\bar{x} \pm s$  %)

Group	Untreated	mAb		
		Unrelated	Anti- $\text{CD}_4^+$	Anti- $\text{CD}_8^+{}^b$
pCR3.1	10.1 $\pm$ 2.1	10.7 $\pm$ 1.9	9.7 $\pm$ 1.2	3.2 $\pm$ 0.8
pCR3.1-S	50.5 $\pm$ 6.4	49.7 $\pm$ 6.1	48.3 $\pm$ 5.9	10.6 $\pm$ 1.4
pCR3.1-S+IL-2	61.9 $\pm$ 7.1	62.0 $\pm$ 6.8	56.2 $\pm$ 7.5	13.5 $\pm$ 1.9
pCR3.1-S+IL-12	73.3 $\pm$ 8.8	69.9 $\pm$ 7.6	75.6 $\pm$ 9.1	16.9 $\pm$ 2.3

$^bP < 0.01$  vs unrelated mAb or  $\text{CD}_4^+$  mAb

### DNA vaccine inhibits the formation of subcutaneous translating tumor derived from P815-HBV-S

After inoculated with P815-HBV-S, all five mice with or without pCR3.1 (100 %) formed the tumor. The rate of tumor formation was 20 % (1/5) in mice immunized with pCR3.1-S and there was no tumor formed in mice coimmunized with pCR3.1-S and IL-12. The survival rate of mice immunized with pCR3.1-S alone or coimmunized with IL-12 increased significantly (Figure 2) and the tumor growth was evidently slower than that of mice immunized with or without pCR3.1 (Figure 3).

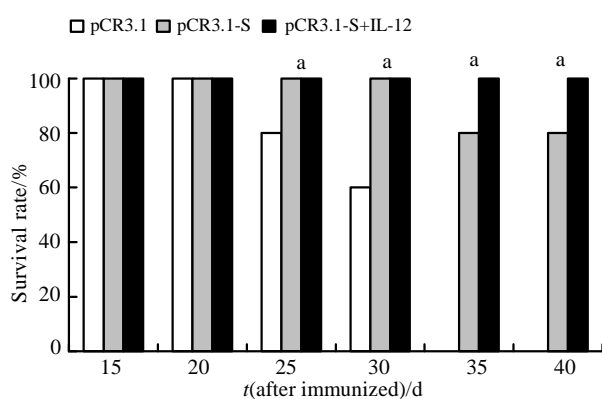


**Figure 2** Survival rate in different group. <sup>a</sup> $P < 0.05$  vs pCR3.1

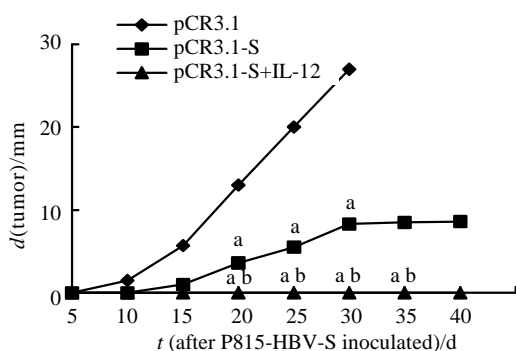


**Figure 3** Growth curve of subcutaneous translating tumor in different group of mice. <sup>b</sup> $P < 0.01$  vs pCR3.1; <sup>a</sup> $P < 0.05$  vs pCR3.1-S

## DISCUSSION

HBV infection is very common in China<sup>[16-23]</sup>. It is estimated that approximately 130 million people in the world is infected by hepatitis B virus (HBV). These people are at risk of developing chronic hepatitis leading to liver cirrhosis and hepatocellular carcinoma. Up to now, vaccination is a main way in prevention<sup>[24-31]</sup>.

It has been suggested that the MHC class II and I restricted T cell responses to the virus are relatively weak during chronic HBV infection<sup>[28]</sup> and there are no specific therapies to cope with it. DNA vaccine contains the gene for an antigenic portion of a pathogen, such as the core or the envelope protein, usually under the transcriptional control of a viral promoter<sup>[29,30]</sup>. In DNA-based vaccination, immunogenic proteins are expressed in transfected cells of the vaccine recipients in their native conformation with correct post-translational modifications from antigen-encoding expression plasmid DNA *in vivo*. This ensures the integrity of antibody-defined epitopes and supports the generation of protective antibody. DNA vaccination is furthermore an exceptionally potent strategy to stimulate CD8+ cytotoxic T lymphocyte (CTL) responses because antigenic peptides are efficiently generated by endogenous processing of intracellular protein antigen<sup>[31]</sup>.

The results of our experiment indicate that the plasmids expressing either IL-2 or IL-12 can enhance the specific humoral and cellular immune responses against HBV infection elicited by pCR3.1-S in mice. The former mainly enhances the level of the HBsAg specific antibody and the latter mainly enhances the HBsAg specific CTL activity.

IL-2 can enhance the immune responses through promoting proliferation and differentiation of B cells and the antibody development. The proliferation and activation of many kinds of T-cells and the production of various cytokins can also be promoted and stimulated by IL-2. The effect of IL-2 enhancing the level of antibody may be related to its ability to induce the

increase of the Th1 cells but not Th2 cells. This can increase IgG2a type of antibody and lead to the increase of the total level of the antibody subsequently<sup>[32-34]</sup>. IL-12 is so far the most potent cytokine with the widest scope of modulation of immune responses. The immune responses can be modulated by IL-12 promoting the production of Th1 type T cells and secretion of other cytokines, stimulating the polarization and proliferation of T cells and through promoting the maturity of CTL cells and LAK cells. All of these can enhance the ability of the host to kill and eliminate pathogens. The adjuvant activities of cytokines were also observed by others<sup>[25,32-36]</sup>.

The situations *in vivo* are different from that *in vitro* after all. In order to search the preventive and therapeutic effects of HBV DNA vaccine to the HBV infection *in vivo*, we serve the mouse injected with P815-HBV-S cells subcutaneously for an animal model of HBV infection. The preventive and therapeutic effects of pCR3.1-S on HBV infectious animal model were investigated by observing the inhibiting effects of pCR3.1-S on the neoplasia of P815-HBV-S cells inoculated by subcutaneous injection. The result indicates that the pCR3.1-S can reduce the formative rate of the subcutaneous translating tumor significantly, inhibit the growth of tumor, prolong the living periods and promote the survival rate of mice injected with the P815-HBV-S cells. Maybe all of these relate to the specific killing effect of CTLs to P815-HBV-S cells induced by DNA vaccine. Furthermore, these effects of pCR3.1-S can be enhanced obviously by IL-12 gene as shown in the experiment. The therapeutic potential of DNA-based immunization for the chronic HBV carrier states has also been demonstrated in a transgenic mouse model<sup>[37]</sup>. This mode of immunization has been shown to successfully eliminate HBsAg in circulation.

These features of DNA-based immunization make it an attractive strategy for prophylactic and therapeutic vaccination against extra- and intracellular pathogens. Recently, DNA vaccines induced the specific humoral<sup>[38]</sup> and cellular<sup>[39-41]</sup> immune responses were observed in human experiments. The results of these experiments suggest that DNA vaccine might be a potential therapy for chronic HBV infection.

## REFERENCES

- Loirat D, Lemonnier FA, Michel ML. Multiepitopic HLA-A\*0201-restricted immune response against hepatitis B surface antigen after DNA-based immunization. *J Immunol* 2000; **165**: 4748-4755
- Dunham SP, Flynn JN, Rigby MA, Macdonald J, Bruce J, Cannon C, Golder MC, Hanlon L, Harbour DA, Mackay NA, Spibey N, Jarrett O, Neil JC. Protection against feline immunodeficiency virus using replication defective proviral DNA vaccines with feline interleukin-12 and -18. *Vaccine* 2002; **20**: 1483-1496
- Huang ZH, Zhuang H, Lu S, Guo RH, Xu GM, Cai J, Zhu WF. Humoral and cellular immunogenicity of DNA vaccine based on hepatitis B core gene in rhesus monkeys. *World J Gastroenterol* 2001; **7**: 102-106
- Le TP, Coonan KM, Hedstrom RC, Charoenvit Y, Sedegah M, Epstein JE, Kumar S, Wang R, Doolan DL, Maguire JD, Parker SE, Hobart P, Norman J, Hoffman SL. Safety, tolerability and humoral immune responses after intramuscular administration of a malaria DNA vaccine to healthy adult volunteers. *Vaccine* 2000; **18**: 1893-1901
- Cox RJ, Mykkeltvedt E, Robertson J, Haaheim LR. Non-lethal viral challenge of influenza haemagglutinin and nucleoprotein DNA vaccinated mice results in reduced viral replication. *Scand J Immunol* 2002; **55**: 14-23
- Strasser JE, Arnold RL, Pachuk C, Higgins TJ, Bernstein DI. Herpes simplex virus DNA vaccine efficacy: effect of glycoprotein D plasmid constructs. *J Infect Dis* 2000; **182**: 1304-1310
- Fuller DH, Rajakumar PA, Wilson LA, Trichel AM, Fuller JT, Shipley T, Wu MS, Weis K, Rinaldo CR, Haynes JR, Murphey-Corb M. Induction of mucosal protection against primary, heterologous simian immunodeficiency virus by a DNA vaccine. *J Virol*

- 2002; **76**: 3309-3017
- 8 **Gavarrasana S**, Kalasapudi R S, Rao T D, Thirumala S. Prevention of carcinoma of cervix with human papillomavirus vaccine. *Indian J Cancer* 2000; **37**: 57-66
- 9 **Thirdborough SM**, Radcliffe JN, Friedmann PS, Stevenson FK. Vaccination with DNA encoding a single-chain tcr fusion protein induces antitumor immunity and protects against t-cell lymphoma. *Cancer Res* 2002; **62**: 1757-1760
- 10 **Horner AA**, Van Uden JH, Zubeldia JM, Broide D, Raz E. DNA-based immunotherapeutics for the treatment of allergic disease. *Immunol Rev* 2001; **179**: 102-118
- 11 **Lee YL**, Ye YL, Yu CI, Wu YL, Lai YL, Ku PH, Hong RL, Chiang BL. Construction of single-chain interleukin-12 DNA plasmid to treat airway hyperresponsiveness in an animal model of asthma. *Hum Gene Ther* 2001; **12**: 2065-2079
- 12 **Garren H**, Ruiz PJ, Watkins TA, Fontoura P, Nguyen LT, Estline ER, Hirschberg DL, Steinman L. Combination of gene delivery and DNA vaccination to protect from and reverse Th1 autoimmune disease via deviation to the Th2 pathway. *Immunity* 2001; **15**: 15-22
- 13 **Chaplin PJ**, De Rose R, Boyle JS, McWaters P, Kelly J, Tennent JM, Lew AM, Scheerlinck JP. Targeting improves the efficacy of a DNA vaccine against *Corynebacterium pseudotuberculosis* in sheep. *Infect Immun* 1999; **67**: 6434-6438
- 14 **Li WB**, Yao ZQ, Zhou YY, Feng ZH. Studies on immunization with HBV gene vaccine plus HBsAg protein in mice. *Shijie Huaren Xiaohua Zazhi* 1999; **7**: 188-190
- 15 **Rakhmievich AL**, Turner J, Ford MJ, McCabe D, Sun WH, Sondel PM, Grotz K, Yang NS. Gene gun-mediated skin transfection with interleukin 12 gene results in regression of established primary and metastatic murine tumors. *Proc Natl Acad Sci USA* 1996; **93**: 6291-6296
- 16 **Guan XJ**, Wu YZ, Jia ZC, Shi TD, Tang Y. Construction and characterization of an experimental ISCOMS-based hepatitis B polypeptide vaccine. *World J Gastroenterol* 2002; **8**: 294-297
- 17 **Chen XS**, Wang GJ, Cai X, Yu HY, Hu YP. Inhibition of hepatitis B virus by oxymatrine *in vivo*. *World J Gastroenterol* 2001; **7**: 49-52
- 18 **Huang ZH**, Zhuang H, Lu S, Guo RH, Xu GM, Cai J, Zhu WF. Humoral and cellular immunogenicity of DNA vaccine based on hepatitis B core gene in rhesus monkeys. *World J Gastroenterol* 2001; **7**: 102-106
- 19 **Fang JN**, Jin CJ, Cui LH, Quan ZY, Choi BY, Ki MR, Park HB. A comparative study on serologic profiles of virus hepatitis B. *World J Gastroenterol* 2001; **7**: 107-110
- 20 **Guo SP**, Wang WL, Zhai YQ, Zhao YL. Expression of nuclear factor- $\kappa$ B in hepatocellular carcinoma and its relation with the X protein of hepatitis B virus. *World J Gastroenterol* 2001; **7**: 340-344
- 21 **You J**, Zhuang L, Tang BZ, Yang H, Yang WB, Li W, Zhang HL, Zhang YM, Zhang L, Yan SM. Interferon alpha with Thymopeptide in the treatment of chronic hepatitis B. *Shijie Huaren Xiaohua Zazhi* 2001; **9**: 388-391
- 22 **He XS**, Huang JF, Chen GH, Fu Q, Zhu XF, Lu MQ, Wang GD, Guan XD. Orthotopic liver transplantation for fulminant hepatitis B. *World J Gastroenterol* 2000; **6**: 398-399
- 23 **Zhao LS**, Qin S, Zhou TY, Tang H, Liu L, Lei BJ. DNA-based vaccination induces humoral and cellular immune responses against hepatitis B virus surface antigen in mice without activation of C-myc. *World J Gastroenterol* 2000; **6**: 239-243
- 24 **Du DW**, Zhou YX, Feng ZH, Li GY, Yao ZQ. Study on immunization of anti-subcutaneous transplanting tumor induced by gene vaccine. *Shijie Huaren Xiaohua Zazhi* 1999; **7**: 955-957
- 25 **Du DW**, Zhou YX, Feng ZH, Yao ZQ, Li GY. Immune responses to interleukin 12 and hepatitis B gene vaccine in H<sup>2</sup>-d mice. *Shijie Huaren Xiaohua Zazhi* 2000; **8**: 128-130
- 26 **Liu HB**, Meng ZD, Ma JC, Han CQ, Zhang YL, Xing ZC, Zhang YW, Liu YZ, Cao HL. A 12-year cohort study on the efficacy of plasma-derived hepatitis B vaccine in rural newborns. *World J Gastroenterol* 2000; **6**: 381-383
- 27 **Li H**, Wang L, Wang SS, Gong J, Zeng XJ, Li RC, Nong Y, Huang YK, Chen XR, Huang ZN. Research on optimal immunization strategies for hepatitis B in different endemic areas in China. *World J Gastroenterol* 2000; **6**: 392-394
- 28 **Geissler M**, Tokushige K, Wakita T, Zurawski VR Jr, Wands JR. Differential cellular and humoral immunization using chimeric constructs. *Vaccine* 1998; **16**: 857-867
- 29 **Reyes-Sandoval A**, Ertl H C. DNA vaccines. *Curr Mol Med* 2001; **1**: 217-243
- 30 **Kwissa M**, Unsinger J, Schirmbeck R, Hauser H, Reimann J. Poly-valent DNA vaccines with bidirectional promoters. *J Mol Med* 2000; **78**: 495-506
- 31 **Schirmbeck R**, Reimann J. Revealing the potential of DNA-based vaccination: lessons learned from the hepatitis B virus surface antigen. *Biol Chem* 2001; **382**: 543-452
- 32 **Du DW**, Liu QQ, Chen HM, Li JG, Lian JQ, Feng ZH, Zhou YX, Yao ZQ. Immune adjuvant effect of eukaryotic expression vector with Interleukin-2 on hepatitis B gene vaccine. *Shanghai Mianyixue Zazhi* 2001; **21**: 77-79
- 33 **Geissler M**, Bruss V, Michalak S, Hockenjos B, Ortman D, Offensperger WB, Wands JR, Blum HE. Intracellular retention of hepatitis B virus surface proteins reduces interleukin-2 augmentation after genetic immunizations. *J Virol* 1999; **73**: 4284-4292
- 34 **Li WB**, Yao ZQ, Zhou YX, Feng ZH. Effect of interleukin-2 on the potency of genetic vaccines of hepatitis B virus. *Di-si Junyi Daxue Xuebao* 1999; **20**: 747-749
- 35 **Scheerlinck JP**, Casey G, McWaters P, Kelly J, Woollard D, Lightowler MW, Tennent JM, Chaplin PJ. The immune response to a DNA vaccine can be modulated by co-delivery of cytokines gene using a DNA prime-protein boost strategy. *Vaccine* 2001; **19**: 4053-4060
- 36 **Noormohammadi AH**, Hochrein H, Curtis JM, Baldwin TM, Handman E. Paradoxical effects of IL-12 in leishmaniasis in the presence and absence of vaccinating antigen. *Vaccine* 2001; **19**: 4043-4052
- 37 **Oka Y**, Akbar SM, Horiike N, Joko K, Onji M. Mechanism and therapeutic potential of DNA-based immunization against the envelope proteins of hepatitis B virus in normal and transgenic mice. *Immunology* 2001; **103**: 90-97
- 38 **Tacket CO**, Roy MJ, Widera G, Swain WF, Broome S, Edelman R. Phase 1 safety and immune response studies of a DNA vaccine encoding hepatitis B surface antigen delivered by a gene delivery device. *Vaccine* 1999; **17**: 2826-2829
- 39 **Roy MJ**, Wu MS, Barr LJ, Fuller JT, Tussey LG, Speller S, Culp J, Burkholder JK, Swain WF, Dixon RM, Widera G, Vessey R, King A, Ogg G, Gallimore A, Haynes JR, Heydenburg Fuller D. Induction of antigen-specific CD8<sup>+</sup> T cells, T helper cells, and protective levels of antibody in humans by particle-mediated administration of a hepatitis B virus DNA vaccine. *Vaccine* 2001; **19**: 764-778
- 40 **Weber R**, Bossart W, Cone R, Luethy R, Moelling K. Phase I clinical trial with HIV-1 gp160 plasmid vaccine in HIV-1-infected asymptomatic subjects. *Eur J Clin Microbiol Infect Dis* 2001; **20**: 800-803
- 41 **Swain WE**, Heydenburg Fuller D, Wu MS, Barr LJ, Fuller JT, Culp J, Burkholder J, Dixon RM, Widera G, Vessey R, Roy MJ. Tolerability and immune responses in humans to a PowderJect DNA vaccine for hepatitis B. *Dev Biol (Basel)* 2000; **104**: 115-119

Edited by Zhang JZ

## Expression of hepatitis B virus X protein in transgenic mice

Jun Xiong, Yu-Cheng Yao, Xiao-Yuan Zi, Jian-Xiu Li, Xin-Min Wang, Xu-Ting Ye, Shu-Min Zhao, Yong-Bi Yan, Hong-Yu Yu, Yi-Ping Hu

**Jun Xiong, Yu-Cheng Yao, Xiao-Yuan Zi, Jian-Xiu Li, Xin-Min Wang, Xu-Ting Ye, Shu-Min Zhao, Yong-Bi Yan, Yi-Ping Hu,** Department of Cell Biology, Second Military Medical University, Shanghai 200433, China

**Hong-Yu Yu,** Department of Pathology, Changzheng Hospital, Second Military Medical University, Shanghai 200433, China

**Supported by** Projects of the Science Development Foundation of Shanghai (No.994919033) and Tackling Key Problems in Science and Technology from the State Science and Technology Ministry (No.TJ99-LA01)

**Correspondence to:** Yi-Ping Hu, Department of Cell Biology, Department of Basic Medicine, Second Military Medical University, Shanghai, 200433, China. yphu@smmu.edu.cn

**Telephone:** +86-21-25070291 **Fax:** +86-21-25070291

**Received:** 2002-01-14 **Accepted:** 2002-07-26

### Abstract

**AIM:** To establish a mice model harboring hepatitis B virus *x* gene (adr subtype) for studying the function of hepatitis B virus X protein, a transactivator of viral and cellular promoter/enhancer elements.

**METHODS:** Expression vector pcDNA3-*HBx*, containing CMV promoter and hepatitis B virus *x* gene open reading fragment, was constructed by recombination DNA technique. Hela cells were cultured in DMEM and transfected with pcDNA3-*HBx* or control pcDNA3 plasmids using FuGENE6 Transfection Reagent. Expression of pcDNA3-*HBx* vectors in the transfected Hela cells was confirmed by Western blotting. After restriction endonuclease digestion, the coding elements were microinjected into male pronuclei of mice zygotes. The pups were evaluated by multiplex polymerase chain reaction (PCR) at genomic DNA level. The *x* gene transgenic mice founders were confirmed at protein level by Western blotting, immunohistochemistry and immunogold transmission electron microscopy.

**RESULTS:** Expression vector pcDNA3-*HBx* was constructed by recombination DNA technique and identified right by restriction endonuclease digestion and DNA direct sequencing. With Western blotting, hepatitis X protein was detected in Hela cells transfected with pcDNA3-*HBx* plasmids, suggesting pcDNA3-*HBx* plasmids could express in eukaryotic cells. Following microinjection of coding sequence of pcDNA3-*HBx*, the embryos were transferred to oviducts of pseudopregnant females. Four pups were born and survived. Two of them were verified to have the *HBx* gene integrated in their genomic DNA by multiplex PCR assay, and named C57-TgN(*HBx*)SMMU1 and C57-TgN(*HBx*)SMMU3 respectively. They expressed 17KD X protein in liver tissue by Western blotting assay. With the immunohistochemistry, X protein was detected mainly in hepatocytes cytoplasm of transgenic mice, which was furthermore confirmed by immunogold transmission electron microscopy.

**CONCLUSION:** We have constructed the expression vector pcDNA3-*HBx* that can be used to study the function of *HBx* gene in eukaryotic cells *in vitro*. We also established *HBx*

gene (adr subtype) transgenic mice named C57-TgN (*HBx*)SMMU harboring *HBx* gene in their genome and express X protein in hepatocytes, Which might be a valuable animal system for studying the roles of *HBx* gene in hepatitis B virus life cycle and development of hepatocellular carcinoma *in vivo*.

Xiong J, Yao YC, Zi XY, Li JX, Wang XM, Ye XT, Zhao SM, Yan YB, Yu HY, Hu YP. Expression of hepatitis B virus X protein in transgenic mice. *World J Gastroenterol* 2003; 9(1): 112-116  
<http://www.wjgnet.com/1007-9327/9/112.htm>

### INTRODUCTION

Human hepatitis B virus (HBV) is the prototype for a family of viruses, referred to as *Hepadnaviridae*<sup>[1,2]</sup>. It has at least 4 subtypes, ayw, adr, ayr, and adw, among which adr is the most prevailing subtype in China. The complete genomic DNA of subtype adr has been cloned and demonstrated only 3.2kbp in length, and which is different from the other 3 subtypes in DNA and protein sequence<sup>[3]</sup>. HBV genome has 4 open reading frames (ORFs), including envelope genes coding region (*pre-s1*, *pre-s2* and *s* gene coding region), precore (*pc*) gene and core(*c*) gene coding region, polymerase (*p*) gene coding region, *x* gene coding region<sup>[4-6]</sup>.

Chronic HBV infection is associated with a high incidence of liver disease, including hepatocellular carcinoma (HCC)<sup>[7-9]</sup>. Based on epidemiologic studies involving chronic HBV infection, it is estimated that the relative risk of developing HCC for HBV carriers may be 100- to 200-fold higher than that for non-carriers. It is proposed that the role of HBV played in HCC predisposition is modifying host gene regulation. Integration of viral DNA into the host genome can mediate host gene deregulation by a variety of mechanisms<sup>[10-15]</sup>. X protein may alter host gene expression leading to the development of HCC<sup>[16]</sup>. It has been demonstrated that X protein is a transactivator of a variety of viral and cellular promoter/enhancer elements and can mediate the activation of signal transduction pathways. Besides, it may affect DNA repair, cell cycle control, and apoptosis<sup>[17-22]</sup>. It is now clear that X-defective virus is unable to initiate infection *in vivo*. However, the physiological role of X protein during the course of an infection remains a major issue unresolved in hepadnavirus biology<sup>[23-27]</sup>.

To explore the function of *HBx* gene *in vivo*, we generated transgenic mice harboring *HBx* gene from subtype adr by microinjection method, in which *HBx* gene could be expressed. This model might be valuable for the study of *HBx* biology and its associated biomedical issues *in vivo*.

### MATERIALS AND METHODS

#### *Reagents, antibodies, cells and animals*

Restriction Endonucleases and T<sub>4</sub> DNA ligase were obtained from Promega Co. (USA). The mouse monoclonal antibody against X protein was purchased from DAKO (USA). Sheep anti mouse IgG-HRP was obtained from CALBIOCHEM (Germany). Gel extraction kit was purchased from QIAGEN. Hela cells were preserved in our laboratory. C57BL/6 mice were maintained in our Transgenic Animal Laboratory (SPF level).

### Plasmid constructions

Plasmids pBR322-HBV (containing two tandem copies of the HBV genome of adr subtype) and pcDNA3 (containing CMV promoter) were preserved in our laboratory. Expression plasmid pcDNA3.1 (containing CMV promoter) was generously provided by Dr. Yu Hong-Yu. An 0.894-Kilobase pair DNA fragment containing *HBx* gene was isolated by gel extraction from plasmid pBR322-HBV after *HindIII* and *BglIII* restriction digest. The fragment was then subcloned into plasmid pcDNA3.1 that has been digested by *HindIII* and *BamHI* to yield intermediate plasmid pcDNA3.1-*HBx*, which was employed as a template for polymerase chain reaction (PCR) amplification of the *HBx* coding fragments. The primers (A: 5'-ACACA AGCTT CATAT GGCTG CTCGG G-3', B: 5'-CATGA ATTCT AGATG ATTAG GCAGA GGTG-3') were synthesized by Sangon Co. (Shanghai). Thirty five cycles of amplification were done in a total volume of 50  $\mu$ l with an annealing temperature of 58 °C. PCR product and pcDNA3 were isolated after *HindIII* and *XbaI* digestion. After ligation, the plasmid of pcDNA3-*HBx* was confirmed by restriction endonucleases digestion and direct DNA sequencing.

### Cell culture and DNA transfection

Hela cells were cultured in DMEM (Gibco) supplemented with 10 % FCS (Gibco) to confluence. Cells at 50 % confluency were transfected with pcDNA3-*HBx* or control pcDNA3 plasmids using FuGENE6 Transfection Reagent (Roche) with a total of 1  $\mu$ g of DNA per 3.5-cm plate of cells. Selection in medium containing geneticin (G418; Gibco) at a concentration of 500  $\mu$ g/ml was started 48 hours later. After 2 weeks selection, positive clones that were named Hela-*HBx* were isolated and further expanded.

### Assay pcDNA3-*HBx* expression in hela cells

Hela-*HBx* cells cultured in 10-cm dishes were rinsed with phosphate-buffered saline (pH7.4) three times and collected in a microcentrifuge tube by trypsinization. Cells were lysed with lysis buffer<sup>[18]</sup>. Supernatants were then diluted 5 times with phosphate-buffered saline (pH7.4) to assay the expression of the transfected pcDNA3-*HBx* vectors in Hela cells by Western blotting.

### Microinjection and production of *HBx* transgenic mice

The pcDNA3-*HBx* plasmid was digested by *SalI* and purified by gel extraction (Qiagen gel extraction kit). Purified coding fragment containing CMV promoter and *HBx* ORF were dissolved in TE buffer (10 mM Tris-HCl, 0.2 mM EDTA, pH7.5) at a final concentration of 2  $\mu$ g/L (-4 000 copies/ $\mu$ l) and microinjected into zygotes. Microinjection and embryo manipulation were performed according to standard protocols.

### Analysis of *HBx* gene integration

Genomic DNA was extracted from tail tissue of pups mice or normal mouse and dissolved in TE buffer. It was used for PCR assays to identify founders of transgenic mice with *HBx* gene. In order to set an internal control of the efficiency of PCR amplification, we developed a multiplex PCR, using two sets of primers to amplify the *HBx* gene and the autosomal *IL3* gene in the same reaction tube<sup>[28,29]</sup>. PCR reaction was performed using 1  $\mu$ l of dissolved DNA, 0.2  $\mu$ M *HBx* gene specific primers (C: 5'-GGACG TCCTT TGTCT ACGTC CCGTC-3', D: 5'-CCTAA TCTCC TCCCC CAACT CCTCC-3', synthesized by Sangon Co. /Shanghai), and 0.1  $\mu$ M *IL3* gene specific primers (E: 5'-GGGAC TCCAA GCTTC AATCA-3', F: 5'-TGGAG GAGGA AGAAA AGCAA-3', synthesized by Sangon Co. /Shanghai) in a total volume of 50  $\mu$ l according to the cycling program: 94 °C, 40 s; 61 °C, 40 s; 72 °C, 60 s; 35 cycles.

### Analysis of *HBx* gene expression in transgenic mice

**Western blotting** Liver samples were obtained from the transgenic mice with *HBx* gene and normal C57BL/6 mice. Specimens (approximately 100 mg) were homogenized in a screw-capped 1.5 ml microcentrifuge tube and lysed in lysis buffer (0.5 % Nonidet P-40, 10 mM Tris (pH7.4), 150 mM NaCl, 1 mM EDTA and 1 mM phenylmethanesulfonyl fluorid). 100 mg lysate was separated via 15 % SDS-polyacrylamide gel electrophoresis with Tris-Glycine buffer (pH8.3). One electrophoresis gel was stained with commassie brilliant blue R-250, and another was blotted to nitrocellulose filter. After blocked with 50 g/L defatted milk, the filter was incubated with X protein mouse monoclonal antibody for 40 min at 37 °C, then washed with TBS (three times, 15 min each time) and incubated with HRP-conjugated sheep anti-mouse IgG for 30 min at 37 °C. Finally, the filter was incubated with peroxidase substrate solution Diaminobenzidine (DAB) for 5 min to visualize the positive bands.

**Immunohistochemistry analysis** Hepatic tissue samples were fixed in 10 % neutral buffered formalin, paraffin-embedded and sectioned. Briefly paraffin-embedded sections were blocked with 3 % hydrogen peroxide (H<sub>2</sub>O<sub>2</sub>) for 10 min at 37 °C and washed with PBS. Subsequently, the sections were incubated in the X protein mouse monoclonal antibody (diluted 1:100) for 2hr at 37 °C. After washing with PBS, the sections were incubated in horseradish peroxidase-labeled sheep anti mouse IgG (diluted 1:50) for 40 min at 37 °C. Washed with PBS three times, the sections were subjected to color reaction with 0.02 % 3, 3-diaminobenzidine tetrahydrochloride containing 0.005 % H<sub>2</sub>O<sub>2</sub> in PBS and counterstained with hematoxylin lightly.

**Immunogold transmission electron microscopy** The immunohistochemical X protein-positive mouse liver tissue was selected to be cut into small pieces (0.1 cm in diameter) and fixed first in 2 % paraformaldehyde and 0.5 % glutaraldehyde mixture buffer for 2hr at 4 °C, washed three times with PBS, acted upon by 0.25 % Triton X-100 for 10 min. After being blocked with blocking buffer, the pieces were incubated with X protein mouse monoclonal antibody over night at 4 °C, washed with TBS and incubated with avidin-gold (15 nm) for 2hr at room temperature; then postfixed in 1 % osmium tetroxide for 1hr at room temperature, dehydrated in gradient ethanol and embedded in epoxy resin. The sections were cut on an LKB Ultralome III, mounted on copper grids, stained with uranyl acetate and lead citrate, and examined by transmission electron microscopy.

## RESULTS

### pcDNA3-*HBx* vector construction and expression in Hela cells

A 0.465kb *HBx* gene was amplified from HBV genomic DNA and subcloned into the expression vector pcDNA3, with which the pcDNA3-*HBx* was constructed. The sequence of *HBx* gene in the plasmid was coincident with that reported before<sup>[3]</sup>, as identified by restriction endonucleases digestion and confirmed by DNA direct sequencing. After purification by gel extraction, pcDNA3-*HBx* plasmids were transfected into Hela cells. Positive clones, Hela-*HBx* cells were isolated by G418 selection. With Western blotting, hepatitis X protein was detected in Hela cells, suggesting pcDNA3-*HBx* plasmids expressed in eukaryotic cells (Figure 1).

### Production of transgenic mice

The pcDNA3-*HBx* plasmid was digested by *SalI* and target fragments containing CMV promoter and *HBx* ORF were purified by gel extraction. Target fragments then were microinjected into male pronuclei of zygotes from C57BL/6



mice. 45 zygotes were microoperated. 41 microinjected eggs were implanted into oviducts of 3 pseudopregnant recipient mice, and 4 pups were born and survived. The born rate was 11 %. By multiplex PCR screening, two of the pups were identified to harbour *HBx* gene in their genomic DNA, named C57-TgN *HMU1* and C57-TgN(*HBx*)SMMU3 (Figure 2).



**Figure 1** Detected hepatitis X protein expression in transfected Hela cells. *M*<sub>r</sub>17 000 X protein was detected in Hela-*HBx* cells. Lane1: control cells; Lane 2: Hela-*HBx* cells.

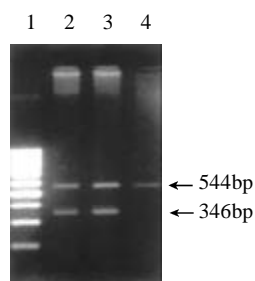


**Figure 2** Analysis of *HBx* gene integration in transgenic mice by PCR. 544 bp *IL3* gene fragment and 346 bp fragment were amplified with positive and negative primers. Lane 1: 100 bp ladder Marker; Lane 2: C57-TgN (*HBx*) SMMU1 transgenic mice; Lane3: C57-TgN(*HBx*)SMMU3 transgenic mice; Lane 4: normal C57BL/6 mice.

#### Expression of *HBx* gene in transgenic mouse

To detect the expression of hepatitis X protein in transgenic mice, liver samples were obtained from C57-TgN(*HBx*) SMMU1 mice and normal C57BL/6 mice. Specimens were homogenized and lysed in lysis buffer. 100 mg lysate was used to assay HBX protein. A component of relative molecular mass 17 000 befitting the X protein was specifically detected with anti X protein monoclonal antibody by Western blotting (Figure 3A), suggesting the transgenic mice with *HBx* gene could express X protein in the liver tissue. The distribution of X protein in hepatocytes was determined by immunohistochemistry and immunogold electron microscopy, which revealed that X protein was mainly distributed in hepatocytic cytoplasm, little on plasm membrane and in nucleus (Figure 3B-3D).

#### DISCUSSION

Transgenic mice are the valuable animal models to study the functions of genes<sup>[30]</sup>. Although transgenic mice containing different HBV genes, including the entire viral genome, have been established and analysed before, there is little evidence to suggest that the virus plays a direct role in inducing hepatocellular carcinoma<sup>[31-41]</sup>. Hepatitis X protein is essential for HBV genes expression and replication<sup>[42,43]</sup>. *In vitro*, X protein exhibits a plethora of activities. From cell culture studies, it is believed that X protein can activate the transcription of host genes, including the major histocompatibility complex and c-myc, as well as viral genes. Aside from the transactivation of many promoters, the other activities linked to X protein include

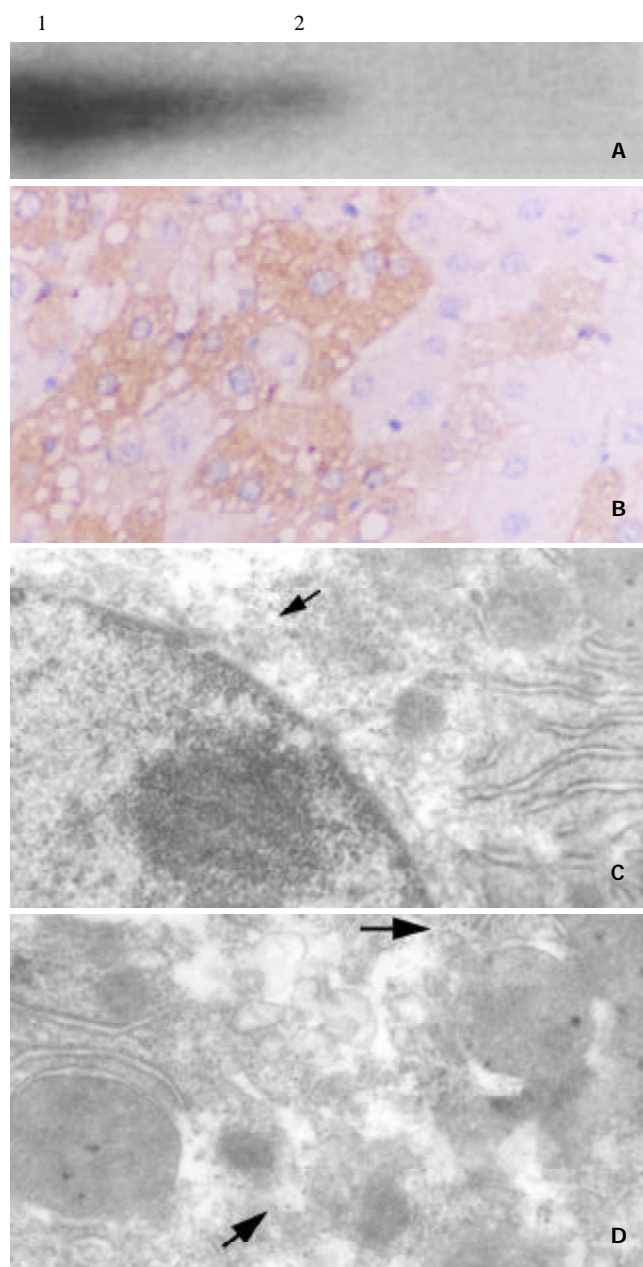


**Figure 3** Expression of *HBx* gene in transgenic mice. (A) Western blot analysis of *HBx* gene expression in liver tissue from transgenic mouse. *M*<sub>r</sub>17 000 X protein was detected with X protein mouse monoclonal antibody; Lane 1: C57-TgN(*HBx*) SMMU1 transgenic mice; Lane 2: normal C57BL/6 mice; (B): *HBx* gene expression mainly in hepatocytes cytoplasm of C57-TgN(*HBx*)SMMU1 transgenic mice demonstrated by immunohistochemistry (×132). (C, D) *HBx* gene Expression in hepatocyte cytoplasm of C57-TgN (*HBx*) SMMU1 transgenic mice detected by immunogold electron microscopy (arrows) 3C: ×20 000; 3D: ×40 000.

stimulation of signal transduction and binding, to various degrees, to well-known protein targets such as p53, proteasome subunit, and UV-damaged DNA binding protein<sup>[44-58]</sup>.

However, the role of *HBx* gene in the course of HBV infection and in inducing HCC is unknown. In the present study, we constructed an *HBx* gene (adr subtype) expression vector pcDNA3-*HBx* containing CMV promoter and *HBx* gene ORF. By Western blotting, we found that it could express X protein in eukaryotic cells. pcDNA3-*HBx* may be a useful vector to study the role of X protein and explore the mechanism of transactivation *in vitro*. We also generated two founders of transgenic mice with *HBx* gene (adr subtype) by microinjections,

named C57-TgN(*HBx*)SMMU1 and C57-TgN(*HBx*)SMMU3, which harboured *HBx* gene in their genomic DNA. The birth rate of the pups was lower than that of other transgenic mice, including entire hepatitis viral genome transgenic mice. This indicated that X protein was probably involved in some phases of development. The hepatitis X protein was expressed in the liver tissue of transgenic mice and distributed mainly in hepacytes cytoplasm by Western blotting, immunohistochemistry and immunogold electron microscopy, which suggested that the transgenic mice could be an important tool in studying the function of *HBx* gene *in vivo*. Besides, we also developed a multiplex PCR to rapidly and accurately screen the transgenic mice with *HBx* gene. This method, using an optimized ratio of primer pairs, allows for the detection of *HBx* gene in transgenic mice, which can not only amplify target genes, but also show its amplification efficiency.

In conclusion, we have established *HBx* (adr subtype) transgenic mice as a model system for defining the function of *HBx* gene (adr subtype) and the role of X protein in the virus life cycle and HCC. And the multiplex PCR is a rapidly and accurately method to detect the transgenic mice with *HBx* gene.

## REFERENCES

- 1 **Tiollais P**, Pourcel C, Dejean A. The hepatitis B virus. *Nature* 1985; **317**: 489-495
- 2 **Ganem D**, Varmus HE. The molecular biology of the hepatitis B viruses. *Annu Rev Biochem* 1987; **56**: 651-693
- 3 **Gan RB**, Chu MJ, Shen LP, Qian SW, Li ZP. The complete nucleotide sequence of the cloned DNA of hepatitis B virus subtype adr in pADR-1. *Sci Sin B* 1987; **30**: 507-521
- 4 **Seeger C**, Mason WS. Hepatitis B virus biology. *Micro Mol Bio Rev* 2000; **64**: 51-68
- 5 **Stuyver LJ**, Locarnini SA, Lok A, Richman DD, Carman WF, Dienstag JL, Schinazi RF. Nomenclature for antiviral-resistance human hepatitis B virus mutations in the polymerase region. *Hepatol* 2001; **33**: 751-757
- 6 **Wu X**, Zhu L, Li ZP, Koshy R, Wang Y. Functional organization of enhancer (EN) of hepatitis B virus. *Virology* 1992; **191**: 490-494
- 7 **Chisari FV**, Ferran C. Hepatitis B virus immunopathogenesis. *Annu Rev Immunol* 1995; **13**: 29-60
- 8 **Chisari FV**. Viruses, immunity, and cancer: lessons from hepatitis B. *Am J Pathol* 2000; **156**: 1117-1132
- 9 **Montalto G**, Cervello M, Giannitrapani L, Dantona F, Terranova A, Castagnetta LA. Epidemiology, risk factors, and natural history of hepatocellular carcinoma. *Ann N Y Acad Sci* 2002; **963**: 13-20
- 10 **Arbuthnot P**, Kew M. Hepatitis B virus and hepatocellular carcinoma. *Int J Exp Pathol* 2001; **82**: 77-100
- 11 **Honda M**, Kaneko S, Kawai H, Shiota Y, Kobayashi K. Differential gene expression between chronic hepatitis B and C hepatic lesion. *Gastroenterology* 2001; **120**: 955-966
- 12 **Liu H**, Wang Y, Zhou Q, Gui SY, Li X. The point mutation of p53 gene exon7 in hepatocellular carcinoma from Anhui Province, a non HCC prevalent area in China. *World J Gastroenterol* 2002; **8**: 480-482
- 13 **Li Y**, Tang ZY, Ye SL, Liu YK, Chen J, Xue Q, Chen J, Gao DM, Bao WH. Establishment of cell clones with different metastatic potential from the metastatic hepatocellular carcinoma cell line MHCC97. *World J Gastroenterol* 2001; **7**: 630-636
- 14 **Cao XY**, Liu J, Lian ZR, Clayton M, Hu JL, Zhu MH, Fan DM, Feitelson M. Differentially expressed genes in hepatocellular carcinoma induced by woodchuck hepatitis B virus in mice. *World J Gastroenterol* 2001; **7**: 575-578
- 15 **Lee JH**, Ku JL, Park YJ, Lee KU, Kim WH, Park JG. Establishment and characterization of four human hepatocellular carcinoma cell lines containing hepatitis B virus DNA. *World J Gastroenterol* 1999; **5**: 289-295
- 16 **Madden CR**, Finegold MJ, Slagle BL. Hepatitis B virus X protein acts as a tumor promoter in development of diethylnitrosamine-induced preneoplastic lesions. *J Virol* 2001; **75**: 3851-3858
- 17 **Koike K**, Moriya K, Yotsuyanagi H, Iino S, Kurokawa K. Induction of cell cycle progression by hepatitis B virus HBx gene expression in quiescent mouse fibroblasts. *J Clin Invest* 1994; **94**: 44-49
- 18 **Shih WL**, Kuo ML, Chuang SE, Cheng AL, Doong SL. Hepatitis B virus X protein inhibits transforming growth factor- $\alpha$ -induced apoptosis through the activation of phosphatidylinositol 3-kinase pathway. *J Bio Chem* 2000; **275**: 25858-25864
- 19 **Benn J**, Schneider RJ. Hepatitis B virus HBx protein deregulates cell cycle checkpoint controls. *Proc Natl Acad Sci* 1995; **92**: 11215-11219
- 20 **Ogden SK**, Lee KC, Barton MC. Hepatitis B viral transactivator HBx alleviates p53-mediated repression of  $\alpha$ -fetoprotein gene expression. *J Bio Chem* 2000; **275**: 27806-27814
- 21 **Su F**, Theodosios CN, Schneider RJ. Role of NK-kappaB and myc proteins in apoptosis induced by hepatitis B virus HBx protein. *J Virol* 2001; **75**: 215-225
- 22 **Diao J**, Garces R, Richardson CD. X protein of hepatitis B virus modulates cytokine and growth factor related signal transduction pathways during the course of viral infections and hepatocarcinogenesis. *Cytokine Growth Factor Rev* 2001; **12**: 189-205
- 23 **Kaneko S**, Miller RH. X-region-specific transcript in mammalian hepatitis B virus-infected liver. *J virol* 1988; **62**: 3979-3984
- 24 **Terradillos O**, Pollicino T, Lecoeur H, Tripodi M, Gougeon ML, Tiollais P, Buendia MA. p53-independent apoptotic effects of the hepatitis B virus HBx protein *in vivo* and *in vitro*. *Oncogene* 1998; **17**: 2115-2123
- 25 **Su F**, Schneider RJ. Hepatitis B virus HBx protein sensitizes cells to apoptotic killing by tumor necrosis factor alpha. *Proc Natl Acad Sci U S A* 1997; **94**: 8744-8749
- 26 **Murakami S**. Hepatitis B virus X protein: a multifunctional viral regulator. *J Gastroenterol* 2001; **36**: 651-660
- 27 **Feitelson MA**, Duan LX. Hepatitis B virus x antigen in the pathogenesis of chronic infections and the development of hepatocellular carcinoma. *Am J Pathol* 1997; **150**: 1141-1157
- 28 **Miyatake S**, Yokota T, Lee F, Arai K. Structure of the chromosomal gene for murine interleukin 3. *Proc Natl Acad Sci USA* 1985; **82**: 316-320
- 29 **Lambert JF**, Benoit BO, Colvin GA, Carlson J, Delville Y, Quesenberry PJ. Quick sex determination of mouse fetuses. *J Neurosci Method* 2000; **95**: 127-132
- 30 **Rall GF**, Lawrence DM, Patterson CE. The application of transgenic and knockout mouse technology for the study of viral pathogenesis. *Virology* 2000; **271**: 220-226
- 31 **Koike K**. Hepatocarcinogenesis in hepatitis viral infection: lessons from transgenic mouse studies. *J Gastroenterol* 2002; **37** (suppl13): 55-64
- 32 **Chen XS**, Wang GJ, Cai X, Yu HY, Hu YP. Inhibition of hepatitis B virus by oxymatrine *in vivo*. *World J Gastroenterol* 2001; **7**: 49-52
- 33 **Aragona E**, Burk RD, Ott M, Shafritz DA, Gupta S. Cell type-specific mechanisms regulate hepatitis B virus transgene expression in liver and other organs. *J Pathol* 1996; **180**: 441-449
- 34 **Xu Z**, Yen TS, Wu L, Madden CR, Tan W, Slagle BL, Ou JH. Enhancement of hepatitis B virus replication by its X protein in transgenic mice. *J Virol* 2002; **76**: 2579-2584
- 35 **Guidotti LG**, Matzke B, Schaller H, Chisari FV. High-level hepatitis B virus replication in transgenic mice. *J Virol* 1995; **69**: 6158-6169
- 36 **Zhu HZ**, Cheng GX, Chen JQ, Kuang SY, Cheng Y, Zhang XL, Li HD, Xu SF, Shi JQ, Qian GS, Gu JR. Preliminary study on the production of transgenic mice harboring hepatitis B virus X gene. *World J Gastroenterol* 1998; **4**: 536-539
- 37 **Chemin I**, Ohgaki H, Chisari FV, Wild CP. Altered expression of hepatic carcinogen metabolizing enzymes with liver injury in HBV transgenic mouse lineages expressing various amounts of hepatitis B surface antigen. *Liver* 1999; **19**: 81-87
- 38 **Schweizer J**, Valenza-Schaerly P, Goret F, Pourcel C. Control of expression and methylation of a hepatitis B virus transgene by strain-specific modifiers. *DNA Cell Biol* 1998; **17**: 427-435
- 39 **Kim CM**, Koike K, Saito I, Miyamura T, Jay G. HBx gene of hepatitis B virus induces liver cancer in transgenic mice. *Nature* 1991; **351**: 317-320
- 40 **Hu YP**, Hu WJ, Zheng WC, Li JX, Dai DS, Wang XM, Zhang SZ, Yu HY, Sun W, Hao GR. Establishment of transgenic mouse harboring hepatitis B virus (adr subtype) genomes. *World J Gastroenterol* 2001; **7**: 111-114
- 41 **Hu YP**, Yao YC, Li JX, Wang XM, Li H, Wang ZH, Lei ZH. The



- cloning of 3' -truncated preS/S gene from HBV genomic DNA and its expression in transgenic mice. *World J Gastroenterol* 2000; **6**: 734-737
- 42 **Ganem D**. The X files-one step closer to closure. *Science* 2001; **294**: 2299-2300
- 43 **Bouchard MJ**, Wang LH, Schneider RJ. Calcium signaling by HBx protein in hepatitis B virus DNA replication. *Science* 2001; **294**: 2376-2378
- 44 **Yun C**, Um HR, Jin YH, Wang JH, Lee MO, Park S, Lee JH, Cho H. NF-kappaB activation by hepatitis B virus X (HBx) protein shifts the cellular fate toward survival. *Cancer Lett* 2002; **184**: 97-104
- 45 **Bergametti F**, Sitterlin D, Transy C. Turnover of hepatitis B virus X protein is regulated by damaged DNA-binding complex. *J Virol* 2002; **76**: 6495-6501
- 46 **Li J**, Xu Z, Zheng Y, Johnson DL, Ou JH. Regulation of hepatocyte nuclear factor 1 activity by wild-type and mutant hepatitis B virus X proteins. *J Virol* 2002; **76**: 5875-5881
- 47 **Han HJ**, Jung EY, Lee WJ, Jang KL. Cooperative repression of cyclin-dependent kinase inhibitor p21 gene expression by hepatitis B virus X protein and hepatitis C virus core protein. *FEBS Lett* 2002; **518**: 169-172
- 48 **Wang XZ**, Jiang XR, Chen XC, Chen ZX, Li D, Lin JY, Tao QM. Seek protein which can interact with hepatitis B virus X protein from human liver cDNA library by yeast two-hybrid system. *World J Gastroenterol* 2002; **8**: 95-98
- 49 **Guo SP**, Wang WL, Zhai YQ, Zhao YL. Expression of nuclear factor-kappa B in hepatocellular carcinoma and its relation with the X protein of hepatitis B virus. *World J Gastroenterol* 2001; **7**: 340-344
- 50 **Lee S**, Tarn C, Wang WH, Chen S, Hullinger RL, Andrisani OM. Hepatitis B virus X protein differentially regulates cell cycle progression in X-transforming versus nontransforming hepatocyte (AML12) cell lines. *J Biol Chem* 2002; **277**: 8730-8740
- 51 **Qiao L**, Leach K, McKinstry R, Gilfor D, Yacoub A, Park JS, Grant S, Hylemon PB, Fisher PB, Dent P. Hepatitis B virus X protein increases expression of p21(Cip-1/WAF1/MDA6) and p27(Kip-1) in primary mouse hepatocytes, leading to reduced cell cycle progression. *Hepatology* 2001; **34**: 906-917
- 52 **Waris G**, Huh KW, Siddiqui A. Mitochondrially associated hepatitis B virus X protein constitutively activates transcription factors STAT-3 and NF-kappa B via oxidative stress. *Mol Cell Biol* 2001; **21**: 7721-7730
- 53 **Nag A**, Datta A, Yoo K, Bhattacharyya D, Chakraborty A, Wang X, Slagle BL, Costa RH, Raychaudhuri P. DDB2 induces nuclear accumulation of the hepatitis B virus X protein independently of binding to DDB1. *J Virol* 2001; **75**: 10383-10392
- 54 **Lin-Marq N**, Bontron S, Leupin O, Strubin M. Hepatitis B virus X protein interferes with cell viability through interaction with the p127-kDa UV-damaged DNA-binding protein. *Virology* 2001; **287**: 266-274
- 55 **Tarn C**, Lee S, Hu Y, Ashendel C, Andrisani OM. Hepatitis B virus X protein differentially activates RAS-RAF-MAPK and JNK pathways in X-transforming versus non-transforming AML12 hepatocytes. *J Biol Chem* 2001; **276**: 34671-34680
- 56 **Jaitovich-Groisman I**, Benlimame N, Slagle BL, Perez MH, Alpert L, Song DJ, Fotouhi-Ardakani N, Galipeau J, Alaoui-Jamali MA. Transcriptional regulation of the TFIIH transcription repair components XPB and XPD by the hepatitis B virus x protein in liver cells and transgenic liver tissue. *J Biol Chem* 2001; **276**: 14124-14132
- 57 **Pan J**, Duan LX, Sun BS, Feitelson MA. Hepatitis B virus X protein protects against anti-Fas-mediated apoptosis in human liver cells by inducing NF-kappa B. *J Gen Virol* 2001; **82**: 171-182
- 58 **Sitterlin D**, Bergametti F, Transy C. UVDDDB p127-binding modulates activities and intracellular distribution of hepatitis B virus X protein. *Oncogene* 2000; **19**: 4417-4426

Edited by Zhu L

# Changes in serum and histology of patients with chronic hepatitis B after interferon alpha-2b treatment

Hong-Lei Han, Zhen-Wei Lang

**Hong-Lei Han, Zhen-Wei Lang**, Department of Pathology, Beijing Youan Hospital, Beijing 100054, Beijing City, China

**Correspondence to:** Professor Zhen-Wei Lang, Department of Pathology, Beijing Youan Hospital, Beijing 100054, Beijing City, China  
**Telephone:** +86-10-63292211-2402

**Received:** 2001-07-19 **Accepted:** 2001-09-21

## Abstract

**AIM:** Chronic hepatitis B is a serious health problem. Interferon has long been used to treat Chronic hepatitis B. To evaluate the effects of interferon on chronic hepatitis B better, we designed the study to investigate the changes in sera and liver histology of patients with chronic hepatitis B after interferon alpha-2b treatment.

**METHODS:** Twenty-four patients with chronic hepatitis B were enrolled in this study. They all received interferon alpha-2b treatment as following: 3 million units, i.m., t.i.w., for 18 weeks. Sera of all patients were obtained respectively for evaluation of ALT, HBsAg, HBcAg, HBeAg, HBV DNA and TIMP-1 before and after interferon treatment, also a liver biopsy pre- and post-treatment was performed for comparison of HAI, HBsAg, HBcAg, HBeAg, TIMP-1 and activated HSC in the liver tissue.

**RESULTS:** Patients who had normalization of serum ALT and seroconversion of HBeAg and/or HBV DNA (blot hybridization) after treatment were defined as responders. The response rate in this study group was 37.5 % (7/24). Compared to pretreatment, the serum HBV DNA and TIMP-1 decreased significantly ( $P < 0.05$ ), so did the HAI, HBcAg, HBeAg, TIMP-1 and activated HSC ( $P < 0.05$ ).

**CONCLUSION:** The significant decrease in HBV DNA in sera, the seroconversion of HBeAg, and the decrease of viral expression in liver indicated that interferon alpha-2b treatment can inhibit viral replication. The normalization of ALT in sera and the improvement of HAI in liver showed that interferon alpha-2b can improve the liver histology of patients with chronic hepatitis B. At the same time, interferon alpha-2b treatment can reduce the TIMP-1 in serum and liver and decrease the number of activated HSC, which may alleviate or inhibit hepatic fibrosis. Although the response rate was unsatisfactory, interferon play a beneficial role on patients with chronic hepatitis B in other respects. We still need further studies to improve the therapy effects.

Han HL, Lang ZW. Changes in serum and histology of patients with chronic hepatitis B after interferon alpha-2b treatment. *World J Gastroenterol* 2003; 9(1): 117-121  
<http://www.wjgnet.com/1007-9327/9/117.htm>

## INTRODUCTION

Chronic hepatitis B is a serious problem threatening public health, especially in our country. Interferon has been used to treat it for a long time. It has been proved that after interferon

treatment, the response rate in patients with chronic hepatitis B is about 30-50 %, with normalization of ALT, seroconversion of HBeAg and HBV DNA and improvement of liver HAI<sup>[1-11]</sup>. However, the effects on hepatic fibrosis and viral antigen in liver tissue have been seldom reported. In this study, we evaluated mainly the effects of interferon treatment on some indexes of sera and liver histology.

## MATERIALS AND METHODS

### Materials

**Patients** Twenty-four patients were enrolled in this study. Of these, 21 were male, 3 were female. The mean age was 38.4. All patients had moderately elevated serum ALT. All patients were negative for hepatitis C and D. None had alcoholic liver disease, autoimmune or drug-induced liver disease, no patients had received antiviral or immunomodulatory therapy. Informed consent was obtained from each patient before the study. All patients were treated with recombinant IFN- $\alpha$ -2b 3MU thrice a week for 18 weeks (The IFN- $\alpha$ -2b was a product of Anke Company of biological technic of Anhui Province). Liver biopsy was performed in each patient before and after IFN treatment and serum specimens were obtained at the same time.  
**Response to IFN- $\alpha$ -2b treatment** Patients who had normalization of serum ALT and seroconversion of HBeAg and/or HBV DNA (blot hybridization) after treatment were defined as responders, while those with negative result were taken as non-responders.

### Methods

**Assay for serum HBV, HCV, CMV and EBV markers** All markers were measured by using the enzyme linked immunosorbent assay (ELISA). Antibodies to HBsAg, anti-HBs, HBeAg, anti-HBe, anti-HBc-IgM, anti-HBc-IgG, anti-HCV-IgG and anti-HCV-IgM were products of American Abbott Company. Anti-CMV-IgG and anti-EBV-IgG were purchased from Italian Deyi Company. The reagents for HBV DNA blot hybridization were products of Yuanli Reagent Company of Shanghai Medical University.

**Quantitative PCR of serum HBV DNA** Blood samples were obtained under fasting conditions before and after the IFN treatment. All sera were stored at -40 °C until assay. Quantitative polymerized chain reaction (PCR) of HBV DNA was performed as the method introduced by American Biotronics Company<sup>[12]</sup>. The logarithms of the HBV DNA levels were statistically analyzed.

**Assay for serum TIMP-1** Serum TIMP-1 was evaluated by using sandwich method of ELISA. Multiclonal antibody to TIMP-1 was bought from Beijing Zhongshan Biological Company, while monoclonal antibody to TIMP-1 was from Fujian Maxim Biological Company. Other reagents for ELISA were purchased from Beijing Zhongshan Biological Company.

**Histological analysis** Liver specimens were graded by 2 pathologists blinded to the response to treatment, using the histological activity index (HAI) described by Knodell<sup>[13]</sup>.

**Assay for viral antigen in liver** Expression of HBsAg, HBcAg and HBeAg in liver were evaluated using immunohistochemical S-P method. S-P kit was produced by Fujian Maxim Biological

Company. The procedures were performed according to the kit instruction. Expression of viral antigen in the liver was evaluated by semi-quantitative scoring system referring to the method introduced by Lindh<sup>[14]</sup>. Based on the ratio of positive cells, the score was 0-3 respectively, corresponding to the positivity in 0 %, 1-20 %, 20-50 %, and more than 50 % of hepatocytes examined.

**Liver fibrosis** (1) Using  $\alpha$ -smooth muscle actin ( $\alpha$ -SMA) as a marker of activated hepatic stellate cell (HSC), the changes of activated HSC in the liver were analysed. (2) The expression of TIMP-1 in the liver was also investigated by using immunohistochemical method. The reagents for both HSC and TIMP-1 were bought from Fujian Maxim Biological Company. Scoring systems were the same as that for viral antigens.

### Statistical analysis

All statistics were performed by using statistical procedure of social science (SPSS), including chi-square test and Wilcoxon's rank sum test. The probability values less than 5 % were considered significant.

## RESULTS

### Responders and non-responders

After interferon treatment, 7/24 (37.5 %) of patients were responders who had normalization of ALT and seroconversion of HBeAg and/or HBV DNA. The other 15 (62.5%) patients were non-responders.

### Changes in serum level of HBV DNA

The average logarithm of serum HBV DNA before interferon treatment was  $8.20 \pm 0.60$  m, which changed to  $7.21 \pm 1.14$  after treatment (Table 1 and Figure 1). Compared to pretreatment, the serum level of HBV DNA decreased significantly ( $P < 0.05$ ). Moreover, the decrease of serum HBV DNA level of responders was significant ( $P < 0.05$ ).

**Table 1** Changes of serum HBV DNA of patients with chronic hepatitis B (Logarithm of the value expressed by copy/ml) ( $\bar{x} \pm s$ )

	responders (n=9)	non-responders (n=15)	all patients (n=24)
pretreatment	$8.52 \pm 0.39$	$8.00 \pm 0.64$	$8.20 \pm 0.60$
post-treatment	$7.24 \pm 0.83$	$7.16 \pm 0.14$	$7.21 \pm 1.14$
P value	$P = 0.028$	$P = 0.051$	$P = 0.002$

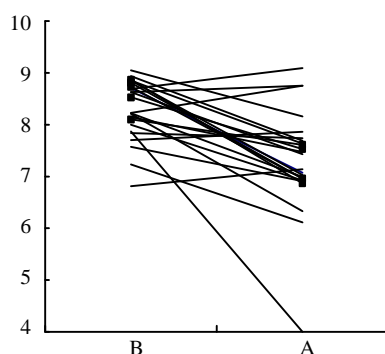


**Figure 1** Changes of the logarithm value of serum HBV DNA of patients with chronic hepatitis B (B: before IFN treatment; A: after IFN treatment)

### Changes in serum TIMP-1

Because of limited samples, only the serum TIMP-1 of 13

patients (4 responders and 9 non-responders) were evaluated. After the IFN treatment was completed, the optical density (OD) values of serum TIMP-1 of 10/13 (76.9 %) of patients decreased. Compared to pretreatment, the decrease was significant (pretreatment  $0.481 \pm 0.199$ , post-treatment  $0.367 \pm 0.210$ ,  $P < 0.05$ ) (Figure 2), regardless of the responders or non-responders.

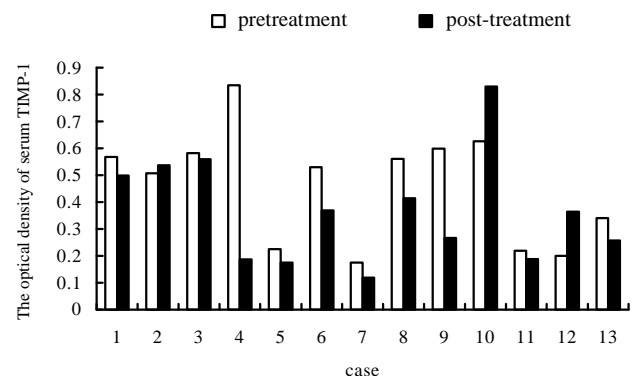


**Figure 2** Changes of OD value of serum TIMP-1 of patients with chronic hepatitis B

### Changes in HAI

Before IFN treatment, there was no significant difference of the HAI between the responders and non-responders ( $P > 0.05$ ). After treatment, the HAI of patients decreased markedly ( $P < 0.05$ ), especially the necrosis and intralobular inflammation ( $P < 0.05$ ), but not the portal inflammation and fibrosis ( $P > 0.05$ ). The changes of HAI of responders was significant ( $P < 0.05$ ), while that of non-responders was insignificant ( $P > 0.05$ ). (Table 2).

**Table 2** Changes of HAI of patients with chronic hepatitis B ( $\bar{x} \pm s$ )

	responders (n=9)		nonresponders (n=15)		all patients (n=24)	
	pre-treatment	post-treatment	pre-treatment	post-treatment	pre-treatment	post-treatment
necrosis	$2.57 \pm 1.51$	$2.14 \pm 1.21$	$2.82 \pm 0.98$	$1.91 \pm 1.04$	$2.72 \pm 1.18^a$	$2.06 \pm 1.11$
lob. inf.	$3.29 \pm 0.49^a$	$1.57 \pm 0.98$	$2.67 \pm 0.82$	$2.36 \pm 0.92$	$2.72 \pm 0.89^a$	$1.78 \pm 1.00$
portal inf.	$3.00 \pm 1.00$	$2.29 \pm 1.25$	$2.32 \pm 0.96$	$2.09 \pm 0.94$	$2.58 \pm 1.00$	$2.39 \pm 0.98$
necrosis	$1.71 \pm 1.25$	$1.57 \pm 1.13$	$1.91 \pm 1.14$	$1.36 \pm 1.12$	$1.82 \pm 1.15$	$1.44 \pm 1.10$
HAI	$10.57 \pm 3.6^a$	$7.57 \pm 4.12$	$9.41 \pm 3.04$	$7.45 \pm 3.11$	$9.86 \pm 3.22^a$	$7.78 \pm 3.30$

<sup>a</sup> $P < 0.05$

### Viral antigens in liver

In the liver, HBsAg was expressed in the following pattern: membranous, submembranous, cytoplasmic or inclusion body. In this study, before IFN treatment, HBsAg was mainly located in the cytoplasm of hepatocytes, and was positive in 22/24 (91.7 %). The positivity of HBsAg in the liver of responders was not considerably different from that of non-responders ( $P > 0.05$ ). After IFN treatment, 17 patients were found to have HBsAg expression in the liver, which was not significantly different from that of pretreatment (pretreatment  $1.50 \pm 1.79$ , post-treatment  $1.11 \pm 0.83$ ,  $P > 0.05$ ), regardless of responders or non-responders (Responders: pretreatment  $1.33 \pm 0.52$ , post-treatment  $1.17 \pm 0.75$ ,  $P > 0.05$ ; Non-responders: pretreatment  $1.50 \pm 0.80$ , post-treatment  $1.08 \pm 0.90$ ,  $P > 0.05$ ). The location of HBsAg switched from a diffuse cytoplasmic pattern to a membranous and/or sub membranous pattern.

HBcAg can be mainly detected in hepatocyte nucleus and cytoplasm (Figure 3). HBcAg expression was positive in 20/

24 (83.3 %). There was no significant difference between HBcAg expression in the liver of the responders and non-responders ( $P>0.05$ ). However 12/20 (60 %) of patients were found to have a decrease in HBcAg expression in liver after IFN treatment, and the location of HBcAg changed to nucleic pattern mostly. Statistics showed that HBcAg expression in the liver declined significantly, Compared to pretreatment ( $1.28\pm0.75$ , post-treatment  $0.61\pm0.85$ ,  $P<0.05$ ). The decrease in the responders was marked, but not that in the non-responders (Responders: pretreatment  $1.67\pm0.52$ , post-treatment  $0.17\pm0.47$ ,  $P<0.05$ ; Non-responders: pretreatment  $1.08\pm0.79$ , post-treatment  $0.83\pm0.94$ ,  $P>0.05$ ).

Positive HBeAg expression in liver was mainly located in cytoplasm and nucleus of hepatocytes (Figure 4). HBeAg was detected in the liver of 12/24 (50 %) of patients before IFN treatment and 4/24 (16.7 %) after treatment. Statistics proved that HBeAg expression decreased remarkably (pre-treatment  $0.78\pm0.94$ , post-treatment  $0.22\pm0.43$ ,  $P<0.05$ ). But the decrease in the responders was not significantly different from that in the non-responders ( $P>0.05$ ).

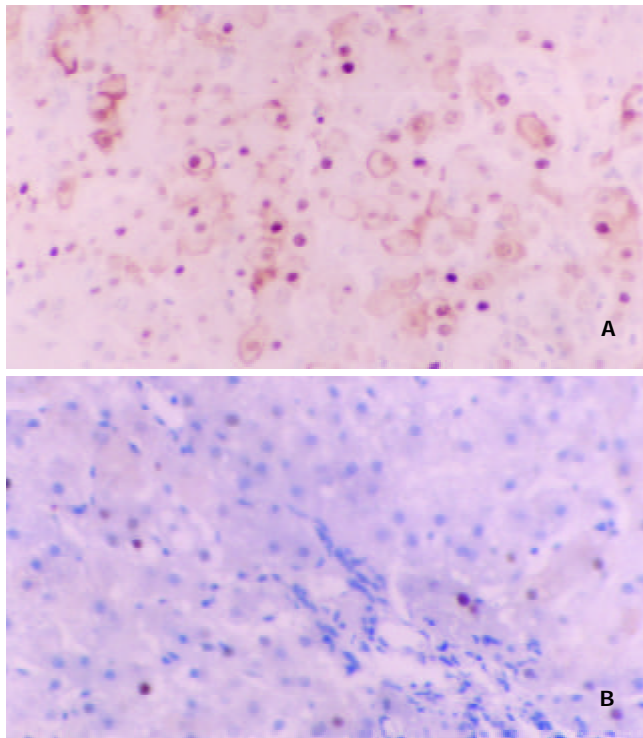


**Figure 3** Changes of HBcAg expression in liver of patients with chronic hepatitis B. A: before IFN treatment; B: after IFN treatment

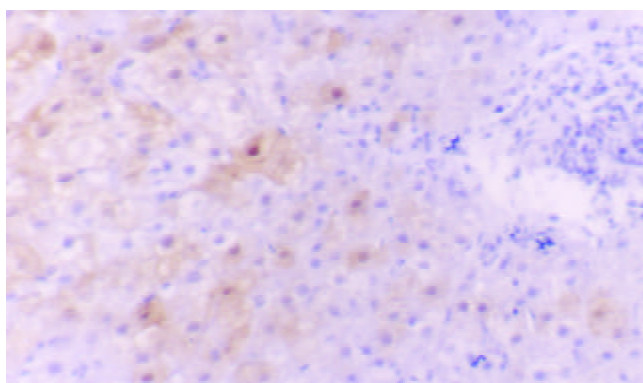


**Figure 4** HBeAg expression in liver of patients with chronic hepatitis B before IFN treatment

### Liver fibrosis

**HSC in liver** Normally, there are only several activated HSCs which contain  $\alpha$ -SMA. But in the liver of patients with chronic hepatitis B, there were large number of  $\alpha$ -SMA-positive HSC, diffusely located in the sinusoids (Figure 5). This showed that the number of  $\alpha$ -SMA-positive HSC in the liver decreased significantly after treatment (pre-treatment  $1.39\pm0.35$ , post-treatment  $0.61\pm0.70$ ,  $P<0.05$ ). The marked change of HSC was related to the change of HAI ( $P<0.05$ ), but not to the fibrosis score in accordance with HAI.

**TIMP-1 in liver** TIMP-1 in the liver was located in cytoplasm of hepatocyte (Figure 6). Before IFN- $\alpha$  treatment, 21/24 (87.5 %) of patients were detected positive TIMP-1 in their livers. In addition, there was no significant difference in TIMP-1 expression between responders and non-responders ( $P>0.05$ ). After treatment, the TIMP-1 in liver of 18/21 (85.6 %) patients decreased. Compared to pretreatment, TIMP-1 in liver decreased significantly (pre-treatment  $1.765\pm1.033$ , post-treatment  $0.588\pm0.441$ ,  $P<0.01$ ), regardless of the responders or non-responders.

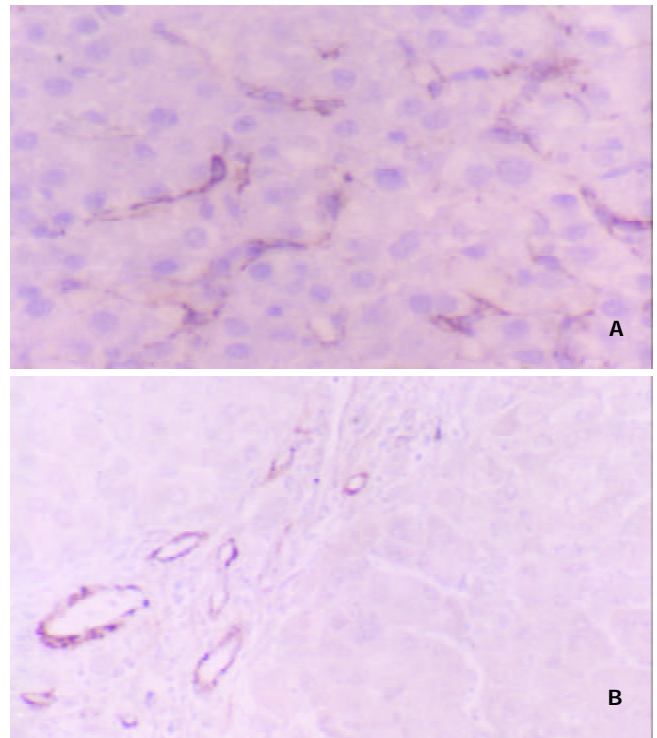


**Figure 5** Changes of  $\alpha$ -SMA-positive HSC in liver of patients with chronic hepatitis B. A: before IFN treatment; B: after IFN treatment

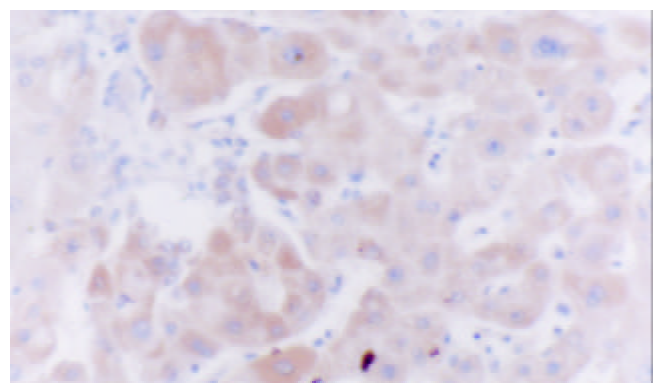


**Figure 6** TIMP-1 in liver of patients with chronic hepatitis B before IFN treatment

## DISCUSSION

Interferon- $\alpha$  treatment is effective in decreasing serum alanine transferase (ALT), converting serum HBeAg and HBVDNA to negative, and improving necroinflammation in the liver of patients with chronic hepatitis B. In this study, we evaluated the effect of interferon- $\alpha$  on both liver histology and serum parameters.

### Viral markers in sera

Among the patients, 9/24 (37.5 %) showed response reaction after interferon treatment, which agreed with other studies<sup>[14]</sup>. The serum ALT of responders became normal, and the serum HBeAg and/or HBVDNA became negative after treatment. Compared to pre-treatment, the serum HBVDNA of the patients decreased significantly ( $P<0.05$ ), especially that of the responders ( $P<0.05$ ). The results suggested that interferon- $\alpha$  could inhibit the viral replication.

### Viral antigen in liver

It was reported that interferon- $\alpha$  can inhibit all hepatitis B virus antigens expression in primary hepatocyte culture<sup>[15]</sup>. Moreover, interferon can change the location of HBsAg in hepatocyte from cytoplasm to the cell membrane or submembrane region<sup>[15]</sup>, which may enhance immune recognition and clearance of infected hepatocytes. Our study evaluated the effect of interferon- $\alpha$  on viral antigen in liver of chronic hepatitis B. In this group, the decline of HBsAg expression in liver was not significant, but the HBsAg expression switched from cytoplasmic to membranous/submembranous, which supported some previous studies<sup>[5,6]</sup>. However, the HBcAg and HBeAg in the liver decreased significantly after interferon treatment, especially in the responders, but not in the non-responders. This might be related to the fact that HBcAg and HBeAg of hepatocytes were target antigens of immune reaction mediated by HBV. IFN could enhance the recognition of immune system on the infected hepatocytes.

### HAI

Shiratori *et al* proved that interferon therapy can improve liver histology of hepatitis C by alleviating hepatic inflammation and fibrosis<sup>[16]</sup>. Our study showed that after interferon treatment, HAI of liver of all the patients decreased significantly ( $P<0.05$ ), mainly in the aspects of necrosis and intralobular inflammation. The change in responders was significant, but not that in the non-responders. This indicated interferon treatment can improve the hepatic lesions of patients with chronic hepatitis B.

### Liver fibrosis

Many patients with chronic hepatitis B progress slowly to liver fibrosis even cirrhosis. During this course, HSC plays a key role in the process of fibrosis. Proliferation and transformation of HSC is basic characteristic of liver fibrosis. On the one hand, liver injury and cytokines released stimulate HSC to proliferate, differentiate and acquire myofibroblast phenotype, with increase of collagen synthesis, expression of  $\alpha$ -SMA, secretion and desposition of extracellular matrix (ECM)<sup>[17,18]</sup>. On the other hand, HSC can secrete matrix metalloproteinase (MMP) which can degrade ECM. It is worth noting that HSC also secretes tissue inhibitor of metalloproteinase (TIMP)-the inhibitor of MMP. TIMP can noncovalently bind with MMP to inhibit the degradation of ECM, and promote liver fibrosis. Researches showed that in liver of patients with liver disease related to hepatitis B, the expression of TIMPs and MMP altered to make the liver tend to develop fibrosis<sup>[19-22]</sup>. Certain medicine can improve liver cirrhosis<sup>[23]</sup>. Several reports suggested that interferon treatment can alleviate hepatic fibrosis caused by viral hepatitis<sup>[24-30]</sup>. The mechanism is not clear. Some evidence

supported that interferon reduced HSCs<sup>[31]</sup>, probably by inducing the apoptosis of HSCs<sup>[32]</sup>. Others believed that interferon changed the amount of enzymes, such as MMP and TIMPs<sup>[33,34]</sup>.

### HSC in liver

In our study, the number of HSC containing  $\alpha$ -SMA decreased significantly after interferon treatment ( $P<0.05$ ). The  $\alpha$ -SMA expression by HSC decreased in 50 % of patients. This suggested that interferon treatment might inhibit the proliferation or transformation of HSC with the same conclusion by Guido's<sup>[31]</sup>. The significant association of  $\alpha$ -SMA to liver HAI ( $P<0.05$ ) suggested that the effect of interferon on HSC maybe related to its anti-inflammatory function. But there was no significant relation between reduction of HSC and change of fibrosis according to Knodell's HAI, which might be due to the small size of our patients.

### TIMP-1 in serum and liver

Mitsuda *et al* found that IFN- $\alpha$  could not only reduce the TIMP-1 in serum to enhance fibrinolysis, but also inhibit the fibrogenesis of patients with chronic hepatitis C<sup>[33]</sup>. Whether IFN- $\alpha$  has similar effect on the patients with chronic hepatitis B remains to be seen.

In this study, TIMP-1 in both serum and liver of patients with chronic hepatitis B decreased markedly after IFN- $\alpha$  treatment. This phenomenon suggests that IFN- $\alpha$  can inhibit production or TIMP-1 expression to improve fibrinolysis and inhibit fibrosis.

In conclusion, our study suggests that IFN- $\alpha$  treatment can inhibit viral replication, alleviate liver injury, inhibit activation of HSC, decrease TIMP-1 in liver and serum and inhibit liver fibrosis. The detailed mechanism and the optimal dose and course of IFN- $\alpha$  still deserve more studies. Although the interval of two biopsy was not very long, evidence suggested that interferon has long-term beneficial effect in patients with chronic hepatitis B<sup>[35]</sup>. The result was not very satisfactory. Maybe we should combine interferon and other medicines to treat chronic hepatitis B, as some study did<sup>[36]</sup>.

## REFERENCES

- 1 Pessoa MG, Wright TL. Update on clinical trials in the treatment of hepatitis B. *J Gastroenterol Hepatol* 1999; **14** (Suppl): S6-S11
- 2 Lau GKK, Carman WF, Locarnini SA, Okuda K, Lu ZM, Williams R, Lam SK. Treatment of chronic hepatitis B virus infection: An Asia-Pacific perspective. *J Gastroenterol Hepatol* 1999; **14**: 3-12
- 3 Yao GB. Treatment of chronic hepatitis B in China. *J Gastroenterol Hepatol* 2000; **15**(Suppl): E61-E66
- 4 Ishikawa T, Kakumu S. Update of liver disease related to chronic hepatitis B virus infection. *Intern Med* 2001; **40**: 178-179
- 5 Liaw YF. Management of patients with chronic hepatitis B. *J Gastroenterol Hepatol* 2002; **17**: 406-408
- 6 Wang XZ, Chen YX, Ma LS, Ma JY, Pan BR. Antiviral therapy of chronic hepatitis B in China. *Shijie Huaren Xiaohua Zazhi* 2002; **10**: 745-748
- 7 Hoofnagle JH, Peters M, Mullen KD, Jones DB, Rustgi V, Bisceglie AD, Hallahan C, Park Y, Meschievitz C, Jones EA. Randomized, controlled trial of recombinant human  $\alpha$ -interferon in patients with chronic hepatitis B. *Gastroenterol* 1988; **95**: 1318-1325
- 8 Oliveri F, Santantonio T, Bellati G, Colombatto P, Mels GC, Carriero L, Dastoli G, Pastore G, Ideo G, Bonino F, Brunetto MR. Long term response to therapy of chronic anti-HBe-Positive Hepatitis B is poor independent of type and schedule of interferon. *Am J Gastroenterol* 1999; **94**: 1366-1372
- 9 Brunetto MR, Oliveri F, Coco B, Leandro G, Colombatto P, Gorin JM, Bonino F. Outcome of anti-HBe positive chronic hepatitis B in alpha-interferon treated and untreated patients: a long term cohort study. *J Hepatol* 2002; **36**: 263-270
- 10 You J, Zhuang L, Tang BZ, Yang WB, Ding SY, Li W, Wu RX,



- Zhang HL, Zhang YM, Yan SM, Zhang L. A randomized controlled clinical trial on the treatment of Thymosin a1 versus interferon- $\alpha$  in patients with hepatitis B. *World J Gastroenterol* 2001; **7**: 411-414
- 11 **Zhuang L**, You J, Tang BZ, Ding SY, Yan KH, Peng D, Zhang YM, Zhang L. Preliminary results of Thymosins-a1 versus interferon- $\alpha$ -treatment in patients with HBeAg negative and serum HBV DNA positive chronic hepatitis B. *World J Gastroenterol* 2001; **7**: 407-410
- 12 **Kaneko S**, Feinstone SM, Miller RH. Rapid and sensitive method for the detection of serum hepatitis B virus DNA using the Polymerase Chain Reaction Technique. *J Clin Microbiol* 1989; **27**: 1930-1933
- 13 **Knodel RG**, Ishak KG, Black WC, Chen TS, Craig R, Kaplowitz N, Kiernan TW, Wollman J. Formulation and application of a numerical scoring system for assessing histological activity in asymptomatic chronic active hepatitis. *Hepatology* 1981; **1**: 431-435
- 14 **Lindh M**, Savage K, Rees J, Garwood L, Horal P, Norkrans G, Dhillon AP. HBeAg immunostaining of liver tissue in various stages of chronic hepatitis B. *Liver* 1999; **19**: 294-298
- 15 **Lau JYN**, Bain VG, Naoumov NV, Smith HM, Alexander GJM, Williams R. Effect of interferon- $\gamma$  on hepatitis B viral antigen expression in primary hepatocyte culture. *Hepatology* 1991; **14**: 975-979
- 16 **Shiratori Y**, Imazeki F, Moriyama M, Yano M, Arakawa Y, Yokosuka O, Kuroki T, Nishiguchi S, Sata M, Yamada G, Fujiyama S, Yoshida H, Omata M. Histological improvement of fibrosis in patients with hepatitis C who have sustained response to interferon therapy. *Ann Intern Med* 2000; **132**: 517-524
- 17 **Qin JP**, Jiang MD. Phenotype and regulation of hepatic stellate cell and liver fibrosis. *Shijie Huaren Xiaohua Zazhi* 2001; **9**: 801-804
- 18 **Huang GC**, Zhang JS. Signal transduction in the cells activated by hepatic stellate cells. *Shijie Huaren Xiaohua Zazhi* 2001; **9**: 1056-1060
- 19 **Xie YM**, Nie QH, Zhou YX, Cheng YQ, Kang WZ. Detection of TIMP-1 and TIMP-2 RNA expressions in cirrhotic liver tissue using digoxigenin labeled probe by in situ hybridization. *Shijie Huaren Xiaohua Zazhi* 2001; **9**: 251-254
- 20 **Nie QH**, Cheng YQ, Xie YM, Zhou YX, Bai XG, Cao YZ. Methodologic research on TIMP-1, TIMP-2 detection as a new diagnostic index for hepatic fibrosis and its significance. *World J Gastroenterol* 2002; **8**: 282-287
- 21 **Liu HL**, Li XH, Wang DY, Yang SP. Matrix metalloproteinase-2 and tissue inhibitor of metalloproteinase -1 expression in fibrotic rat liver. *World J Gastroenterol* 2000; **6**: 881-884
- 22 **Wu CH**. Fibrodynamics-elucidation of the mechanisms and sites of liver fibrogenesis. *World J Gastroenterol* 1999; **5**: 388-390
- 23 **Wang LT**, Zhang B, Jie J. Effect of anti-fibrosis compound on collagen expression of hepatic cells in experimental liver fibrosis of rats. *World J Gastroenterol* 2000; **6**: 877-880
- 24 **Li XQ**, Zeng MX, Ling QH. Effects of interferon- $\gamma$  on DNA synthesis and collagen production of cultured rat hepatocytes. *Shijie Huaren Xiaohua Zazhi* 1998; **6**: 488-490
- 25 **Cheng ML**, Wu YY, Huang KF, Luo TY, Ding YS, Lu YY, Liu RC, Wu J. Clinical study on the treatment of liver fibrosis due to hepatitis B by IFN- $\alpha$ 1 and traditional medicine preparation. *World J Gastroenterol* 1999; **5**: 267-269
- 26 **Cheng ML**, Lu YY, Wu J, Luo TY, Huang KF, Ding YS, Liu RC, Li J, Li Z. Three-year follow-up study on hepatic fibrosis due to chronic hepatitis B is treated by interferon- $\alpha$ -1b and traditional medicine preparation. *World J Gastroenterol* 2000; **6**(suppl 3): 81
- 27 **Zavaglia C**, Airolidi A, Pinzello G. Antiviral therapy of HBV- and HCV-induced liver cirrhosis. *J Clin Gastroenterol* 2000; **30**: 234-241
- 28 **Du XF**, Weng HL, Cai WM. Histological changed in 20 hepatic fibrosis with chronic hepatitis B after human interferon- $\alpha$  treatment. *Chin J Hepatol* 2001; **9**: 273-275
- 29 **Weng HL**, Cai WM, Liu RH. Animal experiment and clinical study of effect of gammaa2interferon on hepatic fibrosis. *World J Gastroenterol* 2001; **7**: 42-48
- 30 **Deuffic-Burban S**, Poynard T, Valleron AJ. Quantification of fibrosis progression in patients with chronic hepatitis C using a Markov model. *J Viral Hepatitis* 2002; **9**: 114-122
- 31 **Guido M**, Rugge M, Chemello L, Leandro G, Fattovich G, Giustina G, Cassaro M, Alberti A. Liver stellate cells in chronic viral hepatitis: the effect of interferon therapy. *J Hepatol* 1996; **24**: 301-307
- 32 **Xu WH**, Lü XX, Zhu JR. Apoptosis of hepatic stellate cell of rats with liver fibrosis. *Shijie Huaren Xiaohua Zazhi* 2002; **10**: 972-974
- 33 **Mitsuda A**, Suou T, Ikuta Y, Kawasaki H. Changes in serum tissue inhibitor of matrix metalloproteinase-1 after interferon alpha treatment in chronic hepatitis C. *J Hepatol* 2000; **32**: 666-672
- 34 **Wang Y**, Gao Y, Yu JL, Huang YQ, Jiang XQ. Effect of interferon-alpha on interstitial collagenase gene expression in rat liver fibrosis. *Shijie Huaren Xiaohua Zazhi* 2001; **9**: 20-23
- 35 **Lin SM**, Sheen IS, Chien RN, Chu CM, Liaw YF. Long term beneficial effect of interferon therapy in patients with chronic hepatitis B virus infection. *Hepatology* 1999; **29**: 971-975
- 36 **You J**, Zhuang L, Tang BZ, Yang H, Yang WB, Li W, Zhang HL, Zhang YM, Zhang L, Yan SM. Interferon alpha with thymopeptide in the treatment of chronic hepatitis B. *Shijie Huaren Xiaohua Zazhi* 2001; **9**: 388-391

Edited by Wu XN

• *H. pylori* •

# Expression of Lewis<sup>b</sup> blood group antigen in *Helicobacter pylori* does not interfere with bacterial adhesion property

Peng-Yuan Zheng, Jiesong Hua, Han-Chung Ng, Khay-Guan Yeoh, Ho Bow

**Peng-Yuan Zheng, Jiesong Hua, Han-Chung Ng, Ho Bow,** Department of Microbiology, Faculty of Medicine, National University of Singapore, 5 Science Drive 2, Singapore 117597, Republic of Singapore

**Khay-Guan Yeoh,** Department of Medicine, Faculty of Medicine, National University of Singapore, 5 Science Drive 2, Singapore 117597, Republic of Singapore

**Supported by** a grant from the National University of Singapore, No. 6431

**Correspondence to:** Peng-Yuan Zheng, MD, PhD, Division of Gastroenterology/Nutrition, The Hospital for Sick Children, University of Toronto, 555 University Ave. Toronto, ON, Canada M5G 1X8. pengyuan.zheng@sickkids.ca

**Telephone:** +1-416-8137072 **Fax:** +1-416-8136531

**Received:** 2002-08-03 **Accepted:** 2002-08-19

## Abstract

**AIM:** The finding that some *Helicobacter pylori* strains express Lewis b (Le<sup>b</sup>) blood group antigen casts a doubt on the role of Le<sup>b</sup> of human gastric epithelium being a receptor for *H. pylori*. The aim of this study was to determine if expression of Le<sup>b</sup> in *H. pylori* interferes with bacterial adhesion property.

**METHODS:** Bacterial adhesion to immobilized Le<sup>b</sup> on microtitre plate was performed in 63 *H. pylori* strains obtained from Singapore using *in vitro* adherence assay. Expression of Lewis blood group antigens was determined by ELISA assay.

**RESULTS:** Among 63 *H. pylori* strains, 28 expressed Le<sup>b</sup> antigen. *In vitro* adhesion assay showed that 78.6 % (22/28) of Le<sup>b</sup>-positive and 74.3 % (26/35) of Le<sup>b</sup>-negative *H. pylori* isolates were positive for adhesion to immobilized Le<sup>b</sup> coated on microtitre plate ( $P=0.772$ ). In addition, blocking of *H. pylori* Le<sup>b</sup> by prior incubation with anti-Le<sup>b</sup> monoclonal antibody did not alter the binding of the bacteria to solid-phase coated Le<sup>b</sup>.

**CONCLUSION:** The present study suggests that expression of Le<sup>b</sup> in *H. pylori* does not interfere with the bacterial adhesion property. This result supports the notion that Le<sup>b</sup> present on human gastric epithelial cells is capable of being a receptor for *H. pylori*.

Zheng PY, Hua J, Ng HC, Yeoh KG, Bow H. Expression of Lewis<sup>b</sup> blood group antigen in *Helicobacter pylori* does not interfere with bacterial adhesion property. *World J Gastroenterol* 2003; 9(1):122-124

<http://www.wjgnet.com/1007-9327/9/122.htm>

## INTRODUCTION

*Helicobacter pylori* is the major etiologic agent of chronic active gastritis, and is generally accepted as a causative factor in the pathogenesis of gastritis, peptic ulcer (PU) disease and gastric adenocarcinoma<sup>[1-3]</sup>. It is estimated that over 50 % of the world's population are infected with *H. pylori*.

The bacterium shows a strict tropism for gastric epithelium and is usually isolated from gastric epithelium and duodenal mucosa with gastric metaplasia. The presence of specific receptors for *H. pylori* on the gastric mucosa may explain its gastric tropism. The Lewis<sup>b</sup> (Le<sup>b</sup>) blood group antigen has been reported to be a receptor of *H. pylori*, and the blood-group antigen-binding adhesin, BabA, has been shown to mediate binding of *H. pylori* to human Le<sup>b</sup> on gastric epithelium<sup>[4]</sup>. Following the finding that Le<sup>b</sup> was expressed in some strains of *H. pylori*<sup>[5]</sup>, the role of host Le<sup>b</sup> as a receptor for *H. pylori* has been questioned considering the *H. pylori* lipopolysaccharide (LPS) Le<sup>b</sup> may interfere with the interaction between the bacteria BabA and Le<sup>b</sup> on gastric epithelium<sup>[5, 6]</sup>. This may be more important for the Asian strains where there is a higher frequency of *H. pylori* strains expressing type 1 blood-group antigens (Le<sup>a</sup>, Le<sup>b</sup>) (43.5 % for Le<sup>b</sup>)<sup>[7, 8]</sup> comparing with Western strains (<10 % for Le<sup>b</sup>). The high frequency of Le<sup>b</sup> expression in *H. pylori* strains in our population offers a unique opportunity to investigate the potential influence of Le<sup>b</sup> in *H. pylori* on the bacterial adhesion property.

## MATERIALS AND METHODS

### *Patients and H. pylori isolates*

*H. pylori* strains were isolated from the gastric biopsies of 108 patients undergoing upper gastrointestinal endoscopy for dyspepsia at the National University Hospital, Singapore. Informed consent was obtained from all the patients for gastroscopy and biopsies. A subset of 63 *H. pylori* strains from these 108 strains which were performed in our previous study<sup>[8]</sup> was randomly chosen for the *in vitro* adherence assay. Of these, 36 were isolated from male patients and 27 were from female patients. The average age of the patients was 43 years (16-78 years). Based on endoscopic and histologic examination, the patients were classified into the following groups: peptic ulcer ( $n=33$ ), and chronic gastritis ( $n=30$ ). The bacteria were isolated and identified as described previously<sup>[8]</sup>. Each strain was cultured on chocolate agar for 3-4 days at 37 °C in a humid incubator (Forma Scientific, Mountain View, USA) supplemented with 5 % CO<sub>2</sub>.

### *In vitro adherence assay*

The adherence assay was performed according to Gerhard *et al*<sup>[9]</sup> with minor modifications. Briefly, for each of the 63 *H. pylori* strains, the 4-day-old culture was harvested and washed twice in 0.05 M carbonate buffer (pH 9.6) before resuspending in 1 ml of the same buffer. A 10 µl of 10 mg·ml<sup>-1</sup> of digoxigenin (Roche Diagnostics, Mannheim, Germany) solution was added to the bacterial suspension and incubated for 60 min at RT. Polysorb 96-well- microtiter plates (Nunc, Rochester, USA) were coated with 50 ng per well of Le<sup>a</sup>, Le<sup>b</sup>, Le<sup>x</sup> and Le<sup>y</sup>, (IsoSep, Tullinge, Sweden) in 50 µl of 0.05 M carbonate buffer (pH 9.6) while 50 µl of the same buffer was added as negative control. Following overnight incubation at RT, the solution was decanted without washing, and 100 µl of blocking buffer (0.5 % non-fat milk/0.2 % Tween-20) was added. After the plate was further incubated at RT for 1 hour, the solution was decanted without washing, and then 50 µl of digoxigenin

labeled bacteria diluted to an OD of 0.5 at 600 nm were added to each well of the plates and incubated for another 1 hour at RT with gentle agitation. After washing with PBS, 50 µl of 150 mU·ml<sup>-1</sup> of anti-digoxigenin-HRP antibody (Roche Diagnostics, Mannheim, Germany) was added and incubated for 1 hour at RT. The plates were washed 3 times with PBS before adding 50 µl of o-phenylenediamine dihydrochloride (Sigma, Louis, USA) (0.4 mg·ml<sup>-1</sup> in citric acid buffer with 0.025 % H<sub>2</sub>O<sub>2</sub>). The reaction was stopped with the addition of 2.5 M sulfuric acid. The OD value was read at 490 nm in an ELISA reader (Bio-Tek, Houston, USA). The strains were considered positive for adhesion to the antigen if the ratio of OD<sub>Ag</sub>/OD<sub>control</sub> was >2.0<sup>[9]</sup>. The assay was carried out in duplicate for all the strains tested.

### Lewis antigen expression

The expression of Lewis blood group antigens (Le<sup>a</sup>, Le<sup>b</sup>, Le<sup>x</sup> and Le<sup>y</sup>) was determined by enzyme-linked immunosorbent assay (ELISA) as described previously<sup>[8, 10]</sup>. The following murine monoclonal antibodies (mAb) were used: mAb 54-1F6A, specific for Lewis<sup>x</sup> (Le<sup>x</sup>); mAb 1E52, specific for Le<sup>y</sup>; mAb 7Le, specific for Le<sup>a</sup> and mAb 225Le, specific for Le<sup>b</sup>. Bacterial whole cells from 3-day cultures (7.5×10<sup>6</sup> ml<sup>-1</sup>) were suspended in 1 ml phosphate buffered saline (PBS) at pH 7.4. One hundred ml of suspension was added to each well of 96-well microtitre plate (Nunc, Rochester, USA) and incubated overnight at room temperature (RT). Plates were then washed three times with PBS containing 0.05 % Tween-20 (PBST). Subsequently, an aliquot of 100 ml of mAbs (100 ng·ml<sup>-1</sup>) was added and incubated overnight at RT. After washing three times with PBST, a 100 ml solution of 1:1 000 horseradish peroxidase-labelled goat anti-mouse immunoglobulin (DAKO, Glostrup, Denmark) diluted in PBST with 0.5 % goat serum was added. Color development occurred with the addition of H<sub>2</sub>O<sub>2</sub> and o-phenylenediamine dihydrochloride (Sigma, St. Louis, USA) in phosphate citrate buffer (pH 5.4) in the dark for 30 min at RT. A 50 ml of 2.5 M H<sub>2</sub>SO<sub>4</sub> solution was added to each well to stop the reaction. The optical density (OD) was read at 490 nm. OD of 0.2 was chosen as the cut-off value because the sum of non-specific background binding value for mAbs never exceeded an OD of 0.1. Synthetic protein-linked Lewis antigens, i.e., Le<sup>a</sup>, Le<sup>b</sup>, Le<sup>x</sup> and Le<sup>y</sup> (IsoSep, Tullinge, Sweden) were used as positive controls for the mAbs.

### Adherence blocking assay by anti-Le<sup>b</sup> mAb

To test if blocking LPS Le<sup>b</sup> would alter the binding of the bacteria to Le<sup>b</sup> on ELISA plate, two chemically characterized strains with Le<sup>b</sup> (H428 and H507)<sup>[7]</sup> were subjected to adherence blocking assay by incubation with mAb 225Le, specific for Le<sup>b</sup><sup>[8, 11]</sup>. The bacteria were incubated with 225Le mAb (1.0, 10.0, and 100.0 µg·ml<sup>-1</sup>) for 1 hour at RT, and then washed twice with PBST (PBS + 0.05 % Tween-20). The adherence assay was performed as described earlier.

### Statistical analysis

Frequencies were compared using 2-tailed Fisher's exact test (SPSS 9.0, Chicago, USA). The ratios of OD values were expressed as means ± standard deviations, and the distributions of the ratios were compared by using Student's *t* test for comparison of means of independent samples. A *P* value <0.05 was considered statistically significant.

## RESULTS

### In vitro adherence assay

Of the 63 *H. pylori* strains tested, 48 (76.2 %) were positive for adhesion to immobilized Le<sup>b</sup> antigen on microtitre plate. The positive *H. pylori* strains showed ratios of OD<sub>Ag</sub>/OD<sub>control</sub>

between 2.0-4.1 while the negative strains exhibited values between 0.89-1.67. None of the *H. pylori* strains bound to Le<sup>a</sup>, Le<sup>x</sup> or Le<sup>y</sup>.

### Effect of Le<sup>b</sup> expression in *H. pylori* on bacterial adhesion property

In the test for expression of Lewis antigen in *H. pylori*, 28 out of the 63 *H. pylori* strains expressed Le<sup>b</sup> while 35 did not express Le<sup>b</sup> based on ELISA. Among these 28 Le<sup>b</sup>-positive strains, 22 (78.6 %) were positive for adhesion to immobilized Le<sup>b</sup> antigen coated on plate as compared to 26 (74.3 %) of 35 Le<sup>b</sup>-negative strains (*P*=0.772). Furthermore, the ratio of OD<sub>Ag</sub>/OD<sub>control</sub> was not significant difference between LPS Le<sup>b</sup>-positive strains and Le<sup>b</sup>-negative strains (2.3±0.7 vs 2.3±0.7, *P*=0.988).

### Adherence blocking assay by anti-Le<sup>b</sup> mAb

Two chemically characterized Le<sup>b</sup> positive *H. pylori* strains H428 and H507<sup>[7]</sup> were subjected to adherence blocking assay by prior incubation with the bacteria with specific mAb 225Le (100.0 µg·ml<sup>-1</sup>). The ratio of OD<sub>Ag</sub>/OD<sub>control</sub> for strain H428 was changed from 2.7 to 2.6 after incubation with mAb 225Le. The value of adhesion assay for strain H507 was showed minimal change from 1.1 to 1.0. No difference of the ratio of OD<sub>Ag</sub>/OD<sub>control</sub> was observed when the bacteria were incubated with different concentrations (1.0, 10.0, and 100.0 µg·ml<sup>-1</sup>) of mAb 225Le, which suggested that Le<sup>b</sup> expression in *H. pylori* did not interfere with the bacterial adhesion to Le<sup>b</sup>.

### Effect of mixed Lewis expression on bacterial adhesion property

Of the 63 *H. pylori* strains tested, 55 expressed 2 or more Lewis antigens (Le<sup>a</sup>, Le<sup>b</sup>, Le<sup>x</sup> or Le<sup>y</sup>), and the remaining 8 strains expressed 1 Lewis antigen. Among the 55 strains with expression of 2 or more Lewis antigens, 42 (76.4 %) were positive for adhesion to immobilized Le<sup>b</sup> compared with 6 (75 %) of 8 strains with 1 Lewis antigen expression (*P*=1.000). Furthermore, the ratio of OD<sub>Ag</sub>/OD<sub>control</sub> was not significant difference between the strains with expression of 2 or more Lewis antigen and strains with 1 Lewis antigen (2.3±0.7 vs 2.2±0.8, *P*=0.836).

## DISCUSSION

Attachment of *H. pylori* to gastric epithelium is important for its colonization and survival. This adhesion property protects the bacteria from the displacement from the stomach by gastric emptying and peristalsis<sup>[12]</sup>. A recent study has demonstrated that the *H. pylori* blood-group antigen-binding adhesin, BabA, facilitates bacterial colonization and augments a nonspecific immune response<sup>[13]</sup>. The fucosylated blood group antigens of Le<sup>b</sup> and H type 1 have been proposed as receptors of *H. pylori*<sup>[14]</sup>. In addition, a study using transgenic mice expressing the human Le<sup>b</sup> epitope in gastric epithelial cells indicated that Le<sup>b</sup> antigen functioned as a receptor for *H. pylori* adhesin and mediated its attachment to gastric pit and surface mucous cells. However, following the observation<sup>[5]</sup> that some *H. pylori* strains also express Le<sup>b</sup>, the question on the possible role of host Le<sup>b</sup> as a receptor for *H. pylori* has been raised by Wirth *et al*<sup>[5]</sup> as well as Clyne and Drumm<sup>[6]</sup>. Furthermore, if host Le<sup>b</sup> is the principle receptor for *H. pylori*, one might then expect a decreased prevalence of *H. pylori* in the secretor subjects because Le<sup>b</sup> present in saliva or gastric mucus in secretor individuals would competitively inhibit the binding of *H. pylori*. However, numerous studies have shown that there is no association between prevalence of *H. pylori* and host secretor status<sup>[14]</sup>, which indicates that competitive inhibition by Le<sup>b</sup> in gastric mucus in secretor individuals may not be able to effectively prevent the colonization of *H. pylori*.



In this study, it was shown that there was no significant difference between Le<sup>b</sup>-positive and Le<sup>b</sup>-negative *H. pylori* strains with respect to their ability to adhere to immobilized Le<sup>b</sup>, mimicking the epithelial cell Le<sup>b</sup> antigen. This suggests that expression of Le<sup>b</sup> in *H. pylori* strains in our study population does not interfere with the bacterial adhesion to immobilized Le<sup>b</sup> *in vitro*. Furthermore, the blocking experiment using anti-Le<sup>b</sup> mAb on two Le<sup>b</sup> expressing strains (H428 and H507) showed that the expression of Le<sup>b</sup> in *H. pylori* had no effect on the adhesion property of *H. pylori*. Additionally, our study population are mainly of Chinese origin which are predominantly Le (b+) phenotype<sup>[8]</sup>, and *H. pylori* strains isolated from Asian population have a tendency to express type 1 Lewis antigen (Le<sup>a</sup> and Le<sup>b</sup>)<sup>[7,8]</sup>. However, a high prevalence of *H. pylori* infection has been found in this population. These data further support our observation that expression of Le<sup>b</sup> in *H. pylori* does not affect the bacterial adhesion.

Our previous study found that increased expression of Lewis antigens in *H. pylori* was associated with peptic ulceration in our population<sup>[8]</sup>. We, therefore, attempted to determine whether strains with Lewis antigen expression have advantage for binding to immobilized Le<sup>b</sup>, but only observed that the increased expression of a combination of Le antigens in *H. pylori* had no influence on bacterial adhesion.

The chemical structures of Le<sup>a</sup>, Le<sup>b</sup>, Le<sup>x</sup>, Le<sup>y</sup>, i antigen, H type 1 and blood group A antigens expressed by *H. pylori* have been elucidated<sup>[7,15,16]</sup>. These antigens are also expressed on gastric mucosa<sup>[14]</sup>. The possible interaction between Lewis antigens expressed by *H. pylori* and gastric epithelium is intriguing. Le<sup>x</sup>-Le<sup>x</sup> homotypic interaction has been found to be important in eukaryotic cell interaction, and Le<sup>x</sup> structure has recently been proven to be involved in the formation of adhesion pedestal between *H. pylori* and gastric epithelium<sup>[14]</sup>. More recently, Le<sup>x</sup> structure in *H. pylori* has been demonstrated to promote the bacterial adhesion to gastric epithelium<sup>[17]</sup>. However, Le<sup>b</sup>-Le<sup>b</sup> homotypic interaction has not been proven, and our *in vitro* study does not support such an interaction of *H. pylori* LPS Le<sup>b</sup> with epithelial Le<sup>b</sup>. The next question is how a *H. pylori* population can manage to exist as single bacterium *in vivo* but not autoaggregative, when bacterium expresses both BabA adhesin and Le<sup>b</sup>? *H. pylori* lectins such as BabA may evolve an ability to distinguish between host and bacterial ligands based on differences in their core structure, and thus avoid bacterial autoaggregation<sup>[18,19]</sup>.

In conclusion, expression of Le<sup>b</sup> blood group antigen in *H. pylori* strains in our Asian population does not interfere with the bacterial adhesion to immobilized Le<sup>b</sup> on microtitre plate. This result supports the notion that host Le<sup>b</sup> present on the gastric epithelium is capable of being a receptor for *H. pylori*.

## ACKNOWLEDGEMENTS

The authors are grateful to Dr. Ben J. Appelmelk (Amsterdam Free University, The Netherlands) for generously providing all the monoclonal antibodies. We thank Dr. Mario A. Monteiro (Institute for Biological Sciences, National Research Council, Ottawa, Canada) for analyzing the chemical structures of the *H. pylori* strains. This work was partly present in the European *Helicobacter pylori* 2000 conference in Rome, Italy.

## REFERENCES

- Hunt RH, Sumanac K, Huang JQ. Should we kill or should we save *Helicobacter pylori*? *Aliment Pharmacol Ther* 2001; **15** (Suppl 1): 51-59
- Cai L, Yu SZ, Zhang ZF. *Helicobacter pylori* infection and risk of gastric cancer in Changle County, Fujian Province, China. *World J Gastroenterol* 2000; **6**: 374-376
- Uemura N, Okamoto S, Yamamoto S, Matsumura N, Yamaguchi S, Yamakido M, Taniyama K, Sasaki N, Schlemper RJ. *Helicobacter pylori* infection and the development of gastric cancer. *N Engl J Med* 2001; **345**: 784-789
- Ilver D, Arnqvist A, Ogren J, Frick IM, Kersulyte D, Incecik ET, Berg DE, Covacci A, Engstrand L, Boren T. *Helicobacter pylori* adhesin binding fucosylated histo-blood group antigens revealed by retagging. *Science* 1998; **279**: 373-377
- Wirth HP, Yang M, Karita M, Blaser MJ. Expression of the human cell surface glycoconjugates Lewis x and Lewis y by *Helicobacter pylori* isolates is related to *cagA* status. *Infect Immun* 1996; **64**: 4598-4605
- Clyne M, Drumm B. Absence of effect of Lewis A and Lewis B expression on adherence of *Helicobacter pylori* to human gastric cells. *Gastroenterology* 1997; **113**: 72-80
- Monteiro MA, Zheng PY, Ho B, Yokota BSI, Amano KI, Pan ZJ, Berg DE, Chan KH, MacLean LL, Perry MB. Expression of histo-blood group antigens by lipopolysaccharides of *Helicobacter pylori* strains from Asian hosts: the propensity to express type 1 blood-group antigens. *Glycobiology* 2000; **10**: 701-713
- Zheng PY, Hua J, Yoeh KG, Ho B. Association of peptic ulcer with increased expression of Lewis antigens but not *cagA*, *iceA* and *vacA* in *Helicobacter pylori* isolates in an Asian population. *Gut* 2000; **47**: 18-22
- Gerhard M, Lehn N, Neumayer N, Boren T, Rad R, Schepp W, Miehke S, Classen M, Prinz C. Clinical relevance of the *Helicobacter pylori* gene for blood-group antigen-binding adhesin. *Proc Natl Acad Sci USA* 1999; **96**: 12778-12783
- Zheng PY, Hua J, Ng HC, Ho B. Unchanged characteristics of *Helicobacter pylori* during its morphological conversion. *Microbios* 1999; **98**: 51-64
- Appelmelk BJ, Monteiro MA, Martin SL, Moran AP, Vandenbroucke-Grauls CM. Why *Helicobacter pylori* has Lewis antigens. *Trends Microbiol* 2000; **8**: 565-570
- Falk PG, Syder AJ, Guruge JL, Kirschner D, Blaser MJ, Gordon JI. Theoretical and experimental approaches for studying factors defining the *Helicobacter pylori*-host relationship. *Trends Microbiol* 2000; **8**: 321-329
- Rad R, Gerhard M, Lang R, Schoniger M, Rosch T, Schepp W, Becker I, Wagner H, Prinz C. The *Helicobacter pylori* blood group antigen-binding adhesin facilitates bacterial colonization and augments a nonspecific immune response. *J Immunol* 2002; **168**: 3033-3041
- Taylor DE, Rasko DA, Sherburne R, Ho C, Jewell LD. Lack of correlation between Lewis antigen expression by *Helicobacter pylori* and gastric epithelial cells in infected patients. *Gastroenterology* 1998; **115**: 1113-1122
- Monteiro MA, Chan KH, Rasko DA, Taylor DE, Zheng PY, Appelmelk BJ, Wirth HP, Yang M, Blaser MJ, Hynes SO, Moran AP, Perry MB. Simultaneous expression of type 1 and type 2 Lewis blood group antigens by *Helicobacter pylori* lipopolysaccharides. Molecular mimicry between *H. pylori* lipopolysaccharides and human gastric epithelial cell surface glycoforms. *J Biol Chem* 1998; **273**: 11533-11543
- Monteiro MA, Appelmelk BJ, Rasko DA, Moran AP, Hynes SO, MacLean LL, Chan KH, Michael FS, Logan SM, O'Rourke J, Lee A, Taylor DE, Perry MB. Lipopolysaccharide structures of *Helicobacter pylori* genomic strains 26695 and J99, mouse model *H. pylori* Sydney strain, *H. pylori* P466 carrying sialyl lewis X, and *H. pylori* UA915 expressing lewis B classification of *H. pylori* lipopolysaccharides into glycoform families. *Eur J Biochem* 2000; **267**: 305-320
- Edwards NJ, Monteiro MA, Faller G, Walsh EJ, Moran AP, Roberts IS, High NJ. Lewis X structures in the O antigen side-chain promote adhesion of *Helicobacter pylori* to the gastric epithelium. *Mol Microbiol* 2000; **35**: 1530-1539
- Karlsson KA. The human gastric colonizer *Helicobacter pylori*: a challenge for host-parasite glycobiology. *Glycobiology* 2000; **10**: 761-771
- Falk P. Why does *Helicobacter pylori* actually have Lewis antigens? *Trends Microbiol* 2001; **9**: 61-62

# N-acetylcysteine attenuates alcohol-induced oxidative stress in the rat

Resat Ozaras, Veysel Tahan, Seval Aydin, Hafize Uzun, Safiye Kaya, Hakan Senturk

**Resat Ozaras**, Department of Infectious Diseases and Clinical Microbiology, University of Istanbul, Istanbul, Turkey

**Veysel Tahan, Hakan Senturk**, Department of Internal Medicine, University of Istanbul, Istanbul, Turkey

**Seval Aydin, Hafize Uzun, Safiye Kaya**, Department of Biochemistry, University of Istanbul, Istanbul, Turkey

This study was presented in Digestive Disease Week, 20-23rd May, 2001, Atlanta, Georgia as an oral presentation

**Supported by** the research Fund of the University of Istanbul. No: T-589/240698

**Correspondence to:** Resat Ozaras, M.D., Altimermer Cad. 27/4, Kucukhamam TR-34303 Fatih, Istanbul, Turkey. rozaras@yahoo.com

**Telephone:** +90-212-5882840 **Fax:** +90-212-5882840

**Received:** 2002-07-26 **Accepted:** 2002-11-22

## Abstract

**AIM:** There is increasing evidence that alcohol-induced liver damage may be associated with increased oxidative stress. We aimed to investigate free-radical scavenger effect of n-acetylcysteine in rats intragastrically fed with ethanol.

**METHODS:** Twenty-four rats divided into three groups were fed with ethanol (6 g/kg/day, Group 1), ethanol and n-acetylcysteine (1 g/kg, Group 2), or isocaloric dextrose (control group, Group 3) for 4 weeks. Then animals were sacrificed under ether anesthesia, intracardiac blood and liver tissues were obtained. Measurements were performed both in serum and in homogenized liver tissues. Malondialdehyde (MDA) level was measured by TBARS method. Glutathione peroxidase (GSH-Px) and superoxide dismutase (SOD) levels were studied by commercial kits. Kruskal-Wallis test was used for statistical analysis.

**RESULTS:** ALT and AST in Group 1 (154 U/L and 302 U/L, respectively) were higher than those in Group 2 (94 U/L and 155 U/L) and Group 3 (99 U/L and 168 U/L) ( $P=0.001$  for both). Serum and tissue levels of MDA in Group 1 (1.84 nmol/mL and 96 nmol/100 mg-protein) were higher than Group 2 (0.91 nmol/mL and 64 nmol/100 mg-protein) and Group 3 (0.94 nmol/mL and 49 nmol/100 mg-protein) ( $P<0.001$  for both). On the other hand, serum GSH-Px level in Group 1 (8.21 U/g-Hb) was lower than Group 2 (16 U/g-Hb) and Group 3 (16 U/g-Hb) ( $P<0.001$ ). Serum and liver tissue levels of SOD in Group 1 (11 U/mL and 26 U/100 mg-protein) were lower than Group 2 (18 U/mL and 60 U/100 mg-protein) and Group 3 (20 U/mL and 60 U/100 mg-protein) ( $P<0.001$  for both).

**CONCLUSION:** This study demonstrated that ethanol-induced liver damage is associated with oxidative stress, and co-administration of n-acetylcysteine attenuates this damage effectively in rat model.

Ozaras R, Tahan V, Aydin S, Uzun H, Kaya S, Senturk H. N-acetylcysteine attenuates alcohol-induced oxidative stress in the rat. *World J Gastroenterol* 2003; 9(1): 125-128  
<http://www.wjgnet.com/1007-9327/9/125.htm>

## INTRODUCTION

Reactive oxygen intermediates contributes to the pathogenesis of various hepatic disorders such as paracetamol intoxication, hemochromatosis, toxic hepatitis, and alcoholic liver injury<sup>[1-4]</sup>. Increased oxygen radical production leads to lipid peroxidation by induced cytochrome P4502E1<sup>[5,6]</sup>. Enhanced generation of acetaldehyde was shown to cause lipid peroxidation in isolated perfused livers<sup>[7]</sup>. Oxidative damage correlates with the amount of ethanol consumed<sup>[8]</sup>.

Antioxidants such as vitamin E have been suggested as therapeutic options in acute and chronic liver diseases<sup>[9,10]</sup>. N-acetylcysteine (NAC) exerts a strong antioxidant activity, and is the treatment of choice in acetaminophen intoxication. NAC provides protection from toxic liver damage by elevating intracellular glutathione concentrations<sup>[11,12]</sup>. It has also been used in the treatment of CCl<sub>4</sub> poisoning<sup>[12]</sup>.

In this study, we tested whether NAC attenuates alcohol-induced free radical damage in the liver in a rat model.

## MATERIALS AND METHODS

Male Wistar-Albino rats weighing 220-250 g obtained from University of Istanbul Animal Research Laboratory were kept in the same unit and fed chow (Eris Chow Industry, Istanbul, Turkey) *ad libitum*. All rats had free access to tap water. All animals received humane care in compliance with the National Institutes of Health criteria for care of laboratory animals.

Twenty-four rats divided into three groups and were given ethanol (Group 1) or both ethanol and NAC (Group 2) or isocaloric dextrose (Group 3). NAC and alcohol were administered respectively 4 hours apart. Ethanol and NAC were given intragastrically at doses of 6 g/kg/day and 1 mg/kg/day respectively.

All rats were sacrificed at 1 month under ether anesthesia. After exploration of the thorax, intracardiac blood and liver samples were quickly obtained. Serum alcohol levels were measured on the day the rats were sacrificed.

Glutathione peroxidase levels in erythrocytes, serum alcohol level and biochemistry were studied immediately. For the remaining studies, serum and liver tissue samples were stored at -70 °C.

**Tissue Homogenization:** Liver samples were weighed and homogenized in 0.15 M NaCl for lipid peroxidation parameters and for the other studies, and homogenates of 20 % were obtained. Tissue homogenates were sonicated two times at 30 sec. intervals. Homogenization and sonication were performed at 4 °C. After sonication, homogenates for lipid peroxidation and biochemical studies were centrifuged at 3 000 rpm for 10 minutes and at 15 000 rpm for 15 minutes respectively. Aliquots of the supernatants were used for both studies<sup>[13]</sup>. The assayed parameters were expressed per mg protein and protein content of the aliquots was determined by the method of Lowry *et al*<sup>[14]</sup>.

## Lipid peroxidation

Lipid peroxidation was measured by thiobarbituric acid method, a modified form of the procedure described by Beuge and Aust<sup>[15]</sup>. This method measures several aldehydes derived

from lipid hydroperoxides and also known as TBARS (thiobarbituric acid reactive substances) method.

### Superoxide dismutase (SOD) level

Serum and homogenized liver tissue SOD levels were measured by using commercial kits. (Randox-Ransod, Cat No:SD 125).

### Glutathione level

Glutathione concentration was determined according to the method of Beutler *et al*<sup>[16]</sup>, using metaphosphoric acid for protein precipitation and 5' 5-dithiobis-2-nitrobenzoic acid for colour development. Erythrocyte and tissue glutathione concentrations were expressed as mg/grHb, mg/gr wet weight respectively.

### Glutathione peroxidase level

Serum and homogenized liver tissue glutathione peroxidase levels were also measured by using commercial kits. (Randox-Ransel, Cat No: RS 505).

Biochemical studies were performed by using autoanalyser (Hitachi 717). Hemoglobin level was measured manually by cyanmethemoglobin method.

### Alcohol level

Serum alcohol level was measured by fluorescent polarizing immunoassay using commercial kits (Abbot TDx, Cat No: 378190100).

### Statistical analysis

All results are expressed as mean  $\pm$  standard deviation. Comparisons between the groups were performed by Kruskal-Wallis variance analysis and a *P* value  $<0.05$  was accepted as statistically significant.

## RESULTS

Blood alcohol levels of Group 1 and 2 were comparable ( $207 \pm 33$  mg/dL vs  $182 \pm 27$  mg/dL).

AST level in Group 1 ( $302.00 \pm 70.68$  U/L), was higher than those in Group 2 ( $155.25 \pm 24.07$  U/L), and in Group 3 ( $168.25 \pm 32.08$  U/L) ( $P=0.001$ ). ALT level also in Group 1 ( $154.13 \pm 33.59$  U/L), was higher than those in Group 2 ( $94.25 \pm 16.02$  U/L), and in Group 3 ( $99.00 \pm 19.86$  U/L) ( $P=0.001$ ) (Figure 1).

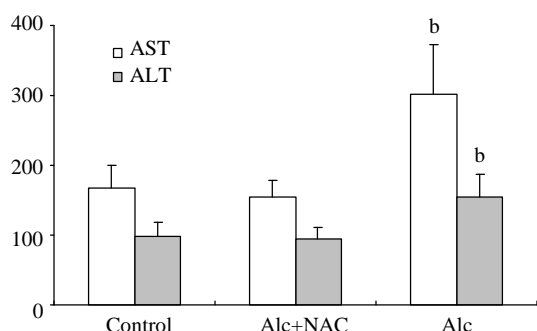


**Figure 1** Serum AST and ALT levels (U/L). Alc: alcohol, NAC: N-acetylcysteine, <sup>b</sup> $P=0.001$  vs control and Alc+NAC group.

Although serum GGT level in Group 1 ( $8.50 \pm 3.16$  U/L) tend to be higher than those in Group 2 ( $8.25 \pm 3.92$  U/L) and Group 3 ( $6.88 \pm 3.76$  U/L), the difference was not significant. However tissue GGT level in Group 1 ( $18.75 \pm 5.90$  U/g-protein) was significantly higher than those in Group 2 ( $7.23 \pm 6.09$  U/g-protein) and Group 3 ( $6.25 \pm 3.33$  U/g-protein) ( $P<0.001$ ) (Figure 2).

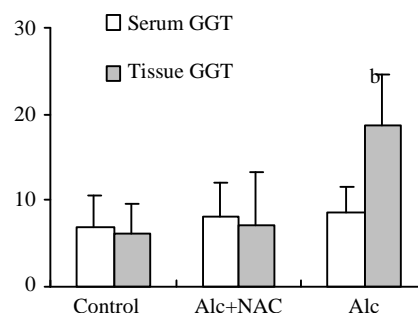


**Figure 2** Serum (U/L) and tissue (U/g-protein) GGT levels. Alc: alcohol, NAC: N-acetylcysteine, <sup>b</sup> $P<0.001$  vs control and Alc+NAC group.

Although serum ALP level in Group 1 ( $131.38 \pm 33.84$  U/L) tend to be higher than those in Group 2 ( $109.50 \pm 49.75$  U/L) and Group 3 ( $93.13 \pm 32.42$  U/L), the difference was not significant either. But tissue ALP level in Group 1 ( $26.88 \pm 3.31$  U/g-protein) was significantly higher than those in Group 2 ( $12.63 \pm 2.67$  U/g-protein) and Group 3 ( $11.25 \pm 2.49$  U/g-protein) ( $P<0.001$ ) (Figure 3).

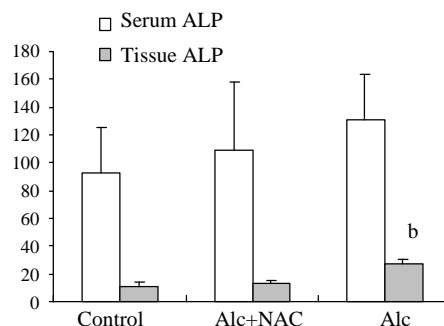


**Figure 3** Serum (U/L) and Tissue (U/g-protein) ALP levels. Alc: alcohol, NAC: N-acetylcysteine, <sup>b</sup> $P<0.001$  vs control and Alc+NAC group.

Erythrocyte glutathione level was lower in Group 1 ( $356.2 \pm 18.3$  mg/g-Hb) when compared to Group 2 ( $387.8 \pm 13.1$  mg/g-Hb) and Group 3 ( $398.0 \pm 18.0$  mg/g-Hb) ( $P<0.01$ ) (Figure 4).

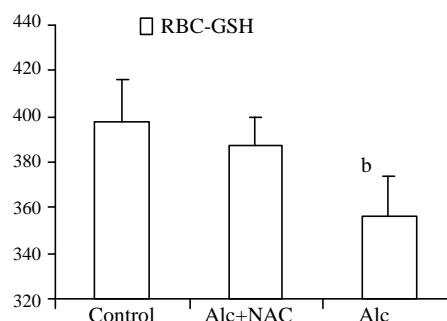


**Figure 4** Erythrocyte glutathione levels (U/g-Hb). Alc: alcohol, NAC: N-acetylcysteine, <sup>b</sup> $P<0.01$  vs control and Alc+NAC group.

Blood glutathione peroxidase level was lower in Group 1 ( $8.21 \pm 1.15$  U/g-Hb) when compared to Group 2 ( $16.04 \pm 2.38$  U/g-Hb) and Group 3 ( $16.84 \pm 2.68$  U/g-Hb) ( $P<0.001$ ) (Figure 5). Also serum SOD level was lower in Group 1 ( $11.08 \pm 1.13$  U/mL) when compared to Group 2 ( $17.92 \pm 0.81$  U/mL) and Group 3 ( $19.68 \pm 1.76$  U/mL) ( $P<0.001$ ). The same was true for the tissue SOD levels: it was lower in Group 1 ( $26.04 \pm 8.49$  U/100 mg-protein) when compared to Group 2 ( $59.96 \pm 10.23$  U/100 mg-protein) and Group 3 ( $60.34 \pm 8.24$  U/100 mg-protein) ( $P<0.001$ ) (Figure 6).

Serum MDA level was significantly higher in Group 1 ( $1.84 \pm 0.14$  nmol/mL) than those in Group 2 ( $0.91 \pm 0.14$  nmol/mL) and Group 3 ( $0.94 \pm 0.11$  nmol/mL) ( $P < 0.001$ ) (Figure 7). For the tissue levels, it was higher also in Group 1 ( $96.00 \pm 18.20$  nmol/100 mg-protein) than those in Group 2 ( $64.00 \pm 11.63$  nmol/100 mg-protein) and Group 3 ( $49.63 \pm 12.11$  nmol/100 mg-protein) ( $P < 0.001$ ) (Figure 8).

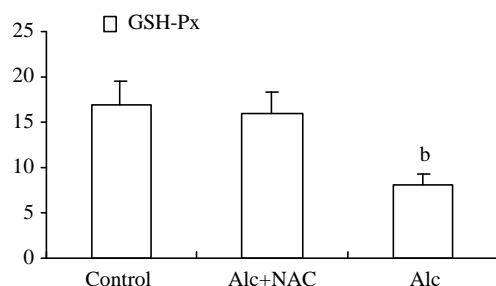


**Figure 5** Blood glutathione peroxidase levels (U/g-Hb). Alc: alcohol, NAC: N-acetylcysteine, <sup>a</sup> $P < 0.001$  vs control and Alc+NAC group.

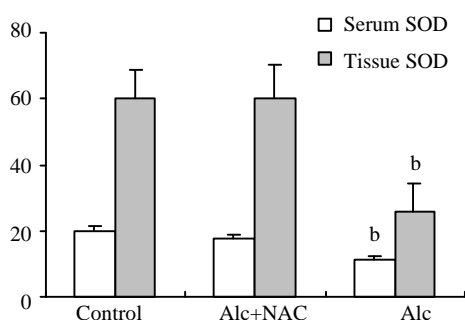


**Figure 6** Serum (U/mL) and tissue (U/100 mg-protein) superoxide dismutase (SOD) levels. Alc: alcohol, NAC: N-acetylcysteine, <sup>b</sup> $P < 0.001$  vs control and Alc+NAC group.

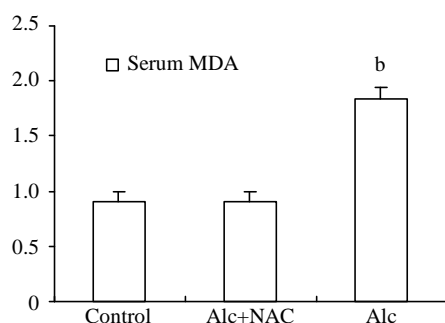


**Figure 7** Serum MDA level (nmol/mL). Alc: alcohol, NAC: N-acetylcysteine, <sup>b</sup> $P < 0.001$  vs control and Alc+NAC group.

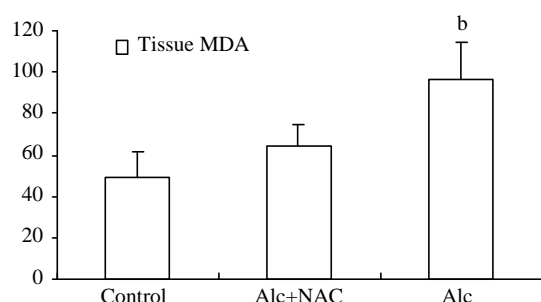


**Figure 8** Tissue MDA level (nmol/100 mg-protein). Alc: alcohol, NAC: N-acetylcysteine, <sup>b</sup> $P < 0.001$  vs control and Alc+NAC group.

## DISCUSSION

Ethanol is capable of generating oxygen radicals, inhibiting glutathione synthesis, producing glutathione loss from the tissue, increasing malonyldialdehyde levels and impairing antioxidant defense systems in humans and experimental animals. Lipid peroxidation results from the increased oxygen radical production by the induced 2E1<sup>[6]</sup>. Enhanced generation of acetaldehyde was also shown to be capable of causing lipid peroxidation in isolated perfused livers<sup>[7]</sup>. Lipid peroxidation is not only a reflection of tissue damage, it may also play a pathogenic role, for instance by promoting collagen production<sup>[17]</sup>. The removal of the toxic metabolites is believed to be the vital initial step in providing cell survival during ethanol intoxication<sup>[18]</sup>.

Genc *et al*<sup>[19]</sup>, used melatonin in preventing lipid peroxidation due to acute alcohol intoxication. They found that melatonin administration prior to alcohol did not alter MDA and GSH levels of the tissue but an antioxidant enzyme (CuZn-SOD) was higher in animals receiving alcohol+melatonin. However since absorption and kinetics of this hormone are not widely known, and its antioxidant effect depend on both the tissue studied and the dose applied, the results of a melatonin study may not reflect the effects of other antioxidants.

Nanji *et al*<sup>[20]</sup>, used thromboxane inhibitors in alcoholic liver disease in rats. They found that treatment with thromboxane inhibitors prevented necrosis and inflammation, and suggested a role for the use of thromboxane inhibitors in the treatment of alcoholic liver disease. Flora *et al*<sup>[21]</sup> tested NAC and a chelator agent meso 2,3-dimercaptosuccinic acid combination in the treatment of arsenic-induced oxidative stress, and found that these agents had a capability of reversing the toxic effects.

Bruck *et al*<sup>[11]</sup>, have used NAC in the treatment of thioacetamide-induced fulminant hepatic failure in the rat model. They found no protective effect of NAC. In this model, total hepatic glutathione content is not affected. Instead, other free radical scavengers, dimethylsulfoxide and dimethylthiourea having additional modes of action such as inhibition of nitric oxide formation prevented liver injury.

The results of our study show that co-administration of NAC diminishes oxidative stress, by increasing antioxidant enzymes. This restoration of oxidant/antioxidant balance is reflected by lower levels of transaminases, ALP, and GGT. Although the decrease in serum level of the latter two enzymes was not significant, tissue levels were lower. NAC has been used in acetaminophen intoxication. It reduces the incidence of organ failure and enhances survival<sup>[22]</sup>. It acts by reducing tissue hypoxia, mediated by the activity of the nitric oxide/soluble guanylate cyclase system<sup>[1]</sup>. Cysteine derived from NAC also serves as a precursor of glutathione which forms conjugates with carbon tetrachloride metabolites<sup>[23]</sup> and increases intracellular glutathione concentrations<sup>[1]</sup>. In a recent study, NAC - in a lower dose than used in the current study - has been shown to prevent the fatty acid changes produced by ethanol and also reduce inflammatory response by reducing the level of prostaglandin<sup>[24]</sup>.

Antioxidant protective mechanisms are both enzymatic and nonenzymatic. Impairments in these defense systems have been shown in alcoholics: alterations in ascorbic acid levels, glutathione, selenium, and vitamin E have been observed<sup>[25,26]</sup>. Reduced hepatic alpha-tocopherol content after long-term ethanol feeding in rats under adequate intake of vitamin E<sup>[27]</sup> and also in alcoholics<sup>[28]</sup> has been reported. Alpha-tocopherol level was found to be reduced in the blood of the alcoholics<sup>[29]</sup>. In addition to acetaldehyde and free radical generation by the ethanol-induced microsomes, these deficient defense systems were suggested to contribute to liver damage via lipid peroxidation<sup>[17]</sup>. Lipid peroxidation is a reflection of tissue

damage and plays a pathogenic role by promoting collagen production<sup>[30]</sup>.

A growing body of experimental and clinical experience shows the importance of free radicals in ethanol-induced liver damage. Free radical scavenging property may be beneficial as ascertained by previous studies of NAC in both acetaminophen and carbon tetrachloride intoxication. In this rat model, we have used NAC to attenuate ethanol-induced free radical damage. In both serum and tissue levels, we observed a favorable result. The results of this study suggest a role for NAC in the management of ethanol-induced liver damage as a safe, cheap, and effective option.

## REFERENCES

- 1 **Bruck R**, Aeed H, Shirin H, Matas Z, Zaidel L, Avni Y, Halpern Z. The hydroxyl radical scavengers dimethylsulfoxide and dimethylthiourea protect rat against thioacetamide-induced fulminant hepatic failure. *J Hepatol* 1999; **31**: 27-38
- 2 **Bacon BR**, Tavill AS, Brittenham GM, Park CH, Recknagel RO. Hepatic lipid peroxidation *in vivo* in rats with chronic iron overload. *J Clin Invest* 1983; **71**: 429-439
- 3 **Kyle ME**, Miccadei S, Nakae D, Farber JL. Superoxide dismutase and catalase protect cultured hepatocytes from the cytotoxicity of acetaminophen. *Biochem Biophys Res Commun* 1987; **149**: 889-896
- 4 **Shaw S**, Jayatilke E, Ross WA, Gordon E, Lieber CS. Ethanol-induced lipid peroxidation: potentiation by long-term alcohol feeding and attenuation by methionine. *J Lab Clin Med* 1981; **98**: 417-424
- 5 **Dai Y**, Rashba-Step J, Cederbaum AI. Stable expression of human cytochrome P4502E1 in HepG2 cells: characterization of catalytic activities and production of reactive oxygen intermediates. *Biochemistry* 1993; **32**: 6928-6937
- 6 **Castillo T**, Koop DR, Kamimura S, Triadafilopoulos G, Tsukamoto H. Role of cytochrome P-450 2E1 in ethanol-, carbon tetrachloride- and iron-dependent microsomal lipid peroxidation. *Hepatology* 1992; **16**: 992-996
- 7 **Muller A**, Sies H. Role of alcohol dehydrogenase activity and the acetaldehyde in ethanol-induced ethane and pentane production by isolated perfused rat liver. *Biochem J* 1982; **206**: 153-156
- 8 **Clot P**, Tabone M, Arico S, Albano E. Monitoring oxidative damage in patients with liver cirrhosis and different daily alcohol intake. *Gut* 1994; **35**: 1637-1643
- 9 **Liu SL**, Esposti SD, Yao T, Diehl AM, Zern MA. Vitamin E therapy of acute CCl<sub>4</sub>-induced hepatic injury in mice is associated with inhibition of nuclear factor kappa B binding. *Hepatology* 1995; **22**: 1474-1481
- 10 **Brown KE**, Poulos JE, Li L, Soweid AM, Ramm GA, O'Neill R, Britton RS, Bacon BR. Effect of vitamin E supplementation on hepatic fibrogenesis in chronic dietary iron overload. *Am J Physiol* 1997; **272**: G116-G123
- 11 **Lauterburg BH**, Corcoran GB, Mitchell JR. Mechanism of action of N-acetylcysteine in the protection against the hepatotoxicity of acetaminophen in rats *in vivo*. *J Clin Invest* 1983; **71**: 980-991
- 12 **Howard RJ**, Blake DR, Pall H, Williams A, Green ID. Allopurinol/N-acetylcysteine for carbon monoxide poisoning. *Lancet* 1987; **2**: 628-629
- 13 **Brown KE**, Kinter MT, Oberley TD, Freeman ML, Frierson HF, Ridnour LA, Tao Y, Oberley LW, Spitz DR. Enhanced gamma-glutamyl transpeptidase expression and selective loss of CuZn superoxide dismutase in hepatic overload. *Free Radic Biol Med* 1998; **24**: 545-555
- 14 **Lowry OH**, Rosebrough NJ, Farr AL, Landall RJ. Protein measurement with Folin phenol reagent. *J Biol Chem* 1951; **193**: 265-275
- 15 **Buege JA**, Aust SD. Microsomal lipid peroxidation. *Methods Enzymol* 1978; **52**: 302-310
- 16 **Beutler E**, Duran O, Kelly MB. Improved method for the determination of blood glutathione. *J Lab Clin Med* 1963; **61**: 882-888
- 17 **Lieber CS**. Alcohol and the liver: 1994 update. *Gastroenterology* 1994; **106**: 1085-1105
- 18 **Nordmann R**, Ribiere C, Rouach, H. Implication of free radical mechanisms in ethanol-induced cellular injury. *Free Radic Biol Med* 1992; **12**: 219-240
- 19 **Genc S**, Gurdol F, Oner-Iyidogan Y, Onaran I. The effect of melatonin administration on ethanol-induced lipid peroxidation in rats. *Pharmacol Res* 1998; **37**: 37-40
- 20 **Nanji AA**, Khwaja S, Rahemtulla A, Miao L, Zhao S, Tahan SR. Thromboxane inhibitors attenuate pathological changes in alcoholic liver disease in the rat. *Gastroenterology* 1997; **112**: 200-207
- 21 **Flora SJS**. Arsenic-induced oxidative stress and its reversibility following combined administration of n-acetylcysteine and meso 2,3-dimercaptosuccinic acid in rats. *Clin Exp Pharmacol Physiol* 1999; **26**: 865-869
- 22 **Prescott LF**, Illingworth RN, Critchley JA, Stewart MJ, Adam RD, Proudfoot AT. Intravenous N-acetylcysteine: the treatment of choice for paracetamol poisoning. *Br Med J* 1979; **2**: 1097-1100
- 23 **Mathiseon PW**, Williams G, MacSweeney JE. Survival after massive ingestional carbon tetrachloride treated by intravenous infusion of acetylcysteine. *Hum Toxicol* 1985; **4**: 627-631
- 24 **Raja, Krishnan V**, Menon VP. Potential role of antioxidants during ethanol-induced changes in the fatty acid composition and arachidonic acid metabolites in male Wistar rats. *Cell Biol Toxicol* 2001; **17**: 11-22
- 25 **Tanner AR**, Bantock I, Hinks L, Lloyd B, Turner NR, Wright R. Depressed selenium and vitamin E levels in alcoholic population. Possible relationship to hepatic injury through increased lipid peroxidation. *Dig Dis Sci* 1986; **31**: 1307-1312
- 26 **Bonjour JP**. Vitamins and alcoholism. I. Ascorbic acid. *Int J Vit Nutr Res* 1979; **49**: 434-441
- 27 **Bjorneboe GE**, Bjorneboe A, Hagen BF, Morland J, Drevon CA. Reduced hepatic a-tocopherol content after long-term administration of ethanol to rats. *Biochem Biophys Acta* 1987; **918**: 236-241
- 28 **Leo MA**, Rosman A, Lieber CS. Differential depletion of carotenoids and tocopherol in liver diseases. *Hepatology* 1993; **17**: 977-986
- 29 **Bjorneboe GE**, Johnsen J, Bjorneboe A, Marklund SL, Skjvl N, Hoiseth A, Bache-Wiig JE, Morland J, Drevon CA. Some aspects of antioxidant status in blood from alcoholics. *Alcohol Clin Exp Res* 1988; **12**: 806-810
- 30 **Geesin JC**, Hendricks LJ, Falkenstein PA, Gordon JS, Berg RA. Regulation of collagen synthesis by ascorbic acid: characterization of the role of ascorbate-stimulated lipid peroxidation. *Arch Biochem Biophys* 1991; **290**: 127-132

Edited by Xu JY and Xu XQ

# Mechanisms for regulation of gastrin and somatostatin release from isolated rat stomach during gastric distention

Yong-Yu Li

**Yong-Yu Li**, Department of Pathophysiology, Medical College of Tongji University, Shanghai 200331, China

**Correspondence to:** Yong-Yu Li, M.D., Professor of Pathophysiology, Department of Pathophysiology, Medical College of Tongji University, Shanghai 200331, China. liyyu@163.net

**Telephone:** +86-21-51030563

**Received:** 2002-09-13 **Accepted:** 2002-10-21

## Abstract

**AIM:** To investigate the intragastric mechanisms for regulation of gastric neuroendocrine functions during gastric distention in isolated vascularly perfused rat stomach.

**METHODS:** Isolated vascularly perfused rat stomach was prepared, then the gastric lumen was distended with either 5, 10 or 15 ml pH7 isotonic saline during a period of 20 min. During the distention, the axonal blocker tetrodotoxin (TTX), the cholinergic antagonist atropine, or the putative somatostatin-antagonist cyclo [7-aminoheptanoyl-Phe-D-Trp-Lys-Thr(Bzl)] were applied by vascular perfusion. The releases of gastrin and somatostatin were then examined by radioimmunoassay.

**RESULTS:** The graded gastric distention caused a significant volume-dependent decrease in gastrin secretion [ $-183 \pm 75$  (5 ml),  $-385 \pm 86$  (10 ml) and  $-440 \pm 85$  (15 ml) pg/20 min] and a significant increase of somatostatin secretion [ $260 \pm 102$  (5 ml),  $608 \pm 148$  (10 ml) and  $943 \pm 316$  (15 ml) pg/20 min]. In response to 10 ml distention, the infusion of either axonal blocker TTX ( $10^{-6}$  M) or cholinergic blocker atropine ( $10^{-7}$  M) had a similar affect. They both attenuated the decrease of gastrin release by approximately 50 %, and attenuated the increase of somatostatin release by approximately 40 %. The infusion of somatostatin-antagonist cyclo [7-aminoheptanoyl-Phe-D-Trp-Lys-Thr(Bzl)] ( $10^{-6}$  M) attenuated the decrease of gastrin release by about 60 %. Furthermore, combined infusion of the somatostatin-antagonist and atropine completely abolished distention-induced inhibition of gastrin release.

**CONCLUSION:** The present data suggest that distention of isolated rat stomach stimulates somatostatin release via cholinergic and non-cholinergic TTX-insensitive pathways. Both somatostatin and intrinsic cholinergic pathways are responsible for distention-induced inhibition of gastrin release.

Li YY. Mechanisms for regulation of gastrin and somatostatin release from isolated rat stomach during gastric distention. *World J Gastroenterol* 2003; 9(1): 129-133  
<http://www.wjgnet.com/1007-9327/9/129.htm>

## INTRODUCTION

Early in 1948, Grossman first proposed that intragastric neurones could regulate gastric neuroendocrine response to gastric distention independent of the extrinsic nervous system<sup>[1]</sup>, and later Schubert and Makhlof reported that

distention of the distal part of the isolated rat stomach activates the intrinsic VIP neurones and the intrinsic cholinergic mechanism, thereby regulating gastrin and somatostatin release<sup>[2]</sup>. However, the intrinsic pathways, independent of extrinsic nerves, which are activated by gastric distention and which modify gastrin release, have remained largely obscure until now.

After finding that distention of isolated rat stomach results in an inhibition of gastrin release and that distention of the extrinsically innervated stomach stimulates gastrin release *in vivo*<sup>[3]</sup>, we performed this study to examine the intragastric mechanisms involved in regulation of gastrin and somatostatin response to gastric distention. For the study, gastric distention was performed *in vitro* in isolated vascularly perfused rat stomach, an extrinsically denervated preparation that retains the integrity of intramural neurones as well as intragastric paracrine pathways<sup>[4-7]</sup>. In this model the effect of graded gastric distention on the release of gastrin and somatostatin was determined. The importance of the intrinsic nervous system and, in particular, its cholinergic part was investigated by performing distention in presence of the axonal blocker tetrodotoxin (TTX) and the cholinergic antagonist atropine. The putative somatostatin-antagonist cyclo [7-aminoheptanoyl-Phe-D-Trp-Lys-Thr(Bzl)] was employed in order to evaluate the role of endogenous somatostatin on regulation of gastrin release during gastric distention.

## MATERIALS AND METHODS

### Materials

Male Wistar rats ( $n=101$ ), body weight 250-300 g (Charles River Wiga GmbH, Sulzfelden, Germany); dextran T-70 (Pharmacia, Uppsala, Sweden); bovine serum albumine (Serva, Heidelberg, Germany); cyclo [7-aminoheptanoyl-Phe-D-Trp-Lys-Thr(Bzl)] (Bachem, Hannover, Germany); commercial gastrin-kit (Becton and Dickinson, Heidelberg, Germany); tetrodotoxin (TTX), atropine, somatostatin-14 and porcine gastrin-releasing peptide (GRP) (Sigma Chemie, Munich, Germany).

### Experimental design

We first prepared the rat stomach. The stomach was isolated from rats fasted overnight using a procedure described by McIntosh *et al*<sup>[8,9]</sup>. The isolated stomach was perfused through the celiac artery in a single pass perfusion system at a rate of 1.5 ml/min with a modified Krebs-Ringer buffer solution. The perfusion medium contained 4 % dextran T-70, 0.2 % bovine serum albumin and 5.5 mM glucose and was gassed with 95 % O<sub>2</sub> and 5 % CO<sub>2</sub>. The gastric venous effluent was collected via a catheter in the portal vein at two-minute intervals and frozen immediately for subsequent radioimmunoassay. A further catheter was placed in the stomach via the esophagus with the tip at the cardia. A distal catheter was placed in the stomach at the ligated pylorus to drain gastric contents.

After insertion of the gastric catheters, the lumen of the stomach was gently rinsed with isotonic pH7 saline until clear. Thereafter gastric lumen was continuously perfused with saline (1.5 ml/min) during an equilibration period of 25 min and a basal period of 10 min and the perfusate was allowed to flow off via a distal catheter. Subsequently, graded gastric distention

was initiated by instillation of 5, 10 or 15 ml saline through the esophageal catheter at a rate of 2 ml per 10 sec while the distal catheter was blocked. After a distention period of 20 min the distal catheter was reopened and the gastric lumen was again perfused for a period of 20 min with saline. After instillation of the saline load, a fluid filled pressure transducer was connected to the esophageal catheter for recording of the intragastric pressure. During distention, intragastric pressure increased to  $5.0 \pm 0.4$  cm water at 5 ml saline load, to  $10.4 \pm 0.9$  cm water at 10 ml saline load and to  $15.0 \pm 1.1$  cm water at 15 ml saline load. The increase in intragastric pressure induced by the tested distention volumes caused no visible mucosal damage and no impairment of vascular perfusion.

For neural blockade, either the neurotoxin TTX ( $10^{-6}$  M) or the cholinergic blocker atropine ( $10^{-7}$  M) was added to the vascular perfusate. In further experiments the putative somatostatin-antagonist cyclo [7-aminoheptanoyl-Phe-D-Trp-Lys-Thr(Bzl)] ( $10^{-6}$  M) was added to the perfusate alone or in combination with atropine ( $10^{-7}$  M). Since the somatostatin-antagonist did not completely abolish distention-induced inhibition of gastrin release, its effectiveness was tested against the inhibitory action of somatostatin-14 ( $10^{-8}$  M) on gastrin release prestimulated by mammalia bombisin peptide GRP ( $10^{-8}$  M), which is well known in stimulating gastrin secretion<sup>[10-12]</sup>. In each stomach only one experiment was performed.

#### Radioimmunoassay

Gastrin levels in the venous effluent were measured by radioimmunoassay as described elsewhere<sup>[13]</sup> employing a commercial gastrin-kit. Somatostatin was determined as described in detail previously<sup>[14]</sup>, by employing antibody 80C which was generously provided by Dr. R.H. Unger (Dallas, TX, USA).

#### Data analysis

All data are expressed as mean  $\pm$  SE. Integrated peptide secretion was calculated as the sum of the differences between the value of each time point during gastric distention and the mean value of the preceding baseline period. For statistical evaluation of the point-to-point variations, the Friedman two-way analysis of variance was used, followed by the Wilcoxon matched-pairs signed rank test if the former allowed rejection of the null hypothesis. The difference in the values between the treatment groups was statistically evaluated by analysis of variance for multiple determinations. Differences resulting in *P*-values of 0.05 or less were considered significant.

## RESULTS

#### Effect of graded gastric distention on release of gastrin and somatostatin

Graded distention of isolated rat stomach elicited a significant and volume dependent decrease in gastrin release from a mean baseline of  $63 \pm 4$  to a minimum of  $50 \pm 3$  pg/min ( $P < 0.05$ ;  $n = 8$ ), during distention with 5 ml, from  $69 \pm 6$  to  $41 \pm 3$  pg/min ( $P < 0.01$ ;  $n = 15$ ), with 10 ml and from  $60 \pm 7$  to  $25 \pm 5$  pg/min, and with 15 ml saline ( $P < 0.01$ ;  $n = 8$ ) (Figure 1). Gastrin secretion decreased throughout the distention period and returned promptly to baseline values after removal of the intragastric saline load. Integrated gastrin release decreased during distention by  $-183 \pm 75$  pg/20 min ( $P < 0.05$ ) at 5 ml, by  $-385 \pm 86$  pg/20 min ( $P < 0.01$ ) at 10 ml, and by  $-440 \pm 85$  pg/20 min ( $P < 0.01$ ) at 15 ml saline distention (Figure 2).

Somatostatin levels rose volume-dependently during gastric distention from a mean baseline of  $41 \pm 5$  to a maximum level of  $61 \pm 6$  pg/min ( $P < 0.05$ ) at 5 ml, from  $40 \pm 5$  to  $92 \pm 12$  pg/min ( $P < 0.01$ ) at 10 ml and from  $39 \pm 6$  to  $116 \pm 22$  pg/min ( $P < 0.01$ ) at 15 ml saline load (Figure 1). After distention,

somatostatin secretion decreased to its baseline level. The integrated incremental somatostatin release was  $260 \pm 102$  pg/20 min ( $P < 0.05$ ) during distention with 5 ml,  $608 \pm 148$  pg/20 min ( $P < 0.01$ ) during distention with 10 ml and  $943 \pm 316$  pg/20 min ( $P < 0.05$ ) during distention with 15 ml saline (Figure 2).

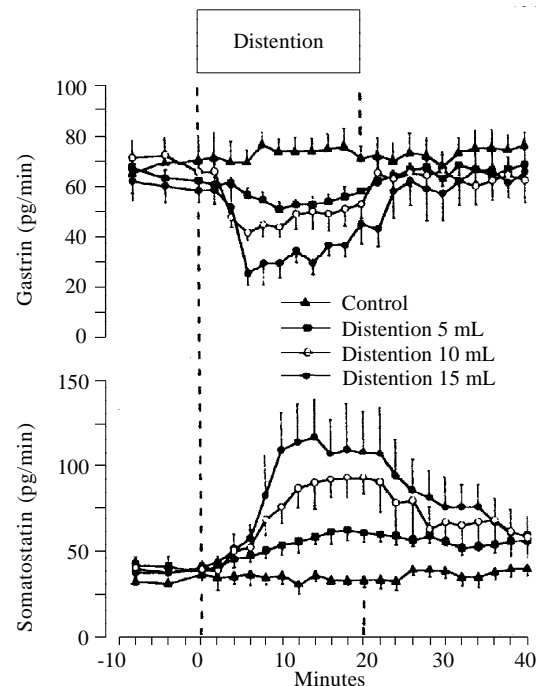


**Figure 1** Release of gastrin and somatostatin from perfused rat stomachs in control ( $n = 8$ ) and during gastric distention with 5 ml ( $n = 8$ ), 10 ml ( $n = 15$ ) and 15 ml ( $n = 8$ ) saline (mean  $\pm$  SE)

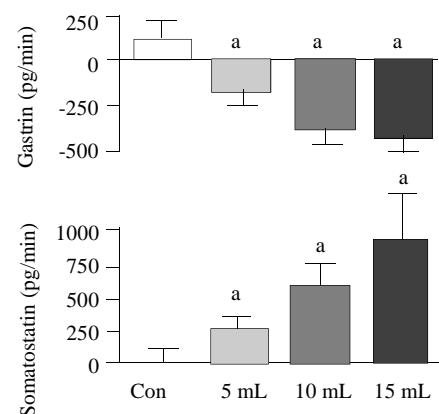


**Figure 2** Integrated release of gastrin, somatostatin from perfused rat stomachs in control ( $n = 8$ ) and during gastric distention with 5 ml ( $n = 8$ ), 10 ml ( $n = 15$ ) and 15 ml ( $n = 8$ ) saline. (mean  $\pm$  SE) <sup>a</sup> $P < 0.05$  vs 10 ml distention in control

#### Effect of TTX and atropine on release of gastrin and somatostatin during gastric distention

The axonal blocker TTX ( $10^{-6}$  M) and the cholinergic antagonist atropine ( $10^{-7}$  M) elicited similar effects on distention-induced inhibition of gastrin. The decrease of gastrin release in response to distention with 10 ml saline was attenuated by approximately 50 % [from  $-385 \pm 86$  pg/20 min to  $-189 \pm 89$  pg/20 min ( $P < 0.05$  vs control)] during infusion of TTX ( $n = 10$ ), and to  $-224 \pm 95$  pg/20 min ( $P < 0.05$  vs control) during infusion of atropine ( $n = 10$ ) (Figure 3). The effects of TTX and atropine on distention-stimulated somatostatin release were also nearly identical, and the incremental somatostatin response to a 10 ml intragastric saline load was reduced about

40 % [from  $608 \pm 148$  pg/20 min to  $370 \pm 100$  pg/20 min ( $P < 0.05$  vs control) in presence of TTX, and to  $404 \pm 77$  pg/20 min ( $P < 0.05$  vs control) during infusion of atropine] (Figure 3).

#### Effect of the somatostatin-antagonist on release of gastrin during gastric distention

In presence of the somatostatin-antagonist ( $10^{-6}$  M), the decrease in gastrin release induced by gastric distention with 10 ml saline was significantly attenuated ( $-167 \pm 73$  pg/20 min with somatostatin-antagonist vs  $-385 \pm 86$  pg/20 min without somatostatin-antagonist;  $P < 0.05$ ,  $n = 15$ ). Combined administration of the somatostatin-antagonist and atropine ( $n = 15$ ) nearly completely abolished distention-induced inhibition of gastrin release (Figure 3).

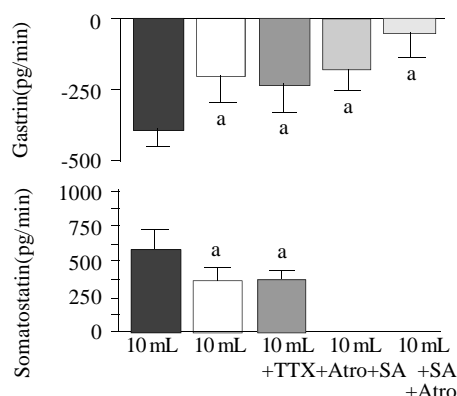


**Figure 3** Integrated release of gastrin and somatostatin from perfused rat stomachs during gastric distention with 10 ml in control ( $n = 15$ ) and in presence of tetrodotoxin (TTX,  $10^{-6}$  M;  $n = 10$ ), atropine (Atro,  $10^{-7}$  M;  $n = 10$ ), somatostatin-antagonist (SA,  $10^{-6}$  M;  $n = 15$ ) and a combination of somatostatin-antagonist and atropine ( $n = 15$ ), (mean  $\pm$  SE). \* $P < 0.05$  vs 10 ml distention in control.

#### Effect of the somatostatin-antagonist on the inhibitory action of exogenous somatostatin-14 on GRP-prestimulated gastrin release

Infusion of GRP ( $10^{-8}$  M) produced a significant increase in gastrin release, from a baseline value of  $58 \pm 6$  to a maximum of  $136 \pm 11$  pg/min. GRP-prestimulated gastrin release was reduced significantly from  $136 \pm 11$  pg/min to  $84 \pm 4$  pg/min by exogenous somatostatin-14 ( $10^{-8}$  M;  $n = 11$ ) ( $P < 0.05$ ). When somatostatin-14 was removed from the perfusate, gastrin release promptly returned to prestimulated levels. At a dose of  $10^{-6}$  M the somatostatin-antagonist did not change the baseline gastrin release, but completely blocked the inhibitory action of exogenous somatostatin-14 on GRP-prestimulated gastrin release ( $n = 9$ ). (Figure 4).

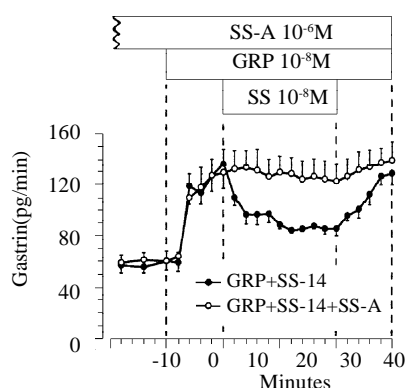


**Figure 4** Effect of somatostatin-14 ( $10^{-6}$  M) on gastrin release from perfused rat stomachs prestimulated by GRP ( $10^{-8}$  M) in control ( $n = 11$ ) and during perfusion with somatostatin-antagonist ( $10^{-6}$  M;  $n = 9$ ). (mean  $\pm$  SE.)

## DISCUSSION

It is well established that gastric distention *in vivo* activates vagal mechanoreceptors within the gastric wall. The afferent vagal nerve fibers activate brainstem neurones which regulate vagal efferent fibers and thereby exocrine and endocrine functions of the stomach<sup>[15-19]</sup>. Apart from this extrinsic nervous system, the stomach itself contains regulatory systems within the gastric wall such as intrinsic neurons and intrinsic paracrine pathways<sup>[20-22]</sup>. The importance of these intragastric mechanisms on regulation of gastrin in response to gastric distention is largely unknown. Isolated perfused stomach allows examination of the remaining intragastric regulatory mechanisms since this model is separated from the extrinsic innervation and the systemic humoral signals, whereas the integrity of intrinsic neurocrine and paracrine pathways is maintained.

As previously reported, distention of the isolated stomach causes a decrease of gastrin release in proportion to the applied intragastric volume and intragastric pressure<sup>[3]</sup>. To examine the functional role of the intragastric nervous system we employed the neurotoxin tetrodotoxin (TTX) which blocks all neural elements that are activated by an influx of  $\text{Na}^+$ . This comprises all the adrenergic and cholinergic neurons and, presumably, the majority of peptidergic neurons as well. The effect was observed while using a very low concentration of TTX ( $10^{-6}$ - $10^{-8}$  M) which had no noticeable effect on other membrane parameters<sup>[23]</sup>. The present data suggest that the inhibition of gastrin release during gastric distention is mediated in part by neural, particularly cholinergic, mechanisms.

However, the classical cholinergic neurotransmitter acetylcholine and its stable analogue carbachol stimulate gastrin release *in vivo* in the isolated stomach preparation and in cultured antral G-cells<sup>[24-27]</sup>. Therefore the inhibitory effect of the cholinergic system on gastrin release in our experiment seems to be indirect, perhaps via peptidergic neurotransmitters. Furthermore, the present data suggest that gastric distention activates endogenous somatostatin through cholinergic and non-cholinergic TTX insensitive pathways, and endogenously released somatostatin can cause distention-induced inhibition of gastrin release. Several studies have shown a reciprocal relationship between stimulation of somatostatin and inhibition of gastrin, suggesting a functional linkage between somatostatin and gastrin release<sup>[28-32]</sup>. Accordingly, the importance of endogenous somatostatin for regulation of gastrin release is supported by studies with antisomatostatin serum, demonstrating an augmented gastrin release after neutralization of endogenously released somatostatin in isolated rat stomach<sup>[33]</sup>. These findings imply that endogenous somatostatin exerts its inhibitory effect on gastrin release via intragastric mechanisms. The secretion and expression of gastrin are under the paracrine control of somatostatin, produced by D cells situated in close contact with gastrin-producing G cells, and gastric D-cells extend the long cytoplasmatic processes that terminate close to gastrin-secreting G-cells in antral mucosa of both humans and rats<sup>[34,35]</sup>. This morphological evidence for a paracrine mode of action is consistent with the functional study results.

The putative somatostatin-antagonist cyclo [7-aminoheptanoyl-Phe-D-Trp-Lys-Thr (Bzl)] has been described as an antagonist of somatostatin in some peripheral tissues such as endocrine rat pancreas, the papillary muscle of the guinea pig heart and the ferret trachea, as well as in neural tissues such as avian choroid, rat cortex, rat hippocampus and rat pituitary<sup>[36]</sup>. In the present study the somatostatin antagonist completely blocked the inhibitory effect of a high infusion rate of somatostatin-14 on gastrin release. During infusion of somatostatin-14 ( $10^{-8}$  M), somatostatin measured in the portal venous effluent of the isolated rat stomach rose to levels



between 1 000 and 1 600 pg/min, whereas somatostatin secretion during gastric distention was only between 60 and 120 pg/min. Since the inhibitory effect of exogenous somatostatin was sufficiently antagonized by the dose of the somatostatin-antagonist employed, it seems most likely that a sufficient amount of antagonist was administered to block all the effects of endogenously released somatostatin during gastric distention. Therefore the residual inhibition of gastrin during gastric distention in presence of the somatostatin-antagonist seems to be independent of endogenous somatostatin and may be mediated by inhibitory cholinergic pathways.

Schubert and Makhlof have previously shown that low distention of the antral part of the isolated rat stomach stimulated somatostatin and inhibited gastrin release probably via VIP-dependent mechanisms, whereas high distention caused an increase in gastrin and a decrease in somatostatin secretion via cholinergic pathways<sup>[2]</sup>. Distention of the whole stomach seems to activate other regulatory mechanisms than selective distention of the distal part of the stomach, since Debas *et al.* have shown that distention of the oxyntic gland area of the stomach can modulate antral gastrin release<sup>[37]</sup>. Furthermore the mechanoreceptors in the antrum have been reported to respond mainly to gastric contractions, while those located in the corpus and fundus respond primarily to distention<sup>[38]</sup>.

In conclusion, the present data suggest that distention of the isolated rat stomach inhibits gastrin release via intrinsic neurocrine and paracrine pathways. Both somatostatin and intrinsic cholinergic pathways are responsible for distention-induced inhibition of gastrin release. Somatostatin release is activated by gastric distention through cholinergic and non-cholinergic TTX-insensitive pathways.

## ACKNOWLEDGEMENT

The author sincerely thanks Dr. N. Weigert and Professor V. Schusdziaarra in the Department of Internal Medicine II, Technical University of Munich, Germany, for their expert guidance in this experimental research.

## REFERENCES

- Grossman MI, Robertson CR, Ivy AC. The proof of a hormonal mechanism for gastric secretion: the humoral transmission of the distention stimulus. *Am J Physiology* 1948; **153**: 1-9
- Schubert ML, Makhlof GM. Gastrin secretion induced by distention is mediated by gastric cholinergic and vasoactive intestinal peptide neurons in rats. *Gastroenterology* 1993; **104**: 834-839
- Weigert N, Li YY, Schick RR, Coy DH, Classen M, Schusdziaarra V. Role of vagal fibers and bombesin/gastrin-releasing peptide-neurons in distention-induced gastrin release in rats. *Regul pept* 1997; **69**: 33-40
- Lippl F, Schusdziaarra V, Huepgens K, Allescher HD. Inhibitory effect of nociceptin on somatostatin secretion of the isolated perfused rat stomach. *Regul Pept* 2002; **107**: 37-42
- Weigert N, Schepp W, Haller A, Schusdziaarra V. Regulation of gastrin, somatostatin and bombesin release from the isolated rat stomach by exogenous and endogenous gamma-aminobutyric acid. *Digestion* 1998; **59**: 16-25
- Weigert N, Schaffler A, Reichenberger J, Madaus S, Classen M, Schusdziaarra V. Effect of endogenous opioids on vagally induced release of gastrin, somatostatin and bombesin-like immunoreactivity from the perfused rat stomach. *Regul Pept* 1995; **55**: 207-215
- Saffouri B, DuVal JW, Makhlof GM. Stimulation of gastrin secretion in vitro by intraluminal chemicals: regulation by intramural cholinergic and noncholinergic neurons. *Gastroenterology* 1984; **87**: 557-561
- McIntosh CH, Pederson RA, Koop H, Brown JC. Gastric inhibitory polypeptide stimulated secretion of somatostatin-like immunoreactivity from the stomach: inhibition by acetylcholine or vagal stimulation. *Can J Physiol Pharmacol* 1981; **59**: 468-472
- Li YY. Effect of neuromedin C on gastrin secretion from isolated and perfused rat stomach. *Shengli Xuebao* 1996; **48**: 77-82
- Tokita K, Hocart SJ, Coy DH, Jensen RT. Molecular basis of the selectivity of gastrin-releasing peptide receptor for gastrin-releasing peptide. *Mol Pharmacol* 2002; **61**: 1435-1443
- Schubert ML, Jong MJ, Makhlof GM. Bombesin/GRP-stimulated somatostatin secretion is mediated by gastrin in the antrum and intrinsic neurons in the fundus. *Am J Physiol* 1991; **261**: G885-889
- Schepp W, Prinz C, Hakanson R, Schusdziaarra V, Classen M. Bombesin-like peptides stimulate gastrin release from isolated rat G-cells. *Regul Pept* 1990; **28**: 241-253
- Barber WD, Burks TF. Brain stem response to phasic gastric distension. *Am J Physiol* 1983; **245**: G242-248
- Blackshaw LA, Grundy D, Scratcherd T. Involvement of gastrointestinal mechano- and intestinal chemoreceptors in vagal reflexes: an electrophysiological study. *J Auton Nerv Syst* 1987; **18**: 225-234
- Ladabaum U, Minoshima S, Hasler WL, Cross D, Chey WD, Owyang C. Gastric distention correlates with activation of multiple cortical and subcortical regions. *Gastroenterology* 2001; **120**: 369-376
- Tuo BG, Yan YH, Ge ZL, Ou GW, Zhao K. Ascorbic acid secretion in the human stomach and the effect of gastrin. *World J Gastroenterol* 2000; **6**: 704-708
- Voutilainen M, Juhola M, Pitkanen R, Farkkila M, Sipponen P. Immunohistochemical study of neuroendocrine cells at the gastric cardia mucosa. *J Clin Pathol* 2002; **55**: 767-769
- Mailliard ME, Wolfe MM. Effect of antibodies to the neuropeptide GRP on distention-induced gastric acid secretion in the rat. *Regul Pept* 1989; **26**: 287-296
- Kovacs TO, Walsh JH, Maxwell V, Wong HC, Azuma T, Katt E. Gastrin is a major mediator of the gastric phase of acid secretion in dogs: proof by monoclonal antibody neutralization. *Gastroenterology* 1989; **97**: 1406-1413
- Lindstrom LM, Ekblad E. Origins and projections of nerve fibres in rat pyloric sphincter. *Auton Neurosci* 2002; **97**: 73-82
- Kawashima K, Ishihara S, Karim Rumi MA, Moriyama N, Kazumori H, Suetsugu H, Sato H, Fukuda R, Adachi K, Shibata M, Onodera S, Chiba T, Kinoshita Y. Localization of calcitonin gene-related peptide receptors in rat gastric mucosa. *Peptides* 2002; **23**: 955-966
- Blackshaw LA, Grundy D, Scratcherd T. Vagal afferent discharge from gastric mechanoreceptors during contraction and relaxation of the ferret corpus. *J Auton Nerv Syst* 1987; **18**: 19-24
- Ulbricht W. Kinetics of drug action and equilibrium results at the node of Ranvier. *Physiol Rev* 1981; **61**: 785-828
- Weigert N, Schaffer K, Wegner U, Schusdziaarra V, Classen M, Schepp W. Functional characterization of a muscarinic receptor stimulating gastrin release from rabbit antral G-cells in primary culture. *Eur J Pharmacol* 1994; **264**: 337-344
- Leib MS, Wingfield WE, Twedt DC, Williams AR, Bottoms GD. Gastric distention and gastrin in the dog. *Am J Vet Res* 1985; **46**: 2011-2015
- Konturek SJ. Cholinergic control of gastric acid secretion in man. *Scand J Gastroenterol Suppl* 1982; **72**: 1-5
- Schiller LR, Walsh JH, Feldman M. Distention-induced gastrin release: effects of luminal acidification and intravenous atropine. *Gastroenterology* 1980; **78**: 912-917
- Chiba T, Taminato T, Kadowaki S, Abe H, Chihara K, Seino Y, Matsukura S, Fujita T. Effects of glucagon, secretin and vasoactive intestinal polypeptide on gastric somatostatin and gastrin release from isolated perfused rat stomach. *Gastroenterology* 1980; **79**: 67-71
- Buscail L, Vernejoul F, Faure P, Torrisani J, Susini C. Regulation of cell proliferation by somatostatin. *Ann Endocrinol* 2002; **63**: 2S13-18
- Soehartono RH, Kitamura N, Yamagishi N, Taguchi K, Yamada J, Yamada H. An immunohistochemical study of endocrine cells in the abomasum of vagotomized calf. *J Vet Med Sci* 2002; **64**: 11-15

- 31 **Zavros Y**, Rieder G, Ferguson A, Samuelson LC, Merchant JL. Hypergastrinemia in response to gastric inflammation suppresses somatostatin. *Am J Physiol Gastrointest Liver Physiol* 2002; **282**: G175-183
- 32 **Li YY**, Gao JT. Somatostatin: the important factor for regulating digestive functions. *Shengli Kexue Jinzhan* 1995; **26**: 65-68
- 33 **Short GM**, Doyle JW, Wolfe MM. Effect of antibodies to somatostatin on acid secretion and gastrin release by the isolated perfused rat stomach. *Gastroenterology* 1985; **88**: 984-988
- 34 **Larsson LI**, Goltermann N, DeMagistris L, Rehfeld JF, Schwartz TW. Somatostatin cell processes as pathways for paracrine secretion. *Science* 1979; **205**: 1393-1395
- 35 **Larsson LI**. Developmental biology of gastrin and somatostatin cells in the antropyloric mucosa of the stomach. *Microsc Res Tech* 2000; **48**: 272-281
- 36 **Shibata S**, Koga Y, Hamada T, Watanabe S. Facilitation of 2-deoxyglucose uptake in rat cortex and hippocampus slices by somatostatin is independent of cholinergic activity. *Eur J Pharmacol* 1993; **231**: 381-388
- 37 **Debas HT**, Walsh JH, Grossman MI. Evidence for oxyntopyloric reflex for release of antral gastrin. *Gastroenterology* 1975; **68**: 687-690
- 38 **Andrews PL**, Grundy D, Scratcherd T. Vagal afferent discharge from mechanoreceptors in different regions of the ferret stomach. *J Physiol* 1980; **298**: 513-524

**Edited by** Zhang JZ

# Effects of tetrandrine on calcium and potassium currents in isolated rat hepatocytes

Hong-Yi Zhou, Fang Wang, Lan Cheng, Li-Ying Fu, Ji Zhou, Wei-Xing Yao

**Hong-Yi Zhou, Fang Wang, Lan Cheng, Li-Ying Fu, Ji Zhou, Wei-Xing Yao**, Department of Pharmacology, Tongji medical college of Huazhong university of science and technology, Wuhan 430030, Hubei Province, China

**Correspondence to:** Hong-Yi Zhou, Department of Pharmacology, Tongji medical college of Huazhong university of science and technology, 13 hangkong Road, Wuhan 430030, China. zhouhy518@yahoo.com.cn  
**Telephone:** 027-83644206

**Received:** 2002-06-27 **Accepted:** 2002-07-25

## Abstract

**AIM:** To study the effects of tetrandrine (Tet) on calcium release-activated calcium current ( $I_{CRAC}$ ), delayed rectifier potassium current ( $I_K$ ), and inward rectifier potassium currents ( $I_{K1}$ ) in isolated rat hepatocytes.

**METHODS:** Hepatocytes of rat were isolated by using perfusion method. Whole cell patch-clamp techniques were used in our experiment.

**RESULTS:** The peak amplitude of  $I_{CRAC}$  was  $-508 \pm 115$  pA ( $n=15$ ), its reversal potential of  $I_{CRAC}$  was about 0 mV. At the potential of -100 mV, Tet inhibited the peak amplitude of  $I_{CRAC}$  from  $-521 \pm 95$  pA to  $-338 \pm 85$  pA ( $P < 0.01$  vs control,  $n=5$ ), with the inhibitory rate of 35 % at 10  $\mu$ mol/L and from  $-504 \pm 87$  pA to  $-247 \pm 82$  pA ( $P < 0.01$  vs control,  $n=5$ ), with the inhibitory rate of 49 % at 100  $\mu$ mol/L, without affecting its reversal potential. The amplitude of  $I_{CRAC}$  was dependent on extracellular  $Ca^{2+}$  concentration. The peak amplitude of  $I_{CRAC}$  was  $-205 \pm 105$  pA ( $n=3$ ) in tyrode's solution with  $Ca^{2+}$  1.8 mmol/L ( $P < 0.01$  vs the peak amplitude of  $I_{CRAC}$  in external solution with  $Ca^{2+}$  10 mmol/L). Tet at the concentration of 10 and 100  $\mu$ mol/L did not markedly change the peak amplitude of delayed rectifier potassium current and inward rectifier potassium current ( $P > 0.05$  vs control).

**CONCLUSION:** Tet protects hepatocytes by inhibiting  $I_{CRAC}$ , which is not related to  $I_K$  and  $I_{K1}$ .

Zhou HY, Wang F, Cheng L, Fu LY, Zhou J, Yao WX. Effects of tetrandrine on calcium and potassium currents in isolated rat hepatocytes. *World J Gastroenterol* 2003; 9(1): 134-136  
<http://www.wjgnet.com/1007-9327/9/134.htm>

## INTRODUCTION

Tetrandrine (Tet) is a bisbenzylisoquinoline alkaloid from a Chinese medicinal herb (*Stephania tetrandra* S. Moore). In the past decade, lots of studies demonstrated that Tet possessed multiple bioactivities, such as potential immunomodulating, anticarcinoma<sup>[1]</sup> and protective effect on CCl<sub>4</sub>-injured hepatocytes<sup>[2]</sup>. It has also been used in the treatment of ischemic heart diseases<sup>[3]</sup> and hypertension<sup>[3,4]</sup>. Recently, the antifibrotic effects of Tet have been received considerable attention<sup>[1,5-10]</sup>. The former researches of Tet on the liver have probed into cellular and molecular levels<sup>[9,10]</sup>. In the present paper, we used

whole-cell patch-clamp technique to observe the effects of Tet on  $I_{CRAC}$ ,  $I_K$ ,  $I_{K1}$  in normal isolated rat hepatocytes, in order to have a better understanding its hepatoprotective and antifibrotic effects.

## MATERIALS AND METHODS

### Solutions and drugs

Tet was from Jinhua Pharmaceutical Co. The stock solution (10 mmol/L) was dissolved in distilled water after acidification with 0.1 mol/L HCl and neutralized with 0.1 mol/L NaOH.  $Ca^{2+}$ -free Hank's solution was prepared without  $Ca^{2+}$  and  $Mg^{2+}$ . KB solution contained (mmol/L): glutamic acid 70, taurine 15, KCl 130,  $KH_2PO_4$  10, HEPES 10, glucose 11, egtazic acid 0.5, pH was adjusted to 7.4 with KOH. The external solution used to record  $I_{crac}$  contained (mmol/L): NaCl 140, KCl 2.8,  $CaCl_2$  10,  $MgCl_2$  0.5, glucose 11, HEPES 10, pH was adjusted to 7.4 with NaOH. The internal solution used to record  $I_{CRAC}$  contained (mmol/L): potassium-glutamate 145, NaCl 8,  $MgCl_2$  1, Mg-ATP 0.5, egtazic acid 10, HEPES 10, pH was adjusted to 7.2 with KOH. The external solution used to record  $I_K$  contained (mmol/L): NaCl 144, KCl 4,  $CaCl_2$  1.8,  $MgCl_2$  0.53,  $NaH_2PO_4$  0.33, glucose 5.5, HEPES 5, pH was adjusted to 7.4 with NaOH. The internal solution used to record  $I_K$  contained (mmol/L): KCl 130,  $K_2ATP$  5, creatine phosphate 5, HEPES 5, pH was adjusted to 7.2 with KOH. The same external and internal solutions used to record  $I_{K1}$  contained (mmol/L): KCl 7,  $MgCl_2$  2, egtazic acid 1, potassium-glutamate 130, HEPES 10, pH was adjusted to 7.4 with KOH.

### Isolation of single hepatocytes

Hepatocytes were isolated with the modified method reported by Seglen<sup>[11]</sup>. Briefly, adult wistar rats of either sex ( $175 \pm 25$  g) were anesthetized by intraperitoneal injection of pentobarbital sodium (50 mg/kg). The portal vein was cannulated and perfused with oxygenated  $Ca^{2+}$ -free Hank's solution 30 ml/min at 37 °C for 4-5 min followed by perfusion with  $Ca^{2+}$ -free Hank's solution containing collagenase (Type 1, Sigma) (0.3g/L) for 10 min. The liver was chopped in 10 ml  $Ca^{2+}$ -free Hank's solution. The cell suspension was filtered through 200 mesh gauze and then centrifuged three times (50 g, 2 min) to separate liver cells. Cells were plated onto the coverslips and incubated in KB medium for 2 hour and preserved in DMEM at 4 °C.

### Electrophysiologic recording

Whole-cell recordings were performed using a PC-II patch clamp amplifier (Huazhong university of science and technology). The recording chamber (1.5 ml) was perfused with the corresponding external solution. The pipettes were pulled in two stages from hard glass capillaries using a vertical microelectrode puller (Narishige, Japan). Electrode has a resistance of 2-5 M $\Omega$  for whole-cell recording when filled with electrode internal solution. All experiments were conducted at  $22 \pm 2$  °C.

### Statistic analysis

The data were expressed as  $\bar{x} \pm s$ . Statistical significances were analyzed by a unpaired *t*-test. A value of  $P < 0.05$  was considered significant.

## RESULTS

### Effect of Tet on calcium release-activated calcium current ( $I_{CRAC}$ )

$I_{CRAC}$  was elicited for 200 ms from the holding potential of 0 mV to various potentials ranging from -10 mV to +80 mV with the step of 20 mV every 5 s<sup>[12]</sup>. The peak amplitude of  $I_{CRAC}$  was  $-508 \pm 115$  pA ( $n=15$ ) and the reversal potential of  $I_{CRAC}$  was about 0 mV, the current was steady and without run-down in 5 mins. Tet inhibited the peak amplitude of  $I_{CRAC}$  from  $-521 \pm 95$  pA to  $-338 \pm 85$  pA ( $P < 0.01$  vs control,  $n=5$ ), with the inhibitory rate of 35 % at 10  $\mu\text{mol/L}$  and from  $-504 \pm 87$  pA to  $-247 \pm 82$  pA ( $P < 0.01$  vs control,  $n=5$ ), with the inhibitory rate of 49 % at 100  $\mu\text{mol/L}$ . Tet did not affect the shape of its current voltage curve (Figure 1,2).

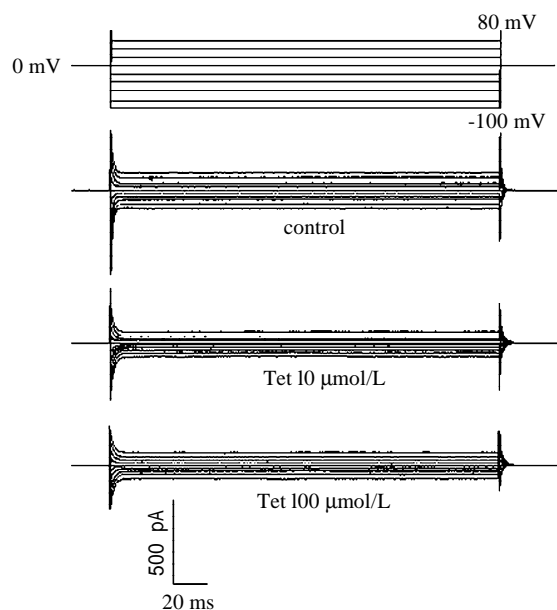


**Figure 1** Effect of Tet on  $I_{CRAC}$  in isolated rat hepatocytes.  $I_{CRAC}$  traces before and after Tet 10  $\mu\text{mol/L}$  and 100  $\mu\text{mol/L}$ .  $I_{CRAC}$  was elicited for 200 ms from the holding potential of 0 mV to various potentials ranging from -100 mV to +80 mV with step of 20 mV.

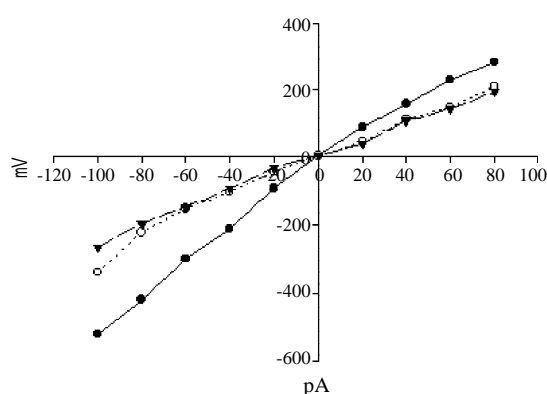


**Figure 2** Effect of Tet on I-V relationship of  $I_{CRAC}$  in isolated rat hepatocytes. Especially at the potential of -100 mV, Tet inhibited the peak amplitude of  $I_{CRAC}$  with the inhibitory rate of 35 % at 10  $\mu\text{mol/L}$  and with the inhibitory rate of 49 % at 100  $\mu\text{mol/L}$ . ● control; ○ 10  $\mu\text{mol/L}$ ; □ 100  $\mu\text{mol/L}$ .

The amplitude of  $I_{CRAC}$  was dependent on extracellular  $\text{Ca}^{2+}$  concentration. The peak amplitude of  $I_{CRAC}$  was  $-205 \pm 105$  pA ( $n=3$ ) in tyrode's solution with  $\text{Ca}^{2+}$  1.8 mmol/L ( $P < 0.01$  vs the peak amplitude of  $I_{CRAC}$  in external solution with  $\text{Ca}^{2+}$  10 mmol/L). Tet at 10  $\mu\text{mol/L}$  decreased  $I_{CRAC}$  from  $-205 \pm 105$  pA to  $-148 \pm 96$  pA ( $n=3$ ).

### Effect of Tet on delayed rectifier potassium current ( $I_K$ )

$I_K$  was elicited by 900 ms depolarization steps from +30 mV to +140 mV with step of 10 mV at holding potential of -50 mV<sup>[13]</sup>. Tet at 10 and 100  $\mu\text{mol/L}$  did not change the peak amplitude of  $I_K$  [from  $2014 \pm 686$  pA to  $2030 \pm 692$  pA and  $2047 \pm 710$  pA respectively,  $n=5$ , cells from 3 rats,  $P > 0.05$ ]. Tet did not affect the shape of its current voltage curve.

### Effect of Tet on inward rectifier potassium current ( $I_{K1}$ )

$I_{K1}$  was elicited by a number of step pulses (40 ms) from the holding potential ( $E_h$ ) of 0 mV to test potentials from -200 mV to +175 mV with the step of 10 mV<sup>[14]</sup>. Tet at 10 and 100  $\mu\text{mol/L}$  did not change the peak amplitude of  $I_{K1}$  [from  $2254 \pm 718$  pA to  $2239 \pm 700$  pA and  $2224 \pm 658$  pA respectively,  $n=5$ , cells from 3 rats,  $P > 0.05$ ]. Tet did not affect the shape of its current voltage curve.

## DISCUSSION

Hepatic fibrosis is a common consequence of chronic liver injury from many causes<sup>[15-19]</sup>, and the sustained hepatic injury is a primary factor for hepatic fibrogenesis<sup>[20-28]</sup>. Preventing hepatocyte from injury is a matter of primary importance in blocking the fibrogenic pathway. Tet has been considered as an effective antifibrotic and hepatoprotective agent<sup>[1,2,5-10]</sup>, but its protection against toxic cell death has never been well illustrated.

The  $\text{Ca}^{2+}$  influx is mainly mediated by voltage-operated  $\text{Ca}^{2+}$  channels and receptor-activated  $\text{Ca}^{2+}$  channels. Voltage-operated  $\text{Ca}^{2+}$  channels are not present in hepatocytes<sup>[29]</sup>. Calcium influx in isolated hepatocytes mainly depend on receptor-mediated  $\text{Ca}^{2+}$  entry which has been identified by indirect methods<sup>[30]</sup>. Previous studies have shown that one type of receptor-activated  $\text{Ca}^{2+}$  channels, most likely a store-operated  $\text{Ca}^{2+}$  channel, in freshly isolated rat hepatocytes is inhibited by high concentrations of L-type voltage-operated  $\text{Ca}^{2+}$  channels antagonists<sup>[30,31]</sup>. Besides, the mRNA encoding isoforms of L-type voltage-operated  $\text{Ca}^{2+}$  channels has been detected in rat hepatocytes, these observation suggested that receptor-activated  $\text{Ca}^{2+}$  channels in rat hepatocytes exhibit some characteristics of voltage-operated  $\text{Ca}^{2+}$  channels<sup>[32]</sup>. Cui *et al* reported that  $I_{CRAC}$  (an important sub-type of store-operated  $\text{Ca}^{2+}$  channels) existed in isolated rat hepatocytes and 50  $\mu\text{mol/L}$  of verapamil, diltiazem and nifedipine could decrease the amplitude of  $I_{CRAC}$  effectively<sup>[12]</sup>. The results in our experiment showed that Tet at the concentration of 10 and 100  $\mu\text{mol/L}$  could decrease the peak amplitude of  $I_{CRAC}$ . The concentration that Tet made a half-maximal inhibition of  $I_{CRAC}$  was approximately 100  $\mu\text{mol/L}$ , which was substantially higher than that needed for the half-maximal inhibition of L-type voltage-operated  $\text{Ca}^{2+}$  channels by Tet. It suggested that Tet could protect hepatocytes by inhibiting  $I_{CRAC}$  and decreasing intracellular  $\text{Ca}^{2+}$  concentration, in which a higher concentration of Tet was needed.

Nietsch's study demonstrated that the activation of potassium and chloride channels by TNF- $\alpha$  induced apoptosis and death of the HTC rat hepatoma cells, which could be significantly delayed by  $\text{K}^+$  channel blockers ( $\text{Ba}^{2+}$  and quinine)<sup>[33]</sup>. Our result showed that Tet had no effect on  $I_K$  and  $I_{K1}$ , which suggested that the hepatoprotection of Tet might not relate to potassium channels. However, whether calcium activated potassium channels exist in rat hepatocytes or not remains controversial<sup>[34,35]</sup>. The effect of Tet on potassium channels requires further investigation.

In conclusion, Tet protects hepatocytes by inhibiting  $I_{CRAC}$ , which is not related to  $I_K$  and  $I_{K1}$ .

## REFERENCES

1. Li DG, Wang ZR, Lu HM. Pharmacology of tetrandrine and its therapeutic use in digestive diseases. *World J Gastroenterol* 2001; 7: 627-629

- 2 **Chen XH**, Hu YM, Liao YQ. Protective effects of tetrandrine on CCl<sub>4</sub>-injured hepatocytes. *Acta Pharmacol Sin* 1996; **17**: 348-350
- 3 **Wong TM**, Wu S, Yu XC, Li HY. Cardiovascular actions of Radix Stephaniae Tetrandrae: a comparison with its main component, tetrandrine. *Acta Pharmacol Sin* 2000; **21**: 1083-1088
- 4 **Cheng D**, Chen W, Mo X. Acute effect of tetrandrine pulmonary targeting microspheres on hypoxic pulmonary hypertension in rats. *Chin Med J (Engl)* 2002; **115**: 81-83
- 5 **Lee SH**, Nan JX, Sohn DH. Tetrandrine prevents tissue inhibitor of metalloproteinase-1 messenger RNA expression in rat liver fibrosis. *Pharmacol Toxicol* 2001; **89**: 214-216
- 6 **Liu D**, Li G, Liu D, Cao Y. Effects of tetrandrine on the synthesis of collagen and scar-derived fibroblast DNA. *Zhonghua Shaoshang Zazhi* 2001; **17**: 222-224
- 7 **Park PH**, Nan JX, Park EJ, Kang HC, Kim JY, Ko G, Sohn DH. Effect of tetrandrine on experimental hepatic fibrosis induced by bile duct ligation and scission in rats. *Pharmacol Toxicol* 2000; **87**: 261-268
- 8 **Ma JY**, Barger MW, Hubbs AF, Castranova V, Weber SL, Ma JK. Use of tetrandrine to differentiate between mechanisms involved in silica-versus bleomycin-induced fibrosis. *J Toxicol Environ Health A* 1999; **57**: 247-266
- 9 **Li DG**, Lu HM, Chen YW. Progression on antifibrotic effects of tetrandrine. *Shijie Huaren Xiaohua Zazhi* 1999; **7**: 171-172
- 10 **Li DG**, Lu HM, Chen YW. Progress in studies of tetrandrine against hepatofibrosis. *World J Gastroenterol* 1998; **4**: 377-379
- 11 **Seglen PO**. Preparation of isolated rat liver cells. *Methods Cell Biol* 1976; **13**: 29-83
- 12 **Cui GY**, Li JM, Cui H, Hao LY, Liu DJ, Zhang KY. Effects of calcium channel blockers on calcium release-activated calcium currents in rat hepatocytes. *Acta Pharmacol Sin* 1999; **20**: 415-418
- 13 **Li JM**, Cui GY, Liu DJ, Cui H, Chang TH, Wang YP, Zhang KY. Effects of N-methyl berbamine on delayed outward potassium current in isolated rat hepatocytes. *Acta Pharmacol Sin* 1998; **19**: 24-26
- 14 **Henderson RM**, Graf J, Boyer JL. Inward-rectifying potassium channels in rat hepatocytes. *Am J Physiol* 1989; **256**: G1028-1035
- 15 **Wu CH**. Fibrodynamics-elucidation of the mechanisms and sites of liver fibrogenesis. *World J Gastroenterol* 1999; **5**: 388-390
- 16 **Albanis E**, Friedman SL. Hepatic fibrosis. Pathogenesis and principles of therapy. *Clin Liver Dis* 2001; **5**: 315-334
- 17 **Friedman SL**. Molecular regulation of hepatic fibrosis, an integrated cellular response to tissue injury. *J Biol Chem* 2000; **275**: 2247-2250
- 18 **Brenner DA**, Waterboer T, Choi SK, Lindquist JN, Stefanovic B, Burchardt E, Yamauchi M, Gillan A, Rippe RA. New aspects of hepatic fibrosis. *J Hepatol* 2000; **32**(Suppl 1): 32-38
- 19 **Maddrey WC**. Alcohol-induced liver disease. *Clin Liver Dis* 2000; **4**: 115-131
- 20 **Liu Y**, Shimizu I, Omoya T, Ito S, Gu XS, Zuo J. Protection effect of estradiol on hepatocytic oxidative damage. *World J Gastroenterol* 2002; **8**: 363-366
- 21 **Wei HS**, Li DG, Lu HM, Zhan YT, Wang ZR, Huang X, Zhang J, Cheng JL, Xu QF. Effects of AT1 receptor antagonist, losartan, on rat hepatic fibrosis induced by CCl<sub>4</sub>. *World J Gastroenterol* 2000; **6**: 540-545
- 22 **Hu YY**, Liu CH, Wang RP, Liu C, Liu P, Zhu DY. Protective actions of salvianolic acid A on hepatocyte injured by peroxidation *in vitro*. *World J Gastroenterol* 2000; **6**: 402-404
- 23 **Chen PS**, Zhai WR, Zhou XM, Zhang JS, Zhang YE, Ling YQ, Gu YH. Effects of hypoxia, hyperxia on the regulation of expression and activity of matrix metalloproteinase-2 in hepatic stellate cells. *World J Gastroenterol* 2001; **7**: 647-651
- 24 **Hamasaki K**, Nakashima M, Naito S, Akiyama Y, Ohtsuru A, Hamanaka Y, Hsu CT, Ito M, Sekine I. The sympathetic nervous system promotes carbon tetrachloride-induced liver cirrhosis in rats by suppressing apoptosis and enhancing the growth kinetics of regenerating hepatocytes. *J Gastroenterol* 2001; **36**: 111-120
- 25 **Hu Y**, Wang R, Zhang X, Liu C, Liu C, Liu P, Zhu D. Effects of carbon tetrachloride-injured hepatocytes on hepatic stellate cell activation and salvianolic acid A preventive action *in vitro*. *Zhonghua Ganzangbing Zazhi* 2000; **8**: 299-301
- 26 **Kim KY**, Choi I, Kim SS. Progression of hepatic stellate cell activation is associated with the level of oxidative stress rather than cytokines during CCl<sub>4</sub>-induced fibrogenesis. *Mol Cells* 2000; **10**: 289-300
- 27 **Shi J**, Aisaki K, Ikawa Y, Wake K. Evidence of hepatocyte apoptosis in rat liver after the administration of carbon tetrachloride. *Am J Pathol* 1998; **153**: 515-525
- 28 **Greenwel P**, Dominguez-Rosales JA, Mavi G, Rivas-Estilla AM, Rojkind M. Hydrogen peroxide: a link between acetaldehyde-elicited alpha1 (I) collagen gene up-regulation and oxidative stress in mouse hepatic stellate cells. *Hepatology* 2000; **31**: 109-116
- 29 **Sawanobori T**, Takanashi H, Hiraoka M, Iida Y, Kamisaka K, Maezawa H. Electrophysiological properties of isolated rat liver cells. *J Cell Physiol* 1989; **139**: 580-585
- 30 **Strigrow F**, Bohnensack R. Verapamil and diltiazem inhibit receptor-operated calcium channels and intracellular calcium oscillations in rat hepatocytes. *FEBS Lett* 1993; **318**: 341-344
- 31 **Hughes BP**, Milton SE, Barritt GJ, Auld AM. Studies with verapamil and nifedipine provide evidence for the presence in the liver cell plasma membrane of two types of Ca<sup>2+</sup> inflow transporter which are dissimilar to potential-operated Ca<sup>2+</sup> channels. *Biochem Pharmacology* 1986; **35**: 3045-3052
- 32 **Brereton HM**, Harland ML, Frosco M, Petronijevic T, Barritt GJ. Novel variants of voltage-operated calcium channel alpha 1-subunit transcripts in a rat liver-derived cell line: deletion in the IVS4 voltage sensing region. *Cell Calcium* 1997; **22**: 39-52
- 33 **Nietsch HH**, Roe MW, Fiekers JF, Moore AL, Lidofsky SD. Activation of potassium and chloride channels by tumor necrosis Factor  $\alpha$  role in liver cell death. *J Biol Chem* 2000; **275**: 20556-20561
- 34 **Takanashi H**, Sawanobori T, Kamisaka K, Maezawa H, Hiraoka M. Ca<sup>2+</sup>-activated K<sup>+</sup> channel is present in guinea-pig but lacking in rat hepatocytes. *Jpn J Physiol* 1992; **42**: 415-430
- 35 **Duszynski J**, Elensky M, Cheung JY, Tillotson DL, Lanoue KF. Hormone-regulated Ca<sup>2+</sup> channel in rat hepatocytes revealed by whole cell patch clamp. *Cell Calcium* 1995; **18**: 19-29

Edited by Zhu L

# Influence of intrauterine injection of rat fetal hepatocytes on rejection of rat liver transplantation

Yan-Ling Yang, Ke-Feng Dou, Kai-Zong Li

**Yan-Ling Yang, Ke-Feng Dou, Kai-Zong Li**, Department of Hepatobiliary Surgery, Xijing Hospital, Fourth Military Medical University, Xi'an 710032, Shaanxi Province, China  
**Supported by** the National Nature Science Foundation of China, No. 30070741

**Correspondence to:** Kai-Zong Li, Department of Hepatobiliary Surgery, Xijing Hospital, Fourth Military Medical University, 710032 Xi'an, Shaanxi Province, China. gdwk@fmmu.edu.cn  
**Telephone:** +86-29-3375259 **Fax:** +86-29-3375561  
**Received:** 2002-08-01 **Accepted:** 2002-08-27

## Abstract

**AIM:** To investigate the influence of immune tolerance induced by intrauterine exposure to fetal hepatocytes on liver transplantation in the adult rat.

**METHODS:** LOU/CN rat fetal hepatocytes were injected into the fetuses of pregnant CHN rats (14-16 days of gestation). At 7-9 weeks of age, the surviving male rats received orthotopic liver transplantation (OLT) from male LOU/CN donors and the survival period was observed and monitored by mixed lymphocyte reaction assay and cytotoxicity test.

**RESULTS:** (1) A total of 31 pregnant CHN rats with 172 fetuses received fetal hepatocytes from LOU/CN rats via intrauterine injection. Among them, thirteen pregnant rats showed normal parturition, with 74 neonatal rats growing up normally. (2) The mean survival period after OLT in rats with fetal exposure to fetal hepatocytes was  $32.1 \pm 3.7$  days, which was significantly different from the control ( $11.8 \pm 2.3$  days,  $P < 0.01$ ) in rats without fetal induction of immune tolerance. (3) Mixed lymphocyte proliferation assays yielded remarkable discrepancies between the groups of rats with- or without fetal exposure to fetal hepatocytes, with values of  $8411 \pm 1361$  and  $22473 \pm 1856$  (CPM  $\pm$  SD,  $P < 0.01$ ) respectively. (4) Cytotoxicity assays showed values of  $21.2 \pm 6.5\%$  and  $64.5 \pm 7.2\%$  ( $P < 0.01$ ) in adult rats with or without fetal induction of immune tolerance.

**CONCLUSION:** Intrauterine injection of fetal hepatocytes into rat fetuses can prolong the survival period of liver transplant adult male rats recipients, inducing immune tolerance in OLT.

Yang YL, Dou KF, Li KZ. Influence of intrauterine injection of rat fetal hepatocytes on rejection of rat liver transplantation. *World J Gastroenterol* 2003; 9(1): 137-140  
<http://www.wjgnet.com/1007-9327/9/137.htm>

## INTRODUCTION

In both experimental study and clinical practice, rejection responses induced by organ transplants necessitate the use of potent immunosuppressive drugs<sup>[1-7]</sup>. It should be noted, however, that excessive dosage of immunosuppressive agents may result in severe side effects such as hypertension and

hepatic and/or renal toxicity. Moreover, prolonged usage of immunosuppressants often leads to severe infection and increased susceptibility to malignancy, thus critically affecting the health of recipients. Particularly in juvenile patients, immunosuppressive drugs can lead to stunted growth. It is therefore imperative to assess, as an alternative to immunosuppressants, the protective effect of induced immune tolerance on organ transplantation. The ideal strategy is to induce a low responsiveness or irresponsiveness in the recipients toward donors' grafts, while preserving normal immunological functions for the recognition of tumor antigens and prevention of infection. Thus immunosuppressive agents can be avoided or be used at dramatically reduced dosage. The key steps toward successful transplantation therefore include either attenuated immune reactions or induced immune tolerance to grafts<sup>[8-15]</sup>.

In utero, the stem cell transplantation represents a new therapeutic approach of experimental nature toward the treatment of hematopoietic diseases, immunodeficiency diseases, metabolic disorders and genetic diseases<sup>[16-19]</sup>. Some reports support the possibility of using this method to induce immunologic tolerance in both human subjects and animals receiving organ transplantation<sup>[20-22]</sup>. But the effect of *in utero* fetal exposure to fetal hepatocytes on liver transplantation in adulthood is unclear. In the present study, we injected fetal hepatocytes intraperitoneally into rat fetuses and then performed orthotopic liver transplantation (OLT) in surviving adult male rats. Some parameters were tested in order to confirm the anti-rejection effect of *in utero* injection of fetal hepatocytes.

## MATERIALS AND METHODS

### Animals

Male and female LOU/CN and CHN rats weighing 200-250 g were obtained from the Laboratory Animal Center of The Fourth Military Medical University, and fed with standard rat chow.

### Timed pregnancy of CHN rats

Male CHN rats, or male LOU/CN rats, were housed individually in standard cages with a metal divider with 0.25-inch holes. One female CHN or LOU/CN rat was placed in the corresponding empty side. The cage divider was then removed 48 hrs later. Pairs of CHN or LOU/CN rats were allowed to mate overnight separately. The pairs were then separated with the females placed singly in cages. The presence of vaginal plug marked day 0 of gestation. Normal gestation is about 21 days.

### Preparation of LOU/CN fetal rat hepatocytes

Pregnant LOU/CN females were killed by cervical dislocation at 15 to 16 days of gestation. All subsequent handling was done under sterile conditions. The uterine horns were removed and dissected in phosphate-buffered saline (PBS). Fetuses were separated from decidua and extraembryonic membranes and transferred to 35 mm petri dishes filled with PBS. Fetal livers were removed, with 5 to 10 livers placed in 1 to 2 ml RPMI 1640 medium (GIBCO BRL, Grand Island, CA) with 15 % fetal calf serum (FCS, GIBCO BRL, Grand Island, CA). Cell suspensions were prepared by repeated pipetting of the livers

through a 23-gauge needle attached to a 1ml pipette. The mononuclear cells were separated by centrifugation at 500 g for 20 minutes and filtered through a Nitex filter with a 41  $\mu$ m pore size (Huamei chemical company, Henan province, China). Cell viability counting (usually greater than 90 %) was done using trypan blue exclusion test, and the final cell suspension was prepared in PBS/15 % FCS at a concentration of  $5 \times 10^7$ /ml. The cell suspension was used for intrauterine injection within 4 hours of preparation.

#### ***In utero intraperitoneal injection into CHN rat fetuses with LOU/CN fetal rat hepatocytes***

Micropipettes were prepared from capillaries using a Brown and Flaming micropipette puller. The end of the needle was cut under a microscope with ophthalmological forceps, and the tip was sharpened on a micro-grinding wheel. Pregnant (11 to 13 days of gestation) CHN rats were anesthetized i.p. with sodium pentobarbital, and the uterine horns were exteriorized with ophthalmological forceps. Fetal hepatocytes from LOU/CN rats were injected into CHN fetuses through a hand-drawn glass micropipette with a beveled edge. The placenta was penetrated at an oblique angle. The number of cells injected per fetus was  $10^6$  (about  $5 \times 10^{10}$  cells/kg of recipient weight), except in experiments in which the effects of different cell concentrations and volumes of cell suspension used were examined. Muscle layers were closed with 4-0 silk suture, and 1-0 silk thread was used for skin suture.

#### ***Orthotopic liver transplantation (OLT)***

Orthotopic whole-liver transplantation was performed<sup>[23-26]</sup> using the simplified cuff technique for portal and intrahepatic vena cava anastomosis, whereas the hepatic artery was not reconstructed. The twenty male CHN rats, aged 7 to 9 weeks that survived intraperitoneal injection with fetal liver cells from LOU/CN rats, were taken as graft recipients, with normal male LOU/CN rats as liver donors. Both donors and recipients were anesthetized with methoxyflurane. After explantation, livers were stored at 0-4 °C for 1 hr in UW solution. Grafts were connected to suprahepatic vena cava with a running 7-0 prolene suture. We insert cuffs into the corresponding vessels, and anastomose the bile duct and hepatic artery over an intraluminal polyethylene splint. Transplantation required less than 40 min, while the portal vein was clamped for 12-15 min during this period. After transplantation, the recipients had free access to standard laboratory chow and tap water. Animals that died within 3 days were considered technical failures and were excluded from data collection. The rate of success of liver transplantation was more than 90 % in this study. Five rats were sacrificed at 5 days after OLT. Immediately before sacrifice, the livers were removed for histological investigation. Liver samples from 10 normal male CHN rats were taken as controls.

#### ***Mixed lymphocyte reaction assay***

Mixed spleen cells were used for setting up lymphocyte cultures. Briefly, the spleens were aseptically removed from experimental CHN rats that survived *in utero* intraperitoneal injection of fetal LOU/CN rat liver cell, and from control CHN rats. Then they were separately disrupted mechanically using a pair of sterile forceps. LOU/CN spleen cells were treated with 25  $\mu$ g/ml mitocin-C (Kyowa Hakko Kogyo, Tokyo, Japan) at 37 °C for 45 min. Then the two groups of cells were washed by PBS, followed by lysis of erythrocytes in Tris-NH<sub>4</sub>Cl solution (pH 7.2). After further washes, the cells were finally resuspended in RPMI 1640 with 10 % FCS. The numbers of two groups of spleen cells were adjusted, and  $5 \times 10^5$  spleen cells from each of the two sources were mixed together (final

volume 0.2 ml) and added to triplicate wells of 96-well round-bottomed microtiter plates. Cells were cultured for 120 hr, and 1  $\mu$ Ci [3H]-thymidine was added into wells 18hr before cell harvesting. Radioactive thymidine incorporation rate was measured by a liquid scintillation counter (1205 Betaplate), with data expressed as CPM $\pm$ SD<sup>[27,28]</sup>.

#### ***Complement-dependent cytotoxicity test***

Recipient CHN rats were tested one week after OLT for complement-dependent cytotoxicity test against lymphocytes suspensions from LOU/CN donor rats. Sera from recipients were prepared and added into the wells of 96-well round-bottomed microtiter plates (1  $\mu$ l per well). Then 1  $\mu$ l lymphocytes (about 2 000 cells per 1  $\mu$ l volume) were added into the same wells. They were gently mixed and incubated for 30 min at 22 °C $\pm$ 2 °C, then 5  $\mu$ l rabbit complement (Huamei chemical company, Henan province, China) was added, and the mixture incubated for 60 min at 22 °C $\pm$ 2 °C. Afterwards, the mixtures were stained with eosin (50 g/L) for 5 min. The cells were fixed in 36 % formalin for 2 hr and observed with an inverted phase-contrast microscope (Olympus, Tokyo, Japan). Cytotoxicity was determined by eosin exclusion and percentage enumeration of cells killed by sera from OLT<sup>[29,30]</sup>.

#### ***Histology***

Livers from CHN rats that underwent OLT were fixed in 10 % neutral formalin for five days and then embedded in paraffin. Five micron sections were cut and stained with hematoxylin and eosin for histological examination. Sections from normal rat livers served as controls.

#### ***Diagnostic criterion of graft rejection***

Several diagnostic criteria were used to determine the existence of rejection response following hepatic transplantation. The first is survival of recipients over 7 days post-transplantation. The second entails the occurrence of acute hepatic dysfunction as typified by inappetence, weight loss, auricle or nail jaundice, depressed mood, with incidental diarrhea or ascites in some cases. The third criterion involves typical histological changes, such as enlarged liver bulk, yellowish white appearance of the liver, and the presence of liver conglutination to muscles or abdominal walls, and viscera. Also frequently encountered are apparent degeneration or necrosis of hepatic cells, and infiltration of numerous lymphocytes, especially at liver sinusoidal area. The fourth denotes the presence in good condition of the recipients plus good appetite, accompanied with normal weight 3 days after successful transplantation. The recipients that died from post-surgical complications such as necrosis of bile duct, intra-abdominal hemorrhage and infection were excluded from data collection.

#### ***Statistics***

All the data were analyzed by Student's *t* test and expressed as mean  $\pm$  S. The statistical difference  $P < 0.05$  was considered significant and  $P < 0.01$  as very significant.

## **RESULTS**

#### ***Influence of intraperitoneal injection into fetus in utero on survival of neonatal CHN rats***

Thirty-one pregnant CHN recipients who later delivered 172 fetal CHN rats were injected into their fetuses with isolated fetal hepatocytes from LOU/CN rats. Among them, eleven pregnant females died from various surgical complications, and seven females aborted or consumed their litters. There were 17 pregnant rats with normal parturition, and 74 neonatal rats grew up normally.

### Suppression of rejection response to rat liver transplantation after intrauterine injection

The mean survival period of rats with fetal intraperitoneal injection of fetal hepatocytes prior to OLT was  $32.1 \pm 3.7$  day, in comparison to control values of  $11.8 \pm 2.3$  day ( $P < 0.01$ ) obtained from rats without this procedure.

### Inhibitory effect of intraperitoneal injection in utero on mixed lymphocytes reaction assay

Mixed lymphocytes reaction assay showed significant differences in [ $^3\text{H}$ ]-thymidine incorporation rates in groups of CHN rats that were either fetally exposed ( $8411 \pm 1361$ , CPM $\pm$ SD) or not ( $22473 \pm 1856$ , CPM $\pm$ SD) to intraperitoneal injection of fetal hepatocytes in utero ( $P < 0.01$ ).

### Suppressive effect of fetal intraperitoneal injection in utero on cytotoxicity test after rat liver transplantation in adulthood

Cytotoxicity test revealed percentage values of dead cells to be  $21.2 \pm 6.5\%$  vs  $64.5 \pm 7.2\%$  ( $P < 0.01$ ) respectively from the two groups of CHN rats with or without fetal intraperitoneal injection in utero prior to OLT in the adult rats, the difference being statistically significant.

## DISCUSSION

With rapid advances in antenatal diagnostic technology, many prenatal diseases (congenital metabolic liver disorders, congenital heart disease and hemophilia, e.g.) can be diagnosed. Therefore organ transplantation becomes a very useful choice for treating these diseases in afflicted children. However, routine regime of immunosuppression in use today suffered from many serious side effects, including stunted growth seen in children using most immunosuppressive drugs<sup>[31-34]</sup>. If we can induce low responsiveness or even irresponsiveness in the recipients to the donors' grafts, immunosuppressive drugs can then be used at much reduced dosage. Until now, low responsiveness or irresponsiveness to the graft has not been achieved in clinical practice. Therefore, induction of immunologic tolerance becomes imperative in clinical transplantation<sup>[35-42]</sup>.

Clonal deletion theory maintains that burst of cell proliferation during embryonic period is very frequent, with resultant formation of multiple specific clones of lymphocytes capable of responding to respective antigens<sup>[43,44]</sup>. During embryonic period, the lymphocyte clones encounter internal antigens or artificially introduced antigens, with consequent damage to, or suppression of these clones, the so-called abstinence clones. In postnatal life, the abstinence clone remains inactive to an internal antigen or an artificially introduced foreign antigen that has been present in utero, a status of immunologic tolerance in the adult to an antigen following prior exposure during the embryonic period. On the contrary, if a lymphocyte clone meets an antigen that has never been introduced during the embryonic period, the specific immunological response would ensue. According to the theory, intrauterine injection is considered a useful tool for the induction of immunologic tolerance, especially for clinical transplantation. Some advantages of intrauterine injection for evoking immunologic tolerance should be noted. Firstly, because the host at fetal stage can't recognize a foreign substance and thus display immunologic tolerance to a xenogen (the earlier the fetal stage of the host, the stronger the tolerance effect to the antigen), no immunologic reaction is seen between the host and ecdemic grafts. Therefore intrauterine injection spares tissue-matching work needed in routine transplantation and makes easier graft transplantation. Meanwhile, immunologic tolerance induced by intrauterine injection makes unnecessary pretreatment with immunosuppressive drugs, thus

avoiding possible side effects of immunosuppressive agents on the body. Secondly, fewer fetal liver cells are needed for transplanting into the recipients during embryonic period because of their small body size and weight. The latter assures little influence and gentle torture for the recipients. Thirdly, in addition to exempt from infection due to microorganism, the maternal body offers adequate nutrition and energy to the fetuses, thus the uterus can be seen as an ideal 'isolation room'<sup>[45-51]</sup>.

We also compared the effect of using rat spleen or bone marrow cells, with that of fetal liver cells, for intraperitoneal injection in utero into fetuses in pregnant rats. It was observed that the survival birth rate using fetal liver cells was much greater than that with spleen or bone marrow cells. Several factors may help to explain the discrepancy. The most important one may be that the response against the host is induced by active lymphocytes located in the spleen or bone marrow cells. In contrast, the main components of fetal liver cells are hematopoietic stem cells possessing two effects, with the first reducing graft versus host reaction, and the other for the maintenance of chimerism because hematopoietic stem cells are characterized by self-renewal and multipotential for differentiation<sup>[52,53]</sup>.

As evidenced by both *in vivo* and *in vitro* data in the present study, the method of fetal hepatocytes in utero injection can prolong the survival period of rat liver transplants. Although complete immune tolerance can not be induced, partial immune tolerance observed in our study is sufficient for liver transplantation. Further work will be needed to reveal if chimerism is induced by transplantation itself, as well as its possible influence on the immune system in the grafted recipients.

## REFERENCES

- 1 **Karim M**, Steger U, Bushell AR, Wood KJ. The role of the graft in establishing tolerance. *Front Biosci* 2002; **7**: 129-154
- 2 **Riordan SM**, Williams R. Transplantation of primary and reversibly immortalized human liver cells and other gene therapies in acute liver failure and decompensated chronic liver disease. *World J Gastroenterol* 2000; **6**: 636-642
- 3 **Tang ZY**. Hepatocellular carcinoma-cause, treatment and metastasis. *World J Gastroenterol* 2001; **7**: 445-454
- 4 **Zhu XF**, Chen GH, He XS, Lu MQ, Wang GD, Cai CJ, Yang Y, Huang JF. Liver transplantation and artificial liver support in fulminant hepatic failure. *World J Gastroenterol* 2001; **7**: 566-568
- 5 **Platell CF**, Coster J, McCauley RD, Hall JC. The management of patients with the short bowel syndrome. *World J Gastroenterol* 2002; **8**: 13-20
- 6 **Ouyang EC**, Wu CH, Walton C, Promrat K, Wu GY. Transplantation of human hepatocytes into tolerized genetically immunocompetent rats. *World J Gastroenterol* 2001; **7**: 324-330
- 7 **Waldmann H**, Cobbold S. Approaching tolerance in transplantation. *Int Arch Allergy Immunol* 2001; **126**: 11-22
- 8 **Yu X**, Carpenter P, Anasetti C. Advances in transplantation tolerance. *Lancet* 2001; **357**: 1959-1963
- 9 **Qian YB**, Cheng GH, Huang JF. Multivariate regression analysis on early mortality after orthotopic liver transplantation. *World J Gastroenterol* 2002; **8**: 128-130
- 10 **Shi LB**, Peng SY, Meng XK, Peng CH, Liu YB, Chen XP, Ji ZL, Yang DT, Chen HR. Diagnosis and treatment of congenital choledochal cyst: 20 years' experience in China. *World J Gastroenterol* 2001; **7**: 732-734
- 11 **Bramhall S**, Minford E, Gunson B, Buckels JA. Liver transplantation in the UK. *World J Gastroenterol* 2001; **7**: 602-611
- 12 **Womer KL**, Lee RS, Madsen JC, Sayegh MH. Tolerance and chronic rejection. *Philos Trans R Soc Lond B Biol Sci* 2001; **356**: 727-738
- 13 **Zavazava N**, Kabelitz D. Alloreactivity and apoptosis in graft rejection and transplantation tolerance. *J Leukoc Biol* 2000; **68**: 167-174
- 14 **Hong JC**, Kahan BD. Immunosuppressive agents in organ transplantation: past, present, and future. *Semin Nephrol* 2000; **20**: 108-125
- 15 **Bartlett A**, McCall J, Munn S. Co-stimulatory blockade and tolerance induction in transplantation. *BioDrugs* 2001; **15**: 491-500



- 16 **Jones DR**. In utero stem cell transplantation: two steps forward but one step back? *Expert Opin Biol Ther* 2001; **1**: 205-212
- 17 **Hayashi S**, Flake AW. In utero hematopoietic stem cell therapy. *Yonsei Med J* 2001; **42**: 615-629
- 18 **Flake AW**. In utero transplantation of haemopoietic stem cells. *Best Pract Res Clin Haematol* 2001; **14**: 671-683
- 19 **Cowan MJ**, Chou SH, Tarantal AF. Tolerance induction post in utero stem cell transplantation. *Ernst Schering Res Found Workshop* 2001; **33**: 145-171
- 20 **Kim HB**, Shaaban AF, Milner R, Fichter C, Flake AW. In utero bone marrow transplantation induces donor-specific tolerance by a combination of clonal deletion and clonal anergy. *J Pediatr Surg* 1999; **34**: 726-729
- 21 **Rubin JP**, Cober SR, Butler PE, Randolph MA, Gazelle GS, Ierino FL, Sachs DH, Lee WP. Injection of allogeneic bone marrow cells into the portal vein of swine in utero. *J Surg Res* 2001; **95**: 188-194
- 22 **Takahashi T**, Kakita A, Sakamoto I, Takahashi Y, Hayashi K, Tadokoro F, Yamashina S. Immunohistochemical and electron microscopic study of extrinsic hepatic reinnervation following orthotopic liver transplantation in rats. *Liver* 2001; **21**: 300-308
- 23 **Boros P**, Tarcsafalvi A, Wang L, Megyesi J, Liu J, Miller CM. Intrahepatic expression and release of vascular endothelial growth factor following orthotopic liver transplantation in the rat. *Transplantation* 2001; **72**: 805-811
- 24 **Okano S**, Eto M, Tomita Y, Yoshizumi T, Yamada H, Minagawa R, Nomoto K, Sugimachi K, Nomoto K. Cyclophosphamide-induced tolerance in rat orthotopic liver transplantation. *Transplantation* 2001; **71**: 447-456
- 25 **He XS**, Huang JF, Chen GH, Zheng KL, Ye XM. A successful case of combined liver and kidney transplantation for autosomal dominant polycystic liver and kidney disease. *World J Gastroenterol* 1999; **5**: 79-80
- 26 **Zhang SG**, Wu MC, Tan JW, Chen H, Yang JM, Qian QJ. Expression of perforin and granzyme B mRNA in judgement of immunosuppressive effect in rat liver transplantation. *World J Gastroenterol* 1999; **5**: 217-220
- 27 **Genden EM**, Mackinnon SE, Yu S, Hunter DA, Flye MW. Pre-treatment with portal venous ultraviolet B-irradiated donor alloantigen promotes donor-specific tolerance to rat nerve allografts. *Laryngoscope* 2001; **111**: 439-447
- 28 **Horimoto H**, Nakai Y, Nakahara K, Nomura Y, Mieno S, Sasaki S. HMG-CoA reductase inhibitor cerivastatin prolonged rat cardiac allograft survival by blocking intercellular signals. *J Heart Lung Transplant* 2002; **21**: 440-445
- 29 **Helmke B**, Schroder D, Kloting I, Kohnert KD. Complement-dependent antibody-mediated cytotoxicity (CAMC) to pancreatic islet cells in the spontaneously diabetic BB/OK rat: interference from cell-bound and soluble inhibitors. *J Clin Lab Immunol* 1991; **35**: 71-81
- 30 **Tange S**, Scherer MN, Graeb C, Weiss T, Justl M, Frank E, Andrassy J, Jauch KW, Geissler EK. The antineoplastic drug Paclitaxel has immunosuppressive properties that can effectively promote allograft survival in a rat heart transplant model. *Transplantation* 2002; **73**: 216-223
- 31 **Reyes J**, Mazariegos GV, Bond GM, Green M, Dvorchik I, Kosmach-Park B, Abu-Elmagd K. Pediatric intestinal transplantation: Historical notes, principles and controversies. *Pediatr Transplant* 2002; **6**: 193-207
- 32 **Bassas AF**, Chehab MS, Al-Shahed MS, Djurberg HG, Al-Shurafa HA, Jawdat MT, Al-Hussaini HF, Zuleika MA, Al-Hebby HA, Wali SH. Pediatric living-related liver transplantation in Saudi Arabia. *Saudi Med J* 2002; **23**: 640-644
- 33 **Robinson LG**, Hilinski J, Graham F, Hymes L, Beck-Sague CM, Hsia J, Nesheim SR. Predictors of cytomegalovirus disease among pediatric transplant recipients within one year of renal transplantation. *Pediatr Transplant* 2002; **6**: 111-118
- 34 **Samsonov D**, Briscoe DM. Long-term care of pediatric renal transplant patients: from bench to bedside. *Curr Opin Pediatr* 2002; **14**: 205-210
- 35 **Rela M**, Dhawan A. Liver transplantation in children. *Indian J Pediatr* 2002; **69**: 175-183
- 36 **Fine RN**. Growth following solid-organ transplantation. *Pediatr Transplant* 2002; **6**: 47-52
- 37 **Bucuvalas JC**, Ryckman FC. Long-term outcome after liver transplantation in children. *Pediatr Transplant* 2002; **6**: 30-36
- 38 **Shneider BL**. Pediatric liver transplantation in metabolic disease: clinical decision making. *Pediatr Transplant* 2002; **6**: 25-29
- 39 **He XS**, Huang JF, Chen GH, Fu Q, Zhu XF, Lu MQ, Wang GD, Guan XD. Orthotopic liver transplantation for fulminant hepatitis B. *World J Gastroenterol* 2000; **6**: 398-399
- 40 **Guan WX**, Li KZ, Dou KF. Hepatocellular carcinoma and liver transplantation. *Shijie Huaren Xiaohua Zazhi* 2001; **9**: 1292-1295
- 41 **Song WL**, Wang WZ, Wu GS, Dong GL, Ling R, Ji G, Zhao JX. Evaluation of perioperative serum cytokine level in acute rejection in human living-related small bowel transplantation. *Shijie Huaren Xiaohua Zazhi* 2001; **9**: 401-404
- 42 **He XS**, Huang JF, Chen GH, Zheng KL, Ye XM. A successful case of combined liver and kidney transplantation for autosomal dominant polycystic liver and kidney disease. *World J Gastroenterol* 1999; **5**: 79-80
- 43 **Prevot A**, Martini S, Guignard JP. Exposure in utero to immunosuppressives. *Rev Med Suisse Romande* 2001; **121**: 283-291
- 44 **Tanaka SA**, Hiramatsu T, Oshitomi T, Imai Y, Koyanagi H. Induction of donor-specific tolerance to cardiac xenografts in utero. *J Heart Lung Transplant* 1998; **17**: 888-891
- 45 **Mackenzie TC**, Shaaban AF, Radu A, Flake AW. Engraftment of bone marrow and fetal liver cells after in utero transplantation in MDX mice. *J Pediatr Surg* 2002; **37**: 1058-1064
- 46 **Taylor PA**, McElmurry RT, Lees CJ, Harrison DE, Blazar BR. Allogenic fetal liver cells have a distinct competitive engraftment advantage over adult bone marrow cells when infused into fetal as compared with adult severe combined immunodeficient recipients. *Blood* 2002; **99**: 1870-1872
- 47 **Barker JE**, Deveau S, Lessard M, Hamblen N, Vogler C, Levy B. In utero fetal liver cell transplantation without toxic irradiation alleviates lysosomal storage in mice with mucopolysaccharidosis type VII. *Blood Cells Mol Dis* 2001; **27**: 861-873
- 48 **Casal ML**, Wolfe JH. In utero transplantation of fetal liver cells in the mucopolysaccharidosis type VII mouse results in low-level chimerism, but overexpression of beta-glucuronidase can delay onset of clinical signs. *Blood* 2001; **97**: 1625-1634
- 49 **Surbek DV**, Holzgreve W, Nicolaides KH. Haematopoietic stem cell transplantation and gene therapy in the fetus: ready for clinical use? *Hum Reprod Update* 2001; **7**: 85-91
- 50 **Surbek DV**, Gratwohl A, Holzgreve W. In utero hematopoietic stem cell transfer: current status and future strategies. *Eur J Obstet Gynecol Reprod Biol* 1999; **85**: 109-115
- 51 **Flake AW**, Zanjani ED. In utero transplantation for thalassemia. *Ann N Y Acad Sci* 1998; **850**: 300-311
- 52 **Pschera H**. Stem cell therapy in utero. *J Perinat Med* 2000; **28**: 346-354
- 53 **Stanworth SJ**, Newland AC. Stem cells: progress in research and edging towards the clinical setting. *Clin Med* 2001; **1**: 378-382

# Functional changes of dendritic cells derived from allogeneic partial liver graft undergoing acute rejection in rats

Ming-Qing Xu, Zhen-Xiang Yao

**Ming-Qing Xu, Zhen-Xiang Yao**, Department of General Surgery, The First affiliated Hospital, Chongqing University of Medical Science, Chongqing 400016, China

**Supported by** the Medical Scientific Foundation of Chongqing City, No. 01-2-029

**Correspondence to:** Dr. Ming-Qing Xu, Liver Transplantation Center, West China Hospital, Sichuan University, Chengdu 610041, Sichuan Province, China. xumingqing@hotmail.com

**Telephone:** +86-28-85400588

**Received:** 2002-07-04 **Accepted:** 2002-09-12

## Abstract

**AIM:** To investigate functional change of dendritic cells (DCs) derived from allogeneic partial liver graft undergoing acute rejection in rats.

**METHODS:** Allogeneic (SD rat to LEW rat) whole and 50 % partial liver transplantation were performed. DCs from liver grafts 0 hr and 4 days after transplantation were isolated and propagated in the presence of GM-CSF *in vitro*. Morphological characteristics of DCs propagated for 4 days and 10 days were observed by electron microscopy. Phenotypical features of DCs propagated for 10 days were analyzed by flow cytometry. Expression of IL-12 protein and IL-12 receptor mRNA in DCs propagated for 10 days was also measured by Western blotting and semiquantitative RT-PCR, respectively. Histological grading of rejection were determined.

**RESULTS:** Allogeneic whole liver grafts showed no features of rejection at day 4 after transplantation. In contrast, allogeneic partial liver grafts demonstrated moderate to severe rejection at day 4 after transplantation. DCs derived from allogeneic partial liver graft 4 days after transplantation exhibited typical morphological characteristics of DC after 4 days' culture in the presence of GM-CSF. DCs from allogeneic whole liver graft 0 hr and 4 days after transplantation did not exhibit typical morphological characteristics of DC until after 10 days' culture in the presence of GM-CSF. After 10 days' propagation *in vitro*, DCs derived from allogeneic whole liver graft exhibited features of immature DC, with absence of CD40, CD80 and CD86 surface expression, and low levels of IL-12 proteins (IL-12 p35 and IL-12 p40) and IL-12 receptor (IL-12R $\beta_1$  and IL-12R $\beta_2$ ) mRNA, whereas DCs from allogeneic partial liver graft 4 days after transplantation displayed features of mature DC, with high levels of CD40, CD80 and CD86 surface expression, and as a consequence, higher expression of IL-12 proteins (IL-12 p35 and IL-12 p40) and IL-12 receptors (IL-12R $\beta_1$  and IL-12R $\beta_2$ ) mRNA than those of DCs both from partial liver graft 0 hr and whole liver graft 4 days after transplantation ( $P < 0.001$ ) was observed.

**CONCLUSION:** DCs derived from allogeneic partial liver graft undergoing acute rejection display features of mature DC.

Xu MQ, Yao ZX. Functional changes of dendritic cells derived from allogeneic partial liver graft undergoing acute rejection in rats. *World J Gastroenterol* 2003; 9(1): 141-147  
<http://www.wjgnet.com/1007-9327/9/141.htm>

## INTRODUCTION

The shortage of donor organs remains a major obstacle to the widespread application of liver transplantation in patients with end-stage liver disease. Although split grafting was used to increase the number of donor livers, the accelerated rejection induced by liver regeneration<sup>[1,2]</sup> can interfere with the outcome of these liver grafts. Therefore, It is important to investigate the mechanism responsible for the accelerated rejection of split liver grafting.

After organ transplantation, interstitial donor dendritic cells (DCs) migrate to recipient lymphoid tissue. In the case of experimental skin, heart, or kidney allografts, these cells have been implicated as the principal instigators of rejection. Despite similar patterns of donor DCs migration, liver grafts are accepted without immunosuppressive therapy between MHC-mismatched mouse, and certain rat strains, and induce donor-specific tolerance. These phenomena and the persistence of donor hematopoietic cells, including DCs, in successful, long-term graft recipients, have raised important questions about the possible role of donor DCs in liver transplant tolerance. The capacity of DCs to initiate immune responses is determined by their surface expression of MHC gene products and costimulatory molecules (CD40, CD80 and CD86), and the secretion of the immune regulator, interleukin (IL)-12<sup>[3-12]</sup>. Immature DCs resident in nonlymphoid tissues such as normal liver are deficient at antigen capture and progressing<sup>[3,13]</sup>, whereas mature DCs, resident in secondary lymphoid tissues, are potent antigen-presenting cells, which can induce naive T-cell activation and proliferation<sup>[3-7]</sup>. Immature DCs that express surface MHC class II, but that are deficient in surface costimulatory molecules, can induce T-cell hyporesponsiveness<sup>[13-15]</sup> and inhibit immune reactivity<sup>[16,17]</sup>. It has been observed that liver-derived<sup>[13,18]</sup> or bone marrow-derived immature DCs<sup>[17]</sup>, propagated *in vitro* and lacking surface costimulatory molecules, can prolong heart or pancreatic islet allograft survival. Whereas, marked augmentation of DCs numbers and maturation of DCs in liver allografts by donor treatment with the hematopoietic growth factor fms-like tyrosine kinase 3 (Flt3) ligand (FL) results in acute liver graft rejection<sup>[19,20]</sup>.

Recent findings have revealed increased immune responses to regenerating allogeneic partial liver graft in rats<sup>[1,2]</sup>, but little is known about the mechanism responsible for the accelerated rejection. The purpose of this study was to investigate the property of DCs isolated from allogeneic partial liver graft in comparison with DCs isolated from allogeneic whole liver graft, in an attempt to elucidate the possible mechanism responsible for the accelerated rejection of allogeneic partial liver graft. Given mature DC can induce naive T-cell activation and proliferation<sup>[3-7]</sup>, and consequently induce acute rejection<sup>[19,20]</sup>, we suspected that maturation of DCs derived from liver graft would be a key inducer of the accelerated rejection of allogeneic partial liver graft. In the present study, we first demonstrated that DCs derived from partial liver graft undergoing acute rejection displayed features of mature DC, including positive expression of costimulatory molecules, higher level expression of IL-12 protein and IL-12 receptor mRNA in these mature DCs.

## MATERIALS AND METHODS

### Animals

One hundred male LEW rats and one hundred male SD rats weighing 220-300 g were used in all the experiments. Allogeneic whole and 50 % partial liver transplantation were performed using a combination of SD rats to LEW rats. The animals were purchased from Chinese Academy of Science and Sichuan University. They were maintained with a 12-hr light/dark cycle in a conventional animal facility with water and commercial chow provided ad libitum, with no fasting before the transplantation.

### Liver transplantation

All operation were performed under ether anesthesia in clean but not sterile conditions. All surgical procedures were performed from 8 a.m. to 5 p.m. Donors and recipients of similar weight ( $\pm 10$  g) were chosen. Liver reduction was achieved by removing the left lateral lobe and the two caudate lobes, which resulted in a 50 % reduction of the liver mass. Whole liver transplantation (WLT) and partial liver transplantation (PLT) were performed with the two-cuff method described by Kammada and Calne<sup>[21]</sup>, Knoop *et al*<sup>[22]</sup> and Uchiyama *et al*<sup>[23]</sup>. Briefly, the whole and partial liver were perfused with 20 ml of chilled lactated Ringer's solution containing 200 U of heparin through the aorta. The liver was removed and immersed in chilled University of Wisconsin solution. Immediately after cuffs were placed on the portal vein and the infrahepatic vena cava, the liver graft was perfused with 8 ml of chilled University of Wisconsin solution through the portal vein and 2 ml of the same solution through the hepatic artery, and then the hepatic artery was ligated. Cold preservation time was approximately 1 hr in all experiments. After a total hepatectomy was performed in the recipient, the suprahepatic vena cava was anastomosed in a continuous fashion with 8-0 sutures. The portal vein and infrahepatic vena cava were then connected by a 6-FG and 8-FG polyethylene tube cuff, respectively. The bile duct was internally stented with a 22-gauge i.v. catheter. The portal vein was clamped for <18 min in all animals. In each group, the survival rate after grafting was >89 % at 24 hr after surgery. Deaths that occurred within this period were defined as resulting from technical failure. Penicillin was given perioperatively.

### Histology

Part of liver graft tissues 4 days after transplantation were sectioned and preserved in 10 % Formalin, embedded in paraffin, cut with microtome, and stained with hematoxylin and eosin.

### Propagation and purification of liver graft-derived DC populations

DCs from liver graft 0 hr and 4 days after transplantation were propagated in GM-CSF from nonparenchymal cells (NPC) isolated from collagenase-digested liver graft tissue, as described by Lu<sup>[18]</sup>. Nonadherent cells, released spontaneously from proliferating cell clusters, were collected after 4 days' and 10 days' culture, and purified by centrifugation 500 $\times$ g, 10 min at room temperature on a 16 % w/v metrizamide gradient (DC purity 80-85 %).

### Morphological and Phenotypical features of DCs

Morphological characteristics of DCs derived from liver graft were observed by electron microscopy. Expression of cell surface molecules was quantitated by flow cytometry as described by Mehling *et al*<sup>[4]</sup>. Aliquots of  $2 \times 10^5$  DCs propagated for 10 days *in vitro* were incubated with the following primary mouse anti-rat mAbs against OX62, CD40, CD80, CD86

(Serotec, USA), or rat IgG as an isotype control for 60 min on ice (1  $\mu$ g/ml diluted in PBS/1.0 % FCS). The cells were washed with PBS/1.0 % FCS and labeled with FITC-conjugated goat anti-mouse IgG, diluted 1/50 in PBS/1.0 % FCS for 30 min on ice. At the end of this incubation cells were washed, PBS were added, and the cells were subsequently analyzed in an FACS-4200 flow cytometer (Becton-Dickinson, USA).

### Semiquantitative RT-PCR for expression of IL-12R mRNA in DCs

Analysis of expression of IL-12R $\beta_1$  and IL-12R $\beta_2$  mRNA was determined by reverse transcription-PCR (RT-PCR) amplification in contrast with house-keeping gene GAPDH. Total RNA from  $1 \times 10^7$  DCs propagated for 10 days *in vitro* was isolated using Tripure<sup>TM</sup> reagent (Promega, USA). First-strand cDNA was transcribed from 1  $\mu$ g RNA using AMV and an Oligo (dT)<sub>15</sub> primer. PCR was performed in a 25  $\mu$ l reaction system containing 10  $\mu$ l cDNA, 2  $\mu$ l 10 mM dNTP, 2.5  $\mu$ l 10 $\times$  buffer, 2.5  $\mu$ l 25 mmol $\cdot$ L<sup>-1</sup> MgCl<sub>2</sub>, 2  $\mu$ l specific primer, 5  $\mu$ l water and 1  $\mu$ l Taq. IL-12R $\beta_1$  and IL-12R $\beta_2$  were amplified using specific primer for IL-12R $\beta_1$ <sup>[24]</sup> and IL-12R $\beta_2$ <sup>[25]</sup>. Specific primers for GAPDH<sup>[26]</sup> were also used for control. Thermal cycling of IL-12R $\beta_1$  and IL-12R $\beta_2$  and GAPDH primers were performed as follows<sup>[25]</sup>: denaturation at 94  $^{\circ}$ C for 1 min, annealing at 55  $^{\circ}$ C for 1 min, and extension at 72  $^{\circ}$ C for 1 min, all cycling were performed for 35 cycles. The predicted PCR product size were 331 bp for IL-12R $\beta_1$ , 1 200 bp for IL-12R $\beta_2$  and 576 bp for GAPDH. PCR products of each sample were subjected to electrophoresis in a 15g $\cdot$ L<sup>-1</sup> agarose gel containing 0.5 mg $\cdot$ L<sup>-1</sup> ethidium bromide. Densitometrical analysis using NIH image software was performed for semiquantification of PCR products, and the expression level of each sample were expressed by IL-12R mRNA/GAPDH mRNA (%).

### Western blotting for IL-12 protein expression in DCs

DCs cultured for 10 days *in vitro* were starved in serum-free medium for 4hr at 37  $^{\circ}$ C. These cells were washed twice in cold PBS, resuspended in 100  $\mu$ l lysis buffer (1 % Nonidet P-40, 20mM Tris-HCl, pH8.0, 137mM NaCl, 10 % glycerol, 2mM EDTA, 10  $\mu$ g/ml leupeptin, 10  $\mu$ g/ml aprotinin, 1mM PMSF, and 1 mM sodium orthovanadate), and total cell lysates were obtained. The homogenates were centrifuged at 10 000 $\times$ g for 10 min at 4  $^{\circ}$ C. Cell lysates (20  $\mu$ g) were electrophoresed on SDS-PAGE gels, and transferred to PVDC membranes for Western blot analysis. Briefly, PVDC membranes were incubated in a blocking buffer for 1 hr at room temperature, then incubated for 2 hr with Abs raised against IL-12 p35 (M-19, goat anti-rat, Santa Cruz, CA), IL-12p40 (H-306, rabbit anti-rat, Santa Cruz, CA). The membranes were washed and incubated for 1 hr with HRP-labeled horse anti-goat or HRP-labeled goat anti-rabbit IgG. Immunoreactive bands were visualized by ECL detection reagent.

### Statistics

Statistic analysis of data was performed using the Student's *t*-test; *P*<0.05 was considered statistically significant.

## RESULTS

### Histological rejection

Histology features of allografted livers were compared between the whole and partial groups on Day 4 after transplantation, allogeneic whole liver grafts demonstrated no rejection. In contrast, partial liver grafts demonstrated moderate to severe rejection, including inflammatory cellular infiltration in the portal tract, and endothelialitis and bile duct damage.

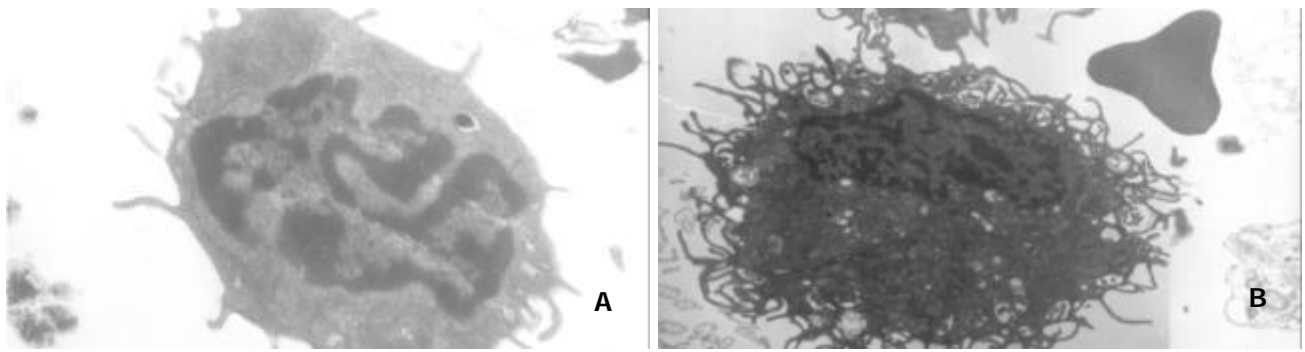


**Figure 1** Morphological characteristics of liver graft-derived DCs propagated for 4 days in the presence of GM-CSF. **A:** DC from whole liver graft 4 days after transplantation ( $\times 200$  b). **B:** DC from partial liver graft 4 days after transplantation ( $\times 600$ b).

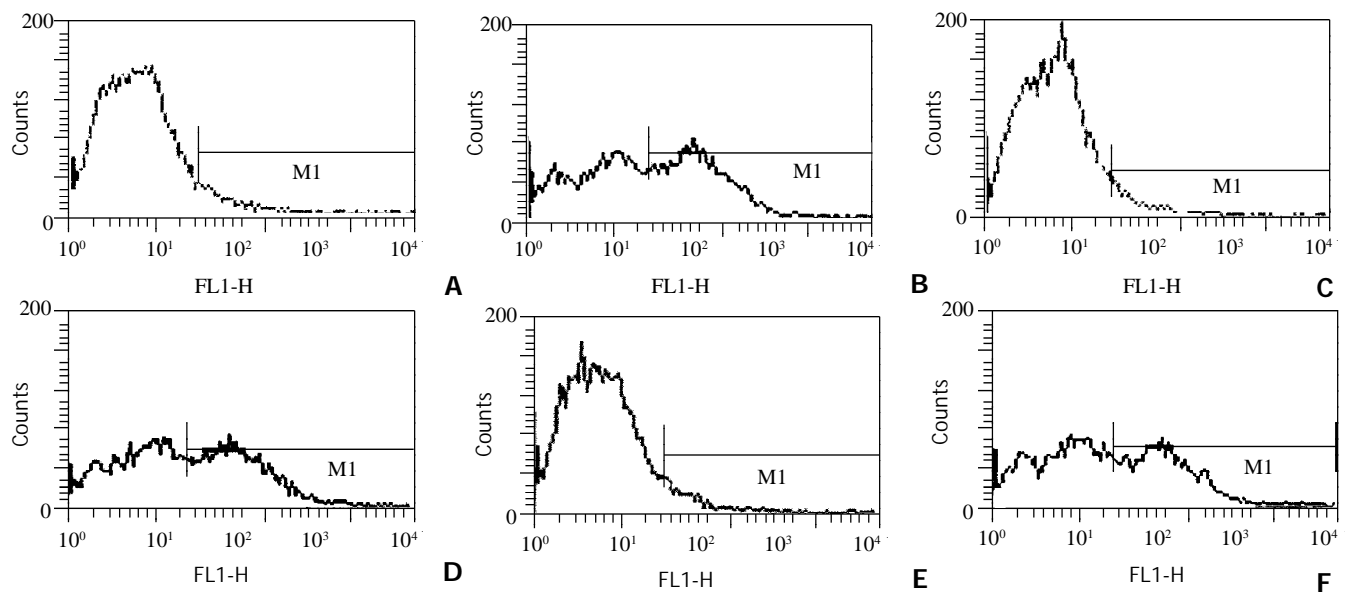


**Figure 2** Expression of costimulatory molecules in DCs from liver grafts 4 days after transplantation by FCM. **A:** Expression of CD40 in whole liver graft-derived DCs; **B:** Expression of CD40 in partial liver graft-derived DCs; **C:** Expression of CD80 in whole liver graft-derived DCs; **D:** Expression of CD80 in partial liver graft-derived DCs; **E:** Expression of CD86 in whole liver graft-derived DCs; **F:** Expression of CD86 in partial liver graft-derived DCs.

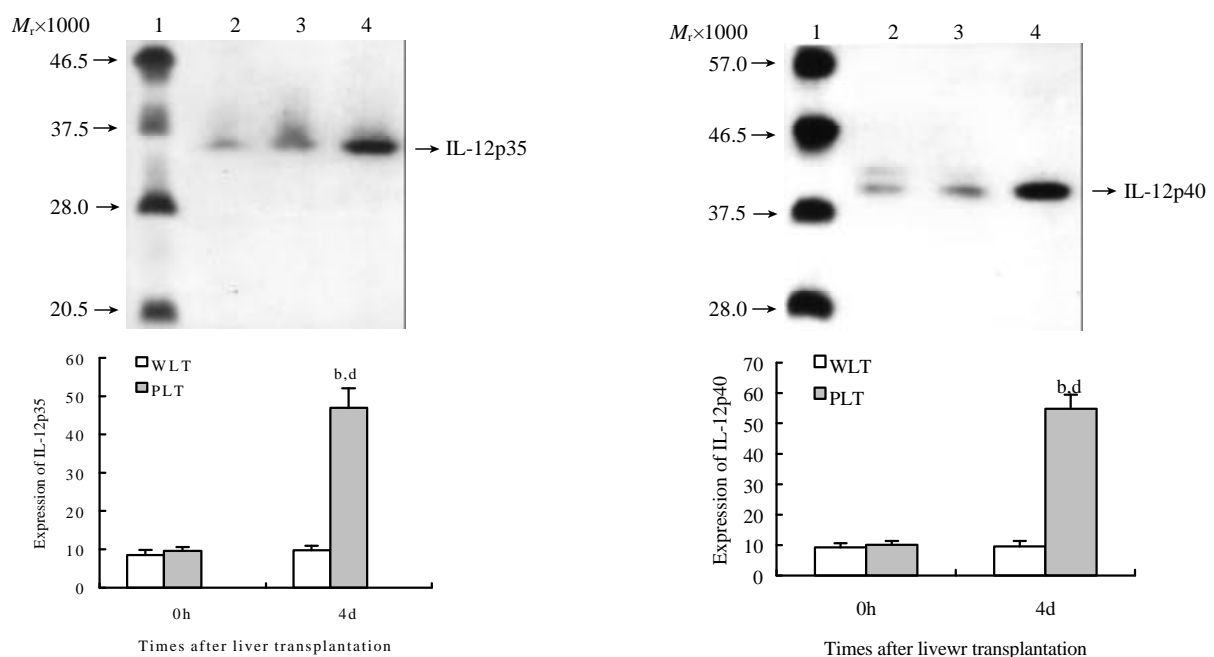


**Figure 3** Detection of IL-12 proteins in liver graft-derived DCs by Western blotting. Lanes 1: protein marker. Lanes 2-4: extracts derived from DCs from liver graft 0 h after transplantation, whole liver graft (WLT) and partial liver graft (PLT) 4 days after transplantation, respectively. Compared with 4 d WLT group,  $^bP < 0.001$ ; Compared with 0 h PLT group,  $^dP < 0.001$ .

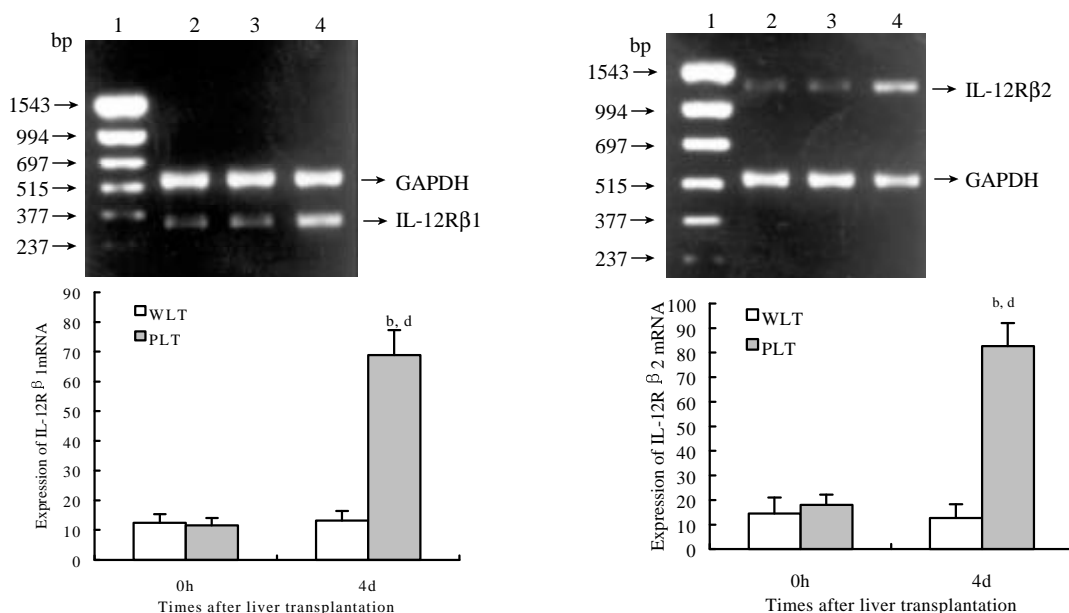


**Figure 4** Detection of IL-12 R mRNA in liver graft-derived DCs by RT-PCR. Lanes 1: marker; Lanes 2- 4: extracts derived from DCs from liver graft 0 h after transplantation, whole liver graft (WLT) and partial liver graft (PLT) 4 days after transplantation, respectively. Compared with 4 d WLT group, <sup>b</sup> $P < 0.001$ ; Compared with 0 h PLT group, <sup>d</sup> $P < 0.001$ .

### Phenotypic characteristics of liver graft-derived DCs propagated in vitro

After 4 days' culture in the presence of GM-CSF, liver graft-derived DCs were observed with electron microscopy, DCs from whole liver grafts 0 hr and 4 days after transplantation exhibited round shape, smaller body, bigger nucleus, and a few shorter dendrites, whereas DCs derived from partial liver graft 4 days after transplantation displayed typical morphological features of DC including anomalous shape, bigger body, and numerous longer dendrites (as shown in Figure 1). Flow cytometry showed 80-85 % of DCs both from whole and partial liver grafts strongly expressed rat DC-specific OX62 antigen molecule (as shown in Table 1), which was suggested high purity DCs were obtained. After 10 day' culture in the presence of GM-CSF, although DCs both from whole and partial liver grafts exhibited typical morphological features of DC by electron microscopy, flow cytometric analysis showed (as shown in Figure 2 and Table 1) whole liver graft-derived DCs displayed low amounts of costimulatory molecules (CD40, CD80 and CD86), whereas DCs from partial liver graft 4 days after transplantation expressed moderate to high levels of these markers. These results suggested allogeneic partial liver transplant could promote maturation of DCs derived from partial liver graft.

**Table 1** Comparison of expression of DC surface markers from whole liver graft and partial liver graft ( $\bar{x} \pm s$ ,  $n=13$ )

Groups	OX62	CD40	CD80	CD86
Whole liver graft-DC	85.63±3.81	7.24±1.87	6.58±2.39	7.01±2.54
Partial liver graft-DC	88.42±5.75	50.18±3.26 <sup>b</sup>	45.31±3.67 <sup>b</sup>	43.29±2.03 <sup>b</sup>

<sup>b</sup> $P < 0.001$  vs whole liver graft-DC

### IL-12 protein expression in liver graft-derived DCs

To investigate the functional change of DCs derived from liver grafts, we evaluated IL-12 protein expression in these DCs. As shown in Figure 3, DCs derived from both whole and liver grafts 0 hr after transplantation expressed detectable but low levels of IL-12 p35 and IL-12 p40, and expression levels of

IL-12 p35 and IL-12 p40 in DCs from whole liver graft 4 days after transplantation were similar to those of DCs from whole liver graft 0 hr after transplantation ( $P > 0.05$ ). However, expression of IL-12 p35 and IL-12 p40 in DCs from partial liver graft 4 days after transplantation was markedly increased, and their expression levels were significantly higher than those of DCs both from partial liver graft 0 hr and whole liver graft 4 days after transplantation ( $P < 0.001$ ).

### IL-12R mRNA expression in liver graft-derived DCs

As shown in Figure 4, semiquantitative RT-PCR analysis revealed detectable but low levels of IL-12R $\beta_1$  and IL-12R $\beta_2$  mRNA expression in DCs both from whole and partial liver grafts 0 hr after transplantation, expression levels of IL-12R $\beta_1$  and IL-12R $\beta_2$  mRNA in DCs from whole liver graft 4 days after transplantation were not markedly changed compared with those of DCs from whole liver graft 0 hr after transplantation ( $P > 0.05$ ). Whereas DCs from partial liver graft 4 days after transplantation expressed higher levels of IL-12R $\beta_1$  mRNA and IL-12R $\beta_2$  mRNA, and their expression levels were markedly higher than those of DCs both derived from partial liver graft 0 hr and whole liver graft 4 days after transplantation ( $P < 0.001$ ).

### DISCUSSION

DCs play critical roles in the initiation and modulation of immune responses<sup>[27-34]</sup>. After vascularized organ transplantation, donor passenger leukocytes (mainly interstitial DCs) are mobilized out of the graft via peripheral blood to the recipient lymphoid and nonlymphoid tissues<sup>[35-39]</sup>. Maturation of donor DC from thyroid, pancreatic islet, skin, or kidney allografts in recipient lymphoid organs lead to the activation of naive, alloreactive Th0 lymphocytes, and thus provides the primary stimulus for acute allograft rejection. However, in mouse and certain rat strain combinations, fully MHC-mismatched liver allografts accepted without any of immune suppression, and fail to elicit an effective rejection response<sup>[38,39]</sup>. Moreover, in humans, the liver is considered the least immunogenic of transplanted whole organs. In a tolerant rat strain combination, depletion of interstitial leukocytes from liver by pretransplant donor radiation prevents the tolerogenic effect, and results in acute rejection<sup>[40]</sup>. On the other hand, it has been reported that

immature, costimulatory molecule-deficient DCs (such as normal liver or bone marrow-derived DCs) propagated *in vitro* can promote graft survival in allogeneic recipients<sup>[14,41,42]</sup>, and posttransplant administration of donor leukocytes induces long-term acceptance of liver transplants<sup>[43]</sup>.

Therefore, passenger leukocytes (most likely DCs) may have a dualistic role with potential to elicit T cell activation and graft rejection, or induce T cell tolerance and graft acceptance. The sustained release from the transplanted liver of immature DCs, may contribute to allogeneic liver graft tolerance induction. These liver-derived DCs migrate *in vivo* to T cells areas of secondary lymphoid tissue, where they persisted for weeks in allogeneic recipients<sup>[18, 44]</sup>. It is accepted that alloantigen-specific Th1 cells initiate allograft rejection, and that Th2 cells exert an inhibitory influence on the development of Th1 clones. It has been proposed that preferential induction of alloantigen-specific Th2 lymphocytes could suppress the development of Ag-specific Th1 cells, and as a consequence, inhibit allograft rejection. Liver-derived DCs might induce the proliferation of Th2 clones with capacity to inhibit Th1 responses<sup>[18]</sup>. Liver-derived DCs display an immature phenotype with absence of costimulatory molecules (CD40, CD80 and CD86) surface expression, low levels of MHC class I and II, and as a consequence, low stimulatory capacity for naive allogeneic T cells. Unlike mature DC, these liver-derived DCs do not induce detectable levels of intracytoplasmic IFN- $\gamma$  in allogeneic CD4<sup>+</sup> cells in 72-h MLR, and elicited very low levels of CTLs *in vitro*<sup>[3,13,18]</sup>. In contrast, acute liver graft rejection would be induced by maturation of liver grafts derived-DCs<sup>[20]</sup>. These findings point to a pivotal role for donor immature or mature DCs in determining the outcome of liver transplantation. Mature DCs express high levels of costimulatory molecules such as CD40, CD80 and CD86. Activation of T cells by mature DCs has been shown to require direct contact between T cells and DCs through CD40-CD40L interaction<sup>[45]</sup>, upon ligation of CD40L on T cells with CD40 on DCs, DCs are triggered to produce even high quantities of IL-12, thus consigning T cells to Th1 responses<sup>[46]</sup>.

IL-12 is an important immune regulator produced primarily by DCs and macrophages that drives the preferential induction of Th1 immune responses. IL-12 appears to be a central mediator of acute graft-vs-host disease in mice<sup>[47]</sup>, whereas neutralization of bioactive IL-12 enhances allogeneic myoblast survival<sup>[48]</sup>. Moreover, exogenous IL-12 mediates liver allograft rejection<sup>[49]</sup>, and IL-12 antagonism could promote liver graft tolerance<sup>[19]</sup>. IL-12 binds to a unique, high affinity receptor on activated Th cells and NK cells, enhances the expression of antiapoptotic factors (bcl<sub>2</sub> and bcl<sub>xl</sub>), and facilitates activated T cell and NK-lymphokine activated killer cell expansion. IL-12 indirectly promotes Th1 and inhibits Th2 development by inducing the secretion of IFN- $\gamma$  by Th1 and NK cells<sup>[19, 50-54]</sup>. Recent investigation showed IL-12 also induce autologous IL-12 production of DC by interaction with IL-12 receptor<sup>[25]</sup>. Previous studies have shown that IL-12R is detected in T cells and NK cells, and IL-12R plays a crucial role for IL-12 mediated activation of these cell types<sup>[25, 55-60]</sup>. IL-12R $\beta_1$  is the subunit primarily responsible for binding IL-12, and IL-12R $\beta_2$  plays an essential role in mediating the biological functions of IL-12. IL-12-induced phosphorylation of STAT4 and IFN- $\gamma$  production are absent in Con A and anti-CD3-activated splenocytes from IL-12R $\beta_2$ <sup>-/-</sup> mice<sup>[56]</sup>. Recent investigations suggested that DCs exhibited expression of IL-12R $\beta_1$  and IL-12R $\beta_2$ <sup>[25,61-66]</sup>, and mature DCs express high level of IL-12R $\beta_1$  and IL-12R $\beta_2$ <sup>[25, 64]</sup>.

Although Omura T *et al*<sup>[1]</sup> and Shiraishi M *et al*<sup>[2]</sup> reported that allogeneic partial liver grafts exhibited increased immune response compared with allogeneic whole liver grafts as early as 3 days after transplantation, little is known about the exact

mechanism responsible for the accelerated rejection. In the present study, accelerated rejection was demonstrated in allogeneic partial liver graft 4 days after transplantation. Our results first demonstrated that DCs derived from allogeneic whole liver graft without acute rejection 4 days after transplantation exhibited an immature phenotype with absence of CD40, CD80 and CD86 surface expression, and low expression of IL-12 proteins (IL-12 p35 and IL-12 p40) and IL-12 receptor (IL-12R $\beta_1$  and IL-12R $\beta_2$ ) mRNA. In contrast with immature DCs derived from whole liver graft, DCs derived from partial liver graft undergoing acute rejection 4 days after transplantation displayed a mature phenotype with high level of CD40, CD80 and CD86 surface expression, and as a consequence, high level expression of IL-12 proteins (IL-12 p35 and IL-12 p40) and IL-12 receptors (IL-12R $\beta_1$  and IL-12R $\beta_2$ ) mRNA. Given immature DCs can induce T-cell hyporesponsiveness<sup>[13-15]</sup> and immune reactivity inhibition<sup>[16,17]</sup>, whereas mature DCs can stimulate Th1 response and the development of alloantigen-specific CTLs<sup>[3-7, 27-34]</sup>, together with IL-12 is an important inducer of liver graft rejection, we suggest that maturation of liver graft-derived DCs may be an important mechanism of the accelerated rejection of allogeneic partial liver graft, and inhibition of maturation of liver graft-derived DCs may suppress rejection of allogeneic partial liver graft.

## REFERENCES

- 1 **Omura T**, Nakagawa T, Randall HB, Lin Z, Huey M, Ascher NL, Emond JC. Increased immune responses to regenerating partial liver grafts in the rat. *J Surg Res* 1997; **70**: 34-40
- 2 **Shiraishi M**, Csete ME, Yasunaga C, Drazen KE, Jurim O, Cramer DV, Busuttill RW, Shaked A. Regeneration-induced accelerated rejection in reduced-size liver grafts. *Transplantation* 1994; **57**: 336-340
- 3 **Morelli AE**, O'Connell PJ, Khanna A, Logar AJ, Lu LN, Thomson AW. Preferential induction of Th1 responses by functionally mature hepatic (CD8 $\alpha$  and CD8 $\alpha$ <sup>+</sup>) dendritic cells. *Transplantation* 2000; **69**: 2647-2657
- 4 **Mehling A**, Grabbe S, Voskort M, Schwarz T, Luger TA, Beissert S. Mycophenolate mofetil impairs the maturation and function of murine dendritic cells. *J Immunol* 2000; **165**: 2374-2381
- 5 **Stuart LM**, Lucas M, Simpson C, Lamb J, Savill J, Lacy HA. Inhibitory effects of apoptotic cell ingestion upon endotoxin-driven myeloid dendritic cell maturation. *J Immunol* 2002; **168**: 1627-1635
- 6 **Ismaili J**, Rennesson J, Aksoy E, Vekemans J, Vincart B, Amraoui Z, Van Laethem F, Goldman M, Dubois PM. Monophosphoryl lipid A activates both human dendritic cells and T cells. *J Immunol* 2002; **168**: 926-932
- 7 **Sato K**, Nagayama H, Enomoto M, Tadokoro K, Juji T, Takahashi TA. Autocrine activation-induced cell death of T cells by human peripheral blood monocyte-derived CD4<sup>+</sup> dendritic cells. *Cellular Immunology* 2000; **199**: 115-125
- 8 **Zheng H**, Dai J, Stoilova D, Li Z. Cell surface targeting of heat shock protein gp96 induces dendritic cell maturation and antitumor immunity. *J Immunol* 2001; **167**: 6731-6735
- 9 **Morel Y**, Truneh A, Sweet RW, Olive D, Costello RT. The TNF superfamily members LIGHT and CD154 (CD40 ligand) costimulate induction of dendritic cell maturation and elicit specific CTL activity. *J Immunol* 2001; **167**: 2479-2486
- 10 **Kobayashi M**, Azuma E, Ido M, Hirayama M, Jiang Q, Iwamoto S, Kumamoto T, Yamamoto H, Sakurai M, Komada Y. A pivotal role of Rho GTPase in the regulation of morphology and function of dendritic cells. *J Immunol* 2001; **167**: 3585-3591
- 11 **Hertz CJ**, Kiertscher SM, Godowski PJ, Bouis DA, Norgard MV, Roth MD, Modlin RL. Microbial lipopeptides stimulate dendritic cell maturation via Toll-like receptor 2. *J Immunol* 2001; **166**: 2444-2450
- 12 **Thoma-Uszynski S**, Kiertscher SM, Ochoa MT, Bouis DA, Norgard MV, Miyake K, Godowski PJ, Roth MD, Modlin RL. Activation of toll-like receptor 2 on human dendritic cells triggers induction of IL-12, but not IL-10. *J Immunol* 2000; **165**: 3804-3810

- 13 **Khanna A**, Morelli AE, Zhong CP, Takayama T, Lu LN, Thomson AW. Effects of liver-derived dendritic cell progenitors on Th1- and Th2-like cytokine responses *in vitro* and *in vivo*. *J Immunol* 2000; **164**: 1346-1354
- 14 **Hirano A**, Luke PP, Specht SM, Fraser MO, Takayama T, Lu L, Hoffman R, Thomson AW, Jordan ML. Graft hyporeactivity induced by immature donor-derived dendritic cells. *Transpl Immunol* 2000; **8**: 161-168
- 15 **Lee WC**, Zhong C, Qian S, Wan Y, Gaudie J, Mi Z, Robbins PD, Thomson AW, Lu L. Phenotype, function, and *in vivo* migration and survival of allogeneic dendritic cell progenitors genetically engineered to express TGF-beta. *Transplantation* 1998; **66**: 1810-1817
- 16 **Hayamizu K**, Huie P, Sibley RK, Strober S. Monocyte-derived dendritic cell precursors facilitate tolerance to heart allografts after total lymphoid irradiation. *Transplantation* 1998; **66**: 1285-1291
- 17 **Khanna A**, Steptoe RJ, Antonyamy MA, Li W, Thomson AW. Donor bone marrow potentiates the effect of tacrolimus on nonvascularized heart allograft survival: association with microchimerism and growth of donor dendritic cell progenitors from recipient bone marrow. *Transplantation* 1998; **65**: 479-485
- 18 **Lu L**, Woo J, Rao AS, Li Y, Watkins SC, Qian S, Starzl TE, Demetris AJ, Thomson AW. Propagation of dendritic cell progenitors from normal mouse liver using granulocyte/macrophage colony-stimulating factor and their maturational development in the presence of type-1 collagen. *J Exp Med* 1994; **179**: 1823-1834
- 19 **Li W**, Lu L, Wang Z, Wang L, Fung JJ, Thomson AW, Qian S. IL-12 antagonism enhances apoptotic death of T cells within hepatic allografts from Flt3 ligand-treated donors and promotes graft acceptance. *J Immunol* 2001; **166**: 5619-5628
- 20 **Steptoe RJ**, Fu F, Li W, Drakes ML, Lu L, Demetris AJ, Qian S, McKenna HJ, Thomson AW. Augmentation of dendritic cells in murine organ donors by Flt3 ligand alters the balance between transplant tolerance and immunity. *J Immunol* 1997; **159**: 5483-5491
- 21 **Kamada N**, Calne RY. A surgical experience with five hundred thirty liver transplantation in the rat. *Surgery* 1983; **93**: 64-69
- 22 **Knoop M**, Bachmann S, Keck H, Steffen R, Neuhaus P. Experience with cuff rearterialization in 600 orthotopic liver grafts in the rat. *Am J Surg* 1994; **167**: 360-363
- 23 **Uchiyama H**, Yanaga K, Nishizaki T, Soejima Y, Yoshizumi T, Sugimachi K. Effects of deletion variant of hepatocyte growth factor on reduced-size liver transplantation in rats. *Transplantation* 1999; **68**: 39-44
- 24 **Collison K**, Saleh S, Parhar R, Meyer B, Kwaasi A, Al-Hussein K, Al-Sedairy S, Al-Mohanna F. Evidence for IL-12-activated Ca<sup>2+</sup> and tyrosine signaling pathways in human neutrophils. *J Immunol* 1998; **161**: 3737-3745
- 25 **Nagayama H**, Sato K, Kawasaki H, Enomoto M, Morimoto C, Tadokoro K, Juji T, Asano S, Takahashi TA. IL-12 responsiveness and expression of IL-12 receptor in human peripheral blood monocyte-derived dendritic cells. *J Immunol* 2000; **165**: 59-66
- 26 **Vos TA**, Hooiveld GJ, Koning H, Childs S, Meijer DK, Moshage H, Jansen PL, Muller M. Up-regulation of the multidrug resistance genes, Mrp1 and Mdr1b, and down-regulation of the organic anion transporter, Mrp2, and the bile salt transporter, Spgp, in endotoxemic rat liver. *Hepatology* 1998; **28**: 1637-1644
- 27 **Zhang JK**, Chen HB, Sun JL, Zhou YQ. Effect of dendritic cells on LPAK cells induced at different times in killing hepatoma cells. *Shijie Huaren Xiaohua Zazhi* 1999; **7**: 673-675
- 28 **Li MS**, Yuan AL, Zhang WD, Chen XQ, Tian XH, Piao YJ. Immune response induced by dendritic cells induce apoptosis and inhibit proliferation of tumor cells. *Shijie Huaren Xiaohua Zazhi* 2000; **8**: 56-58
- 29 **Luo ZB**, Luo YH, Lu R, Jin HY, Zhang PB, Xu CP. Immunohistochemical study on dendritic cells in gastric mucosa of patients with gastric cancer and precancerous lesions. *Shijie Huaren Xiaohua Zazhi* 2000; **8**: 400-402
- 30 **Li MS**, Yuan AL, Zhang WD, Liu SD, Lu AM, Zhou DY. Dendritic cells *in vitro* induce efficient and special anti-tumor immune response. *Shijie Huaren Xiaohua Zazhi* 1999; **7**: 161-163
- 31 **Wang FS**, Xing LH, Liu MX, Zhu CL, Liu HG, Wang HF, Lei ZY. Dysfunction of peripheral blood dendritic cells from patients with chronic hepatitis B virus infection. *World J Gastroenterol* 2001; **7**: 537-541
- 32 **Zhang JK**, Li J, Chen HB, Sun JL, Qu YJ, Lu JJ. Antitumor activities of human dendritic cells derived from peripheral and cord blood. *World J Gastroenterol* 2002; **8**: 87-90
- 33 **Tang ZH**, Qiu WH, Wu GS, Yang XP, Zou SQ, Qiu FZ. The immunotherapeutic effect of dendritic cells vaccine modified with interleukin-18 gene and tumor cell lysate on mice with pancreatic carcinoma. *World J Gastroenterol* 2002; **8**: 908-912
- 34 **Zhang J**, Zhang JK, Zhuo SH, Chen HB. Effect of a cancer vaccine prepared by fusions of hepatocarcinoma cells with dendritic cells. *World J Gastroenterol* 2001; **7**: 690-694
- 35 **Maestroni GJ**. Dendritic cell migration controlled by alpha 1b-adrenergic receptors. *J Immunol* 2000; **165**: 6743-6747
- 36 **Qian S**, Demetris AJ, Murase N, Rao AS, Fung JJ, Starzl TE. Murine liver allograft transplantation: tolerance and donor cell chimerism. *Hepatology* 1994; **19**: 916-924
- 37 **Thomson AW**, Lu L, Murase N, Demetris AJ, Rao AS, Starzl TE. Microchimerism, dendritic cell progenitors and transplantation tolerance. *Stem Cells* 1995; **13**: 622-639
- 38 **Jonsson JR**, Hogan PG, Thomas R, Steadman C, Clouston AD, Balderson GA, Lynch SV, Strong RW, Powell EE. Peripheral blood chimerism following human liver transplantation. *Hepatology* 1997; **25**: 1233-1236
- 39 **Spriewald BM**, Wassmuth R, Carl HD, Kockerling F, Reichstetter S, Kleeberger A, Klein M, Hohenberger MW, Kalden JR. Microchimerism after liver transplantation: prevalence and methodological aspects of detection. *Transplantation* 1998; **66**: 77-83
- 40 **Sun J**, McCaughan GW, Gallagher ND, Sheil AG, Bishop GA. Deletion of spontaneous rat liver allograft acceptance by donor irradiation. *Transplantation* 1995; **60**: 233-236
- 41 **Rastellini C**, Lu L, Ricordi C, Starzl TE, Rao AS, Thomson AW. Granulocyte/macrophage colony-stimulating factor-stimulated hepatic dendritic cell progenitors prolong pancreatic islet allograft survival. *Transplantation* 1995; **60**: 1366-1370
- 42 **Gao JX**, Madrenas J, Zeng W, Cameron MJ, Zhang Z, Wang JJ, Zhong R, Grant D. CD40-deficient dendritic cells producing interleukin-10, but not interleukin-12, induce T-cell hyporesponsiveness *in vitro* and prevent acute allograft rejection. *Immunology* 1999; **98**: 159-170
- 43 **Yan Y**, Shastri S, Richards C, Wang C, Bowen DG, Sharland AF, Painter DM, McCaughan GW, Bishop GA. Posttransplant administration of donor leukocytes induces long-term acceptance of kidney or liver transplants by an activation-associated immune mechanism. *J Immunol* 2001; **166**: 5258-5264
- 44 **Thomson AW**, Lu L, Subbotin VM, Li Y, Qian S, Rao AS, Fung JJ, Starzl TE. In vitro propagation and homing of liver-derived dendritic cell progenitors to lymphoid tissues of allogeneic recipients. Implications for the establishment and maintenance of donor cell chimerism following liver transplantation. *Transplantation* 1995; **59**: 544-551
- 45 **Kitamura H**, Iwakabe K, Yahata T, Nishimura SI, Ohta A, Ohmi Y, Sato M, Takeda K, Okumura K, Van Kaer L, Kawano T, Taniguchi M, Nishimura T. The natural killer T (NKT) cell ligand  $\alpha$ -galactosylceramide demonstrates its immunopotentiating effect by inducing interleukin (IL)-12 production by dendritic cells and IL-12 receptor expression on NKT cells. *J Exp Med* 1999; **189**: 1121-1127
- 46 **Cella M**, Scheidegger D, Palmer-Lehmann K, Lane P, Lanzavecchia A, Alber G. Ligation of CD40 on dendritic cells triggers production of high levels of interleukin-12 and enhances T cell stimulatory capacity: T-T help via APC activation. *J Exp Med* 1996; **184**: 747-752
- 47 **Williamson E**, Garside P, Bradley JA, Mowat AM. IL-12 is a central mediator of acute graft-versus-host disease in mice. *J Immunol* 1996; **157**: 689-699
- 48 **Kato K**, Shimozato O, Hoshi K, Wakimoto H, Hamada H, Yagita H, Okumura K. Local production of the p40 subunit of interleukin 12 suppresses T-helper 1-mediated immune responses and prevents allogeneic myoblast rejection. *Proc Natl Acad Sci USA* 1996; **93**: 9085-9089
- 49 **Thai NL**, Li Y, Fu F, Qian S, Demetris AJ, Duquesnoy RJ, Fung JJ. Interleukin-2 and interleukin-12 mediate distinct effector mechanisms of liver allograft rejection. *Liver Transpl Surg* 1997; **3**: 118-129
- 50 **Heuffer C**, Koch F, Stanzl U, Topar G, Wysocka M, Trinchieri G, Enk A, Steinman RM, Romani N, Schuler G. Interleukin-12 is



- produced by dendritic cells and mediates T helper 1 development as well as interferon-gamma production by T helper 1 cells. *Eur J Immunol* 1996; **26**: 659-668
- 51 **Shibuya K**, Robinson D, Zonin F, Hartley SB, Macatonia SE, Somoza C, Hunter CA, Murphy KM, O'Garra A. IL-1 alpha and TNF- $\alpha$  are required for IL-12-induced development of Th1 cells producing high levels of IFN- $\gamma$  in BALB/c but not C57BL/6 mice. *J Immunol* 1998; **160**: 1708-1716
- 52 **Sin JI**, Kim JJ, Arnold RL, Shroff KE, McCallus D, Pachuk C, McElhiney SP, Wolf MW, Pompa-de Bruin SJ, Higgins TJ, Ciccarelli RB, Weiner DB. IL-12 gene as a DNA vaccine adjuvant in a herpes mouse model: IL-12 enhances Th1-type CD4 $^{+}$  T cell-mediated protective immunity against herpes simplex virus-2 challenge. *J Immunol* 1999; **162**: 2912-2921
- 53 **Bhardwaj N**, Seder RA, Reddy A, Feldman MV. IL-12 in conjunction with dendritic cells enhances antiviral CD8 $^{+}$  CTL responses *in vitro*. *J Clin Invest* 1996; **98**: 715-722
- 54 **Schmidt CS**, Mescher MF. Adjuvant effect of IL-12: conversion of peptide antigen administration from tolerizing to immunizing for CD8 $^{+}$  T cells *in vivo*. *J Immunol* 1999; **163**: 2561-2567
- 55 **Kim J**, Uyemura K, Van Dyke MK, Legaspi AJ, Rea TH, Shuai K, Modlin RL. A role for IL-12 receptor expression and signal transduction in host defense in leprosy. *J Immunol* 2001; **167**: 779-786
- 56 **Wu CY**, Wang X, Gadina M, O'Shea JJ, Presky DH, Magram J. IL-12 receptor  $\beta$ 2 (IL-12R  $\beta$ 2)-deficient mice are defective in IL-12-mediated signaling despite the presence of high affinity IL-12 binding sites. *J Immunol* 2000; **165**: 6221-6228
- 57 **Wang KS**, Frank DA, Ritz J. Interleukin-2 enhances the response of natural killer cells to interleukin-12 through up-regulation of the interleukin-12 receptor and STAT4. *Blood* 2000; **95**: 3183-3190
- 58 **Chang JT**, Shevach EM, Segal BM. Regulation of interleukin (IL)-12 receptor  $\beta$ 2 subunit expression by endogenous IL-12: a critical step in the differentiation of pathogenic autoreactive T cells. *J Exp Med* 1999; **189**: 969-978
- 59 **Kawashima T**, Kawasaki H, Kitamura T, Nojima Y, Morimoto C. Interleukin-12 induces tyrosine phosphorylation of an 85-kDa protein associated with the interleukin-12 receptor  $\beta$ 1 subunit. *Cell Immunol* 1998; **186**: 39-44
- 60 **Lawless VA**, Zhang S, Ozes ON, Bruns HA, Oldham I, Hoey T, Grusby MJ, Kaplan MH. Stat4 regulates multiple components of IFN- $\gamma$ -inducing signaling pathways. *J Immunol* 2000; **165**: 6803-6808
- 61 **Ohteki T**, Fukao T, Suzue K, Maki C, Ito M, Nakamura M, Koyasu S. Interleukin 12-dependent interferon  $\gamma$  production by CD8 $\alpha^{+}$  lymphoid dendritic cells. *J Exp Med* 1999; **189**: 1981-1986
- 62 **Fukao T**, Matsuda S, Koyasu S. Synergistic effects of IL-4 and IL-18 on IL-12-dependent IFN-gamma production by dendritic cells. *J Immunol* 2000; **164**: 64-71
- 63 **Fukao T**, Frucht DM, Yap G, Gadina M, O'Shea JJ, Koyasu S. Inducible expression of Stat4 in dendritic cells and macrophages and its critical role in innate and adaptive immune responses. *J Immunol* 2001; **166**: 4446-4455
- 64 **Fukao T**, Koyasu S. Expression of functional IL-2 receptors on mature splenic dendritic cells. *Eru J Immunol* 2000; **30**: 1453-1457
- 65 **Grohmann U**, Belladonna ML, Bianchi R, Orabona C, Ayroldi E, Fioretti MC, Puccetti P. IL-12 acts directly on DC to promote nuclear localization of NF- $\kappa$ B and primes DC for IL-12 production. *Immunity* 1998; **9**: 315-323
- 66 **Grohmann U**, Bianchi R, Belladonna ML, Vacca C, Silla S, Ayroldi E, Fioretti MC, Puccetti P. IL-12 acts selectively on CD8 $\alpha$  dendritic cells to enhance presentation of a tumor peptide *in vivo*. *J Immunol* 1999; **163**: 3100-3105

Edited by Zhang JZ

# Cloning and analyzing the up-regulated expression of transthyretin-related gene ( $LR_1$ ) in rat liver regeneration following short interval successive partial hepatectomy

Cun-Shuan Xu, Yu-Chang Li, Jun-Tang Lin, Hui-Yong Zhang, Yun-Han Zhang

**Cun-Shuan Xu, Yu-Chang Li, Jun-Tang Lin, Hui-Yong Zhang,**  
College of Life Science, Henan Normal University, Xinxiang 453002,  
Henan Province, China

**Yun-Han Zhang,** Henan Key Laboratory for Tumor Pathology,  
Zhengzhou, 450052, Henan Province, China

**Supported by** grants from National Natural Science Foundation of  
China, No. 39970362; Tackle Key of Scientific and Technical Problem  
of Henan Province, No. 0122031900

**Correspondence to:** Prof. Dr. Cun-Shuan Xu, College of Life  
Science, Henan Normal University, Xinxiang, 453002, Henan  
Province, China. xucs@x263.net

**Telephone:** +86-373-3326341/3326609 **Fax:** +86-373-3326524

**Received:** 2002-03-12 **Accepted:** 2002-04-20

## Abstract

**AIM:** Cloning and analyzing the up-regulated expression of transthyretin-related gene following short interval successive partial hepatectomy (SISPH) to elucidate the mechanism of differentiation, division, dedifferentiation and redifferentiation in rat liver regeneration (LR).

**METHODS:** Lobus external sinister and lobus centralis sinister, lobus centralis, lobus dexter, lobus candatus were removed one by one from rat liver at four different time points 4, 36, 36 and 36 hr (total time: 4 hr, 40 hr, 76 hr, 112 hr) respectively. Suppression subtractive hybridization (SSH) was carried out by using normal rat liver tissue as driver and the tissue following short interval successive partial hepatectomy (SISPH) as tester to construct a highly efficient forward-subtractive cDNA library. After screening, an interested EST fragment was selected by SSH and primers were designed according to the sequence of the EST to clone the full-length cDNA fragment using RACE (rapid amplification of cDNA end). Homologous detection was performed between the full-length cDNA and Genbank.

**RESULTS:** Forward suppression subtractive hybridization (FSSH) library between 0 h and 112 h following SISPH was constructed and an up-regulated full-length cDNA (named  $LR_1$ ), which was related with the transthyretin gene, was cloned by rapid amplification of cDNA end. It was suggested that the gene is involved in the cellular dedifferentiation in LR following SISPH.

**CONCLUSION:** Some genes were up-regulated in 112 h following SISPH in rat.  $LR_1$  is one of these up-regulated expression genes which may play an important role in rat LR.

Xu CS, Li YC, Lin JT, Zhang HY, Zhang YH. Cloning and analyzing the up-regulated expression of transthyretin-related gene ( $LR_1$ ) in rat liver regeneration following short interval successive partial hepatectomy. *World J Gastroenterol* 2003; 9 (1): 148-151

<http://www.wjgnet.com/1007-9327/9/148.htm>

## INTRODUCTION

In mammals, liver is the only organ that possesses the strong capability of regeneration<sup>[1-7]</sup>. Since Higgins and Anderson<sup>[8]</sup> established the model of partial hepatectomy (PH), it has been widely used to study the reconstruction and regeneration of tissue and organs, cellular multiplication, dedifferentiation, stress response and the regulation of physiology and biochemistry<sup>[8-16]</sup>. But due to the complexity of liver regeneration, the molecular mechanism of LR remains to be elucidated. In order to better understand the mechanism of PH, researchers have established a series of successive partial hepatectomy (SPH) models. These included the long interval successive partial hepatectomy (LISPH) that involved an interval of more than three weeks and short interval successive partial hepatectomy (SISPH) which had an interval of 4 and/or 36 hr<sup>[17]</sup>. Because the hepatocytic initiation, dedifferentiation, division and redifferentiation mainly occurred within 144 hr following PH<sup>[18-22]</sup>. It is doubtless that the study on the change of liver tissue, cellular morphology, structure, physiology and biochemistry in every crucial point following SISPH can offer more data about LR. In this paper, we used the normal liver tissue as control and the liver tissue in 112 hr SISPH as experimental materials, and adopted the whole-mount research strategy of genome and resorted to SSH technique to construct a differential expressed forward-subtracted cDNA library. From the library, we picked some significant expressed sequence tags (ESTs) clones. Then the primers were designed according to these ESTs. By RACE PCR, some full-length cDNAs were obtained. After sequencing these full-length cDNAs, it showed that one of them belonged to the gene of related transthyretin, termed  $LR_1$  gene, which was up-regulated expression in LR.

## MATERIALS AND METHODS

### *Making SISPH model and preparation of samples*

Adult Spargue-Dawley rats (weighing 200-250 g) were provided by the experimental animal house of Henan Normal University and 0-4-36-36-36 hr SISPH model was made according to the method of Xu *et al*<sup>[17]</sup>. Lobus external sinister and lobus centralis sinister, lobus centralis, lobus dexter, lobus candatus were removed one by one at four different time points 4, 36, 36 and 36 hr (total time: 4 hr, 40 hr, 76 hr, 112 hr) respectively. The control and the four resected liver hepatic lobus were washed with precooled phosphate-buffered saline (PBS) thoroughly before these samples were frozen in liquid nitrogen and transferred to the -80 °C freezer for storage.

### *Preparation of control mRNA and the 112 hr SISPH mRNA*

Isolation of total RNA and mRNA was carried out according to the protocol of RNAase kit and oligotex mRNA spin column purification kit (Qiagen). The quantity and integrity of mRNA were detected by ultraviolet spectrometer and by electrophoresing on a denaturing formaldehyde agarose

stained by EtBr. Chemicals and reagents used were at least of analytical grade.

### Generating of a subtracted cDNA library

SSH was performed between the aforementioned tester and driver liver tissue mRNA preparations using a PCR select™ cDNA subtraction kit and 50×PCR enzyme kit (Clontech, Heidelberg, Germany) following the instructions of the manufacturer. Briefly, 2 µg aliquots each of poly (A<sup>+</sup>) mRNA from the tester and the pooled driver were subjected to cDNA synthesis. Thereafter, the tester and driver cDNAs were digested with Rsa I. The tester cDNA was subdivided into two portions, and each was ligated with a different cDNA adaptor. In the first hybridization reaction, an excess of driver was added to each sample of tester. The samples were heat denatured and allowed to anneal. Due to the second-order kinetics of hybridization, the concentration of high- and low-abundance sequence is equalized among the single-stranded tester molecules. At the same time, single-stranded tester molecules are significantly enriched for differentially expressed sequences. During the second hybridization, the two primary hybridization samples were mixed together without denaturation, only the remaining equalized and subtracted single-stranded tester cDNAs can reassociate to form double-stranded tester molecules with different ends. After filling in the ends with DNA polymerase, the entire population of molecules was subjected to nested PCR with two adaptor-specific primer pairs. The tester control was amplified with primer1 and nested primer 1 and 2 provided in the kit. The subtraction efficiency was evaluated by house-keeping gene *g3pdh*.

### Cloning the subtracted library into a TA vector

Products from the secondary PCR reactions were ligated into a pGEM-T vector (Promega) and the resultant ligation products were then transformed into JM109 *E. coli* competent cells. The bacterial were subsequently grown in 800 µl of liquid Luria-Bertani medium and allowed to incubate for 45 min at 37 °C with shaking at 150 rpm. Thereafter, the cells were plated onto agar plates containing ampicillin (50 µg/ml), 5-bromo-4-chloro-3-indolyl-β-D-galactoside (x-gal; 20 µg/cm<sup>2</sup>) and isopropyl-β-D-thiogalactoside (IPTG; 12.1 µg/cm<sup>2</sup>) and incubated overnight at 37 °C. Individual recombinant white clones were picked and grown in single line pattern onto Luria-Bertani agar solid medium containing ampicillin and allowed to incubate at 37 °C for 6-7 hr before single clone was picked from single-line pattern agar medium and allowed to grow in Luria-Bertani liquid medium containing ampicillin overnight at 37 °C with shaking of 150 rpm.

### Identifying the subtracted clones

Plasmids were isolated from bacterial clones harboring differentially expressed cDNA sequences as described by Sambrook *et al.* Plasmids containing cDNA inserts were amplified by PCR with nested primer 1 and primer 2 and the amplified product of every plasmid was detected by agarose gel electrophoresis. After that, the inserts that appeared as distinct bands were sequenced by T7/SP6 chain termination reaction in TaKaRa (DaLian, China). Nucleic acid homology searches were subsequently performed at the National Center of Biotechnology Information (National Institutes of Health, Bethesda, Md., NCBI).

### RACE

An interested EST fragment was chosen from the established cDNA library for primer design according to the instructions of the 5' /3' RACE kit (Roche) manufacturer. RACE, a procedure to amplify nucleic acid sequences from a mRNA template between a defined internal site and unknown

sequences at 5' -and 3' -end of mRNA, was then performed by using 5' /3' RACE kit and following the supplier's protocol. The primer used for 3' RACE was SP5: 5' -AGCTGGGAG CCGTTTGC-3' and the primer used for 5' RACE was SP1: 5' -TGCTGTAGGAGTACGGGCT-C3' , SP2: 5' -A C C A G A G T C A T T G G C T G T -3' , SP3: 5' -G C C C G T G C A G C T C T -3' respectively. Proofreading *pfu* DNA polymerase was purchased from MBI and the 3' RACE PCR parameters were: predenaturation at 94 °C for 2 min before amplification was done for 40 cycles at 94 °C for 45 sec, annealing at 65 °C for 1 min and extension at 72 °C for 1 min and 30 sec followed by an additional extension period at 72 °C for 5 min. The 5' RACE used touchdown PCR and amplification was carried out with the following conditions: 94 °C for 2 min, 25 cycles including a denaturation step at 94 °C for 15 sec, an annealing step from 68 °C to 55 °C for 30 sec, and extension at 72 °C for 1 min and 30 sec; 15 cycles as above except that the annealing step at 55 °C; a final extension step at 72 °C for 7 min ended the PCR reaction. The products were subjected to electrophoresis in a 1 % agarose gel, purified according to qiaquick PCR purification kit protocol and added dATP-tailing to blunt-ended fragments at 70 °C for 30 min in the presence of Taq DNA polymerase before ligated into the pGEM-T vector. Transformation, screening, and sequencing were then performed as described above.

### Splicing the full-length nucleotide sequence

Alignment of the sequences was spliced, in light of contig of 5' /3' sequencing result, to get a full-length nucleotide sequence. Homology search was performed using the BLAST program at NCBI.

## RESULTS

### Construction of the subtracted cDNA library and screening of the differential fragments

By means of suppression subtractive hybridization (SSH) technique, we prepared driver cDNAs and tester cDNAs of liver tissue from control and liver tissue 112 hr following SISPH. After two rounds hybridization and two PCR reactions, we obtained the forward-subtractive cDNA library (Figure 1). The subtracted cDNA was evaluated by the house-keeping gene *g3pdh* (Figure 2). Our results showed that the constructed forward-subtracted cDNA library was highly efficient after cDNA library was subcloned into pGEM-T vector and transformed into JM109, we obtained 120 white clones and 40 clones randomly selected were then subjected to sequencing (Figure 3). The sequencing results were sent to NCBI for BLAST searches.

### Determination of the full-length nucleotide sequence of *LR<sub>i</sub>* cDNA by RACE

The original cDNA isolated from the cDNA subtraction screening was about 311bp long. This cDNA fragment was used to design primers according to 5' /3' RACE kit. After amplification, ligation, screening and sequencing, we obtained the sequence of the 3' end and 5' end (Figure 4). Alignment of contig sequences enabled us to delineate the entire cDNA sequence (Figure 5). We found a single long ORF starting with a methionine codon ATG at nucleotide 47 and ending with a TAA stop codon at 625 and a putative polyadenylation signal AATAAA upstream from the poly (A<sup>+</sup>). Homology search using *LR<sub>i</sub>* cDNA sequence revealed that it is 88.8 % homologous to rat transthyretin gene and 88.4 % homologous to albumin gene. Protein homology (Swissport database) search of the peptide encoded by the *LR<sub>i</sub>* ORF revealed that it is 91% homologous to rat transthyretin, submitting this full-length cDNA to NCBI and obtain GenBank Accession No. AF479660.

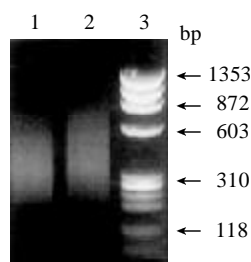


**Figure 1** Gel electrophoresis of SSH results. 1. Control; 2. Forward subtractive; 3. Marker.

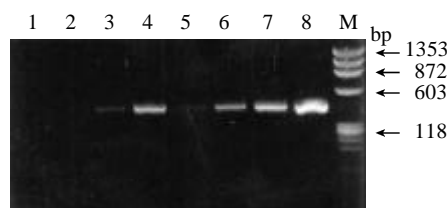


**Figure 2** Efficiency of subtracted library. 1-4. Subtracted products with *g3pdh* primer; 5-8. Control products with *g3pdh* primer; M. Marker.

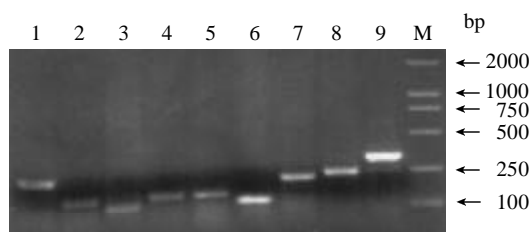


**Figure 3** Gel electrophoresis of clones inserted fragments. 1-9. Different EST fragments; M. Marker.

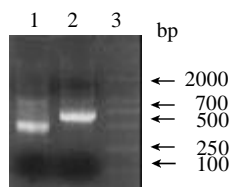


**Figure 4** RACE PCR results. 1. 3' RACE result; 2. 5' RACE result; 3. Marker.

```

1   ggccattacg gccggggatc gtagagatcc gctggtctct gacaggatgg cttcccttcg
61  cctgttctc ctctgcctcg ctggactgat atttgcgtct gaagctggcc ctgggggtgc
121 tggagaatcc aagtgtcctc tgaatgtcaa agtctcgat gctgtccgag gcagccctgc
181 tgtcgatgtg gccgtgaaag tgttcaaaaa gactgcagac ggaagctggg agccgtttgc
241 ctctgggaag accgccgagt ctggagagct gcacgggctc accacagatg agaagttcac
301 ggaaggggtg tacagggtag aactggacac caaatctgac tggaaaggctc ttggcatttc
361 cccattccat gaatacgcag aggtgtgttt cacagccaat gactctgtgc atcgccaata
421 caccatcgca gccctgtcta gcccggtact ctacagcacc actgctgtcg tcagtaaccc
481 ccgaactga gggaccacgc ccaggaggac caggatcttg ccaagcagt agcttcccat
541 ttgtactgaa acagtgttct tgccttataa accgtgttag caactcggga agatgccgtg
601 aaacgttctt attaaaccac ctttatttca tccaaaaaaa aaaaaaaaaa aaaaaaaaaa
661 a

```

**Figure 5** Full-length cDNA of *LR<sub>1</sub>*

## DISCUSSION

SSH technique was developed based primarily on a recently described technique called cDNA suppression PCR which combines normalization and subtraction in a single procedure

to generate subtracted cDNA library<sup>[23-25]</sup>. Compared to the methods of mRNA differential display<sup>[26]</sup>, representational difference analysis of DNA<sup>[27]</sup>, it has two distinct advantages: (1) it has a high subtraction efficiency; (2) it harbors an equalized representation of differentially expressed sequences which can separate effectively both high and low copy expressed genes mainly because of normalization. The normalization step equalizes the abundance of cDNAs within the target population and the subtraction step excludes the common sequences between the target and the driver populations<sup>[23,28,29]</sup>. The experimental results showed the SSH technique can enrich for rare sequences over 1 000-5 000 fold in one round of subtractive hybridization<sup>[23,24,30]</sup>. By resorting to SSH and high-density array scanning technique, using non-metastatic counterpart Bsp73-1AS as driver, metastatic adenocarcinoma cell line Bsp73-ASML as tester, Von Stein<sup>[31]</sup> found up to 252 over-expressed clones among 625 clones with no homologous sequences in GenBank. By using a EST fragment derived from the forward-subtracted cDNA library as probe, we have cloned a novel gene from the liver tissue 112 hr cDNA library following SISPH. These results suggest that SSH technique is applicable to many molecular genetic and positional cloning studies for the identification of disease, developmental, tissue-specific or other differentially expressed genes.

With the aim to shed light on the molecular mechanism of PH, Xu *et al*<sup>[17]</sup> established the SISPH model which selected the intervals at the crucial periods, e.g. the peak of cell activation (4 hr after PH), the peak of cell division (36 hr after PH) and the peak of re-differentiation (48 hr after PH). We have examined some biological activated factors, heat shock proteins (HSPs), proteases, proteins related to cell proliferation and dephosphorylation<sup>[13,14,17,18,32]</sup>. These data have provided useful information to reveal the molecular mechanism of LR. The results suggested that SISPH model may offer more abundant data than that of PH. In present study, We took 0 h and 112 hr as driver and tester respectively in 0-4-36-36-36hr SISPH model when resorting to SSH strategy, then we constructed a forward-subtractive cDNA library in short time by using RACE, subsequently we cloned a full-length cDNA and blast search showed that the cDNA is 88.8 % and 88.4 % homologous to the transthyretin and albumin in rat respectively. This suggested that the gene may exert partial function identical to transthyretin. It is well known that thyroxine and its metabolic products integrated thyroxine-binding prealbumin and albumin is derived from liver to operate. In the physiological conditions, 99.9 % 3,3', 5,5' -tetraiodothyronine ( $T_4$ ) and 99.7 % 3,3' 5-triiodothyronine ( $T_3$ ) are complexed with proteins which contain over 60 % transthyretin and 15-30 % thyroxine-binding prealbumin and 10 % albumin. Our present study showed that the injured liver released abundant analogs of transthyretin. As we know, the changes of transthyretin concentration is regarded as one of the important reasons that metabolic or biochemical abnormality in thyroid gland responsible for hepatopathy<sup>[33,34]</sup>. The up-regulations of transthyretin in liver tissue is speculated to have following functions: (1) breaking the balance of HSS (hepatocyte stimulate substrate) and inhibitor and thus enhancing the dedifferentiation. We have cloned two up-regulated genes, one of which is 78.6 % homologous to rat transferring gene and the other is 72 % homologous to mouse embryonic stem cell gene from 112 hr cDNA library following SISPH (remains to be published). It is also known that over-expression of transferring gene and embryonic stem cell gene have close relations with the cellular dedifferentiation; (2) influencing the induction of enzyme and consumption of oxygen. Compensatory respiration was promoted in mitochondrion responsible for partial hypoxia following PH, but the energy produced from tricarboxylic acid cycle couldn't meet the

structural recovery of damaged liver due to successive partial hepatectomy and thus triggered the related genes to express in hypoxia metabolism. The over-expressed gene of alcohol dehydrogenase have cloned from 112 hr cDNA library following SISPH (remains to be published) seems to explain this hypothesis which is consistent with the result of Cheng Lingzhong.

In conclusion, complicated physiological and biochemical reaction changed in the liver tissue following SISPH, we postulated that this kind of up-regulated gene *LR<sub>1</sub>* expression involve in liver regeneration may (1) relate with compensated increase of stress molecules following SISPH; (2) lead to the initiation of other metabolism; (3) maintain the homeostasis in the body. As to, whether severe dedifferentiation happened following SISPH and what are the key dedifferential factors and how they influence the dedifferentiation, remain to be further investigated.

## REFERENCES

- 1 **Michael M**, Awad, Philip A. Gruppuso. Cell cycle control during liver development in the rat: Evidence indicating a role for cyclin d1 posttranscriptional regulation. *Cell Growth Differ* 2000; **11**: 325-334
- 2 **Jiang YP**, Ballou LM, Lin RZ. Apamycin-insensitive regulation of 4E-BP1 in regenerating rat Liver. *J Biol Chem* 2001; **276**: 10943-10951
- 3 **Zakko WF**, Berg CL, Gollan JL, Green RM. Hepatocellular expression of glucose-6-phosphatase is unaltered during hepatic regeneration. *Am J Physiol Gastrointest Liver Physiol* 1998; **275**: 717-722
- 4 **Iimuro YJ**, Nishiura T, Hellerbrand C, Behrns KE, Schoonhoven R, Grisham JW, Brenner DA. NFκB prevents apoptosis and liver dysfunction during liver regeneration. *J Clin. Invest* 1998; **101**: 802-811
- 5 **Laconi E**, Oren R, Mukhopadhyay DK, Hurston E, Laconi S, Pani P, Dabeva MD, Shafritz DA. Long-Term. Near-total liver replacement by transplantation of isolated hepatocytes in rats treated with retrorsine. *Am J Pathol* 1998; **153**: 319-329
- 6 **Ying C**, Rory O, Conolly B, Russell S, Thomas, Yihua X, Melvin E, Andersen, Laura S, Chubb, Henry C, Pitot, Raymond S, Yang H. A clonal growth model: time-course simulations of liver foci growth following penta-or hexachlorobenzene treatment in a medium-term bioassay. *Cancer Res* 2001; **61**: 1879-1889
- 7 **Kooby DA**, Zakian KL, Challa SN, Matei C, Petrowsky H, Yoo HH, Koutcher JA, Fong Y. Use of phosphorous-31 nuclear magnetic resonance spectroscopy to determine safe timing of chemotherapy after hepatic resection. *Cancer Res* 2000; **60**: 3800-3806
- 8 **Michalopoulos GK**, DeFrance MC. Liver regeneration. *Science* 1997; **275**: 60-66
- 9 **Sigal SH**, Rajvanshi P, Gorla GR, Sokhi RP. Partial hepatectomy-induced polyploidy attenuates hepatocyte replication and activates cell aging events. *Am J Physiol Gastrointest Liver Physiol* 1999; **276**: 1260-1272
- 10 **Ikeda Y**, Matsumata T, Utsunomiya T, Yamagata M, Takenaka K, Sugimachi K. Effects of doxorubicin on cancer cells after two-thirds hepatectomy in rats. *J Surg Onco* 1995; **58**: 101-103
- 11 **Shih HH**, Xiu M, Berasi SP, Sampson EM, Leiter A, Yee AS. HMG box transcriptional repressor hbp1 maintains a proliferation barrier in differentiated liver tissue. *Mol Cell Biol* 2001; **21**: 5723-5732
- 12 **Xu CS**, Xia M, Lu AL, Li XY, Li YH, Zhao XY, Hu YH. Changes in the content and activity of HSC70/HSP68, proteinase and phosphatases during liver regeneration. *Sheng Li Xue Bao* 1999; **51**: 546-556
- 13 **Hayami S**, Yaita M, Ogiri Y, Sun F, Nakata R, Kojo S. Change in caspase-3-like protease in the liver and plasma during rat liver regeneration following partial hepatectomy. *Biochem Pharmacol* 2000; **60**: 1883-1886
- 14 **Rissler P**, Torndal UB, LC Eriksson. Induced drug resistance inhibits selection of initiated cells and cancer development. *Carcinogenesis* 1997; **18**: 649-655
- 15 **Aaron W**, Bell, Jie-Gen Jiang, Qiuyan Chen, Youhua Liu, Reza Zarnegar. The upstream regulatory regions of the hepatocyte growth factor gene promoter are essential for its expression in transgenic mice. *J Biol Chem* 1998; **273**: 6900-6908
- 16 **Lu AL**, Xu CS. Effect of heat shock before and after rat partial hepatectomy on HSC/HSP68, acid and alkaline phosphatases. *World J Gastroenterol* 2000; **6**: 730-733
- 17 **Xu CS**, Li YH, Duan RF, Lu AL, Xia M, Ji AL. Effects of the short interval successive partial hepatectomy on rat survival and liver tissue structure. *Dongwu Xuebao* 2001; **47**: 659-665
- 18 **Ankoma-Sey V**. Hepatic regeneration-revisiting the myth of Prometheus. *News in physiological Sciences* 1999; **14**: 149-155
- 19 **Diehl AM**. Liver regeneration. *Front Biosci* 2002; **7**: e301-314
- 20 **Russell WE**, Dempsey PJ, Sitaric S, Peck AJ, Coffey RJ. Transforming growth factor-alpha concentrations increase in regenerating rat liver: evidence for a delayed accumulation of mature TGF alpha. *Endocrinology* 1993; **133**: 1731-1738
- 21 **Schirmacher P**, Geerts A, Pietrangelo A, Dienes HP, Rogler CE. Hepatocyte growth factor/hepatopoietin A is expressed in fat-storing cells from rat liver but not myofibroblast-like cells derived from fat-storing cells. *Hepatology* 1992; **15**: 5-11
- 22 **Yamada Y**, Kirillova I, Peschon JJ, Fausto N. Initiation of liver growth by tumor necrosis factor deficient liver regeneration in mice lacking type I tumor necrosis factor receptor. *Proc Acad Sci USA* 1997; **94**: 1441-1446
- 23 **Diatchenko L**, Lukyanov S, Lau YF, Siebert PD. Suppression subtractive hybridization: a versatile method for identifying differentially expressed genes. *Methods Enzymol* 1999; **303**: 349-380
- 24 **Nishizuka S**, Tsujimoto H, Stanbridge EJ. Detection of differentially expressed genes in hela x fibroblast hybrids using subtractive suppression hybridization. *Cancer Res* 2001; **61**: 4536-4540
- 25 **Shridhar V**, Sen A, Chien J, Staub J, Avula R, Kovats S, Lee J, Lillie J, Smith DI. Identification of under expressed genes in early- and late-stage primary ovarian tumors by suppression subtraction hybridization. *Cancer Res* 2002; **62**: 262-270
- 26 **Liang P**, Pardee AB. Differential display of eukaryotic messenger RNA by means of the polymerase chain reaction. *Science* 1992; **257**: 967-971
- 27 **Duguin JL**, Dinauer MC. Library subtraction of in vitro cDNA libraries to identify differentially expressed genes in scrapie infection. *Nucleic Acids Res* 1990; **18**: 2789-2792
- 28 **Hara E**, Kato T, Nakada S, Sekiya L, Oda K. Subtractive cDNA cloning using oligo (dT)30-latex and PCR: isolation of cDNA clones specific to undifferentiated human embryonal carcinoma cells. *Nucleic Acids Res* 1991; **19**: 7097-7104
- 29 **Hubank M**, Schatz DG. Identifying differences in mRNA expression by representational analysis of cDNA. *Nucleic Acids Res* 1994; **22**: 5640-5648
- 30 **Fabrikant JL**. The kinetics of the cellular proliferation in the regeneration liver. *Cell Biol* 1968; **36**: 551-565
- 31 **Von Stein OD**, Thies WG, Hofmann MA. High through put screening for rarely transcribed differentially expressed genes. *Nucleic Acids Research* 1997; **25**: 2598-2602
- 32 **Joan M**, Boylan, Padmanabhan Anand, Philip A, Gruppuso. Ribosomal protein S6 phosphorylation and function during Late Gestation liver development in the rat. *J Biol Chem* 2001; **276**: 44457-44463
- 33 **Schreiber G**. The evolutionary and integrative roles of transthyretin in thyroid hormone homeostasis. *J Endocrinol* 2002; **175**: 61-73
- 34 **Toshi D**, Shen CN, Slack JM. Differentiated properties of hepatocytes induced from pancreatic cells. *Hepatology* 2002; **36**: 534-543

Edited by Zhao M

# Effects of pentoxifylline on the hepatic content of TGF- $\beta$ 1 and collagen in Schistosomiasis japonica mice with liver fibrosis

Li-Juan Xiong, Jian-Fang Zhu, Duan-De Luo, Lin-Lan Zen, Shu-Qing Cai

**Li-Juan Xiong, Duan-De Luo, Lin-Lan Zen, Shu-Qing Cai**, Department of Infectious Diseases, Union Hospital, Tongji Medical College, Huazhong University of Science and Technology, Wuhan 430022, Hubei Province, China

**Jian-Fang Zhu**, Department of Central Laboratory, Union Hospital, Tongji Medical College, Huazhong University of Science and Technology, Wuhan 430022, Hubei Province, China

**Supported by** the Science Research Foundation of Schistosomiasis of Hubei Province, No.2000

**Correspondence to:** Dr. Li-Juan Xiong, Department of Infectious Disease, Union Hospital, Tongji Medical College, Huazhong University of Science and Technology, Wuhan 430022, Hubei Province, China. kljxiong@public.wh.hb.cn

**Telephone:** +86-27-85726109

**Received:** 2002-08-15 **Accepted:** 2002-09-12

## Abstract

**AIM:** To study the effects of pentoxifylline (PTX) on the content of hepatic TGF- $\beta$ 1, type I and type III collagen in schistosomiasis japonica mice with liver fibrosis and its mechanism of anti-fibrosis.

**METHODS:** Forty mice with schistosomiasis were divided into four groups: one group as control without any treatment, other three were treated with Praziquantel 500 mg/(kg·d) for 2 d, high dose PTX 360 mg/(kg·d) for 8 wk, and low dose PTX 180 mg/(kg·d) for 8 wk respectively. Immunohistochemical technique and multimedia color pathographic analysis system were applied to observe the content change of hepatic TGF- $\beta$ 1, type I and type III collagen in schistosomiasis japonica mice with liver fibrosis before and after PTX treatment.

**RESULTS:** Effects of PTX on the content change of hepatic TGF- $\beta$ 1, type I and type III collagen in schistosomiasis japonica mice with liver fibrosis were related to the dosage of PTX, high dose PTX treated group could significantly reduce the content of TGF- $\beta$ 1 ( $0.709 \pm 0.111$ ), type I ( $0.644 \pm 0.108$ ) and type III ( $0.654 \pm 0.152$ ) collagen compared with those of control group ( $0.883 \pm 0.140$ ,  $0.771 \pm 0.156$ ,  $0.822 \pm 0.129$ ) with statistical significance ( $P < 0.05$ ). Low dose PTX could also reduce the hepatic content of TGF- $\beta$ 1 ( $0.752 \pm 0.152$ ), type I ( $0.733 \pm 0.117$ ) and type III ( $0.788 \pm 0.147$ ) collagen, but without statistical significance ( $P > 0.05$ ). Both high dose and low dose PTX groups have significant differences on the content of TGF- $\beta$ 1, type I and type III collagen ( $P < 0.05$ ,  $P < 0.05$ ,  $P < 0.01$ , respectively).

**CONCLUSION:** High dose of PTX treatment could reduce the content of hepatic TGF- $\beta$ 1, type I and type III collagen significantly in schistosomiasis japonica mice with liver fibrosis, and thus plays its role of antifibrosis.

Xiong LJ, Zhu JF, Luo DD, Zen LL, Cai SQ. Effects of pentoxifylline on the hepatic content of TGF- $\beta$ 1 and collagen in Schistosomiasis japonica mice with liver fibrosis. *World J Gastroenterol* 2003; 9(1): 152-154

<http://www.wjgnet.com/1007-9327/9/152.htm>

## INTRODUCTION

Liver fibrosis is the main reason for portal hypertension and hemorrhagic of upper digestive tract in schistosomiasis and there fore the main reason for the mortality of schistosomiasis. The basic pathological changes of liver fibrosis are the disturbance and degradation of extracellular matrix (ECM), which causes accumulation of ECM in the liver<sup>[1,2]</sup>. Within the major components of ECM, type I and type III collagen constitute more than 95 % of the total content of increased collagen in liver fibrosis<sup>[3-5]</sup>. It is well known that fibrosis is reversible whereas cirrhosis is irreversible, so it is important to prevent fibrosis progressing to cirrhosis<sup>[6,7]</sup>. However, there is no ideal antifibrosis drug to date. Recent researches found that PTX has antifibrosis function<sup>[8,9]</sup>, while its effects on hepatic fibrosis of schistosomiasis japonica are still unknown. Since the main pathological characteristic of schistosomiasis japonica is the deposition of type I and III collagen and TGF $\beta$ 1 has very important influence on the fibrosis development, it is considered the key cytokine to accelerate cirrhotic procession<sup>[10-15]</sup>, we studied the effects of PTX on the expression of collagen I and III and TGF $\beta$ 1 in mice with schistosomiasis japonica and intended to evaluate the roles of PTX in hepatic fibrosis.

## MATERIALS AND METHODS

### Materials

Forty female Kunming mice, weighted 16-20 g and aged 4-6 w, provided by Experimental Animal Center of Tongji Medical College, were infected with 25 cercaria of schistosoma japonica (provided by Wuhan Institute of Schistosomiasis Prophylactic and Therapy) and fed for 2 weeks and then divided randomly and equally into 4 groups: one group as control without any treatment, other three were treated with Praziquantel 500 mg/(kg·d) for 2 d, high dose PTX (provided as SHUANLIN tablet by Shijiazhuang Pharmaceutics CO.) 360 mg/(kg·d) for 8 wk, and low dose PTX 180 mg/(kg·d) for 8 wk respectively. The mice were then deceased and hepatic tissue sections were prepared for examination. Immunohistochemical technique and multimedia color pathographic analysis system were applied to observe the content of hepatic TGF- $\beta$ 1, type I and type III collagen before and after treatment.

### Assay of TGF $\beta$ 1, collagen I and collagen III

Rabbit anti-mouse TGF $\beta$ 1 was purchased from Santa Cruz. Rabbit anti-mouse collagen I and III, and SABC kit were provided by Boster Biological Technology Co., Ltd. The immunohistochemical studies were performed by the avidin-biotin-peroxidase method, briefly described as following. The tissue sections were blocked in 3 % hydrogen peroxide, washed in buffer solution, and then incubated in mixed digestive solution for 5 min in room temperature. The sections were washed in PBS and then incubated in goat serum blocking solution for 10 min. The sections were then incubated with the primary antibodies at 37 °C for 30 min, washed and then incubated with biotin conjugated secondary antibodies at 37 °C for 20 min, washed with PBS, and then labeled with peroxidase-conjugated streptavidin for 20 min at 37 °C. The washed

sections were then incubated with Diaminobenzidine (DAB), counterstained and prepared for microscopic examination.

### Results analysis

The sections were analyzed with MPZAS-500 multimedia color pathological graph analyzing system. The average integral light density (ILD) of positive staining in each section was obtained and presented as  $\bar{x} \pm s$ . Results were then analyzed with student *t* test.

## RESULTS

### Effects of PTX on TGF- $\beta$ 1 expression

The contents of TGF $\beta$ 1 in praziquantel group, high dose PTX group and low dose PTX group decrease by 44.62 %, 19.71 %, 14.84 % respectively compared with control group. The difference between praziquantel group and control group is very significant ( $P < 0.01$ ). The effect of PTX on TGF $\beta$ 1 content is dose related and there is significant difference on TGF $\beta$ 1 contents between high and low dose groups. The TGF $\beta$ 1 content in high dose PTX group is significantly ( $P < 0.05$ ) different from that of control group while no significant difference between low dose PTX group and control group. Both high dose and low dose PTX groups have significant difference on TGF $\beta$ 1 contents between praziquantel group and themselves. The results are shown in Table 1.

**Table 1** Content of TGF- $\beta$ 1, collagen I and III in liver of each treated group and control group ( $\bar{x} \pm s$ , ILD,  $n = 10$ )

Group	TGF- $\beta$ 1	Collagen I	Collagen III
Control	0.883 $\pm$ 0.140	0.771 $\pm$ 0.156	0.822 $\pm$ 0.129
Praziquantel	0.489 $\pm$ 0.105 <sup>a</sup>	0.596 $\pm$ 0.103 <sup>a</sup>	0.613 $\pm$ 0.116 <sup>a</sup>
High dose PTX	0.709 $\pm$ 0.111 <sup>bd</sup>	0.644 $\pm$ 0.108 <sup>bd</sup>	0.654 $\pm$ 0.152 <sup>be</sup>
Low dose PTX	0.752 $\pm$ 0.152 <sup>cd</sup>	0.733 $\pm$ 0.117 <sup>cd</sup>	0.788 $\pm$ 0.147 <sup>cdg</sup>

<sup>a</sup> $P < 0.01$ , vs control group; <sup>b</sup> $P < 0.05$ , vs control group; <sup>c</sup> $P > 0.05$ , vs control group; <sup>d</sup> $P < 0.01$ , vs praziquantel group; <sup>e</sup> $P > 0.05$ , vs praziquantel group; <sup>f</sup> $P < 0.05$ , vs high dose PTX group; <sup>g</sup> $P < 0.01$ , vs high dose PTX group.

### Effects of PTX on collagen I expression

The contents of collagen I in praziquantel group, high dose PTX group and low dose PTX group decrease by 22.70 %, 16.47 %, 4.93 % respectively compared with control group. The difference between praziquantel group and control group is very significant ( $P < 0.01$ ). The effect of PTX on collagen I content is dose related and there is significant difference on collagen I contents between high and low dose groups. The collagen I content in high dose PTX group is significantly ( $P < 0.05$ ) different from that of control group while no significant difference between low dose PTX group and control group. Both high and low dose PTX groups have significant difference on collagen I contents between praziquantel group and themselves. The results are shown in Table 1.

### Effects of PTX on collagen III expression

The contents of collagen III in praziquantel group, high dose PTX group and low dose PTX group decrease by 25.43 %, 20.44 %, 4.14 % respectively compared with control group. The difference between praziquantel group and control group is very significant ( $P < 0.01$ ). The effect of PTX on collagen III content is dose related and there is significant difference on collagen III contents between high and low dose groups ( $P < 0.01$ ). The collagen III content in high dose PTX group is significantly ( $P < 0.05$ ) different from that of control group while no

significant difference between low dose PTX group and control group ( $P > 0.05$ ). Compared with praziquantel group, high dose PTX group has no difference on collagen III contents ( $P > 0.05$ ), whereas low dose PTX group has significant difference ( $P < 0.01$ ). The results are shown in Table 1.

## DISCUSSION

PTX is a trimethylated xanthine derivative product. As an inhibitor of phosphodiesterase, it can induce the increase of intracellular cAMP, dilation of the blood vessels and smooth muscles, ameliorating the microcirculation. It has been used to improve the peripheral blood vessel disease for many years<sup>[16,17]</sup>. Recently, PTX has been found to have antifibrosis effect. *In vitro* studies show that PTX can inhibit the proliferation of myofibroblast from hepatitis patients and depress the synthesis of collagen. Treatment with PTX in early stage can alleviate the hepatic lesion and inflammatory reaction<sup>[18]</sup>. In animal hepatic fibrosis models, PTX also has anti-fibrosis effect. It has been reported that treated with PTX prior to the inducing of hepatic fibrosis with CCL<sub>4</sub>-acetone can alleviate the proliferation of hepatic stellate cell (HSC), and previous treatment with PTX decelerate the differentiation of HSC in mouse with hepatic fibrosis induce by bile duct ligation<sup>[19]</sup>. It was reported that previous treatment with PTX could improve the regeneration and function of liver after partial hepatectomy in mice with hepatic fibrosis and alleviate the hepatic fibrosis. But there is no report on the effects of PTX on schistosomal hepatic fibrosis<sup>[20]</sup>. The fibrosis in schistosomal has its special characteristics against those caused by hepatic cell lesion or bile duct obstruction. Therefore, the effects of PTX in the schistosomal hepatic fibrosis should be explored.

Hepatic stellate cell (HSC) plays a pivotal role in the fiber synthesis and degradation. The activation of HSC is mediated by various cytokines and reactive oxygen species released from the damaged hepatocytes and activated Kupffer cells<sup>[21-26]</sup>. HSC can release TGF $\beta$ 1 by autocrine<sup>[27,28]</sup> and TGF $\beta$ 1 has been proved to be a strong mitogen to HSC. This autocrine effect is upgraded when HSC has been activated. TGF $\beta$ 1 depresses the regeneration of hepatic cells, activates and promotes HSC to synthesize extracellular matrix such as collagen, fibronectin, proteinopolysaccharide, promotes the synthesis of TIMP and inhibits the synthesis of MMPs<sup>[29-37]</sup>.

We established a mouse hepatic fibrosis model induced by cercaria of schistosomiasis japonica infection and studied the effect of PTX on the fibrosis development in the early stage. We found that PTX could inhibit the development of fibrosis in this model significantly. The quantitative immunohistochemical evaluation of TGF $\beta$ 1, type I and III collagens shows that, high dose of PTX can reduce the content of TGF $\beta$ 1, type I and III collagens in hepatic tissue of mice with schistosomal hepatic fibrosis. Its capability to reduce the hepatic content of type III collagen is similar to praziquantel ( $P > 0.05$ ) and its effects on TGF $\beta$ 1 and type I collagen are weaker than praziquantel. Compared with the control group, low dose of PTX can also reduce the contents of TGF $\beta$ 1, type I and III collagens but the effects have no statistical significance.

The results indicate that PTX treatment in the early stage inhibits the development of schistosomal hepatic fibrosis by reducing the content of TGF $\beta$ 1, type I and III collagens.

## REFERENCES

- 1 **Qing JP**, Jiang MD. Phenotype and regulation of hepatic stellate cell and liver fibrosis. *Shijie Huaren Xiaohua Zazhi* 2001; **9**: 801-804
- 2 **Dai WJ**, Jiang HC. Advances in gene therapy of liver cirrhosis: a review. *World J Gastroenterol* 2001; **7**: 1-8



- 3 **Wang GQ**, Lu HQ, Wang H, Kong XT, Zhong RQ, Huang C, Gao F. Effects of Decorin on collagen of hepatic stellate cells. *Xin Xiaohuabingxue Zazhi* 2001; **9**: 1395-1398
- 4 **Wang JY**, Guo JS, Yang CQ. Expression of exogenous rat collagenase *in vitro* and in a rat model of liver fibrosis. *World J Gastroenterol* 2002; **8**: 901-907
- 5 **Zhang YT**, Chang XM, Li X, Li HL. Effects of spironolactone on expression of type I/III collagen proteins in rat hepatic fibrosis. *Xin Xiaohuabingxue Zazhi* 2001; **9**: 1120-1124
- 6 **Jiang SL**, Yao XX, Sun YF. Therapy of liver fibrosis. *Shijie Huaren Xiaohua Zazhi* 2000; **8**: 684-686
- 7 **Okazaki I**, Watanabe T, Hozawa S, Niioka M, Arai M, Maruyama K. Reversibility of hepatic fibrosis: from the first report of collagenase in the liver to the possibility of gene therapy for recovery. *Keio J Med* 2001; **50**: 58-65
- 8 **Reis LF**, Ventura TG, Souza SO, Arana-Pino A, Pelajo-Machado M, Pereira MJ, Lenzi HL, Conceicao MJ, Takiya CM. Quantitative and qualitative interferences of pentoxifylline on hepatic *Schistosoma mansoni* granulomas: effects on extracellular matrix and eosinophil population. *Mem Inst Oswaldo Cruz* 2001; **96**: 107-112
- 9 **Raetsch C**, Jia JD, Boigk G, Bauer M, Hahn EG, Riecken EO, Schuppan D. Pentoxifylline downregulates profibrogenic cytokines and procollagen I expression in rat secondary biliary fibrosis. *Gut* 2002; **50**: 241-247
- 10 **Jiang HQ**, Zhang XL. Mechanism of liver fibrosis. *Shijie Huaren Xiaohua Zazhi* 2000; **8**: 687-689
- 11 **Kanzler S**, Baumann M, Schirmacher P, Dries V, Bayer E, Gerken G, Dienes HP, Lohse AW. Prediction of progressive liver fibrosis in hepatic C infection by serum and tissue levels of transforming growth factor-beta. *J Viral Hepat* 2001; **8**: 430-437
- 12 **Chen WX**, Li YM, Yu CH, Cai WM, Zheng M, Chen F. Quantitative analysis of transforming growth factor beta1 mRNA in patients with alcoholic liver disease. *World J Gastroenterol* 2002; **8**: 379-381
- 13 **Kmiec Z**. Cooperation of liver cells in health and disease. *Adv Anat Embryol Cell Biol* 2001; **161**: 1-151
- 14 **Du WD**, Zhang YE, Zhai WR, Zhou XM. Dynamic changes of type I,III and IV collagen synthesis and distribution of collagen-producing cells in carbon tetrachloride-induced rat liver fibrosis. *World J Gastroenterol* 1999; **5**: 397-403
- 15 **Bissell DM**. Chronic liver injury, TGF-beta, and cancer. *Exp Mol Med* 2001; **33**: 179-190
- 16 **Schuppan D**, Koda M, Bauer M, Hahn EG. Fibrosis of liver, pancreas and intestine: common mechanisms and clear targets? *Acta Gastroenterol Belg* 2000; **63**: 366-370
- 17 **Windmeier C**, Gressner AM. Pharmacological aspects of pentoxifylline with emphasis on its inhibitory actions on hepatic fibrogenesis. *Gen Pharmacol* 1997; **29**: 181-196
- 18 **Preaux AM**, Mallat A, Rosenbaum J, Zafrani ES, Mavrier P. Pentoxifylline inhibits growth and collagen synthesis of cultured human hepatic myofibroblast-like cells. *Hepatology* 1997; **26**: 315-322
- 19 **Desmouliere A**, Xu G, Costa AM, Yousef LM, Gabbiani G, Tuchweber B. Effects of pentoxifylline on early proliferation and phenotypic modulation of fibrogenic cells in two rat models of liver fibrosis and on cultured hepatic stellate cells. *J Hepatol* 1999; **30**: 621-631
- 20 **Moser M**, Zhang M, Gong Y, Johnson J, Kneteman N, Minuk GY. Effects of preoperative interventions on outcome following liver resection in a rat model of cirrhosis. *J Hepatol* 2000; **32**: 287-292
- 21 **Wu J**, Zern MA. Hepatic stellate cells: a target for the treatment of liver fibrosis. *J Gastroenterol* 2000; **35**: 665-672
- 22 **Reeves HL**, Friedman SL. Activation of hepatic stellate cells-a key issue in liver fibrosis. *Front Biosci* 2002; **7**: D808-826
- 23 **Tsukamoto H**. Cytokine regulation of hepatic stellate cells in liver fibrosis. *Alcohol Clin Exp Res* 1999; **23**: 911-916
- 24 **Battaller R**, Brenner DA. Hepatic stellate cells as a target for the treatment of liver fibrosis. *Semin Liver Dis* 2001; **21**: 437-451
- 25 **Beljaars L**, Meijer DK, Poelstra K. Targeting hepatic stellate cells for cell-specific treatment of liver fibrosis. *Front Biosci* 2002; **7**: e214-222
- 26 **Wu J**, Zern MA. Hepatic stellate cells: a target for the treatment of liver fibrosis. *J Gastroenterol* 2000; **35**: 665-672
- 27 **Liu T**, Hu JH, Cai Q, Ji YP. The signal transducing molecular in HSC. *Shijie Huaren Xiaohua Zazhi* 2001; **9**: 805-807
- 28 **Huang GC**, Zhang JS. Activated *in vivo* signal transduction of HSC. *Xin Xiaohuabingxue Zazhi* 2001; **9**: 1056-1060
- 29 **Dooley S**, Delvoux B, Streckert M, Bonzel L, Stopa M, Ten Dijke P, Gressner AM. Transforming growth factor beta signal transduction in hepatic stellate cells via Smad2/3 phosphorylation, a pathway that is abrogated during *in vitro* progression to myofibroblasts. TGFbeta signal transduction during transdifferentiation of hepatic stellate cells. *FEBS Lett* 2001; **502**: 1-3
- 30 **Garcia-Trevijano ER**, Iraburu MJ, Fontana L, Dominguez-Rosales JA, Auster A, Covarrubias-Pinedo A, Rojkind M. Transforming growth factor beta1 induces the expression of alpha1(I) procollagen mRNA by a hydrogen peroxide-C/EBPbeta-dependent mechanism in rat hepatic stellate cells. *Hepatology* 1999; **29**: 960-970
- 31 **Yata Y**, Gotwals P, Koteliansky V, Rockey DC. Dose-dependent inhibition of hepatic fibrosis in mice by a TGF-beta soluble receptor: implications for antifibrotic therapy. *Hepatology* 2002; **35**: 1022-1030
- 32 **Tahashi Y**, Matsuzaki K, Date M, Yoshida K, Furukawa F, Sugano Y, Matsushita M, Himeno Y, Inagaki Y, Inoue K. Differential regulation of TGF-beta signal in hepatic stellate cells between acute and chronic rat liver injury. *Hepatology* 2002; **35**: 49-61
- 33 **Okuno M**, Akita K, Moriwaki H, Kawada N, Ikeda K, Kaneda K, Suzuki Y, Kojima S. Prevention of rat hepatic fibrosis by the protease inhibitor, camostat mesilate, via reduced generation of active TGF-beta. *Gastroenterology* 2001; **120**: 1784-1800
- 34 **Breitkopf K**, Lahme B, Tag CG, Gressner AM. Expression and matrix deposition of latent transforming growth factor beta binding proteins in normal and fibrotic rat liver and transdifferentiating hepatic stellate cells in culture. *Hepatology* 2001; **33**: 387-396
- 35 **Suzuki C**, Kayano K, Uchida K, Sakaida I, Okita K. Characteristics of the cell proliferation profile of activated rat hepatic stellate cells *in vitro* in contrast to their fibrogenesis activity. *J Gastroenterol* 2001; **36**: 322-329
- 36 **Liu F**, Liu JX. The role of transforming growth factor beta1 in liver fibrosis. *Shijie Huaren Xiaohua Zazhi* 2000; **8**: 86-88
- 37 **Preaux AM**, Mallat A, Nhieu JT, D'ortho MP, Hembry RM, Mavrier P. Matrix metalloproteinase-2 activation in human hepatic fibrosis regulation by cell-matrix interactions. *Hepatology* 1999; **30**: 944-950

Edited by Ren SY

# Effects of Tetrandrine and QYT on ICAM-1 and SOD gene expression in pancreas and liver of rats with acute pancreatitis

Yong-Yu Li, Xue-Li Li, Cui-Xiang Yang, Hong Zhong, Hong Yao, Ling Zhu

**Yong-Yu Li, Hong Zhong, Hong Yao, Ling Zhu**, Department of Pathophysiology, Medical College of Tongji University, Shanghai 200331, China

**Xue-Li Li, Cui-Xiang Yang**, Department of Biochemistry, Medical College of Tongji University, Shanghai 200331, China

**Supported by** the National Natural Scientific Foundation of China, No. 30060031

**Correspondence to:** Yong-Yu Li, M.D., Professor of Pathophysiology, Department of Pathophysiology, Medical College of Tongji University, Shanghai 200331, China. liyyu@163.net

**Telephone:** +86-21-51030563

**Received:** 2002-09-13 **Accepted:** 2002-10-21

## Abstract

**AIM:** Available experimental evidence from both clinical and animal models shows that both Chinese medicines tetrandrine (Tet) and Qing Yi Tong (QYT) have positive treatment effects on acute pancreatitis (AP). This investigation was conducted to explore the treatment mechanisms of Tet and QYT on AP at the molecular level and thereby explain their therapeutic affects. It included an investigation of the effects of these drugs on gene expression of both intercellular adhesion molecule 1 (ICAM-1) and superoxide dismutase (Mn-SOD and Cu, Zn-SOD) in a rat model with AP.

**METHODS:** AP in the test rats was induced by subjecting them to laparotomy followed by a retrograde injection of 4 % sodium taurocholate into the bilio-pancreatic duct. The test rats with AP were divided into three groups. One was treated with Tet, one with QYT, and one with normal saline solution. The sham-operated control group (SO) rats were only subjected to laparotomy. They were given no further treatment. For the Tet group, Tet was injected intraperitoneally, and for the QYT group, QYT was given with a nose-gastric catheter. These procedures were done at both 10 min and 5 h after AP induction. The levels of ICAM-1 mRNA expression and of SOD (Mn-SOD and Cu, Zn-SOD) mRNA expression in the pancreas and liver tissues were measured by RT-PCR at 1, 5, and 10 h after AP induction.

**RESULTS:** When compared with the SO group during the observation time, rats with AP showed a higher expression of ICAM and a lower expression of Mn-SOD in both pancreas and liver tissues, and a lower expression of Cu, Zn-SOD in the pancreas. Tet treatment attenuated changes in the expression of both ICAM-1, and SOD (Mn-SOD and Cu, Zn-SOD) to a significant degree. A similar effect on the expression of SOD (Mn-SOD and Cu, Zn-SOD) was also found in the QYT group, but no obvious suppressive effect on ICAM-1 expression was observed.

**CONCLUSION:** The results of this study suggest that one of the main mechanisms of Tet and QYT in treating AP is to enhance anti-oxidation of the body. The results also suggest that the anti-inflammatory effect of Tet is involved in the reduction of ICAM-1 expression. This explains why Tet and QYT are beneficial in treating AP.

Li YY, Li XL, Yang CX, Zhong H, Yao H, Zhu L. Effects of Tetrandrine and QYT on ICAM-1 and SOD gene expression in pancreas and liver of rats with acute pancreatitis. *World J Gastroenterol* 2003; 9(1): 155-159

<http://www.wjgnet.com/1007-9327/9/155.htm>

## INTRODUCTION

Acute pancreatitis (AP) is a severe disease with both high morbidity and high mortality. Therefore, much research has been focused on the specific and effective therapies for AP<sup>[1-6]</sup>. Tetrandrine (Tet) is a kind of dibenzyl quinoline alkaloid extracted from the root of *Stephania tetrandra* S., a Chinese herbal medicine. Qing Yi Tang (QYT) is a medicine composed of several Chinese herbs. Both Tet and QYT have shown positive treatment effects on AP clinical patients and on animal models. These include attenuation of clinical symptoms, improvement of morphology and biochemistry changes in the tissues and blood, prolongation of survival time, and decrease of mortality<sup>[7-10]</sup>. In order to explore some of the molecular mechanisms combating AP, the effects of Tet and QYT on gene expression of both intercellular adhesion molecule 1 (ICAM-1) and superoxide dismutase (Mn-SOD and Cu, Zn-SOD) were investigated in a rat model with AP.

## MATERIALS AND METHODS

### Chemicals

Chemicals used in this experiment were purchased as follows: Sodium pentobarbital and sodium taurocholate (NaTc) from Shanghai Chemical Reagent Company; TRIzol reagent and Superscript<sup>TM</sup> II from GIBCO-BRL (Shanghai); Oligonucleotide primer pairs from Chinese Academy of Science, Institute of Cell and Biology (Shanghai); Taq DNA polymerase from Promega (Shanghai); Tet from the Department of Pharmacology of Second Military Medical University (Shanghai); QYT from Zunyi Medical College (Zunyi); other reagents from Sigma Chemical (Shanghai).

### Animals and AP model

The subjects for the experiment were adult male and female Sprague-Dawley rats weighing 170-230 g ( $n=36$ ; the Animal Center, Fudan University Medical College, Shanghai). After fasting with free access to water overnight, the rats were anesthetized by an intraperitoneal (ip) injection of 40 mg/kg sodium pentobarbital. AP was induced by a retrograde injection of 4 % NaTc into the bilio-pancreatic duct (BPD) according to the method of Aho *et al*<sup>[11]</sup>. Briefly, a small median laparotomy was performed first, and then the pancreas was exteriorized and the BPD was temporarily closed at the liver hilum with a soft microvascular clamp to prevent reflux of the infused material into the liver. A retrograde injection of 4 % NaTc into the distal BPD was then given (100  $\mu$ l/100body wt, pressure 50cmH<sub>2</sub>O). The clamp was removed 5 min after the injection. In the sham-operated control group (SO) rats only underwent laparotomy. Finally, the abdomen was closed with a silk suture and the rats were placed back into their cages with free access to water and food.

### Animal group

The test rats with AP were divided into three groups: Tet, QYT and normal saline (NS). The Tet group ( $n=9$ ) received an injection (ip) of 4 % Tet at a dosage of 80 mg/kg body wt. The QYT group ( $n=9$ ) received an infusion of QYT (1 ml/100 g body wt), and the NS group ( $n=9$ ) received an infusion of NS (1 ml/100 g body wt), by use of a nose-gastric catheter. Rats in the SO group received the same infusion as the NS group. All groups were treated two times (at 10 min and 5 h after the AP operation).

### Preparation of RNA and RT-PCR assay

At selected times (1,5,10 h) after the AP induction or sham operation, the rats ( $n=3$  at each time point) underwent relaparotomy under pentobarbital anesthesia, and samples of the pancreas and liver were rapidly collected. Total RNA was extracted from pancreatic and liver tissues using the TRIzol reagent. RNA quality was verified by ethidium bromide staining of ribosomal RNA bands on agarose gel. Total RNA was precipitated and re-suspended in diethylpyrocarbonate-treated sterile  $H_2O$ , quantified by spectrophotometry (A260/A280 ratio  $>1.80$ ) and diluted to a concentration of 1.0  $\mu\text{g}/\mu\text{l}$ . Then the extracted RNA was used for a semi-quantitative reverse transcription-polymerase chain reaction (RT-PCR). Total RNA (5  $\mu\text{g}/\text{sample}$ ) was reverse-transcribed using oligo (dT) as a primer. The oligonucleotide primer pairs were designed from published sequences for each gene studied. The sequences used as G3PDH, SOD and ICAM-1 specific primers are shown in Table 1.

**Table 1** Sequence of primers and length of fragments

Gene	Primer (5' → 3')	Length
G3PDH	ACCACAGTCCATGCCATCAC	452 bp
	TCCACCACCCTGTTGCTGTA	
Mn-SOD	ATTAACGCGCAGATCATGCAG	483 bp
	TTTCAGATAGTCAGGTCTGACGTT	
CuZn-SOD	TTCGAGCAGAAGGCAAGCGGTGAA	396 bp
	AATCCCAATCACACCACAAGCCAA	
ICAM-1	CCTTAGGAAGGTGTGATATCCGG	415 bp
	AGGTGGTCACCCATGCTGGTGCT	

Two-microliter aliquots of cDNA were used as a target for separate PCR reactions in the presence of 0.5 units of Taq DNA polymerase, 50  $\mu\text{mol/L}$  of a primer pair specific for G3PDH, SOD or ICAM-1, and amounts of the corresponding constructs. The total volume of the reaction fluid was 25  $\mu\text{l}$ .

The amplification cycles were carried out in a DNA Thermalcycler (Perkin Elmer) under the following conditions: initial denaturation at 94 for 2 min, followed by amplification cycles of 1min at 94  $^{\circ}\text{C}$ , 1min at 58  $^{\circ}\text{C}$  and 1 min at 72  $^{\circ}\text{C}$ . This procedure was repeated for 30 cycles. PCR products were separated by polyacrylamide gel electrophoresis and then visualized by ethidium bromide staining. The intensities of gene-specific bands were photographed and quantified by measuring the optical density (OD) of the bands in a UVP (white/UV transilluminator, GDS 7500). In the same sample, mRNA levels were normalized to the density of an internal control housekeeping gene RT-PCR product, glyceraldehyde-3-phosphate dehydrogenase (G3PDH), which is commonly used as an internal standard control in mRNA expression studies. RT-PCR was performed independently at least twice starting from the same RNA.

### Statistical analysis

Data were expressed as mean  $\pm$  SE. Statistical differences between values from two groups were determined by the unpaired Student's *t*-test and statistical significance was set at  $P<0.05$ .

## RESULTS

### G3PDH level

The level of G3PDH was approximately the same for all pancreas and liver samples tested (Figure 1), which indirectly showed that the cDNA concentration did not differ in the samples from each group.

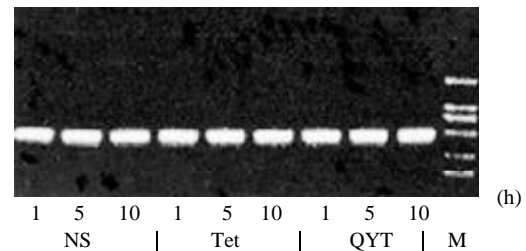


**Figure 1** GAPDH mRNA expression in the liver in the parts of different group.

### ICAM-1 mRNA expression in the pancreas and liver

Semi-quantitative evaluation of ICAM-1 level was obtained by measuring its gene expression by RT-PCR. As shown in Figure 2 and Figure 2B, the pancreas showed an increased ICAM-1 mRNA expression in the NS group at 5 h and 10 h after AP induction when compared to the SO group. Tet attenuated the increase at the same time-points. But QYT showed an increase effect for ICAM-1 mRNA expression at 10 h after AP. In the liver, compared with the SO group, the level of ICAM-1 mRNA expression in the NS group was elevated at 1 h and sustained up to 10 h, with a maximum increase (2-fold) at 5 h after AP induction. A similar change but at a lower level was observed in the Tet group. And in the QYT group a modest increase of ICAM mRNA expression occurred only at 5 h and 10 h after AP induction. (Figure 3 and Figure 3B).

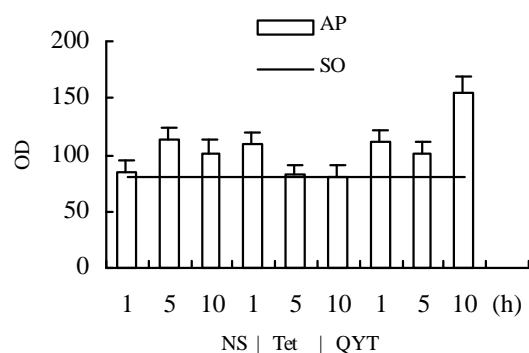


**Figure 2A** ICAM-1 mRNA expression in the pancreas in the different groups.

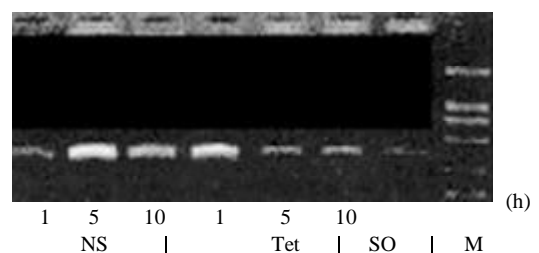


**Figure 2B** ICAM-1 mRNA expression in the pancreas in the different groups.

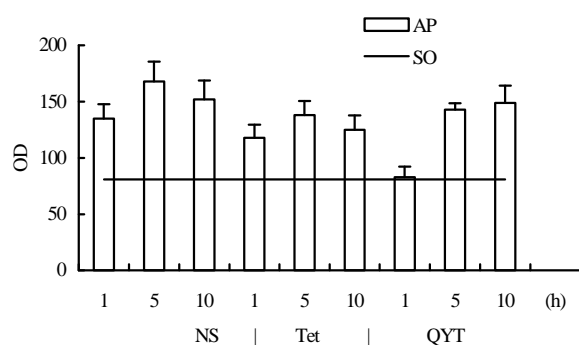


**Figure 3A** ICAM-1 mRNA expression in the liver in the different groups.

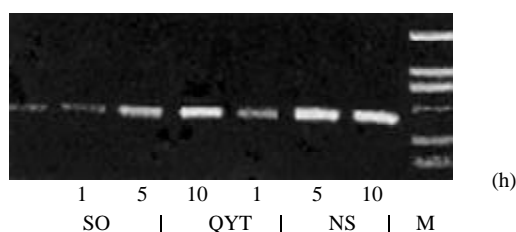


**Figure 3B** ICAM-1 mRNA expression in the liver in the parts of different groups.

#### *Mn-SOD mRNA expression in the pancreas and liver*

As shown in Figure 4 and Figure 4B, in the pancreas, compared to the SO group, Mn-SOD mRNA expression in the NS group was lower from 1 h to 5 h after AP induction. The Tet-treated group had a higher expression at the same time-points, and the QYT-treated group had a much higher expression at 10 h, nearly a 2-fold increase compared to that of the NS group. As shown in Figure 5 and Figure 5B, the NS group showed a similar decrease of Mn-SOD mRNA expression in the liver to that in the pancreas at 1 h and 5 h. When compared to the NS group, the Tet-treated group had a higher Mn-SOD mRNA expression from 1 h to 10 h, and the QYT group had a higher Mn-SOD mRNA expression from 5 h to 10 h, after AP induction.

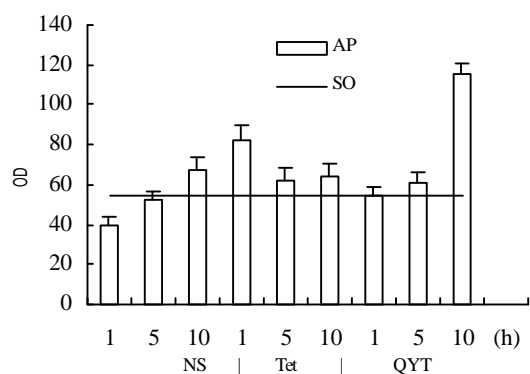


**Figure 4A** Mn-SOD mRNA expression in the pancreas in the different groups.

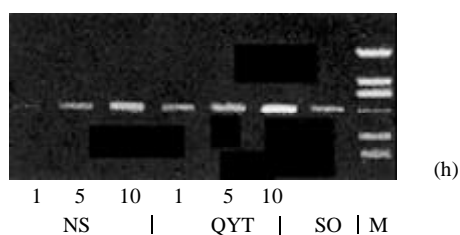


**Figure 4B** Mn-SOD mRNA expression in the pancreas in the parts of different groups.

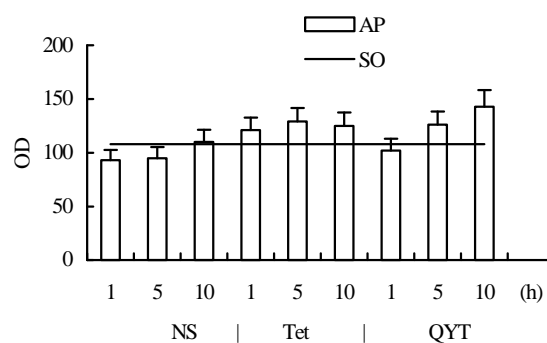


**Figure 5A** Mn-SOD mRNA expression in the liver in the different groups.

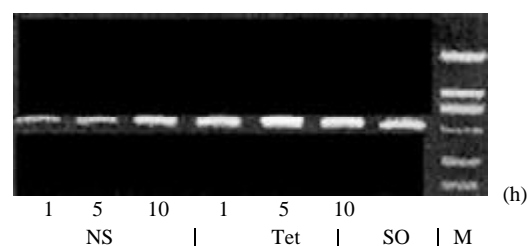


**Figure 5B** Mn-SOD mRNA expression in the liver in the parts of different groups.

#### *Cu,Zn-SOD mRNA expression in the pancreas and the liver*

As shown in Figure 6 and Figure 6B, in the pancreas, the NS group decreased significantly in Cu, Zn-SOD mRNA expression after AP induction to 1/3 of that in SO group. The Tet and QYT-treated groups had much higher levels of Cu, Zn-SOD mRNA expression at 1 h and 10 h respectively. These high levels were a 2-fold increase when compared with the SO group, and a 4-fold increase when compared with the NS group at the same time points. In the liver, no obvious changes of SOD expression were observed (Figure 7).

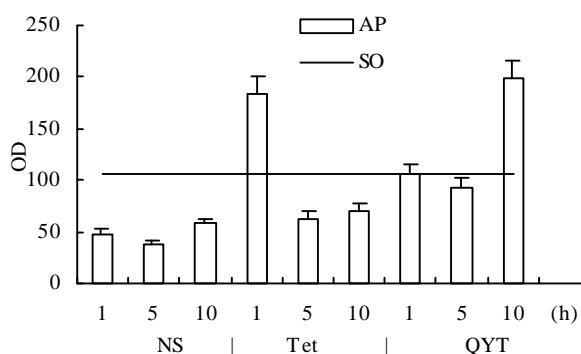


**Figure 6A** Cu, Zn-SOD mRNA expression in the pancreas in the different groups.

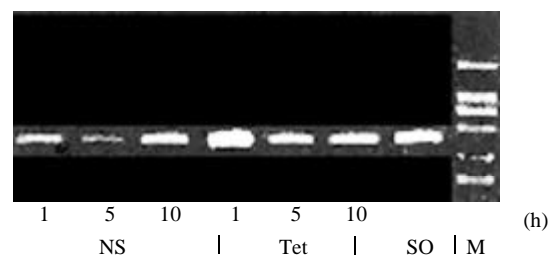


**Figure 6B** Cu, Zn-SOD mRNA expression in the pancreas in the parts of different groups.

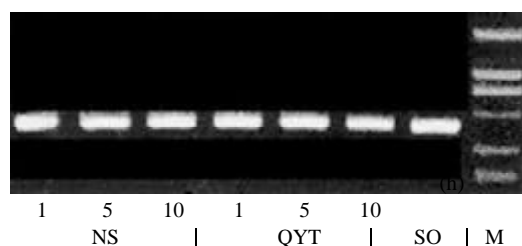


**Figure 7** Cu, Zn-SOD mRNA expression in the liver in the parts of different groups.

## DISCUSSION

Research on AP can be traced back at least one hundred years, yet the treatment of AP continues to be a difficult aspect of clinical practice, especially for severe acute pancreatitis (SAP). SAP is recognized to be a multiple-stage disease where the pathological events at the pancreatic acinar cell level are paralleled by an exaggerated local and systemic inflammatory response (SIRS), and even by multiple-organ damage (MODS) or failure (MOF), with a high mortality<sup>[12-15]</sup>. Considerable progress in understanding of pathophysiologic events during the early stage of AP has been made over the years, but the underlying pathogenic processes responsible for the inflammatory cascade and MOF are still unknown to a large extent. Most recent studies have revealed that the excessive releases of oxygen-derived free radicals (OFRs), destructive inflammatory mediators and cytokines, such as TNF- $\alpha$ , IL-1 $\beta$ , IL-6, IL-8, IL-10, PAF, ICAM-1, play key roles in the AP process<sup>[16-19]</sup>. Recent evidence suggests that, besides their directly detrimental effects on AP, OFRs may activate certain gene transcription factors, notably the nuclear transcription factor-kappa B (NF- $\kappa$ B) and activator protein-1 (AP-1), which then mediate the induction of certain adhesion molecules (ICAM, VCAM, etc.) and other cytokines<sup>[15,20-23]</sup>. These factors prompt neutrophil aggregation, adherence and activation, then tremendous amounts of inflammatory mediators and cytokines are released. The pancreas and remote organs are then severely injured and MOF occurs. Meanwhile, activation of leukocyte may release more OFRs, and the vicious circle continues<sup>[24-27]</sup>.

The manganese superoxide dismutase (Mn-SOD) and copper/zinc superoxide dismutase (Cu, Zn-SOD) existing in the mitochondria or cytoplasm of cells are the major OFR scavengers of the body. Previous experiments have demonstrated that the pathological changes in AP could be reduced by SOD<sup>[28,29]</sup>. By immunohistochemistry, Su *et al* have proved the localization of SOD in acinar cells and have found Mn-SOD mRNA expression peaked at 2 hours after the addition of arginine to the cell culture medium<sup>[30]</sup>. These data suggest that increased SOD expression reflects a defensive mechanism of acinar cells against oxidative stress. G. Teleck *et al* discovered that the increase of OFRs and ICAM expression could be measured within one hour and lasted for the 24 hour observation period<sup>[31]</sup>. These findings, along with others from different laboratories, suggest that OFRs and ICAM induce morphologic change, aggregation, adherence, and activation of polymorphonuclears (PMNs), which then shift out of blood vessels and consequently cause microcirculation dysfunction<sup>[32,33]</sup>. Our experimental results showed that during the process of AP, the expression of ICAM-1 in both the pancreas and the liver (especially in liver) was significantly increased, while the expressions of Mn-SOD and Cu-Zn-SOD were decreased in the pancreas by 1/3 as compared to the SO control group. This was similar to the finding of the experiment by L. Czako *et al*<sup>[28]</sup>. These results provide further evidence that the increased ICAM-1 and decreased OFRs scavengers take part in the

pathophysiologic processes of AP.

Tet is a kind of dibenzyl quinoline alkaloid extracted from the root of *Stephania tetrandra* S., a Chinese herbal medicine with the effect of a non-selective calcium channel blocker (CCB). It has recently been found that Tet also has a widely anti-inflammatory effect by reducing the activity of PLA2 from inflammatory leukocytes, inhibiting the release of inflammatory mediators, eliminating OFRs and dilating blood vessels, and then improving microcirculation function of the body<sup>[7,8,34,35]</sup>. QYT is a combined medication of Chinese herbs containing *Rheum officinale* Baillon, *ructus gardeniae*, etc., and also has the effects of anti-inflammation, cleaning OFRs, eliminating hazardous metabolite, dilating blood vessels and improving microcirculation<sup>[9,10]</sup>. We found in this experiment that Tet reduced ICAM expression in the pancreatic and hepatic tissues during AP, while increasing the expression of Mn-SOD, and Cu, Zn-SOD. QYT had no significant effect on the expression of ICAM-1, but significantly enhanced the expression of Mn-SOD, and Cu, Zn-SOD. These findings suggest that Tet and QYT demonstrate the potentially useful effects of eliminating OFRs and reducing their damage, and also demonstrate the ability of Tet inhibiting ICAM production. The experiment provided a molecular level explanation of why clinical treatment of AP using Tet and QYT has been successful.

It is generally recognized that the induction of AP follows a uniform mechanism independent of different etiologic causes such as gallstones, alcohol, ischemia, hyperlipidemia, hypercalcemia, heredity and others. Firstly, each cause seems to affect primarily the acinar cell, resulting in intracellular activation of trypsinogen and other digestive enzymes and over-production of OFRs, which injure the acinar cells and pancreatic tissue. Then tremendous amounts of inflammatory mediators and cytokines, mentioned above, are released into the tissue and result in microcirculation disturbance. This not only worsens the local damage, but also influences the remote organs and causes systemic inflammatory response syndrome (SIRS). In the final stage of the pathophysiological process, multi-organ damage develops and multi-organ failure (MOF) may happen due to the combined effects of all the factors. Klar *et al* pointed out<sup>[36]</sup> that since the initial enzyme activation and cytokine release were irreversible by the time of clinical presentation, specific therapy must be directed towards microperfusion failure as a secondary pathogenic stage. The beneficial therapeutic principles of this included the inhibition of leukocyte-endothelium interaction with ICAM-1 antibodies and the control of local vasoconstriction to stop the progression of the disease. Therefore, based on previously observed clinical effects and on the experimental results with Tet and QYT in this study, we conclude that Tet and QYT which inhibit ICAM-1 and enhance SOD expression are beneficial in treating AP.

## REFERENCES

- 1 Slavín J, Ghaneh P, Sutton R, Hartley M, Rowlands P, Garvey C, Hughes M, Neoptolemos J. Management of necrotizing pancreatitis. *World J Gastroenterol* 2001; **7**: 476-481
- 2 Masamune A, Shimosegawa T, Satoh A, Fujita M, Sakai Y, Toyota T. Nitric oxide decreases endothelial activation by rat experimental severe pancreatitis-associated ascitic fluids. *Pancreas* 2000; **20**: 297-304
- 3 Hughes CB, el-Din AB, Kotb M, Gaber LW, Gaber AO. Calcium channel blockade inhibits release of TNF alpha and improves survival in a rat model of acute pancreatitis. *Pancreas* 1996; **13**: 22-28
- 4 Eibl G, Buhr HJ, Foitzik T. Therapy of microcirculatory disorders in severe acute pancreatitis: what mediators should we block? *Intensive Care Med* 2002; **28**: 139-146
- 5 Rau B, Bauer A, Wang A, Gansauge F, Weidenbach H, Nevalainen T, Poch B, Beger HG, Nussler AK. Modulation of

- endogenous nitric oxide synthase in experimental acute pancreatitis: role of anti-ICAM-1 and oxygen free radical scavengers. *Ann Surg* 2001; **233**: 195-203
- 6 **Deng Q**, Wu C, Li Z. The prevention of infection complicating acute necrotizing pancreatitis: an experimental study. *Zhonghua Waike Zazhi* 2000; **38**: 625-629
  - 7 **Leng DY**, Yu J, Luo JR, Yu JB. Tet was used in the treatment of patients with severe acute pancreatitis. *Dangdai Yishi* 1997; **2**: 59-60
  - 8 **Zhang H**, Li YY. Therapeutic effect of Tetrandrine on experimental acute pancreatitis. *Zunyi Xueyuan Xuebao* 2000; **23**: 91-95
  - 9 **Li ZL**, Wu CT, Lu LR, Zhu XF, Xiong DX. Traditional Chinese medicine Qing Yi Tang alleviates oxygen free radical injury in acute necrotizing pancreatitis. *World J Gastroenterol* 1998; **4**: 357-359
  - 10 **Wu C**, Li Z, Xiong D. An experimental study on curative effect of Chinese medicine qing yi tang in acute necrotizing pancreatitis. *Zhongguo Zhongxiyi Jiehe Zazhi* 1998; **18**: 236-238
  - 11 **Aho HJ**, Koskensalo SM, Nevelainen TJ. Experimental pancreatitis in the rat. Sodium taurocholate-induced acute haemorrhagic pancreatitis. *Scand J Gastroenterol* 1980; **15**: 411-416
  - 12 **Zhang H**, Li YY. The study progresses on the mechanisms of pancreatitis. *Zhongguo Weizhongbing Jijiu Yixue* 2000; **12**: 116-119
  - 13 **Li YY**, Zhang H. The pathogenesis role of intracellular calcium overload in acute pancreatitis. *Zhongguo Zhongxiyi Jiehe Waike Zazhi* 2001; **7**: 123-125
  - 14 **Li YY**, Gao ZF. The possible role of nuclear factor-kB in the pathogenesis of acute pancreatitis. *Shijie Huaren Xiaohua Zazhi* 2001; **9**: 420-421
  - 15 **Wu XZ**. Therapy of acute severe pancreatitis awaits further improvement. *World J Gastroenterol* 1998; **4**: 285-286
  - 16 **Telek G**, Regoly-Merei J, Kovacs GC, Simon L, Nagy Z, Hamar J, Jakab F. The first histological demonstration of pancreatic oxidative stress in human acute pancreatitis. *Hepatogastroenterology* 2001; **48**: 1252-1258
  - 17 **Bhatia M**, Neoptolemos JP, Slavin J. Inflammatory mediators as therapeutic targets in acute pancreatitis. *Curr Opin Investig Drugs* 2001; **2**: 496-501
  - 18 **Menger MD**, Plusczyk T, Vollmar B. Microcirculatory derangements in acute pancreatitis. *J Hepatobiliary Pancreat Surg* 2001; **8**: 187-194
  - 19 **Bhatia M**, Brady M, Shokuhi S, Christmas S, Neoptolemos JP, Slavin J. Inflammatory mediators in acute pancreatitis. *J Pathol* 2000; **190**: 117-125
  - 20 **Blanchard JA 2nd**, Barve S, Joshi-Barve S, Talwalker R, Gates LK Jr. Antioxidants inhibit cytokine production and suppress NF-kappaB activation in CAPAN-1 and CAPAN-2 cell lines. *Dig Dis Sci* 2001; **46**: 2768-2772
  - 21 **Vaquero E**, Gukovsky I, Zaninovic V, Gukovskaya AS, Pandol SJ. Localized pancreatic NF-kappaB activation and inflammatory response in taurocholate-induced pancreatitis. *Am J Physiol Gastrointest Liver Physiol* 2001; **280**: G1197-1208
  - 22 **Jaffray C**, Yang J, Carter G, Mendez C, Norman J. Pancreatic elastase activates pulmonary nuclear factor kappa B and inhibitory kappa B, mimicking pancreatitis-associated adult respiratory distress syndrome. *Surgery* 2000; **128**: 225-231
  - 23 **Han B**, Logsdon CD. Cholecystokinin induction of mob-1 chemokine expression in pancreatic acinar cells requires NF-kappaB activation. *Am J Physiol* 1999; **277**: C74-82
  - 24 **Chang CK**, Albarillo MV, Schumer W. Therapeutic effect of dimethyl sulfoxide on ICAM-1 gene expression and activation of NF-kB and Ap-1 in septic rats. *J Surg Res* 2001; **95**: 181-187
  - 25 **Yeh LH**, Kinsey AM, Chatterjee S, Alevriadou BR. Lactosylceramide mediates shear-induced endothelial superoxide production and intercellular adhesion molecule-1 expression. *J Vasc Res* 2001; **38**: 551-559
  - 26 **Zaninovic V**, Gukovskaya AS, Gukovsky I, Mouria M, Pandol SJ. Cerulein upregulates ICAM-1 in pancreatic acinar cells, which mediates neutrophil adhesion to these cells. *Am J Physiol Gastrointest Liver Physiol* 2000; **279**: G666-676
  - 27 **Jaffray C**, Yang J, Norman J. Elastase mimics pancreatitis-induced hepatic injury via inflammatory mediators. *J Surg Res* 2000; **90**: 95-101
  - 28 **Czako L**, Takacs T, Varga IS, Tiszlavicz L, Hai DQ, Hegyi P, Matkovics B, Lonovics J. Oxidative stress in distant organs and the effects of allopurinol during experimental acute pancreatitis. *Int J Pancreatol* 2000; **27**: 209-216
  - 29 **Rau B**, Poch B, Gansauge F, Bauer A, Nussler AK, Nevalainen T, Schoenberg MH, Beger HG. Pathophysiologic role of oxygen free radicals in acute pancreatitis: initiating event or mediator of tissue damage. *Ann Surg* 2000; **231**: 352-360
  - 30 **Su SB**, Motoo Y, Xie MJ, Mouri H, Asayama K, Sawabu N. Superoxide dismutase is induced during rat pancreatic acinar cell injury. *Pancreas* 2002; **24**: 146-152
  - 31 **Telek G**, Ducroc R, Scoazec JY, Pasquier C, Feldmann G, Roze C. Differential upregulation of cellular adhesion molecules at the sites of oxidative stress in experimental acute pancreatitis. *J Surg Res* 2001; **96**: 56-67
  - 32 **Zhou ZG**, Chen YD, Sun W, Chen Z. Pancreatic microcirculatory impairment in experimental acute pancreatitis in rats. *World J Gastroenterol* 2002; **8**: 933-936
  - 33 **Masamune A**, Shimosegawa T, Kimura K, Fujita M, Sato A, Koizumi M, Toyota T. Specific induction of adhesion molecules in human vascular endothelial cells by rat experimental pancreatitis-associated ascitic fluids. *Pancreas* 1999; **18**: 141-150
  - 34 **Jiang JM**, Dai DZ. The study progress for tetrandrine-a calcium channel blocker. *Zhongguo Yaolixue Tongbao* 1998; **14**: 297-300
  - 35 **Zhang H**, Li YY. Therapeutic effect of tetrandrine on pancreas and lung injury in rats with experimental acute pancreatitis. *Tongji Daxue Xuebao (Yixue Branch)* 2002; **23**: 363-367
  - 36 **Klar E**, Werner J. New pathophysiologic knowledge about acute pancreatitis. *Chirurg* 2000; **71**: 253-264

Edited by Zhang JZ

• ESOPHAGEAL CANCER •

# Alterations of p53 and PCNA in cancer and adjacent tissues from concurrent carcinomas of the esophagus and gastric cardia in the same patient in Linzhou, a high incidence area for esophageal cancer in northern China

Hong Chen, Li-Dong Wang, Mei Guo, She-Gan Gao, Hua-Qin Guo, Zong-Min Fan, Ji-Lin Li

**Hong Chen, Li-Dong Wang, She-Gan Gao, Zong-Min Fan, Hua-Qin Guo**, Laboratory for Cancer Research, College of Medicine, Zhengzhou University, Zhengzhou, Henan Province, 450052, China  
**Mei Guo**, Anyang City Tumor Hospital, Anyang, Henan Province, 455000, China

**Ji-Lin Li**, Yaocun Esophageal Hospital of, Anyang, Henan Province, 456592, China

**Supported by** National Outstanding Young Scientist Award of China, No.30025016 and Foundation of Henan Education Committee

**Correspondence to:** Li-Dong Wang, Laboratory for Cancer Research, College of Medicine, Zhengzhou University, Zhengzhou 450052, Henan Province, China. ldwang@371.net

**Telephone:** +86-371-6970165 **Fax:** +86-371-6970165

**Received:** 2002-07-23 **Accepted:** 2002-08-07

## Abstract

**AIM:** To characterize the alteration and significance of p53 and PCNA in cancer and adjacent tissues of concurrent cancers from the esophagus and gastric cardia in the same patient.

**METHODS:** P53 and PCNA protein accumulation in 25 patients with concurrent cancers from the esophagus and gastric cardia (CC, concurrent carcinomas of esophageal squamous cell carcinoma and gastric cardia adenocarcinoma) were detected by immunohistochemical method (ABC).

**RESULTS:** In CC patients, both esophageal squamous cell carcinoma (SCC) and gastric cardia adenocarcinoma (GCA) tissues showed different positive immunostaining extent of p53 and PCNA protein ( $P > 0.05$ ). The positive immunostaining rates for p53 and PCNA were 60 % (15/25) and 92 % (23/25), respectively in SCC; and 40 % (10/25) and 88 % (22/25), respectively in GCA. "Diffuse" immunostaining pattern was frequently observed in both p53 and PCNA. High coincidence rates for p53 and PCNA positive staining were observed in SCC and GCA from the same patients, and accounted for 56 % and 96 %. In SCC patients, with the lesions progressed from normal esophageal epithelium (NOR) to basal cell hyperplasia (BCH) to dysplasia (DYS) to carcinoma *in situ* (CIS) to SCC, the positive rates for p53 were 27 %, 50 %, 50 %, 29 % and 72 %, and 55 %, 70 %, 75 %, 71 % and 93 % for PCNA, respectively. In GCA, with the lesions progressed from normal gastric cardia epithelium to DHS to CIS to GCA, the positive rates of p53 expression were 44 %, 27 %, 22 % and 36 % respectively, the difference was not significant; the positive rates of PCNA protein expression were 67 %, 64 %, 67 % and 86 %, respectively. The  $\chi^2$  test, Fisher's Exact Test, Mantel-Haenszel  $\chi^2$  Test and Kappa Test were used for the statistics.

**CONCLUSION:** The high coincident alterations for P53 and PCNA in SCC and GCA from the same patient indicate the possibility of similar molecular basis, which provides important molecular basis and etiological clue for similar geographic distribution and risk factors in SCC and GCA.

Chen H, Wang LD, Guo M, Gao SG, Guo HQ, Fan ZM, Li JL. Alterations of p53 and PCNA in cancer and adjacent tissues from concurrent carcinomas of the esophagus and gastric cardia in the same patient in Linzhou, a high incidence area for esophageal cancer in northern China. *World J Gastroenterol* 2003; 9(1): 16-21

<http://www.wjgnet.com/1007-9327/9/16.htm>

## INTRODUCTION

Esophageal squamous cell carcinoma (SCC) and gastric cardia adenocarcinoma (GCA) are the two most frequent malignant diseases in the world<sup>[1-3]</sup>. SCC is characterized by its remarkable geographic distribution; the ratio between the incident rates of high- and low-risk areas can be as high as 500:1. Consistent geographic distribution with SCC in the same high-incidence area (HIA) is the remarkable epidemiological characteristic of GCA<sup>[3]</sup>, and in America and Europe the incidence of GCA increased dramatically in recent decades<sup>[4-8]</sup>. Linzhou and the nearby counties in Henan province, have the highest incidence and mortality for SCC and GCA in the world, SCC and GCA remain the leading cause of cancer-related death in these areas<sup>[9]</sup>.

It is noteworthy that the concurrent cancers from esophagus and gastric cardia in the same patient (CC) is not uncommon in this area, with an incidence of 0.4-2.5 %<sup>[10-13]</sup>. This special pattern indicates that there may be same or similar risk factors and mechanism involved in the carcinogenesis. The molecular mechanism of SCC/GCA is still not clear, and the information from the concurrent cancers of SCC & GCA in the same patient in the HIA is very limited. It is apparent to further characterize the molecular changes of CC patients may provide not only more information on the molecular mechanism but also the etiological clues for SCC and GCA.

Recent studies indicate that esophageal and gastric cardia carcinogenesis is a multistep progressive process involving multiple genetic changes (accumulation or overlap). The accumulation of p53 protein and p53 gene mutation were observed in the very early stage of esophageal carcinogenesis, even in the microscopically normal esophageal epithelium, with positive immunostaining and mutation rates increasing with the progression of lesions<sup>[14-24]</sup>. In addition, recent study showed that PCNA protein overexpression was also observed in the carcinogenesis of GCA<sup>[25]</sup>.

To elucidate the molecular mechanisms of SCC/GCA carcinogenesis and to expand the knowledge for early detection of SCC/GCA and screening high-risk population, the present study was undertaken to analyze the alternations of p53 and PCNA in cancer tissues and adjacent cancerous tissues with different degrees of precancerous lesions in CC patients.

## MATERIALS AND METHODS

### Tissue collection and processing

25 cases with concurrent cancers of SCC & GCA enrolled in this study were from Linzhou City Hospital, Yaocun



Esophageal Cancer Hospital and Anyang City Tumor Hospital, the high-incidence area for EC, including 16 males and 9 females, with a mean age of 59 (59±9.88) in male and 60.6 (60.6±11.44) in female. None of these patients received any treatment of chemotherapy or radiotherapy before operation. All the resected tissues and biopsied tissues were fixed with 85 % alcohol, embedded with paraffin and serially sectioned at 5 µm. The sections were mounted onto the histostick-coated slides. Four or five adjacent ribbons were collected for histopathological diagnosis (hematoxylin and eosin stain) and immunohistochemical staining.

### Histopathology analysis

Histopathological diagnosis for esophageal and gastric cardia epithelia was based on the changes in cellular morphology and tissue architecture using previously established criteria<sup>[26-32]</sup>. The normal esophageal epithelium (NOR) contained 1 to 3 basal-cell layers; the papillae were confined to the lower half of the epithelium. In basal cell hyperplasia (BCH), the number of proliferating basal cells was increased to more than 3-cell layers. Dysplasia (DYS) was characterized by the partial loss of cell polarity and nuclear atypia. SCC was characterized by confluent and invasive sheets of cohesive, polymorphous cells with hyperchromatic nuclei. The following histopathological classification was used for the gastric-cardia epithelia: dysplasia (DYS), neoplastic features including nuclear atypia and/or architectural abnormalities confined to the gastric epithelium, without invasion; GCA: invasion of neoplastic gastric cells through the basement membrane. The diagnosis of CC was based on the following criteria: (1) the tumors must be clearly separated on histological phenotype; (2) the tumors must be malignant; (3) Metastasis must be excluded.

### Immunohistochemical staining (IHC)

Anti-p53 antibody is a monoclonal mouse anti-serum against p53 of human origin, and recognizes both wild and mutant type p53 (Ab-6, Oncogen Science, Manhasset, NY). Anti-PCNA antibody is a monoclonal mouse anti-serum against PCNA of human origin (Mab, DAKO, Carpinteria, CA). The avidin-biotin-peroxidase complex method was used for the immunostaining of p53, PCNA. In brief, after dewaxing, inactivating endogenous peroxidase activity and blocking cross-reactivity with normal serum (Vectastain Elite Kit; Vector, Burlingame, CA), the sections were incubated overnight at 4 °C with a diluted solution of the primary antibodies (1:500 for p53 and 1:200 for PCNA). Location of the primary antibodies was achieved by subsequent application of a biotinylated anti-primary antibody, an avidin-biotin complex conjugated to horseradish peroxidase, and diaminobenzidine (Vectastain Elite Kit, Vector, Burlingame, CA). The slides were counter-stained by hematoxylin. Negative controls were established by replacing the primary antibody with PBS and normal mouse serum. Known immunostaining-positive slides were used as positive controls.

Specific staining for each protein was categorized as either positive or negative based on the presence of brown coloration staining. More than 10 % positively stained cells were graded as positive<sup>[33,34]</sup>. Clear staining for nuclei was the criterion for a positive reaction. Immunostaining patterns<sup>[26]</sup> were graded into the “focus”, “scattered”, “diffuse”, according to cell distribution in one microscopic eyeshot (×40). All the immunostaining slides were observed by two pathologists independently. The slides with different diagnosis by two pathologists were reviewed again (less than 5 %) until the agreed diagnosis was made.

### Statistics analysis

The  $\chi^2$  test, Fisher's Exact Test, Mantel-Haenszel  $\chi^2$  Test and

Kappa Test were used for the statistics ( $P < 0.05$  was considered significant).

## RESULTS

### Histopathological results

Histopathologically, primary SCC and GCA in the same patient were verified in all 25 cases by two pathologists using an Olympus microscope independently. Of the 14 CC patients (both with cancer and adjacent tissues) examined, in esophagus 11 samples were diagnosed as normal, 10 as BCH, 8 as DYS, 7 as CIS and 14 as SCC; in gastric cardia 9 as normal, 11 as DYS, 9 as CIS and 14 as GCA.

### Expression of p53 protein in CC patients (Table 1)

P53 positive immunostaining was observed in the epithelial and tumor cells of esophagus and gastric cardia. In CC patients, both SCC and GCA tissues showed a different extent positive immunostaining of p53 protein (Figure 1,2). In 25 CC patients, the immunostaining rate of p53 protein in SCC was 60 % (15/25) and in GCA was 40 % (10/25), and statistical analysis showed that the difference was not significant ( $P > 0.05$ ). “Diffuse” was the most frequent immunostaining pattern observed in both SCC (60 %, 9/15) and GCA (70 %, 7/10). High coincidence alteration for positive staining of p53 was observed in SCC and GCA from the same patients, and accounted for 56 %.

**Table 1** Expression of P53 protein in 25 CC patients

Number	Sex/age	P53 immunostaining			
		SCC		GCA	
		(+/-) <sup>a</sup>	Immunostaining pattern	(+/-) <sup>a</sup>	Immunostaining pattern
001	M/63	+ <sup>a</sup>	Diffuse	- <sup>a</sup>	-
002	M/60	-	-	+	Focus & Scattered
003	M/55	+	Diffuse	-	-
004	M/71	+	Diffuse & Scattered	+	Scattered
005	F/56	+	Scattered & Diffuse	-	-
006	M/59	-	-	-	-
007	F/67	-	-	-	-
008	M/62	+	Diffuse	+	Diffuse
009	F/61	+	Diffuse	-	-
010	F/64	+	Scattered	-	-
011	M/65	+	Diffuse	-	Diffuse
012	M/68	+	Diffuse	-	Diffuse
013	M/57	-	-	-	-
014	M/51	+	Diffuse	-	-
015	M/50	-	-	-	-
016	M/67	+	Scattered	-	Diffuse
017	M/70	+	Focus	-	-
018	M/67	+	Scattered	-	Scattered
019	F/74	-	-	+	Diffuse
020	M/49	-	-	+	Diffuse
021	M/36	-	-	-	-
022	M/70	+	Diffuse	-	-
023	F/74	-	-	-	-
024	F/56	-	-	-	-
025	F/38	+	Scattered	+	Diffuse & Scattered

<sup>a</sup>+: positive immunostaining of P53, -: negative immunostaining of P53.

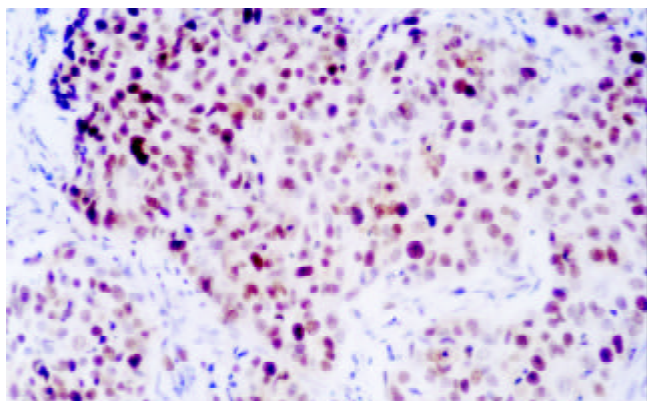


**Figure 1** Expression of p53 in SCC ( $\times 200$ )

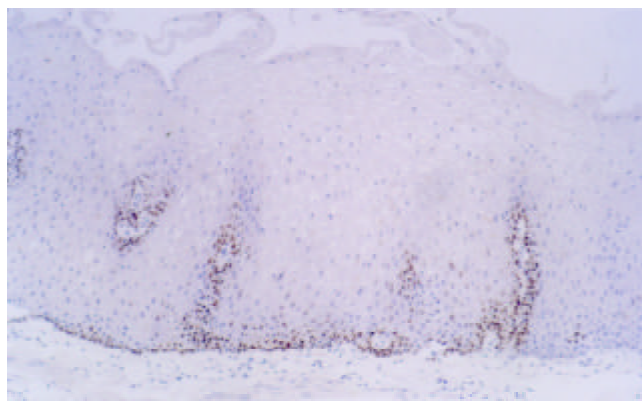


**Figure 5** Expression of p53 in NOR (Esophagus) ( $\times 200$ )

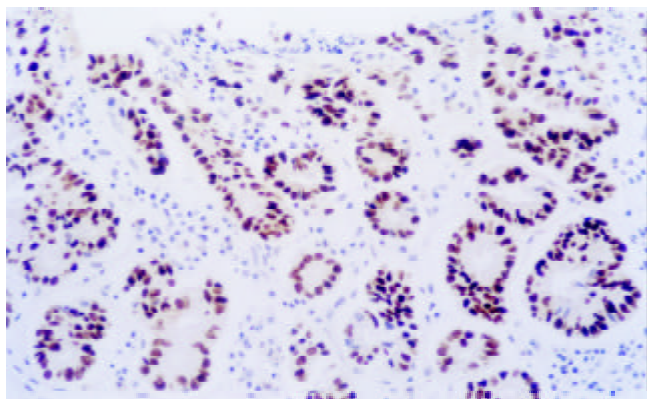


**Figure 2** Expression of p53 in GCA ( $\times 200$ )

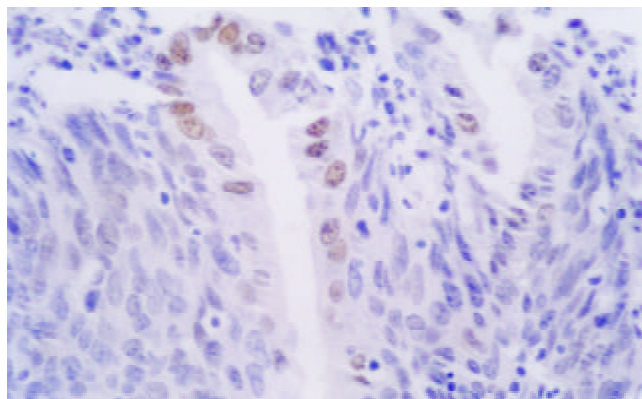


**Figure 6** Expression of p53 in NOR (Gastric cardia) ( $\times 400$ )

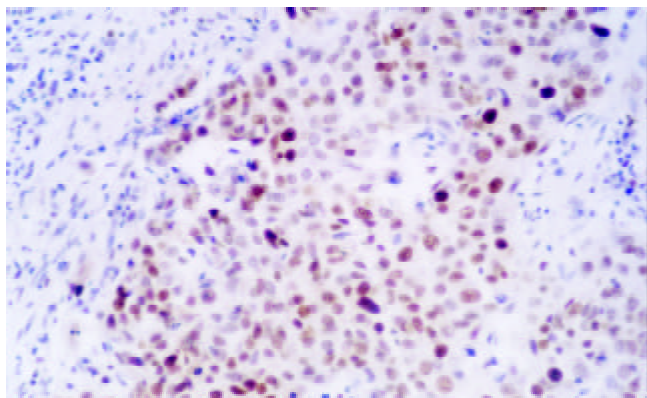


**Figure 3** Expression of PCNA in SCC ( $\times 200$ )

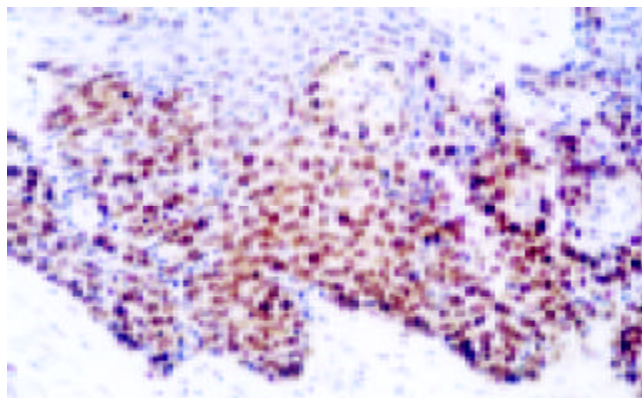


**Figure 7** Expression of p53 in CIS (Esophagus) ( $\times 200$ )

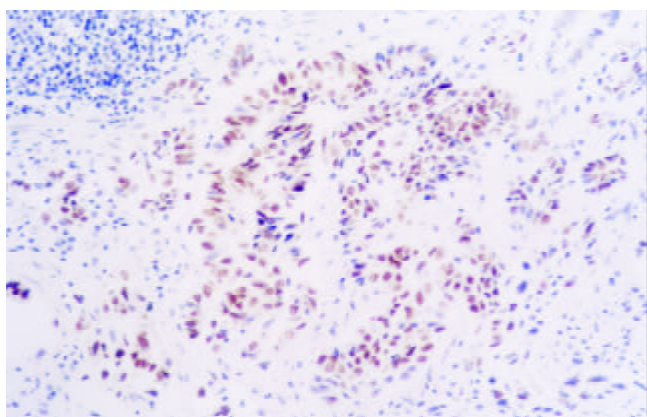


**Figure 4** Expression of PCNA in GCA ( $\times 200$ )

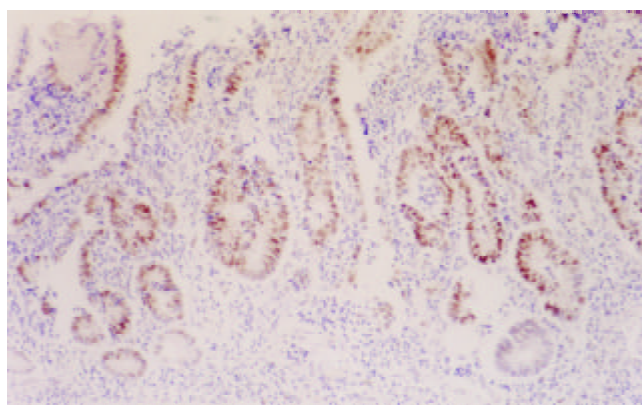


**Figure 8** Expression of p53 in DYS (Gastric cardia) ( $\times 100$ )

**Expression of PCNA protein in CC patients (Table 2)**

In CC patients, both SCC and GCA tissues showed a different extent positive immunostaining of PCNA protein (Figure 3,4). And the positive immunostaining was observed in the cell nuclei of tumor and epithelial tissues. In 25 CC patients, the immunostaining rate of PCNA protein in SCC was 92 % (23/25) and in GCA was 86 % (19/22), and statistical analysis showed that the difference was not significant ( $P>0.05$ ). “Diffuse” was the most frequent immunostaining pattern observed in both SCC 57 % (13/23) and GCA 86 % (19/22). High coincidence alteration for positive staining of PCNA was observed in SCC and GCA from the same patients, and accounted for 96 % (24/25).

**Table 2** Expression of PCNA protein in 25 CC patients

Number	Sex/age	PCNA immunostaining			
		SCC		GCA	
		(+/-) <sup>a</sup>	Immunostaining pattern	(+/-) <sup>a</sup>	Immunostaining pattern
001	M/63	+	Diffuse	+	Diffuse
002	M/60	+	Scattered	+	Focus & Scattered
003	M/55	+	Diffuse	+	Diffuse
004	M/71	+	Scattered & Focus	+	Diffuse
005	F/56	+	Scattered & Diffuse	+	Diffuse
006	M/59	+	Scattered & Focus	+	Diffuse
007	F/67	+	Diffuse	+	Focus
008	M/62	+	Diffuse	+	Diffuse
009	F/61	+	Diffuse	+	Diffuse
010	F/64	+	Scattered	+	Diffuse
011	M/65	+	Focus	+	Diffuse
012	M/68	+	Diffuse	+	Diffuse
013	M/57	-	-	-	-
014	M/51	+	Diffuse	-	-
015	M/50	+	Scattered	+	Diffuse
016	M/67	+	Scattered	+	Diffuse
017	M/70	+	Focus	+	Scattered & Focus
018	M/67	+	Diffuse	+	Scattered
019	F/74	+	Diffuse	+	Diffuse
020	M/49	+	Scattered & Focus	+	Diffuse
021	M/36	+	Diffuse	+	Diffuse
022	M/70	-	-	-	-
023	F/74	+	Diffuse	+	Diffuse
024	F/56	+	Scattered & Focus	+	Diffuse
025	F/38	+	Scattered	+	Diffuse

<sup>a</sup>+: positive immunostaining of PCNA, -: negative immunostaining of PCNA.

**Expression of p53 and PCNA in adjacent cancerous tissues**

In SCC patients, with the lesions progressed from normal esophageal epithelium to BCH to DYS to CIS to SCC, an increasing tendency of p53 protein accumulation and PCNA expression were observed, the positive rates for p53 were 27 %, 50 %, 50 %, 29 % and 72 %, and 55 %, 70 %, 75 %, 71 % and 93 % for PCNA, respectively. In GCA, with the lesions progressed from normal gastric cardia epithelium to DYS to

CIS to GCA, the positive rates of p53 expression were 44 %, 27 %, 22 % and 36 % respectively, the difference was not significant; the positive staining of PCNA protein expression were 67 %, 64 %, 67 % and 86 %, respectively, positive rates of PCNA expression in GCA was generally higher than those in precancerous lesions (Table 3) (Figure 5-8).

**Table 3** Expression of P53 & PCNA in precancerous lesions of adjacent cancerous tissues

Number of samples		P53		PCNA	
		+	%	-	%
Esophagus					
NOR	11	3	27	6	55
BCH	10	5	50	7	70
DYS	8	4	50	6	75
CIS	7	2	29	5	71
SCC	14	10	71	13	93
Gastric cardia					
NOR	9	4	44	6	67
DYS	11	3	27	7	64
CIS	9	2	22	6	67
CGA	14	5	36	12	86

**DISCUSSION**

In this study, indistinguishable overexpressions of p53 and PCNA protein and the same main immunostaining pattern (Diffuse) of immunoreaction were observed in primary SCC and GCA from the same patient. We also found that in CC patient p53 and PCNA had high coincident alteration in both SCC and GCA. These results indicated that SCC and GCA in the same patient might have the similar molecular basis and mechanism of carcinogenesis. These results might be a molecular explanation of the consistent geographic distribution of SCC and GCA. That further characterized the molecular alterations in different stages of SCC and GCA and their relations with morphological changes would provide more information to elucidate the carcinogenesis of SCC and GCA. In this study, high PCNA positive staining rates were observed in CC patient, both in esophageal and gastric cardia epithelia. It inferred that in this high-incidence area, the alimentary canal of patients exposed to similar risk factor might lead the esophageal and gastric cardia epithelial cells to become the hotspot of hyperproliferation, which might be a molecular evidence of hypothesis of field cancerization<sup>[35,36]</sup>. The hypothesis of field cancerization is an explanation of multiple primary malignant neoplasms, which consider the tissues of similar architecture exposed to similar pathogen might occur independently as precancerous lesions in multiple sites of the organ.

It is very important for the diagnosis of CC and multiple primary SCC/GCA to exclude local metastasis. In this study, microscopic observation showed that mixed of SCC and GCA tissue was observed occasionally in some patients, and the tissues adjacent to SCC and GCA had different patterns of precancerous lesions, which were characterized by either isolated or in succession. These unique information provided important clues to study the molecular basis of SCC/GCA carcinogenesis and sensibility.

Through the contrast study of adjacent cancerous tissues of SCC and GCA, we found that different extent of overexpressions of p53 and PCNA were already observed in the apparently normal epithelia and very early precancerous



lesions of esophagus and gastric cardia. Especially, from normal epithelia (NOR) to different precancerous lesions to SCC, of both p53 and PCNA protein positive staining rate increased accordingly in the esophagus, and PCNA increased in gastric cardia, but did not show the tendency of increase. Other researchers' results showed that from NOR to precancerous lesions to SCC/GCA, positive staining of p53 and PCNA showed a continuous increasing tendency<sup>[14,25,37-44]</sup>. So the explanation of our result might be that IHC qualitative analysis cannot reflect the number of immunostaining cells, and only show the alteration of immunostaining rates. The use of quantitative analysis may solve this problem. In this study we also found that in the stage of CIS, both esophagus and gastric cardia tissues showed a decrease of positive staining rate of p53. It might due to that precancerous lesions have an instable characteristic of bidirectional development, that is, in the multistage progression course of carcinogenesis precancerous lesions might progress to cancer, or reverse to low-grade lesion or even normal<sup>[14]</sup>. These results inferred that the molecular changes of SCC and GCA not only were similar in the ultimate stages but also in the early stages, so the CC patient might have similar carcinogenetic course in primary SCC and GCA, but their precise mechanism and biological significance need further study.

## REFERENCES

- 1 **Wang LD**, Zhou Q, Yang CS. Esophageal and gastric cardia epithelial cell proliferation in northern Chinese subjects living in a high-incidence area. *J Cell Biochem Suppl* 1997; **28/29**: 159-165
- 2 **Correa P**. Precursors of gastric and esophageal cancer. *Cancer* 1982; **50**: 2554-2565
- 3 **Lu JB**, Yang WX, Zu SK, Chang QL, Sun XB, Lu WQ, Quan PL, Qin YM. Cancer mortality and mortality trends in Henan, China, 1974-1985. *Cancer Detect Prev* 1988; **13**: 167-173
- 4 **Blot WJ**, Devesa SS, Kneller RW, Fraumeni JF. Rising incidence of adenocarcinoma of the esophagus and gastric cardia. *JAMA* 1991; **265**: 2960
- 5 **Blot WJ**, Devesa SS, Fraumeni JF. Continuing climb in rates of esophageal adenocarcinoma: An update. *JAMA* 1993; **270**: 1320
- 6 **Pera M**, Cameron AJ, Trastek VF, Carpenter HA, Zinsmeister AR. Increasing incidence of adenocarcinoma of the esophagus and esophagogastric junction. *Gastroenterology* 1993; **104**: 510-513
- 7 **Botterweck AA**, Schouten LJ, Volovics A, Dorant E, van den Brandt PA. Trends in incidence of adenocarcinoma of the oesophagus and gastric cardia in ten European countries. *Int J Epidemiol* 2000; **29**: 645-654
- 8 **Hainaut P**, Soussi T, Shomer B, Hollstein M, Greenblatt M, Hovig E, Harris CC, Montesano R. Database of p53 gene somatic mutation in human tumors and cell lines: updated compilation and future prospects. *Nucleic Acid Res* 1997; **25**: 151-157
- 9 **Gao SS**, Zhou Q, Li YX, Bai YM, Zheng ZY, Zou JX, Liu G, Fan ZM, Qi YJ, Zhao X, Wang LD. Comparative studies on epithelial lesions at gastric cardia and pyloric antrum in subjects from a high incidence area for esophageal cancer in Henan, China. *World J Gastroenterol* 1998; **4**: 332-333
- 10 **Zhou HP**, Cao XF. Six cases of esophageal carcinoma with concomitant tumors of the gastric cardia. *Zhonghua Waike Zazhi* 1987; **25**: 700
- 11 **Yao SC**. Nine cases report of primary esophageal and gastric cardia cancers. *Zhongliu* 1987; **7**: 121
- 12 **Zhou FY**, Ma JS, Han XC. Repetitive primary carcinomas concurrently occurring in the esophagus and gastric cardia. *Henan Zhongliuxue Zazhi* 1996; **9**: 357-358
- 13 **Wang L**, Zhang S. Twenty-eight cases report of the concurrent cancers of esophagus and gastric cardia. *Jining Yixueyuan Xuebao* 1996; **19**: 43-44
- 14 **Wang LD**, Chen H. Alterations of tumor suppressor gene p53-Rb system and human esophageal esophageal carcinogenesis. *Shijie Huaren Xiaohua Zazhi* 2002; **9**: 367-371
- 15 **Gao H**, Wang LD, Zhou Q, Hong JY, Huang TY, Yang CS. p53 tumor suppressor gene mutation in early esophageal precancerous lesions and carcinoma among high-risk populations in Henan, China. *Cancer Res* 1994; **54**: 4342-4346
- 16 **Hainaut P**, Hernandez T, Robinson A, Rodriguez-Tome P, Flores T, Hollstein M, Harris CC, Montesano R. IARC database of p53 gene mutation in human tumors and cell lines: updated compilation, revised formats and new visualization tools. *Nucleic Acids Res* 1998; **26**: 205-213
- 17 **Bennett WP**, Hollstein MC, He A, Zhu SM, Resau JH, Trump BF, Metcalf RA, Welsh JA, Midgley C, Lane DP. Archival analysis of p53 genetic and protein alterations in Chinese esophageal Cancer. *Oncogene* 1991; **6**: 1779-1784
- 18 **Shi ST**, Yang GY, Wang LD, Xue Z, Feng B, Ding W, Xing EP, Yang CS. Role of P53 gene mutations in human esophageal carcinogenesis: results from immunohistochemical and mutation analysis of carcinomas and nearby non-cancerous lesions. *Carcinogenesis* 1999; **20**: 591-597
- 19 **Harris CC**. Structure and function of the p53 tumor suppressor gene: clues for rational cancer therapeutic strategies. *J Natl Cancer Inst* 1996; **88**: 1442-1455
- 20 **Sidransky D**, Hollstein M. Clinical implications of the p53 gene. *Annu Rev Med* 1996; **47**: 285-301
- 21 **Li HC**, Lu SX. Mutation of p53 gene in human cancers of the esophagus and gastric cardia. *Zhonghua Zhongliu Zazhi* 1994; **16**: 172-176
- 22 **Yue WB**, Wang LD, Ding I. Detection of angiogenic growth factors in patients with precancerous and cancerous lesions of esophagus from high-risk area in Henan, China. *World J Gastroenterol* 1998; **4**(Suppl 2): 109
- 23 **He LJ**, Wu M. The distribution of esophageal and cardiac carcinoma and precancerous of 2238. *World J Gastroenterol* 1998; **4**(Suppl 2): 100
- 24 **Xu T**, Fang LP, Li J, Liu WQ, Zhou ZY, Qiu CP, Yu XH, Si TP, He LJ, Fang XL, Meng ZH, Li YH, Jiang LH, Luo DY. A pathologic analysis of 4451 cases with digestive tract cancer. *World J Gastroenterol* 1998; **4**(Suppl 2): 65-66
- 25 **Gerdies J**, Schwab U, Seeub H. Production of a mouse monoclonal antibody reactive with a human nuclear antigen associated with cell proliferation. *Int J Cancer* 1983; **31**: 13-20
- 26 **Wang LD**, Hong JY, Qiu SL, Gao HG, Yang CS. Accumulation of p53 protein in human esophageal precancerous lesions: a possible early biomarker for carcinogenesis. *Cancer Res* 1993; **53**: 1783-1787
- 27 **Hermanek P**, Hutter RVP, Sobin LH. International Union Against Cancer (UICC). TNM atlas, 4th edition. *Berlin: Springer* 1997
- 28 **Warren S**, Gates P. Multiple primary malignant tumors. A survey of literature and a statistical study. *Am J Cancer* 1932; **16**: 1358-1414
- 29 **Moertel CG**. Multiple primary malignant neoplasms. *Cancer* 1977; **40**: 1786
- 30 **Esophageal Cancer**. Du BL (editor). *Beijing: Chinese Science And Technology Publishing Company* 1994
- 31 **Wang LD**, Shi ST, Zhou Q, Goldstein S, Hong JY, Shao P, Qiu SL, Yang CS. Changes in P53 and cyclin D1 protein level and cell proliferation in different stages of Henan esophageal and gastric-cardia Carcinogenesis. *Int J Cancer* 1994; **59**: 514-519
- 32 **Shen MZ**, Wang G, Qiu SL. Stomach cancer, Chinese stomach tumor collaborative research group editor. *Shenyang: Liaoning People Publishing Company* 1981
- 33 **Biemer-Huttmann AE**, Walsh MD, McGuckin MA, Ajioka Y, Watanabe H, Leggett BA, Jass JR. Immunohistochemical staining patterns of Mucin1, Mucin2, Mucin4 and Mucin5AC mucins in hyperplastic polyps, serrated adenomas, and traditional adenomas of the colorectum. *J Histochem Cytochem* 1999; **47**: 1039-1048
- 34 **Reis CA**, David L, Correa P, Carneiro F, de Bolos C, Garcia E, Mandel U, Clausen H, Sobrinho-Simoes M. Intestinal metaplasia of human stomach displays distinct patterns of mucin expression. *Cancer Res* 1999; **59**: 1003-1007
- 35 **Moertel CG**, Dockerty MB. Multiple primary malignant neoplasms: tumors of different tissues or organs. *Cancer* 1961; **14**: 231-237
- 36 **Slaught TP**, Soutwick HW, Smejkel W. Field cancerization in

- oral stratified epithelium. *Cancer* 1953; **6**: 963-968
- 37 **Lu SX**. Alterations of oncogenes and tumor suppressor genes in esophageal cancer in China. *Mutation Res* 2000; **462**: 343-353
- 38 **Liu B**, Wang LD. Barrett's esophagus. *Huaren Xiaohua Zazhi* 1999; **3**: 3-7
- 39 **Mandard AM**, Hainaut P, Hollstein M. Genetic steps in the development of squamous cell carcinoma of the esophagus. *Mutation Res* 2000; **462**: 335-342
- 40 **Zou JX**, Wang LD, Shi Stephanie T, Yang GY, Xue ZH, Gao SS, Li YX, Yang Chung S. p53 gene mutations in multifocal esophageal precancerous and cancerous lesions in patients with esophageal cancer in high-risk northern China. *Shijie Huaren Xiaohua Zazhi* 1999; **7**: 280-284
- 41 **Wang YK**, Ji XL, Gu YG, Zhang SC, Xiao JH. P53 and PCNA expression in glandular dilatation of gastric mucosa. *China Natl J New Gastroenterol* 1996; **2**: 106-108
- 42 **Wang LD**, Zhou Q, Gao SS, Li YX, Yang WC. Measurements of cell proliferation in esophageal and gastric cardia epithelia of subjects in a high incidence area for esophageal cancer. *China Natl J New Gastroenterol* 1996; **2**: 82-85
- 43 **Wang LD**, Yang WC, Zhou Q, Xing Y, Jia YY, Zhao X. Changes of p53 and Waf1p21 and cell proliferation in esophageal carcinogenesis. *China Natl J New Gastroenterol* 1997; **3**: 87-89
- 44 **Wang LD**, Zhou Q, Wei JP, Yang WC, Zhao X, Wang LX, Zou JX, Gao SS, Li YX, Yang CS. Apoptosis and its relationship with cell proliferation, p53, Waf1p21, bcl-2 and *c-myc* in esophageal carcinogenesis studied with a high-risk population in northern China. *World J Gastroenterol* 1998; **4**: 287-293

**Edited by** Wu XN

# Relationship between overexpression of NK-1R, NK-2R and intestinal mucosal damage in acute necrotizing pancreatitis

Xin Shi, Nai-Rong Gao, Qing-Ming Guo, Yong-Jiu Yang, Ming-Dong Huo, Hao-Lin Hu, Helmut Friess

**Xin Shi, Nai-Rong Gao, Yong-Jiu Yang, Ming-Dong Huo, Hao-Lin Hu**, Department of General Surgery, Zhong-Da Hospital, Southeast University, Nanjing 210009, Jiangsu Province, China  
**Qing-Ming Guo**, Department of Pathology, Zhong-Da Hospital, Southeast University, Nanjing 210009, Jiangsu Province, China  
**Helmut Friess**, Department of General Surgery, University of Heidelberg, Im Neuenheimer Feld 110, D-69120 Heidelberg, Germany  
**Supported by** the scientific research funding for the returned overseas Chinese scholars, State Personnel Ministry, No. 7690004027  
**Correspondence to:** Dr. Xin Shi, Department of General Surgery, Zhong-Da Hospital, Southeast University, Nanjing, 210009, Jiangsu Province, China. shixined@hotmail.com  
**Telephone:** +86-25-3272196 **Fax:** +86-25-3272196  
**Received:** 2002-07-01 **Accepted:** 2002-08-05

## Abstract

**AIM:** To study the expression of neurokinin-1 receptor (NK-1R) and neurokinin-2 receptor (NK-2R) in distal ileum of acute necrotizing pancreatitis (ANP) and to evaluate the relationship between expression of these two receptors and intestinal mucosal damage.

**METHODS:** A total of 130 adult Sprague-Dawley rats were randomly divided into two groups: the rats in ANP group ( $n=80$ ) were induced by the retrograde intraductal infusion of  $30\text{ g} \cdot \text{L}^{-1}$  sodium taurocholate. And the rats in normal control group ( $n=50$ ) received laparotomy only. Sacrifices were made 6 h, 12 h, 24 h and 48 h later in ANP and normal control group after induction respectively. Intestinal mucosal permeability was studied by intrajejunal injection of  $1.5\text{mCi}$  radioactive isotope  $^{99\text{m}}\text{Tc}$ -diethylene triamine pentacetic acid (DTPA) and the radioactivity of  $^{99\text{m}}\text{Tc}$ -DTPA content in urine was measured 6 h, 12 h, 24 h and 48 h after induction. Then the pancreas and intestine were prepared for pathology. Reverse transcription polymerase chain reaction (RT-PCR) was used to determine the mRNA expression of NK-1R and NK-2R, and Western blot was used to investigate the protein level of NK-1R and NK-2R.

**RESULTS:** In ANP rats, serious histologic damages in intestinal mucosa were observed, and the radioactivity of  $^{99\text{m}}\text{Tc}$ -DTPA in urine increased significantly in the ANP group. RT-PCR revealed that NK-1R and NK-2R mRNA level was overexpressed in the distal ileum of ANP as compared with the normal control group. Western blot discovered stronger NK-1R (14-fold increase) and NK-2R (9-fold increase) immunoreactivity in the intestinal mucosa of ANP rats. Moreover, the overexpression of NK-1R was associated with mucosal pathological score ( $r=0.77$ ,  $P<0.01$ ) and intestinal permeability ( $r=0.68$ ,  $P<0.01$ ) in ANP rats.

**CONCLUSION:** NK-1R and NK-2R contribute to disrupted neuropeptides loop balance, deteriorate intestinal damage, and are involved in pathophysiological changes in ANP.

Shi X, Gao NR, Guo QM, Yang YJ, Huo MD, Hu HL, Friess H. Relationship between overexpression of NK-1R, NK-2R and intestinal mucosal damage in acute necrotizing pancreatitis. *World J Gastroenterol* 2003; 9(1): 160-164  
<http://www.wjgnet.com/1007-9327/9/160.htm>

## INTRODUCTION

Acute necrotizing pancreatitis (ANP) has a complicated and ill-defined pathophysiology. It is associated with a high complication rate and unpredictable outcome, with a mortality rate of 10-45 %<sup>[1]</sup>. The hypothesis that ANP promotes bacterial translocation, leading to infection in the inflamed pancreas and peripancreatic tissue, has been studied in rats fed with fluorescent beads, sensitive inert markers of translocation<sup>[2]</sup>. The results suggested a translocated bacteria route for pancreatic infection. Normal intestinal mucosal barrier can keep the bacteria from translocation, however, this barrier is damaged in ANP<sup>[3,4]</sup>. The mechanism, which leads to the dysfunction of mucosal barrier, remains unclear<sup>[5-9]</sup>.

Recent studies have revealed the important role of Substance P (SP) and its receptors in ANP<sup>[10-13]</sup>. However, the expression of SP's two receptors- neurokinin-1 receptor (NK-1R) and neurokinin-2 receptor (NK-2R) in intestinal mucosa of ANP, remains unclear. And their roles in mucosal damage has not been revealed.

Therefore, in the present study the mRNA of NK-1R and NK-2R in intestinal mucosa of ANP was analyzed using reverse transcription polymerase chain reaction (RT-PCR), the protein level of these two receptors was analyzed by Western blot. And the relationship between mRNA level and intestinal mucosal damage/intestinal permeability was also investigated.

## MATERIALS AND METHODS

### Animals

Adult Sprague-Dawley rats weighing 250-300 g were obtained from the Laboratory Animal Center of Southeast University, and fed with standard rat chow. Animals were fasted overnight and anesthetized with  $20\text{ g} \cdot \text{L}^{-1}$  sodium pentobarbital (intraperitoneal injection). ANP models ( $n=80$ ) were induced by the retrograde intraductal infusion of  $30\text{ g} \cdot \text{L}^{-1}$  sodium taurocholate ( $0.1\text{ ml} \cdot \text{min}^{-1} \cdot \text{kg}^{-1}$ ). And the rats in normal control group ( $n=50$ ) received laparotomy, the duodenum was taken out of the abdominal cavity and the pancreas was turned over for three times.

Sacrifices were made 6 h, 12 h, 24 h and 48 h later in ANP and normal control group after induction respectively. The distal ileum, pancreas and blood in portal vein were obtained for further studies. Freshly removed tissue samples were immediately fixed in paraformaldehyde solution for 12-24 hours and paraffin-embedded for routine histopathologic analysis. Concomitantly, tissue samples destined for RNA and protein extraction were immediately snap-frozen in liquid nitrogen and maintained at  $-80\text{ }^{\circ}\text{C}$  until use. Blood was obtained for serum amylase determinations.

### Pathological examination for intestinal mucosa and pancreas

Paraffin-embedded tissue sections (2-3 mm thick) were subjected to hematoxylin & eosin staining. Intestinal mucosal damage was evaluated blindly under microscope by two pathologists<sup>[14, 15]</sup>.

### Determinants of intestinal mucosal permeability

Intestinal mucosal permeability was investigated by intrajejunal

injection of 1.5mCi radioactive isotope  $^{99m}\text{Tc}$  (Chinese Institute of Nuclear Power)-diethylene triamine pentacetic acid (DTPA, Chinese Institute of Nuclear Power) and the radioactivity of  $^{99m}\text{Tc}$ -DTPA content in urinary were measured 6 h, 12 h, 24 h and 48 h after induction. Urinary volume was measured and radioactive impulse was determined using radio-immunity  $\gamma$  counter. Intestinal mucosal permeability was calculated using the following formula: Intestinal mucosal permeability (%) =  $\frac{^{99m}\text{Tc}\text{-DTPA excretory rate}(\%) - [(\text{urine-background}) \times \text{volume}] / (\text{standard-background}) \times 100\%}{100\%}$  [16, 17].

### RNA extraction and RT-PCR

Total RNA was extracted using the single-step guanidinium isothiocyanate method, as previously reported [18,19]. Following DNase treatment, total RNA was reversely transcribed into cDNA using random hexamers according to the manufacturer's instructions (Roche Diagnostics, Rotkreuz, Switzerland). The primers were designed using Primer Express software (Germany) and synthesized by Amplimmun (Amplimmun AG, Madulain, Switzerland). The sequence is shown in Table 1.

**Table 1** The sequence of primers used for RT-PCR

Primers	Sequence	Primer size (bp)	PCR products size (bp)
NK-1R			
Forward primer	5'- CAT CAA CCC AGA TCT CTA CC -3'	20	380
Reverse primer	5'- GCT GGA GCT TTC TGT CAT GGA -3'	21	
NK-2R			
Forward primer	5'-CAT CAC TGT GGA CGA GGG GG-3'	20	491
Reverse primer	5'-TGT CTT CCT CAG TTG GTG TC-3'	20	
GAPDH			
Forward primer	5'-TGA AGG TCG GTG TCA ACG GAT TTG GC-3'	26	999
Reverse primer	5'- CAT GTA GGC CAT GAG GTC CAC CAC-3'	24	

PCR amplification was carried out using either NK-1R or NK-2R or GAPDH in a final volume of 25  $\mu\text{l}$  with a Perkin-Elmer GeneAmp System 9 700 and 0.625 U of Taq DNA polymerase (Roche Diagnostics GmbH, Mannheim, Germany). Cycling conditions were as follows: 35 cycles of denaturation at 94 °C for 1 min, annealing at 62 °C for 1 min and elongation at 72 °C for 2.5 min. The first PCR cycle was preceded by denaturation at 94 °C for 3 min, and last PCR cycle was followed by incubation at 72 °C for 10 min.

For each PCR reaction, an identical tube containing the same amount of reagent, and same amount of water was substituted for cDNA in these tubes. These tubes served as negative control of PCR.

RNA concentrations and PCR were titrated to establish standard curves to document linearity and to permit semiquantitative analysis of signal strength [20-22]. Amplified PCR products were separated by electrophoresis through a 1 % agarose gel at 45 V for 120 min. The cDNA bands were visualized by ultraviolet illumination after the gels were stained with 0.5  $\text{g} \cdot \text{L}^{-1}$  ethidium bromide dissolved in Tris-borate-EDTA buffer (89 mM Tris, 89 mM boric acid, 2.5 mM EDTA, pH 8.2). The gels were photographed, and the films were scanned and analyzed with a computerized densitometer (Image-Pro Plus, Version 3.0.01).

### Western blot

Western blot for NK-1R and NK-2R was performed as previously reported with certain modifications [18,19]. Briefly, 200 mg of tissue samples were powered in liquid nitrogen and

then homogenized in lysis buffer (50 mM Tris-HCl, pH 7.5, 150 mM NaCl, 2 mM EDTA, 1 % SDS) supplemented with a protease inhibitor cocktail (Roche Diagnostics, Rotkreuz, Switzerland). The lysate was collected and centrifuged at 4 °C for 10 min with 14 000 rpm to remove the insoluble material. The protein concentration was measured by spectrophotometry using the BCA protein assay (Pierce, Rockford, IL, USA). For each sample, 40 mg of protein was separated on 12 % SDS-polyacrylamide gels and electroblotted onto nitrocellulose membranes.

The blots were incubated in blocking solution (50  $\text{g} \cdot \text{L}^{-1}$  non-fat milk in 20 mM Tris-HCl, 150 mM NaCl, 1  $\text{g} \cdot \text{L}^{-1}$  Tween-20 [TBS-T]), followed by incubation with 1:1 000 dilution of goat anti-rat NK-1R antibody (Santa Cruz Biotechnology, Santa Cruz, CA, USA) or 1:1 000 dilution of goat anti-rat NK-2R antibody (Santa Cruz Biotechnology, Santa Cruz, CA, USA) at 4 °C overnight. The membranes were then washed with TBS-T and incubated with donkey anti-goat IgG (1:3 000 dilution) for 60 min at room temperature. Antibody detection was performed with an enhanced chemiluminescence reaction (ECL Western blotting detection, Amersham Life Science, Amersham, UK).

### Statistical analysis

Results were expressed as mean  $\pm$  SD. Statistical analysis was made using the Prism software (Prism, GraphPad Software Inc., San Diego, CA, USA). The comparative statistical evaluations among groups were done using the Mann-Whitney U test or Chi-square test. Spearman correlation analysis was used for correlation analysis of the parameters. Significance was defined as  $P < 0.05$ .

## RESULTS

### Serum amylase and pathological examination

Serum amylase increased significantly in ANP group as compared with normal controls ( $P < 0.01$ ). The diagnoses of ANP were confirmed by gross appearance and microscopy. In ANP group, mucosal edema, epithelia degeneration, necrosis or even abscission were observed after 6 h. Hemangiectasia, hemorrhage and inflammatory cell infiltration were revealed in mucosa or submucosa (Table 2).

**Table 2** The pathological score of intestinal mucosa

Groups	0 h	6 h	12 h	24 h	48 h
Control	0.92 $\pm$ 0.47	0.90 $\pm$ 0.35	0.93 $\pm$ 0.38	0.93 $\pm$ 0.29	1.07 $\pm$ 0.36
ANP		2.11 $\pm$ 0.47 <sup>a</sup>	2.65 $\pm$ 0.49 <sup>b</sup>	3.91 $\pm$ 0.82 <sup>b</sup>	4.89 $\pm$ 1.21 <sup>b</sup>

<sup>a</sup> $P < 0.05$  vs each time point of control group, respectively; <sup>b</sup> $P < 0.01$  vs each time point of control group, respectively

### Intestinal mucosal permeability change in ANP rats

The intestinal mucosal permeability was determined using isotope. The results revealed that permeability increased significantly after 6 h (Table 3).

**Table 3** Changes of intestinal mucosal permeability

Groups	0 h	6 h	12 h	24 h	48 h
Control	0.0411 $\pm$ 0.0156	0.0455 $\pm$ 0.0174	0.0532 $\pm$ 0.0188	0.0693 $\pm$ 0.0153	0.0698 $\pm$ 0.0223
ANP		0.2367 $\pm$ 0.1132 <sup>a</sup>	0.3457 $\pm$ 0.0473 <sup>a</sup>	0.6651 $\pm$ 0.1411 <sup>a</sup>	0.7021 $\pm$ 0.1523 <sup>a</sup>

<sup>a</sup> $P < 0.01$  vs each time point of control group, respectively



### mRNA expression of NK-1R and NK-2R in distal ileum

The rats were sacrificed 6 h, 12 h, 24 h or 48 h after model inducing, distal ileum was obtained for determination of NK-1R and NK-2R mRNA. Figure 1 shows the amplification plot at the time point of 6 h. The gene above had been amplified effectively, and amplification of GAPDH was comparable in each sample, which suggested comparable mRNA in each sample (Figure 1B, 1D), whereas amplification of NK-1R in normal controls was so weak that some of the samples could only be observed in the gel. In contrast, the amplification of NK-1R in ANP group was relatively stronger (Figure 1A). The expression of NK-2R was similar to NK-1R (Figure 1C). After 12 h, 24 h or 48 h, the expression of above genes maintained the same pattern as before.

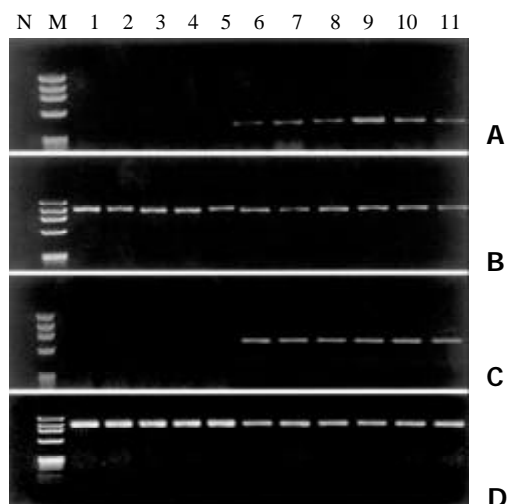


**Figure 1** Amplification results of NK-1R, NK-2R and GAPDH from RT-PCR in control and ANP intestinal tissue. A: amplification results of NK-1R; C: amplification results of NK-2R; B, D: amplification results of GAPDH. N: PCR negative control; M: PCR Marker (upper to lower: 1 000, 800, 600, 400, 200 and 100bp); 1-5: group of normal control; 6-11: group of ANP

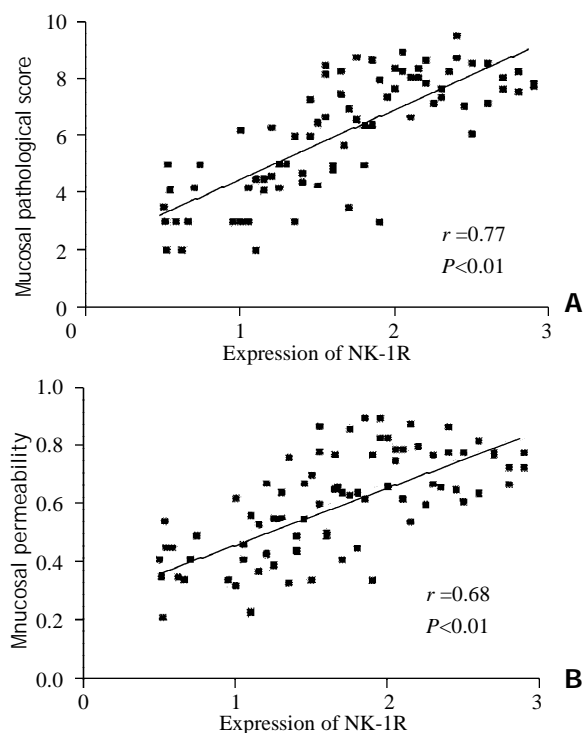


**Figure 2** The expression level of NK-AR mRNA was correlated with intestinal mucosal pathological score (A) and mucosal permeability (B) in ANP rats

### Correlation of expression of NK-1R and NK-2R with intestinal mucosal damage

We then evaluated whether there was a relationship between the expression levels of these two genes and intestinal mucosal pathological score and permeability. A significant relationship between NK-1R mRNA and mucosal pathological score ( $r=0.77$ ,  $P<0.01$ ) was found (Figure 2A). Furthermore, statistical analysis revealed a significant relationship between NK-1R mRNA and mucosal permeability ( $r=0.68$ ,  $P<0.01$ , Figure 2B). Although NK-2R mRNA was overexpressed in ANP, there was no significant relationship between this gene expression and intestinal mucosal pathological score ( $r=0.32$ ,  $P=0.31$ ) and permeability ( $r=0.28$ ,  $P=0.21$ ).

### NK-1R and NK-2R protein expression in distal ileum

We then performed the Western blot analysis in controls and ANP group. All the normal controls exhibited approximately 46 kDa band of NK-1R protein of weak intensity. In contrast, the ANP samples showed a more intense signal (Figure 3A). The densitometric analysis demonstrated a 14-fold increase of NK-1R protein level in ANP ileum compared with the normal ileum ( $P<0.01$ ).

When Western blot analysis for NK-2R was performed, similar pattern was observed, protein signal was weak in normal control, but much stronger in ANP group (Figure 3B). Densitometry revealed a 9-fold increase of NK-2R in ANP ileum ( $P<0.01$ ).

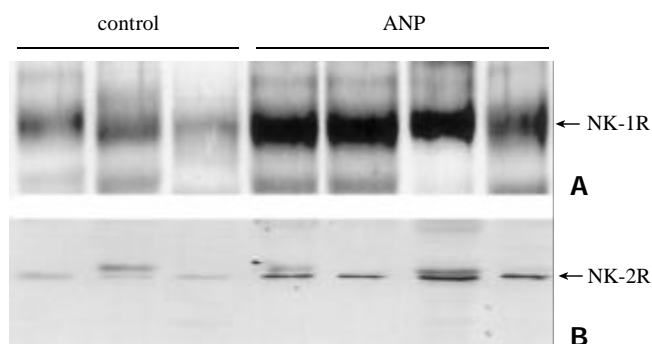


**Figure 3** Western blot revealed the protein level of NK-1R (A) and NK-2R (B) in normal control and ANP intestinal tissue

### DISCUSSION

Intestinal bacterial translocation is the main source leading to infection of pancreas, whereas this translocation is dependent, to some degree, on the function of intestinal mucosal barrier. Intestinal mucosal barrier is made up of mechanical, biological, immunologic and chemical barrier, while the mechanical barrier is the fundamental one, which can prevent large molecule and bacteria from passing through<sup>[23,24]</sup>. More and more evidence showed that gut barrier dysfunction is related to multiorgan system failure in sepsis and immune dysregulation<sup>[25-35]</sup>. Pancreatitis-induced hypovolaemia due to endothelial barrier leakage and gut arteriovenous shunting causes intestinal ischaemia and reperfusion injury with concomitant gut barrier dysfunction. Gut endothelial barrier dysfunction probably plays a central role. Potential molecular mechanisms could be associated with alterations in intracellular signal transduction, intercellular signal and expression of adhesion molecules on endothelial cells. Bacterial infections are often seen during the progression of ANP, concomitant with the potential development of multiple organ dysfunction<sup>[36,37]</sup>. The mechanisms underlying gut barrier dysfunction in acute pancreatitis are thus complex and still not fully elucidated.

SP is synthesized by small-diameter C sensory 'pain' fibers, and release of this peptide into the dorsal horn of the spinal cord following intense peripheral stimulation was thought to promote central hyperexcitability (central sensitization)<sup>[38,39]</sup>. In addition, it could result in plasma extravasation, neutrophil infiltration, and vasodilatation. In rats, both SP and NK-1R selective agonist stimulated pancreatic plasma extravasation, and this response was blocked by the NK-1R antagonist. Selective agonist of NK-2R showed no effect<sup>[12]</sup>. Continuous infusion of SP stimulated plasma extravasation in rat pancreas via activation of NK-1R<sup>[40-42]</sup>.

In the present study, expression of NK-1R and NK-2R mRNA was investigated by RT-PCR and the protein levels of NK-1R and NK-2R were determined using Western blot analysis in normal control and ANP intestines. The results revealed that both NK-1R and NK-2R were overexpressed in ANP intestines, and the overexpression of NK-1R was correlated with mucosal damage in ANP rats. Increased level of SP<sup>[43]</sup> in ANP, together with overexpression of its receptors-NK-1R and NK-2R, results in excessive biological effect, such as aggregation of neutrophilic granulocyte, cascade release of inflammatory transmitter, tissue fluid and plasma extravasation, thus resulting in deterioration of intestinal pathological changes and gut barrier dysfunction, and facilitating gut bacterial translocation.

Better understanding of the molecular biological changes in ANP will provide novel therapies to this disease. Once specific receptors were identified, selective antagonists which blocked these receptors would have therapeutic effects. Antagonists against NK-1R have showed some effects in acute pancreatitis on animal models<sup>[12,42]</sup>. Knowledge about the regulating events will probably make future pharmacological therapy available for prevention and treatment of the severe complications of ANP, including gut barrier dysfunction.

## REFERENCES

- Buchler MW**, Gloor B, Muller CA, Friess H, Seiler CA, Uhl W. Acute necrotizing pancreatitis: treatment strategy according to the status of infection. *Ann Surg* 2000; **232**: 619-626
- Medich DS**, Lee TK, Melhem MF, Rowe MI, Schraut WH, Lee KK. Pathogenesis of pancreatic sepsis. *Am J Surg* 1993; **165**: 46-50
- Juononen PO**, Alhava EM, Takala JA. Gut permeability in patients with acute pancreatitis. *Scand J Gastroenterol* 2000; **35**: 1314-1318
- Liu Q**, Djuricin G, Nathan C, Gattuso P, Weinstein RA, Prinz RA. The effect of interleukin-6 on bacterial translocation in acute canine pancreatitis. *Int J Pancreatol* 2000; **27**: 157-165
- Li JY**, Lu Y, Hu S, Sun D, Yao YM. Preventive effect of glutamine on intestinal barrier dysfunction induced by severe trauma. *World J Gastroenterol* 2002; **8**: 168-171
- Simsek I**, Mas MR, Yasar M, Ozyurt M, Saglamkaya U, Deveci S, Comert B, Basustaoglu A, Kocabalkan F, Refik M. Inhibition of inducible nitric oxide synthase reduces bacterial translocation in a rat model of acute pancreatitis. *Pancreas* 2001; **23**: 296-301
- Colak T**, Ipek T, Paksoy M, Polat E, Uygun N, Kayabasi B. The effects of cefepim, G-CSF, and sucralbate on bacterial translocation in experimentally induced acute pancreatitis. *Surg Today* 2001; **31**: 502-506
- Cicalese L**, Sahai A, Sileri P, Rastellini C, Subbotin V, Ford H, Lee K. Acute pancreatitis and bacterial translocation. *Dig Dis Sci* 2001; **46**: 1127-1132
- Buttenschoen K**, Berger D, Hiki N, Buttenschoen DC, Vasilescu C, Chikh-Torab F, Seidelmann M, Beger HG. Endotoxin and antiendotoxin antibodies in patients with acute pancreatitis. *Eur J Surg* 2000; **166**: 459-466
- Bhatia M**, Neoptolemos JP, Slavin J. Inflammatory mediators as therapeutic targets in acute pancreatitis. *Curr Opin Investig Drugs* 2001; **2**: 496-501
- Steer ML**. Relationship between pancreatitis and lung diseases. *Respir Physiol* 2001; **128**: 13-16
- Grady EF**, Yoshimi SK, Maa J, Valeroso D, Vartanian RK, Rahim S, Kim EH, Gerard C, Gerard N, Bunnett NW, Kirkwood KS. Substance P mediates inflammatory oedema in acute pancreatitis via activation of the neurokinin-1 receptor in rats and mice. *Br J Pharmacol* 2000; **130**: 505-512
- Bhatia M**, Brady M, Shokuhi S, Christmas S, Neoptolemos JP, Slavin J. Inflammatory mediators in acute pancreatitis. *J Pathol* 2000; **190**: 117-125
- Denham JW**, Hauer-Jensen M, Kron T, Langberg CW. Treatment-time-dependence models of early and delayed radiation injury in rat small intestine. *Int J Radiat Oncol Biol Phys* 2000; **48**: 871-887
- Park PO**, Haglund U, Bulkley GB, Falt K. The sequence of development of intestinal tissue injury after strangulation ischemia and reperfusion. *Surgery* 1990; **107**: 574-580
- Weiss DJ**, Evanson OA, MacLeay J, Brown DR. Transient alteration in intestinal permeability to technetium Tc99m diethylenetriaminopentaacetate during the prodromal stages of alimentary laminitis in ponies. *Am J Vet Res* 1998; **59**: 1431-1434
- Li YS**, Li JS, Jiang JW, Liu FN, Li N, Qin WS, Zhu H. Glycyl-glutamine-enriched long-term total parenteral nutrition attenuates bacterial translocation following small bowel transplantation in the pig. *J Surg Res* 1999; **82**: 106-111
- Kleeff J**, Shi X, Bode HP, Hoover K, Shrikhande S, Bryant PJ, Korc M, Buchler MW, Friess H. Altered expression and localization of the tight junction protein ZO-1 in primary and metastatic pancreatic cancer. *Pancreas* 2001; **23**: 259-265
- Koliopanos A**, Friess H, Kleeff J, Shi X, Liao Q, Pecker I, Vlodavsky I, Zimmermann A, Buchler MW. Heparanase expression in primary and metastatic pancreatic cancer. *Cancer Res* 2001; **61**: 4655-4659
- King KA**, Hu C, Rodriguez MM, Romaguera R, Jiang X, Piedimonte G. Exaggerated neurogenic inflammation and substance P receptor upregulation in RSV-infected weanling rats. *Am J Respir Cell Mol Biol* 2001; **24**: 101-107
- Piedimonte G**, Rodriguez MM, King KA, McLean S, Jiang X. Respiratory syncytial virus upregulates expression of the substance P receptor in rat lungs. *Am J Physiol* 1999; **277(4 Pt 1)**: L831-840
- Kaltreider HB**, Ichikawa S, Byrd PK, Ingram DA, Kishiyama JL, Sreedharan SP, Warnock ML, Beck JM, Goetzl EJ. Upregulation of neuropeptides and neuropeptide receptors in a murine model of immune inflammation in lung parenchyma. *Am J Respir Cell Mol Biol* 1997; **16**: 133-144
- Andersson R**, Wang XD. Gut barrier dysfunction in experimental acute pancreatitis. *Ann Acad Med Singapore* 1999; **28**: 141-146
- Wang XD**, Borjesson A, Sun ZW, Wallen R, Deng XM, Zhang HY, Hallberg E, Andersson R. The association of type II pneumocytes and endothelial permeability with the pulmonary macrophage system in experimental acute pancreatitis. *Eur J Clin Invest* 1998; **28**: 778-785
- Hirsh M**, Dyugovskaya L, Bashenko Y, Krausz MM. Reduced rate of bacterial translocation and improved variables of natural killer cell and T-cell activity in rats surviving controlled hemorrhagic shock and treated with hypertonic saline. *Crit Care Med* 2002; **30**: 861-867
- Shimizu T**, Tani T, Endo Y, Hanasawa K, Tsuchiya M, Kodama M. Elevation of plasma peptidoglycan and peripheral blood neutrophil activation during hemorrhagic shock: plasma peptidoglycan reflects bacterial translocation and may affect neutrophil activation. *Crit Care Med* 2002; **30**: 77-82
- Doty JM**, Oda J, Ivatury RR, Blocher CR, Christie GE, Yelon JA, Sugerman HJ. The effects of hemodynamic shock and increased intra-abdominal pressure on bacterial translocation. *J Trauma* 2002; **52**: 13-17
- Koyluoglu G**, Bakici MZ, Elagoz S, Arpacik M. The effects of pentoxifylline treatment on bacterial translocation after hemorrhagic shock in rats. *Clin Exp Med* 2001; **1**: 61-66
- Ling YL**, Meng AH, Zhao XY, Shan BE, Zhang JL, Zhang XP. Effect of cholecystokinin on cytokines during endotoxic shock in rats. *World J Gastroenterol* 2001; **7**: 667-671
- Cui DX**, Zeng GY, Wang F, Xu JR, Ren DQ, Guo YH, Tian FR, Yan XJ, Hou Y, Su CZ. Mechanism of exogenous nucleic acids and their precursors improving the repair of intestinal epithelium after gamma-irradiation in mice. *World J Gastroenterol* 2000; **6**: 709-717
- Wu XN**. Current concept of pathogenesis of severe acute

- pancreatitis. *World J Gastroenterol* 2000; **6**: 32-36
- 32 **Indaram AV**, Nandi S, Weissman S, Lam S, Bailey B, Blumstein M, Greenberg R, Bank S. Elevated basal intestinal mucosal cytokine levels in asymptomatic first-degree relatives of patients with Crohn's disease. *World J Gastroenterol* 2000; **6**: 49-52
- 33 **Zhu L**, Yang ZC, Li A, Cheng DC. Protective effect of early enteral feeding on postburn impairment of liver function and its mechanism in rats. *World J Gastroenterol* 2000; **6**: 79-83
- 34 **Meng AH**, Ling YL, Zhang XP, Zhao XY, Zhang JL. CCK-8 inhibits expression of TNF-alpha in the spleen of endotoxic shock rats and signal transduction mechanism of p38 MAPK. *World J Gastroenterol* 2002; **8**: 139-143
- 35 **Zhu L**, Yang ZC, Li A, Cheng DC. Reduced gastric acid production in burn shock period and its significance in the prevention and treatment of acute gastric mucosal lesions. *World J Gastroenterol* 2000; **6**: 84-88
- 36 **Schwarz M**, Thomsen J, Meyer H, Buchler MW, Beger HG. Frequency and time course of pancreatic and extrapancreatic bacterial infection in experimental acute pancreatitis in rats. *Surgery* 2000; **127**: 427-432
- 37 **Hongo H**, Takano H, Imai A, Yamaguchi T, Boku Y, Fujii T, Naito Y, Yoshida N, Yoshikawa T, Kondo M. Pancreatic phospholipase A2 induces bacterial translocation in rats. *Immunopharmacol Immunotoxicol* 1999; **21**: 717-726
- 38 **Duggan AW**, Hendry IA, Morton CR, Hutchison WD, Zhao ZQ. Cutaneous stimuli releasing immunoreactive substance P in the dorsal horn of the cat. *Brain Res* 1988; **451**: 261-273
- 39 **Cao YQ**, Mantyh PW, Carlson EJ, Gillespie AM, Epstein CJ, Basbaum AI. Primary afferent tachykinins are required to experience moderate to intense pain. *Nature* 1998; **392**: 390-394
- 40 **Maa J**, Grady EF, Kim EH, Yoshimi SK, Hutter MM, Bunnett NW, Kirkwood KS. NK-1 receptor desensitization and neutral endopeptidase terminate SP-induced pancreatic plasma extravasation. *Am J Physiol Gastrointest Liver Physiol* 2000; **279**: G726-732
- 41 **Maa J**, Grady EF, Yoshimi SK, Drasin TE, Kim EH, Hutter MM, Bunnett NW, Kirkwood KS. Substance P is a determinant of lethality in diet-induced hemorrhagic pancreatitis in mice. *Surgery* 2000; **128**: 232-239
- 42 **Kirkwood KS**, Kim EH, He XD, Calauastro EQ, Domush C, Yoshimi SK, Grady EF, Maa J, Bunnett NW, Debas HT. Substance P inhibits pancreatic exocrine secretion via a neural mechanism. *Am J Physiol* 1999; **277**(2 Pt 1): G314-320
- 43 **Bhatia M**, Saluja AK, Hofbauer B, Frossard JL, Lee HS, Castagliuolo I, Wang CC, Gerard N, Pothoulakis C, Steer ML. Role of substance P and the neurokinin 1 receptor in acute pancreatitis and pancreatitis-associated lung injury. *Proc Natl Acad Sci U S A* 1998; **95**: 4760-4765

Edited by Ma JY

# Effect of oxytocin on contraction of rabbit proximal colon *in vitro*

Dong-Ping Xie, Lian-Bi Chen, Chuan-Yong Liu, Jing-Zhang Liu, Ke-Jing Liu

**Dong-Ping Xie, Lian-Bi Chen, Chuan-Yong Liu, Jing-Zhang Liu, Ke-Jing Liu**, Department of Physiology, Medical School, Shandong University, Jinan 250012, Shandong Province, China

**Supported by** Scientific Initiating Grants of Shandong University and Shandong Science Foundation

**Correspondence to:** Lian-Bi Chen, Department of Physiology, School of Medicine, Shandong University, Jinan 250012, Shandong Province, China. clb@sdu.edu.cn

**Telephone:** +86-531-8382037 **Fax:** +86-531-8382156

**Received:** 2002-06-08 **Accepted:** 2002-07-03

## Abstract

**AIM:** To investigate the effects of oxytocin (OT) on isolated rabbit proximal colon and its mechanism.

**METHODS:** Both longitudinal muscle (LM) and circular muscle (CM) were suspended in a tissue chamber containing 5 mL Krebs solution (37 °C), bubbled continuously with 950 mL·L<sup>-1</sup> O<sub>2</sub> and 50 mL·L<sup>-1</sup> CO<sub>2</sub>. Isometric spontaneous contractile responses to oxytocin or other drugs were recorded in circular and longitudinal muscle strips.

**RESULTS:** OT (0.1 U·L<sup>-1</sup>) failed to elicit significant effects on the contractile activity of proximal colonic smooth muscle strips ( $P > 0.05$ ). OT (1 to 10 U·L<sup>-1</sup>) decreased the mean contractile amplitude and the contractile frequency of CM and LM. Hexamethonium (10 μmol·L<sup>-1</sup>) partly blocked the inhibition of oxytocin (1 U·L<sup>-1</sup>) on the contractile frequency of CM. N<sup>ω</sup>-nitro-L-arginine-methylester (L-NAME, 1 μmol·L<sup>-1</sup>), progesterone (32 μmol·L<sup>-1</sup>) and estrogen (2.6 μmol·L<sup>-1</sup>) had no effects on OT-induced responses.

**CONCLUSION:** OT inhibits the motility of proximal colon in rabbits. The action is partly relevant with N receptor, but irrelevant with that of NO, progesterone or estrogen.

Xie DP, Chen LB, Liu CY, Liu JZ, Liu KJ. Effect of oxytocin on contraction of rabbit proximal colon *in vitro*. *World J Gastroenterol* 2003; 9(1): 165-168

<http://www.wjgnet.com/1007-9327/9/165.htm>

## INTRODUCTION

Oxytocin (OT) is a very abundant neuropeptide. The structure of the OT gene was elucidated in 1984<sup>[1]</sup>, and the sequence of the OT receptor was reported in 1992<sup>[2]</sup>. OT exerted a wide spectrum of central and peripheral effects<sup>[3-5]</sup>. It was reported that hypothalamic paraventricular nucleus is a site of controlling gastric function<sup>[6]</sup>, oxytocin facilitated the manifestation of inhibitory effects of hypothalamus on the motor function of gastrointestinal tract<sup>[7]</sup>. The experiments on rats had shown that gastric motility was inhibited by microinjection of oxytocin into the dorsal motor nucleus of the vagus (DMN), and that the inhibition of gastric motility after electrical stimulation of the hypothalamic paraventricular nucleus was blocked by microinjection of an oxytocin receptor antagonist directly into the DMN. These results suggested that oxytocin acted on the gastric motility via DMN<sup>[8]</sup>. The reports on peripheral action of oxytocin to influence gastrointestinal

(GI) motility were controversial: OT decreases the contractions of the guinea pig stomach *in vitro*, and inhibits the tone and peristaltic contractions of stomach and small intestines in fasting dogs *in vivo*<sup>[9]</sup>; but increases the gastric emptying of semisolid food in normal human and the contractions of gastric smooth muscle strips in rats<sup>[10]</sup>. The effect of oxytocin on colonic motility is still unknown.

OTR is functionally coupled to GTP binding proteins, stimulates the activity of phospholipase C-β isoforms. Finally, a variety of cellular events are initiated. For example, the forming Ca<sup>2+</sup>-calmodulin complexes triggers the activation of neuronal and endothelial isoforms of nitric oxide (NO) synthase<sup>[11]</sup>. Steroid hormones were reported to control oxytocin receptor (OTR) activity via both genomic and nongenomic pathways<sup>[12]</sup>. Estrogen induces the OTR mRNA expression, and then increases the OTR density on the membrane of the uterus smooth muscle and central nervous system<sup>[13,14]</sup>; on the other hand, progesterone inhibits the nuclear OTR mRNA expression, and decreases the sensitivity of the target cell on OT stimulation<sup>[15,16]</sup>; progesterone was also reported to bind to OTR with high affinity and inhibit the receptor function<sup>[17]</sup>. In this study, we investigated the effect of OT on proximal colonic motility of rabbits; We also investigated if the OT-induced responses were relevant with NO, steroid hormones or N receptor.

## MATERIALS AND METHODS

### Animal preparation

Rabbits of both sexes, weighing 1.5-2 kg, were fasted for 24-hour and sacrificed. The proximal colon (1 cm from the cecocolonic junction) was removed. The segment of the colon was opened along the mesentery. Muscle strips (8×2 mm) were cut, parallel to either the circular or the longitudinal fibers, and named circular muscle (CM) and longitudinal muscle (LM). The mucosa on each strip was carefully removed.

### Experiments

The muscle strip was suspended in a tissue chamber containing 5 mL Krebs solution (37 °C) and bubbled continuously with 950 mL·L<sup>-1</sup> O<sub>2</sub> and 50 mL·L<sup>-1</sup> CO<sub>2</sub><sup>[18]</sup>. One end of the strip was fixed to a hook on the bottom of the chamber. The other end was connected to an external isometric force transducer (JZ-BK, BK). Motility of colonic strips (under an initial tension of 1 g) in 2 tissue chambers were simultaneously recorded on ink-writing recorders (LMS-ZB, Cheng-Du). After 1 h equilibration, OT (0.1, 1, 10 U·L<sup>-1</sup>) was added in the tissue chamber to observe their effects on proximal colon; N<sup>ω</sup>-nitro-L-arginine-methylester (L-NAME, 1 μmol·L<sup>-1</sup>), hexamethonium (10 μmol·L<sup>-1</sup>), progesterone (32 μmol·L<sup>-1</sup>) or estrogen (2.6 μmol·L<sup>-1</sup>), given 3 min before the administration of OT (1 U·L<sup>-1</sup>), was added separately to investigate whether the actions of OT were relevant with NO, N receptor or steroids. The resting tension, the contractile frequency, and the mean contractile amplitude of LM and CM were measured.

### Drugs preparation

The following agents were used: oxytocin (Biochemical Pharmaceutical Company, Shanghai, China), N<sup>ω</sup>-nitro-L-arginine-methylester (L-NAME) and hexamethonium (Sigma Chemical Company), progesterone and estrogen (The Ninth Pharmaceutical Factory in Shanghai).

### Data analysis

The results were presented as  $\bar{x} \pm s$ , and statistically analyzed by paired *t* test,  $P < 0.05$  was considered to be significant.

## RESULTS

### Effect of OT on the spontaneous contraction of colonic smooth muscle strips

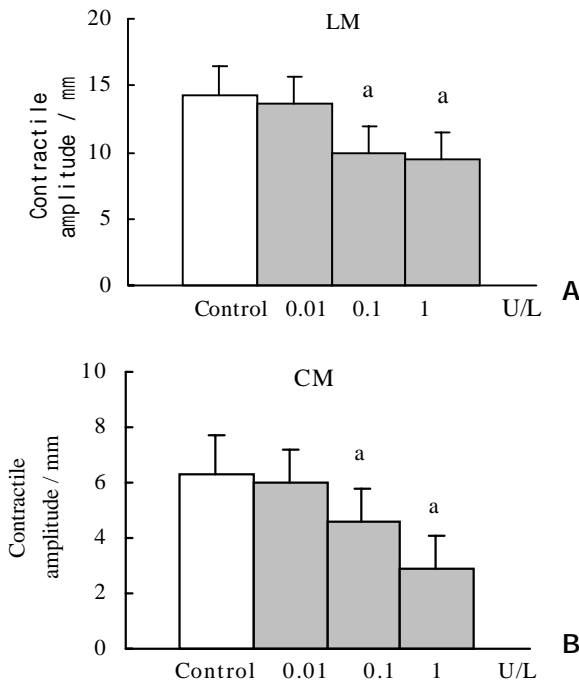


**Figure 1** A: Effect of oxytocin on the mean contractile amplitude of longitudinal muscle (LM) of proximal colon in rabbits. B: Effect of oxytocin on the mean contractile amplitude of circular muscle (CM) of proximal colon in rabbits. <sup>a</sup> $P < 0.05$  vs control,  $n = 10$ .

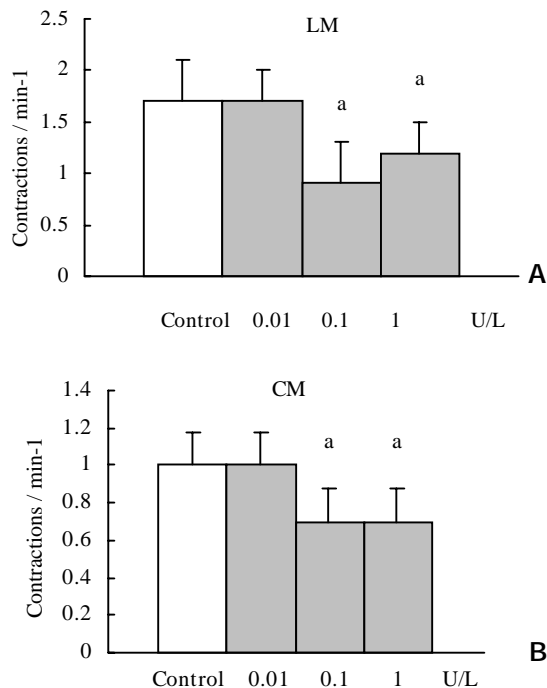


**Figure 2** A: Effect of oxytocin on the contractile frequency of longitudinal muscle (LM) of proximal colon in rabbits. B: Effect of oxytocin on the contractile frequency of circular muscle (CM) of proximal colon in rabbits. <sup>a</sup> $P < 0.05$  vs control,  $n = 10$ .

OT ( $0.1 \text{ U} \cdot \text{L}^{-1}$ ) failed to elicit significant effects on the contractile activity of proximal colonic smooth muscle strips ( $P > 0.05$ ). OT ( $1$  to  $10 \text{ U} \cdot \text{L}^{-1}$ ) decreased the mean contractile amplitude and the contractile frequency of CM and LM (Figure 1, Figure 2). It had no significant effects on the resting tension of CM and LM.

### Effect of hexamethonium on the OT-induced responses

Hexamethonium ( $10 \text{ } \mu\text{mol} \cdot \text{L}^{-1}$ ) had no significant effect on the contractile activity of each colonic smooth muscle strip. Hexamethonium given 3 minute before administration of OT ( $1 \text{ U} \cdot \text{L}^{-1}$ ) decreased OT-induced inhibition on the contractile frequency of CM (Figure 3). It had no significant effects on the other action of OT.

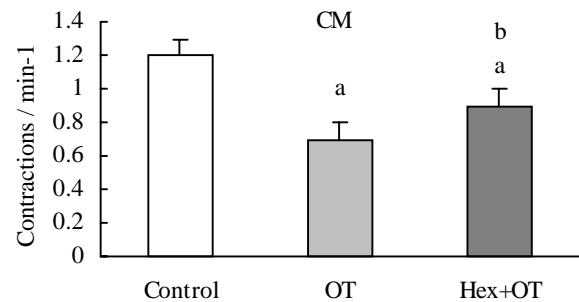


**Figure 3** Effect of oxytocin on the contractile frequency of circular muscle (CM) of proximal colon after hexamethonium pretreatment in rabbits. OT, oxytocin; Hex, hexamethonium. <sup>a</sup> $P < 0.05$  vs control, <sup>b</sup> $P < 0.05$  vs oxytocin,  $n = 6$ .

### Effect of L-NAME on the OT-induced responses

L-NAME ( $1 \text{ } \mu\text{mol} \cdot \text{L}^{-1}$ ) itself had no significant effects on proximal colon in rabbits. When given 3 min before the administration of OT ( $1 \text{ U} \cdot \text{L}^{-1}$ ), It had no significant effects on OT-induced responses.

### Effect of progesterone and estrogen on the OT-induced responses

Progesterone ( $32 \text{ } \mu\text{mol} \cdot \text{L}^{-1}$ ) and estrogen ( $2.6 \text{ } \mu\text{mol} \cdot \text{L}^{-1}$ ) had no significant effects on proximal colonic motility. When given 3 min before the administration of OT ( $1 \text{ U} \cdot \text{L}^{-1}$ ), neither progesterone nor estrogen had significant effects on OT-induced responses.

## DISCUSSION

The present study revealed that oxytocin  $1 \text{ U} \cdot \text{L}^{-1}$  to  $10 \text{ U} \cdot \text{L}^{-1}$  inhibited the spontaneous contractile motility of proximal colonic smooth muscle in rabbits. Petring *et al* reported that vein injection of oxytocin could increase the gastric emptying of semisolid food in normal human<sup>[10]</sup>. Oxytocin  $10$ – $100 \text{ U} \cdot \text{L}^{-1}$  stimulated the spontaneous contractile motility of gastric body and gastric antrum in rats *in vitro*. But oxytocin ( $10 \text{ pmol} \cdot \text{L}^{-1}$ – $10 \text{ nmol} \cdot \text{L}^{-1}$ ) suppressed the spontaneous contractions of circular smooth muscle from guinea-pig gastric antrum and gastric emptying in male rats<sup>[19,20]</sup>. Therefore, it seems that there are species, region and OT concentration differences in OT-induced contractions in gastrointestinal tract.

Our results showed that hexamethonium partly blocked the decreasing action of oxytocin on the contractile frequency of colonic strips, but not that of the contractile amplitude of the strips. These results suggested that oxytocin partly inhibited the contractile frequency of colonic strips via ganglion N receptor.

NO is found to be an inhibitory neurotransmitter of enteric neurons. NOS neurons has been identified in the myenteric plexus<sup>[21–23]</sup>. The action of OT has been reported to relevant

with NO<sup>[24]</sup> We observed the effect of L-NAME (inhibitor of NOS activity) on the inhibitory action of oxytocin to decide whether oxytocin inhibits the colonic contraction via NO synthetic pathway. The results showed that L-NAME had no effect on the inhibitory action of oxytocin, which suggested that the inhibitory action of oxytocin on colonic motility was irrelevant with NO.

OT has been identified to exert the actions via OT receptors in many tissues, including the hypothalamus, uterus, kidney, pancreas, heart, vasculature, and thymus<sup>[25-30]</sup>. Oxytocin receptor are suggested to be present on the members of guinea-pig antral smooth muscle cells<sup>[19]</sup>. OT might act on the proximal colonic smooth muscle via selective oxytocin receptor, which still need to be further studied.

The function and physiological regulation of the OT system has been reported to be strongly steroid dependent<sup>[31,32]</sup>. But our results showed that both progesterone and estrogen had no significant effects on OT-induced responses.

Effects on the gastrointestinal tract muscle during pregnancy are caused primarily by hormonal changes, such as progesterone, estrogen, and other hormones<sup>[33]</sup>. Motility changes occur throughout the gastrointestinal tract during pregnancy, including colonic transit manifested primarily as abdominal bloating and constipation<sup>[34]</sup>. Both progesterone and estrogen have been shown to inhibit colonic motility and transit in rats<sup>[35]</sup>. But Hinds and associates<sup>[36]</sup> reported that no significant differences in colon transit were found between phase of the menstrual cycle or between women and men. Our results also showed that neither progesterone nor estrogen affected the proximal colonic motility in rabbits. OT was another hormone relate to pregnancy, and its plasma concentration was higher in late pregnancy<sup>[37,38]</sup>. Our results showed that OT inhibited the colonic motility. Results from these studies provided new insight into the mechanisms controlling colonic motility during pregnancy and may form the basis for drug treatments of colonic motility disorders.

In conclusion, oxytocin inhibit the contractile activity of proximal colonic smooth muscle of rabbits *in vitro*. The action is partly relevant with N receptor, but irrelevant with that of NO, progesterone or estrogen.

## REFERENCES

- Ivell R, Richter D. Structure and comparison of the oxytocin and vasopressin genes from rat. *Proc Natl Acad Sci USA* 1984; **81**: 2006-2010
- Kimura T, Tanizawa O, Mori K, Brownstein MJ, Okayama H. Structure and expression of a human oxytocin receptor. *Nature* 1992; **356**: 526-529
- Arletti R, Bertolini A. Oxytocin acts as an antidepressant in two animal models of depression. *Life Sci* 1987; **41**: 1725-1730
- Arletti R, Benelli A, Bertolini A. Influence of oxytocin on feeding behavior in the rat. *Peptides* 1989; **10**: 89-93
- Ackerman AE, Lange GM, Clemens LG. Effects of paraventricular lesions on sex behavior and seminal emission in male rats. *Physiol Behav* 1997; **63**: 49-53
- Flanagan LM, Dohanics J, Verbalis JG, Stricker EM. Gastric motility and food intake in rats after lesions of hypothalamic paraventricular nucleus. *Am J Physiol* 1992; **263**: R39-44
- Dobrovol'skaia ZA, Kosenko AF. The role of oxytocin in realizing hypothalamic effects on the motor function of the digestive tract. *Fiziol Zh SSSR* 1989; **75**: 734-737
- Flanagan LM, Olson BR, Sved AF, Verbalis JG, Stricker EM. Gastric motility in conscious rats given oxytocin and an oxytocin antagonist centrally. *Brain Research* 1992; **578**: 256-260
- Milenov K, Barth T, Jost K, Kasakov L. Effect of deamino-dicarboxy oxytocin and oxytocin on myoelectrical and mechanical activity of uterus, stomach and small intestine in dog. *Endocrinol Exp* 1979; **13**: 177-183
- Petring OU. The effect of oxytocin on basal and pethidine - induced delayed gastric emptying. *Br J Clin Pharmacol* 1989; **28**: 329-332
- Melis MR, Argiolas A. Reduction of drug-induced yawning and penile erection and of noncontact erections in male rats by the activation of GABAA receptors in the paraventricular nucleus: involvement of nitric oxide. *Eur J Neurosci* 2002; **15**: 852-860
- Zingg HH, Grazzini E, Breton C, Larcher A, Rozen F, Russo C, Guillon G, Mouillac B. Genomic and non - genomic mechanisms of oxytocin receptor regulation. *Adv Exp Med Biol* 1998; **449**: 287-295
- Engstrom T, Bratholm P, Christensen NJ, Vilhardt H. Up-regulation of oxytocin receptors in non-pregnant rat myometrium by isoproterenol: effects of steroids. *J Endocrinol* 1999; **161**: 403-411
- Terenzi MG, Jiang QB, Cree SJ, Wakerley JB, Ingram CD. Effect of gonadal steroids on the oxytocin-induced excitation of neurons in the bed nuclei of the stria terminalis at parturition in the rat. *Neuroscience* 1999; **91**: 1117-1127
- Behrendt-Adam CY, Adams MH, Simpson KS, McDowell KJ. Oxytocin - neurophysin I mRNA abundance in equine uterine endometrium. *Domes Anim Endocrinol* 1999; **16**: 183-192
- Murata T, Murata E, Liu CX, Narita K, Honda K, Higuchi T. Oxytocin receptor gene expression in rat uterus: regulation by ovarian steroids. *J Endocrinol* 2000; **166**: 45-52
- Grazzini E, Guillon G, Mouillac B, Zingg HH. Inhibition of oxytocin receptor function by direct binding of progesterone. *Nature* 1998; **392**: 509-512
- Xie DP, Li W, Qu SY, Zheng TZ, Yang YL, Ding YH, Wei YL, Chen LB. Effect of areca on contraction of colonic muscle strips in rats. *World J Gastroenterol* 2002; **8**: 350-352
- Duridanova DB, Nedelcheva MD, Gagov HS. Oxytocin induced changes in single cell K<sup>+</sup> currents and smooth muscle contraction of guinea-pig gastric antrum. *Eur J Endocrinol* 1997; **136**: 531-538
- Liu CY, Chen LB, Liu PY, Xie DP, Wang PS. Effects of progesterone on gastric emptying and intestinal transit in male rats. *World J Gastroenterol* 2002; **8**: 338-341
- Peng X, Feng JB, Yan H, Zhao Y, Wang SL. Distribution of nitric oxide synthase in stomach myenteric plexus of rats. *World J Gastroenterol* 2001; **7**: 852-854
- Venkova K, Krier J. A nitric oxide and prostaglandin-dependent component of NANC off-contractions in cat colon. *Am J Physiol* 1994; **266**: G40-G47
- Powell AK, Bywater RA. Endogenous nitric oxide release modulates the direction and frequency of colonic migrating motor complexes in the isolated mouse colon. *Neurogastroenterol Motil* 2001; **13**: 221-228
- Haraldsen L, Soderstrom-Lauritzen V, Nilsson GE. Oxytocin stimulates cerebral blood flow in rainbow trout (*Oncorhynchus mykiss*) through a nitric oxide dependent mechanism. *Brain Res* 2002; **929**: 10-14
- Adan RA, Van Leeuwen FW, Sonnemans MA, Brouns M, Hoffman G, Verbalis JG, Burbach JP. Rat oxytocin receptor in brain, pituitary, mammary gland, and uterus: partial sequence and immunocytochemical localization. *Endocrinology* 1995; **136**: 4022-4028
- Jasper JR, Harrell CM, O'Brien JA, Pettibone DJ. Characterization of the human oxytocin receptor stably expressed in 293 human embryonic kidney cells. *Life Sci* 1995; **57**: 2253-2261
- Jeng YJ, Lolait SJ, Strakova Z, Chen C, Copland JA, Mellman D, Hellmich MR, Soloff MS. Molecular cloning and functional characterization of the oxytocin receptor from a rat pancreatic cell line (RINm5F). *Neuropeptides* 1996; **30**: 557-565
- Jankowski M, Hajjar F, Kawas SA, Mukaddam DS, Hoffman G, McCann SM, Gutkowska J. Rat heart: a site of oxytocin production and action. *Proc Natl Acad Sci USA* 1998; **95**: 14558-14563
- Jankowski M, Wang D, Hajjar F, Mukaddam DS, McCann SM, Gutkowska J. Oxytocin and its receptors are synthesized in the rat vasculature. *Proc Natl Acad Sci USA* 2000; **97**: 6207-6211
- Elands J, Resink A, De Kloet ER. Neurohypophysial hormone receptors in the rat thymus, spleen, and lymphocytes. *Endocrinology* 1990; **126**: 2703-2710
- Gimpl G, Fahrenholz F. The oxytocin receptor system: structure, function, and regulation. *Physiol Rev* 2001; **81**: 629-683

- 32 **Soloff MS**, Grzonka Z. Binding studies with rat myometrial and mammary gland membranes on effects of mannanase on relative affinities of receptors for oxytocin analogs. *Endocrinology* 1986; **119**: 1564-1569
- 33 **Everson GT**. Gastrointestinal motility in pregnancy. *Gastroenterol Clin North Am* 1992; **21**: 751-776
- 34 **Baron TH**, Ramirez B, Richter JE. Gastrointestinal motility disorder during pregnancy. *Ann Intern Med* 1993; **118**: 366-375
- 35 **Ryan JP**, Bhojwani A. Colonic transit in rats: effect of ovariectomy, sex steroid hormones, and pregnancy. *Am J Physiol* 1986; **251**:G46-50
- 36 **Hinds JP**, Stoney B, Wald A. Does gender or the menstrual cycle affect colonic transit? *Am J Gastroenterol* 1989; **84**: 123-126
- 37 **Mizutani S**, Hayakawa H, Akiyama H, Sakura H, Yoshino M, Oya M, Kawashima Y. Simultaneous determinations of plasma oxytocin and serum placental leucine aminopeptidase (P-LAP) during late pregnancy. *Clin Biochem* 1982; **15**: 141-145
- 38 **Kumaresan P**, Subramanian M, Anandarangam PB, Kumaresan M. Radioimmunoassay of plasma and pituitary oxytocin in pregnant rats during various stages of pregnancy and parturition. *J Endocrinol Invest* 1979; **2**: 65-70

Edited by Wu XN



# A new cytokine: the possible effect pathway of methionine enkephalin

Xin-Hua Liu, Dong-Ai Huang, Fei-Yi Yang, Yan-Sheng Hao, Guo-Guang Du, Ping-Feng Li, Gang Li

**Xin-Hua Liu, Fei-Yi Yang, Yan-Sheng Hao, Guo-Guang Du, Ping-Feng Li, Gang Li**, Department of Biochemistry and Molecular Biology, Health Science Center, Peking University, Beijing 100083, China  
**Dong-Ai Huang**, Department of Biochemistry, Hainan Medical College, Haikou 571101, Hainan Province China

**Supported by** National Science Foundation of China, No. 30060091  
**Correspondence to:** Dr. Gang Li and Ping-Feng Li, Department of Biochemistry and Molecular Biology, Peking University Health Science Center, Beijing 100083, China. ligang55@263.net

**Telephone:** +86-10-62092454

**Received:** 2002-06-01 **Accepted:** 2002-07-06

## Abstract

**AIM:** To investigate experimentally the effects of methionine enkephalin on signal transduction of mouse myeloma NS-1 cells.

**METHODS:** The antigen determinate of delta opioid receptor was designed in this lab and the polypeptide fragment of antigen determinate with 12 amino acids residues was synthesized. Monoclonal antibody against this peptide fragment was prepared. Proliferation of Mouse NS-1 cells treated with methionine enkephalin of  $1 \times 10^{-6}$  mol·L<sup>-1</sup> was observed. The activities of protein kinase A (PKA) and protein kinase C (PKC) were measured and thereby the mechanism of effect of methionine enkephalin was postulated.

**RESULTS:** The results demonstrated that methionine enkephalin could enhance the proliferation of NS-1 cells and the effect of methionine enkephalin could be particularly blocked by monoclonal antibody. The activity of PKA was increased in both cytosol and cell membrane. With reference to PKC, the intracellular activity of PKC in NS-1 cells was elevated at  $1 \times 10^{-7}$  mol·L<sup>-1</sup> and then declined gradually as the concentration of methionine enkephalin was raised. The effects of methionine enkephalin might be reversed by both naloxone and monoclonal antibody.

**CONCLUSION:** Coupled with the findings, it indicates that the signal transduction systems via PKA and PKC are involved in the effects of methionine enkephalin by binding with the traditional opioid receptors, and therefore resulting in different biological effects.

Liu XH, Huang DA, Yang FY, Hao YS, Du GG, Li PF, Li G. A new cytokine: the possible effect pathway of methionine enkephalin. *World J Gastroenterol* 2003; 9(1): 169-173  
<http://www.wjgnet.com/1007-9327/9/169.htm>

## INTRODUCTION

A number of studies have documented the involvement of endogenous opioid peptide on the cellular functions. It has been known that opioid receptors exist on the surface of cells pertinent to immune function, and that the activation or inhibition of these receptors may enhance or down regulate

some cell activities. Methionine enkephalin, the native opioid peptide, has been identified and defined as a cytokine because of its non-neurotransmitter function and sharing all of the major properties of cytokines<sup>[1-4]</sup>. Although numerous studies have shown that opioid-induced alteration of cellular function can be mediated indirectly via the central nervous system (CNS) or through direct interaction with cells, the precise cellular mechanisms underlying the immunomodulatory effects of opioids are largely unknown.

It is especially true that the opioid receptors contain consensus sites for phosphorylation by numerous protein kinases. Protein kinase C (PKC) has been shown to catalyze the *in vitro* phosphorylation of delta-opioid receptors and to potentiate agonist-induced receptor desensitization<sup>[5,6]</sup>. On the other hand, studies suggest that acute and chronic opioid can regulate the cAMP-dependent protein kinase (PKA) signaling pathway and the changes in this pathway may be involved in opioid tolerance<sup>[7-9]</sup>. It has been documented that increased PKA activity can maintain cellular tolerance to opioid receptor agonist by chronic opioid treatment<sup>[10]</sup>.

Although there is mounting evidence supporting the concept that opioids are members of the cytokine-like family, the relative contribution of the opioids to immunoregulation remains unclear. Furthermore, little has been studied how methionine enkephalin acts as binding with the receptor of cell surface and trigger the intracellular biological events via some kinases. In this series of experiments, we analyzed the effect of methionine enkephalin, the endogenous opioid, on the activities of PKA and PKC at various dosages. The effects of monoclonal antibody and naloxone were also determined so that the mechanism of effect of methionine enkephalin on the signal transduction will be further clarified.

## MATERIALS AND METHODS

### Materials

Methionine enkephalin, naloxone, dithiothreitol (DTT), leupeptin, histone, phosphatidyl serine (PS), diacylglycerol (DG) and ATP were purchased from SIGMA; DMEM medium, bovine serum albumin (BSA) and 1-eth-3-3-dimethylaminopropyl carbodimide-HCl (EDC) were purchased from GIBCO; phenylmethyl sulfonyl fluoride (PMSF) and egtazic acid (EGTA) were from SERVAL.

### Methods

#### Design of polypeptide fragment of delta opioid receptor

Delta opioid receptor is composed of 372 amino acids residues. Hydrophilic analysis and structure prediction were performed in our laboratory by typing the sequence of opioid receptor into a special computer program designed according to the principle of prediction of antigen determinants, and by which fragment of antigen determinant was selected<sup>[11]</sup>. The amino acids residues sequence of antigen determinant was selected from the 3<sup>rd</sup> hydrophilic peak based on the feature of possibility of antigen determinant and listed as follows: NH<sub>2</sub>-Gly-Ser-Leu-Arg-Arg-Pro-Arg-Gln-Ala-Thr-Thr-Arg-COOH.

**Synthesis of polypeptide fragment and preparation of monoclonal antibody** Polypeptide fragment with 12 amino

acids residues of delta opioid receptor was synthesized in North West University, USA. Monoclonal antibody against this polypeptide fragment was prepared according to the routine procedure. In short, BABL/C mice was immunized with synthesized polypeptide fragment conjugated with bovine serum albumin in complete Freund's adjuvant at 2- to 3-week intervals. The splenic cells separated from mice were fused with myeloma cells to form a stable antibody-producing hybridoma cell line. Positive clones were screened by the method of ELISA and inoculated into BALB/C mice. The antibody was harvested from ascitic fluid and purified with affinity chromatography. The titers of monoclonal antibodies were higher than 3 000. The specificity and effects of monoclonal antibody were verified in this experiment.

**Effect of methionine enkephalin on proliferation of NS-1 cell lines** NS-1, Mouse myeloma cell line, was cultured in DMEM medium containing 10 % fetal calf serum at 37 °C in a humidified atmosphere of 5 % CO<sub>2</sub>. After the cell growth occupied full of the bottom of the flasks, the cells were washed once and resuspended in medium at a density of  $5 \times 10^4$  cells per ml. 1 ml of the cells per well was liquated in a 24 wells plate. When the cells were grown about 70 % full of wells, the supernatant was taken out. Then the cells were resuspended in 1 ml of medium without serum and cultured for one more day. After 1 d, supernatants in all wells were removed and the cells were resuspended in 1 ml of medium (with 10 % fetal calf serum). The cells were administrated with  $1 \times 10^{-6}$  mol·L<sup>-1</sup> of methionine enkephalin. Different concentrations of monoclonal antibody ( $0.1$ – $10 \times 10^{-9}$  mol·L<sup>-1</sup>) were used to block the effect of methionine enkephalin. The culture was continued for 2 d and then pulsed with  $18.5 \times 10^3$  Bq of <sup>3</sup>H-TdR in each well. 4 h later, the cells were harvested onto glass microfiber filter using a multiple sample harvester. The incorporation of <sup>3</sup>H-TdR was measured by using LKB 1209 Rackbeta liquid scintillation counter.

**Determination of protein kinase A activity** NS-1 cells were adjusted to  $5 \times 10^4$  cells per ml with DME medium (containing 10 % fetal calf serum) and aliquot into 24 well plate at 1 ml cell suspension per well. When the cells were grown about 70 % full of the wells, the supernatant was taken out. Then the cells were resuspended in 1 ml of medium without serum, cultured for one more day and added  $1 \times 10^{-6}$  mol·L<sup>-1</sup> of methionine enkephalin. For the blocking assay, the different concentration of monoclonal antibody ( $0.1$ – $10 \times 10^{-6}$  mol·L<sup>-1</sup>) and naloxone ( $0.1$ – $10 \times 10^{-6}$  mol·L<sup>-1</sup>) were added at the same time. After 24 h, the cells were collected, resuspended in 500 µl of buffer A (containing 200 mmol·L<sup>-1</sup> Tris-HCl pH 7.5, 0.25 mol·L<sup>-1</sup> sucrose, 2 mmol·L<sup>-1</sup> edetic acid, 2 mmol·L<sup>-1</sup> dithiothreitol, 10 mg·L<sup>-1</sup> leupeptin and 0.5 mmol·L<sup>-1</sup> PMSF) and destroyed by supersonic instrument for 2 min in ice bath. The supernatants were collected following a spin at 10 000 g for 45 min and defined as the cytosol fraction. The pellet was resuspended in 400 µl of buffer A containing 0.5 % Triton X-100, supersonically destroyed for 2 min and defined as the membrane fraction. The measurement of PKA activity was carried out as described with modifications<sup>[12]</sup>. In short, 40 µl of extracted enzyme fractions were mixed with 160 µl of the solution at the final concentration of 20 mmol·L<sup>-1</sup> Tris-HCl pH 7.5, 5 mmol·L<sup>-1</sup> MgCl<sub>2</sub>, 0.25 g·L<sup>-1</sup> BSA, 0.5 g·L<sup>-1</sup> histone,  $2 \times 10^{-7}$  mol·L<sup>-1</sup> ATP ( $\gamma$ -<sup>32</sup>P ATP,  $3.7 \times 10^4$  Bq) and 8.0 µmol·L<sup>-1</sup> of cAMP at 37 °C for 10 min. After followed by incubation in ice bath for 5 min to terminate the reaction, 150 µl of the solution from each sample was collected onto Whatmen GF/C filter paper. After washing 2× with 10 % TCA-2 % phosphoric acid for 30 min at room temperature followed by 2× wash with 5 % TCA for 30 min, the activities of PKA were measured by using liquid scintillation counter and expressed as pmol value of <sup>32</sup>P in histone catalyzed by per mg protein per min.

**Determination of protein kinase C activity** The procedures of cell treatment and enzyme extraction were similar to that described in the determination of PKA instead of cells resuspended in 500 µl of buffer B (buffer A+10 mmol·L<sup>-1</sup> egtazic acid). The final volume was 200 µl with final concentration of 20 mmol·L<sup>-1</sup> Tris-HCl pH 7.5, 5 mmol·L<sup>-1</sup> MgCl<sub>2</sub>, 0.25 g·L<sup>-1</sup> BSA, 0.5 g·L<sup>-1</sup> histone,  $2 \times 10^{-5}$  mol·L<sup>-1</sup> ATP ( $\gamma$ -<sup>32</sup>P ATP,  $3.7 \times 10^4$  Bq), and 40 µl of extracted enzyme fraction. The measurement of activity of PKC was performed as described by Choi *et al.* with modification<sup>[13]</sup>. Briefly, 5 mmol·L<sup>-1</sup> CaCl<sub>2</sub>, 80 mg·L<sup>-1</sup> PS and 3 mg·L<sup>-1</sup> DG were added into reaction system. The collection and assay of samples and the addition of methionine enkephalin, also monoclonal antibody and naloxone, were according to the measurement of PKA. The activities of PKC were expressed with pmol value of <sup>32</sup>P in histone catalyzed by per mg protein per min (pmol·mg<sup>-1</sup>·min<sup>-1</sup>).

### Statistical analysis

The data were expressed as  $\bar{x} \pm s$  obtained from at least 3 independent experiments and analyzed by *t* test.

## RESULTS

### Effects of methionine enkephalin on the proliferation of NS-1 cells

Methionine enkephalin could stimulate the proliferation of NS-1 cells. When  $1 \times 10^{-6}$  mol·L<sup>-1</sup> of methionine enkephalin was added into the cultured cells, the cells could proliferate up to 109 %. Monoclonal antibody at a lower concentration of  $0.1 \times 10^{-9}$  mol·L<sup>-1</sup> could not block the effect of methionine enkephalin. Whereas 1 and  $10 \times 10^{-9}$  mol·L<sup>-1</sup> of monoclonal antibody could reverse the enhancing effect of methionine enkephalin on the cell proliferation that showed significantly the differences as compared with treatment group of methionine enkephalin alone (Figure 1).

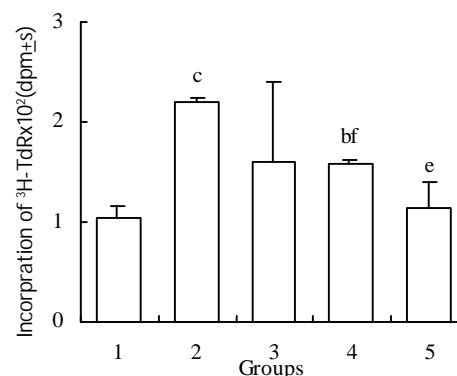


**Figure 1** Blockage of monoclonal antibody to the effect of methionine enkephalin on the proliferation of NS-1 cells. Treatment groups; 1: control group; 2:  $1 \times 10^{-6}$  mol·L<sup>-1</sup> methionine enkephalin; 3:  $1 \times 10^{-6}$  mol·L<sup>-1</sup> methionine enkephalin plus  $1 \times 10^{-10}$  mol·L<sup>-1</sup> monoclonal antibody; 4:  $1 \times 10^{-6}$  mol·L<sup>-1</sup> methionine enkephalin plus  $1 \times 10^{-9}$  mol·L<sup>-1</sup> monoclonal antibody; 5:  $1 \times 10^{-6}$  mol·L<sup>-1</sup> methionine enkephalin plus  $1 \times 10^{-8}$  mol·L<sup>-1</sup> monoclonal antibody. *n*=3 from 3 independent experiments. <sup>b</sup>*P*<0.05 and <sup>c</sup>*P*<0.01 vs control group, <sup>e</sup>*P*<0.05 and <sup>f</sup>*P*<0.01 vs group 2

### Effects of methionine enkephalin on the activity of PKA

Methionine enkephalin at various concentrations could enhance the level of activity of PKA in cytosol and cell membrane. The effects could be observed at the concentration of  $0.1$ – $10 \times 10^{-6}$  mol·L<sup>-1</sup> in cytosol and  $0.01$ – $10 \times 10^{-6}$  mol·L<sup>-1</sup> in cell membrane. The effects of methionine enkephalin on the activity of PKA were consistent in the cytosol and the cell membrane (Figure 2).

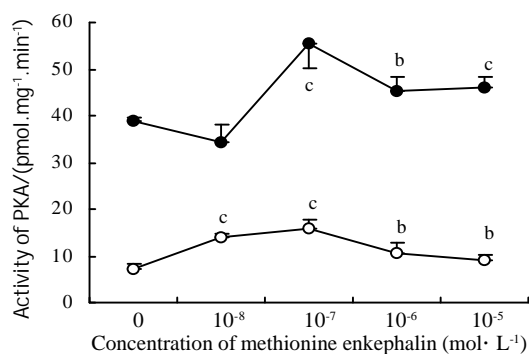


**Figure 2** The influences of different concentrations of methionine enkephalin on the activity of PKA in cytosol (●) and cell membrane (○) of NS-1 cells.  $n=3$  from 3 independent experiments. <sup>b</sup> $P<0.05$  and <sup>c</sup> $P<0.01$  vs control ( $0 \text{ mol} \cdot \text{L}^{-1}$ )

### Antagonism of monoclonal antibody and naloxone on the activity of PKA

$1 \times 10^{-6} \text{ mol} \cdot \text{L}^{-1}$  of methionine enkephalin was used for the blocking assay of monoclonal antibody on the activity of PKA. The reversed effects could be observed at the concentration of  $1 \times 10^{-10}$  and  $1 \times 10^{-9} \text{ mol} \cdot \text{L}^{-1}$  of antibody (Table 1). After administration of different concentrations of naloxone in the case of cytosol, the reversed effects were also obvious (Figure 3).

**Table 1** Antagonism of different of concentrations of monoclonal antibody (Mab) to methionine enkephalin (MENK) at  $1 \times 10^{-6} \text{ mol} \cdot \text{L}^{-1}$  on the activity of PKA in cytosol and membrane of NS-1 cells.  $n=3$  from 3 independent experiments. <sup>b</sup> $P<0.05$  and <sup>c</sup> $P<0.01$  vs control, <sup>e</sup> $P<0.05$  and <sup>f</sup> $P<0.01$  vs group 2

MENK+MAB	Activity of PKA in cytosol / $\text{pmol} \cdot \text{mg}^{-1} \cdot \text{min}^{-1}$	Activity of PKA in membrane / $\text{pmol} \cdot \text{mg}^{-1} \cdot \text{min}^{-1}$
Control	$21.10 \pm 1.09$	$6.81 \pm 1.63$
MENK	$24.69 \pm 0.49^c$	$10.42 \pm 0.71^b$
MENK+ $10^{-11} \text{ mol} \cdot \text{L}^{-1}$ MAB	$29.98 \pm 0.59^{cf}$	$13.73 \pm 1.84^{ce}$
MENK+ $10^{-10} \text{ mol} \cdot \text{L}^{-1}$ MAB	$20.03 \pm 1.47$	$7.59 \pm 0.35^e$
MENK+ $10^{-9} \text{ mol} \cdot \text{L}^{-1}$ MAB	$12.99 \pm 0.95^{cf}$	$7.11 \pm 2.04^e$

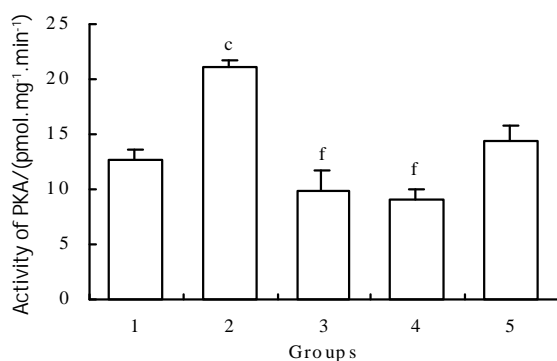


**Figure 3** The effects of different concentration of naloxone on the activity of PKA in cytosol of NS-1 cells. Treatment groups: 1: control; 2:  $1 \times 10^{-6} \text{ mol} \cdot \text{L}^{-1}$  methionine enkephalin; 3:  $1 \times 10^{-6} \text{ mol} \cdot \text{L}^{-1}$  methionine enkephalin plus  $1 \times 10^{-7} \text{ mol} \cdot \text{L}^{-1}$  naloxone; 4:  $1 \times 10^{-6} \text{ mol} \cdot \text{L}^{-1}$  methionine enkephalin plus  $1 \times 10^{-6} \text{ mol} \cdot \text{L}^{-1}$  naloxone; 5:  $1 \times 10^{-6} \text{ mol} \cdot \text{L}^{-1}$  methionine enkephalin plus  $1 \times 10^{-5} \text{ mol} \cdot \text{L}^{-1}$  naloxone.  $n=3$  from 3 independent experiments. <sup>c</sup> $P<0.01$  vs control, <sup>f</sup> $P<0.01$  vs group 2

### Effects of methionine enkephalin on the activity of PKC

In Figure 4, a narrow effective range of methionine enkephalin was displayed. At the concentration of  $1 \times 10^{-7} \text{ mol} \cdot \text{L}^{-1}$ ,

methionine enkephalin could enhance the intracellular activity of PKC (Figure 4), but the higher concentration ( $10^{-6}$ – $10^{-5} \text{ mol} \cdot \text{L}^{-1}$ ) of methionine enkephalin showed a suppressive effect compared with control ( $0 \text{ mol} \cdot \text{L}^{-1}$ ).

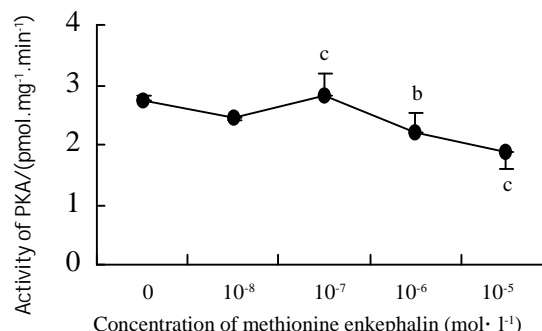


**Figure 4** The influences of different concentrations of methionine enkephalin on the intracellular activity of PKC in NS-1 cells.  $n=3$  from 3 independent experiments. <sup>b</sup> $P<0.05$  and <sup>c</sup> $P<0.01$  vs control ( $0 \text{ mol} \cdot \text{L}^{-1}$ ).

### Antagonism of monoclonal antibody and naloxone on the activity of PKC

Based on the data in Figure 4,  $1 \times 10^{-6} \text{ mol} \cdot \text{L}^{-1}$  of methionine enkephalin was used to inhibit the PKC. Like observed in the case of PKA, the effect of methionine enkephalin could be blocked by different concentrations of monoclonal antibody (Table 2). Naloxone at concentrations of  $1 \times 10^{-6}$  and  $1 \times 10^{-5} \text{ mol} \cdot \text{L}^{-1}$  could also reverse the suppressed effect of methionine enkephalin in the cytosol (Figure 5).

**Table 2** Antagonism of different of concentrations of monoclonal antibody (Mab) to methionine enkephalin (MENK) at  $1 \times 10^{-6} \text{ mol} \cdot \text{L}^{-1}$  on the intracellular activity of PKC in NS-1 cells.  $n=3$  from 3 independent experiments. <sup>b</sup> $P<0.05$  vs control, <sup>e</sup> $P<0.05$  and <sup>f</sup> $P<0.05$  vs group 2

MENK+MAB	Activity of PKC ( $\text{pmol} \cdot \text{mg}^{-1} \cdot \text{min}^{-1}$ )
Control	$3.06 \pm 0.19$
MENK	$2.26 \pm 0.03^b$
MENK+ $10^{-11} \text{ mol} \cdot \text{L}^{-1}$ MAB	$2.92 \pm 0.02^e$
MENK+ $10^{-10} \text{ mol} \cdot \text{L}^{-1}$ MAB	$2.80 \pm 0.4^e$
MENK+ $10^{-9} \text{ mol} \cdot \text{L}^{-1}$ MAB	$3.13 \pm 0.45^{ff}$

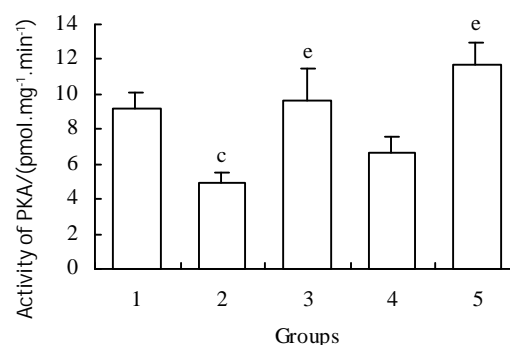


**Figure 5** The effects of different concentration of naloxone on the intracellular activity of PKC in NS-1 cells. Treatment groups: 1: control; 2:  $1 \times 10^{-6} \text{ mol} \cdot \text{L}^{-1}$  methionine enkephalin; 3:  $1 \times 10^{-6} \text{ mol} \cdot \text{L}^{-1}$  methionine enkephalin plus  $1 \times 10^{-7} \text{ mol} \cdot \text{L}^{-1}$  naloxone; 4:  $1 \times 10^{-6} \text{ mol} \cdot \text{L}^{-1}$  methionine enkephalin plus  $1 \times 10^{-6} \text{ mol} \cdot \text{L}^{-1}$  naloxone; 5:  $1 \times 10^{-6} \text{ mol} \cdot \text{L}^{-1}$  methionine enkephalin plus  $1 \times 10^{-5} \text{ mol} \cdot \text{L}^{-1}$  naloxone.  $n=3$  from 3 independent experiments. <sup>c</sup> $P<0.01$  vs control, <sup>e</sup> $P<0.05$  vs group 2

## DISCUSSION

The biological and clinical effects of opiate interaction with immune cells are well appreciated. In recent years, investigations from several laboratories have indicated that opioids can operate as cytokines, the principal communication signals of the immune system<sup>[1,2]</sup>. Our previous studies have also proved the cellular modulation of methionine enkephalin<sup>[3,4]</sup>. In this experiment, the results that methionine enkephalin could enhance the proliferation of NS-1 cells and perform the effect of growth factor-like, were consistent with the conclusion.

One possible component in the receptor signal cascade that can be responsible for these differences is the ligand-receptor interaction site. Receptor chimera studies followed by mutational analysis have revealed that functions of receptor domains were different for various opioid alkaloids and opioid peptides<sup>[14-19]</sup>. Based on the principle of antigen determinant, we prepared the monoclonal antibody against delta opioid receptor. Our data showed that the effects of methionine enkephalin were reversible in the presence of different concentration of monoclonal antibody, which indicating the existence of a functional domain at the peptides segment.

Although some laboratories have provided evidences that supporting agonist-induced down-regulation of opioid receptors appear to require the phosphorylation of the receptor protein<sup>[20-24]</sup>, the identities of the specific protein kinases that perform this task remain uncertain. Moreover, it is unknown whether the change of protein kinase activation was dependent on the effect of methionine enkephalin. Our data showed that the activities of PKA were up-regulated in both cytosol and membrane of NS-1 cells in a variety of concentrations of methionine enkephalin. The elevation of PKA activity showed dose-independent and the most efficient concentration of methionine enkephalin was at  $10^{-7}$  mol·L<sup>-1</sup>. It had been shown that increased PKA activity related to the maintenance of cellular tolerance to opioid receptor agonists<sup>[10, 25, 26]</sup>.

However, in the case of PKC, the enzyme activity was elevated when methionine enkephalin at the concentration of  $1 \times 10^{-7}$  mol·L<sup>-1</sup> and declined gradually at  $1 \times 10^{-6}$  to  $10^{-5}$  mol·L<sup>-1</sup>. The coincident results have also been observed in other laboratory. It had been reported that a biphasic response of opioid on expression of some cytokines had been demonstrated that nanomolar concentration of opioid augmented the secretion of both IL-6 and TNF- $\alpha$ , whereas micromolar concentration inhibited their synthesis<sup>[27]</sup>. It had also been reported that opioid-induced PKC translocation followed a time-dependent and biphasic pattern beginning 2 h after opioid addition, when a pronounced translocation of PKC to the plasma membrane occurred. When exposure to opioids was lengthened to >12 h, both cytosolic and particulate PKC levels dropped significantly below those of control-treated cells because of the decrease of membrane-bound PKC density<sup>[15, 28]</sup>.

From our data, the effect of methionine enkephalin could be reversed by a lower concentration of monoclonal antibody. Although little previous information was available to compare the usage of antibody, it was postulated that a complex ligand-receptor interaction was involved. The results that an antagonism of monoclonal antibody to the effect of methionine enkephalin on the activity of PKA or PKC indicated that the antigen determinant of the receptor fragment was also the functional domain of the receptor. The postulate was reinforced by studies involving  $\mu/\delta$  receptor chimeras that investigated the function of each domain<sup>[14, 15]</sup>. Likewise, the same results could be observed in the assay of naloxone, the antagonist of opioid receptor. The effect of naloxone abolishing the effect of opioid on the activity of PKA had been reported<sup>[29, 30]</sup>. Thus, a traditional opioid mechanism on signaling pathway of PKA and PKC was thereby involved.

## REFERENCES

- 1 **Peterson PK**, Molitor TW, Chao CC. The opioid-cytokine connection. *J Neuroimmunology* 1998; **83**: 63-69
- 2 **Plotnikoff NP**, Faith RE, Murgo AJ, Herberman RB, Good RA. Methionine enkephalin: a new cytokine-human studies. *Clin Immunol Immunopathol* 1997; **82**: 93-101
- 3 **Li G**, Fraker PJ. Methionine enkephalin alteration of mitogenic and mixed lymphocyte culture responses in zinc-deficient mice. *Acta Pharmacol Sin* 1989; **10**: 216-221
- 4 **Li G**, Yu J. Inhibition of bone marrow immature B lymphocytes from zinc deficient mice by methionine enkephalin. *Acta Pharmacol Sin* 1991; **12**: 500-503
- 5 **Kramer HK**, Simon EJ. Role of protein kinase C(PKC) in agonist-induced mu-opioid receptor down-regulation:II. Activation and involvement of the alpha, epsilon, and zeta isoform of PKC. *J Neurochem* 1999; **72**: 594-604
- 6 **Narita M**, Mizoguchi H, Kampine JP, Tseng LF. Role of protein kinase C in desensitization of spinal delta-opioid-mediated antinociception in the mouse. *Br J Pharmacol* 1996; **118**: 1829-1835
- 7 **Shen J**, Benedict GA, Gallagher A, Stafford K, Yoburn BC. Role of camp-dependent protein kinase (PKA) in opioid agonist-induced mu-opioid receptor downregulation and tolerance in mice. *Synapse* 2000; **38**: 322-327
- 8 **Avidor-Reiss T**, Bayewitch M, Levy R, Matus-Leibovitch N, Nevo I, Vogel Z. Adenylylcyclase supersensitization in mu-opioid receptor-transfected Chinese hamster ovary cells following chronic opioid treatment. *J Biol Chem* 1995; **270**: 29732-29738
- 9 **Liu JG**, Anand KJ. Protein kinases modulate the cellular adaptations associated with opioid tolerance and dependence. *Brain Res Brain Res Rev* 2001; **38**: 1-19
- 10 **Wagner EJ**, Ronnekleiv OK, Kelly MJ. Protein kinase A maintains cellular tolerance to mu opioid receptor agonists in hypothalamic neurosecretory cells with chronic morphine treatment: convergence on a common pathway with estrogen in modulating mu opioid receptor/effector coupling. *J Pharmacol Exp Ther* 1998; **285**: 1266-1273
- 11 **Hopp TP**, Woods KR. Prediction of protein antigenic determinants from amino acid sequences. *Proc Natl Acad Sci USA* 1981; **78**: 3824-3828
- 12 **Li MS**, Li PF, He SP, Du GG, Li G. The promoting molecular mechanism of alpha-fetoprotein o the growth of human hepatoma Bel7402 cell line. *World J Gastroenterol* 2002; **8**: 469-475
- 13 **Choi SW**, Park HY, Rubeiz NG, Sachs D, Gilchrist BA. Protein kinase C- $\alpha$  levels are inversely associated with growth rate in cultured human dermal fibroblasts. *J Dermatological Sci* 1998; **18**: 54-63
- 14 **Fukuda K**, Kato S, Mori K. Location of regions of the opioid receptor involved in selective agonist binding. *J Biol Chem* 1995; **270**: 6702-6709
- 15 **Pepin MC**, Yue SY, Roberts E, Wahlestedt C, Walker P. Novel "restoration of function" mutagenesis strategy to identify amino acids of the  $\delta$ -opioid receptor involved in ligand binding. *J Biol Chem* 1997; **272**: 9260-9267
- 16 **Meng F**, Ueda Y, Hoversten MT, Thompson RC, Taylor L, Watson SJ, Akil H. Mapping the receptor domains critical for the binding selectivity of delta-opioid receptor ligands. *Eur J Pharmacol* 1996; **311**: 285-292
- 17 **Metzger TG**, Paterlini MG, Ferguson DM, Portoghese PS. Investigation of the selectivity of oxymorphone- and naltrexone-derived ligands via site-directed mutagenesis of opioid receptors: exploring the "address" recognition locus. *J Med Chem* 2001; **44**: 857-862
- 18 **Ide S**, Sakano K, Seki T, Awamura S, Minami M, Satoh M. Endomorphin-1 discriminates the mu-opioid receptor from the delta- and kappa-opioid receptors by recognizing the difference in multiple regions. *Jpn J Pharmacol* 2000; **83**: 306-311
- 19 **Bonner G**, Meng F, Akil H. Selectivity of mu-opioid receptor determined by interfacial residues near third extracellular loop. *Eur J Pharmacol* 2000; **403**: 37-44
- 20 **Krupnick JG**, Benovic JL. The role of receptor kinases and arrestins in G protein-coupled receptor regulation. *Ann Rev Pharmacol Toxicol* 1998; **38**: 289-319
- 21 **Whistler JL**, Tsao P, von Zastrow M. A phosphorylation-regulated brake mechanism controls the initial endocytosis of opioid

- receptors but is not required for post-endocytic sorting to lysosomes. *J Biol Chem* 2001; **276**: 34331-34338
- 22 **Chaturvedi K**, Bandari P, Chinen N, Howells RD. Proteasome involvement in agonist-induced down-regulation of mu and delta opioid receptors. *J Biol Chem* 2001; **276**: 12345-12355
- 23 **Law PY**, Kouhen OM, Solberg J, Wang W, Erickson LJ, Loh HH. Deltorphin II-induced rapid desensitization of delta-opioid receptor requires both phosphorylation and internalization of the receptor. *J Biol Chem* 2000; **275**: 32057-32065
- 24 **Kramer HK**, Andria ML, Esposito DH, Simon EJ. Tyrosine phosphorylation of the delta-opioid receptor. Evidence for its role in mitogen-activated protein kinase activation and receptor internalization. *Biochem Pharmacol* 2000; **60**: 781-792
- 25 **Yoshikawa M**, Nakayama H, Ueno S, Hirano M, Hatanaka H, Furuya H. Chronic fentanyl treatments induce the up-regulation of mu opioid receptor mRNA in rat pheochromocytoma cells. *Brain Res* 2000; **859**: 217-223
- 26 **Wang Z**, Sadee W. Tolerance to morphine at the mu-opioid receptor differentially induced by camp-dependent protein kinase activation and morphine. *Eur J Pharmacol* 2000; **389**: 165-171
- 27 **Roy S**, Cain KJ, Chapin RB, Charboneau RG, Barke RA. Morphine modulates NF kappa B activation in macrophages. *Biochem Biophys Res Commun* 1998; **245**: 392-396
- 28 **Kramer HK**, Simon EJ. Role of protein kinase C(PKC) in agonist-induced mu-opioid receptor down-regulation: I. PKC translocation to the membrane of SH-SY5Y neuroblastoma cells is induced by mu-opioid agonists. *J Neurochem* 1999; **72**: 585-593
- 29 **Chakrabarti S**, Law PY, Loh HH. Distinct differences between morphine-and [D-Ala2,N-MePhe4,Gly-ol5]-enkephalin-mu-opioid receptor complexes demonstrated by cyclic AMP-dependent protein kinase phosphorylation. *J Neurochem* 1998; **71**: 231-239
- 30 **Sharma P**, Kumar Bhardwaj S, Kaur Sandhu S, Kaur G. Opioid regulation of gonadotropin release: role of signal transduction cascade. *Brain Res Bull* 2000; **52**: 135-142

**Edited by** Wu XN

• CLINICAL RESEARCH •

# Is analysis of lower esophageal sphincter vector volumes of value in diagnosing gastroesophageal reflux disease?

Robert E. Marsh, Christopher L. Perdue, Ziad T. Awad, Patrice Watson, Mohamed Selima, Richard E. Davis, Charles J. Filipi

**Robert E. Marsh, Christopher L. Perdue, Ziad T. Awad, Mohammed Selima, Richard E. Davis, Charles J. Filipi**, Department of Surgery, Creighton University School of Medicine, Omaha Nebraska USA  
**Patrice Watson**, Department of Preventive Medicine, Creighton University School of Medicine, Omaha Nebraska USA

**Correspondence to:** Dr. Charles J. Filipi, Department of Surgery, Creighton University School of Medicine, 601 N 30<sup>th</sup> Street, Suite 3740, Omaha, NE 68131. [cjfilipi@creighton.edu](mailto:cjfilipi@creighton.edu)  
**Telephone:** +402-280-4213 **Fax:** +402-280-4278

**Received:** 2002-07-23 **Accepted:** 2002-07-27

## Abstract

**AIM:** With successful surgical treatment of gastroesophageal reflux disease (GERD), there is interest in understanding the anti-reflux barrier and its mechanisms of failure. To date, the potential use of vector volumes to predict the DeMeester score has not been adequately explored.

**METHODS:** 627 patients in the referral database received esophageal manometry and ambulatory 24-hour pH monitoring. Study data included LES resting pressure (LESP), overall LES length (OL) and abdominal length (AL), total vector volume (TVV) and intrabdominal vector volume (IVV).

**RESULTS:** In cases where LESP, TVV or IVV were all below normal, there was an 81.4 % probability of a positive DeMeester score. In cases where all three were normal, there was an 86.9 % probability that the DeMeester score would be negative. Receiver-operating characteristics (ROC) for LESP, TVV and IVV were nearly identical and indicated no useful cut-off values. Logistic regression demonstrated that LESP and IVV had the strongest association with a positive DeMeester score; however, the regression formula was only 76.1 % accurate.

**CONCLUSION:** While the indices based on TVV, IVV and LESP are more sensitive and specific, respectively, than any single measurement, the measurement of vector volumes does not add significantly to the diagnosis of GERD.

Marsh RE, Perdue CL, Awad ZT, Watson P, Selima M, Davis RE, Filipi CJ. Is analysis of lower esophageal sphincter vector volumes of value in diagnosing gastroesophageal reflux disease? *World J Gastroenterol* 2003; 9(1): 174-178

<http://www.wjgnet.com/1007-9327/9/174.htm>

## INTRODUCTION

With the recognition of gastroesophageal reflux disease (GERD) as a surgical pathology, there is deep interest in understanding the anatomical and physiological anti-reflux barrier and its mechanisms of failure<sup>[1-8]</sup>. The anatomical components of the barrier include the crural fibers of the diaphragmatic esophageal hiatus, the smooth muscle sling fibers of the gastric cardia, and the semicircular and clasp fibers of the distal esophagus<sup>[1-5]</sup>. Augmented by positive intrabdominal pressure over the most

distal portion of the lower esophagus and proximal cardia, the sphincter approximates the mucosal epithelium covering the internal surface area of the esophagogastric junction. This distinct high-pressure zone is a critical factor in the barrier against reflux of gastric contents<sup>[5-8]</sup>. The anatomical function of the lower esophageal sphincter (LES) is complemented by neutralization of refluxate by alkaline oral secretions and rapid clearance of esophageal contents by intermittent and reflex peristalsis<sup>[8]</sup>.

Various means have been devised to measure the mechanical integrity of the LES<sup>[8-11]</sup>. Traditional pull-through manometry has been succeeded in some laboratories by sophisticated equipment and software that allows measurement of the closure pressure generated by the three-dimensional sphincter mechanism. Directional pressures can be summated over the length of the sphincter to produce a vector volume that describes the overall physical resistance of the barrier to continuous reflux<sup>[11,12]</sup>. Other measures of the sphincter competence include resting pressure of the LES at various points along its length, the vector volume of the intrabdominal portion of the LES as well as overall and intrabdominal lengths of the LES. While many observers have noted the relationship between abnormal manometry and GERD<sup>[4-14]</sup>, we have sought to quantify this relationship in a way that describes the comparative ability of such measurements to predict positive ambulatory pH monitoring as described by DeMeester and colleagues<sup>[15]</sup>. It was our goal to compare traditional manometric measurements, vector volume analysis and results of 24-hour pH monitoring. We postulated that one or more of the manometric measurements would yield a statistically significant relationship to a positive DeMeester score. Because of the complexity of the procedure, expense, and general discomfort to the patient, it was hoped that detection of a defective LES would obviate the need for subsequent pH monitoring in certain cases.

## MATERIALS AND METHODS

### Materials

Manometric studies were performed using a 9-lumen catheter (ESM38R, Arndorfer, Greendale, Wisconsin) coupled to a hydraulic capillary infusion system (Arndorfer). The catheter consisted of a central lumen of 1.8 mm internal diameter surrounded by 8 lumens of 0.8 mm internal diameter. Four channels extended to the distal end of the catheter with ports at the same level and oriented radially at 90° intervals. The remaining 4 ports were spaced contiguously at 5 cm intervals proximal to, and offset by 45° from, the radial ports, providing 20 cm of working length. The central lumen was not used. The catheter was pulled at a 3 mm/second using a mechanical puller. The transducer information was translated into digital information using a polygraph (Medtronic Synectics, Shoreview, Minnesota). External transducers were also used to detect swallow and respiratory waves. The information was saved for real-time and retrospective review using Polygram software (Medtronic Synectics).

### Methods

The original audit population consisted of 1 900 patients referred to the Esophageal Function Laboratory in the

Department of Surgery at Creighton University. This population received either esophageal manometry, 24-hour pH monitoring or both. Patients were referred to the laboratory for typical or atypical symptoms thought to represent GERD. Of the 1 900 patients in the referral database, only 627 received both esophageal manometry with measurement of LES vector volumes and ambulatory 24-hour pH monitoring. Vector volume data were available for the total length of the lower esophageal sphincter (total vector volume, TVV) and for the intrabdominal length (intrabdominal vector volume, IVV). The vector volume is a calculated value representing the directional pressures within the LES over a specific portion of the sphincter. Additional data included age, weight, resting pressure of the LES (LESP), overall LES length (OL) and abdominal LES length (AL).

In preparation for station pull-through (SPT), the catheter assembly was introduced through either nare and advanced into the stomach. SPT was performed using a mechanized puller (Medtronic Synectics) at 3 mm/sec to avoid swallowing with pauses every centimeter to allow pressure measurement. Using the gastric baseline pressure as the reference point, a port entered the LES when a sustained positive deflection away from the baseline was observed. A wet swallow of 5 mL tap water was performed at this level to observe relaxation of the LES. The SPT proceeded through the entirety of the LES resulting in five measurements from separate channels which were averaged to produce the final value. The patient was instructed to breathe regularly and not to swallow. Swallowing (except for the wet swallow) required another attempt.

The resting pressure of the LES (LESP) was defined as the mean pressure at the respiratory inversion point (RIP). The RIP was the place on the pressure waveform where the positive deflections in the abdomen caused by inspiration changed to negative deflections in the chest. OL was the distance between the distal and proximal borders of the LES; AL was the distance between the distal border of the LES and the RIP. Both measurements were obtained during SPT.

Measurements for vector volume calculations were obtained from transducers attached to the 4 radial ports located at the same level on the catheter. Each channel yielded a separate pressure and direction (pressure vector) over the length of the LES. The distal border of the LES was defined as the position at which two or more of the four channels deflected positively from the gastric baseline. The crural component, often represented as the distal hump in the bimodal waveform, was intentionally included in the TVV. The proximal border was defined as that position in which two or more of the four channels returned and stayed below the gastric baseline. Computer software summated the pressure vector measurements into a single vector volume (mm Hg<sup>3</sup>). A three-dimensional image was also generated but not included in the database.

IVV was determined similarly. The proximal endpoint of the IVV was the RIP; the distal endpoint was the same as for TVV. As with TVV determination, when two or more of the four channels reached the RIP, all were considered to be at the RIP. Computer software similarly produced a value for the vector volume.

Upon completion of manometry, the pressure catheter was replaced with a pH probe catheter (Ingold Bipolar Glass pH Probe, Mui Scientific, Mississauga, Ontario). All patients had been off their medication (PPI's for 7 days, H2 blockers for 3 days) for the appropriate time. The catheter was passed through the nose and into the stomach to obtain a baseline reading from the ambulatory recording equipment to be carried by the patient (Digitrapper, Medtronic Synectics). The catheter was then withdrawn to a position 5 cm above the LES as determined by SPT. A baseline reading was again obtained. The catheter was secured to the nose and patients were given instructions to eat at

least three meals (limited to foods in which the pH was known), to stay upright at least 4 hours after eating, and to be recumbent for no more than 8 hours during sleep. Patients were instructed to note in a diary the time of each symptom occurrence, when and what they ate, and when they retired for bed.

At the completion of the 24-hour period, the catheter was removed and the information in the Digitrapper was downloaded and analyzed using pH-metry software (EsopHagram, Synectics). A DeMeester score was then tabulated by the computer and recorded for both acid and alkaline reflux. A score <14.8 was considered negative for GERD.

Except for the logistic regression, sensitivities and specificities for the receiver-operating characteristics (ROC) were calculated manually. The purpose of the ROC was to find an optimal cut-off point, if any, for measurements that would yield the greatest combination of sensitivity and specificity. The formulas for calculations involving LESP (for example) were:

$$\text{Sensitivity} = \frac{[\text{'n' patients with GERD and LESP} \leq \text{'x'}]}{[\text{'n' patients with GERD}]}$$

$$\text{Specificity} = \frac{[\text{'n' patient without GERD and LESP} > \text{'x'}]}{[\text{'n' patient without GERD}]}$$

In those calculations, 'x' refers to a progressively larger cut-off value for LESP (following the example above). Therefore, a particular sensitivity represented the probability that a patient with an  $\text{LESP} \leq \text{'x'}$  would have GERD. Likewise, the specificity represents that probability that a patient with an  $\text{LESP} > \text{'x'}$  would not have GERD. Cut-off values were chosen at increments that resulted in enough data points to provide adequate resolution to the curve but with enough cases within each range to reflect real trends. This was done for LESP, TVV, IVV, AL and OL.

All other calculations were performed by SAS statistical software (version 6.12). The logistic regression process was automated and resulted in a formula for predicting GERD-positive or GERD-negative. According to its program, the statistical software started with all predictors in a test formula, then through backward selection, removed predictors that failed to meet the appropriate confidence interval. The software rejected predictors when p-values were >0.05 %. There were no attempts at relating the manometry measurements directly to DeMeester score in a continuous fashion. Rescaling in order to account for outliers consisted of setting values above the 95<sup>th</sup> percentile for any measurement equal to the value of that measurement at the 95<sup>th</sup> percentile. Values for normal were derived from a prior study in this laboratory using 50 healthy (non-GERD) volunteers. No attempts were made to sort patients or data according to age, sex or weight.

## RESULTS

Demographic data with respect to the diagnosis of GERD is presented in Table 1. There were no attempts at age or sex matching. Table 2 includes the means, standard deviations, p-values, sensitivities and specificities for the measured parameters. The sensitivity and specificity of LESP, TVV and IVV, respectively, were 67.3 % and 73.3 %; 72.5 % and 62.6 %; and 58.5 % and 77.3 % at the lower values for normal. The sensitivity and specificity for AL and OL reflect the fact that very few patients had abnormal values of either (4 and 2 patients, respectively); this was also reflected in the similarity relatively large standard deviations between the average AL and OL for GERD and non-GERD sufferers. Because AL and OL were so weakly sensitive for reflux disease, Any-low refers only to cases where LESP, TVV or IVV were below normal. The sensitivity of Any-low indicated an 81.4 % probability a patient with either abnormally low LESP, TVV or IVV will have GERD. Similarly, AL and OL were also excluded from calculations of the All-low values. There was an 86.9 %



probability that a patient with all three normal measurements will not have an abnormal esophageal acid exposure; this is the specificity for All-low.

**Table 1** Demographic data for study cases

	Range	non-GERD mean $\pm$ SD	GERD mean $\pm$ SD
Age (years)	4 – 86	47.0 $\pm$ 16.1 (n=308)	48.5 $\pm$ 14.9 (n=319)
Weight (lbs)	87–397	173.6 $\pm$ 42.2 (n=310)	190.2 $\pm$ 38.0 (n=317)
Sex	F: 313M: 314	F: 101 M: 80	F: 108 M: 162

**Table 2** Summary of manometric data

	Normal range	Range of measurements	non-GERD mean $\pm$ SD	GERD mean $\pm$ SD	P	Sens. %	Spec. %
LESP	6.1–25.6	0–59.3	10.9 $\pm$ 8.4 (n=319)	5.7 $\pm$ 4.8 (n=308)	<0.001	67.3	71.3
IVV	1855–10953	0–45830	4090 $\pm$ 4709 (n=321)	1712 $\pm$ 2080 (n=306)	<0.001	72.5	62.6
TVV	2060–14135	80–60740	5429 $\pm$ 5564 (n=321)	2533 $\pm$ 2626 (n=306)	<0.001	58.5	77.3
AL	1.0–5.0	0–9.8	2.6 $\pm$ 1.0 (n=280)	2.2 $\pm$ 1.0 (n=347)	0.013	4.5	98.4
OL	2.4–5.5	1.2–27.4	4.7 $\pm$ 1.8 (n=287)	4.6 $\pm$ 1.4 (n=340)	<0.047	2.6	99.0
Any low	–	–	–	–	–	81.4	51.0
All ow	–	–	–	–	–	49.3	86.9

LESP=Lower esophageal sphincter resting pressure (mm-Hg), IVV=Intrabdominal vector volume (mm-Hg<sup>3</sup>), TVV=total vector volume (mm-Hg<sup>3</sup>), AL=abdominal length of the LES (mm), OL=overall length of the LES (mm). “Any-low” refers to cases where LESP, IVV or TVV are lower than normal. “All-low” refers to cases where LESP, IVV and TVV are all lower than normal. SD=Standard deviation, Sens.=Sensitivity, Spec.=Specificity. ‘P’ is the probability value from the chi-squared test for GERD vs. non-GERD; P<0.05 is significant. Sensitivities and specificities are calculated using the lowest normal value.

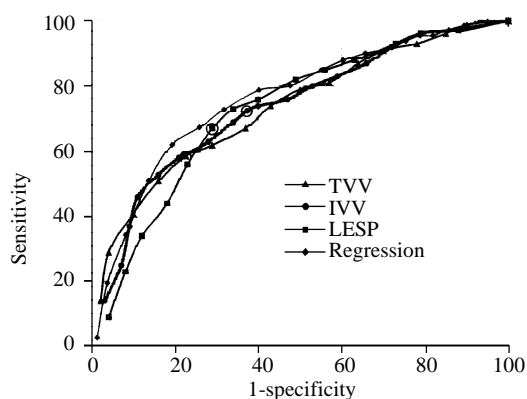


**Figure 1** Receiver-operating characteristics for total vector volume (TVV), intrabdominal vector volume (IVV) and LES resting pressure (LESP). Included is a comparable ROC for the logistic regression. The points on the curves that correspond to the normal values in Table 1 are circled

Figure 1 shows the receiver-operating characteristics for LESP, TVV, and IVV. The curves for AL and OL fell below all of the other curves and (for clarity) have not been depicted. There are no obvious points at which both specificity and sensitivity are optimal for any of the measurements. Cut-off values equal to the lowest normal values are indicated by the circled data points. Also shown in Figure 1 is an ROC curve for the regression formula (below) indicating that it does not

have a better combination of sensitivity and specificity than the measurements themselves.

The logistic regression formula following backward selection was

$$Y = 1.24 + [\text{LESP}](-0.1056) + [\text{IVV}](-0.00019)$$

where Y is equal to a nominal value for GERD (1=the presence and 2=absence of GERD). P-values for the factor estimates were all <0.0001. Various attempts were made at rescaling the data (as described in Materials and Methods) and ranking without effect. The “native” logistic regression (unscaled and unranked) was superior or equal in every case with 76.1 % concordance, 23.6 % discordance and 0.3 % tied. Table 3 contains data from the logistic regression process. TVV, OL and AL were excluded by the software from the regression formula because of P-values >0.05 %. When ranked values were used for logistic regression, similar estimates were obtained for the y-intercept, LESP and IVV factors and the P-values were all <0.0001. The formulas for the ranked and rescaled data were equally good or worse at predicting GERD and have been excluded from further discussion.

**Table 3** Logistic regression with the results of backward selection

Variable	Estimate	P
Intercept	+1.241	<0.0001
LESP	-0.106	<0.0001
IVV	-0.00019	<0.0001
TVV	(rejected)	0.43
AL	(rejected)	0.089
OL	(rejected)	0.79
Concordant = 76.1%		
Discordant = 23.6%		
Tied = 0.3%		

## DISCUSSION

Intraabdominal vector volume is more sensitive than TVV or LESP, but only marginally, and no more than 72.5 % (Table 2). Measurements of TVV and LESP are more specific for GERD; that is, findings of normal TVV and LESP are 77.3 % and 71.3 % likely in a non-GERD patient, respectively. While the mean values for LESP, TVV and IVV are all significantly lower in GERD patients (P<0.0001), the standard deviations are nearly equal to the means themselves in every measurement (Table 2). Intrabdominal length (AL) and overall length (OL) of the LES are clearly unimportant in the assessment of gastroesophageal reflux disease. Only 4 and 2 patients, respectively, had abnormally low values for AL or OL.

When measurements are viewed as ROC curves (Figure 1), there are no points where a measurement has both a high sensitivity and high specificity. That is to say that there appears to be no optimal cut-off value for predicting GERD. Ideally, an ROC curve is a parabolic figure with the apex in the upper right corner (using the axes as in Figure 1) which drops sharply from a point where sensitivity and specificity are both high to a point where sensitivity is very low and specificity is very high. In fact, there are no values for which there is a high sensitivity and even a moderately useful specificity. At cut-off values representing 85 % sensitivity for GERD ( $\leq 1600$  mm-Hg<sup>3</sup> for TVV;  $\leq 1000$  mm-Hg<sup>3</sup> for IVV; and  $\leq 3$  mm-Hg for LESP), the specificities of the measurements fall between 35 % and 45 %. Finding significantly lower-than-average TVV, IVV and LESP in GERD patients (Table 2.) reiterates our understanding of the pathological consequences of a weakened LES. It also confirms our present understanding that there is a more complex relationship between the

anatomical correlates of the LES and function than can be expressed by a single measurement.

Use of the "Any-low," "All-low," and logistic regression models were attempts to use the measurements in a combined fashioned, similar to the calculation of the DeMeester ambulatory pH score. While Any-low had a relatively better sensitivity (81.4 %) and All-low had relatively better specificity (86.9 %) for the DeMeester score than the original measurements, the logistic regression-presumably the more rigorous mathematical model-was little better than the ROC curves for LESP, IVV or TVV. The computer generated a series of sensitivities and specificities for predictions made by the regression formula. This data is represented in Figure 1 as a means of comparison. Interestingly, total vector volume of the LES (TVV) was rejected by the computer due to a failure to meet the 95 % correlation confidence interval. The logistic regression formula was only 76.1 % accurate in predicting the real data. Attempts at ranking the data and rescaling in order to account for a number of outlying measurements made no improvement in the accuracy of the formula. The regression formula was clearly unable to improve on the predictive power of the raw measurements. As such, the formula has no practical use in the laboratory.

We have been motivated to find a way to identify surgical candidates without directly measuring distal esophageal reflux because of the inherent difficulty with ambulatory pH monitoring (patient discomfort, cost, compliance). Recently, Fass and colleagues have suggested that the test itself may have the effect of reducing reflux-provoking activities, thereby reducing the sensitivity of the test<sup>[16]</sup>. In studies of different patient populations where vector volumes were found to have greater use<sup>[11-14]</sup> we are unaware of the degree to which they were able to control patient compliance with ambulatory pH monitoring protocols (either maintaining a normal daily diet and activities or maintaining a controlled regimen). Certainly, patient compliance would be expected to be higher when he or she is made to understand the importance of maintaining normal habits. This is also an uncontrolled factor in the present study. In a sense, this might be a form of "compliance bias" reflected in the sensitivity of the test, where poor compliance (relatively less daily activity, smaller meals, more conservative food choices) results in more falsely negative screening tests. Quigley has also referred to the multiple difficulties with pH-metry as the gold standard for diagnosing GERD, namely the issue of patient compliance with testing conditions<sup>[17]</sup>. It remains to be seen if patient compliance, or any other factors, have any real effect on 24-hour pH monitoring and the treatment indications for GERD.

To improve surgical results, it is helpful but not mandatory to find evidence that a defective lower esophageal sphincter is the cause for GERD. This is based on the reports by numerous authors who have sought to describe the sphincter and its mechanisms of failure<sup>[1-10]</sup>. Studies have demonstrated the effectiveness of anti-reflux surgery to improve symptom scores, esophagitis and LES resting pressure<sup>[2,7,11,13]</sup>. Authors have asserted that measurement of vector volumes would be superior to standard lower esophageal manometry for detecting a defective LES<sup>[11-15]</sup>. Wetscher and colleagues made the observation that IVV was more sensitive than LESP (i.e. standard manometry) and TVV at detecting a defective lower esophageal sphincter<sup>[12]</sup>. They concluded that measurement of vector volumes would be a valuable adjunct to current esophagogastric studies. Our study suggests that measurement of vector volumes is not greatly more valuable than traditional manometry.

There is an 81.4 % chance that a patient with either a low LESP, TVV or IVV (when all three are measured) will have a positive DeMeester score. Whether or not this would suffice

as an indication for surgery would require inclusion of surgical outcome data into the analysis. Alternatively, a priority ranking system used by Martinez-Serna and colleagues might serve as an effective adjunct to manometry data<sup>[18]</sup>. Those authors found a positive association between high symptom priority ranking for heartburn and regurgitation and abnormal pH and manometry results. Analysis of traditional manometry, vector volumes, symptom scores and surgical outcomes will be necessary to confidently define indications for surgery without ambulatory pH monitoring.

Transient relaxation of the lower esophageal sphincter may be an important etiology for pathologic reflux<sup>[8-19]</sup>. Dodds and colleagues found that 65 % of reflux episodes in GERD patients were due to transient relaxation of the LES<sup>[8]</sup>. This finding is difficult to interpret when 82 % of normal reflux in non-GERD patients can also be attributed to transient LES relaxation<sup>[20]</sup>. Sloan and colleagues found that abrupt increases in intrabdominal pressure resulted in a higher occurrence of reflux in GERD patients who also had hiatal hernia and low LES resting tone<sup>[21]</sup>. Kahrilas *et al.* found the degree of separation of the LES from the crura is associated with the transient relaxations<sup>[22]</sup>. This separation can be detected by manometry and is described as the double hump.

Based on our findings, we draw the following conclusions: (1) a patient with a low TVV, IVV or LESP (when all three are measured) is 81.4 % likely to have a positive DeMeester score; and (2) when LESP, TVV and IVV are normal, a patient is 86.9 % likely to have a negative DeMeester score. This is a marginal improvement over the sensitivities and specificities of the native measurements, but the probabilities are not large enough to justify omission of the ambulatory pH study despite its inherent challenge to patient compliance and reliability. It appears that vectors volumes, particularly intrabdominal vector volume, are just as sensitive and specific for GERD as LES resting pressure, and thus cannot be considered superior in the evaluation of GERD.

## REFERENCES

- 1 **Liebermann-Meffert D**, Allgower M, Schmid P, Blum AL. Muscular equivalent of the lower esophageal sphincter. *Gastroenterology* 1979; **76**: 31-38
- 2 **Stein HJ**, Crookes PF, DeMeester TR. Three-dimensional manometric imaging of the lower esophageal sphincter. *Surg Annu* 1995; **27**: 199-214
- 3 **Bonavina L**, Evander A, DeMeester TR, Walther B, Cheng SC, Palazzo L, Concannon JL. Length of the distal esophageal sphincter and competency of the cardia. *Am J Surg* 1986; **151**: 25-34
- 4 **Stein HJ**, Liebermann-Meffert D, DeMeester TR, Siewert JR. Three-dimensional pressure image and muscular structure of the human lower esophageal sphincter. *Surgery* 1995; **117**: 692-698
- 5 **DeMeester TR**, Wernly JA, Bryant GH, Little AG, Skinner DB. Clinical and *in vitro* analysis of determinants of gastroesophageal competence. A study of the principles of antireflux surgery. *Am J Surg* 1979; **137**: 39-46
- 6 **Stein HJ**, Barlow AP, DeMeester TR, Hinder RA. Complications of gastroesophageal reflux disease. Role of the lower esophageal sphincter, esophageal acid and acid/alkaline exposure, and duodenogastric reflux. *Ann Surg* 1992; **216**: 35-43
- 7 **Costantini M**, Zaninotto G, Anselmino M, Boccu C, Nicoletti L, Ancona E. The role of a defective lower esophageal sphincter in the clinical outcome of treatment for gastroesophageal reflux disease. *Arch Surg* 1996; **131**: 655-659
- 8 **Dodds WJ**, Dent J, Hogan WJ, Helm JF, Hauser R, Patel GK, Egide MS. Mechanisms of gastroesophageal reflux in patients with reflux esophagitis. *N Engl J Med* 1982; **307**: 1547-1552
- 9 **Crookes PF**, Kaul BK, DeMeester TR, Stein HJ, Oka M. Manometry of individual segments of the distal esophageal sphincter. Its relation to functional incompetence. *Arch Surg* 1993; **128**: 411-415

- 10 **Byrne PJ**, Stuart RC, Lawlor P, Walsh TN, Hennessy TP. A new technique for measuring lower oesophageal sphincter competence in patients. *Ir J Med Sci* 1993; **162**: 351-354
- 11 **Bombeck CT**, Vaz O, DeSalvo J, Donahue PE, Nyhus LM. Computerized axial manometry of the esophagus. A new method for the assessment of antireflux operations. *Ann Surg* 1987; **206**: 465-472
- 12 **Wetscher GJ**, Hinder RA, Perdakis G, Wiescheimer T, Stalzer R. Three-dimensional imaging of the lower esophageal sphincter in healthy subjects and gastroesophageal reflux. *Dig Dis Sci* 1996; **41**: 2377-2382
- 13 **Stein HJ**, DeMeester TR, Naspetti R, Jamieson J, Perry RE. Three-dimensional imaging of the lower esophageal sphincter in gastroesophageal reflux disease. *Ann Surg* 1991; **214**: 374-383
- 14 **DeMeester TR**, Wang CI, Wernly JA, Pellegrini CA, Little AG, Klementsich P, Bermudez G, Johnson LF, Skinner DB. Technique, indications, and clinical use of 24 hour esophageal pH monitoring. *J Thorac Cardiovasc Surg* 1980; **79**: 656-670
- 15 **Stein HJ**, Korn O, Liebermann-Meffert D. Manometric vector volume analysis to assess lower esophageal sphincter function. *Ann Chir Gynaecol* 1995; **84**: 151-158
- 16 **Fass R**, Hell R, Sampliner RE, Pulliam G, Graver E, Hartz V, Johnson C, Jaffe P. Effect of ambulatory 24-hour esophageal pH monitoring on reflux- provoking activities. *Dig Dis Sci* 1999; **44**: 2263-2269
- 17 **Quigley EM**. 24 h pH monitoring for gastroesophageal reflux disease: already standard but not yet gold? *Am J Gastroenterol* 1992; **87**: 1071-1075
- 18 **Martinez-Serna T**, Tercero F, Jr., Filipi CJ, Dickason TJ, Watson P, Mittal SK, Tasset MR. Symptom priority ranking in the care of gastroesophageal reflux: a review of 1 850 cases. *Dig Dis* 1999; **17**: 219-224
- 19 **Holloway RH**, Kocyan P, Dent J. Provocation of transient lower esophageal sphincter relaxations by meals in patients with symptomatic gastroesophageal reflux. *Dig Dis Sci* 1991; **36**: 1034-1039
- 20 **Schoeman MN**, Tippet MD, Akkermans LM, Dent J, Holloway RH. Mechanisms of gastroesophageal reflux in ambulant healthy human subjects. *Gastroenterology* 1995; **108**: 83-91
- 21 **Sloan S**, Rademaker AW, Kahrilas PJ. Determinants of gastroesophageal junction incompetence: hiatal hernia, lower esophageal sphincter, or both? *Ann Intern Med* 1992; **117**: 977-982
- 22 **Kahrilas PJ**, Shi G, Manka M, Joehl RJ. Increased frequency of transient lower esophageal sphincter relaxation induced by gastric distention in reflux patients with hiatal hernia. *Gastroenterology* 2000; **118**: 688-695

Edited by Zhang JZ

• CLINICAL RESEARCH •

# Role of NF- $\kappa$ B in multiple organ dysfunction during acute obstructive cholangitis

Bin Tu, Jian-Ping Gong, Hu-Yi Feng, Chuan-Xin Wu, Yu-Jun Shi, Xu-Hong Li, Yong Peng, Chang-An Liu, Sheng-Wei Li

**Bin Tu, Jian-Ping Gong, Hu-Yi Feng, Chuan-Xin Wu, Yu-Jun Shi, Xu-Hong Li, Yong Peng, Chang-An Liu, Sheng-Wei Li,** Department of General Surgery, the Second College of Clinical Medicine & the Second Affiliated Hospital of Chongqing University of Medical Science, 74 Linjiang Road, Chongqing 400010, China  
**Supported by** the National Natural Science Foundation of China, No.39970719, 30170919

**Correspondence to:** Dr Jian-Ping Gong, Department of General Surgery, the Second College of Clinical Medicine & the Second Affiliated Hospital of Chongqing University of Medical Science, 74 Linjiang Road, Chongqing 400010, China. gongjianping11@hotmail.com  
**Telephone:** +86-23-63766701 **Fax:** +86-23-63822815  
**Received:** 2002-06-24 **Accepted:** 2002-07-22

## Abstract

**AIM:** To elucidate the role of NF- $\kappa$ B activation in the development of multiple organ dysfunction (MOD) during acute obstructive cholangitis (AOC) in rats.

**METHODS:** Forty-two Wistar rats were divided into three groups: the AOC group, the group of bile duct ligation (BDL group), and the sham operation group (SO group). All the animals in the three groups were killed in the 6th and 48th hour after operation. Morphological changes of vital organs were observed under light and electron microscopy. NF- $\kappa$ B activation was determined with Electrophoretic Mobility Shift Assay (EMSA). Arterial blood gas analyses and the serum levels of lactate dehydrogenase (LDH), alanine aminotransferase (ALT), blood urea nitrogen (BUN) and creatinine were performed. The concentrations of TNF- $\alpha$  and IL-6 in plasma were also measured.

**RESULTS:** The significant changes of histology and ultrastructure of vital organs were observed in AOC group. By contrast, in BDL group, all the features of organs damage were greatly reduced. Expression of NF- $\kappa$ B activation in various tissues increased in AOC group when compared to other two groups. At 6 h, the arterial pH in three groups was  $7.52 \pm 0.01$ ,  $7.46 \pm 0.02$ , and  $7.45 \pm 0.02$ , and the blood pCO<sub>2</sub> was  $33.9 \pm 0.95$  mmHg,  $38.1 \pm 0.89$  mmHg,  $38.9 \pm 0.94$  mmHg, there was difference in three groups ( $P < 0.05$ ). At 48 h, the blood pH values in three groups was  $7.33 \pm 0.07$ ,  $7.67 \pm 0.04$ , and  $7.46 \pm 0.03$ , and blood HCO<sub>3</sub><sup>-</sup> was  $20.1 \pm 1.29$  mmol·L<sup>-1</sup>,  $26.7 \pm 1.45$  mmol·L<sup>-1</sup> and  $27.4 \pm 0.35$  mmol·L<sup>-1</sup>, there was also difference in three groups ( $P < 0.05$ ). In AOC group, Levels of LDH, ALT, BUN and creatinine were  $16359.9 \pm 2278.8$  nkat·L<sup>-1</sup>,  $5796.2 \pm 941.9$  nkat·L<sup>-1</sup>,  $55.7 \pm 15.3$  mg/dl, and  $0.72 \pm 0.06$  mg/dl, which were higher than in SO group ( $3739.1 \pm 570.1$  nkat·L<sup>-1</sup>,  $288.4 \pm 71.7$  nkat·L<sup>-1</sup>,  $12.5 \pm 2.14$  mg/dl, and  $0.47 \pm 0.03$  mg/dl) ( $P < 0.05$ ). Levels of plasma TNF- $\alpha$  and IL-6 in AOC at 48 h were  $429 \pm 56.62$  ng·L<sup>-1</sup> and  $562 \pm 57$  ng·L<sup>-1</sup>, which increased greatly when compared to BDL group ( $139 \pm 16$  ng·L<sup>-1</sup>,  $227 \pm 43$  ng·L<sup>-1</sup>) and SO group ( $74 \pm 10$  ng·L<sup>-1</sup>,  $113 \pm 19$  ng·L<sup>-1</sup>) ( $P < 0.05$ ).

**CONCLUSION:** The pathological damages and the NF- $\kappa$ B activation of many vital organs existed during AOC. These

findings have an important implication for the role of NF- $\kappa$ B activation in MOD during AOC.

Tu B, Gong JP, Feng HY, Wu CX, Shi YJ, Li XH, Peng Y, Liu CA, Li SW. Role of NF- $\kappa$ B in multiple organ dysfunction during acute obstructive cholangitis. *World J Gastroenterol* 2003; 9 (1):179-183

<http://www.wjgnet.com/1007-9327/9/179.htm>

## INTRODUCTION

In humans with acute obstructive cholangitis (AOC) or other sepsis, the onset of multiple organ dysfunction (MOD), especially involving the liver, the heart, the lungs, and the kidneys, is a well known complication that is associated with a high mortality rate<sup>[1-10]</sup>. MOD in either humans or animals appears to emerge as a consequence of progressive development of activation of mononuclear phagocytes system and an unregulated release into the blood of a variety of proinflammatory mediators (interleukins, cytokines, chemokines)<sup>[11-14]</sup>. NF- $\kappa$ B is highly activated at sites of inflammation in diverse diseases and can induce transcription of proinflammatory cytokines<sup>[15-17]</sup>. For example, NF- $\kappa$ B is overexpressed in neutrophil, peripheral blood mononuclear cells (PBMC), dendritic cells (DC), and Kupffer cell, and so on. Its activity may enhance recruitment of inflammatory cells and production of proinflammatory mediators like IL-1, IL-6, IL-8, and TNF- $\alpha$ <sup>[18-21]</sup>. These events may be associated with the development of MOD.

In our original study of patients with AOC, the changes of NF- $\kappa$ B activation were documented<sup>[1]</sup>, but evidence of MOD and the effects of NF- $\kappa$ B were not assessed. In the current studies, we observed the pathological changes of the damages of many vital organs and correlated the role of NF- $\kappa$ B activation with MOD in animal model with AOC.

## MATERIALS AND METHODS

### Reagents

*E. coli* and type IV of collagenase were obtained from Sigma Chemical Company (St. Louis, Mo.). The kits of TNF- $\alpha$  and IL-6 were obtained from Beijing Bang Bing Co.. Other reagents were purchased from Ke Hua Co. or Zhong Sheng Co..

### Animals and experimental groups

Forty-two male Wistar rats, weighing 250-300 g, were obtained from the Laboratory Animal Center of Chongqing University of Medical Science. The animals were fed with standard rat food and water *ad libitum* for 1 wk before use and kept in a climate-controlled environment with a 12 h light-dark cycle. The animals were handled in accordance with the guidelines set by the Experimental Animals Society of Chongqing University of Medical Science. These animals were randomized into three groups: the AOC group, the group of bile duct ligation (BDL), and sham operation (SO). All the animals in these groups were killed in the 6th and 48th hour after operation. Seven rats from each group at each time point were examined.

### Preparation of animal models

All rats were starved overnight and underwent an upper midline laparotomy with an intraperitoneal injection of 30 mg·kg<sup>-1</sup> sodium pentobarbital for anesthesia. In AOC group, a median incision was made on the upper abdomen. The common bile duct was mobilized and doubly ligated. 0.2 ml of the *E. coli* suspension ( $5 \times 10^{12}$  cfu·L<sup>-1</sup>) was injected into the ligated common bile duct. In BDL group, the common bile duct was doubly ligated but no *E. coli* suspension was injected. In SO group, neither *E. coli* suspension injection nor common bile duct ligation was done, but only routine operative procedure was performed.

### Histology

Morphological changes of liver, heart, lungs, and kidneys were observed by light microscope and transmission electron microscope (TEM). These samples from different organs were fixed with 10 % buffered formalin or 2.5 % glutaraldehyde immediately. For optical microscopy, the tissue blocks were embedded in paraffin, and the sections were stained with hematoxylin and eosin (H&E). For TEM, the tissue blocks were embedded in Epon 618 resin and ultrathin sections were stained with uranyl acetate and lead citrate. A transmission electron microscope (JEM-2000) was used.

### Electrophoretic mobility shift assay for NF- $\kappa$ B

**Isolation of nuclear proteins** Nuclear proteins were isolated as previously described<sup>[1,22]</sup>. In brief, the liver, heart, lungs, and kidneys tissues were placed in 0.8 mL of ice-cold hypotonic buffer [10 mmol·L<sup>-1</sup> HEPES (pH7.9), 10 mL KCl, 0.1 mmol·L<sup>-1</sup> EDTA, 0.1 mmol·L<sup>-1</sup> ethylene glycol tetraacetic acid, 1 mmol·L<sup>-1</sup> DTT; Protease inhibitors (aprotinin, pepstatin, and leupeptin, 10 mg·L<sup>-1</sup> each)]. The homogenates were incubated on ice for 20 min, vortexed for 20 s after adding 50  $\mu$ L of 10 per cent Nonidet P-40, and then centrifuged for 1 minute at 4 °C in an Eppendorf centrifuge. Supernatants were decanted, the nuclear pellets after a single wash with hypotonic buffer without Nonidet P-40 were suspended in an ice-cold hypertonic buffer [20 mmol·L<sup>-1</sup> HEPES (pH7.9), 0.4 mol·L<sup>-1</sup> NaCl, 1 mmol·L<sup>-1</sup> EDTA, 1 mmol·L<sup>-1</sup> DTT; Protease inhibitors], incubated on ice for 30 min at 4 °C, mixed frequently, and centrifuged for 15 min at 4 °C. The supernatants were collected as nuclear extracts and stored at -70 °C. Concentrations of total proteins in the samples were determined according to the method of Bradford.

**Electrophoretic mobility shift assay (EMSA)** NF- $\kappa$ B binding activity was performed in a 10- $\mu$ L binding reaction mixture containing 1  $\times$  binding buffer [50 mg·L<sup>-1</sup> of double-stranded poly (dI-dC), 10 mmol·L<sup>-1</sup> Tris-HCl (pH 7.5), 50 mmol·L<sup>-1</sup> NaCl, 0.5 mmol·L<sup>-1</sup> EDTA, 0.5 mmol·L<sup>-1</sup> DTT, 1 mmol·L<sup>-1</sup> MgCl<sub>2</sub>, and 100 mL·L<sup>-1</sup> glycerol], 5  $\mu$ g of nuclear protein, and 35 fmol of double-stranded NF- $\kappa$ B consensus oligonucleotide (5' -AGT TGA GGG GAC TTT CCC AGG-3') that was endly labeled with  $\gamma$ -<sup>32</sup>P(111TBq mmol<sup>-1</sup> at 370GBq L<sup>-1</sup>) using T4 polynucleotide kinase. The binding reaction mixture was incubated at room temperature for 20 min and analyzed by electrophoresis on 7 per cent nondenaturing polyacrylamide gels. After electrophoresis the gels were dried by Gel-Drier (Bio-Rad Laboratories, Hercules, CA) and exposed to Kodak X-ray films at -70 °C. The binding bands were quantified by scanning densitometer of a Bio-Image Analysis System.

### Arterial blood gas analyses

In some animals, a carotid artery catheter was placed through an anterior cervical area, and arterial blood samples were collected to measure blood lactate, pH, pO<sub>2</sub>, pCO<sub>2</sub>, and HCO<sub>3</sub><sup>-</sup> using a blood gas analyzer.

### Measurement of biochemical parameters

Blood was obtained from the inferior vena cava at the time of

sacrifice, heart, liver, kidney injury were assessed by measuring the serum lactate dehydrogenase (LDH), alanine aminotransferase (ALT), blood urea nitrogen (BUN) and creatinine, respectively, which were performed with an Automatic Biochemical Analyser.

### Assay of TNF- $\alpha$ and IL-6 in plasma

The concentrations of TNF- $\alpha$  and IL-6 in plasma were measured by a commercially available enzyme-linked immunosorbent assay (ELISA) according to the manufacture instructions which has a low detection limit of 50 ng·L<sup>-1</sup>. Briefly, microtitre plates were coated with anti TNF- $\alpha$  or IL-6 mAb overnight at room temperature on a plate shaker and then, after they had been blocked, samples were added. The detecting antibody was biotinylated anti TNF- $\alpha$  or IL-6. The results were determined at 492 nm with DG 3022 Enzyme Linkage Essay Instrument.

### Statistical analysis

The results are presented as means  $\pm$  SEM. Data sets were analyzed with a one-way ANOVA. The differences were regarded significant when the *P* value was less than <0.05.

## RESULTS

### The changes of histology and ultrastructure of vital organs

In AOC group, in the liver, there was multifocal and patchy lytic necrosis. hepatocytes showed swelling and partly fatty degeneration, focal cytoplasmic degeneration and many myelin figures could be seen in the cytoplasm (Figure 1), Kupffer cells showed proliferation and many myelin figures in the cytoplasm (Figure 2). In the lungs, polymorphonuclears neutrophil (PMN) aggregated in alveolar capillary. In the heart, mitochondria were swollen or even vacuolated (Figure 3). In the kidneys, there was extensive fusion of foot processes of podocytes in glomeruli. The cells had lost their cell membranes and exhibited mitochondrial swelling together with intracellular edema in proximal convoluted tubules (Figure 4).

### Changes of NF- $\kappa$ B activation

In AOC group, The NF- $\kappa$ B activity increased significantly in liver, nearly fivefold over other organs after 6 h. At 48 h, the NF- $\kappa$ B activity increased also significantly in lung and heart besides liver (Figure 5). In BDL group and SO group, the active form of NF- $\kappa$ B was minimal in hepatic tissue and other tissues.

### Arterial blood gas analyses

In AOC group, arterial blood gases showed early respiratory alkalosis and late metabolic acidosis. At 6 h there was a mild respiratory alkalosis, with the arterial pH rising from  $7.45 \pm 0.02$  to  $7.52 \pm 0.01$ , the blood pCO<sub>2</sub> fell from a value of  $37.9 \pm 0.86$  to  $34.23 \pm 0.89$ . At 48 h, similar group showed evidence of metabolic acidosis, with the blood pH values falling from  $7.46 \pm 0.003$  to  $7.33 \pm 0.007$ , and blood HCO<sub>3</sub><sup>-</sup> (mmol·L<sup>-1</sup>) falling from  $27.4 \pm 0.35$  to  $20.1 \pm 1.29$ . In contrast, in BDL group, the blood pH and pCO<sub>2</sub> values were the same as those values obtained in SO group (Table 1).

### Biochemical parameters

Biochemical parameters in three groups were showed in Table 2.

### Cytokines contents in plasma

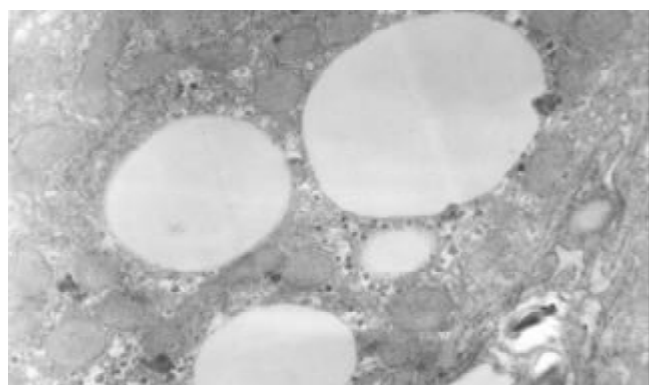
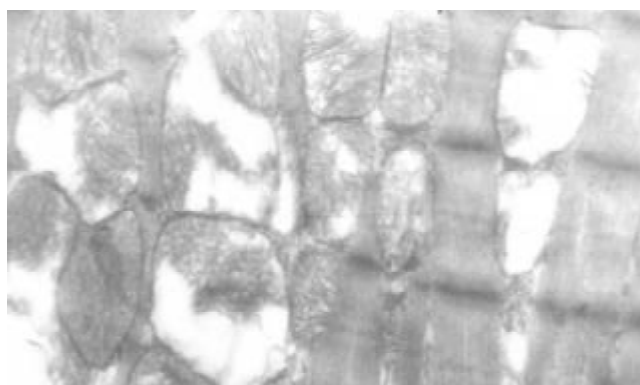
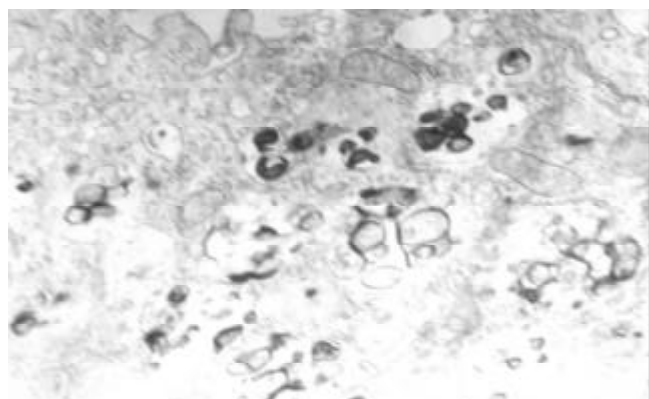
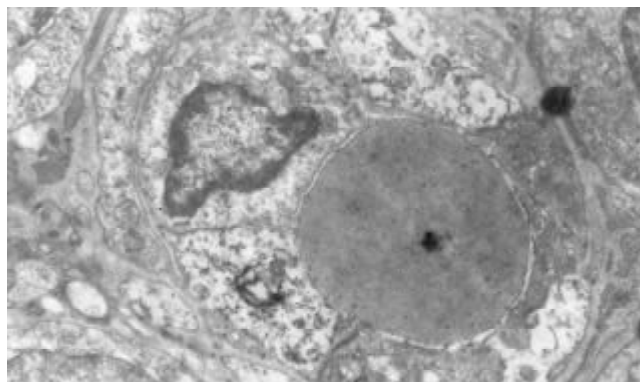
In AOC group, Levels of plasma TNF- $\alpha$  and IL-6 increased greatly in 6 h and 48 h. Levels of two cytokines were over 4-fold and 5-fold higher than that in other two groups. In BDL group, the levels of TNF- $\alpha$  and IL-6 in 48 h increased modestly when compared to that in SO group (*P*<0.05). Low levels of TNF- $\alpha$  and IL-6 was detectable in plasama in SO group (Table 3).

**Table 1** Arterial blood gas analyses in three groups animals

Parameter	Early Phase (6 h)			Late Phase (48 h)		
	AOC	BDL	SO	AOC	BDL	SO
pH	7.52 $\pm$ 0.01 <sup>a</sup>	7.46 $\pm$ 0.02	7.45 $\pm$ 0.02	7.33 $\pm$ 0.07 <sup>a</sup>	7.67 $\pm$ 0.04	7.46 $\pm$ 0.03
pCO <sub>2</sub> (mmHg)	33.9 $\pm$ 0.95 <sup>a</sup>	38.1 $\pm$ 0.89	38.9 $\pm$ 0.94	40.4 $\pm$ 4.23	37.8 $\pm$ 3.51	37.5 $\pm$ 0.72
HCO <sub>3</sub> <sup>-</sup> (mmol/L)	26.6 $\pm$ 0.63	28.3 $\pm$ 0.86	27.8 $\pm$ 1.04	20.1 $\pm$ 1.57 <sup>a</sup>	26.7 $\pm$ 1.45	27.82 $\pm$ 1.25
pO <sub>2</sub> (mmHg)	105.1 $\pm$ 6.4	108.3 $\pm$ 4.2	106.5 $\pm$ 5.8	67.3 $\pm$ 6.9 <sup>a</sup>	104.7 $\pm$ 5.3	110.7 $\pm$ 4.6

<sup>a</sup>*P*<0.05, vs other groups.**Table 2** Biochemical parameters in three groups animals

Parameter	Early Phase (6 h)			Late Phase (48 h)		
	AOC	BDL	SO	AOC	BDL	SO
LDH (nkat·L <sup>-1</sup> )	13632.7 $\pm$ 891.8 <sup>a</sup>	4107.4 $\pm$ 951.9	3655.7 $\pm$ 576.8	16359.9 $\pm$ 2278.8 <sup>a</sup>	6793 $\pm$ 885.1 <sup>c</sup>	3742.4 $\pm$ 570.1
ALT (nkat·L <sup>-1</sup> )	2213.8 $\pm$ 391.7 <sup>a</sup>	343.4 $\pm$ 103.3	311.7 $\pm$ 91.7	5796.2 $\pm$ 941.9 <sup>a</sup>	955.2 $\pm$ 175 <sup>c</sup>	288.4 $\pm$ 75
BUN (mg/dl)	16.3 $\pm$ 13.3	12.9 $\pm$ 2.8	11.8 $\pm$ 2.2	55.7 $\pm$ 15.3 <sup>a</sup>	16.7 $\pm$ 4.6	12.5 $\pm$ 2.14
Cr (mg/dl)	0.48 $\pm$ 0.03	0.42 $\pm$ 0.02	0.41 $\pm$ 0.03	0.72 $\pm$ 0.06 <sup>a</sup>	0.51 $\pm$ 0.03	0.47 $\pm$ 0.03

<sup>a</sup>*P*<0.05, vs other groups. <sup>c</sup>*P*<0.05, vs SO group.**Figure 1** Fatty degeneration, focal cytoplasmic degeneration and myelin figures in the cytoplasm of hepatocyte in AOC group TEM $\times$ 12 000.**Figure 3** Myocyte mitochondria of heart were swollen or even vacuolated in AOC group TEM $\times$ 20 000.**Figure 2** Kupffer cells showed proliferation and focal cytoplasmic degeneration and many myelin figures could be seen in the cytoplasm in AOC group TEM $\times$ 15 000.**Figure 4** Proximal convoluted tubules was full of electron dense phagosomes, the cells had lost their cell membranes and exhibited mitochondrial swelling together with intracellular edema In AOC group TEM $\times$ 3 000.



**Figure 5** Activation of NF- $\kappa$ B in AOC group. Lane 1, 2, 3, and 4 represents the Liver, the lungs, the heart, and the kidneys in 4 kw, respectively. Lane 5, 6, 7, and 8 represents the Liver, the lungs, the heart, and the kidneys in 8 kw, respectively.

**Table 3** TNF- $\alpha$  and IL-6 levels in plasma ( $n=7$ )

Groups	TNF- $\alpha$ (ng·L <sup>-1</sup> )		IL-6 (ng·L <sup>-1</sup> )	
	6 h	48 h	6 h	48 h
AOC	235±39.23 <sup>a</sup>	429±56.62 <sup>a</sup>	253±23.41 <sup>a</sup>	562±57.58 <sup>a</sup>
BDL	73±11.52	139±16.21 <sup>c</sup>	113±21.39	227±43.02 <sup>c</sup>
SO	72±12.45	74±10.53	109±18.37	113±19.81

<sup>a</sup> $P<0.05$ , vs other two groups. <sup>c</sup> $P<0.05$ , vs SO group.

## DISCUSSION

AOC in humans often leads to progressive MOD, which is still associated with a high mortality rate<sup>[1-5]</sup>. Recent studies showed NF- $\kappa$ B is rapidly in response to many pathologic signals that may be relevant during surgical trauma, including cytokines, adhesion molecules, endotoxin, hypoxia, and shear<sup>[23-27]</sup>. Activation of NF- $\kappa$ B results in the transcription of genes that can participate in the inflammatory reaction by inducing the production of cytokines, immunoreceptors, and cell adhesion molecules<sup>[28-32]</sup>. These cytokines and proinflammatory mediators are therefore a potentially attractive target inducing MOD during sepsis and endotoxemia<sup>[33-47]</sup>. Information on the role of NF- $\kappa$ B in sepsis, AOC and MOD is limited but shows that NF- $\kappa$ B is increased during inflammation and sepsis<sup>[1,18]</sup>.

The role of NF- $\kappa$ B activation in sepsis and in complication such as MOD is a debatable issue. Pennington *et al*<sup>[20]</sup> observed the degree of NF- $\kappa$ B activation with severity of acute appendicitis and found that NF- $\kappa$ B binding activity is elevated in these patients and correlates with symptoms longer than 24 hours. Arnalich *et al*<sup>[18]</sup> determined NF- $\kappa$ B activation in peripheral blood mononuclear cells of 34 patients with severe sepsis and serial concentrations of inflammatory cytokines and resulted the prognosis value of early measurement of NF- $\kappa$ B activity in patients with severe sepsis. Gong and Paterson *et al*<sup>[1,20]</sup> determined NF- $\kappa$ B activation in mononuclear and neutrophils from critically ill patients and compared NF- $\kappa$ B activation with circulating concentrations of IL-6, IL-8 and soluble intercellular adhesion molecule (sICAM)-1, and found NF- $\kappa$ B activation in patients systemic inflammatory response syndrome, which increased markedly before death. However, Chen *et al*<sup>[48]</sup> observed intrahepatic changes in TNF- $\alpha$  and NF- $\kappa$ B activation in Sprague-Dawley rats with cecal ligation and puncture, and their results implied NF- $\kappa$ B activation was not linked to the outcome in sepsis. In our original study of patients with AOC, the changes of NF- $\kappa$ B activation were documented, but evidence of MOD and the effects of NF- $\kappa$ B were not assessed. So it would be helpful to further analyze the expression with the inflamed tissues. There is, however, no published information about a key role of NF- $\kappa$ B in

development of multiple organ dysfunction during biliary infection. In this study, we investigated the role NF- $\kappa$ B in the development of MOD in rats with AOC.

The present study shows a correlation among the pathological damages of many vital organs, NF- $\kappa$ B activation and release of proinflammatory cytokines. This is only one published investigation about the correlation of NF- $\kappa$ B activation and MOD during AOC. The present study demonstrated that NF- $\kappa$ B activation plays a key role during AOC. The finding that prompt surgical inflammatory condition of the inflammatory focus results in a rapid normalization of NF- $\kappa$ B activation adds further validity to this assay.

Perhaps other important finding of this study was the marked difference in NF- $\kappa$ B levels among various organs during AOC. During AOC, Expression of NF- $\kappa$ B was observed first in liver at 6 h. At 48 h, NF- $\kappa$ B also expressed in the lung, the heart, and the kidney besides the liver. The liver was the main organ which was injured by bacteria during AOC, liver and other organs influence each other in their function, the liver plays a key role in host defense. Matuschak *et al* reported that the liver failure affected on the incidence and resolution of the adult respiratory distress syndrome. Seki *et al*<sup>[49]</sup> Hepatocytes produce acute phase protein and complement in bacterial infections. KCs are activated by various bacterial stimuli, including LPS and bacterial superantigens, and produce IL-12 and other monokines. So the liver plays a crucial role in the first line of defense against bacterial infections<sup>[50-52]</sup>. However, if this defense system is inadequately activated, sepsis and shock associated with MOD takes place. It was found in our previous study that when liver was injured, especially KCs function failed, gram-negative bacteria normally restricted to the biliary tract invaded the bloodstream and were trapped in vital organs, and NF- $\kappa$ B activation occurred, eventually MOD ensued. Further clinical trials are indicated to confirm that this “molecular biology” marker indeed will be a useful clinical tool in the management of the patients with AOC<sup>[53-56]</sup>.

In conclusion, we have shown the expression of NF- $\kappa$ B and the pathological changes of the damages occurred in many vital organs, especially in liver during AOC. These findings have an important implication for the role of NF- $\kappa$ B activation in MOD during AOC.

## REFERENCES

- Gong JP, Liu CA, Wu CX, Li SW, Shi YJ, Li XH. Nuclear factor  $\kappa$ B activity in patients with acute severe cholangitis. *World J Gastroenterol* 2002; **8**: 346-349
- Huang ZQ. New development of biliary surgery in China. *World J Gastroenterol* 2000; **6**: 187-192
- Kimmings AN, Deventer SIJH, Rauws EAJ, Huibregtse K, Gouma DJ. Systemic inflammatory response in acute cholangitis and after subsequent treatment. *Eur J Surg* 2000; **166**: 700-705
- Lillemoe KD. Surgical treatment of biliary tract infections. *Am Surg* 2000; **66**: 138-144
- Fry DE. Sepsis syndrome. *Am Surg* 2000; **66**: 126-132
- Parker SJ, Watkins PE. Experimental models of gram-negative sepsis. *Br J Surg* 2001; **88**: 22-30
- Tabrizi AR, Zehnbauser BA, Freeman BD, Buchman TG. Genetic markers in sepsis. *J Am Coll Surg* 2001; **192**: 106-117
- Jackson GDF, Dai Y, Sewell WA. Bile mediates intestinal pathology in endotoxemia in rats. *Infect Immun* 2000; **68**: 4714-4719
- Islam AFMW, Moss ND, Dai Y, Smith MSR, Collins AM, Jackson GDF. Lipopolysaccharide-induced biliary factors enhance invasion of *salmonella enteritidis* in a rat model. *Infect Immun* 2000; **68**: 1-5
- Erwin PJ, Lewis H, Dolan S, Tobias PS, Schumann RR, Lamping N, Wisdom GB, Rowlands BJ, Halliday MI. Lipopolysaccharide binding protein in acute pancreatitis. *Crit Care Med* 2000; **28**: 104-109
- Kordzaya DJ, Goderdzishvili VT. Bacterial translocation in obstructive jaundice in rats: role of mucosal lacteals. *Eur J Surg* 2000; **166**: 367-374



- 12 **Kimmings AN**, van Deventer SJH, Obertop H, Rauws EAJ, Huijbregtse K, Gouma DJ. Endotoxin, cytokines, and endotoxin binding proteins in obstructive jaundice and after preoperative biliary drainage. *Gut* 2000; **46**: 725-731
- 13 **Bone-Larson CL**, Simpson KJ, Colletti LM, Lukacs NW, Chen SC, Lira S, Kunkel SL, Hogaboam CM. The role of chemokines in the immunopathology of the liver. *Immunol Rev* 2000; **177**: 8-20
- 14 **Ito Y**, Machen NW, Urbaschek R, McCuskey RS. Biliary obstruction exacerbates the hepatic microvascular inflammatory response to endotoxin. *Shock* 2000; **14**: 599-604
- 15 **Zhao SY**, Qi Y, Liu XC, Jiang QB, Liu SY, Jiang Y, Jiang ZF. Activation of NF- $\kappa$ B in bronchial epithelial cells from children with asthma. *Chin Med J* 2001; **114**: 909-911
- 16 **West MA**, Clair L, Kraatz J, Rodriguez JL. Endotoxin tolerance from lipopolysaccharide pretreatment induces nuclear factor- $\kappa$ B alterations not present in C3H/HeJ mice. *J Trauma* 2000; **49**: 298-305
- 17 **Reddy SAG**, Huang JH, Liao WSL. Phosphatidylinositol 3-kinase as a mediator of TNF-induced NF- $\kappa$ B activation. *J Immunol* 2000; **164**: 1355-1363
- 18 **Paterson RL**, Galley HF, Dhillon JK, Webster NR. Increased nuclear factor  $\kappa$ B activation in critically ill patients who die. *Crit Care Med* 2000; **28**: 1047-1051
- 19 **Arnalich F**, Garcia-Palomero E, Lopez J, Jimenez M, Madero R, Renart J, Vazquez JJ, Montiel C. Predictive value of nuclear factor  $\kappa$ B activity and plasma cytokine levels in patients with sepsis. *Infect Immun* 2000; **68**: 1942-1945
- 20 **Pennington C**, Dunn J, Li C, Ha T, Browder W. Nuclear factor  $\kappa$ B activation in acute appendicitis: a molecular marker for extent of disease? *Am Surgeon* 2000; **66**: 914-919
- 21 **Foulds S**, Galustian C, Mansfield AO, Schachter M. Transcription factor NF- $\kappa$ B expression and postsurgical organ dysfunction. *Ann Surg* 2001; **233**: 70-78
- 22 **Reising H**, Jaeschke H, Bauer I, Patau C, Datene V, Pannen BHJ, Bauer M. Differential activation pattern of redox-sensitive transcription factors and stress-inducible dilator systems heme oxygenase-1 and inducible nitric oxide synthase in hemorrhagic and endotoxic shock. *Crit Care Med* 2001; **29**: 1962-1971
- 23 **Kono H**, Wheeler MD, Rusyn I, Lin M, Seabra V, Rivera CA, Bradford BU, Forman DT, Thurman RG. Gender differences in early alcohol-induced liver injury: role of CD14, NF- $\kappa$ B, and TNF- $\alpha$ . *Am J Physiol Gastrointest Liver Physiol* 2000; **278**: G652-G661
- 24 **Ninomiya-Tsuji J**, Kishimoto K, Hiyama A, Inoue JJ, Cao Z, Matsumoto K. The kinase TAK1 can activate the NIK-I $\kappa$ B as well as the MAP kinase cascade in the IL-1 signalling pathway. *Nature* 1999; **398**: 252-256
- 25 **Hedin KE**, Kaczynski JA, Gibson MR, Urrutia R. Transcription factors in cell biology, surgery, and transplantation. *Surgery* 2000; **128**: 1-5
- 26 **Starkel P**, Horsmans Y, Sempoux C, Saeger CD, Wary J, Lause P, Maiter D, Lambotte L. After portal branch ligation in rat, nuclear factor  $\kappa$ B, interleukin-6, signal transducers and activators of transcription 3, *c-fos*, *c-myc*, and *c-jun* are similarly induced in the ligated and nonligated lobes. *Hepatology* 1999; **29**: 1463-1470
- 27 **Liu Y**, Wang Y, Yamakuchi M, Isowaki S, Nagata E, Kanmura Y, Kitajima I, Maruyama I. Upregulation of Toll-like receptor 2 gene expression in macrophage response to peptidoglycan and high concentration of lipopolysaccharide is involved in NF- $\kappa$ B activation. *Infect Immun* 2001; **69**: 2788-2796
- 28 **Jiang QQ**, Akashi S, Miyake K, Petty HR. Cutting Edge: lipopolysaccharide induces physical proximity between CD14 and Toll-like receptor 4 (TLR4) prior to nuclear translocation of NF- $\kappa$ B. *J Immunol* 2000; **165**: 3541-3544
- 29 **Adib-Conquy M**, Adrie C, Moine P, Asehnoune K, Fitting C, Pinsky MR, Dhainaut JF, Cavaillon JM. NF- $\kappa$ B expression in mononuclear cells of patients with sepsis resembles that observed in lipopolysaccharide tolerance. *Am J Respir Crit Care Med* 2000; **162**: 1877-1883
- 30 **Abraham E**, Arcaroli J, Shenkar R. Activation of extracellular signal-regulated kinases, NF- $\kappa$ B, and cyclic adenosine 5' -monophosphate response element-binding protein in lung neutrophils occurs by differing mechanisms after hemorrhage or endotoxemia. *J Immunol* 2001; **166**: 522-530
- 31 **Belich MP**, Salmeron A, Johnston LH, Ley SC. TPL-2 kinase regulates the proteolysis of the NF- $\kappa$ B-inhibitory protein NF- $\kappa$ B1 p105. *Nature* 1999; **397**: 363-368
- 32 **Choi JH**, Ko HM, Kim JW, Lee HK, Han SS, Chun SB, Im SY. Platelet-activating factor-induced early activation of NF- $\kappa$ B play a crucial role for organ clearance of *Candida albicans*. *J Immunol* 2001; **166**: 5139-5144
- 33 **Han DW**. The clinical sine of subsequent liver injury induced by gut derived endotoxemia. *Shijie Huaren Xiaohua Zazhi* 1999; **7**: 1055-1058
- 34 **Lin E**, Calvano SE, Lowry SF. Inflammatory cytokines and cell response in surgery. *Surgery* 2000; **127**: 117-126
- 35 **Li SW**, Gong JP, Wu CX, Shi YJ, Liu CA. Lipopolysaccharide induced synthesis of CD14 proteins and its gene expression in hepatocytes during endotoxemia. *World J Gastroenterol* 2002; **8**: 124-127
- 36 **Hardaway RM**. A review of septic shock. *Am Surg* 2000; **66**: 22-27
- 37 **Sindram D**, Porte RJ, Hoffman MR, Bentley RC, Clavien PA. Synergism between platelets and leukocytes in inducing endothelial cell apoptosis in the cold ischemic rat liver: a Kupffer cell mediated injury. *FASEB J* 2001; **15**: 1230-1232
- 38 **Wu RQ**, Xu YX, Song XH, Chen LJ, Meng XJ. Adhesion molecule and proinflammatory cytokine gene expression in hepatic sinusoidal endothelial cells following cecal ligation and puncture. *World J Gastroenterol* 2001; **7**: 128-130
- 39 **Baldwin AS**. The transcription factor NF- $\kappa$ B and human disease. *J Clin Invest* 2001; **107**: 3-6
- 40 **Assy N**, Jacob G, Spira G, Edoute Y. Diagnostic approach to patients with cholestatic jaundice. *World J Gastroenterol* 1999; **5**: 252-262
- 41 **Blunck R**, Scheel O, Muller M, Brandenburg K, Seitzer U, Seydel U. New insights into endotoxin-induced activation of macrophages: involvement of a K<sup>+</sup> channel in transmembrane signaling. *J Immunol* 2001; **166**: 1009-1015
- 42 **Tak PP**, Firestein GS. NF- $\kappa$ B: a key role in inflammatory diseases. *J Clin Invest* 2001; **107**: 7-11
- 43 **Ling YL**, Meng AH, Zhao XY, Shan BE, Zhang JL, Zhang XP. Effect of cholecystokinin on cytokines during endotoxic shock in rats. *World J Gastroenterol* 2001; **7**: 667-671
- 44 **Gordon H**. Detection of alcoholic liver disease. *World J Gastroenterol* 2001; **7**: 297-302
- 45 **Bai XY**, Jia XH, Cheng LZ, Gu YD. Influence of IFN- $\alpha$ 2b and BCG on the release of TNF and IL-1 by Kupffer cells in rats with hepatoma. *World J Gastroenterol* 2001; **7**: 419-421
- 46 **Wang LS**, Zhu HM, Zhou DY, Wang YL, Zhang WD. Influence of whole peptidoglycan of bifidobacterium on cytotoxic effectors produced by mouse peritoneal macrophages. *World J Gastroenterol* 2001; **7**: 440-443
- 47 **Zuo GQ**, Gong JP, Liu CH, Li SW, Wu XC, Yang K, Li Y. Expression of lipopolysaccharide binding protein and its receptor CD14 in experimental alcoholic liver disease. *World J Gastroenterol* 2001; **7**: 836-840
- 48 **Chen J**, Raj N, Kim P, Andrejko KM, Deutschman CS. Intrahepatic nuclear factor- $\kappa$ B activity and  $\alpha_1$ -acid glycoprotein transcription do not predict outcome after cecal ligation and puncture in the rat. *Crit Care Med* 2001; **29**: 589-596
- 49 **Seki S**, Habu Y, Kawamura T, Takeda K, Dobashi H, Ohkawa T, Hiraide H. The liver as a crucial organ in the first line of host defense: the roles of Kupffer cells, natural killer (NK) cells and NK 1.1 Ag<sup>+</sup> T cells in T helper 1 immune responses. *Immunol Rev* 2000; **174**: 35-46
- 50 **Wu RQ**, XU YX, Song XH, Chen LJ, Meng XJ. Relationship between cytokine mRNA expression and organ damage following cecal ligation and puncture. *World J Gastroenterol* 2002; **8**: 131-134
- 51 **Gong JP**, Wu CX, Liu CA, Li SW, Shi YJ, Li XH, Peng Y. Liver sinusoidal endothelial cell injury by neutrophils in rats with acute obstructive cholangitis. *World J Gastroenterol* 2002; **8**: 342-345
- 52 **Gong JP**, Dai LL, Liu CA, Wu CX, Shi YJ, Li SW, Li XH. Expression of CD14 protein and its gene in liver sinusoidal endothelial cells during endotoxemia. *World J Gastroenterol* 2002; **8**: 551-554
- 53 **Shang D**, Guan FL, Jin PY, Chen HL, Cui JH. Effect of combined therapy of Yinchenhao Chengqi decoction and endoscopic sphincterotomy for endotoxemia in acute cholangitis. *World J Gastroenterol* 1998; **4**: 443-445
- 54 **Tiscornia OM**, Hamamura S, de Lehmann ES, Otero G, Waisman H, Tiscornia WP, Bank S. Biliary acute pancreatitis: a review. *World J Gastroenterol* 2000; **6**: 157-168
- 55 **Gong JP**, Wu CX, Liu CA, Li SW, Shi YJ, Yang K, Li Y, Li XH. Intestinal damage mediated by Kupffer cells in rats with endotoxemia. *World J Gastroenterol* 2002; **8**: 923-927
- 56 **Zhang WZ**, Chen YS, Wang JW, Chen XR. Early diagnosis and treatment of severe acute cholangitis. *World J Gastroenterol* 2002; **8**: 150-152

• CLINICAL RESEARCH •

# Proliferative activity of bile from congenital choledochal cyst patients

Gao-Song Wu, Sheng-Quan Zou, Xian-Wen Luo, Jian-Hong Wu, Zheng-Ren Liu

**Gao-Song Wu, Sheng-Quan Zou, Xian-Wen Luo, Jian-Hong Wu, Zheng-Ren Liu**, Department of General Surgery, Tongji Hospital, Tongji Medical College, Huazhong University of Science and Technology, Wuhan, 430030, Hubei Province, China

**Correspondence to:** Dr. Gao-Song Wu, Department of General Surgery of Tongji Hospital, 1095 Jiefang Road, Wuhan, 430030, Hubei Province, China. wugaosong9172@sina.com

**Telephone:** +86-27-83662851 **Fax:** +86-27-83662851

**Received:** 2002-07-08 **Accepted:** 2002-07-31

## Abstract

**AIM:** To explore the potential carcinogenicity of bile from congenital choledochal cyst (CCC) patients and the mechanism of the carcinogenesis in congenital choledochal cyst patients.

**METHODS:** 20 bile samples from congenital choledochal cyst patients and 10 normal control bile samples were used for this study. The proliferative effect of bile was measured by using Methabenzthiazuron (MTT) assay; Cell cycle and apoptosis were analyzed by using flow cytometry (FCM), and the PGE<sub>2</sub> levels in the supernatant of cultured cholangiocarcinoma cells were quantitated by enzyme-linked immunoabsorbent assay (ELISA).

**RESULTS:** CCC bile could significantly promote the proliferation of human cholangiocarcinoma QBC939 cells compared with normal bile ( $P=0.001$ ) and negative control group ( $P=0.002$ ), and the proliferative effect of CCC bile could be abolished by addition of cyclooxygenase-2 specific inhibitor celecoxib (20  $\mu$ M). The QBC939 cells proliferative index was increased significantly after treated with 1 % bile from CCC patient ( $P=0.008$ ) for 24 h, the percentage of S phase ( $29.48 \pm 3.27$  %) was increased remarkably ( $P<0.001$ ) compared with normal bile ( $11.72 \pm 2.70$  %), and the percentage of G0/G1 phase ( $54.19 \pm 9.46$  %) was decreased remarkably ( $P=0.042$ ) compared with normal bile ( $69.16 \pm 10.88$  %), however, bile from CCC patient had no significant influence on apoptosis of QBC939 cells ( $P=0.719$ ).

**CONCLUSION:** Bile from congenital choledochal cyst patients can promote the proliferation of human cholangiocarcinoma QBC939 cells via COX-2 and PGE<sub>2</sub> pathway.

Wu GS, Zou SQ, Luo XW, Wu JH, Liu ZR. Proliferative activity of bile from congenital choledochal cyst patients. *World J Gastroenterol* 2003; 9(1): 184-187  
<http://www.wjgnet.com/1007-9327/9/184.htm>

## INTRODUCTION

Congenital choledochal cyst (CCC) is a rare disease in Western countries<sup>[1-3]</sup>. Most of the reported cases come from Asia, particularly from Japan<sup>[4-7]</sup>. In recent years, cases of CCC are reported increasingly in China<sup>[8-17]</sup>. The incidence of carcinoma arising in the wall of a congenital bile duct cyst is high and this lesion is considered as a precancerous state of the biliary

tract, but its underlying precise mechanisms remain unclear. For the purpose of resolving these mechanisms we used the whole bile of CCC patients to act directly on the QBC939 cells to determine the effects of CCC bile on the growth of cholangiocarcinoma cells.

## MATERIALS AND METHODS

### Materials

**Bile samples collection and treatment:** Experiments were classified into CCC bile group, normal control bile group and negative control group. 20 CCC bile samples were obtained from the common bile duct of patients (5 male, 15 female, age range 5-49 years, mean 26.8 years) with CCC underwent operation at the Department of Surgery, Tongji hospital, Wuhan, China. 10 normal control bile samples were obtained from the common bile duct of patients (5 male, 5 female, age range 23-51 years, mean 42.3 years) with a normal hepatobiliary tract underwent surgery at the Department of Surgery, Tongji hospital, Wuhan, China. All patients didn't take any nonsteroid anti-inflammatory drugs, antibiotics or anti-tumor drugs before operation. Bile samples were filtered (0.22  $\mu$ m, Millipore) by sterile technique immediately twice and stored at -80 °C. PBS (pH7.2) instead of bile sample was used as negative control. Human extra-hepatic cholangiocarcinoma cell line QBC939 was established and given to us through the courtesy of professor Xu-Guang Wang (Third Military Medical University, China)<sup>[18]</sup>, cells were maintained as mono-layers in Dulbecco's modified Eagle's medium (DMEM) supplemented with 10 % fetal bovine serum (FBS, Gibco, USA.), 100 units/ml penicillin and 100 mg/ml streptomycin in a humidified atmosphere of 95 % air and 5 % CO<sub>2</sub> at 37 °C. They were subcultivated every 3-5 days and given fresh medium every other day. 70-80 % subconfluent monolayers of human cholangiocarcinoma cells were employed in all experiments. PGE<sub>2</sub> ELISA detection kit was purchased from Jingmei Biotech Co., Wuhan, China. Celecoxib was synthesized and given as a gift by Dr Zhi-Nan Mei (Wuhan University, China)<sup>[19]</sup>. Stock solution was prepared in dimethylsulfoxide (DMSO) and stored at -20 °C. In all experiments DMSO final concentration in the medium was  $\leq 0.1$  %.

### Methods

**Cytotoxicity pretesting** Cytotoxicity pretesting was taken with each of the gradient diluted bile sample to determine the concentration of experimental bile samples. Our results showed that 1 % bile (10  $\mu$ L bile/mL medium) had no significant cytotoxic influence on QBC939 cells.

**MTT assay** The human cholangiocarcinoma cells QBC939 in proliferating status was determined by using MTT assay. Cholangiocarcinoma cells were seeded at a density of  $1 \times 10^4$  cells per well in flat-bottomed 96-well microplates. 12 h after incubation, cells were treated with 1 % bile samples with or without 20  $\mu$ M celecoxib. After 24 h incubation, 20  $\mu$ L MTT (5 g/L) was added to each well, cultured for 4 h. After removed of supernatant, 150  $\mu$ L DMSO was added and shaken for 5 min until the crystal was dissolved. OD490nm value was

measured by using an enzyme-linked immunoabsorbent assay reader. The negative control well had no cells and was used as zero point of absorbance. Each assay was performed three times in triplicate.

**ELISA** The PGE<sub>2</sub> levels in the supernatant of cultured human cholangiocarcinoma cells QBC939 were quantitated by ELISA: Cells were seeded into 24-well microplates (4.0×10<sup>5</sup>/well) and allowed to adhere overnight. The cells were then incubated in the presence 1 % bile samples with or without 20 μM celecoxib for 24 h. The supernatants were aspirated and centrifuged to prepare for the detection of PGE<sub>2</sub>. 0.5 mL supernatant was added into 0.1 mL 1N HCl and centrifuged for 10 min at room temperature; then 0.1 mL 1.2N NaOH was used to neutralize the acidified samples. Standard solution (200 μL per well) or activated samples were added into the microplates. Then the steps were proceeded as instructed. The value of OD of each well was determined at 450nm. The supernatants were harvested in triplicate and the experiment was performed three times.

**Flow cytometric analysis** Cholangiocarcinoma cells QBC939 were trypsinized and plated in 6-well culture dishes in the presence of 1 % CCC bile or 1 % normal bile. After 24 h, cells were harvested, centrifuged at low speed and fixed in 70 % ethanol. After overnight incubation at 4 °C, cells were stained with 50 μg/ml propidium iodide in the presence of Rnase A (10 μg/ml) and 0.1 % Triton X-100 and determined by using a flow cytometer.

### Statistical analysis

Data were expressed as  $\bar{x} \pm s$ . Student's *t*-test was used for statistical analysis. *P*<0.05 indicates significant difference.

## RESULTS

### Assay of COX-2 activity

The COX-2 activity was determined by PGE<sub>2</sub> levels in the supernatant released by the cultured human cholangiocarcinoma cells QBC939. The concentrations of PGE<sub>2</sub> in culture medium of QBC939 cells treated with 1 % CCC bile, 1 % normal bile or 1 % PBS (pH7.2) with or without 20 μM celecoxib for 24 h were quantitated by ELISA (Table 1). CCC bile could induce the release of PGE<sub>2</sub> in QBC939 cells: the PGE<sub>2</sub> level was higher significantly (*P*<0.001) in CCC bile group (184.0±9.7 ng/well) compared with that in normal control bile group (131.0±7.3 ng/well) and negative control group (123.3±8.4). Celecoxib could suppress QBC939 cells PGE<sub>2</sub> production, the PGE<sub>2</sub> concentration was 80.3±7.1 ng/well, 74.1±9.7 ng/well and 72.4±10.8 ng/well in CCC bile group, normal control bile group and negative control bile group respectively, when pre-treated with 20 μM celecoxib, there was no statistical difference (*P*>0.05).

**Table 1** PGE<sub>2</sub> level released by QBC939 in the existence of bile with or without celecoxib

Group	<i>n</i>	PGE <sub>2</sub>	<i>P</i>	+CE PGE <sub>2</sub>	<i>P</i>
A	20	184.0±9.7	<sup>b</sup> <i>P</i> <0.001, <sup>d</sup> <i>P</i> <0.001	80.3±7.1	<sup>b</sup> <i>P</i> =0.057, <sup>d</sup> <i>P</i> =0.055
B	10	131.0±7.3	<sup>b</sup> <i>P</i> =0.087	74.1±9.7	<sup>b</sup> <i>P</i> =0.771
C	5	123.3±8.4		72.4±10.8	

The concentrations of PGE<sub>2</sub> (ng/well) in culture medium of QBC939 cells treated with 1 % CCC bile (A), 1 % normal bile (B) or 1 % PBS (C) with or without 20 μM celecoxib (+CE) for 24 h were quantitated by ELISA. Data were expressed as  $\bar{x} \pm s$ , b vs C, d vs B.

### Effects of bile on the growth of QBC939

QBC939 cells were incubated in 1 % bile samples with or without 20 μM celecoxib, and the cell density was measured by using MTT assay (Table 2). CCC bile could significantly promote the proliferation of human cholangiocarcinoma QBC939 cells compared with normal bile (*P*=0.001) and negative control group (*P*=0.002), and the proliferative effect of CCC bile could be abolished by addition of cyclooxygenase-2 specific inhibitor celecoxib.

**Table 2** Effects of bile on the growth of QBC939 with or without celecoxib

Group	<i>n</i>	OD <sub>490</sub>	<i>P</i>	+CE OD <sub>490</sub>	<i>P</i>
A	20	0.59±0.17	<sup>b</sup> <i>P</i> =0.002, <sup>d</sup> <i>P</i> =0.001	0.29±0.09	<sup>b</sup> <i>P</i> =0.089, <sup>d</sup> <i>P</i> =0.190
B	10	0.47±0.14	<sup>b</sup> <i>P</i> =0.398	0.26±0.07	<sup>b</sup> <i>P</i> =0.052
C	5	0.43±0.10		0.24±0.09	

QBC939 cells were incubated in 1 % CCC bile (A), 1 % normal bile (B) or 1 % PBS (C) with or without 20 μM celecoxib (+CE), and the cells density (OD<sub>490nm</sub>) was measured by using MTT assay. Data were expressed as  $\bar{x} \pm s$ , b vs C, d vs B.

### Flow cytometric analysis of cell cycle and apoptosis

The QBC939 cells proliferative index (PI) increased significantly (*P*=0.008) after treated with 1 % CCC bile (41.53±5.68) compared with normal bile (25.46±4.41), PI=(S+G2/M) % × 100. The percentage of S phase cells was increased remarkably (*P*<0.001) in CCC bile group (29.48±3.27) % compared with that in normal bile group (11.72±2.70) %, and the percentage of G0/G1 phase cells was decreased remarkably (*P*=0.002) in CCC group (54.19±9.46) % compared with that in normal group (69.16±10.88) %, CCC bile had no significant influence on the apoptosis of QBC939 cells compared with normal bile (*P*=0.719). The percentage of apoptotic cells in CCC bile group and normal bile group were (2.38±0.41) % and (2.09±0.36) % respectively (Figure 1).

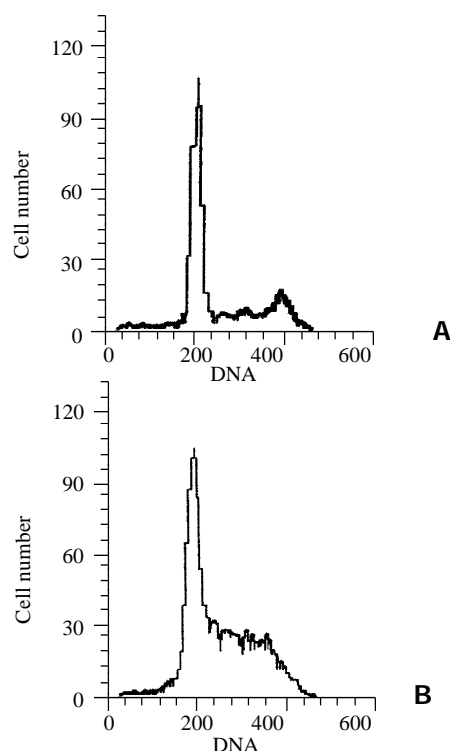


**Figure 1** Representative data of cell cycle and apoptosis from QBC939 cells in the presence of 1 % CCC bile (B) or 1 % normal bile (A) for 24 h was analyzed by using flow cytometry.

## DISCUSSION

As one of the high risk factors of cholangiocarcinoma, CCC is a common disease in eastern countries. Choledochal cysts are associated with a 10 % overall incidence of cholangiocarcinoma: there is a 1 % cumulative risk which plateaus after 15-20 years<sup>[20]</sup>. In almost all cases congenital bile duct cysts are related to anomalous arrangements of the pancreaticobiliary duct system (APBDU) which seems to play a crucial role in the development of cystic bile ducts and biliary carcinogenesis. Bile stasis together with reflux of pancreatic juice causing longstanding inflammation and activation of bile acids might be the factors in carcinogenesis of the exposed bile duct epithelium in the cystic wall<sup>[21]</sup>. Ohtsuka<sup>[22]</sup> have reported that bile presented one possible explanation for the predisposition to carcinoma in choledochocoele as bile containing amylase may stagnate in the choledochocoele and then carcinoma may develop in the inner epithelium of the choledochocoele by the same mechanism as that leading to carcinogenesis in patients with APBDU.

Elevation of the secondary and free bile acid concentrations is considered as a risk factor for biliary carcinogenesis in CCC patients. Yuzuru *et al*<sup>[23]</sup> have suggested that elevation of the lysolecithin (LL) in the bile is one of the factors for development of biliary tract carcinoma in patients with CCC: the LL in the phospholipid, which is produced from lecithin by activated phospholipase A<sub>2</sub> in refluxed pancreatic juice, was significantly elevated in the CCC group. Yoon *et al*<sup>[24]</sup> have indicated that bile acids both induced EGFR phosphorylation and enhanced COX-2 protein expression. EGFR was activated by bile acids and functioned to induce COX-2 expression by a MAPK cascade. The induction of COX-2 might participate in the genesis and progression of cholangiocarcinomas.

In an effort to delineate the underlying mechanisms of the carcinogenesis in CCC patients, we used the whole bile from CCC patients for the first time to act directly on the human cholangiocarcinoma QBC939 cells *in vitro* to determine the effects of CCC bile on the growth of human cholangiocarcinoma cells. Our data showed that CCC bile could significantly promote the proliferation of human cholangiocarcinoma QBC939 cells compared with normal bile, and the proliferative effect of CCC bile could be abolished by addition of cyclooxygenase-2 specific inhibitor celecoxib. Our research indicated that CCC bile promoted the proliferation of human cholangiocarcinoma QBC939 cells via COX-2 and PGE<sub>2</sub> pathway.

Substantial evidences have shown that COX-2 is important in carcinogenesis<sup>[25-33]</sup>. Celecoxib as a new COX-2 selective inhibitor has shown its safety and efficiency in human and animal. Several studies have demonstrated that celecoxib has significant efficacy in animal models: Celecoxib inhibited intestinal tumor multiplicity up to 71 % compared with controls in the Min mouse model, inhibited colorectal tumor burden in the rat azoxymethane (AOM) model<sup>[34-36]</sup>. Recently celecoxib has been approved by FDA to reduce the number of adenomatous colorectal polyps in patients with familial adenomatous polyposis (FAP). Our data suggested that celecoxib as a chemopreventive and chemotherapeutic agent might be effective in cholangiocarcinomas and could be used as a chemopreventive strategy in the people of high-risk conditions for the development of cholangiocarcinoma such as CCC patients. Our research demonstrated that the QBC939 cells proliferative index increased significantly after treated with CCC bile for 24 h, the percentage of S phase was increased remarkably compared with normal bile, and the percentage of G0/G1 phase was decreased remarkably compared with normal bile, however, CCC bile had no significant influence on apoptosis of QBC939 cells. These data suggested that CCC bile could effect on the QBC939 cell proliferation cycle and

the proliferative activity of CCC bile was on cell cycle but not on apoptosis.

In conclusion, CCC bile can promote the proliferation of human cholangiocarcinoma QBC939 cells and these effects are via COX-2 and PGE<sub>2</sub> pathway.

## REFERENCES

- 1 **Cucinotta E**, Palmeri R, Lazzara S, Salamone I, Melita G, Melita P. Diagnostic problems of choledochal cysts in the adult. *Chir Ital* 2002; **54**: 245-248
- 2 **Nassar AH**, Chakhtoura N, Martin D, Parra-Davila E, Sleeman D. Choledochal cysts diagnosed in pregnancy: a case report and review of treatment options. *J Matern Fetal Med* 2001; **10**: 363-365
- 3 **Wienke J**, Falen S, McCartney W. Hepatobiliary scan showing type II choledochal cyst. *Clin Nucl Med* 2001; **26**: 1010-1012
- 4 **Komuro H**, Makino SI, Yasuda Y, Ishibashi T, Tahara K, Nagai H. Pancreatic complications in choledochal cyst and their surgical outcomes. *World J Surg* 2001; **25**: 1519-1523
- 5 **Li L**, Yamataka A, Yian-Xia W, Da-Yong W, Segawa O, Lane GJ, Kun W, Jin-Zhe Z, Miyano T. Ectopic distal location of the papilla of Vater in congenital biliary dilatation: Implications for pathogenesis. *J Pediatr Surg* 2001; **36**: 1617-1622
- 6 **O'Neill JA**. Choledochal cyst. *Curr Probl Surg* 1992; **29**: 361-410
- 7 **Tsuchida Y**, Takahashi A, Suzuki N, Kuroiwa M, Murai H, Toki F, Kawarasaki H, Hashizume K, Honna T. Development of intrahepatic biliary stones after excision of choledochal cysts. *J Pediatr Surg* 2002; **37**: 165-167
- 8 **Shi LB**, Peng SY, Meng XK, Peng CH, Liu YB, Chen XP, Ji ZL, Yang DT, Chen HR. Diagnosis and treatment of congenital choledochal cyst: 20 years' experience in China. *World J Gastroenterol* 2001; **7**: 732-734
- 9 **Liu H**, Lu XH. The diagnosis of choledochal cyst (A report of 50 cases). *Xin Xiaohuabingxue Zazhi* 1996; **4**: 259
- 10 **Zhang Z**, Wei HL. Congenital choledochal dilatation in adult (A report of 3 cases). *Xin Xiaohuabingxue Zazhi* 1996; **4**(Suppl 5): 32
- 11 **Qiao Q**, Sun Z, Huang Y. Diagnosis and treatment of congenital choledochal cysts in adults. *Zhonghua Waike Zazhi* 1997; **35**: 610-612
- 12 **Wang L**, Wang SF, Li YG. Choledochal cyst (A report of 2 cases). *Xin Xiaohuabingxue Zazhi* 1996; **4**(Suppl 5): 210
- 13 **Tao K**, Li K, Dou K. Analysis and prevention of reoperation on congenital choledochal cyst. *Zhonghua Waike Zazhi* 1999; **37**: 344-346
- 14 **Dou K**, Guan W, Li K. Living related liver transplantation: a case report. *Zhonghua Waike Zazhi* 1998; **36**: 203-205
- 15 **Lin JTH**, Chen YH, Ni YH, Lai HS, Peng SS. Magnetic resonance cholangiopancreatography diagnosed pancreatitis associated choledochal cyst: report of one case. *Acta Paediatr Taiwan* 2001; **42**: 363-366
- 16 **Li M**, Jin Q, Feng J. Early postoperative complications of choledochal cyst excision and reconstruction of biliary tract. *Zhonghua Waike Zazhi* 2001; **39**: 686-689
- 17 **Zhao L**, Li Z, Ma H, Zhang X, Mou X, Zhang D, Lin W, Niu A. Congenital choledochal cyst with pancreatitis. *Chin Med J* 1999; **112**: 637-640
- 18 **Wang SG**, Han BL, Duan HC, Chen YS, Peng ZM. Establishment of the extrahepatic cholangiocarcinoma cell line. *Zhonghua Shiyao Waike Zazhi* 1997; **14**: 67-68
- 19 **Mei ZY**, Shi Z, Wang XH, Luo XD. Synthesis of COX-2 Inhibitor Celecoxib. *Zhongguo Yiyao Gongye Zazhi* 2000; **31**: 433-434
- 20 **Chapman RW**. Risk factors for biliary tract carcinogenesis. *Ann Oncol* 1999; **10**(Suppl 4): 308-311
- 21 **Holzinger F**, Baer HU, Schilling M, Stauffer EJ, Buchler MW. Congenital bile duct cyst: a premalignant lesion of the biliary tract associated with adenocarcinoma-a case report. *Z Gastroenterol* 1996; **34**: 382-385
- 22 **Ohtsuka T**, Inoue K, Ohuchida J, Nabae T, Takahata S, Niiyama H, Yokohata K, Ogawa Y, Yamaguchi K, Chijiwa K, Tanaka M. Carcinoma arising in choledochocoele. *Endoscopy* 2001; **33**: 614-619
- 23 **Sugiyama Y**, Kobori H, Hakamada K, Seito D, Sasaki M. Altered bile composition in the gallbladder and common bile duct of patients with anomalous pancreaticobiliary ductal junction. *World J Surg* 2000; **24**: 17-21

- 24 **Yoon JH**, Higuchi H, Werneburg NW, Kaufmann SH, Gores GJ. Bile acids induce cyclooxygenase-2 expression via the epidermal growth factor receptor in a human cholangiocarcinoma cell line. *Gastroenterology* 2002; **122**: 985-993
- 25 **Gao HJ**, Yu LZ, Sun G, Miao K, Bai JF, Zhang XY, Lu XZ, Zhao ZQ. The expression of Cox-2 Proteins in gastric cancer tissue and accompanying tissue. *Shijie Huaren Xiaohua Zazhi* 2000; **8**: 578-579
- 26 **Zhuang ZH**, Wang LD. Non-steroid anti-inflammatory drug and digestive tract tumors. *Shijie Huaren Xiaohua Zazhi* 2001; **9**: 1050-1053
- 27 **Tian G**, Yu JP, Luo HS, Yu BP, Yue H, Li JY, Mei Q. Effect of Nimesulide on proliferation and apoptosis of human hepatoma SMMC-7721 cells. *World J Gastroenterol* 2002; **8**: 483-487
- 28 **Sun B**, Wu YL, Zhang XJ, Wang SN, He HY, Qiao MM, Zhang YP, Zhong J. Effects of Sulindac on growth inhibition and apoptosis induction in human gastric cancer cells. *Shijie Huaren Xiaohua Zazhi* 2001; **9**: 997-1002
- 29 **Tian G**, Yu TP, Luo HS, Yu BP, Li JY. The expression and effect of cyclooxygenase-2 in acute hepatic injury. *Shijie Huaren Xiaohua Zazhi* 2002; **10**: 24-27
- 30 **Li JY**, Yu JP, Luo HS, Yu BP, Huang JA. Effects of nonsteroidal anti-inflammatory drugs on the proliferation and cyclooxygenase activity of gastric cancer cell line SGC7901. *Shijie Huaren Xiaohua Zazhi* 2002; **10**: 262-265
- 31 **Wu YL**, Sun B, Zhang XI, Wang SN, He HY, Qiao MM, Zhong J, Xu JY. Growth inhibition and apoptosis induction of sulindac on human gastric cancer cells. *World J Gastroenterol* 2001; **7**: 796-800
- 32 **Sirica AE**, Lai GH, Zhang Z. Biliary cancer growth factor pathways, cyclo-oxygenase-2 and potential therapeutic strategies. *J Gastroenterol Hepatol* 2001; **16**: 363-372
- 33 **Chariyalertsak S**, Sirikulchayanonta V, Mayer D, Kopp-Schneider A, Furstenberger G, Marks F, Muller-Decker K. Aberrant cyclooxygenase isozyme expression in human intrahepatic cholangiocarcinoma. *Gut* 2001; **48**: 80-86
- 34 **Hosomi Y**, Yokose T, Hirose Y, Nakajima R, Nagai K, Nishiwaki Y, Ochiai A. Increased cyclooxygenase 2 (COX-2) expression occurs frequently in precursor lesions of human adenocarcinoma of the lung. *Lung Cancer* 2000; **30**: 73-81
- 35 **Tsubouchi Y**, Mukai S, Kawahito Y, Yamada R, Kohno M, Inoue K, Sano H. Meloxicam inhibits the growth of non-small cell lung cancer. *Anticancer Res* 2000; **20**: 2867-2872
- 36 **Souza RF**, Shewmake K, Beer DG, Cryer B, Spechler SJ. Selective inhibition of cyclooxygenase-2 suppresses growth and induces apoptosis in human esophageal adenocarcinoma cells. *Cancer Res* 2000; **60**: 5767-5772

Edited by Xu JY

• CLINICAL RESEARCH •

# K-ras gene mutation in the diagnosis of ultrasound guided fine-needle biopsy of pancreatic masses

Min Zheng, Lian-Xin Liu, An-Long Zhu, Shu-Yi Qi, Hong-Chi Jiang, Zhu-Ying Xiao

**Min Zheng, Zhu-Ying Xiao**, Department of Ultrasound, the First Clinical College, Harbin Medical University, Harbin 150001, Heilongjiang Province, China

**Lian-Xin Liu, An-Long Zhu, Hong-Chi Jiang**, Department of Surgery, the First Clinical College, Harbin Medical University, Harbin 150001, Heilongjiang Province, China

**Shu-Yi Qi**, Department of VIP, the First Clinical College, Harbin Medical University, Harbin 150001, Heilongjiang Province, China  
**Support by** Natural Scientific Foundation of Heilongjiang Province, No.97024

**Correspondence to:** Dr. An-Long Zhu, Department of Surgery, the First Clinical College, Harbin Medical University, No.23 Youzheng Street, Nangang District, Harbin 150001, Heilongjiang Province, China. anlonge@163.com

**Telephone:** +86-451-4213684 **Fax:** +86-451-3670428

**Received:** 2002-07-08 **Accepted:** 2002-08-02

## Abstract

**AIM:** To investigate the utility of K-ras mutation analysis of ultrasound guided fine-needle aspirate biopsy of pancreatic masses.

**METHODS:** Sixty-six ultrasound guided fine-needle biopsies were evaluated by cytology, histology and k-ras mutation. The mutation at codon 12 of the k-ras oncogene was detected by artificial restriction fragment length polymorphisms using *Bst* NI approach.

**RESULTS:** The presence of malignant cells was reported in 40 of 54 pancreatic carcinomas and K-ras mutations were detected in 45 of the 54 FNABs of pancreatic carcinomas. The sensitivity of cytology and k-ras mutation were 74 % and 83 %, respectively. The speciality of cytology and k-ras mutation were both 100 %. The sensitivity and speciality of k-ras mutation combined with cytology were 83 % and 100 %, respectively.

**CONCLUSION:** High diagnostic accuracy with acceptable discomfort of FNAB make it useful in diagnosis of pancreatic carcinoma. Ultrasound guided fine-needle biopsy is a safe and feasible method for diagnosing pancreatic cancer. Pancreatic carcinoma has the highest K-ras mutation rate among all solid tumors. The mutation rate of k-ras is about 80-100 %. The usage of mutation of codon 12 of k-ras oncogene combined with cytology is a good alternative for evaluation of pancreatic masses.

Zheng M, Liu LX, Zhu AL, Qi SY, Jiang HC, Xiao ZY. K-ras gene mutation in the diagnosis of ultrasound guided fine-needle biopsy of pancreatic masses. *World J Gastroenterol* 2003; 9(1):188-191 <http://www.wjgnet.com/1007-9327/9/188.htm>

## INTRODUCTION

Pancreatic adenocarcinoma is a very aggressive carcinoma and has the worst prognosis in common abdominal cancer<sup>[1-3]</sup>. Despite the poor prognosis, patients with localized disease may be cured with surgery<sup>[4-6]</sup>. However, it is difficult to diagnose

pancreatic cancer in the earlier stages. This dismal prognosis is a result not only of biological aggressiveness but also of diagnosis late in the chronological progression of the tumor. If pancreatic cancer can be resected when it is small, the prognosis is much better, with a 5-year survival of approximately 40 %<sup>[7-9]</sup>. When pancreatic cancer is clinically suspected and a pancreatic mass identified by ultrasonography or computed tomography scan, a guided percutaneous fine-needle biopsy (FNAB) can be obtained; this may be the only sample available for diagnosis in most patients<sup>[10-12]</sup>.

Even though alternative techniques for sampling cellular or tissue material have been developed, FNAB is still widely used for morphological verification of intra-abdominal malignancies, especially in pancreatic cancer. Although it has been questioned because of the risk of peritoneal seeding and seeding of tumor cells along the needle tract. It is still widely used for the diagnosis of pancreatic cancer combined with modern molecular biological techniques<sup>[13]</sup>.

The high incidence of mutations at codon 12 of the K-ras gene (65-100 %) leads to consider them as a potential tumor marker at the tissue level<sup>[14-19]</sup>. The development of PCR-based techniques for detection of K-ras mutations has allowed its use in the clinical setting. The high incidence of mutation suggests that it may be used as a tumor marker at the tissue level. The role of k-ras detection in the clinical evaluation of pancreatic mass has to be established in a large series of patients. Data suggest that a combination of cytological examination and K-ras mutation detection in cellular material may improve diagnostic accuracy<sup>[20-26]</sup>. In this study we evaluated the diagnostic utility of cytological and histological examination and k-ras mutation detection, alone and in combination under the ultrasound guided FNAB from 66 patients with pancreatic masses.

## MATERIALS AND METHODS

### *Patients and samples*

Between January 1997 and May 2001, 66 consecutive patients (38 men and 28 women, mean age of 54±9 years) with pancreatic masses were included. In all cases FNAB of the masses were percutaneously obtained under ultrasonographic guidance. A portion (50 %) of each FNAB was immediately examined by pathologist. The other 50 % of the same specimen was frozen and stored in liquid nitrogen.

Final diagnosis of pancreatic carcinoma was established if malignant cells were identified in the FNAB or in surgically resected specimens or when death occurred within six months after diagnosis, with clinical evolution compatible with disseminated cancer disease. Other types of neoplasm were diagnosed on the basis of pathological findings. The diagnosis of chronic pancreatitis was based on standard clinical criteria. In chronic pancreatitis, a minimum of 6-month (range, 6-27 months) follow-up period with no evidence of cancer was available. Pancreatic tuberculosis was confirmed by positive Lowenstein culture.

### *Detection of K-ras codon 12 mutations*

DNA was extracted following standard procedures. We utilized

*Bst*NI (Promega, USA) restriction fragment length polymorphism/polymerase chain reaction (RFLP/PCR) method that enriches for the amplification of mutant codon 12 K-ras alleles by cleaving amplified wild-type allele through intermediate digestion between first- and second-round PCR<sup>[27]</sup>. To create the restriction site for the enzyme *Bst*NI [CCTGG], which is lost when a K-ras codon 12 mutation exists, the first-round amplification was performed using the mutant primers K-ras 5' and DD5P (Table 1) in a volume of 50 µL containing PCR buffer (50 mmol/L KCl, 20 mmol/L Tris HCl, pH 8.4), 1.5 mmol/L MgCl<sub>2</sub>, 0.2 mmol/L each dNTP (Promega, USA), 1U of Taq polymerase (Life Technologies, USA), and 150 ng of PCR primers<sup>[28]</sup>. The reactions were 10 cycles of 92 °C(15s), 44 °C(15s) and 72 °C(15s). An aliquot of 5 µL of the amplified product was enzymatically digested with *Bst*NI following the manufacturer's directions. One microliter of the digested product was reamplified using a heminested reaction with mutant amplimers K-ras 5' and K-ras 3' <sup>[28]</sup>. The reaction conditions were 35 cycles of 92 °C(15s), 54 °C(15s) and 72 °C(15s). The latter primer artificially introduces an internal control to assure the completion of enzymatic digestion. After polyacrylamide gel electrophoresis (6 %) and ethidium bromide (0.5 g/L) staining, the 143-bp band depicted the mutant allele, and the 114-bp band the wild-type allele. RFLP/PCR method consistently detected a mutant allele in serial dilutions containing at least 1 mutant allele in 1 000 wild-type alleles. Positive bands were always clearly identifiable when DNA obtained from FNAB was examined. All samples were analyzed in duplicate. Results were available 48-72 h after the tissue sample was obtained.

**Table 1** Primers for K-ras mutation detection

Round	Primer	Sequence
First	K-ras 5'	5'-ACTGAARARAACTTGTGGTAGTTGGACCT-3'
	DD5P	5'-TCATGAAAATGGTCAGAGAA-3'
Second	K-ras 5'	5'-ACTGAATATACTTGTGGTAGTTGGAACCT-3'
	K-ras 3'	5'-TCAAAGAATGGTCCTGGACC-3'

## RESULTS

### Cytological examination

Final diagnoses were as follows: 54 pancreatic carcinomas, 3 other malignancies (1 lymphoma, and 2 cholangio-carcinomas), 6 benign diseases (5 chronic pancreatitis and 1 tuberculosis), and 3 endocrine tumors. The presence of malignant cells was reported in 40 of 54 pancreatic carcinomas with no false positives. However, in 14 of the 54 FNABs of pancreatic carcinomas, the cytological report was not conclusive: 12 because of insufficient material and 2 because of suspicion. The sensitivity of cytology was 74 % in the diagnosis of pancreatic cancer.

### Molecular diagnosis

Molecular analysis was possible in 54 of 66 FNABs. K-ras mutations were detected in 45 of the 54 FNABs of pancreatic carcinomas, with no false positives. The combination of cytology and enriched RFLP/PCR analysis was always informative and showed a sensitivity of 83.3 %, with a specificity of 100 %. Only nine pancreatic carcinomas failed to be correctly classified after the combined cytological and molecular analysis.

In three cases, a K-ras positive analysis in combination with the presence of suspicious cells was considered confirmation of pancreatic cancer, and no further studies were performed. Two of these patients died 1 and 3 months later, respectively,

with a clinical course consistent with advanced pancreatic cancer. In the other, positive peritoneal disease was present at surgery. In one patient with insufficient material at cytology, molecular analysis was the endpoint of the diagnostic work-up, and laparotomy was not performed because of the poor clinical status of the patient. Finally, in the remaining one patient with insufficient material for cytological evaluation and K-ras positive analysis, surgical resection of a histologically confirmed pancreatic carcinoma was performed.

## DISCUSSION

The influence of biopsy on the natural history of pancreatic carcinoma is still unclear, considering the increasing intention to treat and the development of new multimodality therapies<sup>[29,30]</sup>. Our data indicate the FNAB of pancreatic malignancy can be easily performed without serious side effects and is still a safe and useful procedure for establishing the diagnosis of pancreatic carcinoma. High diagnostic accuracy with acceptable patient discomfort has also been reported when using an 18-gauge cutting needle with an automatic spring-loaded sample device. The large amount of tissue obtained could improve the microscopic evaluation, but it has not been verified that microhistology offers advantages over cytology in the diagnosis of pancreatic cancer. The complication rate, including needle tract seeding, in pancreatic carcinoma is lower than in other tumors<sup>[31,32]</sup>.

The main limitation of cytological analysis is the substantial proportion of cases in which a conclusive report is not possible, and where a second procedure to confirm diagnosis is required. FNAB can get a bigger tissues for microhistological examination. The molecular approach allows detection of K-ras mutants even when cells are present in a small proportion. Mutation detection would have complemented the cytological evaluation of FNAB when cellular material was insufficient, suspicious cells were present, or when healthy-appearing duct cells were reported<sup>[33]</sup>.

Pancreatic carcinoma is known to have the highest K-ras mutation rate among all tumors. The codon 12 of this gene is affected in 80-100 % of the cases<sup>[34-36]</sup>. Only a minority of pancreatic cancers (9 cases) failed to be correctly classified by the combined histological and molecular approach in our studies. Although inaccurate sampling of the lesion may account for some of the false negatives observed, the molecular approach has some limitations<sup>[26,37]</sup>. The discrepancies between the results of the various studies are based on the wide range of investigated cases, the selection of lesion types, and the sensitivity of the microdissection and PCR techniques employed. The clinical usefulness of ras mutations relies on the development of rapid, sensitive, and reproducible techniques for their detection. Moreover, a positive molecular diagnosis avoided iterative pancreatic fine-needle aspiration or further diagnostic procedures in these patients.

In Japanese studies, a comparison of the K-ras mutation pattern in ductal lesions with that of the adjacent carcinomas revealed nearly identical mutation patterns<sup>[38,39]</sup>, whereas in a study from North America a concordance rate of only 50 % was reported<sup>[40]</sup>. The results of our analysis showed identical mutation patterns in the primary tumor confirming the results of the Japanese authors. There are large differences in the incidence of ras mutations between Japanese and Western populations, although the reason is still unclear and the number of subjects is limited. In Japan, the frequency of K-ras mutation ranged from 55-80 %<sup>[41-44]</sup>, whereas in West it was relatively low, ranging from 0-31 %<sup>[45,46]</sup>. The current data suggest that most patients have ras gene mutations in the tumor itself, which is similar to previous Japanese reports.

In conclusion, the results of the present study indicate that



K-ras analysis is a highly specific and sensitive approach in pancreatic carcinoma patients and suggest that a k-ras assay may have a role in the diagnostic assessment of these patients. Further investigations are needed to confirm these results, to improve the technique's sensitivity, and to establish its usefulness in the early.

## REFERENCES

- 1 **Yoshida T**, Matsumoto T, Sasaki A, Morii Y, Aramaki M, Kitano S. Prognostic factors after pancreatoduodenectomy with extended lymphadenectomy for distal bile duct cancer. *Arch Surg* 2002; **137**: 69-73
- 2 **Shankar A**, Russell RC. Recent advances in the surgical treatment of pancreatic cancer. *World J Gastroenterol* 2001; **7**: 622-626
- 3 **Zhao XY**, Yu SY, Da SP, Bai L, Guo XZ, Dai XJ, Wang YM. A clinical evaluation of serological diagnosis for pancreatic cancer. *World J Gastroenterol* 1998; **4**: 147-149
- 4 **Ahmad NA**, Lewis JD, Ginsberg GG, Haller DG, Morris JB, Williams NN, Rosato EF, Kochman ML. Long term survival after pancreatic resection for pancreatic adenocarcinoma. *Am J Gastroenterol* 2001; **96**: 2532-2534
- 5 **Guo XZ**, Friess H, Shao XD, Liu MP, Xia YT, Xu JH, Buchler MW. KAI1 gene is differently expressed in papillary and pancreatic cancer: influence on metastasis. *World J Gastroenterol* 2000; **6**: 866-871
- 6 **Ghaneh P**, Slavin J, Sutton R, Hartley M, Neoptolemos JP. Adjuvant therapy in pancreatic cancer. *World J Gastroenterol* 2001; **7**: 482-489
- 7 **Huang JJ**, Yeo CJ, Sohn TA, Lillemoe KD, Sauter PK, Coleman J, Hruban RH, Cameron JL. Quality of life and outcomes after pancreatoduodenectomy. *Ann Surg* 2000; **231**: 890-898
- 8 **Sakorafas GH**, Tsiotou AG. Multi-step pancreatic carcinogenesis and its clinical implications. *Eur J Surg Oncol* 1999; **25**: 562-565
- 9 **Liu B**, Staren E, Iwamura T, Appert H, Howard J. Taxotere resistance in SUIT Taxotere resistance in pancreatic carcinoma cell line SUIT and its sublines. *World J Gastroenterol* 2001; **7**: 855-859
- 10 **Cui JH**, Krueger U, Henne-Bruns D, Kremer B, Kalthoff H. Orthotopic transplantation model of human gastrointestinal cancer and detection of micrometastases. *World J Gastroenterol* 2001; **7**: 381-386
- 11 **Liu B**, Staren E, Iwamura T, Appert H, Howard J. Effects of Taxotere on invasive potential and multidrug resistance phenotype in pancreatic carcinoma cell line SUIT-2. *World J Gastroenterol* 2001; **7**: 143-148
- 12 **Xu HB**, Zhang YJ, Wei WJ, Li WM, Tu XQ. Pancreatic tumor: DSA diagnosis and treatment. *World J Gastroenterol* 1998; **4**: 80-81
- 13 **Linder S**, Blasjo M, Sundelin P, von Rosen A. Aspects of percutaneous fine-needle aspiration biopsy in the diagnosis of pancreatic carcinoma. *Am J Surg* 1997; **174**: 303-306
- 14 **Villanueva A**, Reyes G, Cuatrecasas M, Martinez A, Erill N, Lerma E, Farre A, Lluís F, Capella G. Diagnostic utility of K-ras mutations in fine-needle aspirates of pancreatic masses. *Gastroenterology* 1996; **110**: 1587-1594
- 15 **Yuan P**, Sun MH, Zhang JS, Zhu XZ, Shi DR. APC and K-ras gene mutation in aberrant crypt foci of human colon. *World J Gastroenterol* 2001; **7**: 352-356
- 16 **Wang Q**, Lin ZY, Feng XL. Alterations in metastatic properties of hepatocellular carcinoma cell following H-ras oncogene transfection. *World J Gastroenterol* 2001; **7**: 335-339
- 17 **Yin ZZ**, Jin HL, Yin XZ, Li TZ, Quan JS, Jin ZN. Effect of Boschniakia rossica on expression of GST-P, p53 and p21(ras) proteins in early stage of chemical hepatocarcinogenesis and its anti-inflammatory activities in rats. *World J Gastroenterol* 2000; **6**: 812-818
- 18 **Li J**, Feng CW, Zhao ZG, Zhou Q, Wang LD. A preliminary study on ras protein expression in human esophageal cancer and precancerous lesions. *World J Gastroenterol* 2000; **6**: 278-280
- 19 **Ward R**, Hawkins N, O' Grady R, Sheehan C, O' Connor T, Impey H, Roberts N, Fuery C, Todd A. Restriction endonuclease-mediated selective polymerase chain reaction: a novel assay for the detection of K-ras mutations in clinical samples. *Am J Pathol* 1998; **153**: 373-379
- 20 **Ikeda N**, Nakajima Y, Sho M, Adachi M, Huang CL, Iki K, Kanehiro H, Hisanaga M, Nakano H, Miyake M. The association of K-ras gene mutation and vascular endothelial growth factor gene expression in pancreatic carcinoma. *Cancer* 2001; **92**: 488-499
- 21 **Fukushima H**, Yamamoto H, Itoh F, Nakamura H, Min Y, Horiuchi S, Iku S, Sasaki S, Imai K. Association of matrilysin mRNA expression with K-ras mutations and progression in pancreatic ductal adenocarcinomas. *Carcinogenesis* 2001; **22**: 1049-1052
- 22 **Lohr M**, Muller P, Mora J, Brinkmann B, Ostwald C, Farre A, Lluís F, Adam U, Stubbe J, Plath F, Nizze H, Hopt UT, Barten M, Capella G, Liebe S. p53 and K-ras mutations in pancreatic juice samples from patients with chronic pancreatitis. *Gastrointest Endosc* 2001; **53**: 734-743
- 23 **Mora J**, Puig P, Boadas J, Urgell E, Montserrat E, Lerma E, Gonzalez-Sastre F, Lluís F, Farre A, Capella G. K-ras gene mutations in the diagnosis of fine-needle aspirates of pancreatic masses: prospective study using two techniques with different detection limits. *Clin Chem* 1998; **44**: 2243-2248
- 24 **Pabst B**, Arps S, Binmoeller K, Thul R, Walsemann G, Fenner C, Klapdor R. Analysis of K-ras mutations in pancreatic tissue after fine needle aspirates. *Anticancer Res* 1999; **19**: 2481-2484
- 25 **Li D**, Firozi PF, Zhang W, Shen J, DiGiovanni J, Lau S, Evans D, Friess H, Hassan M, Abbruzzese JL. DNA adducts, genetic polymorphisms, and K-ras mutation in human pancreatic cancer. *Mutat Res* 2002; **513**: 37-48
- 26 **Ha A**, Watanabe H, Yamaguchi Y, Ohtsubo K, Wang Y, Motoo Y, Okai T, Wakabayashi T, Sawabu N. Usefulness of supernatant of pancreatic juice for genetic analysis of K-ras in diagnosis of pancreatic carcinoma. *Pancreas* 2001; **23**: 356-363
- 27 **Kahn SM**, Jiang W, Culbertson TA, Weinstein IB, Williams GM, Tomita N, Ronai Z. Rapid and sensitive nonradioactive detection of mutant K-ras genes via "enriched" PCR amplification. *Oncogene* 1991; **6**: 1079-1083
- 28 **Jiang W**, Kahn SM, Guillem JG, Lu SH, Weinstein IB. Rapid detection of ras oncogenes in human tumors: applications to colon, esophageal, and gastric cancer. *Oncogene* 1989; **4**: 923-928
- 29 **Schramm H**, Urban H, Arnold F, Penzlin G, Bosseckert H. Intrасurgical pancreas cytology. *Pancreas* 2002; **24**: 210-214
- 30 **Freeny PC**. Pancreatic carcinoma: imaging update 2001. *Dig Dis* 2001; **19**: 37-46
- 31 **Chang KJ**, Nguyen P, Erickson RA, Durbin TE, Katz KD. The clinical utility of endoscopic ultrasound-guided fine-needle aspiration in the diagnosis and staging of pancreatic carcinoma. *Gastrointest Endosc* 1997; **45**: 387-393
- 32 **Gloor B**, Todd KE, Reber HA. Diagnostic workup of patients with suspected pancreatic carcinoma: the University of California-Los Angeles approach. *Cancer* 1997; **79**: 1780-1786
- 33 **Puig P**, Urgell E, Capella G, Sancho FJ, Pujol J, Boadas J, Farre A, Lluís F, Gonzalez-Sastre F, Mora J. A highly sensitive method for K-ras mutation detection is useful in diagnosis of gastrointestinal cancer. *Int J Cancer* 2000; **85**: 73-77
- 34 **Suwa H**, Hosotani R, Kogire M, Doi R, Ohshio G, Fukumoto M, Imamura M. Detection of extrapancreatic nerve plexus invasion of pancreatic adenocarcinoma. Cytokeratin 19 staining and K-ras mutation. *Int J Pancreatol* 1999; **26**: 155-162
- 35 **Luttges J**, Kloppel G. Update on the pathology and genetics of exocrine pancreatic tumors with ductal phenotype: precursor lesions and new tumor entities. *Dig Dis* 2001; **19**: 15-23
- 36 **Matsubayashi H**, Watanabe H, Nishikura K, Ajioka Y, Kijima H, Saito T. Determination of pancreatic ductal carcinoma histogenesis by analysis of mucous quality and K-ras mutation. *Cancer* 1998; **82**: 651-660
- 37 **Eskelinen MJ**, Haglund UH. Prognosis of human pancreatic adenocarcinoma: review of clinical and histopathological variables and possible uses of new molecular methods. *Eur J Surg* 1999; **165**: 292-306
- 38 **Tsuchida T**, Kijima H, Hori S, Oshika Y, Tokunaga T, Kawai K, Yamazaki H, Ueyama Y, Scanlon KJ, Tamaoki N, Nakamura M. Adenovirus-mediated anti-K-ras ribozyme induces apoptosis and growth suppression of human pancreatic carcinoma. *Cancer Gene Ther* 2000; **7**: 373-383
- 39 **Kimura W**, Zhao B, Futakawa N, Muto T, Makuuchi M. Significance of K-ras codon 12 point mutation in pancreatic juice in the diagnosis of carcinoma of the pancreas. *Hepatogastroenterology* 1999; **46**: 532-539

- 40 **Futakawa N**, Kimura W, Yamagata S, Zhao B, Ilsoo H, Inoue T, Sata N, Kawaguchi Y, Kubota Y, Muto T. Significance of K-ras mutation and CEA level in pancreatic juice in the diagnosis of pancreatic cancer. *J Hepatobiliary Pancreat Surg* 2000; **7**:63-71
- 41 **Theodor L**, Melzer E, Sologov M, Idelman G, Friedman E, Bar-Meir S. Detection of pancreatic carcinoma: diagnostic value of K-ras mutations in circulating DNA from serum. *Dig Dis Sci* 1999; **44**: 2014-2019
- 42 **Caldas C**. Biliopancreatic malignancy: screening the at risk patient with molecular markers. *Ann Onco* 1999; **10**: 153-156
- 43 **Matsubayashi H**, Watanabe H, Yamaguchi T, Ajioka Y, Nishikura K, Iwafuchi M, Yamano M, Kijima H, Saito T. Multiple K-ras mutations in hyperplasia and carcinoma in cases of human pancreatic carcinoma. *Jpn J Cancer Res* 1999; **90**: 841-848
- 44 **Nakaizumi A**, Uehara H, Takenaka A, Uedo N, Sakai N, Yano H, Ohigashi H, Ishikawa O, Ishiguro S, Sugano K, Tatsuta M. Diagnosis of pancreatic cancer by cytology and measurement of oncogene and tumor markers in pure pancreatic juice aspirated by endoscopy. *Hepatogastroenterology* 1999; **46**: 31-37
- 45 **Castells A**, Puig P, Mora J, Boadas J, Boix L, Urgell E, Sole M, Capella G, Lluís F, Fernandez-Cruz L, Navarro S, Farre A. K-ras mutations in DNA extracted from the plasma of patients with pancreatic carcinoma: diagnostic utility and prognostic significance. *J Clin Oncol* 1999; **17**: 578-584
- 46 **Tamagawa E**, Ueda M, Takahashi S, Sugano K, Uematsu S, Mukai M, Ogata Y, Kitajima M. Pancreatic lymph nodal and plexus micrometastases detected by enriched polymerase chain reaction and nonradioisotopic single-strand conformation polymorphism analysis: a new predictive factor for recurrent pancreatic carcinoma. *Clin Cancer Res* 1997; **3**: 2143-2149

**Edited by** Xu JY

• ESOPHAGEAL CANCER •

# A new three-layer-funnel-shaped esophagogastric anastomosis for surgical treatment of esophageal carcinoma

Han-Lei Dan, Yang Bai, Hui Meng, Cong-Lin Song, Jie Zhang, Yong Zhang, Lei-Chi Wan, Ya-Li Zhang, Zhen-Shu Zhang, Dian-Yuan Zhou

**Han-Lei Dan, Yang Bai, Ya-Li Zhang, Zhen-Shu Zhang, Dian-Yuan Zhou**, Research Institute of Digestive Disease, South Hospital, First Military Medical University, Guangzhou 510515, Guangdong Province, China

**Hui Meng**, Department of Cardio-Thoracic Surgery, South Hospital, First Military Medical University, Guangzhou 510515, Guangdong Province, China

**Cong-Lin Song, Jie Zhang**, Department of Surgery, No. 520 Hospital, Mianyang City 621000, Sichuan Province, China

**Yong Zhang**, Yanting Oncology Research Institute, Yanting County 621042, Sichuan Province, China

**Lei-Chi Wan**, Department of Cardio-Thoracic Surgery, Pearl River Hospital, Guangzhou 510282, Guangdong Province, China

**Correspondence to:** Dr. Han-Lei Dan, M.D., Doctor-in-chief of Surgery Department. Prof. Ya-Li Zhang, M.D., Ph. D., Research Institute of Digestive Disease, South Hospital (Nanfang Hospital), First Military Medical University, Guangzhou 510515, Guangdong Province, China. henrydan@sina.com

**Telephone:** +86-20-85141531 **Fax:** +86-20-85141531

**Received:** 2002-05-14 **Accepted:** 2002-06-16

## Abstract

**AIM:** To reduce the incidence of postoperative anastomotic leak, stenosis, gastroesophageal reflux (GER) for patients with esophageal carcinoma, and to evaluate the conventional method of esophagectomy and esophagogastric anastomosis modified by a new three-layer-funnel-shaped (TLF) esophagogastric anastomotic suturing technique.

**METHODS:** From January 1997 to October 1999, patients with clinical stage I and II (IIa and IIb) esophageal carcinoma, which met the enrollment criteria, were surgically treated by the new method (Group A) and by conventional operation (Group B). All the patients were followed at least for 6 months. Postoperative outcomes and complications were recorded and compared with the conventional method in the same hospitals and with that reported previously by McLarty *et al* in 1997 (Group C).

**RESULTS:** 58 cases with stage I and II (IIa and IIb) esophageal carcinoma, including 38 males and 20 females aged from 34 to 78 (mean age: 57), were surgically treated by the TLF anastomosis and 64 by conventional method in our hospitals from January 1997 to October 1999. The quality of swallowing was improved significantly (*Wilcoxon W*=2 142, *P*=0.001) 2 to 3 months after the new operation in Group A. Only one patient had a blind anastomotic fistula diagnosed by barium swallow test 2 months but healed up 3 weeks later. Postoperative complications occurred in 25 (43 %) patients, anastomotic stenosis in 8 (14 %), and GER in 13 (22 %). The incidences of postoperative anastomotic leak, stenosis and GER were significantly decreased by the TLF anastomosis method compared with that of conventional methods ( $\chi^2=6.566$ , *P*=0.038;  $\chi^2=10.214$ , *P*=0.006;  $\chi^2=21.265$ , *P*=0.000).

**CONCLUSION:** The new three-layer-funnel-shaped

esophagogastric anastomosis (TLFEA) has more advantages to reduce postoperative complications of anastomotic leak, stricture and GER.

Dan HL, Bai Y, Meng H, Song CL, Zhang J, Zhang Y, Wan LC, Zhang YL, Zhang ZS, Zhou DY. A new three-layer-funnel-shaped esophagogastric anastomosis for surgical treatment of esophageal carcinoma. *World J Gastroenterol* 2003; 9(1): 22-25  
<http://www.wjgnet.com/1007-9327/9/22.htm>

## INTRODUCTION

Surgical therapy is considered the major method for treatment of operable esophageal cancer<sup>[1-2]</sup>. Unfortunately, there are many operative complications after classical standard esophagectomy and esophageal reconstruction with stomach in patients with esophageal carcinoma. Anastomotic leak, with a rate of about 12-14 % as reported, is the most severe complication and the principal cause of death after operation<sup>[3-7]</sup>. Anastomotic stenosis and gastroesophageal reflux (GER), with higher rates of about 36.4-40 % and 50-60 % respectively, result in dysphagia, heartburn, regurgitation and nausea<sup>[3-7]</sup>.

We modified the conventional method of esophagectomy and created a new three-layer-funnel-shaped (TLF) esophagogastric anastomotic suturing technique, which significantly reduced postoperative complications of anastomotic leak, stricture and GER.

## MATERIALS AND METHODS

### *Patients and preoperative examination*

From January 1997 to October 1999, the patients with clinical stage I and II (IIa and IIb) esophageal carcinoma, which met the enrollment criteria, were allocated into two groups and surgically treated by a new method (Group A) and the conventional operation (Group B) in our hospitals. All patients were diagnosed by esophagoscopy and biopsy. Barium swallow test confirmed that the cancer length was <5 cm, there was absence of sinus or fistula. No lung or liver metastases were detected by radiography and/or computed tomography (CT) scan of the chest and ultrasonography of the upper abdomen. Supraclavicular lymph nodes were not involved by physical examination in all patients. Karnofsky performance status was >70. All patients assessed by pulmonary functional test were fit for thoracotomy. Patients with stage III or IV esophageal carcinoma, inoperable conditions, receiving chemotherapy or radiotherapy before or after operation were precluded.

### *Methods of operation*

Partial or sub-total resection of esophagus was routinely performed through left or right thoracic incision, some cases need cervical incision, with removal of paraesophageal, subcarinal, supradiaphragmatic, perihilar, as well as left gastric and coeliac lymph node group. Partial gastrectomy was performed with esophagogastric junction carcinoma. The stomach remained and was reconstructed as a tube-like pouch to replace the resected part of the esophagus. The anastomotic

techniques were improved as follows:

When the gastric tube was constructed, an adequate amount of greater omentum was reserved for protecting the right gastroepiploic vessels and the blood supply of the gastric tube. The gastric tube was kept long enough to avoid tension and pulled along the esophageal bed, anchored to the back of the chest wall beside the mediastinum (The cervical cancer need a cervical incision to perform the anastomotic suture in the neck). First, the esophageal muscular layer was cut 3.0-3.5 cm in length into the inclined cycle, and the esophageal mucosa was kept 1.0-1.5 cm longer. Between the short gastric vessel, the sero-muscular layer was incised 4.0-4.5 cm, and its posterior aspect was hand-sewn to the same aspect of esophageal muscular layer. Then, excised the inner circular muscle layer and mucosa of stomach for 2.5-3.0 cm long and anastomosed to the esophageal mucosa by interrupted suture. The anterior aspect of the esophageal muscular and the gastric sero-muscular layer was sewn finally with fundoplication by inversion suture. The fundoplication suture cycle is 1.0 -2.0 cm larger than the suture cycle of the esophageal muscular-to-sero-muscular layer of the stomach (Figure 1). The other procedures were performed as usual.

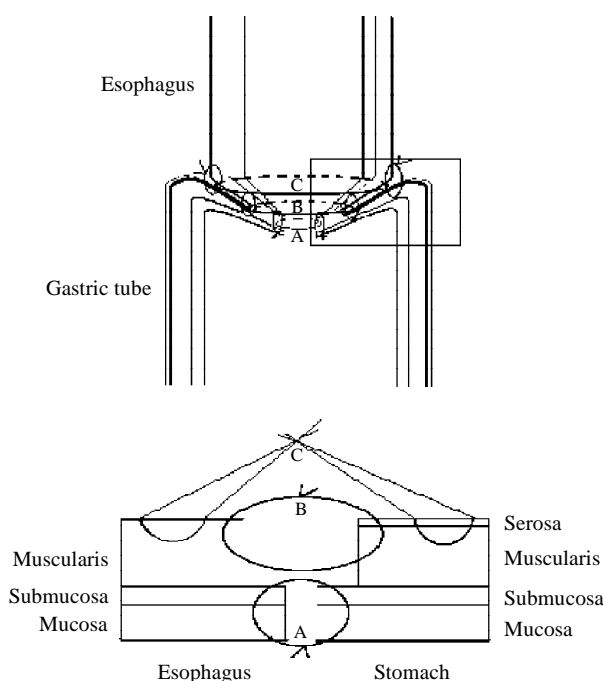


**Figure 1** Technique of three-layer-funnel-shaped (TLF) esophagogastric anastomosis. A: mucosa-to-mucosa suture cycle; B: the esophagus muscular to gastric sero-muscular suture cycle; C: fundoplication suture cycle.

### Postoperative management and follow-up

After the operation, all patients were treated routinely by thoracic drainage, nutrition support, and antibiotics. The swallowing ability and symptoms of anastomotic leak, stricture and GER were observed clinically as reported<sup>[3-7]</sup>. All patients were evaluated clinically by their general condition, eating habits, swallowing ability and barium swallow test or esophagoscopy 2 to 3 months after the completion of all treatments and followed up at intervals of 2-3 months for at least 6 months.

Postoperative anastomotic leak was diagnosed clinically by leakage of gastrointestinal contents and radiographically extravasation of water-soluble contrast medium at the site of anastomosis. The anastomotic stricture was defined as any form of narrowing in the anastomosis region by contrast swallow study ( $\leq 2.0$  cm in diameter in obverse and lateral posture)

and any symptom of dysphagia when swallowing solid food, semisolids or liquids, requiring endoscopic dilation. GER was present if the patient had intermittent or continuous heartburn, regurgitation and nausea, especially that required antacids for relief of heartburn, or barium regurgitation at horizontal posture or Trendelenburg's position on radiographic examination.

### Statistical analysis

All patients' general characteristics, pathological pattern of carcinoma, clinical staging, swallowing ability, postoperative complications, and incidences of anastomotic leak, stricture, and GER were recorded and compared to that treated by conventional methods in the same hospitals and that reported previously by McLarty *et al*<sup>[7]</sup>. Quantitative data were compared by using Independent-Samples *t* test and qualitative data by Chi-square, Fisher's exact test, and Wilcoxon rank test. Statistical significance was assumed at  $P \leq 0.05$ .

### RESULTS

58 patients (Group A), including 38 males and 20 females aged from 34 to 78 (mean age: 57), 54 cases with dysphagia, 4 without any symptom by routine examination, were successfully treated by the new method and 64 (Group B) by the conventional operation. There were no severe intraoperative complications, no operative mortality, no abscesses or uncontrolled infections occurred in all patients. Treated by the new method, the quality of swallowing of the patients improved significantly ( $P=0.001$ ) 2 to 3 months after the operation (Table 1). In Group A, only one patient had a minute blind anastomotic fistula into the immediate paraesophageal soft tissues without causing any symptoms which was diagnosed by barium swallowing test 2 months after the operation, but healed up automatically without any treatment 3 weeks afterwards. Postoperative complications occurred in 25 patients (43 %), including incision and/or thoracic cavity bleeding in 2, wound infection in 1, pneumonia in 1, anastomotic stenosis in 8 (14 %), and GER in 13 (22 %). There were 7 of 8 cases with symptom of dysphagia but dilated successfully by endoscopy, 1 case with moderate stricture could only eat semisolid or liquid food 1 year after the operation.

**Table 1** Evaluation of swallowing quality after operation (Group A,  $n=58$ )

	No symptom of dysphagia	With symptom of dysphagia		
		Solid Food	Semisolids	Liquids
Preoperation	4 (6.9%)	23 (39.7%)	26 (44.8%)	5 (8.6%)
Postoperation	50 (86.2%)	5 (8.6%)	2 (3.4%)	1 (1.7%)

Analysed by wilcoxon rank test (*Wilcoxon W*=2 142,  $P=0.001$ ), swallowing quality of patients after operation increased significantly compared with that before operation.

Except the difference of pathological type of carcinoma in the west from that in China, which was not the major factor that affected the operation modality and the early outcomes, the patients' general characteristics, tumor site and clinical staging in Group A were analogous to those in Group B and that reported previously by Allison *et al* (Table 2). Although the total incidence of postoperative complications were not different due to different method of calculation, the incidences of anastomotic leak, stricture, and GER in our new method therapy group were significantly reduced compared with that of conventional therapy groups (Table 3).

**Table 2** Characteristics and pathological condition of patients in different groups

	A New method (n=58)	B Conventional (n=64)	C Reported <sup>a</sup> (n=107)	Statistical analysis	
				$\chi^2/t$	P Value
Sex (male /female)	46/12	43/21	81/26	2.563	0.279
Mean age (range) (years)	57 (34-78)	54(28-76)	62 (30-81)		
Tumor site					
Upper (include cervical)	4 (7%)	3 (4.6%)	2 (2%)	2.731	0.604
Middle	21 (36%)	24 (37.5%)	43 (40%)		
Lower(junctional part)	33 (57%)	37 (57.8%)	62 (58%)		
Pathological type <sup>b</sup>					
Squamous	32 (55%)	34(53%)	28 (26%)	14.399	0.001 <sup>b</sup>
Adenocarcinoma	22 (38%)	28(44%)	72 (67%)	1.155	0.561 <sup>c</sup>
Others	4 (7%)	2(3%)	7 (7%)		
Tumor Diameter (Mean±SD)(cm)	3.1±1.94	3.6 ± 1.58	ND	1.551(t)	0.084
Clinical Staging					
Stage I	18 (31%)	22 (35%)	34 (32%)	7.272	0.122
StageIIA	31 (53%)	29 (45%)	65 (61%)		
StageIIB	9 (16%)	13 (22%)	8 ( 8%)		

<sup>a</sup>By McLarty AJ, Deschamps C, Trastek VF, *et al.* Ann Thorac Surg, 1997;63:1568-1572. <sup>b</sup>The pathological type of esophageal carcinoma was different as reported in the west from that in China ( $P=0.001$ ), but it was not the major factor that affected the methods and early outcomes of operation. <sup>c</sup>Compared the pathologic type of cancer treated by the new(Group A) and the conventional (Group B) methods. ND: No data available.

**Table 3** Postoperative Outcomes and Complications of Patients in the above Groups

	A New method (n=58)	B Conventional (n=64)	C Reported <sup>a</sup> (n=107)	Statistical analysis	
				$\chi^2/t$	P Value
No complication	33(56.9%)	26(40.6%)	17 (16%)	29.716	0.000
Complications	25 (43%)	38(59.3%)	43 (40%)	2.258	0.353
Anastomotic leak	1 (2%)	4(6%)	13 (12%)	6.566	0.038
Anastomotic stricture					
Dysphagia to food	8 (13%)	24(37.5%)	40 (37%)	10.214	0.006
Postoperative dilation	8 (14%)	23(35.9%)	46(43%)	14.746	0.001
Gastroesophageal reflux					
Reflux Symptoms	13 (22%)	33(52%)	64 (60%)	21.265	0.000
Required antacids	11 (19%)	20(32%)	31 (29%)	2.026	0.363

<sup>a</sup>By McLarty AJ, *et al.* Ann Thorac Surg, 1997;63:1568-1572.

## DISCUSSION

There are clear evidences that patients with earlier stage esophageal carcinoma have relatively good outcomes when treated with resection only, especially through thoracic incision which is easy to remove the regional lymph nodes and to carry out the whole operation<sup>[1,2,8]</sup>. Multimodality treatment with neoadjuvant chemotherapy or chemoradiotherapy was recommended for esophageal carcinoma by some studies but the results are debatable recently by other studies due to poor outcomes at present<sup>[9-12]</sup>. Yet there are still many postoperative complications such as leaks, stricture, and GER, which affect the esophageal function and quality of life, as well as long-term survival of the patients<sup>[3-7]</sup>.

Anastomotic leak is mainly caused by ischemia of the anastomosis and errors in surgical technique<sup>[7]</sup>. Except few recurrence of carcinoma which occurs usually above 6 months after operation, small-bore anastomosis and fibrotic stenosis are the principal causes of anastomotic stricture that results in poor function of swallowing<sup>[3,4,7]</sup>. Some studies show that there is a trend toward slightly higher leaking rate for one-layer

anastomosis and a higher stricture rate for two-layer anastomosis<sup>[4,13,14]</sup>. As for GER, it is basically caused by loss or alteration of normal anatomical structure, location, and function of esophagus, cardia and stomach<sup>[3,5,6]</sup>.

The new three-layer-funnel-shaped esophagogastric anastomotic suturing technique, we report here, has more advantages than the classical ones. First, it not only maintains adequate arterial perfusion and venous drainage by reserving enough amount of greater omentum, protecting the right gastroepiploic vessels, and avoiding excessive tension of gastric tube and esophagus, but also maintains accurate mucosa-to-mucosa, muscular-to-muscular apposition and enhances the anastomosis by three-layer sutures, as well as omentum or pleura covering. This significantly avoids the occurrence of anastomotic leak according to our clinical data.

Second, it forms three inclined suture cycles in different diameters at different levels (Figure 1). The fundoplication suture cycle and the esophageal muscular-to-gastric sero-muscular suture cycle are ellipse like and big enough to form a large-bore anastomosis that reduces stricture formation. That

is why the incidence of anastomotic strictures being low and dilated easily and effectively in our study.

Third, with adequate mucosa-to-mucosa suture, the new method reconstructed a soft mucosa petal which forms the third suture cycle, smaller in diameter and easier to open or shrink automatically, and prevents GER effectively. Although postoperative GER still occurred in 22 % which need further study, it was significantly decreased compared to the conventional method<sup>[15]</sup>. Twenty-four-hour esophageal pH monitor is a new method to diagnose GER and we plan to carry out a further randomized clinical trial to more scientifically evaluate the anti-GER effects of the mucosa petal created by the new anastomosis<sup>[16]</sup>.

Like all conventional anastomotic suture techniques, we also emphasize that it is important for the anastomotic healing to prevent infection, malnutrition, influence of chemotherapy and radiotherapy and other related factors in perioperative stage. To prevent the anastomotic tissue injury from strangulation, one should never suture too tightly, or place an excessive number of sutures. In addition, each suture 'bite' of esophageal muscular layer may be transversely sewn so as to overcome the problem because the longitudinally oriented esophageal muscle holds suture poorly.

Some studies recommend that the stapled esophagogastric anastomosis after resection for esophagogastric or cardia cancer is a simple and expeditious procedure, carrying an acceptable perioperative morbidity and cancer recurrence rate<sup>[17-19]</sup>. But except the technical problems caused by the staples, the stricture rate of stapled anastomosis was higher<sup>[17-21]</sup>. Beitler *et al* systemically reviewed the related randomized controlled trials and pointed out that both stapled and hand-sewn techniques are acceptable but both need further improvement<sup>[22]</sup>. GER is recently demonstrated as a main risk factor for esophageal adenocarcinoma and is the main factor that decreases the quality of life of patients after operation<sup>[7,23-30]</sup>. The new three-layer-funnel-shaped esophagogastric anastomotic suturing technique is a pilot study, its effect on anti-GER has not been very ideal, and we are making further efforts for improvement, especially that on the prevention of anastomotic leak, stricture and GER.

## REFERENCES

- 1 **Simchuk EJ**, Alderson D. Oesophageal surgery. *World J Gastroenterol* 2001; **7**: 760-765
- 2 **Law S**, Fok M, Chow S, Chu KM, Wong J. Preoperative chemotherapy versus surgical therapy alone for squamous cell carcinoma of the esophagus: a prospective randomized trial. *J Thorac Cardiovasc Surg* 1997; **114**: 210-217
- 3 **Whooley BP**, Law S, Alexandrou A, Murthy SC, Wong J. Critical appraisal of the significance of intrathoracic anastomotic leakage after esophagectomy for cancer. *Am J Surg* 2001; **181**: 198-203
- 4 **Swisher SG**, Hunt KK, Holmes EC, Zinner MJ, McFadden DW. Changes in the surgical management of esophageal cancer from 1970 to 1993. *Am J Surg* 1995; **169**: 609-614
- 5 **Urschel JD**. Esophagogastric anastomotic leaks complicating esophagectomy: a review. *Am J Surg* 1995; **169**: 634-640
- 6 **Bruns CJ**, Gawenda M, Wolfgarten B, Walter M. Cervical anastomotic stenosis after gastric tube reconstruction in esophageal carcinoma. Evaluation of a patient sample 1989-1995. *Langenbecks Arch Chir* 1997; **382**: 145-148
- 7 **McLarty AJ**, Deschamps C, Trastek VF, Allen MS, Pairolero PC, Harmsen WS. Esophageal resection for cancer of the esophagus: long-term function and quality of life. *Ann Thorac Surg* 1997; **63**: 1568-1572
- 8 **Miller JD**, Jain MK, de Gara CJ, Morgan D, Urschel JD. Effect of surgical experience on results of esophagectomy for esophageal carcinoma. *J Surg Oncol* 1997; **65**: 20-21
- 9 **Walsh TN**, Noonan N, Hollywood D, Kelly A, Keeling N, Hennessy TP. A comparison of multimodal therapy and surgery for esophageal adenocarcinoma. *N Engl J Med* 1996; **335**: 462-467
- 10 **Bosset JF**, Gignoux M, Triboulet JP, Tiet E, Manton G, Elias D, Lozach P, Ollier JC, Pavy JJ, Mercier M, Sahmoud T. Chemoradiotherapy followed by surgery compared with surgery alone in squamous-cell cancer of the esophagus. *N Engl J Med* 1997; **337**: 161-167
- 11 **Stein HJ**, Sendler A, Fink U, Siewert JR. Multidisciplinary approach to esophageal and gastric cancer. *Surg Clin North Am* 2000; **80**: 659-682
- 12 **Urba SG**, Orringer MB, Turrisi A, Iannettoni M, Forastiere A, Strawderman M. Randomized trial of preoperative chemoradiation versus surgery alone in patients with locoregional esophageal carcinoma. *J Clin Oncol* 2001; **19**: 305-313
- 13 **Zieren HU**, Muller JM, Pichlmaier H. Prospective randomized study of one- or two-layer anastomosis following oesophageal resection and cervical oesophagogastric anastomosis. *Br J Surg* 1993; **80**: 608-611
- 14 **Wang SJ**, Wen DG, Zhang J, Man X, Liu H. Intensify standardized therapy for esophageal and stomach cancer in tumor hospitals. *World J Gastroenterol* 2001; **7**: 80-82
- 15 **Wang Q**, Liu J, Zhao X. Can esophagogastric anastomosis prevent gastroesophageal reflux. *Zhonghua Waike Zazhi* 1999; **37**: 71-73
- 16 **Sun M**, Wang WL, Wang W, Wen DL, Zhang H, Han YK. Gastroesophageal manometry and 24-hour dual pH monitoring in neonates with birth asphyxia. *World J Gastroenterol* 2001; **7**: 695-697
- 17 **Bisgaard T**, Wojdemann M, Larsen H, Heindorff H, Gustafsen J, Svendsen LB. Double-stapled esophagogastric anastomosis for resection of esophagogastric or cardia cancer: new application for an old technique. *J Laparoendosc Adv Surg Tech A* 1999; **9**: 335-339
- 18 **Singh D**, Maley RH, Santucci T, Macherey RS, Bartley S, Weyant RJ, Landreneau RJ. Experience and technique of stapled mechanical cervical esophagogastric anastomosis. *Ann Thorac Surg* 2001; **71**: 419-424
- 19 **Stone CD**, Heitmiller RF. As originally published in 1994: Simplified, standardized technique for cervical esophagogastric anastomosis. Updated in 2000. *Ann Thorac Surg* 2000; **70**: 999-1000
- 20 **Valverde A**, Hay JM, Fingerhut A, Elhadad A. Manual versus mechanical esophagogastric anastomosis after resection for carcinoma: a controlled trial. French Associations for Surgical Research. *Surgery* 1996; **120**: 476-483
- 21 **Berrisford RG**, Page RD, Donnelly RJ. Stapler design and strictures at the esophagogastric anastomosis. *J Thorac Cardiovasc Surg* 1996; **111**: 142-146
- 22 **Beitler AL**, Urschel JD. Comparison of stapled and hand-sewn esophagogastric anastomoses. *Am J Surg* 1998; **175**: 337-340
- 23 **Shaheen N**, Ransohoff DF. Gastroesophageal reflux, Barrett esophagus, and esophageal cancer: clinical applications. *JAMA* 2002; **287**: 1982-1986
- 24 **Lagergren J**, Bergstrom R, Lindgren A, Nyren O. Symptomatic gastroesophageal reflux as a risk factor for esophageal adenocarcinoma. *N Engl J Med* 1999; **340**: 825-831
- 25 **Johanson JF**. Critical review of the epidemiology of gastroesophageal reflux disease with specific comparisons to asthma and breast cancer. *Am J Gastroenterol* 2001; **96**: S19-21
- 26 **El-Serag HB**, Hepworth EJ, Lee P, Sonnenberg A. Gastroesophageal reflux disease is a risk factor for laryngeal and pharyngeal cancer. *Am J Gastroenterol* 2001; **96**: 2013-2018
- 27 **Ferguson MK**, Durkin A. Long-term survival after esophagectomy for Barrett's adenocarcinoma in endoscopically surveyed and nonsurveyed patients. *J Gastrointest Surg* 2002; **6**: 29-35
- 28 **Ye W**, Chow WH, Lagergren J, Yin L, Nyren O. Risk of adenocarcinomas of the esophagus and gastric cardia in patients with gastroesophageal reflux diseases and after antireflux surgery. *Gastroenterology* 2001; **121**: 1286-1293
- 29 **Incarbone R**, Bonavina L, Saino G, Bona D, Peracchia A. Outcome of esophageal adenocarcinoma detected during endoscopic biopsy surveillance for Barrett's esophagus. *Surg Endosc* 2002; **16**: 263-266
- 30 **Shaheen N**, Ransohoff DF. Gastroesophageal reflux, barrett esophagus, and esophageal cancer: scientific review. *JAMA* 2002; **287**: 1972-1981

# Silencing-specific methylation and single nucleotide polymorphism of *hMLH1* promoter in gastric carcinomas

Da-Jun Deng, Jin Zhou, Bu-Dong Zhu, Jia-Fu Ji, Jeffrey C. Harper, Steven M. Powell

**Da-Jun Deng, Jin Zhou, Bu-Dong Zhu, Jia-Fu Ji**, Peking University Health Science Center and Beijing Institute for Cancer Research, Beijing, 100034, China

**Jeffrey C. Harper, Steven M. Powell**, University of Virginia Health Science Center, Charlottesville, VA 22908-0708, USA

**Supported by** grant (2000-A-29) from Peking University Center for Human Disease Genomics, grant (0106) from Peking University Cancer Research Center, grant (3171045) from National Natural Science Foundation of China, and by NIH Grant CA67900

**Correspondence to:** Professor Da-Jun Deng, Department of Cancer Etiology, Peking University School of Oncology and BICR, Da-Hong-Luo-Chang Street, Western District, Beijing, 100034, China. dengdajun@sina.com

**Telephone:** +86-10-66162978 **Fax:** +86-10-66175832

**Received:** 2002-09-13 **Accepted:** 2002-10-18

## Abstract

**AIM:** To investigate CpG methylation and single nucleotide polymorphism (SNP) of a specific promoter region of *hMLH1* in primary gastric carcinoma.

**METHODS:** Primary gastric carcinomas ( $n=80$ ), their corresponding normal mucosal samples, and gastric mucosal biopsies from normal/gastritis control patients ( $n=54$ ) were used. Hypermethylation at -253 nt and -251 nt in relation with the translational start site and SNP of a silencing specific region (-339 nt-46 nt) in the *hMLH1* promoter were analyzed by *Bst* UI-combined bisulfite assay (COBRA), denaturing high performance liquid chromatogram (DHPLC), and sequencing.

**RESULTS:** (A) The specific methylation at -253 nt and -251 nt was observed in 2 of 60 primary gastric carcinomas, but neither in all of the corresponding mucosa nor in normal/gastritis samples, by *Bst* UI-COBA and DHPLC. (B) The *hMLH1* promoter was methylated homogeneously in the xenograft of the primary gastric carcinoma with the methylated and unmethylated *hMLH1*. (C) The pattern of SNP at -93 nt of the *hMLH1* promoter in 54 Chinese patients with gastric carcinoma was the same as that in the control patients: 51 % was A/G heteroalleles, 34 % and 15 % were A/A and G/G homoalleles, respectively.

**CONCLUSION:** Biallelic inactivation of *hMLH1* by epigenetic silencing existed in human primary gastric carcinoma homogeneously. Hypermethylation of *hMLH1* may play a role in the early stage of development of a few gastric carcinomas. The SNP at -93 nt is not related to the susceptibility of gastric carcinomas.

Deng DJ, Zhou J, Zhu BD, Ji JF, Harper JC, Powell SM. Silencing-specific methylation and single nucleotide polymorphism of *hMLH1* promoter in gastric carcinomas. *World J Gastroenterol* 2003; 9(1): 26-29

<http://www.wjgnet.com/1007-9327/9/26.htm>

## INTRODUCTION

Hypermethylation of CpG islands in upstream is an epigenetic

mechanism of lost of functions of tumor suppressor genes, DNA repair genes, *etc*<sup>[1-3]</sup>. The methylated *hMLH1* was observed in most of primary gastric carcinomas with the microsatellite instability-H phenotype (MSI-H)<sup>[4-12]</sup>. Silencing of *hMLH1* by CpG methylation may play an important role in the development of MSI-H tumors. However, the *hMLH1*-methylated proportions in MSI-L and MSI-stable sporadic gastric carcinoma varied greatly (0-75 %) in previous reports. Nakajima *et al.* reported that *hMLH1* methylation was detected in 8 of 100 primary gastric carcinoma cases, but not detected in their corresponding normal mucosa or in intestine metaplastic mucosa<sup>[13]</sup>. Kang *et al.* reported a much higher rate of *hMLH1* methylation in gastric carcinoma (20.3 %), adenoma (9.8 %), and intestine metaplastic mucosa (6.3 %)<sup>[14]</sup>. Different results might result from applications of both different markers used to classify MSI tumors, and different approaches or primers used to detect methylation of CpG island of *hMLH1*. It was reported recently that the methylation of CpGs in a small C-region (-270 nt ~ -199 nt) of the *hMLH1* promoter was invariably correlated with the absence of gene expression<sup>[15-17]</sup>. Thus, it is of interest to further explore the silencing specific methylation of the *hMLH1* promoter in primary gastric carcinomas. In the present study, we analyzed the silencing specific *hMLH1* methylation at -253 nt and -251 nt in the C-region in primary gastric carcinoma and normal/gastritis control.

Deng *et al.* established a novel approach to detect CpG methylation by denaturing high performance liquid chromatography (DHPLC)<sup>[18,19]</sup>, which was further developed to quantify CpG methylation and SNP of CpG islands simultaneously<sup>[20,21]</sup>. It was reported that there is a SNP at -93 nt of the *hMLH1* promoter<sup>[22]</sup>. In order to evaluate the possible role of the SNP in the gastric carcinogenesis, the pattern of the SNP in patients with gastric carcinoma was also compared with that in control patients without malignant diseases using DHPLC.

## MATERIALS AND METHODS

### Gastric samples

60 primary gastric carcinomas and their corresponding normal gastric mucosa were collected: 34 from the Beijing Institute for Cancer Research (BICR) surgically (28 males and 6 females, 29-59 years old, average age: 47.7 years old), and 26 from the University of Virginia Health System (Uva) (18 males and 8 females, 41-84 years old, the average age: 63.8 years old). Three Uva xenografted human GC were obtained from nude mice as described<sup>[23]</sup>. In addition, 56 biopsy samples of gastric epithelial tissues were collected from normal/gastritis patients at BICR (50 males and 4 female, 18-47 years old, the average age: 29.7 years old). All samples were used in the analysis of both methylation and SNP. Additional 18 corresponding normal gastric mucosal samples from BICR (Chinese patients, 13 males and 5 females, 26-78 years old, average age: 48.7 years old) with gastric carcinoma were used in SNP analysis in order to have the same number of cases as control. All clinical samples and histopathological information for each case were obtained according to approved institutional guidelines.



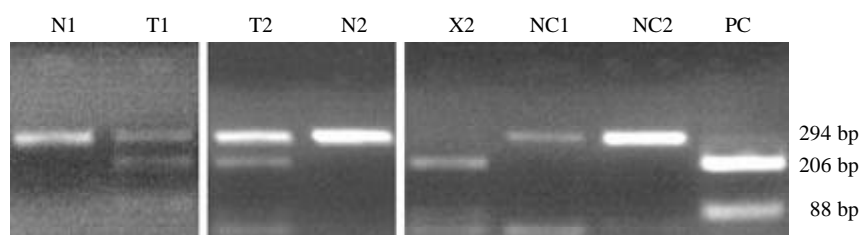


**Figure 1** Detection of *hMLH1* methylation by *Bst*UI-COBRA assay. PCR products and methylated ssPCR products (294 bp) were digested into two small fragments (206 bp and 88 bp). Unmethylated ssPCR products were not digested by *Bst*UI. T1, T2: primary gastric carcinomas; N1, N2: corresponding normal gastric mucosal samples; X2: xenograft of primary gastric carcinomas (T2) with *hMLH1* methylation; NC1, NC2: negative control xenografts of primary gastric carcinomas without *hMLH1* methylation; PC: PCR products of the *hMLH1* templates not treated by bisulfite

### DNA extraction and bisulfite modification

Genomic DNA of tissue samples was isolated with QIAGEN DNA Purification Kits. Two mg genomic DNA was treated with sodium bisulfite in order to convert the unmethylated C to U (T in PCR products) as described<sup>[24]</sup>.

### Design of Primers and PCR Conditions

Primers were designed according to the specific region (-339 nt ~ -46 nt in relation to the translational start site) of CpG islands of the sense strand of *hMLH1* (GenBank accession number U83845, gi: 2511457) as described<sup>[18, 20]</sup>. The strand-specific primers for the modified CpG islands included *hMLH1*-mF (5' -gtattttgtttttattgttgata-3') and *hMLH1*-mR (5' -aatacttcaaccaatcacctcaata-3'). Primers for the templates without bisulfite-treatment included *hMLH1*-wF (5' -gcattctctgctcctattggctggata-3') and *hMLH1*-wR (5' -agtgccttcagccaatcacctcagt-3'). Hot-started touchdown PCR (-1.0 °C per cycle, total 35 cycles) was used to amplify *hMLH1* without bisulfite-treatment (72 °C → 58 °C), and the sense strand templates with bisulfite-treatment (ssPCR, 65 °C → 50 °C for *hMLH1*)<sup>[18, 20]</sup>.

### Detection of CpG methylation by combined bisulfite restriction analysis (COBRA) and DHPLC

The specific region of the methylated CpG island contain a *Bst*UI restriction site (CGCG) that is converted to UGUG in the unmethylated CpG island after bisulfite modification. Hence the methylation of the bisulfite-modified *hMLH1* could be analyzed directly by *Bst*UI-COBRA. In the confirmation study, methylation status was detected further by DHPLC. Basic mechanism to detect methylation by DHPLC is that the retention time of the methylated PCR products is longer than that of the unmethylated ones, because of higher denaturing temperature of the methylated sequence resulted from higher G+C content after bisulfite modification<sup>[20]</sup>.

### Analysis for SNP by DHPLC and sequencing

The SNP at -93 nt in the corresponding normal mucosal samples and the gastric biopsies from the control patients was detected by DHPLC and confirmed by sequencing as described<sup>[20]</sup>. Because all control normal/gastritis samples were collected from Chinese patients, therefore only corresponding normal samples from Chinese cases with gastric carcinomas hospitalized in BICR were used in the SNP analysis.

## RESULTS AND DISCUSSION

### Silencing-specific methylation of *hMLH1* promoter

One *Bst*UI restriction site (CGCG) exists in the silencing-specific C-region of the CpG island that was invariably correlated with the absence of gene expression<sup>[15]</sup>. This site remains only in the methylated templates but not in the

unmethylated ones after bisulfite modification. Therefore, *Bst*UI-COBRA was used to detect the methylation of the specific region<sup>[18]</sup>. If the template is methylated, its ssPCR product (294 bp) is digested into a 206 bp and an 88 bp fragments. If not methylated, not digested. The specific CpG methylation of the *hMLH1* promoter was observed in only 3.3 % (2 of 60) of primary gastric carcinoma cases by this assay (Figure 1-T1, T2). T1 sample was distal adenocarcinoma (mod-poor differentiation) from BICR, and T2 was gastro-esoph junction adenocarcinoma (poor differentiation) from UVa. Such methylation was neither observed in all 60 corresponding normal gastric mucosa (Figure 1-N1, N2) nor in 54 normal/gastritis samples from the BICR control patients. The unmethylated *hMLH1* was detectable in all tested human samples (Figure 1-T1, T2, N1, N2). The same result was observed by DHPLC analysis (Figure 2-A, B).

The positive rate (3.3 %) of the specific CpG hypermethylation of *hMLH1* in the present study was lower than those reported by others. Nakajima *et al.* reported that *hMLH1* methylation was observed in 8 of 100 primary gastric carcinomas (8 %) by *Rsa*I-COBRA (restriction site GTAC)<sup>[13]</sup>. Although the specific C-region was also included in the ssPCR products in Nakajima's work, the *Rsa*I restriction site GTAC is at -76 nt in the D-region where the correlation between CpG methylation and gene expression is not as well as the C-region<sup>[15]</sup>. Kang *et al.* reported that *hMLH1* methylation was detected in 20.3 % of gastric carcinoma cases<sup>[14]</sup>. The possible reason for the higher positive rate might result from detection of CpG methylation in A-region of the *hMLH1* promoter that are methylated partially even in cells expressing *hMLH1*<sup>[15]</sup>. Another reason was that they used a very sensitive assay, methylation-specific PCR (MSP)<sup>[24]</sup>, which would result in a positive result even if 0.1 % of testing cells were methylated. Detection of methylation by *Bst*UI-COBRA used in the present study reflects the exact status of the *hMLH1* methylation in the testing samples. Therefore, the low methylation rate in the present study most likely represents the true state of these gastric cancers.

### Only the methylated *hMLH1* was detectable in the xenograft of primary gastric carcinoma

It was reported that bialleles of *hMLH1* were inactivated by CpG methylation in cell lines<sup>[25]</sup>. Unlike in cell lines, both the methylated and unmethylated *hMLH1* were observed in primary gastric carcinomas (Figure 1-T1, T2). In order to confirm that *hMLH1* is methylated homogeneously in malignant cells, we detected the status of *hMLH1* methylation in UVa xenografts originated from *hMLH1*-methylated and -unmethylated primary gastric carcinomas by *Bst*UI-COBRA. No *hMLH1* methylation was detected in two xenografts from two *hMLH1*-unmethylated primary gastric carcinoma (Figure 1-NC1, NC2). Only methylated *hMLH1* was observed in the X2 xenograft from primary gastric carcinoma T2, in which both the methylated and unmethylated *hMLH1* were observed

(Figure 1-X2, T2). This result was also confirmed by results of DHPLC (Figure 2-B). These results suggested that bialleles of *hMLH1* was methylated homogeneously in all of the malignant cells. The unmethylated *hMLH1* in T2 should come from normal cells such as fibrocytes, fibroblasts, and lymphocytes comprising the primary carcinoma. To best of our knowledge, this is the first report to describe the distribution of methylation status of CpG islands in primary carcinoma.

Thus, all of the malignant cells in the primary gastric cancer T2 appear originate from a single initiated cell with biallelic aberrant methylation of the *hMLH1* promoter. It is useful to study whether certain extent of methylation in the specific C-region of *hMLH1* CpG island is detectable in precancerous gastric lesions by sensitive assays such as MSP<sup>[24]</sup> and Methylight<sup>[26]</sup>. Taken together, the *hMLH1* methylation may play an important role in the initiation stage of a few gastric carcinomas. In addition to inactivation of *hMLH1* by germline defects<sup>[27-32]</sup>, silencing of *hMLH1* by CpG methylation is an alternative way to inactivate *hMLH1*.

**Table 1** Pattern of the SNP at -93 nt of the *hMLH1* promoter in patients with and without gastric carcinoma

Patients	n	G/G	A/G	A/A
Without gastric carcinoma	56	9(16.1%)	29(51.8%)	18(32.1%)
With gastric carcinoma	54	8(14.9%)	27(50.0%)	19(35.2%)
Total	110	17(15.5%)	56(50.9%)	37(33.6%)

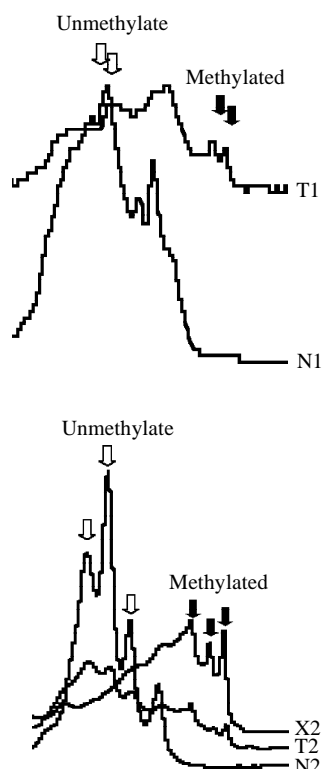


**Figure 2** DHPLC Chromatograms of the specific methylation of the *hMLH1* promoter ssPCR products were analyzed at partial denaturing temperature 54 °C, point mutation mode. T1 and T2, primary gastric carcinomas; N1 and N2, the corresponding normal gastric mucosal samples; X2, the xenograft of T2 in nude mouse

#### SNP at -93 of the *hMLH1* promoter is not correlated with gastric carcinoma

There is a SNP at -93 of the *hMLH1* promoter<sup>[22]</sup>, which is located within the D-region tested in the present study. In order

to evaluate the correlation of the SNP with risk of gastric cancer, we compared the pattern of the SNP in 54 Chinese patients with gastric carcinoma with that in 56 Chinese control patients through DHPLC and sequencing. Similar percentages of homoalleles (G/G and A/A) and heteroalleles (A/G) were observed in samples from both groups (Table 1). The result suggested that this SNP was not correlated with the risk of gastric carcinoma. Similar result was observed in hereditary nonpolyposis colorectal cancer (HNPCC) and non-HNPCC populations<sup>[22]</sup>.

#### REFERENCES

- Bird A. DNA methylation de Novo. *Science* 1999; **286**: 2287-2288.
- Jones PA, Laird PW. Cancer epigenetics comes of age. *Nature Genet* 1999; **21**: 163-167
- Yakoob J, Fan XG, Hu GL, Zhang Z. DNA methylation and carcinogenesis in digestive neoplasms. *World J Gastroenterol* 1998; **4**: 174-177
- Leung SY, Yuen ST, Chung LP, Chu KM, Chan AS, Ho JC. *hMLH1* promoter methylation and lack of *hMLH1* expression in sporadic gastric carcinomas with high-frequency microsatellite instability. *Cancer Res* 1999; **59**: 159-164
- Fleisher AS, Esteller M, Wang S, Tamura G, Suzuki H, Yin J, Zou TT, Abraham JM, Kong D, Smolinski KN, Shi YQ, Rhyu MG, Powell SM, James SP, Wilson KT, Herman JG, Meltzer SJ. Hypermethylation of the *hMLH1* gene promoter in human gastric cancers with microsatellite instability. *Cancer Res* 1999; **59**: 1090-1095
- Kang GH, Shim YH, Ro JY. Correlation of methylation of the *hMLH1* promoter with lack of expression of *hMLH1* in sporadic gastric carcinomas with replication error. *Lab Invest* 1999; **79**: 903-909
- Bevilacqua RA, Simpson AJ. Methylation of the *hMLH1* promoter but no *hMLH1* mutations in sporadic gastric carcinomas with high-level microsatellite instability. *Int J Cancer* 2000; **87**: 200-203
- Pinto M, Oliveira C, Machado JC, Cirnes L, Tavares J, Carneiro F, Hamelin R, Hofstra R, Seruca R, Sobrinho-Simoes M. MSI-L gastric carcinomas share the *hMLH1* methylation status of MSI-H carcinomas but not their clinicopathological profile. *Lab Invest* 2000; **80**: 1915-1923
- Jung HY, Jung KC, Shim YH, Ro JY, Kang GH. Methylation of the *hMLH1* promoter in multiple gastric carcinomas with microsatellite instability. *Pathol Int* 2001; **51**: 445-451
- Sakata K, Tamura G, Endoh Y, Ohmura K, Ogata S, Motoyama T. Hypermethylation of the *hMLH1* gene promoter in solitary and multiple gastric cancers with microsatellite instability. *Br J Cancer* 2002; **86**: 564-567
- Oue N, Sentani K, Yokozaki H, Kitadai Y, Ito R, Yasui W. Promoter methylation status of the DNA repair genes *hMLH1* and *MGMT* in gastric carcinoma and metaplastic mucosa. *Pathobiology* 2001; **69**: 143-149
- Baek MJ, Kang H, Kim SE, Park JH, Lee JS, Paik YK, Kim H. Expression of *hMLH1* is inactivated in the gastric adenomas with enhanced microsatellite instability. *Br J Cancer* 2001; **85**: 1147-1152
- Nakajima T, Akiyama Y, Shiraishi J, Arai T, Yanagisawa Y, Ara M, Fukuda Y, Sawabe M, Saitoh K, Kamiyama R, Hirokawa K, Yuasa Y. Age-related hypermethylation of the *hMLH1* promoter in gastric cancers. *Int J Cancer* 2001; **94**: 208-211
- Kang GH, Shim YH, Jung HY, Kim WH, Ro JY, Rhyu MG. CpG island methylation in premalignant stages of gastric carcinoma. *Cancer Res* 2001; **61**: 2847-2851
- Deng G, Chen A, Hong J, Chae HS, Kim YS. Methylation of CpG in a small region of the *hMLH1* promoter invariably correlates with the absence of gene expression. *Cancer Res* 1999; **59**: 2029-2033
- Deng G, Peng E, Gum J, Terdiman J, Sleisenger M, Kim YS. Methylation of *hMLH1* promoter correlates with the gene silencing with a region-specific manner in colorectal cancer. *Br J Cancer* 2002; **86**: 574-579
- Kang YH, Bae SI, Kim WH. Comprehensive analysis of promoter methylation and altered expression of *hMLH1* in gastric cancer cell lines with microsatellite instability. *J Cancer Res Clin Oncol* 2002; **128**: 119-124

- 18 **Deng DJ**, Deng GR, Zhou J, Xin HJ. Detection of CpG methylations in human mismatch repair gene *hMLH1* promoter by denaturing high-performance liquid chromatography (DHPLC). *Chin J Cancer Res* 2000; **12**: 171-191
- 19 **Deng D**, Deng G, Lu Y. Analysis of the methylation in CpG island by denaturing high-performance liquid chromatography. *Zhonghua Yixue Zazhi* 2001; **81**: 158-161
- 20 **Deng D**, Deng G, Smith MF, Zhou J, Xin H, Powell SM, Lu Y. Simultaneous detection of CpG methylation and single nucleotide polymorphism by denaturing high performance liquid chromatography. *Nucleic Acids Res* 2002; **30**: e13
- 21 **Deng D**, El-Rifai W, Jil J, Zhu B, Trampont P, Li J, Smith MF, Powell SM. Hypermethylation of Metallothionein-3 CpG island in gastric carcinoma. *Carcinogenesis* 2003; **24**: in press
- 22 **Ito E**, Yanagisawa Y, Iwahashi Y, Suzuki Y, Nagasaki H, Akiyama Y, Sugano S, Yuasa Y, Maruyama K. A core promoter and a frequent single-nucleotide polymorphism of the mismatch repair gene *hMLH1*. *Biochem Biophys Res Commun* 1999; **256**: 488-494
- 23 **El-Rifai W**, Frierson HF, Harper JC, Powell SM, Knuutila S. Expression profiling of gastric adenocarcinoma using cDNA array. *Int J Cancer* 2001; **92**: 832-838
- 24 **Herman JG**, Graff JR, Myöhänen S, Nelkin BD, Baylin SB. Methylation-specific PCR: A novel PCR assay for methylation status of CpG islands. *Proc Natl Acad Sci USA* 1996; **93**: 9821-9826
- 25 **Veigl ML**, Kasturi L, Olechnowicz J, Ma AH, Lutterbaugh JD, Periyasamy S, Li GM, Drummond J, Modrich PL, Sedwick WD, Markowitz SD. Biallelic inactivation of *hMLH1* by epigenetic gene silencing, a novel mechanism causing human MSI cancers. *Proc Natl Acad Sci USA* 1998; **95**: 8698-8702
- 26 **Eads CA**, Danenberg KD, Kawakami K, Saltz LB, Blake C, Shibata D, Danenberg PV, Laird PW. MethyLight: a high-throughput assay to measure DNA methylation. *Nucleic Acids Res* 2000; **28**: e32
- 27 **Leach FS**, Nicolaides NC, Papadopoulos N, Liu B, Jen J, Parsons R, Peltomaki P, Sistonen P, Aaltonen LA, Nystrom-Lahti M. Mutations of a *mutS* homolog in hereditary nonpolyposis colorectal cancer. *Cell* 1993; **75**: 1215-1225
- 28 **Kinzler KW**, Vogelstein B. Lessons from hereditary colorectal cancer. *Cell* 1996; **87**: 159-170
- 29 **Eshleman JR**, Markowitz SD. Microsatellite instability in inherited and sporadic neoplasms. *Curr Opin Oncol* 1995; **7**: 83-89
- 30 **Marra G**, Boland CR. Hereditary nonpolyposis colorectal cancer: the syndrome, the genes, and historical perspectives. *J Natl Cancer Inst* 1995; **87**: 1114-1125
- 31 **Zhao B**, Wang ZJ, Xu YF, Wan YL, Li P, Huang YT. Report of 16 kindreds and one kindred with *hMLH1* germline mutation. *World J Gastroenterol* 2002; **8**: 263-266
- 32 **Cai Q**, Sun MH, Lu HF, Zhang TM, Mo SJ, Xu Y, Cai SJ, Zhu XZ, Shi DR. Clinicopathological and molecular genetic analysis of 4 typical Chinese HNPCC families. *World J Gastroenterol* 2001; **7**: 805-810

Edited by Xu XQ

# A novel gene, GCRG224, is differentially expressed in human gastric mucosa

Gang-Shi Wang, Meng-Wei Wang, Ben-Yan Wu, Wei-Di You, Xin-Yan Yang

**Gang-Shi Wang, Meng-Wei Wang, Ben-Yan Wu, Wei-Di You, Xin-Yan Yang**, Department of Gastroenterology, General Hospital of Chinese PLA, Beijing 100853, China

**Supported by** Key project grant in medical sciences from the tenth five-year plan of Chinese PLA; Contract Grant number: 01Z035

**Correspondence to:** Gang-Shi Wang, MD., Ph.D., Department of Gerontal Gastroenterology, General Hospital of Chinese PLA, Beijing 100853, China. wanggangshi@hotmail.com

**Telephone:** +86-10-66937393

**Received:** 2002-03-25 **Accepted:** 2002-04-20

## Abstract

**AIM:** To clone genes that may predispose us to human gastric cancer and to analyze its expression in gastric tissues.

**METHODS:** Specimens of paired tumor, paratumor and normal gastric mucosa tissues collected from fifteen patients who suffered from stomach antrum adenocarcinoma were used for analysis. Seven out of the fifteen cases were first studied by fluorescent differential display reverse transcription polymerase chain reaction (DDTR-PCR) analysis. The differentially expressed bands of interest were cloned, analyzed by Northern blot, sequencing and RT-PCR. Through BLAST, the sequencing results were compared with GenBank database for homology analysis. *In situ* hybridization with DIG-labeled cRNA probes was used to analyze the expression of interesting cDNA bands in paraffin embedded paired normal gastric mucosa and cancer tissues isolated from 30 gastric adenocarcinoma patients.

**RESULTS:** DDRT-PCR showed that one of the interesting cDNA bands, which was named W2, expressed much higher in all seven tested tumor and paratumor samples than in their normal counterparts, it was sub-cloned into a pGEM-T Easy vector. Two subclones were subsequently obtained. One of the subclone, GCRG224, was studied further. The sequencing result showed that GCRG224 consisted of 1 159 base pairs and had one open reading frame (ORF). It located at human chromosome 11q14. No homologue was found in GenBank database with GCRG224-ORF. This nucleotide sequence data were submitted to GenBank with accession No. AF438406. RT-PCR showed that GCRG224 expressed higher in 11/15 gastric cancer tissues than in non-tumor tissues. However, the result of Northern blot analysis showed a higher GCRG224 expression in the non-tumor tissue than in the tumor one. Human multiple tissue Northern blot analysis revealed that GCRG224 also expressed in human normal colon tissue, and peripheral blood leukocyte. *In situ* hybridization analysis showed that only 5/30 adenocarcinoma, 3/18 dysplasia and 6/18 intestinal metaplasia showed higher GCRG224 expression level than the normal gastric glands. However, GCRG224 was over-expressed predominantly in 26/30 cases of normal mucosal epithelium.

**CONCLUSION:** A novel gene named GCRG224 was identified from human gastric mucosal tissue. It

overexpressed in almost all gastric mucosal epithelium but only a small portion of cancer and precancerous lesions. The role of GCRG224 expression in gastric epithelium needs further study.

Wang GS, Wang MW, Wu BY, You WD, Yang XY. A novel gene, GCRG224, is differentially expressed in human gastric mucosa. *World J Gastroenterol* 2003; 9(1): 30-34

<http://www.wjgnet.com/1007-9327/9/30.htm>

## INTRODUCTION

Gastric cancer is one of the most commonly diagnosed malignancies and remains an important cause of mortality world wide<sup>[1]</sup>. Considerable evidence supports the pivotal role of genetic factors in the pathogenesis of gastric cancer<sup>[2-7]</sup>. However, the mechanism of the process of multistage carcinogenesis is still unknown for gastric cancer. Abundant clinical and histopathological data suggest that most, if not all, intestinal-type gastric cancer arise from precancerous lesions, which indicated intestinal-type gastric cancer to be an excellent model for studying the genetic alterations involved in the development of human neoplasms. It would be desirable, therefore, to screen directly from human intestinal-type gastric cancer and its precursor lesions the differentially expressed genes that are closely related to human gastric cancer.

In this study, differential display reverse transcription polymerase chain reaction (DDRT-PCR) analysis was used to identify and characterize differentially expressed genes in human gastric cancer tissues in comparison with their surrounding paratumor and nontumor counterparts. One novel cDNA with a complete cds was identified. We designated this gene as gastric cancer related gene 224 (GCRG224). Expression of GCRG224 in gastric tissues was analyzed using RT-PCR and *In situ* hybridization (ISH).

## MATERIALS AND METHODS

### Tissue acquisition

Fresh primary intestinal-type gastric adenocarcinoma, paratumor tissue which is 1.0 cm away from the tumor mass and their surrounding noncancerous stomach mucosal tissues obtained from 15 patients (11 male, 4 female, with average age 54±15 years) undergoing surgery were used for reverse transcription polymerase chain reaction (RT-PCR) analysis. 7 cases (4 male, 3 female, with average age 51±18 years) out of the 15 patients were used for differential display analyses. Paraffin embedded gastric adenocarcinoma and their corresponding normal gastric mucosal tissues obtained from 30 advanced gastric adenocarcinoma patients (21 male, 9 female, with average age 59±10 years) were used for ISH analysis. All tissues were histologically confirmed by pathologists.

### RNA preparation and differential display

Total RNA was extracted from tissues using TRIzol reagent (Life Technologies, Inc., Rockville, Maryland). The fluorescent

DDRT-PCR procedure was performed essentially as described previously<sup>[8]</sup>. The primers used in the assay included 4 T<sub>12</sub>MN primers and 20 arbitrary oligonucleotide primers (ARP-1 to ARP-20) (Genomix Corporation, Foster City, CA).

### Cloning and sequencing

The cDNA fragment of interest were subcloned into pGEM-T Easy vector (Promega Corporation, Madison, WI) and confirmed by EcoR I (Life Technologies, Bethesda, MD) digestion according to the manufacturer's instruction. Sequence analysis was performed with CEQ<sup>TM</sup> 2000 DNA sequencer (Beckman Coulter, Fullerton, CA). The sequenced cDNA were analyzed via the BLAST program for homology matches in the GenBank database<sup>[9]</sup>.

### Northern blot analysis

Samples containing 20 µg of total nontumor and tumor RNAs were fractionated on an 1.2 % agarose gel containing 5.5 % formaldehyde and 1×MOPS and transferred to a nylon membrane. Fix the RNA to the membrane by baking at 80 °C for 2 hours. Human multiple tissue Northern (MTN) blot II membrane (Clontech Laboratories, Inc., Palo Alto, CA) was used for analysis. Anti-sense cRNA probe labeled with digoxigenin was generated from a digested cDNA insert using Dig Northern Starter Kit (Roche Diagnostic Corporation, Indianapolis, IN) by means of *in vitro* transcription. The membrane was prehybridized and then hybridized according to the manufacturer's protocol. The results were detected using chemiluminescent detection.

### RT-PCR

First-strand cDNAs were synthesized by SuperscriptII Rnase H<sup>-</sup> reverse transcriptase (Life Technologies, Bethesda, MD) using oligo d(T) primers according to the protocol. PCR primers were designed using Primer Premier software (Premier biosoft international, Palo Alto, CA). The PCR primers used were: forward primer: 5' AAGGGTCACCTCTGTTCAAAGTG3', reverse primer: 5' GCAGGGTTTATGGGCTCAATAG3', Product length: 929 bp. G3PDH was used as internal control. Reactions were carried out in 10 µl solutions containing 100 ng cDNA, 0.2 µM of each primer, 50 µM of each dNTP, and 0.5 U of AmpliTaq DNA polymerase (Life Technologies, Bethesda, MD). The amplification conditions were (25 cycles): 1 min at 94 °C, 40 sec at 56 °C, 1 min at 72 °C.

### In situ hybridization

Specimens were fixed in 10 % neutral buffered formalin and embedded in paraffin wax. A series of 5 µm sections were cut for analysis. The antisense cRNA probe was prepared according to procedure described in Northern blot analysis section. ISH was performed as described previously<sup>[10,11]</sup>. Negative control (no probe applied) was performed. Slides were examined using an Olympus microscope. Images were captured using a cooled CCD camera (JVC, Japan). Cytoplasmic staining was noted.

Any appreciable blue staining was considered positive, and graded as ± if very light blue were barely detectable, 1+ if light blue staining were seen diffusely throughout the cytoplasm, 2+ if easily seen fine staining were present throughout the cytoplasm, and 3+ when dark blue were observed. Generally, more than 100 cells (nontumor or tumor) were quantified in each measurement and at least one measurement was taken per slide. H&E slides were then reviewed to determine diagnosis and to map the location of the various histological patterns and correlate with the staining patterns observed in the ISH preparations.

### Informed consents

The study protocol was approved by the Institutional Review Board of the hospital under the guidelines of the 1975 Declaration of Helsinki. Written informed consents were obtained from patients.

## RESULTS

### Isolation of differentially expressed cDNA by DDRT-PCR in gastric cancer

In order to run the assay efficiently, among 80 combinations of primer pairs (4 T<sub>12</sub>MN primers vs 20 ARP primers), 4 pairs able to amplify more bands in one set of paired tissues were chosen and used to amplify cDNA from 7 sets of paired tissues. One primer pair (T<sub>12</sub>GG vs ARP-3: 5' GACCATTGCA3') was found to amplify genes expressed differentially in 7 of 7 sets of the paired tissues. As shown in Figure 1, in comparison with results in the normal tissues, a cDNA fragment (arrowed) was found to be more abundant in the tumor and paratumor samples in all tested patients. The results of mRNA differential display were reproducible. This differentially expressed cDNA band was named as W2.

### Sub-clone and sequence analysis

Two subclones, GCRG213 and GCRG224, were identified from the subcloning procedure. GCRG213 consisted of 1 194 base pairs, while GCRG224 consisted of 1 159 base pairs and had one open reading frame (ORF). The GCRG224-ORF consists of 35 amino acids with an estimated molecular weight of 3.8 kDa. BLAST analysis revealed that GCRG224 nucleotide sequence had 98 % homologue with Homo sapiens clone RP11-718B12, but the deduced amino acid sequence of GCRG224-ORF had no homology with any known peptide in the GenBank database. GCRG224 nucleotide sequence data was submitted to GenBank with accession No.AF438406. Further bioinformatic study in the GenBank database showed that GCRG224 is located at human chromosome 11q14.

### RT-PCR and northern blot analysis

To confirm the expression pattern of GCRG224 in human gastric cancer, we performed RT-PCR analyses in 15 cases of paired gastric adenocarcinoma, paratumor and non-tumor

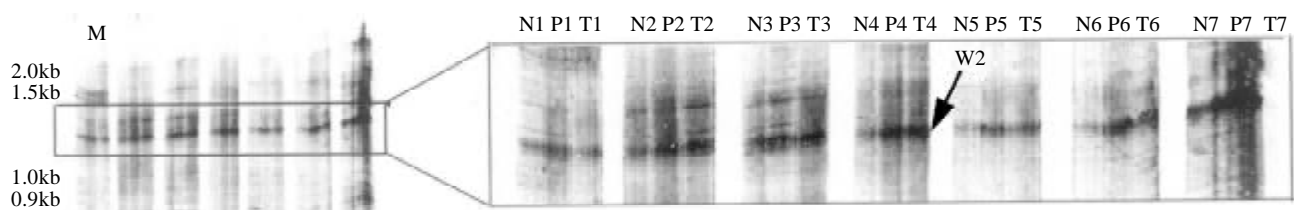


**Figure 1** Differential analysis of expressed genes among human gastric cancer, paratumor and normal stomach mucosal tissues by means of fluorescent differential display. The differentially expressed cDNA fragment W2 (arrowed) showed higher expression in tumor and paratumor tissues than that in normal ones. N: normal; P: paratumor; T: tumor; 1-7: patient number.



tissues. GCRG224 expressed higher in 11/15 gastric cancer tissues than non-tumor tissues. However, the result of Northern blot analysis was contrary to that of DDRT-PCR, the non-tumor tissue showed higher GCRG224 expression level than the tumor did (Figure 2a). MTN results showed that GCRG224 also expressed in human normal colon tissues and peripheral blood leukocyte (Figure 2b).

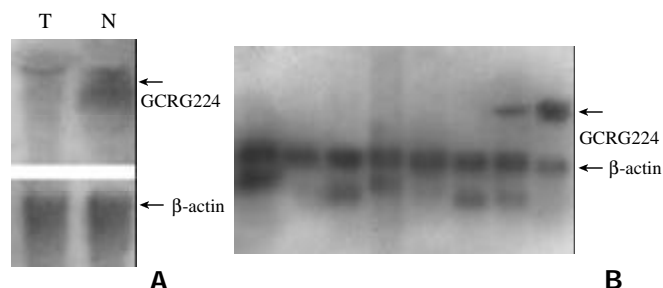


**Figure 2** Northern blot analysis of GCRG224 expression in (a) human gastric cancer T/N pairs. T: tumor, N: non-tumor. (b) various adult human tissues. From left to right: spleen, thymus, prostate, testis, ovary, small intestine, colon, peripheral blood leukocyte.

#### *In situ hybridization*

GCRG224 expression was analyzed at mRNA level. The hybridization signal that appears as blue is restricted to the cytoplasmic portion. All normal gastric glands showed  $\pm$ 1+ staining. Only 5 out of 30 cases of adenocarcinoma had 2+ staining while the rest had  $\pm$ staining. Of the 18 cases of intestinal metaplasia (IM) and dysplasia found in the paratumor site, 6/18 IM and 3/18 dysplasia had 2+ staining, respectively. Interestingly, in 26/30 cases the gastric mucosal epithelial cells were stained 2++3+ (Table 1, Figure 3).

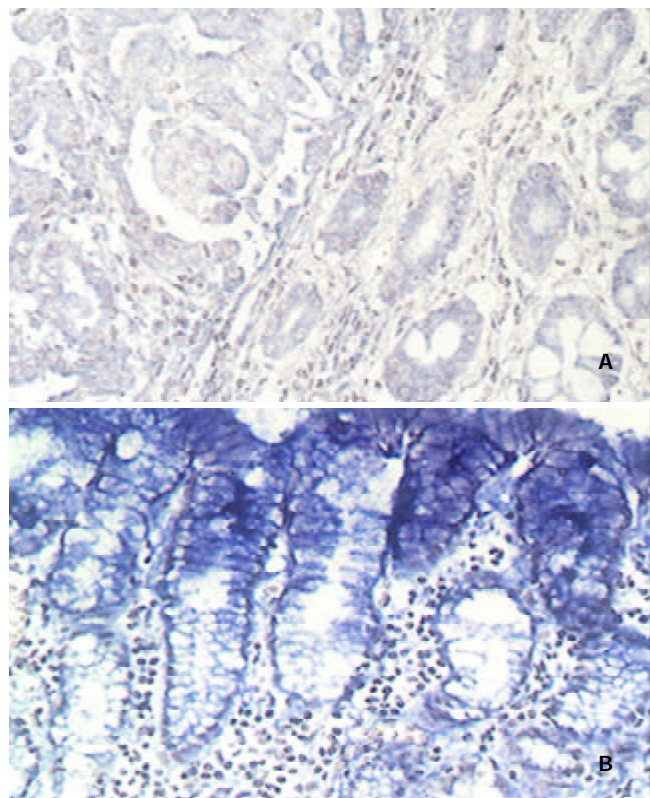


**Figure 3** ISH analysis of GCRG224-ORF mRNA in formaldehyde-fixed, paraffin-embedded gastric tissues with a digoxigenin-labeled anti-sense probe, NBT/BCIP was used as

alkaline phosphatase substrates, the expression appeared as cytoplasmic staining (blue precipitates). (a): Mild expression in tumor (left) and intestinal metaplasia glands (right) (200 $\times$ ); (b): Strong expression in gastric mucosal epithelium cells, while the adjacent normal gastric glands showed little staining (200 $\times$ ).

**Table 1** GCRG224 expression in different types of cells in gastric mucosa

	gastric mucosal epithelium	Gastric glands	IM	DYS	adenocarcinoma
$\pm$	0	19	8	13	25
1+	4	11	4	2	0
2+	15	0	6	3	4
3+	11	0	0	0	1
Total	30	30	18	18	30

#### DISCUSSION

Advances in molecular biology have revealed a consistent set of genetic alterations that may correspond to multi-step stomach cancer development. Aberrant expression and amplification of oncogenes such as c-met, c-myc, K-ras, c-erbB-2<sup>[12-16]</sup>, etc., inactivation of tumor suppressor genes such as p53, p16, Rb, DCC, APC, PTEN<sup>[17-24]</sup>, etc, DNA ploidy and microsatellite instability<sup>[25-28]</sup>, abnormal transcript of genes related to metastasis like nm23, CD44, E-cadherin<sup>[29,30]</sup>, etc., are reported common events in the steps of carcinogenesis. Newly found cancer related genes such as COX-2, survivin, metallothionein II and RUNX3, etc. were also expressed abnormally in gastric cancer<sup>[31-38]</sup>. Recognition of genetic factors had also improved the the treatment of cancer<sup>[39-41]</sup>. However, very little is currently known about genes that may predispose us to gastric cancer. The primary aim of this study was to identify genes that were closely related to human gastric cancer by means of DDRT-PCR.

DDRT-PCR has been widely applied to identify cancer-related genes<sup>[42-47]</sup>, some of these genes look like to be of clinical value. It might reflect the true patterns of genetic changes in human gastric cancer if we identify gastric cancer-related genes directly from human gastric tissues.

One of the defects when using tissues for DDRT-PCR analysis is that some cDNA fragments amplified in the tumor tissues may actually originate from normal cells present in the tumor tissues, which may affect the results of the analyses. In order to decrease the chance of error in this study, we used 7 sets of tumor, paratumor and non-tumor tissues for the assay, displayed the results simultaneously and chose interesting bands showing distinctive patterns in all sets of specimens. One cDNA fragment which is up-regulated in gastric cancer tissues was identified. However, two subclones were identified from the subsequent subcloning procedure. Sequencing results revealed that these two subclones contained nucleotides of nearly the same size but of totally different sequences. This should be the result of PCR amplification in which arbitrary primers were used.

Because the deduced amino acid sequence of GCRG224-ORF had no homology with any known peptide in the GenBank database, further study was focused on this gene. The result of RT-PCR analysis was consistent with that of DDRT-PCR, but Northern blot analysis revealed an opposite result. Furthermore, ISH analysis also failed to see a general higher expression of GCRG224 in tumor cells. On the other hand, ISH showed an extensively strong expression of GCRG224 in gastric mucosal epithelial cells in almost all tested cases. This indicated GCRG224 might come mainly from normal gastric epithelium

other than tumor cells. Although the tissues applied for DDRT-PCR, Northern blot and RT-PCR in this study were examined by pathologists before their usage, they were actually a mixture of different types of cells, the exact percentage of tumor and non-tumor cells in each tissue could not be identified, this resulted in the contradiction we faced. It would be better, therefore, to separate different types of cells using techniques such as microdissection in tissues like gastric mucosa prior to the analyses<sup>[48-51]</sup>.

Correlations between prognoses and the expression of genes such as p53, ras, myc, nm23, etc. were studied extensively in gastric cancer<sup>[15-17,52-57]</sup>. However, the results turned out to be controversial. It is meaningful to find a biomarker that might predict the diagnosis or prognosis of gastric cancer. The consistent over-expression of GCRG224 in all tested tumor tissues in the DDRT-PCR and RT-PCR analyses prompted us to study further the expression pattern of GCRG224 in gastric mucosal tissues using ISH. However, GCRG224 did not show the expression pattern in gastric cancer and its precancerous lesions as RT-PCR revealed. Only around 20 percent tumor and precancerous lesions showed GCRG224 over-expression comparing with their normal gastric glands. Thus, GCRG224 may not serve as a potential marker for the diagnosis of gastric cancer.

A significant finding in this study is the extensive staining of GCRG224 in gastric epithelium. Up till now, the function of gastric mucosal cells is believed to be a barrier of the stomach as well as secretion of alkali and other ions such as Na<sup>+</sup>, K<sup>+</sup> and Cl<sup>-</sup>. It will be of great interest to study the role of GCRG224 expression in gastric mucosal epithelium.

## REFERENCES

- 1 **Stadlander CT**, Waterbor JW. Molecular epidemiology, pathogenesis and prevention of gastric cancer. *Carcinogenesis* 1999; **20**: 2195-2208
- 2 **Becker KF**, Keller G, Hoefler H. The use of molecular biology in diagnosis and prognosis of gastric cancer. *Surg Oncol* 2000; **9**: 5-11
- 3 **Boussioutas A**, Taupin D. Towards a molecular approach to gastric cancer management. *Intern Med J* 2001; **31**: 296-303
- 4 **Palli D**. Epidemiology of gastric cancer: an evaluation of available evidence. *J Gastroenterol* 2000; **35**(Suppl 12): 84-89
- 5 **Yasui W**, Oue N, Kuniyasu H, Ito R, Tahara E, Yokozaki H. Molecular diagnosis of gastric cancer: present and future. *Gastric Cancer* 2001; **4**: 113-121
- 6 **Maltoni M**, Volpi A, Nanni O, Bajorko P, Belletti E, Vecchi AM, Liverani M, Danesi S, Calistri D, Ricotti L, Amadori D. Gastric cancer: epidemiologic and biological aspects. *Forum (Genova)* 1998; **8**: 199-207
- 7 **Meltzer SJ**. Tumor genomics vs. tumor genetics: a paradigm shift? *Gastroenterology* 2001; **121**: 726-729
- 8 **Wang GS**, Wang MW, You WD, Wang HF, Feng MF. Fluorescent mRNA differential display technique. *Zhongguo Yingyong Shenglixue Zazhi* 2000; **16**: 373-376
- 9 **Altschul SF**, Madden TL, Schäffer AA, Zhang J, Zhang Z, Miller W, Lipman DJ. Gapped BLAST and PSI-BLAST: a new generation of protein database search programs. *Nucleic Acids Res* 1997; **25**: 3389-3402
- 10 **Komminoth P**, Merk FB, Leav I, Wolfe HJ, Roth J. Comparison of 35S- and digoxigenin-labeled RNA and oligonucleotide probes for *In situ* hybridization. Expression of mRNA of the seminal vesicle secretion protein II and androgen receptor genes in the rat prostate. *Histochemistry* 1992; **98**: 217-228
- 11 **Komminoth P**. Digoxigenin as an alternative probe labeling for *In situ* hybridization. *Diagn Mol Pathol* 1992; **1**: 142-150
- 12 **Kubicka S**, Claas C, Staab S, Kuhnelt F, Zender L, Trautwein C, Wagner S, Rudolph KL, Manns M. p53 mutation pattern and expression of c-erbB2 and c-met in gastric cancer: relation to histological subtypes, *Helicobacter pylori* infection, and prognosis. *Dig Dis Sci* 2002; **47**: 114-121
- 13 **Hiyama T**, Haruma K, Kitadai Y, Masuda H, Miyamoto M, Tanaka S, Yoshihara M, Shimamoto F, Chayama K. K-ras mutation in *Helicobacter pylori*-associated chronic gastritis in patients with and without gastric cancer. *Int J Cancer* 2002; **97**: 562-566
- 14 **Yokozaki H**, Yasui W, Tahara E. Genetic and epigenetic changes in stomach cancer. *Int Rev Cytol* 2001; **204**: 49-95
- 15 **Nakajima M**, Sawada H, Yamada Y, Watanabe A, Tatsumi M, Yamashita J, Matsuda M, Sakaguchi T, Hirao T, Nakano H. The prognostic significance of amplification and overexpression of c-met and c-erbB-2 in human gastric carcinomas. *Cancer* 1999; **85**: 1894-1902
- 16 **Gurel S**, Dolar E, Yerci O, Samli B, Ozturk H, Nak SG, Gulten M, Memik F. The relationship between c-erbB-2 oncogene expression and clinicopathological factors in gastric cancer. *J Int Med Res* 1999; **27**: 74-78
- 17 **Gurel S**, Dolar E, Yerci O, Samli B, Ozturk H, Nak SG, Gulten M, Memik F. Expression of p53 protein and prognosis in gastric carcinoma. *J Int Med Res* 1999; **27**: 85-89
- 18 **Sato K**, Tamura G, Tsuchiya T, Endoh Y, Usuba O, Kimura W, Motoyama T. Frequent loss of expression without sequence mutations of the DCC gene in primary gastric cancer. *Br J Cancer* 2001; **85**: 199-203
- 19 **He XS**, Su Q, Chen ZC, He XT, Long ZF, Ling H, Zhang LR. Expression, deletion and mutation of p16 gene in human gastric cancer. *World J Gastroenterol* 2001; **7**: 515-521
- 20 **Liu DH**, Zhang XY, Fan DM, Huang YX, Zhang JS, Huang WQ, Zhang YQ, Huang QS, Ma WY, Chai YB, Jin M. Expression of vascular endothelial growth factor and its role in oncogenesis of human gastric carcinoma. *World J Gastroenterol* 2001; **7**: 500-505
- 21 **Liu XP**, Tsushimi K, Tsushimi M, Kawauchi S, Oga A, Furuya T, Sasaki K. Expression of p21(WAF1/CIP1) and p53 proteins in gastric carcinoma: its relationships with cell proliferation activity and prognosis. *Cancer Lett* 2001; **170**: 183-189
- 22 **Fei G**, Ebert MP, Mawrin C, Leodolter A, Schmidt N, Dietzmann K, Malfertheiner P. Reduced PTEN expression in gastric cancer and in the gastric mucosa of gastric cancer relatives. *Eur J Gastroenterol Hepatol* 2002; **14**: 297-303
- 23 **Kang YH**, Lee HS, Kim WH. Promoter methylation and silencing of PTEN in gastric carcinoma. *Lab Invest* 2002; **82**: 285-291
- 24 **Ebert MP**, Fei G, Kahmann S, Muller O, Yu J, Sung JJ, Malfertheiner P. Increased beta-catenin mRNA levels and mutational alterations of the APC and beta-catenin gene are present in intestinal-type gastric cancer. *Carcinogenesis* 2002; **23**: 87-91
- 25 **Laghi L**, Ranzani GN, Bianchi P, Mori A, Heinemann K, Orbetegli O, Spauldo MR, Luinetti O, Franciscani S, Roncalli M, Solcia E, Malesci A. Frameshift mutations of human gastrin receptor gene (hGARE) in gastrointestinal cancers with microsatellite instability. *Lab Invest* 2002; **82**: 265-271
- 26 **Sakata K**, Tamura G, Endoh Y, Ohmura K, Ogata S, Motoyama T. Hypermethylation of the hMLH1 gene promoter in solitary and multiple gastric cancers with microsatellite instability. *Br J Cancer* 2002; **86**: 564-567
- 27 **Baba H**, Korenaga D, Kakeji Y, Haraguchi M, Okamura T, Maehara Y. DNA ploidy and its clinical implications in gastric cancer. *Surgery* 2002; **131** (Suppl): S63-70
- 28 **Russo A**, Bazan V, Migliavacca M, Tubiolo C, Macaluso M, Zanna I, Corsale S, Latteri F, Valerio MR, Pantuso G, Morello V, Dardanoni G, Latteri MA, Colucci G, Tomasino RM, Gebbia N. DNA aneuploidy and high proliferative activity but not K-ras-2 mutations as independent predictors of clinical outcome in operable gastric carcinoma: results of a 5-year gruppo oncologico dell'italia meridionale prospective study. *Cancer* 2001; **92**: 294-302
- 29 **Nesi G**, Palli D, Pernice LM, Saieva C, Paglierani M, Kroning KC, Catarzi S, Rubio CA, Amorosi A. Expression of nm23 gene in gastric cancer is associated with a poor 5-year survival. *Anti-cancer Res* 2001; **21**: 3643-3649
- 30 **Cai J**, Ikeguchi M, Tsujitani S, Maeta M, Liu J, Kaibara N. Significant correlation between micrometastasis in the lymph nodes and reduced expression of E-cadherin in early gastric cancer. *Gastric Cancer* 2001; **4**: 66-74
- 31 **van Rees BP**, Saukkonen K, Ristimäki A, Polkowski W, Tytgat GN, Drilenburg P, Offerhaus GJ. Cyclooxygenase-2 expression during carcinogenesis in the human stomach. *J Pathol* 2002; **196**: 171-179
- 32 **Kikuchi T**, Itoh F, Toyota M, Suzuki H, Yamamoto H, Fujita M, Hosokawa M, Imai K. Aberrant methylation and histone deacetylation of cyclooxygenase 2 in gastric cancer. *Int J Cancer* 2002; **97**: 272-277
- 33 **Krieg A**, Mahotka C, Krieg T, Grabsch H, Muller W, Takeno S,



- Suschek CV, Heydthausen M, Gabbert HE, Gerharz CD. Expression of different survivin variants in gastric carcinomas: first clues to a role of survivin-2B in tumour progression. *Br J Cancer* 2002; **86**: 737-743
- 34 **Ebert MP**, Gunther T, Hoffmann J, Yu J, Miehle S, Schulz HU, Roessner A, Korc M, Malfertheiner P. Expression of metallothionein II in intestinal metaplasia, dysplasia, and gastric cancer. *Cancer Res* 2000; **60**: 1995-2001
- 35 **Bai YQ**, Yamamoto H, Akiyama Y, Tanaka H, Takizawa T, Koike M, Kenji Yagi O, Saitoh K, Takeshita K, Iwai T, Yuasa Y. Ectopic expression of homeodomain protein CDX2 in intestinal metaplasia and carcinomas of the stomach. *Cancer Lett* 2002; **176**: 47-55
- 36 **Li QL**, Ito K, Sakakura C, Fukamachi H, Inoue K, Chi XZ, Lee KY, Nomura S, Lee CW, Han SB, Kim HM, Kim WJ, Yamamoto H, Yamashita N, Yano T, Ikeda T, Itohara S, Inazawa J, Abe T, Hagiwara A, Yamagishi H, Ooe A, Kaneda A, Sugimura T, Ushijima T, Bae SC, Ito Y. Causal relationship between the loss of RUNX3 expression and gastric cancer. *Cell* 2002; **109**: 113-124
- 37 **Saitoh T**, Mine T, Katoh M. Up-regulation of WNT8B mRNA in human gastric cancer. *Int J Oncol* 2002; **20**: 343-348
- 38 **Li Z**, Wang Y, Song J, Kataoka H, Yoshii S, Gao C, Wang Y, Zhou J, Ota S, Tanaka M, Sugimura H. Genomic structure of the human beta-PIX gene and its alteration in gastric cancer. *Cancer Lett* 2002; **177**: 203-208
- 39 **Shinohara H**, Morita S, Kawai M, Miyamoto A, Sonoda T, Pastan I, Tanigawa N. Expression of HER2 in human gastric cancer cells directly correlates with antitumor activity of a recombinant disulfide-stabilized anti-HER2 immunotoxin. *J Surg Res* 2002; **102**: 169-177
- 40 **Takehana T**, Kunitomo K, Kono K, Kitahara F, Iizuka H, Matsumoto Y, Fujino MA, Ooi A. Status of c-erbB-2 in gastric adenocarcinoma: a comparative study of immunohistochemistry, fluorescence in situ hybridization and enzyme-linked immunosorbent assay. *Int J Cancer* 2002; **98**: 833-837
- 41 **Kodera Y**, Nakanishi H, Ito S, Yamamura Y, Kanemitsu Y, Shimizu Y, Hirai T, Yasui K, Kato T, Tatematsu M. Quantitative detection of disseminated free cancer cells in peritoneal washes with real-time reverse transcriptase-polymerase chain reaction: a sensitive predictor of outcome for patients with gastric carcinoma. *Ann Surg* 2002; **235**: 499-506
- 42 **You H**, Xiao B, Cui DX, Shi YQ, Fan DM. Two novel gastric cancer-associated genes identified by differential display. *World J Gastroenterol* 1998; **4**: 334-336
- 43 **Tortola S**, Marcuello E, Risques RA, Gonzalez S, Aiza G, Capella G, Peinado MA. Overall deregulation in gene expression as a novel indicator of tumor aggressiveness in colorectal cancer. *Oncogene* 1999; **18**: 4383-4387
- 44 **Yoshikawa Y**, Mukai H, Hino F, Asada K, Kato I. Isolation of two novel genes, down-regulated in gastric cancer. *Jan J Cancer Res* 2000; **91**: 459-463
- 45 **Wang X**, Lan M, Shi YQ, Lu J, Zhong YX, Wu HP, Zai HH, Ding J, Wu KC, Pan BR, Jin JP, Fan DM. Differential display of vincristine-resistance-related genes in gastric cancer SGC7901 cell. *World J Gastroenterol* 2002; **8**: 54-59
- 46 **Shiozaki K**, Nakamori S, Tsujie M, Okami J, Yamamoto H, Nagano H, Dono K, Umeshita K, Sakon M, Furukawa H, Hiratsuka M, Kasugai T, Ishiguro S, Monden M. Human stomach-specific gene, CA11, is down-regulated in gastric cancer. *Int J Onco* 2001; **19**: 701-707
- 47 **Wang G**, Wang M, You W, Li H. Cloning and primary expression analyses of down-regulated cDNA fragment in human gastric cancer. *Zhonghua Yixue Yichuanxue Zazhi* 2001; **18**: 43-47
- 48 **Fend F**, Kremer M, Quintanilla-Martinez L. Laser capture microdissection: methodical aspects and applications with emphasis on immuno-laser capture microdissection. *Pathobiology* 2000; **68**: 209-214
- 49 **Maitra A**, Wistuba I I, Gazdar A F. Microdissection and the study of cancer pathways. *Curr Mol Med* 2001; **1**: 153-162
- 50 **Rekhter MD**, Chen J. Molecular analysis of complex tissues is facilitated by laser capture microdissection: critical role of upstream tissue processing. *Cell Biochem Biophys* 2001; **35**: 103-113
- 51 **Cor A**, Vogt N, Malfroy B. Microdissection techniques for cancer analysis. *Folia Biol (Praha)* 2002; **48**: 3-8
- 52 **Noda H**, Maehara Y, Irie K, Kakeji Y, Yonemura T, Sugimachi K. Increased proliferative activity caused by loss of p21WAF1/CIP1 expression and its clinical significance in patients with early-stage gastric carcinoma. *Cancer* 2002; **94**: 2107-2112
- 53 **Saadat I**, Saadat M. Glutathione S-transferase M1 and T1 null genotypes and the risk of gastric and colorectal cancers. *Cancer Lett* 2001; **169**: 21-26
- 54 **Kuniyasu H**, Oue N, Wakikawa A, Shigeishi H, Matsutani N, Kuraoka K, Ito R, Yokozaki H, Yasui W. Expression of receptors for advanced glycation end-products (RAGE) is closely associated with the invasive and metastatic activity of gastric cancer. *J Pathol* 2002; **196**: 163-170
- 55 **Mori M**, Mimori K, Yoshikawa Y, Shibuta K, Utsunomiya T, Sadanaga N, Tanaka F, Matsuyama A, Inoue H, Sugimachi K. Analysis of the gene-expression profile regarding the progression of human gastric carcinoma. *Surgery* 2002; **131**: S39-47
- 56 **Endo K**, Maejara U, Baba H, Tokunaga E, Koga T, Ikeda Y, Toh Y, Kohnoe S, Okamura T, Nakajima M, Sugimachi K. Heparanase gene expression and metastatic potential in human gastric cancer. *Anticancer Res* 2001; **21**: 3365-3369
- 57 **Wang CS**, Lin KH, Hsu YC. Alterations of thyroid hormone receptor alpha gene: frequency and association with Nm23 protein expression and metastasis in gastric cancer. *Cancer Lett* 2002; **175**: 121-127

# PTEN encoding product: a marker for tumorigenesis and progression of gastric carcinoma

Lin Yang, Li-Ge Kuang, Hua-Chuan Zheng, Jin-Yi Li, Dong-Ying Wu, Su-Min Zhang, Yan Xin

**Lin Yang, Li-Ge Kuang, Hua-Chuan Zheng, Jin-Yi Li, Dong-Ying Wu, Su-Min Zhang, Yan Xin**, No.4 Lab, Cancer Institute, The First Affiliated Hospital, China Medical University, Shenyang 110001, China

**Ying Chen, Shen Yang**, Gynecology & Obstetrics Hospital, Shenyang 110014, China

**Supported by** the National Natural Science Foundation of China No.30070845, "Outstanding Research Training Program", Ministry of Education No. [1999] 2, and Science Foundation of Liaoning Education Bureau No. 20121031

**Correspondence to:** Prof. Xin Yan, No.4 Lab, Cancer Institute, The First Affiliated Hospital, China Medical University, Shenyang 110001, China. yxin@mail.cmu.edu.cn

**Telephone:** +86-24-23256666 Ext. 6351

**Received:** 2002-04-13 **Accepted:** 2002-06-01

## Abstract

**AIM:** To detect the expression of PTEN encoding product in normal mucosa, intestinal metaplasia (IM), dysplasia and carcinoma of the stomach, and to investigate its clinical implication in tumorigenesis and progression of gastric carcinoma.

**METHODS:** Formalin-fixed paraffin embedded specimens from 184 cases of gastric carcinoma, their adjacent normal mucosa, IM and dysplasia were evaluated for PTEN protein expression by SABC immunohistochemistry. PTEN expression was compared with tumor stage, lymph node metastasis, Lauren's and WHO's histological classification of gastric carcinoma. Expression of VEGF was also detected in 60 cases of gastric carcinoma and its correlation with PTEN was concerned.

**RESULTS:** The positive rates of PTEN protein were 100 % (102/102), 98.5 % (65/66), 66.7 % (4/6) and 47.8 % (88/184) in normal mucosa, IM, dysplasia and carcinoma of the stomach, respectively. The positive rates in dysplasia and carcinoma were lower than in normal mucosa and IM ( $P < 0.01$ ). Advanced gastric cancers expressed less frequent PTEN than early gastric cancer (42.9 % vs 67.6 %,  $P < 0.01$ ). The positive rate of PTEN protein was lower in gastric cancer with than without lymph node metastasis (40.3 % vs 63.3 %,  $P < 0.01$ ). PTEN was less expressed in diffuse-type than in intestinal-type gastric cancer (41.5 % vs 57.8 %,  $P < 0.05$ ). Signet ring cell carcinoma showed the expression of PTEN at the lowest level (25.0 %, 7/28); less than well and moderately differentiated ones ( $P < 0.01$ ). Expression of PTEN was not correlated with expression of VEGF ( $P > 0.05$ ).

**CONCLUSION:** Loss or reduced expression of PTEN protein occurs commonly in tumorigenesis and progression of gastric carcinoma. It is suggested that PTEN can be an objective marker for pathologically biological behaviors of gastric carcinoma.

Yang L, Kuang LG, Zheng HC, Li JY, Wu DY, Zhang SM, Xin Y. PTEN encoding product: a marker for tumorigenesis and progression of gastric carcinoma. *World J Gastroenterol* 2003; 9(1): 35-39

<http://www.wjgnet.com/1007-9327/9/35.htm>

## INTRODUCTION

PTEN/MMAC1/TEP1 gene (phosphatase and tensin homology deleted from chromosome ten/mutated in multiple advanced cancer 1/TGF- $\beta$ -regulated and epithelial cell enriched phosphatase 1) was the firstly defined tumor suppressor which product acted as phosphatase and shared extensive homology with cytoskeletal protein, mapping to human chromosome 10q23.3. PTEN encoding product could not only dephosphorylate the phosphatidylinositol-3, 4, 5-triphosphate (PIP<sub>3</sub>), but also be involved in cytoskeletal reconstruction and cellular mobility<sup>[1-6]</sup>. Recently, many studies showed there were several putative mechanisms relating to tumor suppression as follows: inhibiting cell invasion and metastasis by dephosphorylating focal adhesion kinase (FAK); inhibiting cell apoptosis and increasing cell growth by dephosphorylating PIP<sub>3</sub>; restraining cell differentiation by inhibiting mitogen-activated protein kinase (MAPK) signal pathway<sup>[7-9]</sup>. Mutation or abnormal expression of PTEN protein occurred commonly in multiple tumors and significantly correlates with tumorigenesis and progression of different malignancies<sup>[10-20]</sup>. It was reportedly suggested that deletion or mutation of PTEN could enhance the expression of vascular epithelial growth factor (VEGF) and stimulate the proliferation of microvessels in tumor tissues, which in turn closely correlated with tumor invasion and metastasis<sup>[21-28]</sup>.

Gastric carcinoma was one of the commonest malignancies in the world, and even the most frequent in China<sup>[29]</sup>. Although the achievement of early diagnosis and treatment have somewhat improved the patients' outcome, gastric cancer still remains the major killer among Chinese because the mechanisms of its tumorigenesis and progression were unclear<sup>[30]</sup>. In this study, we detected the expression of PTEN proteins in gastric cancer and its adjacent noncancerous mucosa, compared PTEN protein expression with its pathologically biological behaviors, and discussed the relationship between the expression of PTEN and VEGF in order to explore the role of PTEN gene product in tumorigenesis and progression of gastric cancer, and to provide scientific foundation for evaluating prognosis of gastric carcinoma.

## MATERIALS AND METHODS

### Pathology

One hundred and eighty-four cases of surgically removed specimens of gastric carcinoma were collected from Cancer Institute, China Medical University. This study included 102 cases of adjacent normal mucosa, 63 cases of adjacent IM and 6 cases of adjacent dysplasia. According to clinical staging, 37 cases were early, and 147 cases advanced. According to metastasis, 124 cases were accompanied with lymph node metastasis, 6 with liver metastasis (4 of them with lymph node metastasis) and 2 with ovary metastasis. All gastric specimens were classified according to the Lauren's and WHO's histological classification criteria.

### Immunohistochemistry

All specimens were fixed in 4 % formaldehyde solution,

embedded in paraffin and incised into 5  $\mu$ m sections. The rabbit anti-human polyclonal antibody against PTEN (ready to use) and mouse anti-human monoclonal antibody against VEGF (ready to use) were purchased from Maixim Biotech. SABC complex kit was from Boster Biotech. For negative control, sections were incubated with PBS (0.01 mol/L, pH7.4) instead of the primary antibodies.

Evaluation of PTEN and VEGF expression

Clearly brown staining was restricted to cytoplasm, which was considered as positive for PTEN or VEGF. Slides were scored semi-quantitatively based on staining intensity and distribution. Two pathologists assessed the positive rate according to the percent of positive cells in all counted cells from 5 randomly selected representative fields. The degree of staining was graded in the light of proportion of positive cells as follows: negative (-), positive rate <5 %; weakly positive (+); 5-25 %; moderately positive (++) : 25-50 %; strongly positive (+++~++++): >50 %.

Statistical analysis

Statistical evaluation was performed by chi-square test to differentiate the rates between two groups. *P*-value less than 0.05 was considered as statistically significant. SPSS 10.0 software was employed to analyze all data.

RESULTS

PTEN was expressed in normal mucosa, intestinal metaplasia, dysplasia and carcinoma of the stomach at the rate of 100 % (102/102), 98.5 % (65/66), 66.7 % (4/6), 47.8 % (88/184), respectively. Dysplasia and carcinoma expressed less frequent than normal mucosa or intestinal metaplasia (*P*<0.01) (Table 1, Figure 1,2).

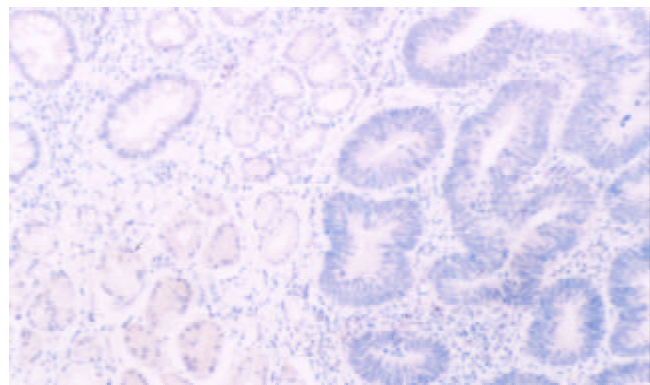


**Figure 1** PTEN protein was restricted to cytoplasm. It was moderately expressed in normal mucosa (below), while decreased in IM (left top) and dysplasia (right), (20 $\times$ )

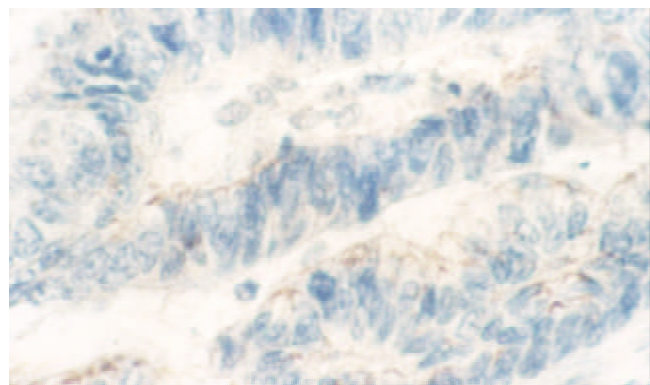


**Figure 2** Well differentiated papillary-tube adenocarcinoma showed weakly positive expression of PTEN protein (40 $\times$ )

**Table 1** PTEN expression in normal mucosa, intestinal metaplasia, dysplasia and carcinoma of the stomach

	<i>n</i>	PTEN expression		
		+~++++	-	%
"Normal" mucosa	102	102	0	100.0
Intestinal metaplasia	66	65	1	98.5
Dysplasia	6	4	2	66.7 <sup>a</sup>
Carcinoma	184	88	96	47.8 <sup>b</sup>

<sup>a</sup>Compared with "normal" mucosa or intestinal metaplasia, *P*<0.01 (modified  $\chi^2$ =18.729, 7.115); <sup>b</sup>Compared with "normal mucosa or intestinal metaplasia, *P*<0.01 ( $\chi^2$ =80.106, 52.499)

Positive rate of PTEN in advanced gastric carcinoma (AGC) was 42.9 % (63/147), lower than in early one (EGC)(67.6 %, 25/37) (*P*<0.01). In 124 cases with lymph node metastasis, 50 expressed PTEN protein (40.3 %), whose positive rate of PTEN was higher than those without lymph node metastasis (63.3 %, 38/60) (*P*<0.01). 41.5 percent of 118 diffuse-type gastric cancers expressed PTEN, less than that of intestinal-type ones (51.8 %, 37/64). Signet ring cell carcinoma expressed PTEN protein at the lowest level (25.0 %, 7/28), more than well and moderately differentiated adenocarcinoma (61.8 %, 21/34) (*P*<0.01).

None of the gastric normal mucosa showed expression of VEGF, while 75.0 percent of gastric carcinoma expressed it (45/60) (*P*<0.05) (Figure 3,4). The PTEN-positive cases expressed VEGF at the rate of 78.1 % (25/32), whereas PTEN-negative ones did it at the rate of 71.4 % (20/28). Both rates were not significantly different by statistical analysis (*P*>0.05).

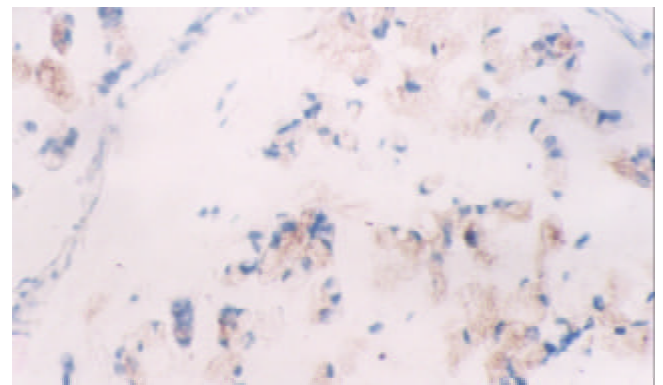


**Figure 3** Mucinous adenocarcinoma of the stomach moderately expressed VEGF (20 $\times$ )

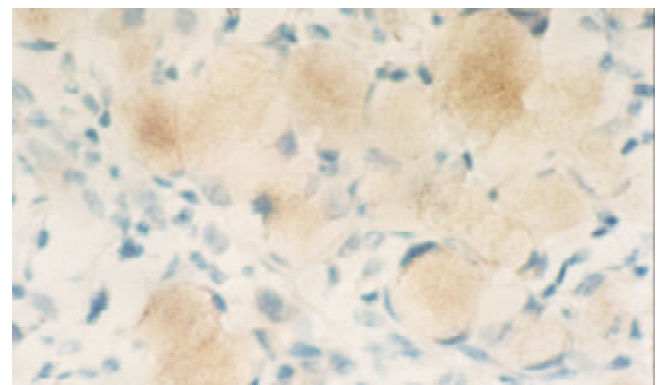


**Figure 4** SRC showed strongly positive expression of VEGF protein (40 $\times$ )

**Table 2** Relationship between expression of PTEN and the biological behaviors of gastric carcinoma

	PTEN expression			%
	n	+	-	
Clinicopathological staging				
Early	37	25	12	67.6
Advanced	147	63	84	42.9 <sup>a</sup>
Lymph node metastasis				
+	124	50	74	40.3 <sup>b</sup>
-	60	38	22	63.3
Lauren's classification				
Intestinal type	64	37	27	57.8
Diffused type	118	49	96	41.5 <sup>c</sup>
Mixed type	2	2	0	100.0
WHO's histological classification				
Papillary adenocarcinoma	20	10	10	50.0
Well-differentiated adenocarcinoma	9	5	4	55.6
Moderated-differentiated adenocarcinoma	25	16	9	64.0
Poorly-differentiated adenocarcinoma	85	39	64	45.9
Undifferentiated adenocarcinoma	5	3	2	60.0
Signet ring-cell carcinoma(SRC)	28	7	21	25.0 <sup>d</sup>
Mucinous adenocarcinoma	10	6	4	60.0
Carcinoid	1	1	0	-
Squamous cell carcinoma	1	1	0	-

<sup>a</sup>Compared with early gastric carcinoma,  $P<0.01(\chi^2=26.504)$ ;

<sup>b</sup>Compared with non-lymph node metastasis,  $P<0.01(\chi^2=8.580)$ ;

<sup>c</sup>Compared with intestinal-type gastric carcinoma,  $P<0.05(\chi^2=4.416)$ ;

<sup>d</sup>Compared with well and moderately differentiated gastric carcinoma,  $P<0.01(\chi^2=8.380)$

## DISCUSSION

Deletion or down-regulation of tumor suppressing genes plays an important role in the multiple steps of tumorigenesis and progression of gastric carcinoma. Previous studies on the relationship between alteration of tumor suppressor genes and the development of gastric carcinoma focused on p53<sup>[31, 32]</sup>, p16<sup>[33]</sup>, p27<sup>[34]</sup>, p33 (ING1)<sup>[35]</sup>, RB<sup>[36]</sup>, DCC<sup>[37]</sup> etc. However, few reports were involved in the newly discovered tumor suppressing gene- PTEN in tumorigenesis and progression of gastric carcinoma.

As a tumor-suppressing gene, PTEN makes great contribution to cellular differentiation, reproduction and apoptosis, as well as cellular adhesion and mobility. Some studies showed down-regulation of PTEN protein expression due to genetic changes like mutation, loss of heterozygosity, hypermethylation in gastric cancer, prostate cancer and breast cancer<sup>[2, 14, 16, 19, 38]</sup>. Our results showed that decreased expression of PTEN during the courses of normal mucosa→intestinal metaplasia→dysplasia→carcinoma. Gastric dysplasia or carcinoma expressed less PTEN than normal mucosa or intestinal metaplasia ( $P<0.01$ ), revealing that genetic changes of PTEN gene may play an important role in malignant transition of epithelial cells of gastric mucosa.

Low expression of PTEN gene product was involved in clinicopathological stage and metastasis of stomach neoplasms. We found that 42.9 percent of AGC expressed PTEN, less than EGC ( $P<0.01$ ). Positive rate of PTEN was lower in gastric cancer with than without lymph node metastasis (40.3 % vs

63.3 %,  $P<0.01$ ). One of the six liver metastases showed negative expression of PTEN in primary or liver metastasis, while the other five cases with liver metastasis showed reduced expression of PTEN protein. These results were similar to other kinds of tumors<sup>[39-46]</sup>. It is suggested that deletion or reduced expression of PTEN protein probably facilitate the metastatic ability of gastric cancer cells. Hwang *et al.* found that PTEN could enhance mobility and metastasis of tumor cells by regulating matrix metalloproteinases (MMPs) and VEGF<sup>[47]</sup>. There was another report that PTEN dephosphorated FAK so as to be involved in cellular adhesion<sup>[7]</sup>. Deletion or reduced expression of PTEN could result in decreasing cellular adhesion, increasing synthesis of MMPs and VEGF, which subsequently contributed to invasion and angiogenesis of cancer cells. These biological effects possibly underlay prelude of invasion and metastasis of tumor. Our results revealed that reduced expression of PTEN was implicated in progression of gastric cancer probably by decreasing cellular adhesion, increasing cellular mobility and angiogenesis and could act as an objective marker to reflect the biological behaviors of gastric cancer.

In addition, signet ring cell carcinoma showed the lowest expression of PTEN among histological classifications, less than well and moderately differentiated adenocarcinoma ( $P<0.01$ ), suggesting that decreased expression of PTEN was closely associated with carcinogenesis of signet ring cell carcinoma. Diffuse-type cancer showed less expression of PTEN at the rate of 41.5 % than intestinal-type one. ( $P<0.05$ ). In this sense, it supported that there were different tumorigenic pathways between diffuse and intestinal -type gastric carcinoma. Diffuse-type gastric cancer, main part of which was signet ring cell carcinoma, showed diffusely invasive growth pattern. It is possible that down-regulation of PTEN could affect the function of cellular skeleton, mobility and adhesion of cancer cells.

Some reports suggested that decreased expression of PTEN encoding product could down-regulate PI<sub>3</sub>K/AKT pathway, leading to increasing synthesis of VEGF induced by hypoxia inducing factor-1 (HIF-1)<sup>[48-50]</sup>. Our study showed that 75.0 percent of gastric carcinomas expressed VEGF (45/60), significantly more than normal mucosa (0/5) ( $P<0.05$ ), indicating that VEGF was up-regulated in gastric cancer. But PTEN was down-regulated in gastric cancer. Both PTEN and VEGF showed negative correlation, which was not statistically significant ( $P>0.05$ ). The relationship between expression of both PTEN and VEGF in tumorigenesis and progression of gastric cancer need proving by amplifying the sample.

In all, loss or reduced expression of PTEN protein occurred commonly in gastric carcinogenesis. Altered expression of PTEN contributed to progression of gastric cancer by increasing cell adhesion, angiogenesis, cell mobility and so on. It was suggested that PTEN could be a useful marker for pathologically biological behaviors of gastric carcinoma. However, the role of PTEN gene and its encoding protein in tumorigenesis and progression of gastric cancer need further investigation.

## REFERENCES

- 1 **Steck PA**, Pershouse MA, Jasser SA, Yung WK, Lin H, Ligon AH, Langford LA, Baumgard ML, Hattier T, Davis T, Frye C, Hu R, Swedlund B, Teng DH, Tavtigian SV. Identification of a candidate tumour suppressor gene, MMAC1, at chromosome 10q23.3 that is mutated in multiple advanced cancers. *Nat Genet* 1997; **15**: 356-362
- 2 **Li J**, Yen C, Liaw D, Podsypanina K, Bose S, Wang SI, Puc J, Miliareis C, Rodgers L, McCombie R, Bigner SH, Giovannella BC, Ittmann M, Tycko B, Hibshoosh H, Wigler MH, Parsons R. PTEN, a putative protein tyrosine phosphatase gene mutated in human brain, breast, and prostate cancer. *Science* 1997; **275**:1943-1947
- 3 **Li DM**, Sun H. TEP1, encoded by a candidate tumor suppressor

- locus, is a novel protein tyrosine phosphatase regulated by transforming growth factor beta. *Cancer Res* 1997; **57**: 2124-2129
- 4 **Cantley LC**, Neel BG. New insights into tumor suppression: PTEN suppresses tumor formation by restraining the phosphoinositide 3-kinase/AKT pathway. *Proc Natl Acad Sci U S A* 1999; **96**: 4240-4245
- 5 **Wu X**, Senechal K, Neshat MS, Whang YE, Sawyers CL. The PTEN/MMAC1 tumor suppressor phosphatase functions as a negative regulator of the phosphoinositide 3-kinase/Akt pathway. *Proc Natl Acad Sci U S A* 1998; **95**: 15587-15591
- 6 **Sun H**, Lesche R, Li DM, Liliental J, Zhang H, Gao J, Gavrilova N, Mueller B, Liu X, Wu H. PTEN modulates cell cycle progression and cell survival by regulating phosphatidylinositol 3,4,5-trisphosphate and Akt/protein kinase B signaling pathway. *Proc Natl Acad Sci U S A* 1999; **96**: 6199-6204
- 7 **Maehama T**, Taylor GS, Dixon JE. PTEN and myotubularin: novel phosphoinositide phosphatases. *Annu Rev Biochem* 2001; **70**: 247-279
- 8 **Besson A**, Robbins SM, Yong VW. PTEN/MMAC1/TEP1 in signal transduction and tumorigenesis. *Eur J Biochem* 1999; **263**: 605-611
- 9 **Waite KA**, Eng C. Protean PTEN: form and function. *Am J Hum Genet* 2002; **70**: 829-844
- 10 **Tanno S**, Tanno S, Mitsuchi Y, Altomare DA, Xiao GH, Testa JR. AKT activation up-regulates insulin-like growth factor I receptor expression and promotes invasiveness of human pancreatic cancer cells. *Cancer Res* 2001; **61**: 589-593
- 11 **Rubin MA**, Gerstein A, Reid K, Bostwick DG, Cheng L, Parsons R, Papadopoulos N. 10q23.3 loss of heterozygosity is higher in lymph node-positive (pT2-3,N+) versus lymph node-negative (pT2-3,N0) prostate cancer. *Hum Pathol* 2000; **31**: 504-508
- 12 **Depowski PL**, Rosenthal SI, Ross JS. Loss of expression of the PTEN gene protein product is associated with poor outcome in breast cancer. *Mod Pathol* 2001; **14**: 672-676
- 13 **Meng Q**, Goldberg ID, Rosen EM, Fan S. Inhibitory effects of Indole-3-carbinol on invasion and migration in human breast cancer cells. *Breast Cancer Res Treat* 2000; **63**: 147-152
- 14 **Garcia JM**, Silva JM, Dominguez G, Gonzalez R, Navarro A, Carretero L, Provencio M, Espana P, Bonilla F. Allelic loss of the PTEN region (10q23) in breast carcinomas of poor pathophenotype. *Breast Cancer Res Treat* 1999; **57**: 237-243
- 15 **Dillon DA**, Howe CL, Bosari S, Costa J. The molecular biology of breast cancer: accelerating clinical applications. *Crit Rev Oncog* 1998; **9**: 125-140
- 16 **Lin WM**, Forgacs E, Warshel DP, Yeh IT, Martin JS, Ashfaq R, Muller CY. Loss of heterozygosity and mutational analysis of the PTEN/MMAC1 gene in synchronous endometrial and ovarian carcinomas. *Clin Cancer Res* 1998; **4**: 2577-2583
- 17 **Shao X**, Tandon R, Samara G, Kanki H, Yano H, Close LG, Parsons R, Sato T. Mutational analysis of the PTEN gene in head and neck squamous cell carcinoma. *Int J Cancer* 1998; **77**: 684-688
- 18 **Hosoya Y**, Gemma A, Seike M, Kurimoto F, Uematsu K, Hibino S, Yoshimura A, Shibuya M, Kudoh S. Alteration of the PTEN/MMAC1 gene locus in primary lung cancer with distant metastasis. *Lung Cancer* 1999; **25**: 87-93
- 19 **Celebi JT**, Shendrik I, Silvers DN, Peacocke M. Identification of PTEN mutations in metastatic melanoma specimens. *J Med Genet* 2000; **37**: 653-657
- 20 **Tsao H**, Zhang X, Fowlkes K, Haluska FG. Relative reciprocity of NRAS and PTEN/MMAC1 alterations in cutaneous. *Cancer Res* 2000; **60**: 1800-1804
- 21 **Huang J**, Kontos CD. PTEN modulates vascular endothelial growth factor-mediated signaling and angiogenic effects. *J Biol Chem* 2002; **277**: 10760-10766
- 22 **Ferrara N**, Gerber HP. The role of vascular endothelial growth factors in angiogenesis. *Acta Haematol* 2001; **106**: 148-156
- 23 **Harmey JH**, Bouchier-Hayes D. Vascular endothelial growth factor (VEGF), a survival factor for tumour cells: implications for anti-angiogenic therapy. *Bioessays* 2002; **24**: 280-283
- 24 **Lin R**, LeCouter J, Kowalski J, Ferrara N. Characterization of endocrine gland-derived vascular endothelial growth factor signaling in adrenal cortex capillary endothelial cells. *J Biol Chem* 2002; **277**: 8724-8729
- 25 **Dias S**, Choy M, Alitalo K, Rafii S. Vascular endothelial growth factor (VEGF)-C signaling through FLT-4 (VEGFR-3) mediates leukemic cell proliferation, survival, and resistance to chemotherapy. *Blood* 2002; **99**: 2179-2184
- 26 **Inoki I**, Shiomi T, Hashimoto G, Enomoto H, Nakamura H, Makino K, Ikeda E, Takata S, Kobayashi K, Okada Y. Connective tissue growth factor binds vascular endothelial growth factor (VEGF) and inhibits VEGF-induced angiogenesis. *FASEB J* 2002; **16**: 219-221
- 27 **Umeda N**, Ozaki H, Hayashi H, Kondo H, Uchida H, Oshima K. Non-paralleled increase of hepatocyte growth factor and vascular endothelial growth factor in the eyes with angiogenic and nonangiogenic fibroproliferation. *Ophthalmic Res* 2002; **34**: 43-47
- 28 **Suzuma K**, Takahara N, Suzuma I, Isshiki K, Ueki K, Leitges M, Aiello LP, King GL. Characterization of protein kinase C beta isoform's action on retinoblastoma protein phosphorylation, vascular endothelial growth factor-induced endothelial cell proliferation, and retinal neovascularization. *Proc Natl Acad Sci U S A* 2002; **99**: 721-726
- 29 **Parkin DM**. Global cancer statistics in the year 2000. *Lancet Oncol* 2001; **2**: 533-543
- 30 **Chen XY**, van Der Hulst RW, Shi Y, Xiao SD, Tytgat GN, Ten Kate FJ. Comparison of precancerous conditions: atrophy and intestinal metaplasia in Helicobacter pylori gastritis among Chinese and Dutch patients. *J Clin Pathol* 2001; **54**: 367-370
- 31 **Gunther T**, Schneider-Stock R, Hackel C, Kasper HU, Pross M, Hackelsberger A, Lippert H, Roessner A. Mdm2 gene amplification in gastric cancer correlation with expression of Mdm2 protein and p53 alterations. *Mod Pathol* 2000; **13**: 621-626
- 32 **Liu XP**, Tsushimi K, Tsushimi M, Oga A, Kawauchi S, Furuya T, Sasaki K. Expression of p53 protein as a prognostic indicator of reduced survival time in diffuse-type gastric carcinoma. *Pathol Int* 2001; **51**: 440-444
- 33 **Jang TJ**, Kim DI, Shin YM, Chang HK, Yang CH. p16(INK4a) Promoter hypermethylation of non-tumorous tissue adjacent to gastric cancer is correlated with glandular atrophy and chronic inflammation. *Int J Cancer* 2001; **93**: 629-634
- 34 **Migaldi M**, Zunarelli E, Sgambato A, Leocata P, Ventura L, De Gaetani C. P27Kip1 expression and survival in NO gastric carcinoma. *Pathol Res Pract* 2001; **197**: 231-236
- 35 **Oki E**, Maehara Y, Tokunaga E, Kakeji Y, Sugimachi K. Reduced expression of p33 (ING1) and the relationship with p53 expression in human gastric cancer. *Cancer Lett* 1999; **147**: 157-162
- 36 **Lee WA**, Woo DK, Kim YI, Kim WH. p53, p16 and RB expression in adenosquamous and squamous cell carcinomas of the stomach. *Pathol Res Pract* 1999; **195**: 747-752
- 37 **Yoshida Y**, Itoh F, Endo T, Hinoda Y, Imai K. Decreased DCC mRNA expression in human gastric cancers is clinicopathologically significant. *Int J Cancer* 1998; **79**: 634-639
- 38 **Kang YH**, Lee HS, Kim WH. Promoter methylation and silencing of PTEN in gastric carcinoma. *Lab Invest* 2002; **82**: 285-291
- 39 **Lee JI**, Soria JC, Hassan KA, El-Naggar AK, Tang X, Liu DD, Hong WK, Mao L. Loss of PTEN expression as a prognostic marker for tongue cancer. *Arch Otolaryngol Head Neck Surg* 2001; **127**: 1441-1445
- 40 **Verma RS**, Manikal M, Conte RA, Godec CJ. Chromosomal basis of adenocarcinoma of the prostate. *Cancer Invest* 1999; **17**: 441-447
- 41 **McMenamin ME**, Soung P, Perera S, Kaplan I, Loda M, Sellers WR. Loss of PTEN expression in paraffin-embedded primary prostate cancer correlates with high Gleason score and advanced stage. *Cancer Res* 1999; **59**: 4291-4296
- 42 **Rustia A**, Wierzbicki V, Marrocco L, Tossini A, Zamponi C, Lista F. Is exon 5 of the PTEN/MMAC1 gene a prognostic marker in anaplastic glioma? *Neurosurg Rev* 2001; **24**: 97-102
- 43 **Nozaki M**, Tada M, Kobayashi H, Zhang CL, Sawamura Y, Abe H, Ishii N, Van Meir EG. Roles of the functional loss of p53 and other genes in astrocytoma tumorigenesis and progression. *Neuro-oncol* 1999; **1**: 124-137
- 44 **Minaguchi T**, Yoshikawa H, Oda K, Ishino T, Yasugi T, Onda T,

- Nakagawa S, Matsumoto K, Kawana K, Taketani Y. PTEN mutation located only outside exons 5, 6, and 7 is an independent predictor of favorable survival in endometrial carcinomas. *Clin Cancer Res* 2001; **7**: 2636-2642
- 45 **Tada K**, Shiraishi S, Kamiryo T, Nakamura H, Hirano H, Kuratsu J, Kochi M, Saya H, Ushio Y. Analysis of loss of heterozygosity on chromosome 10 in patients with malignant astrocytic tumors: correlation with patient age and survival. *J Neurosurg* 2001; **95**: 651-659
- 46 **Mills GB**, Lu Y, Kohn EC. Linking molecular therapeutics to molecular diagnostics: inhibition of the FRAP/RAFT/TOR component of the PI3K pathway preferentially blocks PTEN mutant cells *in vitro* and *in vivo*. *Proc Natl Acad Sci USA* 2001; **98**: 10031-10033
- 47 **Hwang PH**, Yi HK, Kim DS, Nam SY, Kim JS, Lee DY. Suppression of tumorigenicity and metastasis in B16F10 cells by PTEN/MMAC1/TEP1 gene. *Cancer Lett* 2001; **172**: 83-91
- 48 **Laughner E**, Taghavi P, Chiles K, Mahon PC, Semenza GL. HER2 (neu) signaling increases the rate of hypoxia-inducible factor 1alpha (HIF-1alpha) synthesis: novel mechanism for HIF-1-mediated vascular endothelial growth factor expression. *Mol Cell Biol* 2001; **21**: 3995-4004
- 49 **Zhong H**, Chiles K, Feldser D, Laughner E, Hanrahan C, Georgescu MM, Simons JW, Semenza GL. Modulation of hypoxia-inducible factor 1alpha expression by the epidermal growth factor/phosphatidylinositol 3-kinase/PTEN/AKT/FRAP pathway in human prostate cancer cells: implications for tumor angiogenesis and therapeutics. *Cancer Res* 2000; **60**: 1541-1545
- 50 **Zundel W**, Schindler C, Haas-Kogan D, Koong A, Kaper F, Chen E, Gottschalk AR, Ryan HE, Johnson RS, Jefferson AB, Stokoe D, Giaccia AJ. Loss of PTEN facilitates HIF-1-mediated gene expression. *Genes Dev* 2000; **14**: 391-396

**Edited by** Ma JY



# Relationship between lymph node sinuses with blood and lymphatic metastasis of gastric cancer

Tong Yin, Xiao-Long Ji, Min-Shi Shen

**Tong Yin, Xiao-Long Ji, Min-Shi Shen**, General Hospital of PLA, 28 Fu Xing Road, Beijing 100853, China

**Correspondence to:** Dr. Xiao-Long Ji, Department of Pathology of General Hospital of PLA, 28 Fu Xing Road, Beijing 100853, China. xlj@public.bta.net.cn

**Telephone:** +86-10-66936455 **Fax:** +86-10-68228362

**Received:** 2002-03-25 **Accepted:** 2002-04-23

## Abstract

**AIM:** To elucidate the relationship between lymph node sinuses with blood and lymphatic metastasis of gastric cancer.

**METHODS:** Routine autopsy was carried out in the randomly selected 102 patients (among them 100 patients died of various diseases, and 2 patients died of non-diseased reasons), their superficial lymph nodes locating in bilateral necks (include supraclavicle), axilla, inguina, thorax, and abdomen were sampled. Haematoxylin-Eosin staining was performed on 10 % formalin-fixed and paraffin-embedded lymph node tissue sections (5um). The histological patterns of the lymph sinuses containing blood were observed under light microscope. The expression of CD31, a marker for endothelial cell, was detected both in blood and non-blood containing lymph node sinuses with the method of immunohistochemistry.

**RESULTS:** Among the 1322 lymph nodes sampled from the autopsies of 100 diseased cases, lymph node sinuses containing blood were found in 809 lymph nodes sampled from 91 cases, but couldn't be seen in the lymph nodes sampled from the non-diseased cases. According to histology, we divided the blood containing lymph node sinuses into five categories: vascular-opening sinus, blood-deficient sinus, erythrophago-sinus, blood-abundant sinus, vascular-formative sinus. Immunohistochemical findings showed that the expression of CD31 was strongly positive in vascular-formative sinuses and some vascular-opening sinuses while it was faint in blood-deficient sinuses, erythrophago-sinuses and some vascular-opening sinuses. It was almost negative in blood-abundant sinus and non-blood containing sinus.

**CONCLUSION:** In the state of disease, the phenomenon of blood present in the lymph sinus is not uncommon. Blood could possibly enter into the lymph sinuses through the lymphaticovenous communications between the veins and the sinuses in the node. Lymph circulation and the blood circulation could communicate with each other in the lymph node sinuses. The skipping and distal lymphatic metastasis of gastric cancer may have some connection with the blood containing lymph node sinuses.

Yin T, Ji XL, Shen MS. Relationship between lymph node sinuses with blood and lymphatic metastasis of gastric cancer. *World J Gastroenterol* 2003; 9(1): 40-43  
<http://www.wjgnet.com/1007-9327/9/40.htm>

## INTRODUCTION

It is well known that one of the most common behaviours of lymphatic metastasis of gastric cancer is their great tendency to produce skipping metastasis with the tumor emboli traversing the proximal lymph nodes encountered on their route or even bypassing them to form distant nodal metastasis (mainly at left supraclavicle). Skipping metastasis is a peculiar kind of lymphatic metastasis. Until now, there have been few reports of this condition and its pathogenesis has not yet been clarified. Blood present in lymph node sinuses is a phenomenon that haven't been deeply researched too. In the routine lymph node biopsy, erythrocytes in the lymph node sinuses could occasionally be seen. In the early literature, vascular transformation of lymph node sinus (VTS) and haemal lymph node sinus (HLs) have been reported. Their common feature is blood presenting in the lymph node sinus. Since lymph node sinus is also the place where the metastatic malignant tumor is located, we speculated there might be some inner relationships between the two phenomena. The purpose of this study is to find out the relationship between lymph node sinuses with blood and lymphatic metastasis of gastric cancer.

## MATERIALS AND METHODS

When routine autopsy was carried out in the randomly selected 102 patients died of different reasons, their superficial lymph nodes locating in the bilateral necks (include supraclavicle), axilla, inguina, thorax, and abdomen were sampled. Haematoxylin-Eosin staining was performed on 10 % formalin-fixed and paraffin-embedded 5 um lymph node tissue sections. The histological patterns of the lymph node sinuses containing blood were observed under light microscope. The expression of CD31, a marker for endothelial cell, was detected both in blood and non-blood containing lymph node sinuses by immunohistochemistry.

## RESULTS

### *Clinical findings*

The randomly selected 102 cases included 62 males and 38 females whose ages ranged from 2 months to 90 years (mean 45.08 years, median 57 years). Among the 102 cases, 100 patients died of various diseases, and 2 died of non-diseased reasons. The total number of the sampled lymph nodes was 1 362 (1 322 from the 100 patients died of various diseases and 40 from the 2 patients died of non-diseased reasons).

### *Light microscopic findings*

Among the 1 322 lymph nodes sampled from the 100 autopsy diseased cases, blood containing lymph node sinuses were found in 809 lymph nodes sampled from 91 cases, whereas such sinuses couldn't be seen in the lymph nodes sampled from the non-diseased cases. According to the histology, we divided the blood containing lymph node sinuses into five categories: vascular-opening sinus (in 338 lymph nodes from 68 cases), blood-deficient sinus (in 291 lymph nodes from 69 cases), erythrophago-sinus (in 344 lymph nodes from 69 cases), blood-



abundant sinus (in 80 lymph nodes from 34 cases), and vascular-formative sinus (in 364 lymph nodes from 82 cases). In the vascular-opening sinus, venules and/or capillaries in the cortex and medulla extended or opened directly in the lymph node sinuses. Through the opening, blood could enter into the sinus (Figure 1). Blood-deficient sinus was defined as a small quantity of erythrocytes present in the lymph node sinuses (Figure 2). When erythrocytes in the sinuses were phagocytosed, erythrophago-sinus appeared. When the sinuses filled with blood, we called it blood-abundant sinus (Figure 3). Vascular-formative sinus was defined as vascular formation in the sinuses. We could see short to long sinuous vascular slits or vascular channels with round or oval contours lined by flat or plump endothelium. The channels were either empty or filled with an amorphous lymph-like materials and some red cells, occasionally they were markedly engorged with blood (Figure 4).

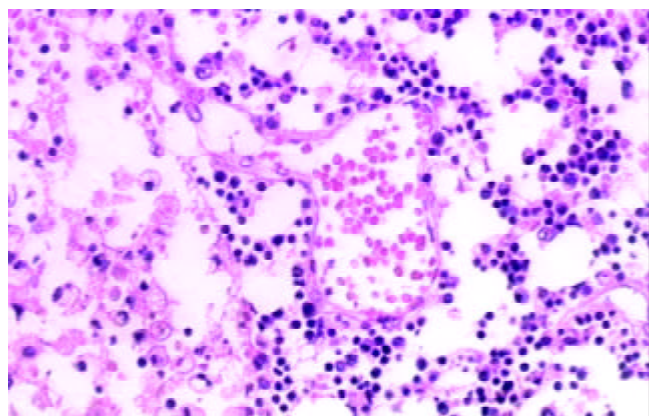


**Figure 1** Vascular-opening lymph node sinus HE×200

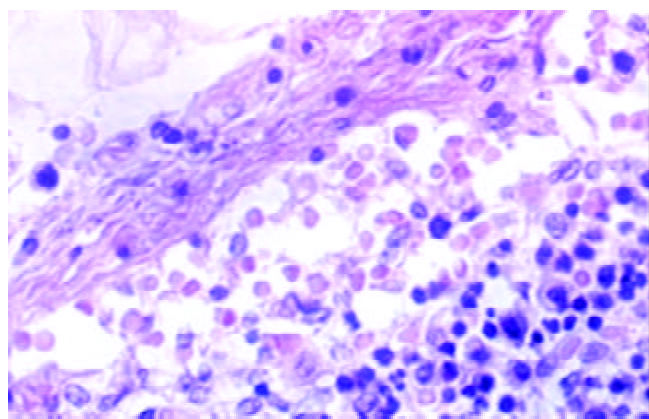


**Figure 2** Blood-deficient lymph node sinus HE×400

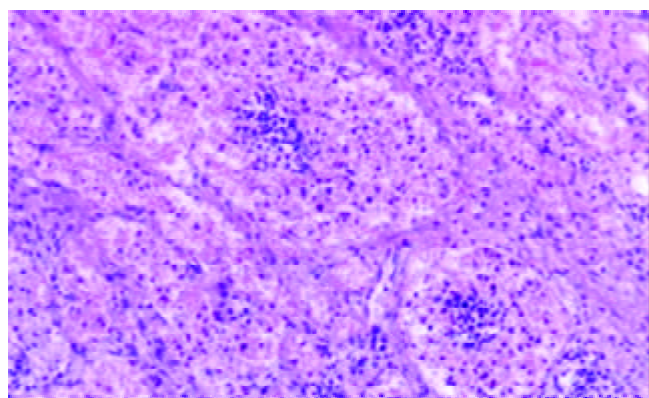


**Figure 3** Blood-abundant lymph node sinus HE×100

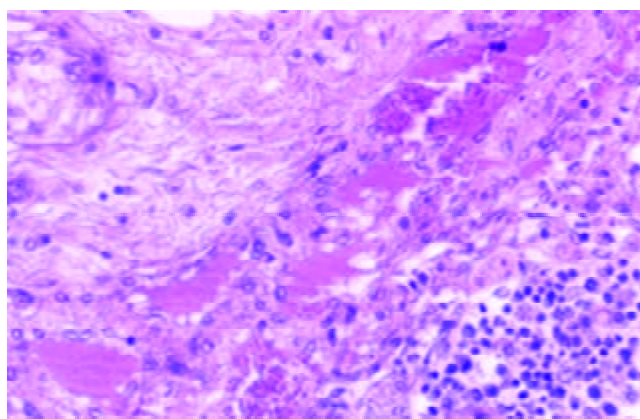


**Figure 4** Vascular-formative lymph node sinus HE×200

### *Immunohistochemical findings*

Immunohistochemical findings showed that the expression of CD31 was strongly positive in vascular-formative sinuses and some vascular-opening sinuses while it was faint in blood-deficient sinuses, erythrophago-sinuses and some vascular-opening sinuses. It was almost negative in blood-abundant sinuses and non-blood containing sinuses.

### DISCUSSION

One of the most prominent features of the behaviour of carcinomas is their great tendency to produce secondary growths in regional lymph nodes. The early lymphatic metastasis of cancers almost invariably appear in the lymph nodes in the direction of normal lymph flow and the marginal sinus is the place where the metastatic growths are initially situated for the afferent lymphatics of lymph node enter the marginal sinus<sup>[1-7]</sup>. As for the spread of the tumor to the lymph nodes in the direction contrary to the normal lymph flow or the lymph nodes far from the primary carcinomas, what is called skipping metastasis, it has always been convinced to be the consequence of the cancerous occlusion of the principal lymphatics; the lymph flow is diverted or sometimes reversed, into collateral channels passing to neighbouring unaffected nodes. Skipping metastasis is a peculiar kind of lymphatic metastasis. It was mostly recognised in the metastasis of gastric cancer to the supraclavicular lymph nodes which could be found as the earliest clinical symptom<sup>[8-11]</sup>. There have been some reports of this condition, but most were concerning with how to detect the metastatic foci and the relationship with clinical nodal stage<sup>[12,13]</sup>. Few mentioned the pathogenesis of skipping metastasis. The presence of previously unknown lymphatic tracts have been reported to explain the phenomenon<sup>[14]</sup>. The skipping of intact lymph nodes can also be explained by anatomically demonstrable intra- and perinodal short circuit connections. Apart from this, preexisting lymph node changes (silicosis, fibrosis) also play an important part<sup>[15]</sup>.

Blood present in lymph node sinus is a phenomenon that haven't been deeply researched. How the blood entering the sinus remains to be elucidated<sup>[16-29]</sup>. It's well recognized that there are two circulations in the lymph node, one is the lymphatic circulation, the other is the blood circulation. They could communicate via the high endothelial venules (HEV) in the paracortex, but it is not certain whether there is some other pathway for the communication in human lymph node. In 1961, Pressman and Simon<sup>[24]</sup> devised experiments in dog to show that there were some other lymphatic-venous communications in lymph node. They inferred that the lymph node contained numerous lymphaticovenous communications between the lymph node sinuses and the veins. This claim has such far

reaching implications that the work should be repeated both in the dog and in other species. When it come to the human lymph node, the studies of blood containing lymph node sinus were concentrated on the vascular transformation of sinuses (VTS) and Hemolymph nodes (HLs). The term VTS was first coined by Haferkamp *et al*<sup>[16]</sup> in 1971 for a distinctive benign vasoproliferative lesion of lymph node, which needed to be distinguished from Kaposi's sarcoma(KS); venous obstruction was thought to be the underlying mechanism, but it was still controversial<sup>[30,31]</sup>. VTS is characterized by conversion of nodal sinuses into capillary-like channels, often accompanied by fibrosis<sup>[21,32]</sup>. Hemolymph nodes (HLs) were another target for the study of the communication between lymph circulation and blood circulation in the lymph node sinuses. HLs are unique lymph nodes, because their lymphatic sinuses contain numerous erythrocytes. In 1969, Turner DR<sup>[25]</sup> reported that blood entered the sinus through the communication between venule and sinuses, but it is still controversial<sup>[26-29]</sup>. From the above-mentioned phenomenons and the researches, we hypothesized that the two circulations in the lymph node could communicate in the lymph node sinus.

In this study, blood in the lymph node sinuses could be found frequently in the lymph nodes sampled from the patients died of disease. The histologic patterns of the changes were not limited to HLs and VTS. According to the histologic patterns, the blood containing lymph node sinuses were divided into 5 categories. Vascular-opening sinus was characterized by venules or capillaries stretching into the sinus with blood in the vascular releasing into the lymph node sinuses (Figure 1). So that, it testified the existence of lymph-venule communication in human lymph node sinuses. Through the vascular-opening sinus, blood could enter the lymph node sinuses directly. This finding was in accordance with Pressman and Simon<sup>[24]</sup>. Blood deficient sinus was possibly formed in the early period of the formation of sinuses containing blood, but the artifact factors should be excluded (Figure 2). The erythrophago-sinus was formed as a result of the phagocytosis of sinus-histocytes in the sinus. The red cells entered into the sinus were recognised as foreign bodies and engulfed by histocytes. When the pressure in venule increased for the stasis, plenty of red cells could rush into the sinus and the blood abundant sinus came into being due to the communication between lymph node sinus and venule (Figure 3). When the blood kept staying in the sinuses, an exceptional sinus containing blood -vascular formative sinus emerged. This kind of sinus was characterized by vascular formation in the lymph node sinus (Figure 4).

In order to clarify the features of endothelial cells of the lymph node sinus containing blood, monoclonal antibody CD31 was used to label the endothelial cells by immunohistochemistry<sup>[33-36]</sup>. The expression of CD31 was different in the 5 blood contained sinuses. It was strongly positive in vascular-formative sinus and some vascular-opening sinus while it was weak in blood-deficient sinus, erythrophago-sinus and some vascular-opening sinus. It was almost negative in blood-abundant sinus and non-blood containing sinus. According to the expression of CD31 in different lymph node sinuses, we could speculated that the endothelial cells might experience the transformation from the lymph node sinus endothelial cells to the vascular endothelial cells. This course may have some connection with the blood in the sinuses<sup>[37]</sup>. The Prompt recognition of the ultrastructure and the mechanism of the phenomenon was needed.

Since lymph node sinus is the place where the metastatic malignant tumor is located and we found in this study that in the state of disease, there was the communication between lymph and blood circulations in the sinus, we speculated there might be some inner relationships between lymphatic skipping metastasis of gastric cancer and blood containing lymph node sinuses.

Early clinical observations let to the impressions that

carcinomas frequently spread and grew in the lymphatic system, whereas tumors of mesenchymal origin spread more frequently by way of the blood stream<sup>[38]</sup>. In fact, this division is arbitrary because these two routes are actually interlinked and inseparable. Cancer cells may invade the lymphatics directly or gain access to them via blood vessels. Tumor cells can readily pass from blood to lymphatic communication via the interstitial spaces of lymph nodes and other tissues exist. When tumor cells entered the local blood circulation and was brought to the distant area, through the communications between the lymph circulation and the blood circulation in lymph node sinuses, they could enter the lymph node and stay in the lymph node sinuses where the foci of skipping metastatic tumors are formed. When the lymph circulation was obstructed, through the communication, blood metastasis of tumor cell could also be accelerated.

Although, lymph node sinus containing blood was only found in the cases died of disease in our study, it was not certain if this kind of lymph node could also be found in non-diseased cases, because such cases were limited. An in-depth study in a larger cohort of gastric cancer patients is needed to confirm whether lymph node sinus containing blood is also very common in such alived human lymph nodes, and their physiological and pathological significance in the skipping metastasis.

## REFERENCES

- 1 **del Regato JA**. Pathways of metastatic spread of malignant tumors. *Semin Oncol* 1977; **4**: 33-38
- 2 **Scanlon EF**. James Ewing lecture. The process of metastasis. *Cancer* 1985; **55**: 1163-1166
- 3 **Wittekind C**. Principles of lymphogenic and hematogenous metastasis and metastasis classification. *Zentralbl Chir* 1996; **121**: 435-441
- 4 **Hermanek P**. Lymph nodes and malignant tumors. *Zentralbl Chir* 2000; **125**: 790-795
- 5 **Passlick B**, Pantel K. Detection and relevance of immunohistochemically identifiable tumor cells in lymph nodes. *Recent Results Cancer Res* 2000; **157**: 29-37
- 6 **Kawaguchi T**. Pathological features of lymph node metastasis. 2) From morphological aspects. *Nippon Geka Gakkai Zasshi* 2001; **102**: 440-444
- 7 **Gendreau KM**, Whalen GF. What can we learn from the phenomenon of preferential lymph node metastasis in carcinoma? *J Surg Oncol* 1999; **70**: 199-204
- 8 **Maruyama K**, Gunven P, Okabayashi K, Sasako M, Kinoshita T. Lymph node metastases of gastric cancer. General pattern in 1931 patients. *Ann Surg* 1989; **210**: 596-602
- 9 **Siewert JR**, Sendlar A. Potential and futility of sentinel node detection for gastric cancer. *Recent Results Cancer Res* 2000; **157**: 259-269
- 10 **Arai K**, Iwasaki Y, Takahashi T. Clinicopathological analysis of early gastric cancer with solitary lymph node metastasis. *Br J Surg* 2002; **89**: 1435-1437
- 11 **Kitagawa Y**, Ohgami M, Fujii H, Mukai M, Kubota T, Ando N, Watanabe M, Otani Y, Ozawa S, Hasegawa H, Furukawa T, Matsuda J, Kumai K, Ikeda T, Kubo A, Kitajima M. Laparoscopic detection of sentinel lymph nodes in gastrointestinal cancer: a novel and minimally invasive approach. *Ann Surg Oncol* 2001; **8**: 86S-89S
- 12 **Ichikura T**, Furuya Y, Tomimatsu S, Okusa Y, Ogawa T, Mukoda K, Mochizuki H, Tamakuma S. Relationship between nodal stage and the number of dissected perigastric nodes in gastric cancer. *Surg Today* 1998; **28**: 879-883
- 13 **Aikou T**, Higashi H, Natsugoe S, Hokita S, Baba M, Tako S. Can sentinel node navigation surgery reduce the extent of lymph node dissection in gastric cancer? *Ann Surg Oncol* 2001; **8**: 90S-93S
- 14 **Yamamoto Y**, Takahashi K, Yasuno M, Sakoma T, Mori T. Clinicopathological characteristics of skipping lymph node metastases in patients with colorectal cancer. *Jpn J Clin Oncol* 1998; **28**: 378-382
- 15 **Junker K**, Gumpich T, Muller KM. Discontinuous lymph node metastases ("skipping") in malignant lung tumors. *Chirurg* 1997;

- 68:** 596-599
- 16 **Haferkamp O**, Rosenau W, Lennert K. Vascular transformation of lymph node sinuses due to venous obstruction. *Arch Pathology* 1971; **92**: 81-83
  - 17 **Steinmann G**, Foldi E, Foldi M, Racz P, Lennert K. Morphologic findings in lymph nodes after occlusion of their efferent lymphatic vessels and veins. *Lab Invest* 1982; **47**: 43-50
  - 18 **Michael M**, Koza V. Vascular transformation of lymph node sinuses-a diagnostic pitfall. Histopathologic and immunohistochemical study. *Pathol Res Pract* 1989; **185**: 441-444
  - 19 **Scherrer C**, Maurer R. Vascular sinus transformation of the lymph nodes. Morphological and immunohistochemical analysis of 6 cases. *Ann Pathol* 1985; **5**:231-238
  - 20 **Lucke VM**, Davies JD, Wood CM, Whitbread TJ. Plexiform vascularization of lymph nodes: an unusual but distinctive lymphadenopathy in cats. *J Comp Pathol* 1987; **97**: 109-119
  - 21 **Chan JKC**, Warnke RA, Dorfman R. Vascular transformation of sinuses in lymph node. A study of its morphological spectrum and distinction from Kaposi's sarcoma. *Am J Surg Pathol* 1991; **15**: 732-743
  - 22 **Ostrowski ML**, Siddiqui T, Barnes RE, Howton MJ. Vascular transformation of lymph node sinuses, a process displaying a spectrum of histologic features. *Arch Pathol Lab Med* 1990; **114**: 656-660
  - 23 **Cook PD**, Czerniak B, Chan JKC, Mackay B, Ordonez NG, Ayala AG, Rosai J. Nodular spindle-cell vascular transformation of lymph nodes. A benign process occurring predominantly in retroperitoneal lymph nodes draining carcinomas that can simulate Kaposi's sarcoma or metastatic tumor. *Am J Surg Pathol* 1995; **19**: 1010-1020
  - 24 **Pressman JJ**, Simon MB. Communication between lymph and blood circulations in lymph node. *Surg Gynec Obstet* 1961; **113**: 537
  - 25 **Turner DR**. The vascular tree of the haemal node in the rat. *J Anat* 1969; **104**: 481
  - 26 **Cerutti P**, Marcaccini A, Guerrero F. A scanning and immunohistochemical study in bovine haemal node. *Anat Histol Embryol* 1998; **27**: 387-392
  - 27 **Hogg CM**, Reid O, Scothorne RJ. Studies on hemolymph nodes. III. Renal lymph as a major source of erythrocytes in the renal hemolymph node of rats. *J Anat* 1982; **135**: 291-299
  - 28 **Abu-Hijleh MF**, Scothorne RJ. Studies on haemolymph nodes. IV. Comparison of the route of entry of carbon particles into parathymic nodes after intravenous and intraperitoneal injection. *J Anat* 1996; **188**: 565-573
  - 29 **He YC**, Shen LS, Yang CL, Fang WN, Li Hong. The distribution of lymphatic channels and red cells in the lymph nodes of rat blood. *Jiepu Xuebao* 1991; **22**: 239-241
  - 30 **Samet A**, Gilbey P, Talmon Y, Cohen H. Vascular transformation of lymph node sinuses. *J Laryngol Otol* 2001; **115**: 760-762
  - 31 **Jindal B**, Vashishta RK, Bhasin DK. Vascular transformation of sinuses in lymph nodes associated with myelodysplastic syndrome-a case report. *Indian J Pathol Microbiol* 2001; **44**: 453-455
  - 32 **Ostrowski ML**, Siddiqui T, Barnes RE, Howton MJ. Vascular transformation of lymph node sinuses. A process displaying a spectrum of histologic features. *Arch Pathol Lab Med* 1990; **114**:656-660
  - 33 **Newman PJ**. The role of PECAM-1 in vascular cell biology. *Ann N Y Acad Sci* 1994; **714**: 165-174
  - 34 **DeLisser HM**, Christofidou-Solomidou M, Strieter RM, Burdick MD, Robinson CS, Wexler RS, Kerr JS, Garlanda C, Merwin JR, Madri JA, Albelda SM. Involvement of endothelial PECAM/CD31 in angiogenesis. *Am J Pathol* 1997; **151**: 671-677
  - 35 **Newman PJ**. The biology of PECAM-1 in vascular cell biology. *J Clin Invest* 1997; **99**: 3-8
  - 36 **Watt SM**, Gschmeissner SE, Bates PA. PECAM-1: its expression and function as a cell adhesion molecule on hemopoietic and endothelial cells. *Leuk Lymphoma* 1995; **17**: 229-244
  - 37 **Fujiwara K**, Masuda M, Osawa M, Kano Y, Katoh K. Is PECAM-1 a mechanoresponsive molecule? *Cell Struct Funct* 2001; **26**: 11-17
  - 38 **Weiss L**, Greep RO. Histology, Fourth Edition. USA: McGraw-Hill, Inc 1977: 523-543

Edited by Zhao M

# Inhibition of conjugated linoleic acid on mouse forestomach neoplasia induced by benzo (a) pyrene and chemopreventive mechanisms

Bing-Qing Chen, Ying-Ben Xue, Jia-Ren Liu, Yan-Mei Yang, Yu-Mei Zheng, Xuan-Lin Wang, Rui-Hai Liu

**Bing-Qing Chen, Ying-Ben Xue, Jia-Ren Liu, Yan-Mei Yang,** Department of Nutrition and Food Hygiene, Public Health College, Harbin Medical University, Harbin 150001, Heilongjiang Province, China  
**Rui-Hai Liu,** Food Science and Toxicology, Department of Food Science, 108 Stocking Hall, Cornell University, Ithaca, NY 14853-7201, USA  
**Supported by** the National Natural Science Foundation of China, No. 30070658

**Correspondence to:** Prof. Bing-Qing Chen, Department of Nutrition and Food Hygiene, Public Health College, Harbin Medical University, 199 Dongdazhi Street, Nangang District, Harbin 150001, Heilongjiang Province, China. bingqingchen@sina.com

**Telephone:** +86-451-3608014 **Fax:** +86-451-3648617

**Received:** 2002-08-24 **Accepted:** 2002-10-12

## Abstract

**AIM:** To explore the inhibition of conjugated linoleic acid isomers in different purity (75 % purity c9,t11-, 98 % purity c9,t11- and 98 % purity t10,c12-CLA) on the formation of forestomach neoplasm and chemopreventive mechanisms.

**METHODS:** Forestomach neoplasm model induced by B(a)P in KunMing mice was established. The numbers of tumor and diameter of each tumor in forestomach were counted; the mice plasma malondialdehyde (MDA) were measured by TBARS assay; TUNEL assay was used to analyze the apoptosis in forestomach neoplasia and the expression of MEK-1, ERK-1, MKP-1 protein in forestomach neoplasm were studied by Western Blotting assay.

**RESULTS:** The incidence of neoplasm in B(a)P group, 75 % purity c9, t11-CLA group, 98 % purity c9,t11-CLA group and 98 % purity t10, c12-CLA group was 100 %, 75.0 % ( $P>0.05$ ), 69.2 % ( $P<0.05$ ) and 53.8 % ( $P<0.05$ ) respectively and the effect of two CLA isomers in 98 % purity on forestomach neoplasia was significant; CLA showed no influence on the average tumor numbers in tumor-bearing mouse, but significantly decreased the tumor size, the tumor average diameter of mice in 75 % purity c9,t11-CLA group, 98 % purity c9,t11-CLA group and 98 % purity t10, c12-CLA group was  $0.157\pm0.047$  cm,  $0.127\pm0.038$  cm and  $0.128\pm0.077$  cm ( $P<0.05$ ) and  $0.216\pm0.088$  cm in B(a)P group; CLA could also significantly increase the apoptosis cell numbers by  $144.00\pm20.31$ ,  $153.75\pm23.25$ ,  $157.25\pm15.95$  ( $P<0.05$ ) in 75 % purity c9,t11-CLA group, 98 % purity c9, t11-CLA group and 98 % purity t10,c12-CLA group ( $30.88\pm3.72$  in BP group); but there were no significant differences between the effects of 75 % purity c9,t11-CLA and two isomers in 98 % purity on tumor size and apoptotic cell numbers; the plasma levels of MDA in were increased by 75 % purity c9,t11-CLA, 98 % purity c9,t11-CLA and 98 % purity t10,c12-CLA. The 75 % purity c9,t11-CLA showed stronger inhibition; CLA could also inhibit the expression of ERK-1 protein and promote the expression of MKP-1 protein, however no influence of CLA on MEK-1 protein was observed.

**CONCLUSION:** Two isomers in 98 % purity show stronger inhibition on carcinogenesis. However, the inhibitory

mechanisms of CLA on carcinogenesis is complicated, which may be due to the increased mice plasma MDA, the inducing apoptosis in tumor tissues. And the effect of CLA on the expression of ERK-1 and MKP-1 may be one of the mechanisms of the inhibition of CLA on the tumor.

Chen BQ, Xue YB, Liu JR, Yang YM, Zheng YM, Wang XL, Liu RH. Inhibition of conjugated linoleic acid on mouse forestomach neoplasia induced by benzo(a)pyrene and chemopreventive mechanisms. *World J Gastroenterol* 2003; 9(1): 44-49

<http://www.wjgnet.com/1007-9327/9/44.htm>

## INTRODUCTION

Conjugated linoleic acid (CLA) refers to a group of dienoic derivatives of linoleic acid that can be found in natural foods, such as the milk fat and meat of ruminant animals<sup>[1-4]</sup>. CLA can also be synthesized in the laboratory and is available commercially as a dietary supplement and has shown to be non-toxic<sup>[5]</sup>. In several animal experiments, supplementation of feeding with CLA showed an anticarcinogenic effect against chemical-induced cancers of the skin, forestomach, colon and breast<sup>[6-9]</sup>. Moreover, of the individual isomers of CLA, c9,t11 isomer has been implicated as most active biologically because it is the predominant isomer incorporated into the phospholipids of cell membrane, however recent evidence showed the t10, c12-CLA isomer might also exert biological activity<sup>[10]</sup>. To date, the sample used for animal experiment or cell experiment is the isomer mixture of conjugated linoleic acid which mainly containing c9,t11-, t10,c12-, t9,t11-, t10,t12-CLA. Potent anticarcinogenic effects have been attributed to a synthetic mixture of CLA containing c9,t11- and t9,c11-CLA (43 %) and t10,c12-CLA (45.3 %)<sup>[7,11-14]</sup>. For example, CLA used in Ha's report contained c9,t11-, t10,c12-, t9,t11-, t10,t12-CLA which accounted for about 90 % of the material<sup>[7]</sup>; Hubbard applied a mixture of CLA isomers with 32.5 % c9,t11-CLA and 32.5 % t10,c12-CLA isomers making up 66 % to mammary tumor metastasis<sup>[14]</sup>, etc. In summary, there were few reports assessing the effects of CLA monomer on the carcinogenesis in animal model.

Now the effect of CLA on carcinogenesis had been confirmed and there were evidences to support CLA action on the every stage of cancer, including initiation<sup>[15,16]</sup>, post-initiation (promotion)<sup>[17,18]</sup>, progression<sup>[19]</sup> and metastasis<sup>[14,20-22]</sup>. However the mechanisms through which CLA inhibits tumorigenesis are moot. Ha *et al*<sup>[7]</sup> suggested an antioxidant mechanism; Schonberg reported that the biochemical mechanisms by which CLA exerted its anticancer activity possibly including the formation of cytotoxic lipid peroxidation products, but this might not be sufficient to explain all the effects of these naturally occurring isomers of CLA<sup>[23]</sup>; Ip's data showed an effect on growth and development of certain types of mammary cells<sup>[24,25]</sup>; Reduced formation of carcinogen-DNA adducts had been implicated<sup>[15,16]</sup>; Durgam's work showed CLA inhibit cancer by influences on the oestrogen response system<sup>[26]</sup>; Others suggested inhibition mechanisms of CLA including its effects on eicosanoid metabolism<sup>[27-31]</sup>, apoptosis<sup>[32,33]</sup>, the gene



expression such as stearoyl-CoA desaturase<sup>[34,35]</sup>, PPRA<sup>[36-38]</sup>, cyclin A,B(1), D(1) cyclin-dependent kinases inhibitors and (CDKI)(P16 and P21)<sup>[39]</sup> ect.

In our research group, we found that 75 % purity c9,t11-CLA inhibit cancer incidence by 40 %; at the same time that 98 % purity c9,t11 and t10,c12-CLA showed stronger inhibition on human gastric cancer (SGC-7901) and breast cancer cells(MCF-7)<sup>[39-42]</sup>. Our study was designed to investigate the inhibition effects of synthetically-prepared individual isomer of CLA in different purity (75 % purity c9,t11-CLA, 98 % purity c9,t11-CLA and 98 % purity t10,c12-CLA) on the forestomach neoplasia induced by B(a)P and the mechanism whereby CLA acted as an anticarcinogen, especially in terms of lipid peroxidation, apoptosis and MAPKs pathway.

## MATERIALS AND METHODS

### Material

BP was purchased from Fluka Chemie AG of Switzerland. Salad oil was purchased from a local grocery. 75 % purity c9, t11-CLA, 98 % purity c9,t11-CLA and 98 % purity t10,c12-CLA were provided by Dr. Ruihai Liu at Cornell University.

### Treatment of mice (43)

KunMing mice, 6 to 7 wk of age, were purchased from Cancer Research Institute of HarBin Medical University in China. Two weeks later the animals were randomized by body weight and divided into 7 groups (15 mice/group). They were then subjected to a forestomach tumorigenesis as follows: each animal except animals in salad control group was given 0.2 ml salad oil solution per 20 mg body weight (1 mg BP in 0.2 ml of salad oil solution) by gavage and animals in salad control group were given 0.2 ml salad oil only twice every week for over after 4 wk. And the following diets were given after 2 weeks of giving BP and continue for 7 wk (Table 1). Beginning with the first intubation and continuing thereafter, the body weight and food intake were recorded twice weekly. All surviving mice were sacrificed 26 wk after the first dose of BP.

**Table 1** The diets given after 2 wk of giving BP

Group	diets
Salad oil Control(A)	Standard diet+salad oil: fat(salad oil) concentration was 20 %
BP Control(B)	Standard diet+salad oil: fat(salad oil) concentration was 20 %
BP+75 % c9,t11-CLA(C)	Standard diet+salad oil+75 %c9,t11-CLA: Fat (salad oil) concentration was 20 %, CLA 0.8 %
BP+98 % c9,t11-CLA(D)	Standard diet+salad oil+98 % c9,t11-CLA: Fat (salad oil) concentration was 20%, CLA 0.5 %
BP+98 %t10,c12-CLA(E)	Standard diet+salad oil+98 %t10,c12-CLA: Fat (salad oil) concentration was 20 %, CLA 0.5 %

### Gross pathology and histopathology

At termination of the study, the forestomach was removed. Tumor numbers and size were recorded, and then fixed in 10 % formalin and paraffin-embedded; 4  $\mu$ m sections were cut and stained with hematoxylin and eosin (HE).

### Lipid peroxidation analysis

The TBARS test was used to measure malonaldehyde (MDA). The mouse plasma MDA levels was determined by TBARs kits (Jiancheng Biotechnology Institute, NanJing, P.R. China).

### Measurement of apoptosis cell numbers in forestomach neoplasia

*In situ* Cell Death Detection Kit, Fluorescein, were purchased from Boehringer Mannheim. Briefly, Fixed and permeabilized

apoptotic tissue sections, incubated the tissue section with the TUNEL reaction mixture containing TdT and fluorescein-dUTP, detected the incorporated fluorescein with an anti-fluorescein antibody POD conjugate and at last visualized the immunocomplex with a substrate reaction were in light microscope. The apoptosis cell number was counted in 10<sup>3</sup> cells.

### Protein extract and western blotting

Three mice forestomaches in each group were homogenated and lysed in RIPA buffer (150 mM NaCl, 0.1 % NP40, 0.5 % deoxycholic acid, 0.1 % SDS, 50 mM Tris, pH 7.4 ) with protease inhibitor, leupeptin and aprotinin. Equal amounts of protein (80  $\mu$ g/lane) were resolved by SDS-polyacrylamide gel electrophoresis, transferred onto nitrocellulose membranes, and immunoblotted with an mouse anti-MEK-1, rabbit anti-ERK-1 and rabbit anti-MKP-1 antibody, then incubated with horseradish peroxidase secondary antibodies. Immunoreactive bands were detected using DAB (diaminobenzidine tetrahydrochloride) substrate and analyzed with a ChemiImager™ 4 000 Low Light Imaging System (Alpha Innotech Corporation, at the same time used GAPDH as house-keeping protein.

## RESULTS

### Establishment of mouse forestomach model

Figure 1(A) showed the normal forestomach with smooth surface and without tumor. However, the white-yellow cauliflower-like neoplasia in different size appeared in the forestomach of mice induced B(a)P(Figure 1B,C). The structure of mouse forestomach in Figure 2(A) was normal and squamous epithelial cells and glandular epithelium cells were in order; The pathological analysis of B(a)P-induced forestomach neoplasia showed atypical hyperplasia in Figure 2(B) with stratified squamous epithelium excessively cornified, with focal proliferative basal cells and hypertrophic echinocyte; The basal cells, proliferating actively and out of order, grew through basement membrane and developed carcinoma *in situ* (Figure 2C).

### Effect of CLA on forestomach neoplasia

The effect of CLA on BP-induced neoplasia of the forestomach in female KunMing mice was shown in Table 2. The incidence of the tumor and average diameter of tumor in 98 % purity c9, t11-CLA group and 98 % purity t10,c12-CLA group were significantly lower than that in B(a)P group ( $P<0.05$ ). 75 % Purity c9,t11-CLA only decreased the tumor incidence which was no significant ( $P>0.05$ ), but its influence on the average diameter being significant ( $P<0.05$ ). The average tumor number of each tumor-bearing mouse showed no statistical significance ( $P>0.05$ ).

**Table 2** Inhibition of BP-induced forestomach neoplasia in female KunMing mice by CLA

Group	No. of mice (No. of tumor-bearing mice) /treatment	Total number of tumors	Tumor incidence (%)	Tumors/ tumor-bearing mouse <sup>d</sup>	Diameter/ tumor (CM)
A	14(0)	0	0	0	0
B	12(12)	31	100	2.58 $\pm$ 0.90	0.216 $\pm$ 0.088
C	12(9)	23	75.0 <sup>a</sup>	2.56 $\pm$ 0.73	0.157 $\pm$ 0.047 <sup>e</sup>
D	13(9)	22	69.2 <sup>bc</sup>	2.44 $\pm$ 0.53	0.127 $\pm$ 0.038 <sup>e</sup>
E	13(7)	21	53.8 <sup>bc</sup>	3.00 $\pm$ 0.58	0.128 $\pm$ 0.077 <sup>e</sup>

<sup>a</sup> $P>0.05$  compared to the group B; <sup>b</sup> $P<0.05$  compared to the group B;

<sup>c</sup> $P>0.05$  compared to the group C; <sup>d</sup> $P>0.05$ , <sup>e</sup> $P<0.05$  compared to the group B

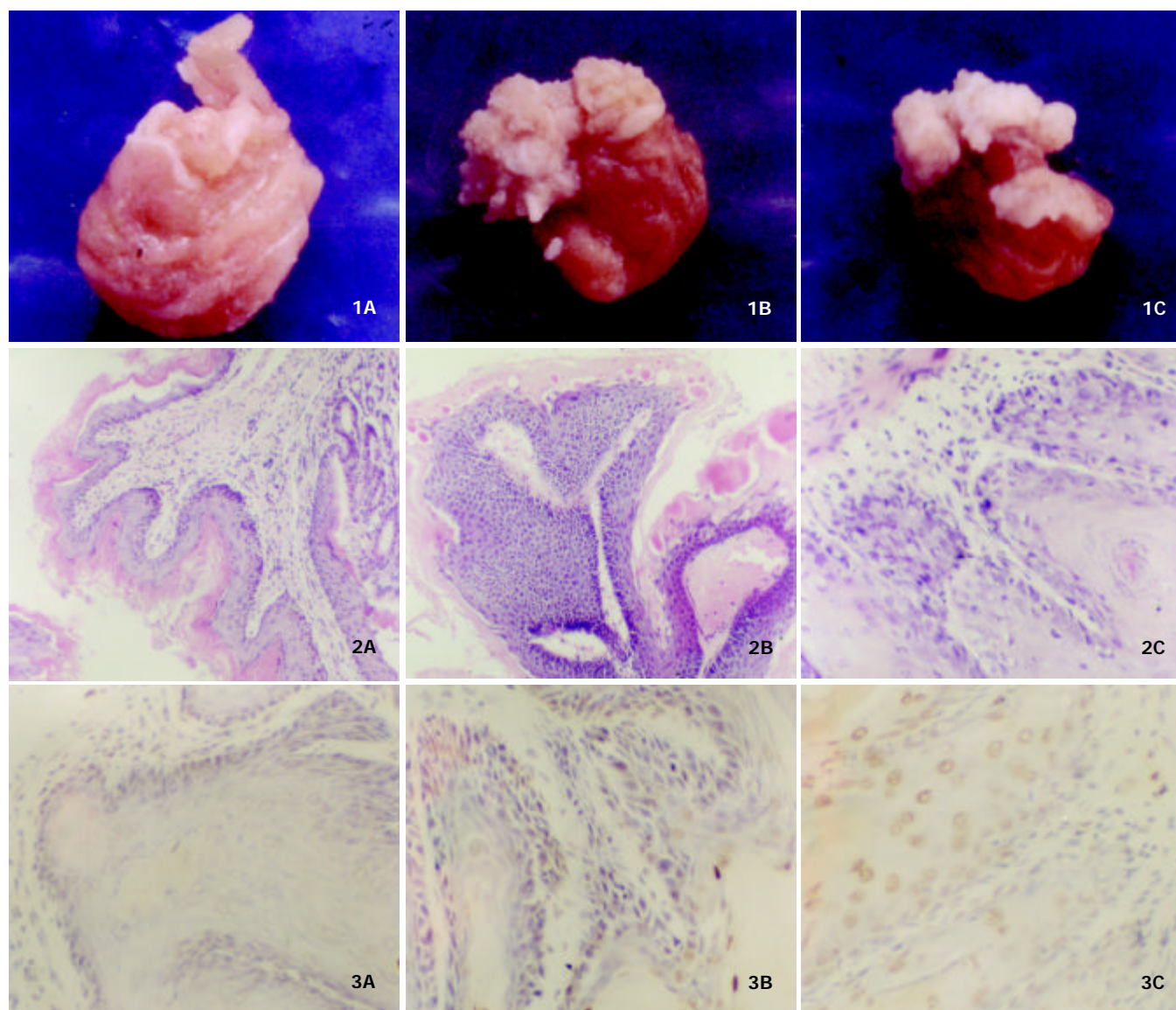


**Figure 1** The establishment of mouse neoplasia model induced by B(a)P. (A): normal forestomach; (B, C): forestomach neoplasia.

**Figure 2** The pathological analysis of mouse forestomach. (A): normal forestomach $\times 10$ ; (B): Atypical hyperplasia $\times 10$ ; (C): Carcinoma *in situ* $\times 4$ .

**Figure 3** Apoptosis induced by CLA in mice forestomach. (A or B): there were few apoptotic cells in group A and B; (C): the apoptosis induced by CLA. Arrow showed apoptotic cells $\times 40$ .

#### Analysis on lipid peroxidation

The plasma levels of MDA measured by the TBARS assay increased in mice treated by 75 % purity c9,t11-CLA, 98 % purity c9,t11-CLA and 98 % purity t10,c12-CLA ( $P < 0.05$ ). Moreover, 75 % purity c9,t11-CLA were more effective than purity 98 % c9,t11-CLA and 98 % purity t10,c12-CLA.

**Table 3** The effects of CLA on mouse plasma lipid peroxidation

Group	MDA in plasma(nmol/L)
A	9.995 $\pm$ 1.634
B	9.937 $\pm$ 1.854
C	17.668 $\pm$ 4.610 <sup>ab</sup>
D	14.005 $\pm$ 4.116 <sup>a</sup>
E	13.303 $\pm$ 3.593 <sup>a</sup>

<sup>a</sup> $P < 0.05$  compared to the group A, B; <sup>b</sup> $P < 0.05$  compared to the group D, E.

#### The effect of CLA on apoptosis in forestomach neoplasia

Figure 3 showed the apoptosis in forestomach neoplasia. Table 4 showed that 75 % c9,t11-CLA, purity 98 % c9,t11-CLA and 98 % purity t10,c12-CLA can significantly induce apoptosis but with no statistical difference ( $P < 0.05$ ).

**Table 4** The effects of CLA on apoptosis in mice stomach( $10^3$  cells)

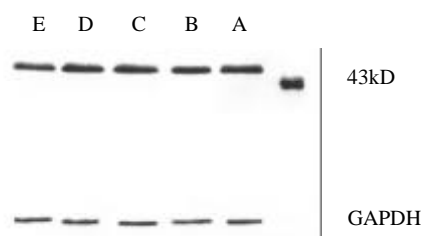
Group	Apoptotic cell numbers
A	42.63 $\pm$ 6.02
B	30.88 $\pm$ 3.72
C	144.00 $\pm$ 20.31 <sup>a</sup>
D	153.75 $\pm$ 23.25 <sup>a</sup>
E	157.25 $\pm$ 15.95 <sup>a</sup>

<sup>a</sup> $P < 0.01$  compared to the group A, B.

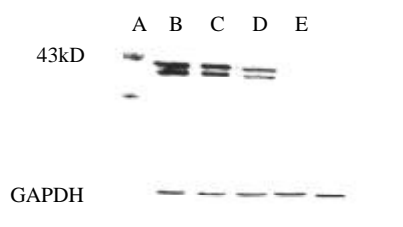
#### The effect of CLA on the MAPKs pathway

Figure 4, 5, 6 showed that 98 % purity t10,c12-CLA decreased

the expression of MEK-1 protein, but no influence was observed in mice treated by 75 % purity c9,t11-CLA and 98 % c9,t11-CLA. The expression of ERK-1 protein in 75 % purity c9,t11-CLA group, 98 % purity c9,t11-CLA group and 98 % purity t10,c12-CLA group was inhibited significantly, and 98 % purity c9,t11-CLA and 98 % purity t10,c12-CLA showed more effective than 75 % purity c9,t11-CLA. The expression of MKP-1 was increased in mice treated by 75 % purity c9,t11-CLA, 98 % purity c9,t11-CLA and 98 % purity t10,c12-CLA.



**Figure 4** The effect of CLA on the expression of MEK-1 protein.



**Figure 5** The effect of CLA on the expression of ERK-1 protein.

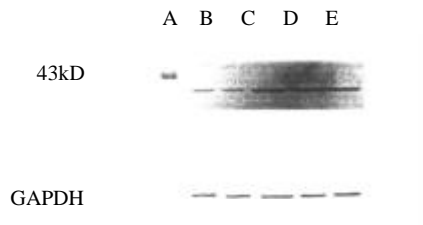


**Figure 6** The effect of CLA on the expression of MKP-1 protein.

## DISCUSSION

To date, all of the *in vivo* work with CLA has been done with a commercial free fatty acid preparation containing a mixture of c9,t11-, t10,c12-, c11, t13-isomers, although food CLA is predominately the c9,t11-isomer present in triacylglycerols (80–90 %). Ha *et al* reported that dietary mixture of c9,t11-CLA, t10,c12-CLA, t9,t11-CLA and t10,t12-CLA significantly decreased the incidence of mouse neoplasm induced B(a)P (up to 20 %) [7]. In DMBA-induced mammary adenocarcinoma model, the incidence in mice treated with dietary 0.05 %, 0.1 %, 0.25 %, 0.5 % CLA isomer mixture was 58 %, 42 %, 34 %, 36 %, respectively (that of the control was 56 %) [9]. In this study, we found that the incidence in mice fed with diet containing 75 % purity c9,t11-CLA (75 %), 98 % purity c9,t11-CLA (69.2 %), 98 % purity t10,c12-CLA (53.8 %) had been decreased, moreover, 98 % purity isomers showed significant influences in the inhibition of carcinogenesis; although 75 % purity c9,t11-CLA decreased tumor incidence with no statistical significance, it still significantly decreased the tumor size; all of which suggested that the effect of CLA on carcinogenesis was possibly related to the CLA purity. In addition, the different isomers of CLA in different purities decreased the average diameter of the tumors, but no influence was observed in

average tumor numbers of each tumor-bearing mouse, which might be one of characteristics of the inhibition of food components on carcinogenesis.

Lu reported that arachidonic acid and linoleic acid may promote HSC proliferation, but increased concentration can be cytotoxic to HSC [44]. As one of the positional and structural isomer of linoleic acid, more interests in conjugated linoleic acid promoting oxidation in cancer cells were paid upon. The study results in Stanton's group showed that CLA could make breast cancer cell more susceptible to lipid peroxidation, moreover, the extent of lipid peroxidation of CLA treated cells was related to CLA-induced cytotoxicity against cancer cell lines. At the same time, they found that milk fat triglyceride-bound CLA, consisting primarily of the c9,t11 isomer, was also cytotoxic towards MCF-7 cells [45–47]. In our study, 75 % purity c9,t11-CLA, 98 % purity c9,t11-CLA and 98 % purity t10,c12-CLA increased the levels of MDA in mouse plasma and 75 % purity c9,t11-CLA was most effective, but 75 % purity c9,t11-CLA did not show strongest inhibition of carcinogenesis, which suggested that the cytotoxic effect of lipid peroxidation to tumor cells might be one of mechanisms by which CLA exerted its biochemical activity. And Schönberg also reported that the formation of MDA induced by 40  $\mu\text{mol} \cdot \text{L}^{-1}$  CLA in lung adenocarcinoma cell lines was completely abolished by 30 microM vitamin E, but the growth rates were only partially restored, which indicated that cytotoxic lipid peroxidation products were only in part responsible for the growth inhibitory effects of CLA [24]. Furthermore, the lipid peroxidation product induced played important role in apoptosis [48]. We found that purity 75 % c9,t11-CLA, purity 98 % c9,t11-CLA and 98 % purity t10,c12-CLA induced significant apoptosis cells in forestomach neoplasia, but there were no differences between 75 % purity c9,t11-CLA group, 98 % purity c9,t11-CLA and 98 % purity t10,c12-CLA groups. The MAPK family consists of at least three different subgroups which include: ERKs, JNKs (SAPKs), and p38 MAPK kinase [49–53]. The Ras-Raf-MEK1/2-ERK1/2 pathway has been explained more clearly. Lavoie found that the transcription of cyclin D1 requires the long-term activation of ERK, which suggests that ERK can regulate cell cycle. In one report, there is a homeostasis between JNK/SAPKs and ERK systems: when ERK cascade is predominant in lymphocyte, cells will proliferate; by contraries, JNK/SAPK cascade will activate cell apoptosis [54]. It is found that the abnormalities of Ras/Raf/MAPK cascade reaction may contribute to malignant transformation of hepatocytes and activation of MAPK proteins may be an early event in hepatocellular carcinogenesis [55]. In summary, The activation of Ras-Raf-MEK-ERK can promote cell proliferation and inhibit cell apoptosis. In addition, The product of the immediate early gene MAP kinase phosphatase (MKP-1), is able to dephosphorylate phosphoserine/threonine as well as phosphotyrosine residues, and shows selectivity for ERKs 1 and 2 *in vitro*, with lower activity toward other MAP kinases such as JNK and P38 MAP kinase [56]. MKP-1 inactivates ERK following growth factor stimulation in intact cells and also suppresses signaling downstream of ERK at the level of gene transcription and proliferation [57], most likely through its inhibitory effects on MAP kinase. In our study, we found that CLA could inhibit the expression of ERK-1 protein, and at the same time inactivate the ERK-1 by increasing the expression of MKP-1, which might be one of mechanisms of CLA anticarcinogen.

In summary, it is confirmed that CLA shows inhibition on forestomach neoplasia induced by B(a)P, which is possibly related with CLA purity. Although the inhibition of different isomers (c9,t11- and t10,c12-CLA) on carcinogenesis is different, they show no significant difference. Moreover, the



inhibition mechanism of CLA is complicated and difficult to be explained by an mechanism.

## ACKNOWLEDGEMENTS

We thank Dr. Rui-Hai Liu at Cornell University for helps and 75 % purity c9,t11-CLA, 98 % purity c9,t11-CLA, 98 % purity t10,c12-CLA.

## REFERENCES

- 1 **Ha YL**, Grimm NK, Pariza MW. Anticarcinogens from fried ground beef: heated-altered derivatives of linoleic acid. *Carcinogenesis* 1987; **8**: 1881-1887
- 2 **Kritchevsky D**. Antimutagenic and some other effects of conjugated linoleic acid. *Br J Nutr* 2000; **83**: 459-465
- 3 **Pariza MW**, Park Y, Cook ME. Mechanisms of action of conjugated linoleic acid: evidence and speculation. *Proc Soc Exp Biol Med* 2000; **223**: 8-13
- 4 **Pariza MW**, Park Y, Cook ME. Conjugated linoleic acid and the control of cancer and obesity. *Toxicol Sci* 1999; **52**: 107-110
- 5 **Scimeca JA**. Toxicological evaluation of dietary conjugated linoleic acid in male Fischer 344 rats. *Food Chem Toxicol* 1998; **36**: 391-395
- 6 **Belury MA**, Nickel KP, Bird CE, Wu Y. Dietary conjugated linoleic acid modulation of phorbol ester skin tumor promotion. *Nutr Cancer* 1996; **26**: 149-157
- 7 **Ha YL**, Storkson J, Pariza MW. Inhibition of benzo(a)pyrene-induced mouse forestomach neoplasia by conjugated dienoic derivatives of linoleic acid. *Cancer Res* 1990; **50**: 1097-1101
- 8 **Xu M**, Dashwood RH. Chemoprevention studies of heterocyclic amine-induced colon carcinogenesis. *Cancer Lett* 1999; **143**: 179-183
- 9 **Ip C**, Singh M, Thompson HJ, Scimeca JA. Conjugated linoleic acid suppresses mammary carcinogenesis and proliferative activity of the mammary gland in the rat. *Cancer Res* 1994; **54**: 1212-1215
- 10 **Sebedio JL**, Gnaedig S, Chardigny JM. Recent advances in conjugated linoleic acid research. *Curr Opin Clin Nutr Metab Care* 1999; **2**: 499-506
- 11 **Ip C**, Chin SF, Scimeca JA, Pariza MW. Mammary cancer prevention by conjugated dienoic derivative of linoleic acid. *Cancer Res* 1991; **51**: 6118-6124
- 12 **Schut HA**, Cummings DA, Smale MH, Josyula S, Friesen MD. DNA adducts of heterocyclic amines: formation, removal and inhibition by dietary component. *Mutation Res* 1997; **376**: 185-194
- 13 **Pariza MW**, Hargraves WA. A beef derived mutagenesis modulator inhibits initiation of mouse epidermal tumors by 7, 12-dimethylbenz(a)anthracene. *Carcinogenesis* 1985; **6**: 591-593
- 14 **Hubbard NE**, Lim D, Summers L, Erickson KL. Reduction of murine mammary tumor metastasis by conjugated linoleic acid. *Cancer Lett* 2000; **150**: 93-100
- 15 **Josyula S**, Schut HA. Effect of dietary conjugated linoleic acid on DNA adduct formation of PhIP and IQ after bolus administration to female F344 rats. *Nutr Cancer* 1998; **32**: 139-145
- 16 **Josyula S**, He YH, Ruch RJ, Schut HA. Inhibition of DNA adduct formation of PhIP in female F344 rats by dietary conjugated linoleic acid. *Nutr Cancer* 1998; **32**: 132-138
- 17 **Ip C**, Jiang C, Thompson HJ, Scimeca JA. Retention of conjugated linoleic acid in the mammary gland is associated with tumor inhibition during the post-initiation phase of carcinogenesis. *Carcinogenesis* 1997; **18**: 755-759
- 18 **Kimoto N**, Hirose M, Futakuchi M, Iwata T, Kasai M, Shirai T. Site-dependent modulating effects of conjugated fatty acids from safflower oil in a rat two-stage carcinogenesis model in female Sprague-Dawley rats. *Cancer Lett* 2001; **168**: 15-21
- 19 **Ip C**, Scimeca JA, Thompson H. Effect of timing and duration of dietary conjugated linoleic acid on mammary cancer prevention. *Nutr Cancer* 1995; **24**: 241-247
- 20 **Xue YB**, Chen BQ, Zheng YM, Yuan LL, Liu RH. Effects of conjugated linoleic acid on the metastasis of mouse melanoma B16-MB. *Weisheng Yanjiu* 2001; **30**: 37-39
- 21 **Chen BQ**, Xue YB, Feng WJ, Zheng YM, Liu RH. The effects of conjugated linoleic acid on the adhesion and migration of B16-MB mouse melanoma cells. *J Health Toxicology* 2001; **1**: 20-23
- 22 **Cesano A**, Visonneau S, Scimeca JA, Kritchevsky D, Santoli D. Opposite effects of linoleic acid and conjugated linoleic acid on human prostatic cancer in SCID mice. *Anticancer Res* 1998; **18**: 1429-1434
- 23 **Visonneau S**, Cesano A, Tepper SA, Scimeca JA, Santoli D, Kritchevsky D. Conjugated linoleic acid suppresses the growth of human breast adenocarcinoma cells in SCID mice. *Anticancer Res* 1997; **17**: 969-973
- 24 **Schonberg S**, Krokan HE. The inhibitory effect of conjugated dienoic derivatives (CLA) of linoleic acid on the growth of human tumor cell lines is in part due to increased lipid peroxidation. *Anticancer Res* 1995; **15**: 1241-1246
- 25 **Ip C**, Banni S, Angioni E, Carta G, McGinley J, Thompson HJ, Barbano D, Bauman D. Conjugated linoleic acid-enriched butter fat alters mammary gland morphogenesis and reduces cancer risk in rats. *J Nutr* 1999; **129**: 2135-2142
- 26 **Durgam VR**, Fernandes G. The growth inhibitory effect of conjugated linoleic acid on MCF-7 cells is related to estrogen response system. *Cancer Lett* 1997; **116**: 121-130
- 27 **Cunningham DC**, Harrison LY, Shultz TD. Proliferative responses of normal human mammary and MCF-7 breast cancer cells to linoleic acid, conjugated linoleic acid and eicosanoid synthesis inhibitors in culture. *Anticancer Res* 1997; **17**: 197-203
- 28 **Liu KL**, Belury MA. Conjugated linoleic acid modulation of phorbol ester-induced events in murine keratinocytes. *Lipids* 1997; **32**: 725-730
- 29 **Igarashi M**, Miyazawa T. The growth inhibitory effect of conjugated linoleic acid on a human hepatoma cell line, HepG2, is induced by a change in fatty acid metabolism, but not the facilitation of lipid peroxidation in the cells. *Biochim Biophys Acta* 2001; **1530**: 162-171
- 30 **Thompson H**, Zhu Z, Banni S, Darcy K, Loftus T, Ip C. Morphological and biochemical status of the mammary gland as influenced by conjugated linoleic acid: implication for a reduction in mammary cancer risk. *Cancer Res* 1997; **57**: 5067-5072
- 31 **Miller A**, Stanton C, Devery R. Modulation of arachidonic acid distribution by conjugated linoleic acid isomers and linoleic acid in MCF-7 and SW480 cancer cells. *Lipids* 2001; **36**: 1161-1168
- 32 **Ip MM**, Masso-Welch PA, Shoemaker SF, Shea-Eaton WK, Ip C. Conjugated linoleic acid inhibits proliferation and induces apoptosis of normal rat mammary epithelial cells in primary culture. *Exp Cell Res* 1999; **250**: 22-34
- 33 **Ip C**, Ip MM, Loftus T, Shoemaker S, Shea-Eaton W. Induction of apoptosis by conjugated linoleic acid in cultured mammary tumor cells and premalignant lesions of the rat mammary gland. *Cancer Epidemiol Biomarkers Prev* 2000; **9**: 689-696
- 34 **Choi Y**, Park Y, Storkson JM, Pariza MW, Ntambi JM. Inhibition of stearoyl-CoA desaturase activity by the cis-9,trans-11 isomer and the trans-10,cis-12 isomer of conjugated linoleic acid in MDA-MB-231 and MCF-7 human breast cancer cells. *Biochem Biophys Res Commun* 2002; **294**: 785-790
- 35 **Choi Y**, Park Y, Pariza MW, Ntambi JM. Regulation of stearoyl-CoA desaturase activity by the trans-10,cis-12 isomer of conjugated linoleic acid in HepG2 cells. *Biochem Biophys Res Commun* 2001; **284**: 689-693
- 36 **Thuillier P**, Anchiraco GJ, Nickel KP, Maldve RE, Gimenez-Conti I, Muga SJ, Liu KL, Fischer SM, Belury MA. Activators of peroxisome proliferator-activated receptor- $\alpha$  partially inhibit mouse skin tumor promotion. *Mol Carcinog* 2000; **29**: 134-142
- 37 **Moya-Camarena SY**, Vanden Heuvel JP, Blanchard SG, Leesnitzer LA, Belury MA. Conjugated linoleic acid is a potent naturally occurring ligand and activator of PPAR $\alpha$ . *J Lipid Res* 1999; **40**: 1426-1433
- 38 **Moya-Camarena SY**, Van den Heuvel JP, Belury MA. Conjugated linoleic acid activates peroxisome proliferator-activated receptor  $\alpha$  and  $\beta$  subtypes but does not induce hepatic peroxisome proliferation in Sprague-Dawley rats. *Biochim Biophys Acta* 1999; **1436**: 331-342
- 39 **Liu JR**, Li BX, Chen BQ, Han XH, Xue YB, Yang YM, Zheng YM, Liu RH. Effect of cis-9, trans-11-conjugated linoleic acid on cell cycle of gastric adenocarcinoma cell line (SGC-7901). *World J Gastroenterol* 2002; **8**: 224-229
- 40 **Liu JR**, Chen BQ, Deng H, Han XH, Liu RH. Cellular Apoptosis Induced by Conjugated Linoleic Acid in Human Gastric Cancer

- (SGC-7901) Cells. *Gongye Weisheng Yu Zhiyebing* 2001; **27**: 129-133
- 41 **Liu JR**, Chen BQ, Xue YB, Han XH, Yang YM, Liu RH. Conjugated linoleic acid inhibits the growth of mammary carcinoma cells. *Zhonghua Yufang Yixue* 2001; **35**: 244-247
  - 42 **Zhu Y**, Qiou J, Chen BQ, Liu RH. The inhibitory effect of conjugated linoleic acid on mice forestomach neoplasia induced by benzo(a)pyrene. *Zhonghua Yufang Yixue* 2001; **35**: 19-22
  - 43 **Wu K**, Shan YJ, Zhao Y, Yu JW, Liu BH. Inhibitory effects of RRR- $\alpha$ -tocopheryl succinate on benzo(a)pyrene (B(a)P)-induced forestomach carcinogenesis in female mice. *World J Gastroenterol* 2001; **7**: 60-65
  - 44 **Lu LG**, Zeng MD, Li JQ, Hua J, Fan JG, Qiu DK. Study on the role of free fatty acids in proliferation of rat hepatic stellate cells (II). *World J Gastroenterol* 1998; **4**: 500-502
  - 45 **Devery R**, Miller A, Stanton C. Conjugated linoleic acid and oxidative behaviour in cancer cells. *Biochem Soc Trans* 2001; **29**: 341-344
  - 46 **O'Shea M**, Stanton C, Devery R. Antioxidant enzyme defence responses of human MCF-7 and SW480 cancer cells to conjugated linoleic acid. *Anticancer Res* 1999; **19**: 1953-1959
  - 47 **O'Shea M**, Devery R, Lawless F, Murphy J, Stanton C. Milk fat conjugated linoleic acid (CLA) inhibits growth of human mammary MCF-7 cancer cells. *Anticancer Res* 2000; **20**: 3591-3601
  - 48 **Hawkins RA**, Sangster K, Arends MJ. Apoptotic death of pancreatic cancer cells induced by polyunsaturated fatty acids varies with double bond number and involves an oxidative mechanism. *J Pathol* 1998; **185**: 61-70
  - 49 **Cobb MH**. MAP kinase pathways. *Prog Biophys Mol Biol* 1999; **71**: 479-500
  - 50 **Chang L**, Karin M. Mammalian MAP kinase signalling cascades. *Nature* 2001; **410**: 37-40
  - 51 **Meng AH**, Ling YL, Zhang XP, Zhao XY, Zhang JL. CCK-8 inhibits expression of TNF- $\alpha$  in the spleen of endotoxic shock rats and signal transduction mechanism of p38 MAPK. *World J Gastroenterol* 2002; **8**: 139-143
  - 52 **Fleischer F**, Dabew R, Goke B, Wagner AC. Stress kinase inhibition modulates acute experimental pancreatitis. *World J Gastroenterol* 2001; **7**: 259-265
  - 53 **Wu K**, Liu BH, Zhao DY, Zhao Y. Effect of vitamin E succinate on expression of TGF- $\beta$ 1, c-Jun and JNK1 in human gastric cancer SGC-7901 cells. *World J Gastroenterol* 2001; **7**: 83-87
  - 54 **Jarvis WD**, Fornari FA, Auer KL, Freermerman AJ, Szabo E, Birrer MJ, Johnson CR, Barbour SE, Dent P, Grant S. Coordinate regulation of stress- and mitogen-activated protein kinases in the apoptotic actions of ceramide and sphingosine. *Mol Pharmacol* 1997; **52**: 935-947
  - 55 **Feng DY**, Zheng H, Tan Y, Cheng RX. Effect of phosphorylation of MAPK and Stat3 and expression of c-fos and c-jun proteins on hepatocarcinogenesis and their clinical significance. *World J Gastroenterol* 2001; **7**: 33-36
  - 56 **Dai T**, Rubie E, Franklin CC, Kraft A, Gillespie DA, Avruch J, Kyriakis JM, Woodgett JR. Stress-activated protein kinases bind directly to the delta domain of c-Jun in resting cells: implications for repression of c-Jun function. *Oncogene* 1995; **10**: 849-855
  - 57 **Sun H**, Charles CH, Lau LF, Tonks NK. MKP-1 (3CH134), an immediate early gene product, is a dual specificity phosphatase that dephosphorylates MAP kinase *in vivo*. *Cell* 1993; **75**: 487-493

Edited by Wu XN

# *Helicobacter pylori* infection and respiratory diseases: a review

Anastasios Roussos, Nikiforos Philippou, Konstantinos I Gourgoulanis

**Anastasios Roussos, Nikiforos Philippou**, 9th Department of Pulmonary Medicine, "SOTIRIA" Chest Diseases Hospital, Athens, Greece  
**Konstantinos I Gourgoulanis**, Pulmonary Department, Medical University of Thessaly, Larisa, Greece  
**Correspondence to:** Dr Anastasios Roussos, 20 Ierosolimon Street, PO: 11252, Athens, Greece. roumar26@yahoo.com  
**Telephone:** +301-8646215 **Fax:** +301-8646215  
**Received:** 2002-10-25 **Accepted:** 2002-11-07

## Abstract

In the past few years, a variety of extradigestive disorders, including cardiovascular, skin, rheumatic and liver diseases, have been associated with *Helicobacter pylori* (*H. pylori*) infection. The activation of inflammatory mediators by *H. pylori* seems to be the pathogenetic mechanism underlying the observed associations. The present review summarizes the current literature, including our own studies, concerning the association between *H. pylori* infection and respiratory diseases.

A small number of epidemiological and serologic, case-control studies suggest that *H. pylori* infection may be associated with the development of chronic bronchitis. A frequent coexistence of pulmonary tuberculosis and *H. pylori* infection has also been found. Moreover, recent studies have shown an increased *H. pylori* seroprevalence in patients with bronchiectasis and in those with lung cancer. On the other hand, bronchial asthma seems not to be related with *H. pylori* infection.

All associations between *H. pylori* infection and respiratory diseases are primarily based on case-control studies, concerning relatively small numbers of patients. Moreover, there is a lack of studies focused on the pathogenetic link between respiratory diseases and *H. pylori* infection. Therefore, we believe that larger studies should be undertaken to confirm the observed results and to clarify the underlying pathogenetic mechanisms.

Roussos A, Philippou N, Gourgoulanis KI. *Helicobacter pylori* infection and respiratory diseases: a review. *World J Gastroenterol* 2003; 9(1): 5-8  
<http://www.wjgnet.com/1007-9327/9/5.htm>

## INTRODUCTION

*Helicobacter pylori* (*H. pylori*) is a slow-growing, microaerophilic, gram-negative bacterium, whose most striking biochemical characteristic is the abundant production of urease. This bacterium colonizes gastric mucosa and elicits both inflammatory and immune lifelong responses, with release of various bacterial and host-dependent cytotoxic substances<sup>[1]</sup>. Pathological studies and extensive clinical trials, carried out in the past few years, have proved the causative role of *H. pylori* in the development of chronic gastritis<sup>[2]</sup> and peptic ulcer disease<sup>[3]</sup>. It seems that this bacterium is also causally related to low-grade B-cell lymphoma of gastric mucosa-associated-lymphoid-tissue (MALT-lymphoma)<sup>[4]</sup>. Moreover, *H. pylori* infection has been established as a risk factor for the development of both diffuse and intestinal types of gastric cancer<sup>[5]</sup>.

Recent studies suggest an epidemiological association

between *H. pylori* infection and several extragastrointestinal pathologies, including cardiovascular, skin, rheumatic and liver diseases (Table 1)<sup>[6,7]</sup>. Unfortunately, such epidemiological studies are influenced by a wide variety of confounding factors, i.e. socioeconomic status, time of acquisition of the infection, presence of different bacterial strains and previous antibiotic therapy. However, according to many authors, the observed associations might be true and explained by a role of *H. pylori* infection in the pathogenesis of certain extradigestive disorders. It is well known that *H. pylori* colonization of the gastric mucosa stimulates the release of various proinflammatory substances, such as cytokines, eicosanoids and proteins of the acute phase<sup>[8]</sup>. Moreover, a cross mimicry between bacterial and host antigens exists in *H. pylori* infected patients<sup>[9]</sup>. Therefore, a pathogenetic link between *H. pylori* infection and diseases characterized by activation of inflammatory mediators and/or induction of autoimmunity might exist.

Chronic inflammation and increased immune response have been observed in a variety of respiratory diseases, including chronic bronchitis<sup>[10,11]</sup> and bronchiectasis<sup>[12]</sup>. Moreover, both chronic obstructive pulmonary disease<sup>[13,14]</sup> and pulmonary tuberculosis<sup>[15]</sup> are more prevalent in peptic ulcer patients than in the general population. Based on these facts, many recent studies have focused on the potential association between *H. pylori* infection and various respiratory disorders. Table 2 summarizes those respiratory diseases whose relation with *H. pylori* infection has been studied in the literature.

The aim of the present report is to provide a critical review of the current literature, including our own studies, as regards the association between *H. pylori* infection and respiratory diseases.

**Table 1**<sup>[6,7]</sup> Extradigestive diseases associated with *H. pylori* infection

### Vascular diseases

Ischaemic heart disease  
Primary Raynaud's phenomenon  
Primary headache

### Skin diseases

Idiopathic chronic urticaria  
Rosacea  
Alopecia areata

### Autoimmune diseases

Sjogren's syndrome  
Autoimmune thyroiditis  
Autoimmune thrombocytopenia  
Schoenlein-Henoch purpura

### Other diseases

Liver cirrhosis  
Growth retardation  
Chronic idiopathic sideropenia  
Sudden infant death  
Diabetes mellitus

**Table 2** Respiratory diseases studied for a relationship with *H. pylori* infection

### Chronic bronchitis

Pulmonary tuberculosis  
Bronchiectasis  
Lung cancer  
Bronchial asthma

## HELICOBACTER PYLORI INFECTION AND CHRONIC BRONCHITIS

Chronic bronchitis is a pulmonary disease characterized by, primarily irreversible, airflow obstruction due to the chronic inflammation of the small airways. The presence of airflow obstruction that is not fully reversible is confirmed by spirometry (postbronchodilator FEV<sub>1</sub><80 % of the predicted value, in combination with an FEV<sub>1</sub>/FVC<70 %). Although its true prevalence remains unknown, it is estimated that approximately 12.5 million persons in the United States suffer from chronic bronchitis<sup>[16]</sup>.

Chronic bronchitis had been associated with gastroduodenal ulcer many years before the identification of *H. pylori* infection as a cause of peptic ulcer disease. Three epidemiological studies, carried out between 1968 and 1986, showed that the prevalence of chronic bronchitis in peptic ulcer patients was increased two-to-three fold compared with that in ulcer-free controls<sup>[13,14,17]</sup>. Moreover, a follow-up study demonstrated that chronic bronchitis was a major cause of death among patients with peptic ulcer disease<sup>[18]</sup>.

The reported association between these two diseases was originally attributed to the known role of cigarette smoking as an independent factor in both ulcerogenesis and development of chronic bronchitis. However, in 1998, Gaseli and colleagues carried out a prospective pilot study in a sample of 60 Italian patients with chronic bronchitis and found an increased seroprevalence of *H. pylori* infection compared to that detected in 69 healthy controls (81.6 % versus 57.9 % respectively,  $P=0.008$ ). In this study, the odds ratio for chronic bronchitis in the presence of *H. pylori* infection, calculated after adjustment for age and social status, was 3.4<sup>[19]</sup>. These results suggested, for the first time, that *H. pylori* infection per se might be related to an increased risk of developing chronic bronchitis. Two years later, a large epidemiological study in 3608 Danish adults showed that chronic bronchitis might be more prevalent in *H. pylori* IgG seropositive women than in uninfected ones (odds ratio 1.6, with a 95 % confidence interval of 1.1-2.5)<sup>[20]</sup>. In order to further investigate the reported association between *H. pylori* infection and chronic bronchitis, we recently performed a case-control study in a cohort of 144 Greek patients with chronic bronchitis and 120 control subjects. Our results were in accordance with those of Gaselli and associates, as we also found that *H. pylori* seropositivity in patients was significantly higher than that in controls (83.3 % vs 60 %,  $P=0.007$ )<sup>[21]</sup>.

The mechanisms underlying the suggested association between *H. pylori* infection and chronic bronchitis remain unclear. This association might reflect either susceptibility induced by common factors or a kind of causal relationship between these two conditions. It is well known that age, sex and socioeconomic status are related with both *H. pylori* infection<sup>[1]</sup> and risk of developing chronic bronchitis<sup>[16]</sup>. However, in all mentioned studies above patients with chronic bronchitis were well matched with control subjects for these parameters. Tobacco use could be another confounding factor. Cigarette smoking is the major cause of chronic bronchitis<sup>[16]</sup>. On the other hand, data on the relation between *H. pylori* infection and smoking habits are controversial. The prevalence of *H. pylori* infection in smokers has been variously reported as low<sup>[22]</sup>, normal<sup>[23]</sup>, and high<sup>[24]</sup>. As the relation between smoking and *H. pylori* infection has not been clarified yet, the possible impact of cigarette smoking on both chronic bronchitis and *H. pylori* infection should be regarded as a potential limitation of the reviewed studies.

Unfortunately, there are no studies in the literature focused on the potential aetio-pathogenetic role of *H. pylori* infection in chronic bronchitis. Some authors hypothesized that the chronic

activation of inflammatory mediators induced by *H. pylori* infection might lead to the development of a non-specific inflammatory process, such as chronic bronchitis<sup>[19,21]</sup>. It is well known that *H. pylori* and particularly those strains bearing the cytotoxin associated gene-A (cagA positive strains), stimulates the release of a variety of proinflammatory cytokines, including interleukin-1 (IL-1), IL-8 and tumour necrosis factor- $\alpha$ <sup>[25,26]</sup>. The eradication of *H. pylori* leads to normalization of serum cytokines levels<sup>[27]</sup>. Recent studies showed that the same cytokines might be released during the course and exacerbations of chronic bronchitis<sup>[10,11,28]</sup>. The underlying mechanisms, which induce and control this inflammatory process in chronic bronchitis, are still unclear. Therefore, we could hypothesize that *H. pylori* infection might play a proinflammatory role and co-trigger chronic bronchitis with other more specific environmental, genetic and unknown yet factors.

In conclusion, the primary evidence for an association between *H. pylori* infection and chronic bronchitis rests on serologic, case-control studies. Studies estimating the relative risk of developing chronic bronchitis for *H. pylori* infected patients and the effect of *H. pylori* eradication on the natural history of chronic bronchitis should be undertaken. The pathogenetic mechanisms underlying this association need also further evaluation. Future studies concerning this aspect should be focused on the prevalence of cagA positive *Helicobacter* strains and their induced proinflammatory markers, in patients with chronic bronchitis.

## HELICOBACTER PYLORI INFECTION AND PULMONARY TUBERCULOSIS

Tuberculosis (TB) is a chronic bacterial infection caused by *Mycobacterium tuberculosis* and characterized by the formation of granulomas in infected tissues and by cell-mediated hypersensitivity. The lungs are primarily infected. However, any other organ may be involved. Although there is a lack of epidemiological evidence concerning the worldwide prevalence of TB, it has been estimated that one third of the world population is infected with *Mycobacterium tuberculosis* and there are ten million new cases of active TB each year. The vast majority of them occur in the developing countries, where TB remains a common health problem<sup>[29]</sup>.

In 1992, Mitchell *et al* carried out a large cross-sectional study concerning the *H. pylori* epidemiology in a southern China population. They found that a history of pulmonary TB might be associated with an increased prevalence of *H. pylori* infection<sup>[30]</sup>. More recently, Woeltje *et al* assessed the prevalence of tuberculin skin test (TST) positivity in a cohort of 346 newly hospitalized patients. A history of peptic ulcer disease was one of the identified risk factors for a positive TST test (odds ratio: 4.53,  $P=0.017$ )<sup>[31]</sup>. In order to further investigate the possible association between pulmonary TB and *H. pylori* infection, Sanaka *et al* performed, in 1998, a serologic case-control study in a hospitalized population. No difference in *H. pylori* seroprevalence among 40 inpatients on antituberculosis chemotherapy for less than three months, 43 TB patients on chemotherapy for more than three months and 60 control subjects was detected (73.3 %, 65 % and 69.8 % respectively,  $P>0.5$  in all comparisons)<sup>[32]</sup>. However, in this study the eradication of *H. pylori* by antituberculosis drugs could not be excluded. Rifampicin and Streptomycin, two drugs commonly used in antituberculosis regimens, are effective against *H. pylori* and decrease in *H. pylori* seroprevalence during antituberculosis therapy has been reported<sup>[33,34]</sup>. Therefore, we recently carried out a case-control study focused on the seroprevalence of *H. pylori* in TB patients, before the initiation of antituberculosis treatment. A total of 80 TB patients and 70 control subjects, well matched for age, sex and social

status, were recruited into this study. We found that the *H. pylori* seropositivity in the TB group was significantly higher than that of controls (87.5 % vs 61.4 %,  $P=0.02$ ). The mean serum concentration of IgG antibodies against *H. pylori* was also significantly higher in TB patients than in control subjects ( $39.0 \pm 25.2$  U/ml vs  $26.1 \pm 21.2$  U/ml,  $P=0.001$ )<sup>[35]</sup>.

Taken together, data in the literature on the relationship between *H. pylori* infection and pulmonary TB are still insufficient. The observed frequent coexistence of both infections must be confirmed in a larger number of patients. This coexistence might reflect susceptibility to both *H. pylori* and *Mycobacterium tuberculosis* induced by common host genetic factors. It has been suggested that HLA-DQ serotype may contribute to enhanced mycobacterial survival and replication<sup>[36]</sup>. Recent studies showed that the same serotype is also associated with increased susceptibility to *H. pylori* infection<sup>[37,38]</sup>. Poor socioeconomic and sanitary conditions during childhood could be another factor responsible for the association between the two infections, as it is well known that in developing countries acquisition of both *H. pylori* and *Mycobacterium tuberculosis* occurs early in life<sup>[39,40]</sup>. Therefore, we believe that studies focused on the common, either genetic or environmental, predisposition to both bacteria are needed.

## HELICOBACTER PYLORI INFECTION AND BRONCHIECTASIS

Bronchiectasis is an abnormal and permanent dilation of bronchi, due to inflammation and destruction of the structural components of the bronchial wall. Persistent or recurrent cough, purulent sputum production and/or hemoptysis are symptoms presented during the clinical course of this disorder. A wide variety of respiratory infections, toxic substances and rare congenital syndromes are associated with the development of bronchiectasis. However, a great percentage of cases are of unknown cause<sup>[41]</sup>.

In 1998, Tsang *et al* found that the *H. pylori* seroprevalence in 100 patients with bronchiectasis (76 %) was higher than that in the controls (54.3 %,  $P=0.001$ ). Further analysis in studied patients revealed an association between *H. pylori* seropositivity and 24-hours sputum volume ( $P=0.03$ )<sup>[42]</sup>.

As far as we know, the study of Tsang *et al* is the only report in the literature concerning the association between *H. pylori* infection and bronchiectasis. The authors hypothesized that the spilling or inhalation of *H. pylori* into the respiratory tract might lead to a chronic bronchial inflammatory disorder such as bronchiectasis. However, although *H. pylori* has been identified in the tracheobronchial aspirates in mechanically ventilated patients<sup>[43]</sup>, neither identification in human bronchial tissue nor isolation from bronchoalveolar lavage (BAL) fluid have been achieved yet<sup>[1]</sup>. On the other hand, recent studies have shown that inflammation in bronchiectasis is primarily cytokine-mediated<sup>[12,44]</sup>. Therefore, the activation of systemic inflammatory mediators by chronic *H. pylori* infection could represent a possible pathogenetic link between these two diseases.

In conclusion, the possible association between *H. pylori* and bronchiectasis seems intriguing and might have a pathogenetic basis. However, studies in larger series are needed to confirm this association and to clarify the underlying mechanisms. As pulmonary TB is a common cause of bronchiectasis, we believe that the increased prevalence of *H. pylori* infection in TB patients should be taken into account in the design of these future studies.

## HELICOBACTER PYLORI INFECTION AND OTHER RESPIRATORY DISEASES

**Lung cancer** A recent study showed a higher *H. pylori* seroprevalence (89.5 %) among 50 patients with lung cancer than that in control subjects (64 %,  $P<0.05$ ). The CagA strain

seropositivity was about thrice as high as in controls. (63 % vs 21.5 % respectively,  $P<0.05$ ). Lung cancer patients were characterized by a significant increase of gastrin concentration in both serum and bronchoalveolar lavage (BAL). An enhanced m-RNA expression for gastrin and its receptor, as well as for cyclooxygenase (COX)-2, in the tumor tissue was also detected. Therefore, the authors hypothesized that *H. pylori* might contribute to lung carcinogenesis, via enhancement of gastrin synthesis. Gastrin might induce increased mucosal cell proliferation of bronchial epithelium and lead to atrophy and induction of COX-2, as it happens in gastric cancer. Finally, the authors proposed that *H. pylori* should be eradicated in lung cancer patients, in order to reduce the *H. pylori* provoked hypergastrinemia and COX-2 expression<sup>[45]</sup>.

Chronic bronchitis, which is associated with both lung cancer and *H. pylori* infection, might be a confounding factor in this study. Moreover, although some authors have also showed an increased gastrin concentration in serum and BAL fluid in lung cancer patients<sup>[46,47]</sup>, others did not confirm this finding<sup>[48]</sup>. Therefore, we believe that before adapting the *H. pylori* eradication in lung cancer patients, further studies are needed to examine whether the reported epidemiological association between these two diseases has a pathogenetic basis. **Bronchial asthma** In 2000, Tsang *et al* estimated the prevalence of *H. pylori* infection in a cohort of 90 patients with bronchial asthma. *Helicobacter pylori* seroprevalence did not differ significantly between asthmatic and control subjects (47.3 % vs 38.1 %,  $P>0.05$ ), while serum concentration of IgG antibodies against *H. pylori* did not correlate with spirometric values and duration of asthma. The authors concluded that bronchial asthma might not be associated with *H. pylori* infection<sup>[49]</sup>. Moreover, as far as we know there is a lack of a theoretical hypothesis that might explain a possible association between these two diseases. Therefore, we believe that our knowledge on the association between *H. pylori* infection and respiratory diseases is unlikely to be advanced by more studies concerning the prevalence of *H. pylori* infection in patients with bronchial asthma.

## CONCLUSIONS-FUTURE CHALLENGES

At present, the primary evidence for a link between *H. pylori* infection and respiratory diseases rests on case-control studies, concerning relatively small numbers of patients. Future studies should be large enough for moderate-sized effects to be assessed or registered reliably. The activation of inflammatory mediators by *H. pylori* infection might be the pathogenetic mechanism underlying the observed associations. Therefore, the role of genetic predisposition of the infected host, the presence of strain-specific virulence factors and the serum concentration of proinflammatory markers in *H. pylori* infected patients with respiratory diseases needs further evaluation. Finally, randomized control studies should be undertaken, in order to clarify the effect of the *H. pylori* eradication on the prevention, development and natural history of these disorders.

## REFERENCES

- 1 **Peterson WL**, Graham DY. *Helicobacter pylori*. In: Feldman M, Scharschmidt BF, Sleisenger MH editors *Gastrointestinal and liver Disease. Pathophysiology, diagnosis, management*. 6th ed. Philadelphia: WB Saunders 1998; p: 604-619
- 2 **Cave DR**. Chronic gastritis and *Helicobacter pylori*. *Semin Gastrointestinal Dis* 2001; **12**: 196-202
- 3 **Cohen H**. Peptic ulcer and *Helicobacter pylori*. *Gastroenterol Clin North Am* 2000; **29**: 775-789
- 4 **Parsonnet J**, Hansen S, Rodriguez L, Gelb AB, Warnke RA, Jellum E, Orentreich N, Vogelstein JH, Friedman GD. *Helicobacter pylori* and gastric lymphoma. *N Engl J Med* 1994; **330**: 1267-1271

- 5 **Xue FB**, Xu YY, Wan Y, Pan BR, Ren J, Fan DM. Association of *H. pylori* infection with gastric carcinoma. A Meta analysis. *World J Gastroenterol* 2001; **7**: 801-804
- 6 **Realdi G**, Dore MP, Fastame L. Extradigestive manifestations of *Helicobacter pylori* infection. Fact and fiction. *Dig Dis Sci* 1999; **44**: 229-236
- 7 **Gasbarrini A**, Franceschi F, Armuzzi A, Ojetti V, Candelli M, Sanz Torre E, Lorenzo AD, Anti M, Pretolani S, Gasbarinni G. Extradigestive manifestations of *Helicobacter pylori* gastric infection. *Gut* 1999; **45**(Suppl 1): 9-12
- 8 **Crabtree JE**. Role of cytokines in pathogenesis of *Helicobacter pylori* induced mucosal damage. *Dig Dis Sci* 1998; **43**(Suppl 9): 46-55
- 9 **Negrini R**, Savio A, Poesi C, Appelmelk BJ, Buffoli F, Paterlini A, Cesari P, Graffeo M, Vaira D, Franzin G. Antigenic mimicry between *H. pylori* and gastric mucosa in the pathogenesis of body atrophic gastritis. *Gastroenterology* 1996; **111**: 655-665
- 10 **Huang SL**, Su CH, Chang SC. Tumor necrosis factor- $\alpha$  gene polymorphism in chronic bronchitis. *Am J Resp Crit Care Med* 1997; **156**: 1436-1439
- 11 **Nelson S**, Summer WR, Mason CM. The role of the inflammatory response in chronic bronchitis: therapeutic implications. *Semin Respir Infect* 2000; **15**: 24-31
- 12 **Silva JR**, Jones JA, Cole P, Poulter L. The immunological component of the cellular inflammatory infiltrate in bronchiectasis. *Thorax* 1989; **44**: 668-673
- 13 **Langman MJ**, Cooke AR. Gastric and duodenal ulcer and their associated diseases. *Lancet* 1976; **1**: 680-683
- 14 **Kellow JE**, Tao Z, Piper DW. Ventilatory function in chronic peptic ulcer. *Gastroenterology* 1986; **91**: 590-595
- 15 **Lundegardh G**, Helmick C, Zack M, Adami HO. Mortality among patients with partial gastrectomy for benign ulcer disease. *Dig Dis Sci* 1994; **39**: 340-346
- 16 **Gomez FP**, Rodriguez-Roisin R. Global Initiative for Chronic Obstructive Lung Disease (GOLD) guidelines for chronic obstructive pulmonary disease. *Curr Opin Pulm Med* 2002; **8**: 81-86
- 17 **Arora OP**, Kapoor CP, Sobti P. Study of gastroduodenal abnormalities in chronic bronchitis and emphysema. *Am J Gastroenterol* 1968; **50**: 289-296
- 18 **Bonnevie O**. Causes of death in duodenal and gastric ulcer. *Gastroenterology* 1977; **73**: 1000-1004
- 19 **Gaselli M**, Zaffoni E, Ruina M, Sartori S, Trevisani L, Ciaccia A, Alvisi V, Fabbri L, Papi A. *Helicobacter pylori* and chronic bronchitis. *Scand J Gastroenterol* 1999; **34**: 828-830
- 20 **Rosenstock SJ**, Jorgensen T, Andersen LP, Bonnevie O. Association of *Helicobacter pylori* infection with lifestyle, chronic disease, body indices and age at menarche in Danish adults. *Scand J Public Health* 2000; **28**: 32-40
- 21 **Roussos A**, Tsimpoukas F, Anastasakou E, Alepopoulou D, Paizis I, Philippou N. *Helicobacter pylori* seroprevalence in patients with chronic bronchitis. *J Gastroenterol* 2002; **37**: 332-335
- 22 **Ogihara A**, Kikuchi S, Hasegawa A, Kurosawa M, Miki K, Kaneko E, Mizukoshi H. Relationship between *Helicobacter pylori* infection and smoking and drinking habits. *J Gastroenterol Hepatol* 2000; **15**: 271-276
- 23 **Brenner H**, Rothenbacher D, Bode G, Adler G. Relation of smoking and alcohol and coffee consumption to active *Helicobacter pylori* infection: cross sectional study. *BMJ* 1997; **315**: 1489-1492
- 24 **Parasher G**, Eastwood GL. Smoking and peptic ulcer in the *Helicobacter pylori* era. *Eur J Gastroenterol Hepatol* 2000; **12**: 843-853
- 25 **Perri F**, Clemente R, Festa V, De Ambrosio CC, Quitadamo M, Fusillo M, Grossi E, Andriulli A. Serum tumour necrosis factor- $\alpha$  is increased in patients with *Helicobacter pylori* infection and CagA antibodies. *Ital J Gastroenterol Hepatol* 1999; **31**: 290-294
- 26 **Russo F**, Jirillo E, Clemente C, Messa C, Chiloiro M, Riezzo G, Amati L, Caradonna L, Di Leo A. Circulating cytokines and gastrin levels in asymptomatic subjects infected by *Helicobacter pylori* (*H. pylori*). *Immunopharmacol Immunotoxicol* 2001; **23**: 13-24
- 27 **Kountouras J**, Boura P, Lygidakis NJ. Omeprazole and regulation of cytokine profile in *Helicobacter pylori*-infected patients with duodenal ulcer disease. *Hepatogastroenterology* 2000; **47**: 1301-1304
- 28 **Keatings VM**, Collins PD, Scott DM, Barnes PJ. Differences in interleukin-8 and tumor necrosis factor- $\alpha$  in induced sputum from patients with chronic obstructive pulmonary disease or asthma. *Am J Respir Crit Care Med* 1996; **153**: 530-534
- 29 **Daniel TM**. Tuberculosis In Harrison's Principles of internal medicine 14<sup>th</sup> edition. New York: McGraw-Hill inc 1998; **p**: 710-718
- 30 **Mitchell HM**, Li YY, Hu PJ, Liu Q, Chen M, Du GG, Wang ZL, Lee A, Hazell SL. Epidemiology of *Helicobacter pylori* in southern China: identification of early childhood as the critical period for acquisition. *J Infect Dis* 1992; **166**: 149-153
- 31 **Woetje KF**, Kilo CM, Johnson K, Primack J, Frases VJ. Tuberculin skin test of hospitalized patients. *Infect Control Hosp Epidemiol* 1997; **18**: 561-565
- 32 **Sanaka M**, Kuyama Y, Iwasaki M, Hanada Y, Tsuchiya A, Haida T, Hiramasa S, Yamaoka S, Yamanaka M. No difference in seroprevalences of *Helicobacter pylori* infection between patients with pulmonary tuberculosis and those without. *J Clin Gastroenterol* 1998; **27**: 331-334
- 33 **Sanaka M**, Kuyama Y, Yamanaka M, Iwasaki M. Decrease of serum concentrations of *Helicobacter pylori* IgG antibodies during antituberculosis therapy: the possible eradication by Rifampicin and Streptomycin. *Am J Gastroenterol* 1999; **94**: 1983-1984
- 34 **Heep M**, Beck D, Bayerdorffer E, Lehn N. Rifampin and rifabutin resistance mechanisms in *Helicobacter pylori*. *Antimicrob Agents Chemother* 1999; **43**: 1497-1499
- 35 **Filippou N**, Roussos A, Tsimboukas F, Tsimogianni A, Anastasakou E, Mavrea S. *Helicobacter pylori* seroprevalence in patients with pulmonary tuberculosis. *J Clin Gastroenterol* 2002; **34**: 189
- 36 **Goldfeld AE**, Delgado JC, Thim S, Bozon MV, Uglieroro AM, Turbay D, Cohen C, Yunis EJ. Association of an HLA-DQ allele with clinical tuberculosis. *JAMA* 1998; **279**: 226-228
- 37 **Azuma T**, Konishi J, Tanaka Y, Hirai M, Ito S, Kato T, Kohli Y. Contribution of HLA-DQA gene to host's response against *Helicobacter pylori*. *Lancet* 1994; **343**: 542-543
- 38 **Beales ILP**, Davey NJ, Pusey CD, Lechler RI, Calam J. Long-term sequelae of *Helicobacter pylori* gastritis. *Lancet* 1995; **346**: 381-382
- 39 **Graham DY**, Adam E, Reddy GT, Agarwal JP, Agarwal R, Evans DJ, Malaty HM, Evans DG. Seroepidemiology of *Helicobacter pylori* infection in India: Comparison of developing and developed countries. *Dig Dis Sci* 1991; **36**: 1084-1088
- 40 **Martin G**, Lazarus A. Epidemiology and diagnosis of tuberculosis. Recognition of at-risk patients is key to prompt detection. *Postgrad Med* 2000; **108**: 42-54
- 41 **Cole PJ**. Bronchiectasis In RL Brewis, B Corrin, DM Geddes, GJ Gibson, editors. Respiratory Medicine. Philadelphia: WB Saunders 1995: 1286-1317
- 42 **Tsang KW**, Lam SK, Lam WK, Karlberg J, Wong BC, Yew WW, Ip MS. High seroprevalence of *Helicobacter pylori* in active bronchiectasis. *Am J Resp Crit Care Med* 1998; **158**: 1047-1051
- 43 **Mitz HS**, Farber SS. Demonstration of *Helicobacter pylori* in tracheal secretions. *J Am Osteopath Assoc* 1993; **93**: 87-91
- 44 **Eller J**, Lapa JR, Poulter RW, Lode H, Cole PJ. Cells and cytokines in chronic bronchial infection. *Ann NY Acad Sci* 1994; **725**: 331-345
- 45 **Gocyk W**, Nikliski T, Olechnowicz H, Duda A, Bielanski W, Konturek P, Konturek S. *Helicobacter pylori*, gastrin and cyclooxygenase-2 in lung cancer. *Med Sci Monit* 2000; **6**: 1085-1092
- 46 **Zhou Q**, Yang Z, Yang J, Tian Z, Zhang H. The diagnostic significance of gastrin measurement of bronchoalveolar lavage fluid for lung cancer. *J Surg Oncol* 1992; **50**: 121-124
- 47 **Zhou Q**, Zhang H, Pang X, Yang J, Tain Z, Wu Z, Yang Z. Pre- and postoperative sequential study on the serum gastrin level in patients with lung cancer. *J Surg Oncol* 1993; **51**: 22-25
- 48 **Dowlati A**, Bury T, Corhay JL, Weber T, Lamproye A, Mendes P, Radermecker M. Gastrin levels in serum and bronchoalveolar lavage of patients with lung cancer: comparison with chronic obstructive pulmonary disease. *Thorax* 1996; **51**: 1270-1272
- 49 **Tsang KW**, Lam WK, Chan KN, Hu W, Wu A, Kwok E, Zheng L, Wong BC, Lam SK. *Helicobacter pylori* seroprevalence in asthma. *Respiratory medicine* 2000; **94**: 756-759

# Association between pepsinogen C gene polymorphism and genetic predisposition to gastric cancer

Hui-Jie Liu, Xiao-Lin Guo, Ming Dong, Lan Wang, Yuan Yuan

**Hui-Jie Liu, Xiao-Lin Guo, Ming Dong, Lan Wang, Yuan Yuan,** Cancer Institute, First Affiliated Hospital, China Medical University, Shenyang, 110001, Liaoning Province, China

**Supported by** The National Basic Research Program (973) of China, No.G1998051203 and National Natural Science Foundation of China, No.30171054

**Correspondence to:** Dr. Yuan Yuan, Cancer Institute, First Affiliated Hospital, China Medical University, 155 Northern Nanjing Street, Heping District, Shenyang 110001, Liaoning Province, China. yyuan@mail.cmu.edu.cn

**Telephone:** +86-24-23256666-6153 **Fax:** +86-24-22703576

**Received:** 2002-06-28 **Accepted:** 2002-07-25

## Abstract

**AIM:** To identify a molecular marker for gastric cancer, and to investigate the relationship between the polymorphism of pepsinogen C (PGC) gene and the genetic predisposition to gastric cancer.

**METHODS:** A total of 289 cases were involved in this study. 115 cases came from Shenyang area, a low risk area of gastric cancer, including 42 unrelated controls and 73 patients with gastric cancer. 174 cases came from Zhuanghe area, a high-risk area of gastric cancer, including 113 unrelated controls, and 61 cases from gastric cancer kindred families. The polymorphism of PGC gene was detected by polymerase chain reaction (PCR) and the relation between the genetic polymorphism of PGC and gastric cancer was examined.

**RESULTS:** Four alleles, 310bp (allele 1), 400bp (allele 2), 450bp (allele 3), and 480bp (allele 4) were detected by PCR. The frequency of allele 1 was higher in patients with gastric cancer than that in controls. Genotypes containing homogenous allele 1 were significantly more frequent in patients with gastric cancer than that in controls (0.33, 0.14,  $\chi^2=3.86$ ,  $P<0.05$ ). There was no significant difference between the control group of Zhuanghe and the group of gastric cancer kindred. But the frequency of allele 1 was higher in control group of Zhuanghe area than that in control group of Shenyang area and genotypes containing homogenous allele 1 were significantly more frequent in the control group of Zhuanghe area than those in control group of Shenyang area (0.33, 0.14,  $\chi^2=4.32$ ,  $P<0.05$ ). In the group of gastric cancer kindred the frequency of allele 1 was significantly higher than that in control group of Shenyang area (0.5164, 0.3571,  $\chi^2=4.47$ ,  $P<0.05$ ). Genotypes containing homogenous allele 1 were significantly more frequent in the group of gastric cancer kindred than those in control group of Shenyang area (0.36, 0.14,  $\chi^2=4.91$ ,  $P<0.05$ ).

**CONCLUSION:** These results suggest that there is some relation between pepsinogen C gene polymorphism and gastric cancer, and the person with homogenous allele 1 predisposes to gastric cancer than those with other genotypes. Pepsinogen C gene polymorphism may be used as a genetic marker for a genetic predisposition to gastric

cancer. The distribution of pepsinogen C gene polymorphism in Zhuanghe, a high-risk area of gastric cancer, is different from that in Shenyang, a low risk area of gastric cancer.

Liu HJ, Guo XL, Dong M, Wang L, Yuan Y. Association between pepsinogen C gene polymorphism and genetic predisposition to gastric cancer. *World J Gastroenterol* 2003; 9(1): 50-53  
<http://www.wjgnet.com/1007-9327/9/50.htm>

## INTRODUCTION

Gastric cancer is the second most common cancer in the world. Especially in China and other eastern Asian countries, the mortality of gastric cancer is still in the leading status of all cancers. The 5-year survival rate of gastric cancer is low, and identification and a better control of risk factors seem to be the most effective means of prevention. It was showed that many factors were ascribing to the cause of gastric cancer, including the living habit, nutrition<sup>[1-3]</sup>, microbe<sup>[4-6]</sup>, and genetic predisposition<sup>[7-10]</sup>. Recently, following the primary completion of Human Genome Project, the association of genetic polymorphisms with diseases came to the study frontier<sup>[11-14]</sup>. Genetic polymorphisms are defined as variations in DNA that are observed in 1 % or more of the population. The study of genetic polymorphisms promises to help define pathophysiologic mechanisms<sup>[15,16]</sup>, to identify individuals at risk for disease<sup>[17-19]</sup> and to suggest novel targets for drug design and treatment<sup>[20-24]</sup>.

Pepsinogen C (PGC), also known as progastricsin, is the precursor of pepsin C or gastricsin. PGC can be detected throughout the stomach and proximal duodenum from the period of late infant stages to adult. Therefore it is also considered to be a mature marker of stomach cells<sup>[25]</sup>. PGC consists of two electrophoretic isozymogens<sup>[26]</sup>. No genetic variation was reported at the protein level. At the DNA level, however, an about 100bp insertion-deletion polymorphism was observed between exon 7 and exon 8 with several restriction enzymes. The polymorphism in PGC gene locus can be identified by both Southern blot and PCR methods.

In this study, we analyzed the PGC gene polymorphism of patients with gastric cancer and members with gastric cancer family history, and then examined the association between PGC gene polymorphism and gastric cancer.

## MATERIALS AND METHODS

### Patients

A total of 289 cases were involved in this study. 42 cases as health control came from the Blood Bank of the First Affiliated Hospital, China Medical University, whose health condition were checked up before blood was collected. 73 gastric cancer patients came from the Department of Oncology. 174 cases came from Zhuanghe, an area with high gastric cancer mortality, in the eastern Liaoning Province, China as described previously<sup>[27]</sup>, including 61 members from seven gastric cancer kindred families and 113 health controls whose family do not have gastric cancer history. In every gastric cancer kindred, at least two persons of the family are gastric cancer patients.



### Analysis of PGC gene polymorphism

The genomic DNA from peripheral blood was amplified by PCR. The primers used were: upstream, 5'-AGCCCTAAGCCTGTTTTTGG-3'; and the downstream, 5'-GGCCAGATCTGCGTGTTTTA-3' [28]. The reaction mixture including 32.15pmol of each primer was subjected to 5 minutes at 95 °C; 35 cycles of one minute at 94 °C, one minute at 57 °C, one minute at 72 °C; with a final extension at 72 °C for 5 minutes. The amplification reaction proceeded in a thermocycler (PE-9 600). 12 µl of reaction mixture (50 µl in total volume) underwent electrophoresis in 2 % agarose gel, and the gel was stained with ethidium bromide.

### Statistical analysis

The association between the polymorphism of PGC gene and gastric cancer was tested using  $\chi^2$  test, with significance assigned to values below  $P<0.05$ .

## RESULTS

### Detection of PGC gene polymorphism

After PCR, four alleles with different size were obtained: 310bp (allele 1), 400bp (allele 2), 450bp (allele 3), and 480bp (allele 4) (Figure 1). These results showed a little difference from the data showed by Southern blot, which demonstrated two different alleles (3.5kb and 3.6kb). According to the study of Ohtaki *et al.*, the 400bp, 450bp and 480bp of the PCR products correspond to the 3.6kb, and the 310bp correspond to 3.5bp of EcoRI fragments in Southern blot [28].

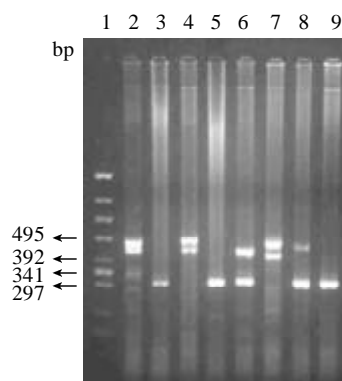


**Figure 1** Analysis of PCR products. 1: The standard of molecule (174 HincII); 2-9: Genotype of samples--450bp/480bp; 310bp/310bp; 450bp/480bp; 310bp/310bp; 310bp/400bp; 400bp/480bp; 310bp/480bp; 310bp/310bp.

### Distribution of PGC gene polymorphism

Ten different genotypes were obtained from the four alleles. Table 1 showed the distribution of these ten genotypes of PGC gene polymorphism in gastric cancer patients, members of gastric cancer kindred, health controls of Shenyang and Zhuanghe areas. Table 2 showed an estimated frequency of the four alleles in the four groups, and Table 3 showed the distribution of allele 1 homogenotype in above four groups. The frequency of allele 1 was higher in patients with gastric cancer than that in controls of Shenyang. Genotypes containing homogenous allele 1 were significantly more frequent in patients with gastric cancer than those in controls of Shenyang ( $P<0.05$ ). In the group of gastric cancer kindred the frequency of allele 1 was significantly higher than that in control group of Shenyang area ( $P<0.05$ ). Genotypes containing homogenous allele 1 were significantly more frequent in the group of gastric cancer kindred than those in control group of Shenyang area ( $P<0.05$ ). The frequency of allele 1 was higher in control group

of Zhuanghe area than that in control group of Shenyang area and genotypes containing homogenous allele 1 were significantly more frequent in the control group of Zhuanghe area than those in control group of Shenyang area ( $P<0.05$ ). There was no significant difference between the control group of Zhuanghe area and the group of gastric cancer kindred.

**Table 1** The distribution of genotypes of PGC gene polymorphism in health control, gastric cancer patients, and gastric cancer kindred group

Genotypes	Controls (Shenyang)	Gastric cancer patients	Controls (Zhuanghe)	Gastric cancer kindred
1:1	6(0.14)	24(0.33)	37(0.33)	22(0.36)
1:2	10(0.24)	10(0.14)	9(0.08)	13(0.21)
1:3	7(0.17)	4(0.05)	14(0.12)	4(0.07)
1:4	1(0.02)	1(0.01)	9(0.08)	2(0.03)
2:2	4(0.10)	8(0.11)	10(0.09)	7(0.11)
2:3	5(0.12)	8(0.11)	9(0.08)	5(0.08)
2:4	1(0.02)	1(0.01)	13(0.12)	1(0.16)
3:3	2(0.05)	10(0.14)	2(0.02)	3(0.05)
3:4	3(0.07)	5(0.07)	8(0.07)	3(0.05)
4:4	3(0.07)	2(0.03)	2(0.02)	1(0.16)
Total	42	73	113	61

**Table 2** The frequency of four alleles of PGC gene polymorphism in health control, gastric cancer patients, and gastric cancer kindred group

	n	Alleles of PGC gene polymorphism			
		1(310bp)	2(400bp)	3(450bp)	4(480bp)
Controls (Shenyang)	42	0.3571	0.2857	0.2262	0.1310
Gastric cancer patients	73	0.4315	0.2397	0.2534	0.0753
Controls (Zhuanghe)	113	0.4663	0.2389	0.1549	0.1504
Gastric cancer kindred	61	0.5164 <sup>a</sup>	0.2705	0.1475	0.0656

<sup>a</sup> $P<0.05$  vs compared with control group of Shenyang  $\chi^2=4.47$ .

**Table 3** The distribution of allele 1 homogenotype in health control, gastric cancer patients, and gastric cancer kindred

	n	1:1	others
Controls (Shenyang)	42	6(0.14)	36
Gastric cancer patients	73	24(0.33) <sup>a</sup>	49
Controls (Zhuanghe)	113	37(0.33) <sup>c</sup>	76
Gastric cancer kindred	61	22(0.36) <sup>c</sup>	39

<sup>a</sup> $P<0.05$  vs compared with control group of Shenyang,  $\chi^2=3.86$ ;

<sup>c</sup> $P<0.05$  vs compared with control group of Shenyang,  $\chi^2=4.32$ ;

<sup>c</sup> $P<0.05$  vs compared with control group of Shenyang,  $\chi^2=4.91$ .

## DISCUSSION

Family members of gastric cancer patients have been found to have a 1.5-fold to 3-fold increase in the risk of developing this cancer [29]. This familial aggregation may be due to genetic or environmental factors shared by family members [30-32]. To understand the genetic predisposition to gastric cancer, we selected pepsinogen C gene as a marker gene, and focused first on the distribution of the PGC gene polymorphism in gastric cancer patient group and health control. After PCR,

four alleles of pepsinogen C gene with different size were obtained. The frequency of allele 1 was higher in patients with gastric cancer than that in controls. Genotypes containing homogenous allele 1 were significantly more frequent in patients with gastric cancer than those in controls. This result showed that there is relation between the pepsinogen C gene polymorphism and gastric cancer, and the person with homogenous allele 1 seems to predispose to gastric cancer than those with other genotypes.

To further study the relation of the PGC gene polymorphism to gastric cancer and the genetic background of Zhuanghe, the high-risk area of gastric cancer, we selected three groups as our next research objects: gastric cancer kindred group in Zhuanghe, the control group of Zhuanghe and the control group of Shenyang. There was no significant difference in the distribution of PGC gene polymorphism between the health control group of Zhuanghe and gastric cancer kindred group, though the frequency of allele 1 in gastric cancer kindred group was a little higher than that in the control group of Zhuanghe. Our understanding for this phenomenon was that the persons who lived in Zhuanghe did not move frequently because of the historical reason, and this consanguinity between the two groups was the main factor responsible for the above result. But the frequency of allele 1 was higher in control group of Zhuanghe area than that in control group of Shenyang area, and genotypes containing homogenous allele 1 were significantly more frequent in the control group of Zhuanghe area than those in control group of Shenyang area. The frequency of allele 1 in the group of gastric cancer kindred was significantly higher than that in control group of Shenyang area. Genotype containing homogenous allele 1 was significantly more frequent in the group of gastric cancer kindred than that in the control group of Shenyang area. The result showed the distribution of PGC gene polymorphism in Shenyang area was different from that in Zhuanghe area.

The mortality of gastric cancer in Zhuanghe area is more than 50 per five hundred thousand. In the low risk area of that cancer, such as Shenyang, however, the mortality is less than 10 per five hundred thousand. From gastric cancer kindred group, the control groups of Zhuanghe and Shenyang, the risk ratio of gastric cancer becomes lower in turn. The data in this study showed that the frequency of allele 1 and Genotype containing homogenous allele 1 in the gastric cancer kindred group, the control groups of Zhuanghe and Shenyang in turn decreases, which is consistent with the risk ratio of gastric cancer in the above three groups. Therefore, we could conclude that the polymorphism of PGC gene may be related to the predisposition of gastric cancer, and the allele 1 associated with the risk of gastric cancer.

The mechanism of the association between PGC gene polymorphism and gastric cancer is not clear, in this study however, several hypotheses can be proposed. One is that the PGC gene itself is one of the genes responsible for gastric cancer. PGC, distributed throughout the stomach and proximal duodenum, is an important enzyme in stomach. It was reported that PGC not only was a digestive enzyme, but also might be a growth factor during the healing of gastric lesions<sup>[33]</sup> and the change of serum PGC was associated with many gastric diseases<sup>[34-37]</sup>. The polymorphism of PGC gene is in the intron between exon 7 and exon 8. Whether this polymorphism could affect the expression of PGC gene or regulate the PGC gene expression when the stomach was attacked by some pathogenetic factors was not known. In the following study, we will concentrate on the association of the PGC gene polymorphism and the PGC gene expression. It is interesting to note that in this study the frequency of allele 1 of PGC in the group of gastric cancer kindred was also higher than that in the group of gastric cancer group. As we know, the members

of the gastric cancer kindred all come from Zhuanghe, a place in which the incidence of gastric cancer is higher, and so is that of some other gastric diseases. In the study of Ohtaki's group, their data showed the polymorphism of PGC gene was associated with gastric body ulcer<sup>[28]</sup>. Comparing with our data, we can conclude the polymorphism of PGC is related to gastric lesions.

Another possible explanation of the association between the PGC gene polymorphism and gastric cancer was that the PGC gene was not itself responsible for the predisposition but one of the responsible genes was closely linked to it. It is interesting to note that the PGC gene was localized to human chromosome 6p21.1-pter by analysis of mouse x human somatic cell hybrids. The recent linkage analysis demonstrated that the PGC gene is 22cM proximal to HLA cluster which has been investigated to determine the associated with gastric disease<sup>[38-41]</sup>, between D6S5 and D6S4, at a distance of 4.5 and 13.1cM. Further molecular biological studies using polymorphism markers for this chromosome region will clarify whether PGC polymorphism is linked to disequilibria of the causative genetic variations for gastric cancer. Lastly, the presence of reduced penetrance, other modifier genes, or an interaction with the environment may explain the association.

## REFERENCES

- 1 **Botterweck AAM**, Van den Brandt PA, Goldbohm RA. Vitamins carotenoids, dietary fiber, and the risk of gastric carcinoma: results from a prospective study after 6.3 years of follow-up. *Cancer* 2000; **88**: 737-748
- 2 **Cai L**, Yu SZ, Zhang ZF. Cytochrome P450 2E1 genetic polymorphism and gastric cancer in Changle, Fujian Province. *World J Gastroenterol* 2001; **7**: 792-795
- 3 **Ye WM**, Yi YN, Luo RX, Zhou TS, Lin RT, Chen GD. Diet and gastric cancer: a case control study in Fujian Province, China. *World J Gastroenterol* 1998; **4**: 516-518
- 4 **Zhang ZF**, Kurtz RC, Klimstra DS, Yu GP, Sun M, Harlap S, Marshall JR. *Helicobacter pylori* infection on the risk of stomach cancer and chronic atrophic gastritis. *Cancer Detect Prev* 1999; **23**: 357-367
- 5 **Melato M**, Sidari L, Rizzardi C, Kovac D, Stimac D, Baxa P, Jonjic N. Gastric epithelium proliferation in early *Hp*+ and *Hp*- gastritis: a flow cytometry study. *Anticancer Res* 2001; **21**: 1347-1353
- 6 **Marinone C**, Martinetti A, Mestriner M, Seregni E, Geuna M, Ferrari L, Strola G, Bonardi L, Fea E, Bombardieri E. p53 evaluation in gastric mucosa of patients with chronic *Helicobacter pylori* infection. *Anticancer Res* 2001; **21**: 1115-1118
- 7 **Oue N**, Shigeishi H, Kuniyasu H, Yokozaki H, Kuraoka K, Ito R, Yasui W. Promoter hypermethylation of MGMT is associated with protein loss in gastric carcinoma. *Int J Cancer* 2001; **93**: 805-809
- 8 **Deguchi R**, Takagi A, Kawata H, Inoko H, Miwa T. Association between CagA+ *Helicobacter pylori* infection and p53, bax and transforming growth factor-beta-RII gene mutations in gastric cancer patients. *Int J Cancer* 2001; **91**: 481-485
- 9 **Yao XX**, Yin L, Sun ZC. The expression of hTERT mRNA and cellular immunity in gastric cancer and precancerosis. *World J Gastroenterol* 2002; **8**: 586-590
- 10 **Zhou Y**, Gao SS, Li YX, Fan ZM, Zhao X, Qi YJ, Wei JP, Zou JX, Liu G, Jiao LH, Bai YM, Wang LD. Tumor suppressor gene p16 and Rb expression in gastric cardia precancerous lesions from subjects at a high incidence area in northern China. *World J Gastroenterol* 2002; **8**: 423-425
- 11 **El-Omar EM**, Carrington M, Chow WH, McColl KEL, Bream JH, Young HA, Herrera J, Lissowska J, Yuan C-C, Hothman N, Lanyon G, Martin M, Fraumeni Jr JF, Rabkin CS. Interleukin-1 polymorphism associated with increased risk of gastric cancer. *Nature* 2000; **404**: 398-402
- 12 **Yea S S**, Yang YI, Jang W H, Lee YJ, Bae HS, Paik KH, Wei Q. Association between TNF- $\alpha$  promoter polymorphism and *Helicobacter pylori* cagA subtype infection. *J Clin Pathol* 2001; **54**: 703-706
- 13 **Shen H**, Xu Y, Zheng Y, Qian Y, Yu R, Qin Y, Wang X, Spitz MR, Wei Q. Polymorphisms of 5, 10-methylenetetrahydrofolate reductase and risk of gastric cancer in a Chinese population: a case-control

- study. *Int J Cancer* 2001; **95**: 332-336
- 14 **Liu MR**, Pan KF, Li ZF, Wang Y, Deng DJ, Zhang L, Lu YY. Rapid screening mitochondrial DNA mutation by using denaturing high-performance liquid chromatography. *World J Gastroenterol* 2002; **8**: 426-430
  - 15 **Pfutzer RH**, Barmada MM, Brunskill AP, Finch R, Hart PS, Neoptolemos J, Furey WF, Whitcomb DC. SPINK1/PSTI polymorphisms act as disease modifiers in familial and idiopathic chronic pancreatitis. *Gastroenterology* 2000; **119**: 615-623
  - 16 **Prkacin I**, Novak B, Sertic J, Mrzljak A. Angiotensin-converting enzyme gene polymorphism in patients with systemic lupus. *Acta Med Croatica* 2001; **55**: 73-76
  - 17 **Wu MS**, Huang SP, Chang YT, Lin MT, Shun CT, Chang MC, Wang HP, Chen CJ, Lin JT. Association of the -160 C a promoter polymorphism of E-cadherin gene with gastric carcinoma risk. *Cancer* 2002; **94**: 1443-1448
  - 18 **Takezaki T**, Gao CM, Wu JZ, Li ZY, Wang JD, Ding JH, Liu YT, Hu X, Xu TL, Tajima K, Sugimura H. hOGG1 Ser(326)Cys polymorphism and modification by environmental factors of stomach cancer risk in Chinese. *Int J Cancer* 2002; **99**: 624-627
  - 19 **Hiyama T**, Tanaka S, Kitadai Y, Ito M, Sumii M, Yoshihara M, Shimamoto F, Haruma K, Chayama K. p53 Codon 72 polymorphism in gastric cancer susceptibility in patients with *Helicobacter pylori*-associated chronic gastritis. *Int J Cancer* 2002; **100**: 304-308
  - 20 **Tsukino H**, Kuroda Y, Qiu D, Nakao H, Imai H, Katoh T. Effects of cytochrome P450 (CYP) 2A6 gene deletion and CYP2E1 genotypes on gastric adenocarcinoma. *Int J Cancer* 2002; **100**: 425-428
  - 21 **Zhang Z**, Zhang X, Hou G, Sha W, Reynolds GP. The increased activity of plasma manganese superoxide dismutase in tardive dyskinesia is unrelated to the Ala-9Val polymorphism. *J Psychiatr Res* 2002; **36**: 317-324
  - 22 **Wootton JC**, Feng X, Ferdig MT, Cooper RA, Mu J, Baruch DI, Magill AJ, Su XZ. Genetic diversity and chloroquine selective sweeps in *Plasmodium falciparum*. *Nature* 2002; **418**: 320-323
  - 23 **Clark AG**. Population genetics: malaria variorum. *Nature* 2002; **418**: 283-285
  - 24 **Feng Z**, Curtis J, Minchella DJ. The influence of drug treatment on the maintenance of schistosome genetic diversity. *J Math Biol* 2001; **43**: 52-68
  - 25 **Kageyama T**, Ichinose M, Tsukada-Kato S, Omata M, Narita Y, Moriyama A, Yonezawa S. Molecular cloning of neonate/infant-specific pepsinogens from rat stomach mucosa and their expression change during development. *Biochem Biophys Res Commun* 2000; **267**: 806-812
  - 26 **Kageyama T**. Pepsinogens, progastricsins, and prochymosins: structure, function, evolution, and development. *Cell Mol Life Sci* 2002; **59**: 288-306
  - 27 **Guo XL**, Wang LE, Wang L, Dong M, Yuan Y. The significant of measuring serum *Hp* CagA on the high risk population in the high-risk area of gastric cancer. *Shijie Huaren Xiaohua Zazhi* 2001; **9**: 595-596
  - 28 **Ohtaki Y**, Azuma T, Konishi J, Ito S, Kuriyama M. Association between genetic polymorphism of the pepsinogen C gene and gastric body ulcer: the genetic predisposition is not associated with *Helicobacter pylori* infection. *Gut* 1997; **41**: 469-474
  - 29 **Brenner H**, Arndt V, Sturmer T, Stegmaier C, Ziegler H, Dhom G. Individual and joint contribution of family history and *Helicobacter pylori* infection to the risk of gastric carcinoma. *Cancer* 2000; **88**: 274-279
  - 30 **Kim JC**, Kim HC, Roh SA, Koo KH, Lee DH, Yu CS, Lee JH, Kim TW, Lee HL, Beck NE, Bodmer WF, hMLH1 and hMSH2 mutations in families with familial clustering of gastric cancer and hereditary non-polyposis colorectal cancer. *Cancer Detect Prev* 2001; **25**: 503-510
  - 31 **Bakir T**, Can G, Erkul S, Siviloglu C. Stomach cancer history in the siblings of patients with gastric carcinoma. *Eur J Cancer Prev* 2000; **9**: 401-408
  - 32 **Dhillon PK**, Farrow DC, Vaughan TL, Chow WH, Risch HA, Gammon MD, Mayne ST, Stanford JL, Schoenberg JB, Ahsan H, Dubrow R, West AB, Rotterdam H, Blot WJ, Fraumeni JF Jr. Family history of cancer and risk of esophageal and gastric cancers in the United States. *Int J Cancer* 2001; **93**: 148-152
  - 33 **Kishi K**, Kinoshita Y, Matsushima Y, Okada A, Maekawa T, Kawanami C, Watanabe N, Chiba T. Pepsinogen C gene product is a possible growth factor during gastric mucosal healing. *Biochem Biophys Res Commun* 1997; **238**: 17-20
  - 34 **Fernandez R**, Vizoso F, Rodriguez JC, Merino AM, Gonzalez LO, Quintela I, Andicoechea A, Truan N, Diez MC. Expression and prognostic significance of pepsinogen C in gastric carcinoma. *Ann Surg Oncol* 2000; **7**: 508-514
  - 35 **Kikuchi S**, Kurosawa M, Sakiyama T, Tenjin H, Miki K, Wada O, Inaba Y. Long-term effect of *Helicobacter pylori* infection on serum pepsinogens. *Jpn J Cancer Res* 2000; **91**: 471-476
  - 36 **Fujisawa T**, Kumagai T, Goto A, Fujimori K, Akamatsu T, Kiyosawa K. Investigation about usefulness of serum antibody of *Helicobacter pylori* and serum pepsinogen I/II ratio as a marker of the judgment after eradication therapy. *Nippon Rinsho* 1999; **57**: 101-106
  - 37 **Araki H**, Miyazaki R, Matsuda T, Gejyo F, Koni I. Significance of serum pepsinogens and their relationship to *Helicobacter pylori* infection and histological gastritis in dialysis patients. *Nephrol Dial Transplant* 1999; **14**: 2669-2675
  - 38 **Magnusson PKE**, Enroth H, Eriksson I, Held M, Nyren O, Engstrand L, Hansson L-E, Gyllenstein UB. Gastric cancer and human leukocyte antigen: distinct DQ and DR alleles are associated with development of gastric cancer and infection by *Helicobacter pylori*. *Cancer Res* 2001; **61**: 2684-2689
  - 39 **Archimandritis A**, Sougioultzis S, Foukas PG, Tzivras M, Davaris P, Moutsopoulos HM. Expression of HLA-DR, costimulatory molecules B7-1, B7-2, intercellular adhesion molecule-1 (ICAM-1) and Fas ligand (FasL) on gastric epithelial cells in *Helicobacter pylori* gastritis; influence of *H. pylori* eradication. *Clin Exp Immunol* 2000; **119**: 464-471
  - 40 **Sakai T**, Aoyama N, Satonaka K, Shigeta S, Yoshida H, Shinoda Y, Shirasaka, D, Miyamoto M, Nose Y, Kasuga M. HLA-DQB1 locus and the development of atrophic gastritis with *Helicobacter pylori* infection. *J Gastroenterol* 1999; **34**: 24-27
  - 41 **Yoshitake S**, Okada M, Kimura A, Sasazuki T. Contribution of major histocompatibility complex genes to susceptibility and resistance in *Helicobacter pylori* related diseases. *Eur J Gastroenterol Hepatol* 1999; **11**: 875-880

Edited by Zhang JZ

• GASTRIC CANCER •

# ***Helicobacter pylori* infection generated gastric cancer through p53-Rb tumor-suppressor system mutation and telomerase reactivation**

Jing Lan, Yong-Yan Xiong, Yi-Xian Lin, Bi-Cheng Wang, Ling-Ling Gong, Hui-Sen Xu, Guang-Song Guo

**Jing Lan, Yong-Yan Xiong, Yi-Xian Lin, Bi-Cheng Wang, Ling-Ling Gong, Hui-Sen Xu, Guang-Song Guo**, Department of Pathology, Zhongnan Hospital, Wuhan University, Wuhan city 430071, Hubei Province, China

**Supported by** the National Science Fund of Hubei Province, No. 98J087 and the Department of Health of Hubei Province, No. WJ01572

**Correspondence to:** Dr. Jing Lan, Department of Pathology, Zhongnan Hospital, Wuhan University, Wuhan 430071, Hubei Province, China. lanjing\_2002@hotmail.com

**Telephone:** +86-27-87661547

**Received:** 2002-03-12 **Accepted:** 2002-04-20

## **Abstract**

**AIM:** To investigate the relationship between *Helicobacter pylori* (*H.pylori*) infection and the expressions of the p53, Rb, c-myc, bcl-2 and hTERT mRNA in a series of diseases from chronic gastritis (CG), intestinal metaplasia type I or II (IMI-II), intestinal metaplasia type III (IMIII), mild or modest dysplasia (DysI-II), severe dysplasia (DysIII) to gastric cancer (GC) and to elucidate the mechanism of gastric carcinogenesis relating to *H.pylori* infection.

**METHODS:** 272 cases between 1998 and 2001 were available for the study including 42 cases of CG, 46 cases of IMI-II, 25 cases of IMIII, 48 cases of DysI-II, 27 cases of DysIII, 84 cases of GC. *H.pylori* infection and the expressions of p53, Rb, c-myc, bcl-2 were detected by means of streptavidin-peroxidase (SP) immunohistochemical method. hTERT mRNA was detected by *in situ* hybridization (ISH).

**RESULTS:** The expressions of p53, Rb, c-myc, hTERT mRNA and bcl-2 were higher in the GC than in CG, IM, Dys. The expression of c-myc was higher in IMIII with *H.pylori* infection (10/16) than that without infection (1/9) and the positive rate in DysI-II and DysIII with *H.pylori* infection was 18/30 and 13/17, respectively, higher than that without infection (4/18 and 3/10, respectively). In our experiment mutated p53 had no association with *H.pylori* infection, the expression of Rb was associated with *H.pylori* infection in GC, but the p53-Rb tumor-suppressor system abnormal in DysI-II cases, DysIII and GC cases with *H.pylori* infection was 21/30, 15/17 and 48/48 respectively, higher than non-infection groups (4/18, 3/10, 28/36). Furthermore the level of hTERT mRNA in GC with *H.pylori* infection (47/48) was higher than that without infection (30/36), however the relationship between bcl-2 and *H.pylori* was only in IMIII. C-myc had a close association with hTERT mRNA in DysIII and GC ( $P=0.0253, 0.0305$  respectively).

**CONCLUSION:** In the gastric carcinogenesis, *H.pylori* might cause the severe imbalance of proliferation and apoptosis in the precancerous lesions (IMIII and GysIII) first, leading to p53-Rb tumor-suppressor system mutation and telomerase reactivation, and finally causes gastric cancer.

Lan J, Xiong YY, Lin YX, Wang BC, Gong LL, Xu HS, Guo GS. *Helicobacter pylori* infection generated gastric cancer through p53-Rb tumor-suppressor system mutation and telomerase reactivation. *World J Gastroenterol* 2003; 9(1): 54-58  
<http://www.wjgnet.com/1007-9327/9/54.htm>

## **INTRODUCTION**

Gastric cancer is one of the most fatal malignancies and in the world about 628 000 persons die of it every year. A close association between *Helicobacter pylori* (*H.pylori*) and gastric cancer has been found<sup>[1-14]</sup>, mainly on the basis of seroepidemiological data. Recently the animal models that developed gastric cancer owing to *H.pylori* infection provided powerful evidence<sup>[15]</sup>. Although *H.pylori* has been classified as a type I carcinogen for gastric cancer by the International Agency for Research on Cancer (IARC)<sup>[16]</sup>, the exact nature and strength of the association with gastric cancer has remained indistinct.

A two-stage pattern has been introduced to explain the escape from senescence of the cultured human cells<sup>[17,18]</sup>. The mortality stage 1 (M1) mechanism causes senescence, where normal human diploid cells become incapable of further division. However this cessation of cellular division can be overcome by the inactivation of human tumor suppressor genes p53 and Rb in fibroblasts<sup>[18,19]</sup> that are mutated in a variety of human neoplasm. In non-neoplastic cells, wild type p53 modulates cell proliferation and differentiation by regulating the transcription of several gene products, inducing p21<sup>waf1</sup> expression which acts as a regulator of the cell cycle at the G1 checkpoint<sup>[20,21]</sup>, and plays a crucial role in repairing damaged DNA through inducing GADD45 (growth arrest and DNA damage)<sup>[22]</sup>. Moreover p53 induces the Bax gene, which is followed by apoptosis, in contrast to bcl-2<sup>[23]</sup>. The cells which have overcome the M1 mechanism are able to divide until crisis occurs, which is caused by the mortality stage 2 (M2) mechanism. It is difficult for human cells to escape from this crisis, but in rare instances some populations can achieve immortality by overcoming this M2 mechanism through the reactivation of the enzyme telomerase<sup>[24-29]</sup>. Telomerase is a unique ribonucleoprotein enzyme that is responsible for adding the telomeric repeats onto the 3' end of chromosomes and composed of a catalytic protein subunit (hTERT, for human telomerase reverse transcription) and a template RNA (TR), and hTERT is the rate-limiting enzyme in the telomerase complex<sup>[30-34]</sup>.

From all the above it is apparent that the understanding of the association of *H.pylori* infection with some genes (for example p53, Rb) as well as telomerase can contribute to the elucidation of the mechanisms that regulate the development of gastric cancer. The aim of the present study, therefore, was to examine this association by detecting the expressions of *H.pylori*, hTERT, p53, Rb, c-myc and bcl-2 in a series of gastric diseases.

## **MATERIALS AND METHODS**

### **Patients**

Two hundred seventy-two patients (174 men, 98 women, ranging in age from 21 to 80 years, mean 54.22 years) underwent endoscopy (noncancerous patients) or curative gastrectomy (gastric cancer patients) in our hospital between 1998 to 2001, including 42 cases of CG, 46 cases of IMI-II, 25 cases of IMIII, 48 cases of DysI-II, 27 cases of DysIII, 84 cases of GC diagnosed according to the updated Sydney System<sup>[35]</sup> and the Japanese Research Society for Gastric Cancer<sup>[36]</sup>. No patients had received chemotherapy or radiation therapy before surgery.

All specimens were fixed in 10 % buffered neutral formalin and embedded in paraffin and serial sections (4 µm thick).

### Histochemical staining

Hematoxylin-eosin (HE) staining was used for the histopathological diagnosis, evaluation and grading of gastritis, atrophy, intestinal metaplasia, dysplasia and cancer. High iron diamine (HID)-alcian blue (AB) (PH 2.5)-periodic acid schiff (PAS) method was used to distinguish sulphates, neutral and acid mucus, which were stained brown-black, red and blue respectively. Using both morphological and histochemical criteria, the cases of intestinal metaplasia were classified into three types<sup>[37]</sup>.

### Immunohistochemistry

Was performed using the streptavidin-peroxidase (sp) method. The following primary antibodies and the kit were used: monoclonal antibodies against p53, Rb, c-myc, bcl-2 and the kit (Maixin-Bio, Fujian), polyclonal antibodies against *H.pylori* (antibody, diagnostica Inc. USA). Dewaxed sections were heated in a microwave oven (700W) for 12 min to retrieve the antigens and cooled to room temperature. Endogenous peroxide was blocked by 3 % hydrogen peroxide (H<sub>2</sub>O<sub>2</sub>) for 15 min in methanol. After being washed with phosphate-buffered-saline (PBS, 0.01M), the sections were further blocked by 10 % rabbit serum for 15 min to reduce nonspecific antibody binding and then incubated with the primary antibodies of p53, Rb, c-myc, bcl-2 or *H.pylori* (1:60 dilution) at 4 °C overnight. After being washed with PBS for 2×5 min, the sections were incubated with the secondary anti-mouse immunoglobulin (Ig) conjugated with biotin at room temperature for 15 min, washed again with PBS, followed by incubation with streptavidin-peroxidase complex for 15 min. The reaction products of peroxidase were visualized by incubation with 0.05 M Tris-HCL buffer (PH7.6) containing 20 mg 3,3'-diaminobenzidine (Maixin-Bio, Fujian) and 100 µl 5 % hydrogen peroxide per 100 ml. Finally, the sections were counterstained for nuclei by hematoxylin solution. To examine the specificity of immunostaining, PBS was used to replace the primary antibodies as the control. The assessment of all the samples was conducted by an observer who did not know any details of this study by calculating the average ratio of positive cells (the nuclei or the plasma, staining brown-yellow) under ten 400× microscopes. If the ratio was more than 10 %, this

sample was considered positive. However the *H.pylori* immunostaining was assessed positive as long as the brown-black dotish, stake or bend material was stained on the surface of mucosa or in the gland's cave.

### In situ hybridization

(ISH) was used to detect hTERT (human telomerase reverse transcriptase) mRNA. The probe (5' -CCCAG GCGCC GCACG AACGT GGCCA GCGGC-3' ) and the kit were bought from Boster Bio (Wuhan). Dewaxed sections were incubated with 3 % hydrogen peroxide for 30 min to reduce the non-specific binding and then with 1 µg/ml pepsin for 5-8 min to improve the penetration of the probe. The prehybridization was performed at 40 °C for 3 h to enhance hybridization efficiency, and the hybridization was conducted in a 42 °C water bath with each section covered with a coverslip, then the thorough washing procedure was followed: 2×SSC (sodium chloride and sodium citrate) at 37 °C for 15 min, 0.5 ×SSC for 15 min, 0.2×SSC for 15 min. Then the sections were visualized according to the kit manufacturer's instructions. We calculated the positive cells ratio to assess the positive sample by calculating the average ratio of positive cells (the plasma was stained brown-yellow) under ten 400× microscopes. If the ratio was more than 10 %, this sample was considered positive.

### Statistics

The chi-square test and the Fisher's exact probability test were used to compute the frequencies by SPSS 10.0 for Windows.  $P < 0.05$  was considered to be statistically significant.

## RESULTS

With the development of the diseases from CG, IM, Dys to GC, the positive expressions of p53, Rb, c-myc, bcl-2 and hTERT mRNA were augmented significantly (Table 1). In particular, the frequencies of Rb, c-myc and hTERT mRNA in IMIII (8/25, 11/25, 4/25, respectively) were statistically higher than those in IMI-II (4/46, 8/46, 1/46, respectively) ( $P < 0.05$ ). The expressions of all variables in GC were statistically higher than in DysIII and IMIII, higher in DysIII e than in IMIII ( $P < 0.05$ ). In general the frequencies of them in *H.pylori* infection groups were higher than those in non-infection groups. The expression of c-myc was 10/10, 18/30,

**Table 1** Expressions of c-myc, bcl-2, p53, Rb and hTERT mRNA in the different gastric diseases (%)

	GC	IMI-II	IMIII	DysI-II	DysIII	GC
c-myc	5(11.90)	8(17.39)	11(44.00)	22(45.83)	16(59.26)	74(88.09)
bcl-2	3(7.14)	17(36.96)	10(40.00)	24(50.00)	18(66.67)	55(65.48)
p53	0(0.00)	3(6.52)	5(20.00)	14(29.17)	10(37.04)	64(76.19)
Rb	3(7.14)	4(8.70)	8(32.00)	14(29.17)	12(44.44)	61(72.62)
HTERTmRNA	0(0.00)	1(2.17)	4(16.00)	10(16.67)	12(44.44)	78(92.86)

**Table 2** The correlations between p53, Rb, c-myc, hTERT, bcl-2 and *H.pylori* in benign diseases and gastric cancer

<i>H.pylori</i>	CG		IMI-II		IMIII		DysI-II		DysIII		GC	
	+(31)	-(11)	+(32)	-(14)	+(16)	-(9)	+(30)	-(18)	+(17)	-(10)	+(48)	-(36)
c-myc	5	0	7	1	10 <sup>a</sup>	1	18 <sup>a</sup>	4	13 <sup>a</sup>	3	44	30
bcl-2	3	0	12	5	9 <sup>a</sup>	1	17	7	13	5	38	17
p53	0	0	2	1	3	2	12 <sup>a</sup>	2	6	4	39	25
Rb	3	0	4	0	6	2	11	3	9	3	40 <sup>a</sup>	21
P53-Rb	3	0	4	1	6	3	21 <sup>a</sup>	4	15 <sup>a</sup>	3	48 <sup>a</sup>	28
hTERT	0	0	1	0	4	0	8	2	9	3	47 <sup>a</sup>	30

<sup>a</sup> $P < 0.05$  vs the non-infected group.

13/17 in IMIII, DysI-II and DysIII with *H.pylori* infection respectively, higher than non-infection group (1/9, 4/18, 3/10, respectively). In our experiment mutated p53 had no association with *H.pylori* infection, the expression of Rb was associated with *H.pylori* infection in GC, but the p53-Rb tumor-suppressor system abnormal in DysI-II cases, DysIII and GC cases with *H.pylori* infection was 21/30, 15/17 and 48/48, respectively, higher than that in non-infection groups (4/18, 3/10, 28/36, respectively). The association between bcl-2 and *H.pylori* only existed in IMIII (9/16, 1/9). The expression of hTERT mRNA in GC with *H.pylori* infection was 47/48, higher than non-infection group (30/36) (Table 2). We also found the association between c-myc and hTERT mRNA in GC and DysIII ( $P<0.05$ ) (Table 3).

**Table 3** Correlation between c-myc and hTERT in the gastric benign diseases and gastric cancer

c-myc	CG		IMI-II		IMIII		DysI-II		DysIII		GC	
	(+)	(-)	(+)	(-)	(+)	(-)	(+)	(-)	(+)	(-)	(+)	(-)
hTERT(+)	0	0	1	0	3	1	7	3	10 <sup>a</sup>	2	70 <sup>a</sup>	7
(-)	5	37	7	39	8	13	15	23	6	9	4	3

<sup>a</sup> $P<0.05$  vs the negative group.

## DISCUSSION

Gastric cancer occurs after a multi-step process of alterations in oncogenes, tumor-suppressor genes, cell-adhesion molecules, telomerase as well as genetic instability at several microsatellite loci. Studies have demonstrated that *H.pylori* infection is closely associated with these abnormal alterations. Konturek's study<sup>[38]</sup> showed that *H.pylori* induced apoptosis in gastric mucosa through upregulation of Bax and bcl-2 expression. The bcl-2 gene family plays an important role in regulating apoptosis. In our studies, *H.pylori* enhanced the expression of c-myc and bcl-2 significantly in IMIII ( $P<0.05$ ). The c-myc protein is a critical component for the control of normal cell growth, but the altered c-myc activity by translocation, amplification, overexpression, and mutation is widespread in tumor cells and important for multi-step carcinogenesis<sup>[39,40]</sup>. C-myc is a strong inducer of proliferation and it is believed to be critical for the oncogenic properties. Some studies showed that the abnormal c-myc expression derived cells inappropriately through the cell cycle, leading to uncontrolled proliferation, a characteristic of neoplastic cells. From our study we found that *H.pylori* infection caused a higher proliferation and a lower apoptosis in IMIII than in CG and IMI-II and accelerated cell proliferation, leaving a good chance for all kinds of genes and proteins to mutate or overexpress, presumably heightening the genetic instability consistent with the development of carcinoma<sup>[41,42]</sup>.

Mutations in the tumor suppressor genes p53 and Rb are common events in human cancers that exert their control on the cell cycle at the G1-S phase transition through independent but interconnected pathways<sup>[43-50]</sup>. Williams' studies showed that germ-line mutation in p53 and Rb might have cooperative tumorigenic effects in mice<sup>[51]</sup>. It has been generally accepted that p53 and Rb tumor-suppressor system, including p53, Rb, p16, p15, p14 and p21waf1<sup>[52-60]</sup>, play an important role in carcinogenesis. Some studies observed this phenomenon that NO (nitric oxide) generated by *H.pylori* caused p53 mutation at the spot C:G to A:T and at the same time p53 was found mutated at the same spot in IM, Dys and GC, thus *H.pylori* probably caused p53 mutation. In our study, we found that the expressions of p53-Rb were continually enhanced from chronic gastritis (3/42) to gastric cancer (76/84) and in the DysIII and

GC which had a close association with *H.pylori* ( $P<0.05$ ). Chen<sup>[61]</sup> reported that the mRNA levels of p53-Rb in gastric cancer were significantly lower than those in their non-cancerous tissues using quantitative analysis method. Some studies favored the view that c-myc drove initial proliferation and subsequent differentiation, concomitant with the activation of the p53 G2 checkpoint and also demonstrated that inactivation of the p53-Rb pathway is required for immortalization through overexpression of Myc<sup>[62,63]</sup>. Although c-myc and p53-Rb had no direct association in our study, *H.pylori* infection might initially provoke the c-myc and bcl-2 more than in non-infection group in IMIII and then inactivate the p53-Rb tumor-suppress system in Dys and they collaborated in GC.

Telomerase activity has been found in 85-90 % of all human cancers but not in adjacent normal cells<sup>[27]</sup>. It has thus been hypothesized that for a cancer cell to undergo sustained proliferation beyond the limits of cell senescence, it must reactivate telomerase or an alternative mechanism in order to maintain telomeres. This makes telomerase a target not only for the novel etiology agent but also a mark for cancer diagnosis. Many studies showed that telomerase activity was higher in cancers than in non-cancerous tissues and higher in IM than in CG<sup>[64-69]</sup>, which was similar to our results. The association between *H.pylori* infection and telomerase activity is still controversial. Suzuki's study<sup>[67]</sup> indicated that hTERT mRNA which was expressed in precancerous lesions and gastric cancer could be induced at an early stage of gastric carcinogenesis, but it was not correlated with *H.pylori*. Kuniyasu<sup>[70]</sup> found that *H.pylori* evidently caused the release of reactive oxygen species (ROMs) and reactive nitrogen species (NO) which might be strong triggers for "stem cell" hyperplastic in IM, followed by telomere reduction and increased telomerase activity as well as hTERT overexpression. We found in GC hTERT expression was significantly higher in infection group (47/48) than in non-infection group (30/36) but had no association in Dys or IM, maybe because there exist two different genetic pathways to two histological types: intestinal-type and diffuse-type gastric cancer. Some studies showed c-myc could stimulate expression of hTERT and thereby enhance telomerase activity which was an important step in carcinogenesis<sup>[71-80]</sup>. In our study c-myc had an association with hTERT in Dys and GC, which suggests that *H.pylori* stimulates telomerase directly or indirectly by the overexpression of c-myc. We did not find the association between hTERT and p53-Rb or bcl-2.

There maybe exit this mechanism of gastric carcinogenesis relating to chronic *H.pylori* infection, which leads to imbalance of proliferation and apoptosis in the early stage, and furthermore p53-Rb tumor-suppressor system mutation, telomerase reactivation and finally gastric cancer generation. Hence this molecular pathology mechanism should be applied in routine diagnostic procedures, classification systems, disease monitoring, and even prognostic assessment.

## ACKNOWLEDGMENTS

The authors thank the faculty of Department of Pathology and Wang Zhifeng of Stomatology of hospital for their excellent technical assistance throughout this investigation.

## REFERENCES

- 1 **Sipponen P**, Kosunen TU, Valle J, Riihela M, Seppala K. *Helicobacter pylori* infection and chronic gastritis in gastric cancer. *J Clin Pathol* 1992; **45**: 319-323
- 2 **Blaser MJ**. Hypotheses on the pathogenesis and natural history of *Helicobacter pylori*-induced inflammation. *Gastroenterology* 1992; **102**: 720-727
- 3 **Forman D**, Newell DG, Fullerton F, Yarnell JW, Stacey AR, Wald

- N, Sitas F. Association between infection with *Helicobacter pylori* and risk of gastric cancer: Evidence from a prospective investigation. *BMJ* 1991; **302**: 1302-1305
- 4 **Parsonnet J**, Friedman GD, Vandersteen DP, Chang Y, Vogelstein JH, Orentreich N, Sibley RK. *Helicobacter pylori* infection and the risk of gastric carcinoma. *N Engl J Med* 1991; **325**: 1127-1131
- 5 **Talley NJ**, Zinsmeister AR, Weaver A, DiMagno EP, Carpenter HA, Perez-perez GI, Blaser MJ. Gastric adenocarcinoma and *Helicobacter pylori* infection. *J Natl Cancer Inst* 1991; **83**: 1734-1739
- 6 **The Eurogast Study Group**. An association between *Helicobacter pylori* infection and gastric cancer: An international study. *Lancet* 1993; **341**: 1359-1362
- 7 **Hansson LE**, Engstrand L, Nyren O, Evans DJ Jr, Lindgren A, Bergstrom R, Andersson B, Athlin L, Bendtsen O, Tracz P. *Helicobacter pylori* infection: Independent risk indicator of gastric adenocarcinoma. *Gastroenterology* 1993; **105**: 1098-1103
- 8 **Blaser MJ**. *Helicobacter pylori* and gastric diseases. *BMJ* 1998; **316**: 1507-1510
- 9 **Wang TC**, Fox JG. *Helicobacter pylori* and gastric cancer: Koch's postulates fulfilled? *Gastroenterology* 1998; **115**: 780-783
- 10 **Vandenplas Y**. *Helicobacter pylori* infection. *World J Gastroenterol* 2000; **6**: 20-31
- 11 **Cai L**, Yu SZ, Zhang ZF. *Helicobacter pylori* infection and risk of gastric cancer in Changle County, Fujian Province, China. *World J Gastroenterol* 2000; **6**: 374-376
- 12 **Zhuang XQ**, Lin SR. Research of *Helicobacter pylori* infection in precancerous gastric lesions. *World J Gastroenterol* 2000; **6**: 428-429
- 13 **Xia HH**, Talley NJ. Apoptosis in gastric epithelium induced by *Helicobacter pylori* infection: implications in gastric carcinogenesis. *Am J Gastroenterol* 2001; **96**: 16-26
- 14 **Meining A**, Bayerdorffer E, Stolte M. Extent, topography and symptoms of *Helicobacter pylori* gastritis. Phenotyping for accurate diagnosis and therapy? *Pathologie* 2001; **22**: 13-18
- 15 **Fujioka T**, Honda S, Tokieda M. *Helicobacter pylori* infection and gastric carcinoma in animal models. *J Gastroenterol Hepatol* 2000; **15**(Suppl): D55-D59
- 16 International Agency for research on Cancer. Schistosomes, Liver flukes and *Helicobacter pylori*. Evaluation of carcinogenic risks to humans. *IARC Monograph Evaluating Carcinogenic Risks to Humans* 1994: 61
- 17 **Wright WE**, Pereira-Smith OM, Shay JW. Reversible cellular senescence: implications for immortalization of normal human diploid fibroblasts. *Mol Cell Biol* 1989; **9**: 3088-3092
- 18 **Shay JW**, Pereira-Smith OM, Wright WE. A role for both RB and p53 in the regulation of human cellular senescence. *Exp Cell Res* 1991; **196**: 33-39
- 19 **Shay JW**, Wright WE, Brasiskyte D, Van der Haegen BA. E6 of human papillomavirus type 16 can overcome the M1 stage of immortalization in human mammary epithelial cells but not in human fibroblasts. *Oncogene* 1993; **8**: 1407-1413
- 20 **el-Deiry WS**, Harper JW, O'Connor PM, Velculescu VE, Canman CE, Jackman J, Pietenpol JA, Burrell M, Hill DE, Wang Y. WAF1/CIP1 is induced in p53-mediated G1 arrest and apoptosis. *Cancer Res* 1994; **54**: 1169-1174
- 21 **Sheikh MS**, Rochefort H, Garcia M. Overexpression of p21WAF1/CIP1 induces growth arrest giant cell formation and apoptosis in human breast carcinoma cell lines. *Oncogene* 1995; **11**: 1899-1905
- 22 **Zhan Q**, Bae I, Kastan MB, Fornace AJ Jr. The p53-dependent gamma-ray response of GADD45. *Cancer Res* 1994; **54**: 2755-2760
- 23 **Zhan Q**, Fan S, Bae I, Guillouf C, Liebermann DA, O'Connor PM, Fornace AJ Jr. Induction of bax by genotoxic stress in human cells correlates with normal p53 status and apoptosis. *Oncogene* 1994; **9**: 3743-3751
- 24 **Harley CB**. Telomere loss: mitotic clock or genetic time bomb? *Mutat Res* 1991; **256**: 271-282
- 25 **Harley CB**, Vaziri H, Counter CM, Allsopp RC. The telomere hypothesis of cellular aging. *Exp Gerontol* 1992; **27**: 375-382
- 26 **Shay JW**, Wright WE, Werbin H. Toward a molecular understanding of human breast cancer: a hypothesis. *Breast Cancer Res Treat* 1993; **25**: 83-94
- 27 **Wright WE**, Shay JW. The two-stage mechanism controlling cellular senescence and immortalization. *Exp Gerontol* 1992; **27**: 383-389
- 28 **Kim NW**, Piatyszek MA, Prowse KR, Harley CB, West MD, Ho PL, Coviello GM, Wright WE, Weinrich SL, Shay JW. Specific association of human telomerase activity with immortal cells and cancer. *Science* 1994; **266**: 2011-2015
- 29 **Shay JW**, Wright WE. Haylick, his limit, and cellular ageing. *Nat Rev Mol cell Biol* 2000; **1**: 72-76
- 30 **Blackburn EH**. Structure and function of telomeres. *Nature* 1991; **350**: 569-573
- 31 **Feng J**, Funk WD, Wang SS, Weinrich SL, Avilion AA, Chiu CP, Adams RR, Chang E, Allsopp RC, Yu J. The RNA component of human telomerase. *Science* 1995; **269**: 1236-1241
- 32 **Kyo S**, Takakura M, Tanaka M, Kanaya T, Sagawa T, Kohama T, Ishikawa H, Nakano T, Shimoya K, Inoue M. Expression of telomerase activity in human chorion. *Biochem Biophys Res Commun* 1997; **241**: 498-503
- 33 **Nakayama J**, Tahara H, Tahara E, Saito M, Ito K, Nakamura H, Nakanishi T, Tahara E, Ide T, Ishikawa F. Telomerase activation by hTERT in human normal fibroblasts and hepatocellular carcinomas. *Nat Genet* 1998; **18**: 65-68
- 34 **Takakura M**, Kyo S, Kanaya T, Tanaka M, Inoue M. Expression of human telomerase subunits and correlation with telomerase activity in cervical cancer. *Cancer Res* 1998; **58**: 1558-1561
- 35 **Dixon MF**, Genta RM, Yardley JH, Correa P. Classification and grading of gastritis. The updated Sydney System. International workshop on the histopathology of gastritis, Houston 1994. *Am J Surg Pathol* 1996; **20**: 1161-1181
- 36 Japanese Research Society for Gastric Cancer: The General Rules for the Gastric Cancer Study, First English Edition. *Kanehara, Tokyo* 1995
- 37 **Jass JR**. Role of intestinal metaplasia in the histogenesis of gastric carcinoma. *J Clin Pathol* 1980; **33**: 801-810
- 38 **Konturek PC**, Pierzchalski P, Konturek SJ, Meixner H, Faller G, Kirchner T, Hahn EG. *Helicobacter pylori* induces apoptosis in gastric mucosa through an upregulation of Bax expression in humans. *Scand J Gastroenterol* 1999; **34**: 375-383
- 39 **Felsher DW**, Bishop JM. Reversible tumorigenesis by MYC in hematopoietic lineages. *Mol Cell* 1999; **4**: 199-207
- 40 **Pelengaris S**, Littlewood T, Khan M, Elia G, Evan G. Reversible activation of c-Myc in skin: induction of a complex neoplasia phenotype by a single oncogenic lesion. *Mol Cell* 1999; **3**: 565-577
- 41 **Conchillo JM**, Houben G, de Bruine A, Stockbrugger R. Is type III intestinal metaplasia an obligatory precancerous lesion in intestinal-type gastric carcinoma? *Eur J Cancer Prev* 2001; **10**: 307-312
- 42 **Rubio CA**, Jonasson JG, Filipe I, Cabanne AM, Hojman R, Kogan Z, Nesi G, Amorosi A, Zampi G, Klimstra D. Gastric carcinoma of intestinal type concur with distant changes in the gastric mucosa. A multicenter study in the Atlantic basin. *Anticancer Res* 2001; **21**: 813-818
- 43 **Jacks T**, Fazeli A, Schmitt EM, Bronson RT, Goodell MA, Weinberg RA. Effects of an Rb mutation in the mouse. *Nature* 1992; **359**: 295-300
- 44 **Donehower LA**, Harvey M, Slagle BL, McArthur MJ, Montgomery CA Jr, Butel JS, Bradley A. Mice deficient for p53 are developmentally normal but susceptible to spontaneous tumours. *Nature* 1992; **356**: 215-221
- 45 **Williams BO**, Remington L, Albert DM, Mukai S, Bronson RT, Jacks T. Cooperative tumorigenic effects of germline mutations in Rb and p53. *Nat Genet* 1994; **7**: 480-484
- 46 **Kamb A**, Gruis NA, Weaver-Feldhaus J, Liu Q, Harshman K, Tavitgian SV, Stockert E, Day RS 3rd, Johnson BE, Skolnick MH. A cell cycle regulator potentially involved in genesis of many tumor types. *Science* 1994; **264**: 436-440
- 47 **Gotz C**, Montenarh M. p53: DNA damage, DNA repair, and apoptosis. *Rev Physiol Biochem Pharmacol* 1996; **127**: 65-95
- 48 **Sherr CJ**. Cancer cell cycles. *Science* 1996; **274**: 1672-1677
- 49 **Platz A**, Hansson J, Mansson-Brahme A, Lagerlof B, Linder S, Lundqvist E, Sevigny P, Inganas M, Ringborg U. Screening of germline mutations in the CDKN2A and CDKN2B genes in Swedish families with hereditary cutaneous melanoma. *J Natl Cancer Inst* 1997; **89**: 697-702
- 50 **Walker DG**, Duan W, Popovic EA, Kaye AH, Tomlinson FH, Lavin M. Homozygous deletion of the multiple tumor suppressor gene 1 in the progression of human astrocytomas. *Cancer Res* 1995; **55**: 20-23
- 51 **Williams BO**, Remington L, Albert DM, Mukai S, Bronson RT,



- Jacks T. Cooperative tumorigenic effects of germline mutations in Rb and p53. *Nat Genet* 1994; **7**: 480-484
- 52 **Sherr CJ**. Tumor surveillance via the ARF-p53 pathway. *Genes Dev* 1998; **12**: 2984-2991
- 53 **Cordon-Cardo C**, Zhang ZF, Dallbagni G, Drobnjak M, Charytonowicz E, Hu SX, Xu HJ, Renter VE, Benedict WF. Cooperative effects of p53 and pRB alterations in primary superficial bladder tumors. *Cancer Res* 1997; **57**: 1217-1221
- 54 **Cote RJ**, Dunn MD, Chatterjee SJ, Stein JP, Shi SR, Tran QC, Hu SX, Xu HJ, Groshen S, Taylor CR, Skinner DG, Benedict WF. Elevated and absent pRb expression is associated with bladder cancer progression and has cooperative effects with p53. *Cancer Res* 1998; **58**: 1090-1094
- 55 **Kastan MB**, Onyekwere O, Sidransky D, Vogelstein B, Craig RW. Participation of p53 protein in the cellular response to DNA damage. *Cancer Res* 1991; **51**: 6304-6311
- 56 **Murakami Y**, Hayashi K, Hirohashi S, Sekiya T. Aberrations of the tumor suppressor p53 and retinoblastoma genes in human hepatocellular carcinoma. *Cancer Res* 1991; **51**: 5520-5525
- 57 **Wang J**, Coltrera MD, Gown AM. Abnormalities of p53 and p110RB tumor suppressor gene expression in human soft tissue tumors: correlations with cell proliferation and tumor grade. *Mod Pathol* 1995; **8**: 837-842
- 58 **Gleich LL**, Li YQ, Biddinger PW, Gartside PS, Stambrook PJ, Pavelic ZP, Gluckman JL. The loss of heterozygosity in retinoblastoma and p53 suppressor genes as a prognostic indicator for head and neck cancer. *Laryngoscope* 1996; **106**: 1378-1381
- 59 **Dosaka-Akita H**, Hu SX, Fujino M, Harada M, Kinoshita I, Xu HJ, Kuzumaki N, Kawakami Y, Benedict WF. Altered retinoblastoma protein expression in nonsmall cell lung cancer: its synergistic effects with altered ras and p53 protein status on prognosis. *Cancer* 1997; **79**: 1329-1337
- 60 **Ferron PE**, Bagni I, Guidoboni M, Beccati MD, Nenci I. Combined and sequential expression of p53, Rb, Ras and Bcl-2 in bronchial preneoplastic lesions. *Tumori* 1997; **83**: 587-593
- 61 **Chen YJ**, Shih LS, Chen YM. Quantitative analysis of CDKN2, p53 and retinoblastoma mRNA in human gastric carcinoma. *Int J Oncol* 1998; **13**: 249-254
- 62 **Pelengaris S**, Rudolph B, Littlewood T. Action of Myc *in vivo* proliferation and apoptosis. *Curr Opin Genet Dev* 2000; **10**: 100-105
- 63 **Dazard JE**, Piette J, Basset-Seguin N, Blanchard JM, Gandarillas A. Switch from p53 to MDM2 as differentiating human keratinocytes lose their proliferative potential and increase in cellular size. *Oncogene* 2000; **19**: 3693-3705
- 64 **Okusa Y**, Ichikura T, Mochizuki H, Shinomiya N. Clinical significance of telomerase activity in biopsy specimens of gastric cancer. *J Clin Gastroenterol* 2000; **30**: 61-63
- 65 **Zhang F**, Zhang X, Fan D. Expression of telomere and telomerase in human primary gastric carcinoma. *Zhonghua Binglixue Zazhi* 1998; **27**: 429-432
- 66 **Kameshima H**, Yagihashi A, Yajima T, Kobayashi D, Denno R, Hirata K, Watanabe N. *Helicobacter pylori* infection: augmentation of telomerase activity in cancer and noncancerous tissues. *World J Surg* 2000; **24**: 1243-1249
- 67 **Suzuki K**, Kashimura H, Ohkawa J, Itabashi M, Watanabe T, Sawahata T, Nakahara A, Muto H, Tanaka N. Expression of human telomerase catalytic subunit gene in cancerous and precancerous gastric conditions. *J Gastroenterol Hepatol* 2000; **15**: 744-751
- 68 **Hur K**, Gazdar AF, Rath A, Jang JJ, Choi JH, Kim DY. Overexpression of human telomerase RNA in *Helicobacter pylori*-infected human gastric mucosa. *Jpn J Cancer Res* 2000; **91**: 1148-1153
- 69 **Hahn WC**, Meyerson M. Telomerase activation, cellular immortalization and cancer. *Ann Med* 2001; **33**: 123-129
- 70 **Kuniyasu H**, Yasui W, Yokozaki H, Tahara E. *Helicobacter pylori* infection and carcinogenesis of the stomach. *Langenbechs Arch Surg* 2000; **385**: 69-74
- 71 **Latil A**, Vidaud D, Valeri A, Fournier G, Vidaud M, Lidereau R, Cussenot O, Biache I. Htert expression correlates with MYC overexpression in human prostate cancer. *Int J Cancer* 2000; **89**: 172-176
- 72 **Kyo S**, Takakura M, Taira T, Kanaya T, Itoh H, Yutsudo M, Ariga H, Inoue M. Sp1 cooperates with c-Myc to active transcription of the human telomerase reverse transcriptase gene (hTERT). *Nucleic Acids Res* 2000; **28**: 669-677
- 73 **Cerni C**. Telomeres, telomerase, and myc. An update. *Mutat Res* 2000; **462**: 31-47
- 74 **Kumamoto H**, Kinouchi Y, Ooya K. Telomerase activity and telomerase reverse transcriptase (TERT) expression in ameloblastomas. *J Oral Pathol Med* 2001; **30**: 231-236
- 75 **Xu D**, Popov N, Hou M, Wang Q, Bjorkholm M, Gruber A, Menkel AR, Henriksson M. Switch from Myc/Max to Mad1/Max binding and decrease in histone acetylation at the telomerase reverse transcriptase promoter during differentiation of HL60 cells. *Proc Natl Acad Sci USA* 2001; **98**: 3826-3831
- 76 **Kyo S**, Takakura M, Inoue M. Telomerase activity in cancer as a diagnostic and therapeutic target. *Histol Histopathol* 2000; **15**: 813-824
- 77 **Eberhardy SR**, D' Cunha CA, Farnham PJ. Direct examination of histone acetylation on Myc target genes using chromatin immunoprecipitation. *J Biol Chem* 2000; **275**: 33798-33805
- 78 **Kitagawa Y**, Kyo S, Takakura M, Kanaya T, Koshida K, Namiki M, Inoue M. Demethylating reagent 5-azacytidine inhibits telomerase activity in human prostate cancer cells through transcriptional repression of hTERT. *Clin Cancer Res* 2000; **6**: 2868-2875
- 79 **Nozawa K**, Maehara K, Isobe K. Mechanism for the reduction of telomerase expression during muscle cell differentiation. *J Biol Chem* 2001; **276**: 22016-22023
- 80 **Sagawa Y**, Nishi H, Isaka K, Fujito A, Takayama M. The correlation of TERT expression with c-myc expression in cervical cancer. *Cancer Lett* 2001; **168**: 45-50

Edited by Pang LH

# Angiostatin up-regulation in gastric cancer cell SGC7901 inhibits tumorigenesis in nude mice

Jing Wu, Yong-Quan Shi, Kai-Chun Wu, De-Xin Zhang, Jing-Hua Yang, Dai-Ming Fan

**Jing Wu, Yong-Quan Shi, Kai-Chun Wu, De-Xin Zhang, Jing-Hua Yang, Dai-Ming Fan**, Institute of Gastrointestinal Diseases Research, Xijing Hospital, Fourth Military Medical University, Xi'an 710032, Shannxi Province, China

**Supported by** the National Natural Science Foundation of China No.39800156

**Correspondence to:** Dr. Jing Wu, Institute of Gastrointestinal Diseases Research, Xijing Hospital, Fourth Military Medical University, Xi'an 710032, Shannxi Province, China. wujingliu@sina.com.cn

**Telephone:** +86-29-3375229

**Received:** 2002-05-16 **Accepted:** 2002-06-09

## Abstract

**AIM:** To explore the influence of angiostatin up-regulation on the biologic behavior of gastric cancer cells *in vitro* and *in vivo*, and the potential of angiostatin gene therapy in the treatment of human gastric cancer.

**METHODS:** Mouse angiostatin cDNA was subcloned into the eukaryotic expression vector pcDNA3.1(+) and identified by restriction endonucleases digestion and sequencing. The recombinant vector pcDNA3.1(+)-angio was transfected into human gastric cancer cells SGC7901 with liposome and paralleled with the vector control and the mock control. Angiostatin transcription and protein expression were examined by RT-PCR and Western blot in the stable cell lines selected by G418. Cell proliferation and growth *in vitro* of the three groups were observed respectively under microscope, cell number counting and FACS. The cells overexpressing angiostatin, vector transfected and untreated were respectively implanted subcutaneously into nude mice. After 30 days the size of tumors formed was measured, and microvessel density count (MVD) in the tumor tissues was assessed by immunohistochemistry with the primary anti-vWF antibody.

**RESULTS:** The recombinant vector pcDNA3.1(+)-angio was confirmed with the correct sequence of mouse angiostatin under the promoter CMV. After 30 d of transfection and selection with G418, macroscopic resistant cell clones were formed in the experimental group transfected with pcDNA 3.1(+)-angio and the vector control. But no untreated cells survived in the mock control. Angiostatin mRNA transcription and protein expression were detected in the experimental group. No significant differences were observed among the three groups in cell morphology, cell growth curves and cell cycle phase distributions *in vitro*. However, in nude mice model, markedly inhibited tumorigenesis and slowed tumor expansion were observed in the experimental group as compared with the controls, which was paralleled with decreased microvessel density in and around tumor tissues ( $P < 0.05$ ).

**CONCLUSION:** Angiostatin does not directly inhibit human gastric cancer cell proliferation and growth *in vitro*, but exerts its anti-tumor functions through antiangiogenesis in a paracrine way *in vivo*.

Wu J, Shi YQ, Wu KC, Zhang DX, Yang JH, Fan DM. Angiostatin up-regulation in gastric cancer cell SGC7901 inhibits tumorigenesis in nude mice. *World J Gastroenterol* 2003; 9(1):59-64  
<http://www.wjgnet.com/1007-9327/9/59.htm>

## INTRODUCTION

Angiogenesis is indispensable for various physiological processes including reproduction, development, wound repair, and tissue regeneration. However, abnormal neovascularization is also involved in the development and progression of pathogenic processes in a variety of disorders, including diabetic retinopathy, psoriasis, chronic inflammation, lepra alphas, rheumatoid arthritis and cardiovascular diseases. Since Folkman put forward the hypothesis that malignant tumor is angiogenesis dependent, direct and indirect evidences have shown that tumor growth and metastasis are accompanied by the growth of new blood vessels, which proves the rationality and feasibility of anti-angiogenic therapy in treatment of cancer<sup>[1,2]</sup>. Shifting the balance within the tumor microenvironment from overproduction of angiogenic stimulators toward an overproduction of angiogenic inhibitors represents one potential anti-angiogenic strategy<sup>[3,4]</sup>. To date, a number of angiogenic inhibitors have been demonstrated to inhibit experimental tumor growth in animal models, and some of them have already entered clinical trials<sup>[5]</sup>.

Gastric cancer is a malignant neoplasm, for which the common treatment is suboptimal and the prognosis of patients remains dismal. It is suggested that tumor-mediated angiogenesis due to high levels of angiogenic stimulators and down-regulation of endogenous angiogenic inhibitors play a fundamental role in the pathogenesis of malignant gastric cancer<sup>[6,7]</sup>. Molecular mechanisms of angiogenesis in gastric cancer have indicated an attractive therapeutic strategy by targeting those angiogenic regulators<sup>[8]</sup>.

Angiostatin, a potent specific inhibitor of proliferating endothelial cells, shows significant antiangiogenic and anticarcinogenic efficacies on various tumors *in vivo*. It specifically inhibits the proliferation, migration, and formation of capillary tubes *in vitro* or *in vivo*, and induces apoptosis in endothelial cells<sup>[9-11]</sup>. Although no directed inhibition on tumor cell growth *in vitro* is observed, evidence shows that angiostatin inhibits the occurrence of the primary as well as metastatic tumor, and remains dormant. Systemic delivery of purified angiostatin protein, however, raises a number of difficult practical problems which make the large-scale implementation inefficient and/or inefficacious. And these problems also make it unavailable logically and pharmaceutically, including difficulties in producing large quantities of biologically active protein, the short half-life of such proteins *in vivo*, and the requirement for long-term intermittent or continuous treatment. The transfer of angiostatin gene, therefore, may represent a useful alternative delivery strategy. Transducing tissues at risk for tumor progression *in vivo* with genes encoding antiangiogenic proteins offers the potential of creating a local antiangiogenic microenvironment that can be stably maintained through continuous expression of the transduced transgene

from surrounding tumor cells.

We have constructed and administered eukaryotic vector encoding mouse angiostatin into human gastric cancer cells to further characterize the antitumor function of angiostatin and explore the potential activity in gene therapy for gastric cancer. Our data demonstrated statistically significant inhibition of tumor formation and growth in nude mice accompanied by decreased microvascular density and upregulation of angiostatin, meanwhile no cytostatic effect on gastric cancer cells was observed *in vitro*. These results suggested that the delivery of angiostatin gene may represent a potentially new treatment modality for malignant gastric cancer, accounting for antiangiogenic activity in a paracrine way on surrounding endothelial cells.

## MATERIALS AND METHODS

### Cell culture and reagents

The human gastric cancer cell line SGC7901 was obtained from the Japanese Cancer Research Resources Bank (Tokyo, Japan). Cells were cultured in RPMI1640 (Gibco) supplemented with 10 % fetal bovine serum (FBS) (Sijiqing, Hangzhou, China), penicillin (100 units/ml) and streptomycin (100 mg/ml) in a humidified atmosphere of 5 % CO<sub>2</sub> at 37 °C. Liposome (Tfx<sup>TM</sup> Reagent) was purchased from Promega Company; total RNA Isolation System (Sino-American Biotechnology Company) G418 from Gibco company; and bicinchoninic acid (BCA) protein assay kit was obtained from Pierce Chemicals (Rockford, Illinois).

### Recombinant eukaryotic expression vector pcDNA3.1(+)-angio construction and transfection

Mouse angiostatin cDNA fragment encoding for the NH<sub>2</sub>-terminal secretory signal sequence(SS) and kringle1-4(K1-4) regions of mouse plasminogen, fused with an antigenic epitope tag HA(HA tag) to the COOH terminus of kringle 4 was inserted into eukaryotic expression vector pcDNA3.1(+). The structure of the recombinant vector pcDNA3.1(+)-angio was confirmed by the restriction enzyme digest and DNA sequencing.

Gastric cancer cells SGC7901 in logarithmic growth phase were planted in 6-well plates at 5×10<sup>5</sup> cells/well, and reached approximately 80 % confluent after overnight incubation on the day of the transfection. DNA/liposome (Tfx<sup>TM</sup> Reagent) complexes were prepared and transfected according to the protocol provided by the manufacturer. The experimental group was transfected with pcDNA3.1(+)-angio 2 µg/liposome 10 µL, the vector control with pcDNA3.1(+) 2 µg/liposome 10 µL and the mock control with liposome 10 µL. After 48 h of transfection, the selective medium containing G418 (400 mg/L) was used to culture cells for 30 d. Then the isolated resistant cell clones were then selected and amplified.

### RNA dot blot analysis of angiostatin transcription

Total RNA was extracted with total RNA isolation system, resuspended in DEPC-treated water, quantitated with OD260 and OD280, and dotted onto nitrocellulose filters. The linear mouse angiostatin cDNA fragment was released from the vector pcDNA3.1(+)-angio and labeled with [ $\alpha$ -<sup>32</sup>P] in nick translation reaction as the probe. The specific activity of the probe was examined by TCA method. Hybrid was performed sequentially: prehybridized at 42 °C for 3 h, the probe denatured in water-bath at 100 °C for 10 min and cooled on ice for 5 min, hybridized at 42 °C overnight, washed in 2×SSC and 0.2×SSC at RT, and then hybrid signals were detected by autoradiograph.

### Western blot analysis of HA-tagged protein

The cells were cultured in conditioned media for 5 d. Cell

supernatants was mixed with Lysine-sepharose and incubated at 4 °C overnight. The resin was washed with 50 mM Tris-HCl (pH8.0), and protein was eluted and stored at -20 °C. Protein concentration was determined by bicinchoninic acid assay (BCA) with bovine serum albumin as standard. Equal aliquots (40 µg) of protein from cell supernatants were subjected to electrophoresis on a 10 % sodium dodecyl sulfate (SDS)-polyacrylamide gel, followed by transfer to PVDF membranes (mMILLIPORE) using the transfer buffer for 2 hours and detection with the rabbit polyclonal anti-HA antibody (diluted 1:500; Santa Cruz Biotechnology, Santa Cruz, CA) overnight at 4 °C and a secondary peroxidase-conjugated goat anti-rabbit antibody (Santa Cruz Biotechnology, Santa Cruz, CA). Final detection was performed by the enhanced chemiluminescence (ECL) Western blotting analysis system.

### Viable cell number counting and FACS analysis of cell cycle

Cell viability and cell growth *in vitro* were determined by cell number counting. Briefly, the three groups of cells were plated on 24-well plates at 1×10<sup>4</sup> cells/well and cultured for 7 d. Everyday viable cell numbers of the three groups were counted under microscope.

Three groups of cells 3×10<sup>5</sup> in the logarithmic growth phase were collected and fixed in 70 % ethanol overnight. After being dyed with PI at 4 °C avoid of light for 30 minutes, the cells through screening were checked in FACS to estimate the changes in cell cycle.

### Animal studies

*In vitro* tumorigenesis assay. BalBc nude mice were randomly divided into three groups, 5 in each group and injected subcutaneously with gastric cancer cells SGC7901 at 1.2×10<sup>7</sup> cells/mouse, the experimental group with pcDNA3.1(+)-angio/SGC7901, the vector control with pcDNA3.1(+)/SGC7901 and the mock control with SGC7901 untransfected. After 30 d, the mice were sacrificed to measure the size of tumor formed and calculate the percentage of inhibition on tumorigenesis *in vivo*.

### Quantitative analyses for microvessel densities (MVD)

The tumor tissues were fixed and embedded in paraffin and MVD were detected by SABC method. Briefly, the sections were incubated with 0.3 % H<sub>2</sub>O<sub>2</sub> and methanol for 30 min, blocked with normal goat serum at RT for 2 h, stained with a primary anti-mouse vWF monoclonal antibody at 4 °C overnight and then biotin-conjugated anti-mouse IgG antibody at RT for 1 h. After being incubated with ABC compounds for 40 min, DAB was used to develop color reaction. Under light microscope, MVD was counted in 4 fields (400×) selected randomly.

### Statistical analysis

The results were verified by variance analysis and  $\chi^2$  analysis with SPLM statistical software offered by the Department of Statistics, the Fourth Military Medical University.

## RESULTS

### Identification of the recombinant eukaryotic expression vector encoding angiostatin cDNA

Angiostatin cDNA was cloned into an eukaryotic expression vector pcDNA3.1(+), under the cytomegalovirus promoter, encoding for the NH-terminal secretory signal sequence (SS), the preactivation peptide (PA), and kringle1-4(K1-4) regions of mouse plasminogen, and an antigenic epitope tag derived from the influenza HA fused to the COOH terminus of kringle4 (Figure 1). As shown in electrophoresis, the linear recombinant plasmid was about 7.0kb, and a fragment 1.4kb was released by restrictive digest with HindIII and XbaI, which confirmed

that the targeted gene was cloned into pcDNA3.1(+)-angio successfully (Figure 2). Gene sequencing showed that it had the same sequence as supposed.

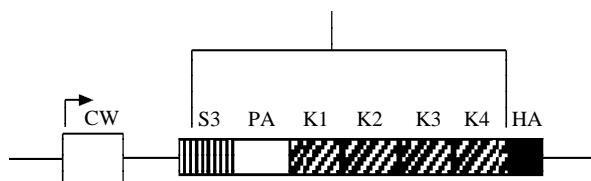


**Figure 1** Schematic diagram of angiostatin cDNA fragment.

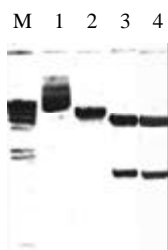


**Figure 2** Identification of angiostatin cDNA insertion in pcDNA3.1(+)-angio. M:  $\lambda$ dsDNA/HindIII marker; 1: pcDNA3.1(+)-angio/ HindIII; 2: pcDNA3.1(+)-angio; 3: pcDNA3.1(+)-angio/HindIII+XbaI; 4: pcDNA3.1(+)-angio/BamHI.

#### Vector-mediated expression and secretion of angiostatin in vitro

To determine the level of transgene-encoded angiostatin transcription and protein expression and secretion, gastric cancer cells SGC7901 transfected with the corresponding vectors were selected by G418 for 30 d and formed macroscopic cell clones in the experimental and vector control groups (Figure 3). The mock group of cells, however, were dead completely after 7 d of selection. Strong RNA hybrid signals of angiostatin mRNA were detected in the experimental group of cell clones genetically engineered but not in the controls (Figure 4). Western blot analysis of cell supernatants (Figure 5) revealed the detected protein of the size consistent with angiostatin in the experiment group, whereas no specific band was observed in the controls.

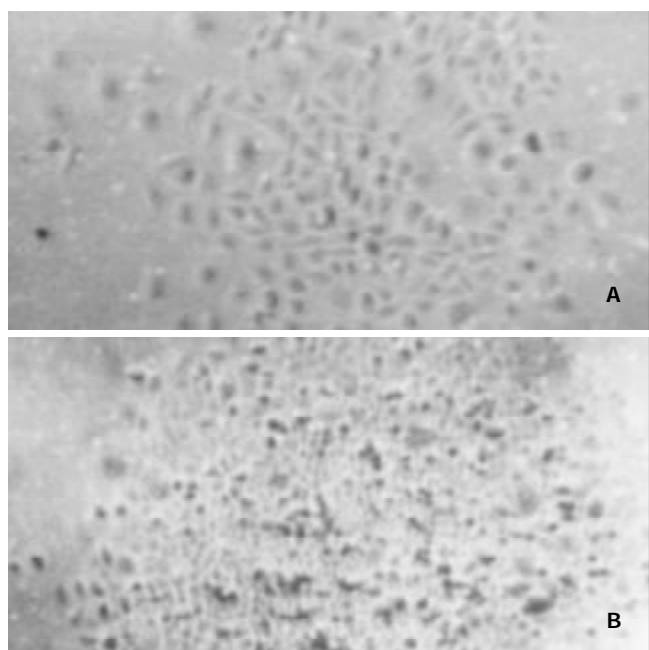


**Figure 3** Cell clones transfected with pcDNA3.1(+)-angio and pcDNA3.1(+) respectively. A: Cell clone pcDNA3.1(+)-angio transfected; B: Cell clone pcDNA3.1(+) transfected.



**Figure 4** Angiostatin mRNA expression by Dot Blot analysis. 1: SGC7901; 2: SGC7901(+); 3:SGC7901-pcDNA3.1(+)-angio.

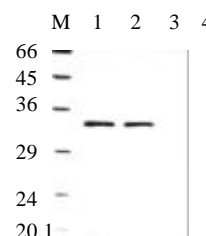


**Figure 5** Angiostatin protein expression by Western Blot analysis. M: Marker; 1: SGC7901pcDNA3.1(+)-angio; 2: SGC7901pcDNA3.1(+)-angio; 3: SGC7901pcDNA3.1(+); 4: SGC7901.

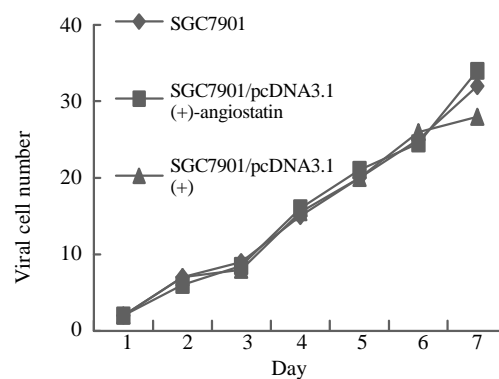


**Figure 6** Cell growth curves.

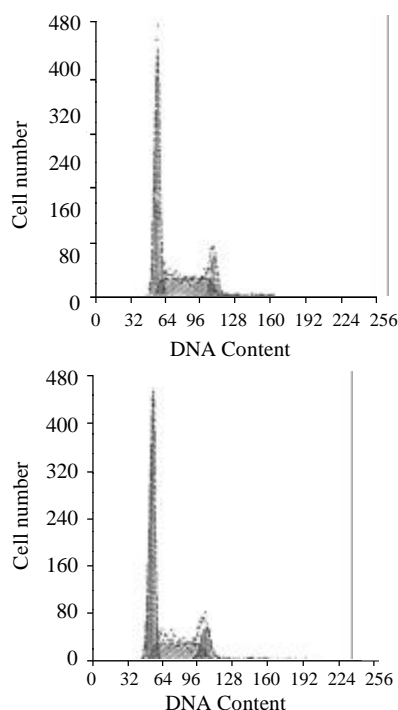


**Figure 7** Cell cycle distributions by FACS analysis. A: SGC7901 transfected with pcDNA3.1(+)-angio; B: SGC7901.

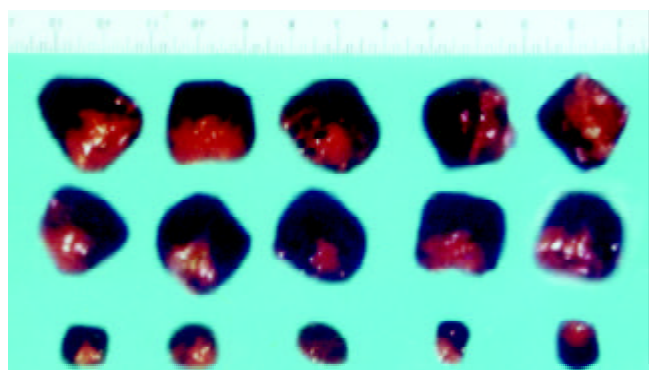


**Figure 8** Tumors formed in nude mice by SGC7901/pcDNA-angio, SGC7901/pcDNA, and SGC7901 cells ( $n=5$ ). A:SGC7901; B: SGC7901/pcDNA3.1(+); C: SGC7901/pcDNA3.1(+)-angio.

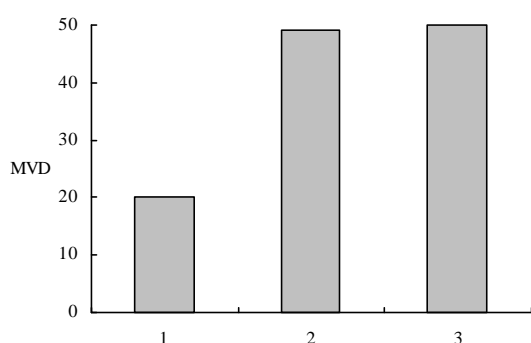


**Figure 9** MVD in immunohistochemistry staining. 1: SGC7901/pcDNA-angio; 2: SGC7901/pcDNA; 3: SGC7901.

#### Biological activity of angiostatin proteins expression *in vitro*

To assay for biological activity of the encoded angiostatin *in vitro*, tumor cells transduced with and without the corresponding vectors were cultured for 7 d to make cell growth curve (Figure 6). Under microscope, no obvious difference was observed in the cell morphology among the three groups of cells. And cell growth curves indicated no change in cell growth speed and doubling time among the three groups. Comparing the cell cycle of the three groups, no significant differences were found in the distribution of G0/G1, S and G2/M (Figure 7). These results indicated that up-regulated angiostatin expression neither directly inhibits cell growth and proliferation nor affects cell cycle *in vitro*.

#### Biological activity of angiostatin proteins expression *in vivo*

The macroscopic tumors were observed on day 7 after injection and expanded fast in the vector and mock control groups of nude mice. However, no tumors were observable until day 10 after injection in the experimental group of nude mice, and tumors expanded slowly. After 30 d of injection, no mice died in the three groups and the tumors were resected and measured. Small, pale tumor nodules were observed in the angiostatin-transfected tumors, whereas large, red and hypervascularized tumors were present in the vector-transfected control and mock control tumor cells. The average size of tumors in the experimental group was  $2.11 \times 0.53 \text{ cm}^3$ , much less than the average size of the vector control  $4.32 \times 1.00 \text{ cm}^3$  and the mock control (Figure 8). The inhibition by angiostatin overexpression reached 72 %.

The tumor tissues in the experimental group showed more typical symptoms of poor vascularization than the control groups. More markedly diminished microvascular densities were detected by immunohistochemical staining in the tumors in the experimental group than in the vector or mock control

groups respectively ( $P<0.01$ ) (Figure 9), which indicated that overexpression of angiostatin probably decreased tumorigenesis by inhibiting neovascularization in tumors *in vivo*. And angiostatin exerted its inhibitory actions in some paracrine ways on ECs surrounding tumor tissues and indirectly inhibited tumorigenesis.

## DISCUSSION

Since Dr. Folkman raised the hypothesis of tumor angiogenic dependence, experimental evidences have validated that tumor growth requires the company of new blood vessel growth. At the prevascular stage, the tumor is unable to grow to a size beyond  $2\text{--}3 \text{ mm}^3$  and remains in its dormant state. However, once the angiogenic phenotype of the tumor is switched on, tumor growth rate changes from linear to exponential<sup>[12-14]</sup>. Metastases are also dependent on angiogenesis in at least two steps of the metastatic events<sup>[15]</sup>. First, metastatic tumor cells must exit from a primary tumor which has been vascularized. Second, upon arrival at their target organ, metastatic tumor cells must undergo neovascularization in order to grow to a clinically detectable size. It is speculated that complete inhibition of tumor angiogenesis may result in a loss of survival factors essential for tumor cells from the endothelial cell as paracrine factors<sup>[16]</sup>. The regulation of tumor angiogenesis is a complex process involving enzymatic and signal-transduction cascades that function in fibrinolysis, matrix remodeling, inflammation, hemodynamic control of oxygenation, and growth regulation<sup>[17-19]</sup>. The local balance between positive and negative factors determines the net tendency toward angiogenesis or angiostasis<sup>[20]</sup>.

Angiogenesis is closely related to gastric cancer as a pertinent predictive factor in addition to having prognostic value<sup>[21]</sup>. The average number of blood vessels is significantly higher in gastric cancer specimens than in normal gastric specimens, higher in advanced disease than in early-stage disease, higher in specimens with metastases or blood vessel invasion than in those without such metastasis or invasion<sup>[22,23]</sup>. VEGF positive immunostaining is observed in the gastric tissues with different severities of lesions, the positive rates increased with the lesion progressing from CAG to IM to DYS<sup>[24]</sup>. And its expression is associated with hematogenous invasion, metastasis, and clinical prognosis of gastric cancer<sup>[25]</sup>. As a malignant disease with the highest mortality rates in China, gastric cancer is refractory to the routine chemotherapy and radiotherapy, which are mainly adopted as the adjunctive therapy during and/or post operation to prolong the survival rates<sup>[26,27]</sup>. Moreover, chemotherapy has obvious toxicity and is subject to drug resistance in the treatment of gastric cancer<sup>[28]</sup>. Until now the only method possible to cure gastric cancer is surgical resection, despite its importance for the late-stage cancer and various types of high-rate recurrences. Meanwhile the chromosomal instability in DNA of gastric cancer cells unfavorably obstructs the curative effects of the methods directly attacking tumor cells.

Thus antiangiogenic treatment may be necessary and potential for gastric cancer, which has been validated in many experiments. In *in vivo* experiments, antiangiogenic agents with cytotoxic anticancer drugs formed a highly effective modulator combination for the treatment against primary and metastatic carcinoma. The combination of anti-VEGF antibody with mitomycin C markedly enhanced anti-tumor and anti-metastasis effects in nude mice transplanted with human gastric cancer SGC-7901<sup>[29]</sup>. The VEGF receptor KDR/Flk-1 antisense strategy significantly increases the number of gastric cancer cells undergoing apoptosis, and decreases tumor dissemination<sup>[30]</sup>. Angiogenesis inhibitor endostatin inhibits both tumor growth and metastasis of human gastric cancer in nude mice<sup>[31]</sup>. And

octreotide inhibits the migration and invasion of SGC-7901 gastric cancer cells *in vitro* and the metastasis of cancer *in vivo* through down-regulation of MMP-2 expression and tumor angiogenesis<sup>[32]</sup>. And the clinical applications of antivasular, anti-angiogenic and angiostatic agents for the treatment of gastric carcinoma may be valuable for long-term administration to maintain tumor dormancy because drug resistance does not develop, and these agents have a sustained effect with less side effects than the traditional methods.

Angiostatin was firstly isolated as a circulating angiogenesis inhibitor, whose sequence has greater than 98 % identity with an internal fragment of plasminogen, containing the first four of five triple loop disulfide-linked kringle structures. Purified angiostatin specifically and reversibly inhibits proliferation of endothelial lineages in a dose-dependent manner, but not proliferation of normal and neoplastic nonendothelial cell lines<sup>[9-11]</sup>. Systemic administration of human angiostatin potently inhibits the growth of transplanted human breast carcinoma by 95 %, colon carcinoma by 97 % and prostate carcinoma by almost 100 % in mice, without obvious weight loss or other toxicity observed<sup>[33,34]</sup>. It causes human primary carcinomas to regress to a dormant state by a net balance of tumor cell proliferation and apoptosis. And in the presence of angiostatin, metastatic tumor cells form microscopic perivascular cuffs around the pre-existing microvessel, rarely expanding beyond 0.3 mm in diameter<sup>[35-37]</sup>. Although angiostatin is a potent inhibitor of angiogenesis and tumor growth, the need of high dosages, repeated injections and long-term administration of this protein into the body have made it less attractive for clinical trials.

In order to develop alternative strategies for therapy, the potential of angiostatin in gene therapy has been investigated. In our study, human gastric cancer cells SGC7901 are transfected with mouse angiostatin cDNA and stable cell lines expressing the secreted form of angiostatin are established. Despite the high levels of its expression in cell clones, angiostatin has no direct influence on tumor-cell growth *in vitro*. Implantation of the stable cell clones in nude mice produces inhibition of primary tumor growth by an average of 72 %. Inhibition of tumor growth is correlated with reduced vascularization, suggesting that angiostatin exerts the antitumor effects through antiangiogenesis. These results are similar to the previously report that angiostatin cDNA transfection into the murine T241 fibrosarcoma cells inhibits primary tumor growth by an average of 77 % in C57Bl6/J mice<sup>[38]</sup>. Thus angiostatin gene therapy is possibly available for gastric cancer, especially for its simple manipulation, highly specificity, wide-spectrum inhibitory effects on various tumors. It has been observed that retroviral transduction of angiostatin in rat glioma cells inhibits tumor growth by 70 % *in vivo*, however, a relatively ineffective process<sup>[39]</sup>. Stable gene transfer of the angiostatin cDNA by retroviral vectors in Kaposi' s sarcoma KS-IMM cells resulted in delayed tumor growth in nude mice, which was associated with reduced vascularization<sup>[40]</sup>. Direct injections of replication-deficient angiostatin-expressing adenoviral vector inhibit tumor growth, and represent a potentially new treatment modality for malignant ascites, which are efficient and capable of transducing dividing cells as well as non-dividing cells *in vivo*<sup>[39,41]</sup>. The specific targeting of tumors to inhibit angiogenesis using an adenovirus expressing angiostatin, may deliver localized concentrations of protein having a greater impact on inhibition of tumor growth<sup>[42]</sup>. AAV-mediated antiangiogenesis gene therapy offers efficient and sustained systemic delivery of the therapeutic product, which in turn effectively suppresses glioma growth in the brain<sup>[43]</sup>. Considering the possibility of viral immunoreaction and toxicity, non-viral angiostatin-delivery system has also been explored. Intravenous injection of cationic liposome-

angiostatin cDNA complex produced a significant antimetastatic effect on murine B16 melanoma compared to either reporter gene-treated and untreated controls<sup>[44]</sup>. These results support that angiostatin-gene therapy is a potential strategy in the clinical treatment of gastric cancer.

In order to modify the specificity, we are exploiting gastric cancer specific single-chained antibodies to guide the angiostatin-gene therapy. Another potential pathway is delivering angiostatin gene directly into gastric cancer tissues under the endoscope. Because neovascularization in tumors is a multi-step process, the key molecules involved in various steps are potentially combined to improve anti-cancer efficacy of angiogenic gene therapy, including inhibition of endothelial cell proliferation, migration, invasion and matrix degradation. More effective inhibition has been observed in the combined gene therapy of angiostatin and endostatin than the angiostatin-or endostatin-therapy respectively<sup>[45]</sup>. Meanwhile, angiogenic genes are possibly combined with other curative molecules, such as immunoregulators, suppressors of oncogene, enzymatic precursor drugs. When angiostatin-mediated antiangiogenic therapy is used in combination with intratumor delivery of the IL-12 gene, this produces a synergistic therapeutic effect<sup>[46]</sup>. It has been validated the potential of combining a destructive strategy directed against the tumor cells with an anti-angiogenic approach to fight cancer. The combination of radiotherapy and angiostatin intratumoral injection reveals a significant inhibition of tumor growth as compared with either treatment<sup>[47]</sup>. These combined therapies will open new possibilities of being less toxic and more effective than the traditional therapies in the clinical treatment of gastric cancer.

In conclusion, it is the first time that approves the potential of angiostatin anti-cancer effect has been proved on gastric cancer and its functional mechanism of antiangiogenesis in tumor has been revealed. And these data offers a new way to comeover the disadvantages in traditional therapies in clinic.

## REFERENCES

- 1 **Hayes AJ**, Li LY, Lippman ME. Science,medicine,and the future antivasular therapy:a new approach to cancer treatment. *BMJ* 1999; **318**: 353-356
- 2 **Rosen LS**. Angiogenesis inhibition in solid tumors. *Cancer J* 2001; **7** (Suppl 3): S120-128
- 3 **Sugimachi K**, Tanaka S, Terashi T, Taguchi K, Rikimaru T, Sugimachi K. The mechanisms of angiogenesis in hepatocellular carcinoma: angiogenic switch during tumor progression. *Surgery* 2002; **131**(Suppl 1): S135-141
- 4 **Cao Y**. Endogenous angiogenesis inhibitors and their therapeutic implications. *Int J Biochem Cell Biol* 2001; **33**: 357-369
- 5 **Hagedorn M**, Bikfalvi A. Target molecules for anti-angiogenic therapy: from basic research to clinical trials. *Crit Rev Oncol Hematol* 2000; **34**: 89-110
- 6 **Saito H**, Tsujitani S. Angiogenesis, angiogenic factor expression and prognosis of gastric carcinoma. *Anticancer Res* 2001; **21**: 4365- 4372
- 7 **Kakeji Y**, Maehara Y, Sumiyoshi Y, Oda S, Emi Y. Angiogenesis as a target for gastric cancer. *Surgery* 2002; **131**(1 Suppl): S48-54
- 8 **Gibaldi M**. Regulating angiogenesis: a new therapeutic strategy. *J Clin Pharmacol* 1998; **38**: 898-903
- 9 **Gupta N**, Nodzenski E, Khodarev NN, Yu J, Khorasani L, Beckett MA, Kufe DW, Weichselbaum RR. Angiostatin effects on endothelial cells mediated by ceramide and RhoA. *EMBO Rep* 2001; **2**: 536-540
- 10 **Lucas R**, Holmgren L, Garcia I, Jimenez B, Mandriota SJ, Borlat F, Sim BK, Wu Z, Grau GE, Shing Y, Soff GA, Bouck N, Pepper MS. Multiple forms of angiostatin induce apoptosis in endothelial cells. *Blood* 1998; **92**: 4730-4741
- 11 **Hari D**, Beckett MA, Sukhatme VP, Dhanabal M, Nodzenski E, Lu H, Mauceri HJ, Kufe DW, Weichselbaum RR. Angiostatin induces mitotic cell death of proliferating endothelial cells. *Mol Cell Biol Res Commun* 2000; **3**: 277-282



- 12 **Papetti M**, Herman IM. Mechanisms of normal and tumor-derived angiogenesis. *Am J Physiol Cell Physiol* 2002; **282**: C947-970
- 13 **Ellis LM**, Liu W, Ahmad SA, Fan F, Jung YD, Shaheen RM, Reinmuth N. Overview of angiogenesis: Biologic implications for antiangiogenic therapy. *Semin Oncol* 2001; **28** (5 Suppl 16): 94-104
- 14 **Cavallaro U**, Christofori G. Molecular mechanisms of tumor angiogenesis and tumor progression. *J Neurooncol* 2000; **50**: 63-70
- 15 **Bashyam MD**. Understanding cancer metastasis: an urgent need for using differential gene expression analysis. *Cancer* 2002; **94**: 1821-1829
- 16 **Reinmuth N**, Stoeltzing O, Liu W, Ahmad SA, Jung YD, Fan F, Parikh A, Ellis LM. Endothelial survival factors as targets for antineoplastic therapy. *Cancer J* 2001; **7** (Suppl 3): S109-119
- 17 **VanMeter TE**, Rooprai HK, Kibble MM, Fillmore HL, Broaddus WC, Pilkington GJ. The role of matrix metalloproteinase genes in glioma invasion: co-dependent and interactive proteolysis. *J Neurooncol* 2001; **53**: 213-235
- 18 **Izumi Y**, Xu L, di Tomaso E, Fukumura D, Jain RK. Tumour biology: herceptin acts as an anti-angiogenic cocktail. *Nature* 2002; **416**: 279-280
- 19 **Giatromanolaki A**, Harris AL. Tumour hypoxia, hypoxia signaling pathways and hypoxia inducible factor expression in human cancer. *Anticancer Res* 2001; **21**: 4317-4324
- 20 **Dixelius J**, Cross M, Matsumoto T, Sasaki T, Timpl R, Claesson-Welsh L. Endostatin regulates endothelial cell adhesion and cytoskeletal organization. *Cancer Res* 2002; **62**: 1944-1947
- 21 **Saito H**, Tsujitani S. Angiogenesis, angiogenic factor expression and prognosis of gastric carcinoma. *Anticancer Res* 2001; **21**: 4365-4372
- 22 **Chen CN**, Cheng YM, Lin MT, Hsieh FJ, Lee PH, Chang KJ. Association of color Doppler vascularity index and microvessel density with survival in patients with gastric cancer. *Ann Surg* 2002; **235**: 512-518
- 23 **Erenoglu C**, Akin ML, Uluutku H, Tezcan L, Yildirim S, Batkin A. Angiogenesis predicts poor prognosis in gastric carcinoma. *Dig Surg* 2000; **17**: 581-586
- 24 **Feng C**, Wang L, Jiao L, Liu B, Zheng S, Xie X. Expression of p53, inducible nitric oxide synthase and vascular endothelial growth factor in gastric precancerous and cancerous lesions: correlation with clinical features. *BMC Cancer* 2002; **2**: 8
- 25 **Tao HQ**, Lin YZ, Wang RN. Significance of vascular endothelial growth factor messenger RNA expression in gastric cancer. *World J Gastroenterol* 1998; **4**: 10-13
- 26 **Meyerhardt JA**, Fuchs CS. Chemotherapy options for gastric cancer. *Semin Radiat Oncol* 2002; **12**: 176-186
- 27 **Wilson KS**. Postoperative chemoradiotherapy helps in gastric adenocarcinoma. *BMJ* 2002; **324**: 977
- 28 **Wang X**, Lan M, Shi YQ, Lu J, Zhong YX, Wu HP, Zai HH, Ding J, Wu KC, Pan BR, Jin JP, Fan DM. Differential display of vincristine-resistance-related genes in gastric cancer SGC7901 cell. *World J Gastroenterol* 2002; **8**: 54-59
- 29 **Tao HQ**, Lin YZ, Wang RN. Significance of vascular endothelial growth factor messenger RNA expression in gastric cancer. *World J Gastroenterol* 1998; **4**: 10-13
- 30 **Kamiyama M**, Ichikawa Y, Ishikawa T, Chishima T, Hasegawa S, Hamaguchi Y, Nagashima Y, Miyagi Y, Mitsuhashi M, Hyndman D, Hoffman RM, Ohki S, Shimada H. VEGF receptor antisense therapy inhibits angiogenesis and peritoneal dissemination of human gastric cancer in nude mice. *Cancer Gene Ther* 2002; **9**: 197-201
- 31 **Zhang GF**, Wang YH, Zhang MA, Wang Q, Luo YB, Han CR, Lu YQ, Rao YY. Inhibition of growth and metastasis of human gastric cancer implanted in nude mice by the angiogenesis inhibitor endostatin. [Article in Chinese]. *Zhonghua Waike Zazhi* 2002; **40**: 59-61
- 32 **Wang CH**, Tang CW. Inhibition of human gastric cancer metastasis by ocreotide *in vitro* and *in vivo*. [Article in Chinese] *Zhonghua Yixue Zazhi* 2002; **82**: 19-22
- 33 **Sim BK**, O'Reilly MS, Liang H, Fortier AH, He W, Madsen JW, Lapcevic R, Nacy CA. A recombinant human angiostatin protein inhibits experimental primary and metastatic cancer. *Cancer Res* 1997; **57**: 1329-1334
- 34 **Kirsch M**, Strasser J, Allende R, Bello L, Zhang J, Black PM. Angiostatin suppresses malignant glioma growth *in vivo*. *Cancer Res* 1998; **58**: 4654-4659
- 35 **Apte RS**, Niederkorn JY, Mayhew E, Alizadeh H. Angiostatin produced by certain primary uveal melanoma cell lines impedes the development of liver metastases. *Arch Ophthalmol* 2001; **119**: 1805-1809
- 36 **Yanagi K**, Onda M, Uchida E. Effect of angiostatin on liver metastasis of pancreatic cancer in hamsters. *Jpn J Cancer Res* 2000; **91**: 723-730
- 37 **Drixler TA**, Rinkes IH, Ritchie ED, van Vroonhoven TJ, Gebbink MF, Voest EE. Continuous administration of angiostatin inhibits accelerated growth of colorectal liver metastases after partial hepatectomy. *Cancer Res* 2000; **60**: 1761-1765
- 38 **Cao Y**, O'Reilly MS, Marshall B, Flynn E, Ji RW, Folkman J. Expression of angiostatin cDNA in a murine fibrosarcoma suppresses primary tumor growth and produces long-term dormancy of metastases. *J Clin Invest* 1998; **101**: 1055-1063
- 39 **Indraccolo S**, Morini M, Gola E, Carrozzino F, Habeler W, Minghelli S, Santi L, Chieco-Bianchi L, Cao Y, Albini A, Noonan DM. Effects of angiostatin gene transfer on functional properties and *in vivo* growth of Kaposi's sarcoma cells. *Cancer Res* 2001; **61**: 5441-5446
- 40 **Gyorffy S**, Palmer K, Gaudie J. Adenoviral vector expressing murine angiostatin inhibits a model of breast cancer metastatic growth in the lungs of mice. *Am J Pathol* 2001; **159**: 1137-1147
- 41 **Tanaka T**, Cao Y, Folkman J, Fine HA. Viral vector-targeted antiangiogenic gene therapy utilizing an angiostatin complementary DNA. *Cancer Res* 1998; **58**: 3362-3369
- 42 **Hampf M**, Tanaka T, Albert PS, Lee J, Ferrari N, Fine HA. Therapeutic effects of viral vector-mediated antiangiogenic gene transfer in malignant ascites. *Hum Gene Ther* 2001; **12**: 1713-1729
- 43 **Ma HI**, Guo P, Li J, Lin SZ, Chiang YH, Xiao X, Cheng SY. Suppression of intracranial human glioma growth after intramuscular administration of an adeno-associated viral vector expressing angiostatin. *Cancer Res* 2002; **62**: 756-763
- 44 **Rodolfo M**, Cato EM, Soldati S, Ceruti R, Asioli M, Scanziani E, Vezzoni P, Parmiani G, Sacco MG. Growth of human melanoma xenografts is suppressed by systemic angiostatin gene therapy. *Cancer Gene Ther* 2001; **8**: 491-496
- 45 **Scappaticci FA**, Smith R, Pathak A, Schloss D, Lum B, Cao Y, Johnson F, Engleman EG, Nolan GP. Combination angiostatin and endostatin gene transfer induces synergistic antiangiogenic activity *in vitro* and antitumor efficacy in leukemia and solid tumors in mice. *Mol Ther* 2001; **3**: 186-196
- 46 **Wilczynska U**, Kucharska A, Szary J, Szala S. Combined delivery of an antiangiogenic protein (angiostatin) and an immunomodulatory gene (interleukin-12) in the treatment of murine cancer. *Acta Biochim Pol* 2001; **48**: 1077-1084
- 47 **Griscelli F**, Li H, Cheong C, Opolon P, Bennaceur-Griscelli A, Vassal G, Soria J, Soria C, Lu H, Perricaudet M, Yeh P. Combined effects of radiotherapy and angiostatin gene therapy in glioma tumor model. *Proc Natl Acad Sci USA* 2000; **97**: 6698-6703



# Synergistic effect of cell differential agent-II and arsenic trioxide on induction of cell cycle arrest and apoptosis in hepatoma cells

Jian-Wei Liu, Yi Tang, Yan Shen, Xue-Yun Zhong

**Jian-Wei Liu**, Department of General Surgery, **Yi Tang**, **Yan Shen**, Cell Culture Laboratory, Guangzhou Red Cross Hospital, Jinan University, Guangzhou 510220, Guangdong Province, China  
**Xue-Yun Zhong**, Department of Pathology, Jinan University Medical College, Guangzhou 510632, Guangdong Province, China  
**Supported by** the Scientific Research Fund of Guangdong Province, No.1998110

**Correspondence to:** Dr. Jian-Wei Liu, Department of General Surgery, Guangzhou Red Cross Hospital, Jinan University, Guangzhou 510220 Guangdong Province, China. mabeliu@public.guangzhou.gd.cn  
**Telephone:** +86-20-84412233 **Fax:** +86-20-84429803  
**Received:** 2002-06-03 **Accepted:** 2002-07-03

## Abstract

**AIM:** To illustrate the possible role of cell differential agent-II (CDA-II) in the apoptosis of hepatoma cells induced by arsenic trioxide ( $As_2O_3$ ).

**METHODS:** Hepatoma cell lines BEL-7402 and HepG2 were treated with  $As_2O_3$  together with CDA-II. Cell surviving fraction was determined by MTT assay; morphological changes were observed by immunofluorescence staining of Hoechst 33 258; and cell cycle and the apoptosis index were determined by flow cytometry (FCM).

**RESULTS:** Cytotoxicity of CDA-II was low. Nevertheless, CDA-II could strongly potentiate arsenic trioxide-induced apoptosis. At 1.0 g/L CDA-II,  $IC_{50}$  of  $As_2O_3$  in hepatoma cell lines was reduced from 5.0  $\mu$ mol/L to 1.0  $\mu$ mol/L ( $P < 0.01$ ). The potentiation of apoptosis was dependent on the dosage of CDA-II. FCM indicated that in hepatoma, cell growth was inhibited by CDA-II at lower concentrations ( $< 2.0$  g/L) primarily by arresting at S and  $G_2$  phase, and at higher concentrations ( $> 2.0$  g/L) apoptotic cell and cell cycle arresting at  $G_1$  phase increased proportionally. The combination of two drugs led to much higher apoptotic rates, as compared with the either drug used alone.

**CONCLUSION:** CDA-II can strongly potentiate  $As_2O_3$ -induced apoptosis in hepatoma cells, and two drugs can produce a significant synergic effect.

Liu JW, Tang Y, Shen Y, Zhong XY. Synergistic effect of cell differential agent-II and arsenic trioxide on induction of cell cycle arrest and apoptosis in hepatoma cells. *World J Gastroenterol* 2003; 9(1): 65-68  
<http://www.wjgnet.com/1007-9327/9/65.htm>

## INTRODUCTION

It has been reported that arsenic trioxide ( $As_2O_3$ ), a newly found apoptosis inducer, possesses a greater apoptotic effect on hepatoma cells as compared with some drugs used in chemotherapy<sup>[1-5]</sup>. However, because of its toxicity and the drug resistance of cancer cells, it has not been widely used in the treatment of cancers<sup>[6-10]</sup>. As a biological preparation purified from human urine, cell differential agent-II (CDA-II) can

effectively induce cell differentiation and reverse drug resistance of cancer cells against chemotherapeutic agents<sup>[11,12]</sup>. Clinical application of CDA-II has demonstrated its low toxicity and satisfactory therapeutic effect<sup>[13-15]</sup>. This report is intended to investigate the effect of CDA-II on  $As_2O_3$ -induced apoptosis of hepatoma cells in an attempt to find a better combination therapy for hepatoma.

## MATERIALS AND METHODS

### Materials

Human hepatoma cell lines HepG2 and Bel-7402 were obtained from the cell laboratory in the Medical School of Zhongshan University; cell differential agent (CDA-II) was provided by Everlife Pharmaceutical Co. Ltd, Hefei; arsenic trioxide ( $As_2O_3$ ,  $M_r=197.84$ ), MTT, Hoechst 33 258 and PI were purchased from Sigma Co., USA; PRMI 1 640 was purchased from GIBCO, USA; agar, RNase, proteinase were purchased from Huamei Company; DEME purchased from Evergreen Company, Hangzhou, dimethyl sulfoxide (DMSO) was imported and individually packed, and  $\lambda$ -DNA Marker VII was purchased from Roche Company, USA.

### Experimental group

The preliminary experiment showed that 1.0-5.0  $\mu$ mol/L of  $As_2O_3$  could induce apoptosis in hepatoma cells to various degrees, and 1.0-5.0 g/L of CDA-II could inhibit proliferation and induce differentiation of hepatoma cells. The experiment was divided into 4 groups: group A, control without any drug; group B,  $As_2O_3$  was added only to final concentrations of 1.0, 2.0, 3.0, 4.0 and 5.0  $\mu$ mol/L; group C, CDA-II was added to final concentrations of 1.0, 2.0, 3.0, 4.0 and 5.0 g/L; and group D, 1.0 g/L of CDA-II + various concentrations of  $As_2O_3$  used in the group A.

### Cell culture and survival rate tested with MTT

Cells were cultured in PRMI1640 with 10 % calf serum, 100 U/ml penicillin and 100  $\mu$ g/ml streptomycin in a humidified atmosphere of 5 %  $CO_2$  at 37 °C. With a density between  $2 \times 10^6$  and  $6 \times 10^6$ , two cell lines grew in the same way as typical epithelial cells, and reproduced once every two days. During the experiment, the density of cells was adjusted to  $1 \times 10^6$ /mL with culture medium PRMI1640, and transferred to 96-well plates, 100  $\mu$ L cell suspension per well, to incubate for 24 hours. Drugs of different concentrations were added to the plate, 4 plate wells for each drug concentration according to the aforementioned group division: 100  $\mu$ L drug and 100  $\mu$ L culture medium were added to each well with a total volume of 200  $\mu$ L for group B and C; 100  $\mu$ L of two drugs each was added with a total volume of 200  $\mu$ L for group D; and 200  $\mu$ L culture medium was added to each well of control group. All the groups had concentrations of 4 compound wells. After incubation for 24 h, 48 h, 72 h and 96 h, 20  $\mu$ L of 0.5 % MTT was added to each well and incubated for another 4 hours. The supernatant was discarded and 200  $\mu$ L of DMSO was added. When the stain was dissolved, the optical density ABS value of each well was read on MinireaderII at 570 nm. Cell survival

rate was calculated with the following equation: average A value of experimental group/average A value of control group $\times 100\%$ . Each experiment was repeated at least three times.

### The rate of apoptosis tested by fluorescence of live cells

After the aforementioned cells were cultured with drugs for 72 h, cells were harvested and fixed with 1:3 glacial acetic acid/methanol twice, first for 5 min and then 10 min and washed with phosphate buffer solution (PBS). Hoechst 33 258 was put into cell suspension to a final concentration of 1.0 mg/L and the cells were stained fluorescent for 15 minutes away from light. An Olympus BH-2 fluorescence microscope was used to observe the fluorescent associated with DNA of cells nuclei. Graphs were drawn based on different concentrations of drugs and apoptotic rate of cells.

### Agarose gel electrophoresis of DNA

Cells treated with drugs for 96 h were collected. After lysis with Nicoletti lysis buffer, DNA was extracted with an equal volume of phenol, phenol/chloroform and chloroform once each, incubated with RNase and precipitated with ethanol and sodium acetate. DNA was sedimented by centrifugation, air dried and dissolved in Tris-EDTA buffer. Each DNA sample was analyzed by gel electrophoreses in 1.2 % agarose gel for 1.5 h and visualized under ultra-violet light.

### Apoptosis index (PI) determined by flow cytometry (FCM)

The cells described above were harvested, and  $1 \times 10^6$  cells were centrifuged to get rid of supernatant, fixed with ethanol, and incubated with 200  $\mu$ L RNase A at 37 °C for 1 h; 800  $\mu$ L PI staining solution was mixed into it and the subsequent mixture was stored in the refrigerator at 4 °C for 30 minutes. Flow cytometry was then used to analyze the cell cycle. The cells with content of DNA in sub  $G_1$  were apoptotic cells.

### Statistics

Software SPSS 10.1 was employed to process the data with test of index deviation, and to analyze the causes of the deviation in data concerning multiple factors of the experimental design.

## RESULTS

### Effects of CDA-II and $As_2O_3$ on the growth of hepatoma cells

Cytotoxicity of CDA-II was low. At 1.0 g/L, the respective survival rate of cell lines HepG2 and BEL-7402 were 92 % and 89 %. When the concentration was increased to 3.0 g/L, the survival rate dropped to 76 % and 65 % respectively. The combined usage of two drugs markedly increased the cytotoxicity of  $As_2O_3$  on the two cell lines. The addition of 1.0 g/L CDA-II caused  $IC_{50}$  of  $As_2O_3$  to fall from 5.0  $\mu$ mol/L to 1.0  $\mu$ mol/L ( $P < 0.01$ , Table 1).

**Table 1** Survival rate of hepatoma cell lines HepG2 treated with drugs ( $\bar{x} \pm s$ ) %

Groups	$c_{B,B}/(\mu\text{mol} \cdot \text{L}^{-1})^a$ or $\rho_{B,C}/(\text{g} \cdot \text{L}^{-1})^b$				
	1.0	2.0	3.0	4.0	5.0 <sup>c</sup>
A (Controls)	100	100	100	100	100
B ( $As_2O_3$ , $c_B$ ) <sup>d</sup>	80.06 $\pm$ 3.27	70.58 $\pm$ 5.42	67.82 $\pm$ 3.43	59.33 $\pm$ 7.33	49.12 $\pm$ 4.25
C (CDA-II, $\rho_B$ ) <sup>e</sup>	92.41 $\pm$ 4.25	81.22 $\pm$ 7.34	70.23 $\pm$ 2.32	68.22 $\pm$ 4.56	67.12 $\pm$ 9.23
D (B+C <sub>1.0</sub> ) <sup>f</sup>	50.67 $\pm$ 3.56	47.88 $\pm$ 6.42	47.34 $\pm$ 4.25	45.54 $\pm$ 8.22	41.55 $\pm$ 3.75

<sup>a</sup> $c_{B,B}/(\mu\text{mol} \cdot \text{L}^{-1})$  is for group B( $As_2O_3$ ,  $c_B$ );  $\rho_{B,C}/(\text{g} \cdot \text{L}^{-1})$  is for group C (CDA-II,  $\rho_B$ ); <sup>b</sup>group D (B+C<sub>1.0</sub>) refers to every each group B

( $As_2O_3$ ,  $c_{B,B}$ ) plus  $\rho_{B,C}=1.0 \text{ g} \cdot \text{L}^{-1}$ ; <sup>c</sup>Concentration grads effect:  $F=32.270$ , sig.=0.000,  $P < 0.05$ ; <sup>d</sup>Main effect for group B ( $As_2O_3$ ,  $c_B$ ):  $F=22.856$ , sig.=0.000,  $P < 0.05$ ; <sup>e</sup>Main effect for group C (CDA-II,  $\rho_B$ ):  $F=0.831$ , sig.=0.059,  $P > 0.05$ ; <sup>f</sup>Interaction effect for group D (B+C<sub>1.0</sub>):  $F=27.178$ , sig.=0.000,  $P < 0.05$

### Effect of two drugs on apoptosis in hepatoma cells

Under fluorescent microscope, cell nuclei of the control group displayed fluorescence evenly. Treated by the two drugs in combination, a large proportion of cells underwent apoptosis. Uneven and more dense particulate fluorescence could be observed in cell nuclei (Figure 1). The rate of apoptosis of 500 cells was calculated. The result showed (Figure 2) that when  $As_2O_3$  was employed at 1.0  $\mu$ mol/L, the number of apoptotic cells was only slightly above that of control, and the difference was not significant ( $P=0.063$ ). However, the apoptotic rate rose greatly with the increase of drug concentrations above 1.0  $\mu$ mol/L, and the significance of differences became obvious as against the control ( $P < 0.01$ ). When CDA-II was used alone, the concentration must be above 3.0 g/L showed significant difference from the control ( $P < 0.015$ ). CDA-II greatly potentiated the apoptosis induced by  $As_2O_3$ . The apoptotic rate of 1.0  $\mu$ mol/L of  $As_2O_3$  together with 1.0 g/L of CDA-II approached that of 4.0  $\mu$ mol/L  $As_2O_3$ .

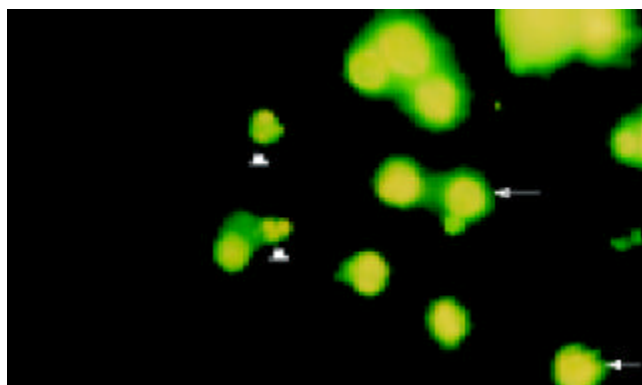


**Figure 1** Immunofluorescence staining of Hoechst 33 258 72 h after 1.0  $\mu$ mol/L  $As_2O_3$ +1.0 g/L CDA-II administrated in HepG2 cells ( $\times 400$ ).  $\rightarrow$ : dispersive fluorescences in normal cells nuclei;  $\triangle$ : compact particulate fluorescences in apoptosis cell nuclei

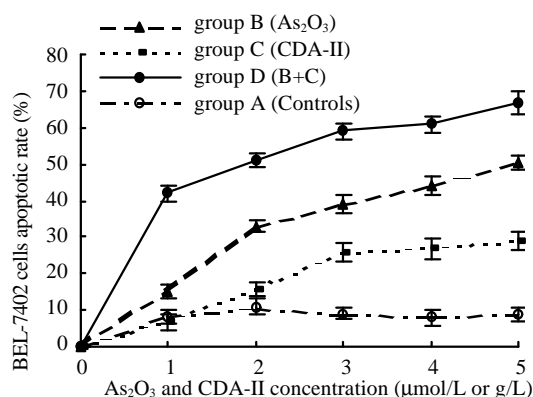


**Figure 2** Comparison of different groups on numbers of BEL-7402 cell apoptosis. A. Main effect( $As_2O_3$ ):  $F=0.387$ , sig.=0.063,  $P > 0.05$ ; B. Main effect(CDA-II):  $F=0.670$ , sig.=0.785,  $P > 0.05$ ; C. Interaction ( $As_2O_3$ + CDA-II):  $F=22.450$ , sig.=0.000,  $P < 0.05$

DNA of cells undergoing apoptosis showed a ladder pattern in agarose gel electrophoresis. In the present study, DNA ladders were characteristically identified in the cells treated with 5.0  $\mu$ mol/L  $As_2O_3$  or 1.0 g/L CDA-II+1  $\mu$ M  $As_2O_3$  for 72 h as shown in Figure 3.

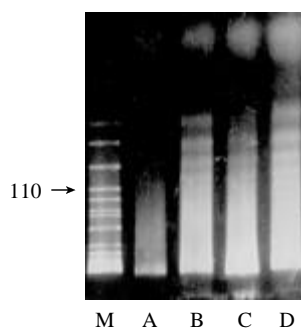


**Figure 3** DNA agarose gel electrophoresis of hepatoma cell lines treated by  $\text{As}_2\text{O}_3$  or CDA-II+ $\text{As}_2\text{O}_3$  for 72 h. M:  $\lambda$ -DNA Marker VII; A (HepG2): controls; B (HepG2):  $1.0 \mu\text{mol} \cdot \text{L}^{-1} \text{As}_2\text{O}_3 + 1.0 \text{ g} \cdot \text{L}^{-1} \text{CDA-II}$ ; C (BEL-7402):  $1.0 \mu\text{mol} \cdot \text{L}^{-1} \text{As}_2\text{O}_3 + 1.0 \text{ g} \cdot \text{L}^{-1} \text{CDA-II}$ ; D (HepG2):  $5.0 \mu\text{mol} \cdot \text{L}^{-1} \text{As}_2\text{O}_3$

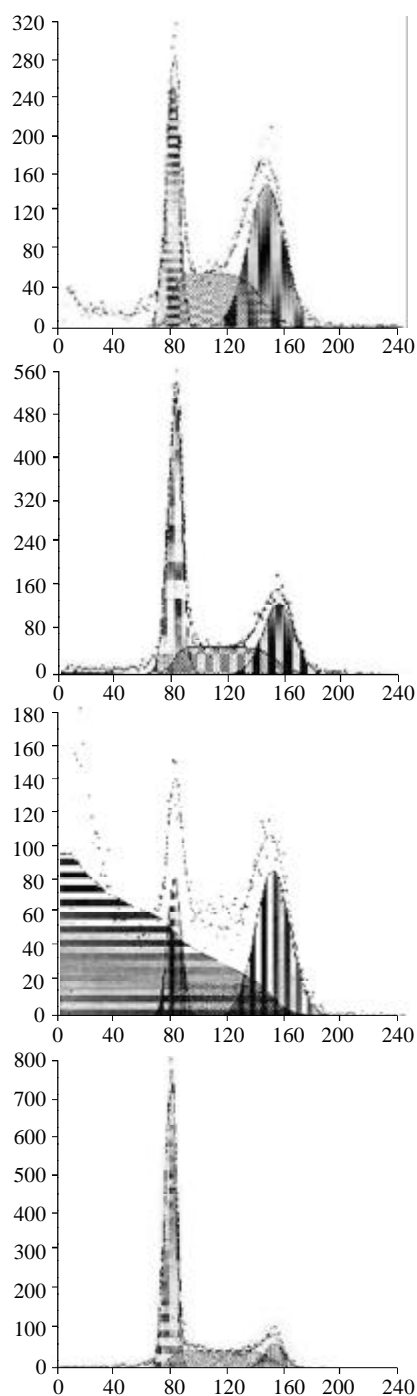


**Figure 5** Flow cytometry 4 days after medicinal treatment. (A).  $1.0 \mu\text{mol/L} \text{As}_2\text{O}_3$ ; (B).  $1.0 \text{ g/L} \text{CDA-II}$ ; (C).  $1.0 \mu\text{mol/L} \text{As}_2\text{O}_3 + 1.0 \text{ g/L} \text{CDA-II}$ ; (D). Control.

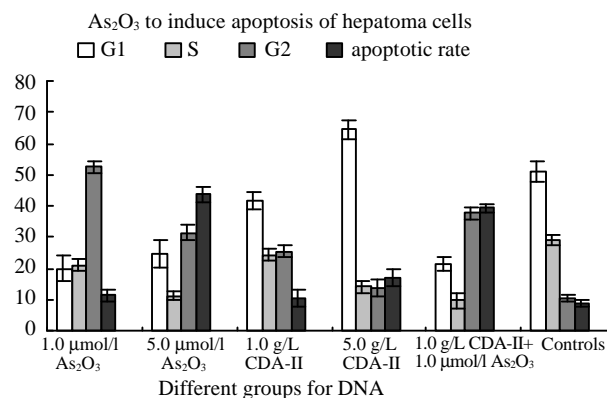


**Figure 4** Comparison of DNA in various groups 4 days after medicinal treatment.  $P < 0.05$  Compared with the controls

### Flow cytometry study of cell apoptosis

Four days after treatment with  $\text{As}_2\text{O}_3$ , sub- $\text{G}_1$  cells, namely apoptotic cells, became evident in HepG2 and BEL-7402, and the number of apoptotic cells was in direct proportion to drug concentration (Figure 4).  $\text{As}_2\text{O}_3$  at  $5.0 \mu\text{mol/L}$  induced 46.7 % of HepG2 and 53.1 % of BEL-7402, respectively to undergo apoptosis. When CDA-II was employed alone below  $2.0 \text{ g/L}$ , the apoptotic rate of hepatoma cells was not significantly different from that of the control. At such low concentration ( $< 2.0 \text{ g/L}$ ), the cells arrested in  $\text{G}_2$  exceeded those in the control, whereas at concentrations above  $2.0 \text{ g/L}$ , both apoptotic cells and cells arrested in  $\text{G}_1$  increased. The combination of  $1.0 \text{ g/L} \text{CDA-II}$  and  $1.0 \mu\text{mol/L} \text{As}_2\text{O}_3$  in hepatoma cells resulted in reduced vitality of the two cell lines, and the apoptotic rate rose from 11.3 % in the presence of  $1.0 \mu\text{mol/L} \text{As}_2\text{O}_3$  alone to 40.2 % (Figure 5). The potentiation of  $\text{As}_2\text{O}_3$ -induced apoptosis by CDA-II was concentration-dependent. The percentage of sub- $\text{G}_1$  cells induced by  $3.0 \text{ g/L} \text{CDA-II}$  and  $1.0 \mu\text{mol/L} \text{As}_2\text{O}_3$  reached 63 %, as against 57 % caused by  $5.0 \mu\text{mol/L} \text{As}_2\text{O}_3$ . All these findings indicated that CDA-II could synergistically potentiate  $\text{As}_2\text{O}_3$  to induce apoptosis of hepatoma cells.

### DISCUSSION

Toxicity of cell apoptotic agents and drug resistance of cancer cells are major factors contributing to the failure of chemotherapy. It has been reported by Cai *et al.*<sup>[16]</sup>, that one-third of 47 patients with normal liver function but suffering from recurrent acute promyelocytic leukemia who were treated with  $\text{As}_2\text{O}_3$ , had their livers damaged. Obviously, the patients with damaged liver function must choose smaller dosage of  $\text{As}_2\text{O}_3$ . In this regard it particularly fits the recommend combination therapy with CAD-II, because CAD-II is a very effective drug to protect liver from hepatotoxin-induced injuries<sup>[17-20]</sup>. In vitro, hepatoma cell growth and proliferation were only inhibited by arsenic trioxide at lower concentrations ( $0.25-2.0 \mu\text{mol/L}$ ), with no significant apoptosis, at higher concentration ( $> 2.0 \mu\text{mol/L}$ ) can induce cell apoptosis<sup>[21-26]</sup>. According to the sensitive standard of chemotherapeutic agents devised by Abe *et al.*<sup>[27,28]</sup>, hepatoma cells in this experiment are sensitive to the dosage of  $5.0 \mu\text{mol/L} \text{As}_2\text{O}_3$ . Based on the following formula<sup>[29]</sup>: drug concentration ( $\text{mg/L}$ ) = [(drug  $\text{mg} \times \text{surface size}$ )/body weight]  $\times (100/60)$ , the sensitive dosage in clinical application is  $20 \text{ mg/m}^2$ . In the presence of  $1 \text{ g/L}$  of CDA-II,  $\text{IC}_{50}$  of  $\text{As}_2\text{O}_3$  can be reduced from  $5.0 \mu\text{mol/L}$  to  $1.0 \mu\text{mol/L}$ . That means  $4 \text{ mg/m}^2$  is equally as effective in the combination protocol as  $20 \text{ mg/m}^2$  of single  $\text{As}_2\text{O}_3$ . CAD-II is a biological preparation purified from human urine which is a selective inhibitor of abnormal cancer methylation enzymes<sup>[16,30,31]</sup>. DNA hypermethylation attributable to abnormal methylation enzymes is related to the evolution of drug resistance of cancer cells<sup>[32,33]</sup>. It is likely that the modulation of abnormal

methylation enzymes is responsible for the reverse of drug resistance and the potentiation of  $As_2O_3$ -induced apoptosis. Shen *et al.* reported that abnormal DNA methylation plays an important role in the process of hepatocellular carcinogenesis. DNA methylation level is closely correlated with the biological characteristic of liver cancer, the lower the level of DNA methylation, the stronger the infiltration and metastatic capacity<sup>[34-36]</sup>. Animal experiments on have demonstrated that CAD-II could effectively prevent the growth and metastasis of xenografted hepatoma<sup>[37]</sup>.<sup>[38]</sup> Analysis of cell cycle revealed that CAD-II at low concentrations could arrest more hepatoma cells in  $G_2$  and S, and at high concentrations could bring about more apoptosis and relatively more cells arrested in  $G_1$ . It is remarkable that CAD-II at a low dosage is not capable to induce apoptosis, nevertheless, it can strongly potentiate  $As_2O_3$ -induced apoptosis. With 1.0 g/L of CAD-II, the apoptosis-inducing capability of  $As_2O_3$  can be reduced from 5.0 to 1.0  $\mu\text{mol/L}$ . Therefore, only 4.0  $\text{mg/m}^2$  of  $As_2O_3$  is needed in clinical treatment giving an equivalence of 20  $\text{mg/m}^2$  of  $As_2O_3$ . Thus, the combined therapy of  $As_2O_3$  and CAD-II offers a great advantage to reduce toxic side effect and to improve the therapeutic efficacy for hepatoma.

## REFERENCES

- Wang W, Qin SK, Chen BA, Chen HY. Experimental study on antitumor effect of arsenic trioxide in combination with cisplatin or doxorubicin on hepatocellular carcinoma. *World J Gastroenterol* 2001; **7**: 702-705
- Pu YS, Hour TC, Chen J, Huang CY, Guan JY, Lu SH. Arsenic trioxide as a novel anticancer agent against human transitional carcinoma-characterizing its apoptotic pathway. *Anticancer Drugs* 2002; **13**: 293-300
- Qian J, Qin SK, He ZM, Wang L, Chen YX, Shao ZJ, Liu XF. Arsenic trioxide for the treatment of medium and advanced primary liver cancer. *Zhonghua Ganzhangbing Zazhi* 2002; **10**: 63
- Qian J, Qin S, He Z. Arsenic trioxide in the treatment of advanced primary liver and gallbladder cancer. *Zhonghua Zhongliu Zazhi* 2001; **23**: 487-489
- Chen JQ, Li SS, Peng MH, Lu YF, Qiu QM, Lu BY, Liao QH. Experimental study on arsenic trioxide and other 6 kinds of anti-tumor drugs' effects on human hepatic cancer cell lines BEL-7404, SMMC-7721. *Zhongguo Puwai Jichu Yu Linchuang Zazhi* 2001; **8**: 367-369
- Vernhet L, Allain N, Payen L, Anger JP, Guillouzo A, Fardel O. Resistance of human multidrug resistance-associated protein 1-overexpressing lung tumor cells to the anticancer drug arsenic trioxide. *Biochem Pharmacol* 2001; **61**: 1387-1391
- Gartenhaus RB, Prachand SN, Paniaqua M, Li Y, Gordon LI. Arsenic trioxide cytotoxicity in steroid and chemotherapy-resistant myeloma cell lines: enhancement of apoptosis by manipulation of cellular redox state. *Clin Cancer Res* 2002; **8**: 566-572
- Hu X, Ma L, Hu N, Ailing No. I in treating 62 cases of acute promyelocytic leukemia. *Zhongguo Zhongxiyi Jiehe Zazhi* 1999; **19**: 473-476
- Kundu SN, Mitra K, Bukhsh AR. Efficacy of a potentized homeopathic drug (Arsenicum-album-30) in reducing cytotoxic effects produced by arsenic trioxide in mice: III. Enzymatic changes and recovery of tissue damage in liver. *Complement Ther Med* 2000; **8**: 76-81
- Jing Y, Wang L, Xia L, Chen GQ, Chen Z, Miller WH, Waxman S. Combined effect of all-trans retinoic acid and arsenic trioxide in acute promyelocytic leukemia cells *in vitro* and *in vivo*. *Blood* 2001; **97**: 264-269
- Xu JY, Zhou Q, Lu P, Tang W, Tong LF. Induction of apoptosis and reversal of drug resistance in human tumor cell line KBV 200 by cell differentiation agent-II. *Zhonghua Neiye Zazhi* 2000; **39**: 37-39
- Xu JY, Zhou Q, Lu P, Tang W, Dong LF. Research on induction of apoptosis and reversal of multidrug resistance in human tumor cell line KBV200 by hyperthermia. *Zhonghua Liliu Zazhi* 2000; **23**: 33-36
- Chen ZS, Ni M, Cheng HH, Ouyang XN, Lin J, Dai XH, Tu XH, Wu XG, Guo WH. Therapeutic efficacy of CDA-II on advanced cancer patients a comparison with cytotoxin chemotherapy. *Zhongguo Zhong Liu Linchuang Yu Kangfu* 1999; **6**: 84-87
- Gao YT, Shi SQ, Gu FL, Wu MC. The effect of uroacitides on advanced liver cancer in 15 case. *Zhongguo Zhongliu* 2002; **11**: 110-112
- Feng FY, Li Q, Wang ZJ. The effect of uroacitides on improving quality of life in advanced cancer patients. *Zhongguo Zhongliu* 2002; **11**: 108-110
- Cai X, Shen YL, Zhu Q, Jia PM, Yu Y, Zhou L, Huang Y, Zhang JW, Xiong SM. Arsenic trioxide-induced apoptosis and differentiation are associated respectively with mitochondrial transmembrane potential collapse and retinoic acid signaling pathways in acute promyelocytic leukemia. *Leukemia* 2000; **14**: 262-270
- Lin WC, Wu YW, Lai TY, Liao MC. Effect of CDA-II, urinary preparation, on lipofuscin lipid peroxidation and antioxidant systems in young and middle-aged rat brain. *Am J Chin Med* 2001; **29**: 91-99
- Lai TY, Wu YW, Lin WC. Effect of a urinary preparation on liver injury by short-term carbon tetrachloride treatment in rats. *Am J Chin Med* 1999; **27**: 241-250
- Lai TY, Wu YW, Lin JG, Lin WC. Effect of pretreatment of rats with a urinary preparation on liver injuries induced by carbon tetrachloride and alpha-naphthylisothiocyanate. *Am J Chinese Med* 1998; **26**: 343-351
- Lai TY, Wu YW, Lin WC. Ameliorative effect of an urinary preparation on acetaminophen and D-galactosamine induced hepatotoxicity in rats. *Am J Chinese Med* 1999; **27**: 73-81
- Li JT, Ou QJ, Wei J. Studies on arsenic trioxide induces apoptosis in hepatoma cell lines Bel-7402. *Aizheng* 2000; **19**: 1087-1089
- Xu HY, Yang YL, Gao YY, Wu QL, Gao GQ. Effect of arsenic trioxide on human hepatoma cell line BEL-7402 cultured *in vitro*. *World J Gastroenterol* 2000; **6**: 681-687
- Oketani M, Kohara K, Tuvdendorj D, Ishitsuka K, Komorizono Y, Ishibashi K, Arima T. Inhibition by arsenic trioxide of human hepatoma cell growth. *Cancer Lett* 2002; **183**: 147-153
- Siu KP, Chan JY, Fung KP. Effect of arsenic trioxide on human hepatocellular carcinoma HepG2 cells: inhibition of proliferation and induction of apoptosis. *Life Sci* 2002; **71**: 275-285
- Kito M, Akao Y, Ohishi N, Yagi K, Nozawa Y. Arsenic trioxide-induced apoptosis and its enhancement by buthionine sulfoximine in hepatocellular carcinoma cell lines. *Biochem Biophys Res Commun* 2002; **291**: 861-867
- Chen H, Qin SK, Pan QH, Chen HY, Ma J. Antitumor effect of arsenic trioxide on mice experimental liver cancer. *Zhonghua Ganzhangbing Zazhi* 2000; **8**: 27-29
- Abe R, Ueo H, Akiyoshi T. Evaluation of MTT assay in agarose for chemosensitivity testing of human cancers: comparison with MTT assay. *Oncology* 1994; **51**: 416-425
- Van Thiel DH, Brems J, Holt D, Hamdani R, Yong S. Chemosensitivity of primary hepatic neoplasms: a potential new approach to the treatment of hepatoma. *Hepatogastroenterology* 2002; **49**: 730-734
- Zhong XY, Chen YX, Sun XD. Study of apoptotic threshold of cis-diamminedichloroplatinum and adriamycin on hepatocellular carcinoma. *Zhongguo Bingli Shengli Zazhi* 2000; **16**: 199-202
- Liao MC. Differentiation therapy for cancer. *Zhongguo Zhongliu* 2002; **11**: 104-107
- Liao MC, Liao CP. Methyltransferase inhibitors as excellent differentiation helper inducers for differentiation therapy of cancer. *Zhongguo Zhongliu* 2002; **11**: 166-168
- Plumb JA, Strathdee G, Sludden J, Kaye SB, Brown R. Reversal of drug resistance in human tumor xenografts by 2'-deoxy-5-azacytidine-induced demethylation of the hMLH1 gene promoter. *Cancer Res* 2000; **60**: 6039-6044
- Wang C, Mirkin BL, Dwivedi RS. DNA (cytosine) methyltransferase overexpression is associated with acquired drug resistance of murine neuroblastoma cells. *Int J Oncol* 2001; **18**: 323-329
- Shen L, Fang J, Qiu D, Zhang T, Yang J, Chen S, Xiao S. Correlation between DNA methylation and pathological changes in human hepatocellular carcinoma. *Hepatogastroenterology* 1998; **45**: 1753-1759
- Shen L, Ahuja N, Shen Y, Habib NA, Toyota M, Rashid A, Issa JP. DNA methylation and environmental exposures in human hepatocellular carcinoma. *J Natl Cancer Inst* 2002; **94**: 755-761
- Shen L, Qui D, Fang J. Correlation between hypomethylation of c-myc and c-N-ras oncogenes and pathological changes in human hepatocellular carcinoma. *Zhonghua Zhongliu Zazhi* 1997; **19**: 173-176
- Wu MF, Han CH, Liu CC, Lai JM, Li ZJ, Xu KS. Establishment of animal models for the evaluation of differentiation inducing agents. *Zhongguo Zhongliu* 2002; **11**: 163-165
- Sun JJ, Zhou XD, Liu YK, Wang ZY. Effect of CDA-II on prevention and therapy for metastasis and recurrence of liver cancer in nude mice. *Zhonghua Gangdan Waikie Zazhi* 1999; **5**: 14-16

# Relationship between the imaging features and pathologic alteration in hepatoma of rats

Jia-He Yang, Tian-Geng You, Nan Li, Qi-Jun Qian, Ping Wang, Zhen-Lin Yan, Meng-Chao Wu

**Jia-He Yang, Tian-Geng You, Nan Li, Qi-Jun Qian, Ping Wang, Zhen-Lin Yan, Meng-Chao Wu**, Eastern Hepatobiliary Hospital, 225 Changhai Road, Shanghai 200433, China

**Supported by** two National Natural Science Foundation of China, No. 39870760 and No. 39970838

**Correspondence to:** Dr. Jie-He Yang, Department of Comprehensive Treatment III, Eastern Hepatobiliary Hospital, Second Military Medical University, Changhai Road 225, Shanghai 200433, China. tgyou59@hotmail.com

**Telephone:** +86-21-25070786 **Fax:** +86-21-65562400

**Received:** 2001-12-05 **Accepted:** 2002-02-23

## Abstract

**AIM:** The imaging features of MRI and DSA, using the models of implanted and induced hepatoma, were investigated in rats.

**METHODS:** CBRH3 cancer cells were implanted for different liver site of rat liver and the diethylnitrosamine was given orally to rats in order to induce liver cancer. Both experimental groups were detected by magnetic resonance imaging (MRI), digital subtraction angiography (DSA) and morphologic assay.

**RESULTS:** Hypointensity on T1WI and homogenous high signal intensity on T2WI in MRI, and ring-like abnormal stain on DSA were found in implanted cancer. Induced cancers appeared as homogeneous or heterogeneous hypointensity on T1WI (10 cases), and equal or slight high intensity on T2WI (8 cases), but some as hypointensity on T2WI (2 cases).

**CONCLUSION:** The imaging features of implanted cancers were similar to that of human liver metastases. Therefore, it could serve as an experimental model of human liver metastatic tumor. The imaging feature of induced cancers, whereas, were similar to that of human primary liver cancer. It could be use as an experimental model of human primary liver cancer.

Yang JH, You TG, Li N, Qian QJ, Wang P, Yan ZL, Wu MC. Relationship between the imaging features and pathologic alteration in hepatoma of rats. *World J Gastroenterol* 2003; 9(1): 69-72  
<http://www.wjgnet.com/1007-9327/9/69.htm>

## INTRODUCTION

It is important to investigate the relationship between the biologic properties of liver tumor and the findings with modern imaging techniques. MRI affords the possibility in coronal and sagittal views, which are very helpful in liver surgery because surgical techniques are described in these planes<sup>[1-2]</sup>. In addition, targeted gene therapy, for instance, cytokines gene therapy, angiogenesis inhibitor and granulocyte-macrophage colony-stimulating factor (GM-CSF) gene-transduced tumor vaccine for patients, may be useful in developing anticancer drugs that prolong or stabilize the progression of tumors with minimal systemic toxicities. These drugs may also be used as novel imaging and radiomunotherapeutic agents in cancer therapy<sup>[3-7]</sup>.

However, little is known on experimental work of both scan imaging and liver cancer. The present study, using the model of

implanted and induced hepatoma of rats, was undertaken to investigate the relationship between the morphologic alterations and imaging characteristics of magnetic resonance imaging (MRI) and digital subtraction angiography (DSA), and more to improve level of diagnostic and treatment for liver cancer. Finally, interleukin 2 was therapeutic effect on liver tumors<sup>[8]</sup>, so the our further study of interleukin gene therapy for liver cancer was based on the present outcome of implanted and induced hepatoma.

## MATERIALS AND METHODS

### *Imaging Instruments*

MRI equipment was produced by Siemens AG (1.0 T). Its SE rank, 128\*128 matrix, T1-weighted sequence (T1WI) were TR/TE 350-480/15 ms; T2-weighted sequence (T2WI) was TR/TE 2 200/90 ms. Slice thickness was 2 mm and scan space was 0.5 mm. Both of coronal and sagittal scanning was fulfilled. Hepatic artery was scanned by DSA (Toshiba DFP-0.3A) with perfusing iodized oil (Lipiodol). Instruments and drugs were sterilized routinely.

### *Animals and Hepatoma cell*

Male Wister rats (200-250 g wt) were obtained from Animal Center of Chinese Academy of Sciences. Animals were maintained on a standard diet. Cellular strains of hepatoma CBRH3 were provided kindly by Prof. Xie Hong (Shanghai Institute of Biochemistry and Cell Biology, Chinese Academy of Science).

### *Implanted liver cancer model in rat*

Hepatoma CBRH3 cells were injected into abdominal cavity of rat. Rats were sacrificed and tumors were removed from abdominal cavity 7-9 days late. The tumors were cut into pieces of 0.05-0.75 cm and then was inoculated into rat liver for one or more locations respectively. The tumor was grown up to diameter in 0.6-1 cm after 7-10 days of inoculation.

### *Induced liver cancer model in rat*

Male Wister rats (age for 8 weeks) took orally 1:10 000 diethylnitrosamine for 80 days to induce liver cancer. The micro-nodules of hepatoma were developed 14 weeks late and 0.2-1 cm of tumor masses were observed 16-18 weeks late. There were poly-cysts in rat liver. This model was used to study for poly-nodules of hepatoma. The success rate of induced cancer was 100 %<sup>[9,10]</sup>.

### *Experimental procedure*

Both of 10 implanted tumor rats (age of 9 days) and 10 induced tumor rats (age of 16-18 weeks) was divided to experimental group and control group, randomly. While rats were scanned by MRI, they were anesthetized by injecting ketamine into muscle. In addition, the hepatic artery and gastroduodenal artery were isolated carefully and micro-catheter was inserted into these artery for injection of iodine oil before DSA<sup>[11]</sup>.

## RESULTS

A stable model of rat hepatoma was established by either implanted tumor with cancer piece or inducing tumor with diethylnitrosamine.



Imaging features of the implanted tumors in MRI and DSA and the pathology: The 10 implanted models showed 18 nodules of tumor in MRI and DSA. 11 nodules of them were round shape and 7 of them were ellipse. The margin of tumors was smooth. Implanted cancer showed homogeneous hypointensity on T1WI (Figure 1) and homogeneous hyperintensity on T2WI. The rat liver showed normal signal and normal organ shape.

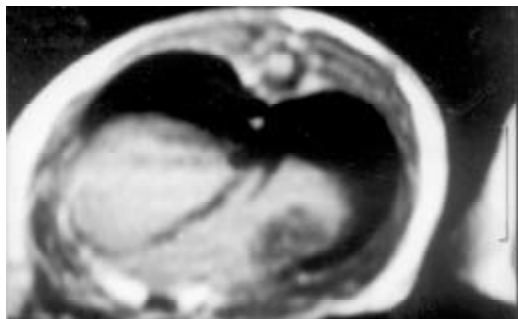


**Figure 1** MR imaging showed low signal on T1WI in implanted hepatoma of rat

In DSA, the tumors showed no stain for blood vessels in the center of tumor (vacancy of vessel) and abnormal ring-like staining of vessel around tumor. The liver tissues were normal. Necrosis and colliquational cavity were shown on the core of tumors in all of 18 tumor mass and the yellow-gray tissue could be seen in cross section of tumors. The cancer cells were small or mediate in size with great nucleus. The parenchyma of liver was normal (Figure 2).

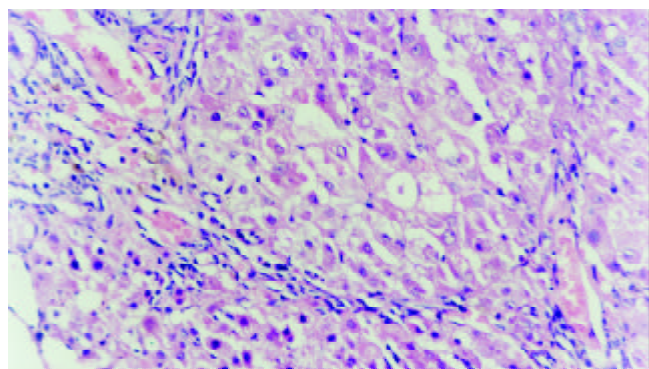


**Figure 2** Distribution of microscopy ( $\times 200$ ) in implanted liver cancer that abnormal type and arrangement of cancer cell. There were abundant vascular proliferation and lymphocyte infiltration growth around tumor

The scanning pictures of MRI and DSA and the pathological alteration in induced cancer: Liver cirrhosis with different degree and multiple nodules of cancer were observed in 10 tumor cases. Eight among 10 tumors showed homogeneous slight hypo-intensity on T1WI (Figure 3) and inhomogeneous slight hyper-intensity on T2WI with different shapes, but some of them were with normal signal or more contrast enhancement (Figure 4). Two among 10 tumor livers were shown inhomogeneous slight low signal on T1WI, but equal signal was found in interval. Hypointensity was observed on T2WI.

In DSA the distribution of internal hepato-vascularity was disorder and the angio-clumps were different in sizes in tumor (Figure 5). Pathology: Tumor liver showed poly-nodules, tumor diffusion and inequality of size. The tumor was light yellow. In microscopy examination, distribution of tumor and liver tissue was in interval. The cancer tissue showed plenty and dilation of vessel. The cell plasma of cancer was not abundant. The arrangement of tumor cell was nest and bunch. Liver tissue was

easy for proliferation of nodule with acid-like change and water-alteration. The dilation of lymphatic tube and the proliferation of bile duct were shown between hepato-lobule. Hepato-lobule was divided by proliferation of fibre. The artery and vein were not distinguished because of dilation of vessel (Figure 6).

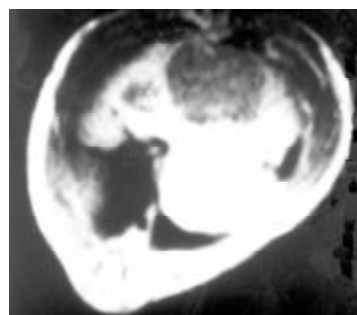


**Figure 3** Homogeneous slight hypointensity on T1WI was found in poly-nodules of tumor

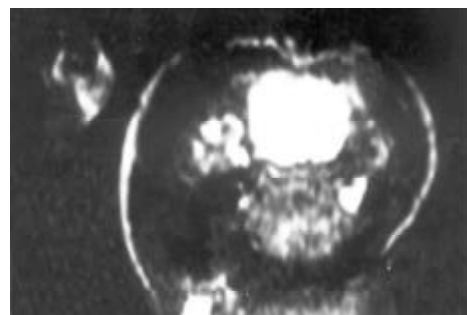


**Figure 4** Inhomogeneous slight hyperintensity was indicated on T2WI in different shape, but some of them were showed normal signal or more contrast enhancement in interval

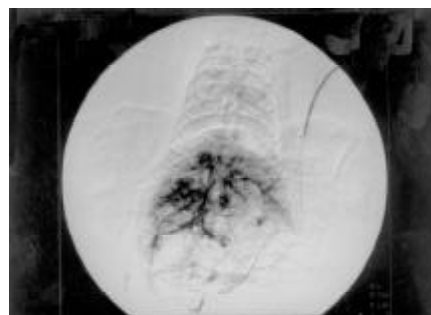


**Figure 5** The disorder of distribution of internal hepato-vascularity was found and the angio-clump showed different size in tumor in DSA

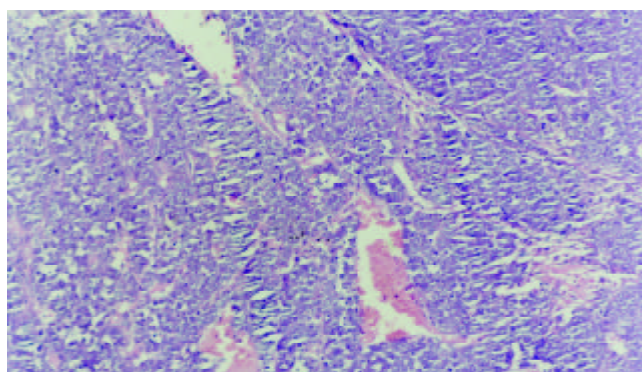


**Figure 6** Distribution of microscopy ( $\times 100$ ) in induced liver cancer that tumor and liver tissue was in interval. There was plenty and dilation of vessel

## DISCUSSION

### Characterization of image technique of rat

The available MR image photos were taken because technique is as follow. (1) Technique of eye surface loop: To avoid disturbing factors for image definition that focus on the location of rat liver, this technique was used. (2) Folium technique keeps away the cabin effect on conceal of small tumor nodules. (3) False shadow caused by move of body act and breath was prevented by suitable anesthesia for rats. On DSA image, deep anesthesia and careful anatomy of hepatic artery with catheter were necessary. But it is difficulty to puncture femoral artery. In order to find available condition of exposure time, we try to test more times<sup>[12]</sup>.

### The relation of image and pathology in implanted cancer

The component of tumor is of long longitudinal relaxation time (T1) and long transverse relaxation time (T2) since the implanted cancer show low signal on T1WI and equal signal on T2WI in MRI. Equal signal intensity implies that there are no tissue component in the core of tumor apart from necrosis, liquefaction and cystic change. Therefore, the situation of blood supply was not described due to no-contrast enhancement of Gadolinium-DTPA<sup>[13,14]</sup>.

On DSA, the imaging of blood vessel around tumor was found such as folium annularity, whereas central liquefaction and necrosis were existed in tumor. Thus, cancer cell on the border of tumor grows actively because of blood supply in plenty and cancer cell in center of tumor does not grow because of insufficient blood supply. There is no liver cirrhosis because signal intensity of liver tissue in MRI and distribution of blood vessel in DSA are normal compared to normal liver parenchyma<sup>[19]</sup>.

Necrosis at core of tumor and the proliferated nodule of tumor cell were found around blood sinus and dilation of blood vessel after 9 days of implanted cancer<sup>[16,17]</sup>. The change in MRI and DSA was accord to pathology.

### The relation of image and pathology in induced cancer

Resent study has suggested that a random clonal origin of hepatocyte carcinoma from mature hepatocytes is seen in the diethylnitrosamine model of hepatocarcinogenesis<sup>[18]</sup>.

Induced cancer is of two different signal intensities including 1. slight low signal intensity on T1WI and slight high signal intensity on T2WI in 8 cases and 2. inhomogeneous low signal on T1WI and low signal on T2WI with regular appearance in 2 cases. We hypothesize that both signals is caused by the difference in hepatoma component and hepatoma cellular arrange. Amount of fibrocyte, apart from tumor cells, is found in these 2 cases which result in extended longitudinal relaxation time (T1) and contracted transverse relaxation time (T2) with low signal on T1WI and low signal on T2WI. Irregular liver shape and liver nodule proliferation in deferent degree with liver cyst could be manifested on MRI because of liver cirrhosis and degeneration resulting from taking carcinogen for long time. To differentiate with cirrhosis nodules and tumor nodules, some investigators reported that the early-enhancing single nodule with cirrhosis is high predictive to hepatocyte cancer in patient. This phenomenon is also seen in our data of photo and microscopy examination<sup>[20,21]</sup>. On DAS, the tumor stain is displayed by reason of disorder of blood vessel and angio-clamp<sup>[22]</sup>.

### Comparison imaging of implanted, induced and human hepatoma

**Primary liver cancer** Based on the liver cirrhosis, primary liver cancer display the slight low signal intensity on T1WI and equal or slight high signal intensity following extended echo time without raise of signal in MRI<sup>[23]</sup>. In DSA, the plenty

amateur vessel is observed<sup>[24]</sup>.

**Liver metastases** MRI shows the low signal intensity on T1WI, high signal on T2WI and annular enhancement by Gadolinium. In DSA, annular staining is displayed without background of cirrhosis<sup>[15]</sup>.

Compared with manifestation of MRI and DSA, studies confirm that implanted hepatoma lead that the signal intensity is high following the extended echo time and annular staining around tumor is occurred without liver cirrhosis<sup>[25]</sup>.

In induced cancer, liver cirrhosis with slight high signal or low signal due to extended echo time without raise of signal is observed in MRI. The abundant malignant vessel stain is indicated that it is similar to human primary liver cancer<sup>[26]</sup>.

In conclusion, the imaging features of implanted cancers were similar to human liver metastases in manifestation of MRI and DSA. Therefor, it could serve as an experimental model of human liver metastatic tumor. The imaging feature of induced cancers, whereas, were similar to that of human primary liver cancer. It could be use as an experimental model of human primary liver cancer.

## REFERENCES

- Foley LM**, Towner RA, Painter DM. *In vivo* image-guided H-magnetic resonance spectroscopy of the serial development of hepatocarcinogenesis in an experimental animal model. *Biochim Biophys Acta* 2001; **15**: 230-236
- Eliat PA**, Lechaux D, Gervais A, Rioux-Leclerc N, Franconi F, Lemaire L, Dazord L, Catros-Quemener V, de Certaines JD. Is magnetic resonance imaging texture analysis a useful tool for cell therapy *in vivo* monitoring? *Anticancer Res* 2001; **21**: 3857-3860
- Scappaticci FA**. Mechanisms and future directions for angiogenesis-based cancer therapies. *J Clin Oncol* 2002; **20**: 3906-3927
- Kawai K**, Tani K, Yamashita N, Tomikawa S, Eriguchi M, Fujime M, Okumura K, Kakizoe T, Clift S, Ando D, Mulligan R, Yamauchi A, Noguchi M, Asano S, Akaza H. Advanced renal cell carcinoma treated with granulocyte-macrophage colony-stimulating factor gene therapy: A clinical course of the first Japanese experience. *Int J Urol* 2002; **9**: 462-466
- Parkes AT**, Speirs V. British cancer research meeting, 30 june-3 july 2002, glasgow. *Breast Cancer Res* 2002; **4**: 202-204
- Zhang L**, Gu J, Lin T, Huang X, Roth JA, Fang B. Mechanisms involved in development of resistance to adenovirus-mediated proapoptotic gene therapy in DLD1 human colon cancer cell line. *Gene Ther* 2002; **9**: 1262-1270
- Gillies SD**, Lan Y, Brunkhorst B, Wong WK, Li Y, Lo KM. Bi-functional cytokine fusion proteins for gene therapy and antibody-targeted treatment of cancer. *Cancer Immunol Immunother* 2002; **51**: 449-460
- Zhao W**, Kobayashi M, Ding W, Yuan L, Seth P, Cornain S, Wang J, Okada F, Hosokawa M. Suppression of *in vivo* tumorigenicity of rat hepatoma cell line KDH-8 cells by soluble TGF-beta receptor type II. *Cancer Immunol Immunother* 2002; **51**: 381-388
- Balansky RM**, Ganchev G, D'Agostini F, De Flora S. Effects of N-acetylcysteine in an esophageal carcinogenesis model in rats treated with diethylnitrosamine and diethyldithiocarbamate. *Int J Cancer* 2002; **98**: 493-497
- Rao MS**, Kashireddy P. Effect of castration on dehydroepiandrosterone-induced hepatocarcinogenesis in male rats. *Anticancer Res* 2002; **22**: 1409-1411
- Thorlacius H**, Larmark M, Randell M, Hultberg B, Jeppsson B. Isolated liver perfusion permits administration of high doses of chemotherapeutic agents. Comparison with hepatic artery infusion. *Eur Surg Res* 2001; **33**: 342-347
- Zhang H**, Liu Y, Cao W, Liu Y, Fan A. Establishment of modified model of Vx-2 carcinoma in rabbit liver and DSA imaging features of the tumor. *Zhonghua Ganzangbing Zazhi* 2002; **10**: 149
- Krupski G**, Ameis D, Cataldegirmen G, Herbst H, Henschel MG, Nicolas V, Rogiers X, Bucheler E. Native magnetic resonance tomography imaging of the Morris hepatoma (MH-7777A) in the rat. *Rofu Fortschr Geb Rontgenstr Neuen Bildgeb Verfahr* 2001; **173**: 639-642



- 14 **Lauenstein TC**, Goehde SC, Herborn CU, Treder W, Ruehm SG, Debatin JF, Barkhausen J. Three-dimensional volumetric interpolated breath-hold MR imaging for whole-body tumor staging in less than 15 minutes: a feasibility study. *Am J Roentgenol* 2002; **179**: 445-449
- 15 **Turler A**, Schaefer H, Schaefer N, Wagner M, Maintz D, Qiao JC, Hoelscher AH. Experimental low-level direct current therapy in liver metastases: influence of polarity and current dose. *Bioelectromagnetics* 2000; **21**: 395-401
- 16 **Kuppen PJ**, Gorter A, Hagenaars M, Jonges LE, Giezeman-Smits KM, Nagelkerke JF, Fleuren G, van de Velde CJ. Role of NK cells in adoptive immunotherapy of metastatic colorectal cancer in a syngeneic rat model. *Immunol Rev* 2001; **184**:236-243
- 17 **Nakamoto T**, Inagawa H, Nishizawa T, Honda T, Kanou J, Nagasue N, Soma G. Antitumor effects of isolated hypoxic hepatic perfusion (IHHP) with high-dose TNF against colonic liver metastases in a rat model. *Anticancer Res* 2002; **22**: 2455-2459
- 18 **Bralet MP**, Pichard V, Ferry N. Demonstration of direct lineage between hepatocytes and hepatocellular carcinoma in diethylnitrosamine-treated rats. *Hepatology* 2002; **36**: 623-630
- 19 **Guo WJ**, Li J, Ling WL, Bai YR, Zhang WZ, Cheng YF, Gu WH, Zhuang JY. Influence of hepatic arterial blockage on blood perfusion and VEGF, MMP-1 expression of implanted liver cancer in rats. *World J Gastroenterol* 2002; **8**: 476-479
- 20 **Dean CE Jr**, Benjamin SA, Chubb LS, Tessari JD, Keefe TJ. Non-additive hepatic tumor promoting effects by a mixture of two structurally different polychlorinated biphenyls in female rat livers. *Toxicol Sci* 2002; **66**: 54-61
- 21 **Stoker J**, Romijn MG, de Man RA, Brouwer JT, Weverling GJ, van Muiswinkel JM, Zondervan PE, Lameris JS, Ijzermans JN. Prospective comparative study of spiral computer tomography and magnetic resonance imaging for detection of hepatocellular carcinoma. *Gut* 2002; **51**: 105-107
- 22 **Carroll NM**, Alexander HR Jr. Isolation perfusion of the liver. *Cancer J* 2002; **8**: 181-193
- 23 **Jeong YY**, Mitchell DG, Kamishima T. Small (<20 mm) enhancing hepatic nodules seen on arterial phase MR imaging of the cirrhotic liver: clinical implications. *AJR Am J Roentgenol* 2002; **178**:1327-1334
- 24 **Vogl TJ**, Balzer JO, Mack MG, Bett G, Oppelt A. Hybrid MR interventional imaging system: combined MR and angiography suites with single interactive table. Feasibility study in vascular liver tumor procedures. *Eur Radiol* 2002; **12**: 1394-1400
- 25 **Teng GJ**, He SC, Guo JH, Cai XL, Gao GR. Preoperative transcatheterhepatic arterial embolization for hepatic malignancy. *Investradiol*, 1993; **28**: 235-241
- 26 **An Y**, Bie P, Dong J. Hepatic artery and portal vein dual perfusion chemotherapy in combination with injection of lipiodol-ethanol in treatment of advanced primary hepatocellular carcinoma. *Zhonghua Waike Zazhi* 2001; **39**: 593-595

Edited by Pang LH

# Synergetic anticancer effect of combined quercetin and recombinant adenoviral vector expressing human wild-type p53, GM-CSF and B7-1 genes on hepatocellular carcinoma cells *in vitro*

Ming Shi, Fu-Sheng Wang, Zu-Ze Wu

**Ming Shi, Fu-Sheng Wang**, Division of Biological Engineering, Institute of Infectious Disease, the 302 Hospital of PLA, Beijing 100039, China

**Zu-Ze Wu**, Institute of Radiation Medicine, Academy of Military Medical Sciences, Beijing 100850, China

**Correspondence to:** Dr. Fu-Sheng Wang, Division of Biological Engineering, Institute of Infectious Disease, the 302 Hospital of PLA, 26 Fengtai Lu, Beijing 100039, China. fswang@public.bat.net.cn

**Telephone:** +86-10-66933332 **Fax:** +86-10-63831870

**Received:** 2002-07-26 **Accepted:** 2002-08-16

## Abstract

**AIM:** This study investigated the anti-cancer effect of combined quercetin and a recombinant adenovirus vector expressing the human p53, GM-CSF and B7-1 genes (designated BB-102) on human hepatocellular carcinoma (HCC) cell lines *in vitro*.

**METHODS:** The sensitivity of HCC cells to anticancer agents was evaluated by 3-(4,5-dimethylthiazol-2-yl)-2,5-diphenyl tetrazolium bromide (MTT) assay. The viability of cells infected with BB-102 was determined by trypan blue exclusion. The expression levels of human wild-type p53, GM-CSF and B7-1 genes were determined by Western blot, enzyme-linked immunosorbent assay (ELISA) and flow cytometric analysis, respectively. The apoptosis of BB-102-infected or quercetin-treated HCC cells was detected by terminal deoxynucleotidyl transferase (TdT) assay or DNA ladder electrophoresis.

**RESULTS:** Quercetin was found to suppress proliferation of human HCC cell lines BEL-7402, HuH-7 and HLE, with peak suppression at 50  $\mu\text{mol/L}$  quercetin. BB-102 infection was also found to significantly suppress proliferation of HCC cell lines. The apoptosis of BB-102-infected HCC cells was greater in HLE and HuH-7 cells than in BEL-7402 cells. Quercetin did not affect the expression of the three exogenous genes in BB-102-infected HCC cells ( $P>0.05$ ), but it was found to further decrease proliferation and promote apoptosis of BB-102-infected HCC cells.

**CONCLUSION:** BB-102 and quercetin synergetically suppress HCC cell proliferation and induce HCC cell apoptosis, suggesting a possible use as a combined anti-cancer agent.

Shi M, Wang FS, Wu ZZ. Synergetic anticancer effect of combined quercetin and recombinant adenoviral vector expressing human wild-type p53, GM-CSF and B7-1 genes on hepatocellular carcinoma cells *in vitro*. *World J Gastroenterol* 2003; 9(1): 73-78

<http://www.wjgnet.com/1007-9327/9/73.htm>

## INTRODUCTION

Hepatocellular carcinoma (HCC) is one of the most malignant diseases known. Surgical resections are incapable of removing

all HCC cells and the disease is very resistant to anticancer agents, making chemotherapy an equally ineffective option<sup>[1]</sup>. Therefore, anti-tumor gene therapy strategies seem a good future option for the treatment of HCC<sup>[2]</sup>. Numerous studies have shown that tumor occurrence and progression are often related to mutations in tumor suppressor genes or loss of host anti-tumor immunity<sup>[3-9]</sup>. Therefore, a promising approach is transfer of tumor suppressor genes to cause tumor cell growth arrest or apoptosis, combined with cytokine genes to induce an effective immune response directly against both the genetically modified and the parental tumor cells<sup>[10]</sup>.

In HCC, mutation or loss of tumor suppressor gene p53 is associated with malignancy and chemoresistance<sup>[11-13]</sup>, making the wild-type p53 (WT-p53) gene a good candidate for replacement by gene therapy. Granulocyte-macrophage colony stimulating factor (GM-CSF) has been proven to be a potent, long-lasting inducer of antitumor immunity that promotes maturation of dendritic cells and enhances the function of antigen-presenting cells and natural killer (NK) cells<sup>[14-17]</sup>. In addition, the expression of members of the B7 gene family has been shown to be important in antitumor responses in both mice and humans<sup>[18-20]</sup>. However, most tumor cells, including HCC cells, lack B7-1 molecules on their surface, and as a result they escape recognition by the immune system<sup>[21]</sup>. Kim *et al.* found an increased antitumor effect with the combined expression of GM-CSF and B7-1 in athymic nude mice, suggesting that coexpression of GM-CSF and B7-1 may enhance antitumor activity<sup>[22]</sup>. Recombinant adenovirus vector BB-102, which expresses p53, GM-CSF and B7-1 genes<sup>[23]</sup>, has been shown to inhibit the growth of various human carcinoma cells, such as hepatocellular carcinoma, lung cancer<sup>[24]</sup>, and laryngeal cancer<sup>[25]</sup>, and enhances carcinoma cell chemosensitivity to anti-cancer agents.

Quercetin (3,3',4',5,7-pentahydroxyflavone) is one of most widely distributed bioflavonoids in the plant kingdom and is a common component of most edible fruits and vegetable. Humans consume approximately 1 g of dietary flavonoid daily. This compound has been shown to inhibit the growth of various human cancer cell lines<sup>[26-34]</sup>, including leukemia, hepatocellular carcinoma, and estrogen-receptor positive breast carcinoma MCF-7, suggesting that quercetin may have anti-cancer and anti-metastasis potential<sup>[35-39]</sup>. The growth inhibitory effect of quercetin on tumor cells is found to be consequence of its ability to interfere with the enzymatic processes involved in the regulation of cellular proliferation: DNA, RNA and protein biosynthesis<sup>[40-43]</sup>. Quercetin also has shown to down-regulate or inhibit the phosphatidylinositol (PI) and phosphatidylinositol phosphate (PIP) kinase activities in human carcinoma cells, leading to a marked reduction of second messengers IP3 concentration and cell death<sup>[44,45]</sup>. Therefore, quercetin may be useful in the treatment of carcinomas with increased or down-regulated signal transduction capacity<sup>[45-47]</sup>.

These results suggest that the combination of quercetin with BB-102 may synergetically suppress the growth of carcinoma cells. Accordingly, this study addressed the synergetic action of quercetin combined with BB-102 against HCC cells *in vitro*.

## MATERIALS AND METHODS

### Agents

Quercetin was purchased from Sigma (St Louis, MO). Western blot detection system ECL+plus Kit was purchased from Amersham Pharmacia Biotech (Arlinton Heights, IL). GM-CSF ELISA kit was bought from Genzyme (Cambridge, MA). The TdT FragEL™ DNA fragmentation detection kit was from Calbiochem (Cambridge, MA). Ad-GFP (Ad5 vector expressing green fluorescence protein) was kindly provided by the Gene Therapy Unit, Baxter Healthcare Corporation, USA. BB-102 was reconstructed by Dr ZH Qu. Quercetin was dissolved in medium containing 0.1 % dimethyl sulfoxide (DMSO), and the same concentration of DMSO was used in control experiments.

### Quercetin inhibits the growth of HCC cells

The BEL-7402, HLE and HuH-7 cell lines were seeded in 96-well plates at a density of  $5 \times 10^3$  cells/well. After 24 h, the cells were exposed to various concentrations of quercetin from 3.125  $\mu\text{mol/L}$  to 100  $\mu\text{mol/L}$ . After 72 h, the number of viable cells was determined by MTT assay.

### Growth suppression in BB-102-infected HCC cells

HCC cell lines were seeded in six-well plates at a density of  $5 \times 10^5$  cells/well. Twelve hours later, the cells were infected with BB-102 and Ad-GFP at a MOI of 50 pfu/cell. Culture medium was used for mock infection. Triplicate wells of each treatment group were counted every 2 days for a total of four times after infection. The viability of the cells was determined by trypan blue exclusion.

### Assay of apoptosis

Apoptosis induced by BB-102 was analyzed by terminal deoxynucleotidyl transferase (TdT) assay. Briefly, HCC cells were seeded in 12-well plates at a density of  $5 \times 10^5$  cells/well. After 24 h, they were infected with BB-102 or Ad-GFP at a MOI of 50 pfu/cell. Culture medium was used for mock infection. Seventy-two hours later, cell monolayers were fixed with 4 % formaldehyde diluted in phosphate-buffered saline (PBS) for 15 min at room temperature. Apoptosis of the cells was detected using a TdT FragEL™ DNA fragmentation detection kit according to the protocol.

Cellular apoptosis induced by quercetin or quercetin combined with BB-102 was analyzed by agarose gel-electrophoresis as described based on the pattern of DNA cleavage. Briefly, cells ( $1 \times 10^6$ ) were lysed with 0.5 ml lysis buffer, followed by the addition of RNase A to a final concentration of 200  $\mu\text{g/ml}$ , and incubated for 1 h at 37 °C. Cells were then treated with 300  $\mu\text{g/ml}$  of proteinase K for 1 h at 37 °C. After addition of 4  $\mu\text{l}$  loading buffer, 20  $\mu\text{l}$  samples in each lane were subjected to electrophoresis on a 1.5 % agarose at 50 V for 3 h. DNA was stained with ethidium bromide and laddering was visualized under UV light.

### p53 gene expression by western blot

Three cell lines were seeded in 6-well plates at a density of  $1 \times 10^5$  cells/well. Group II was treated with 100  $\mu\text{mol/L}$  quercetin, group III was infected with BB-102 at a MOI of 50 pfu/cell, group IV was infected with BB-102 and then treated with 100  $\mu\text{mol/L}$  quercetin, and group I was mock-infected with culture medium infected with empty adenovirus vector as control. After 48 h incubation, cells were washed with phosphate buffered saline, disrupted by addition of lysing buffer (100 mmol/L Tris·Cl pH 6.8, 200 mmol/L DTT, 4 % SDS, 0.2 % bromophenol blue, 20 % glycerol), and electrophoresed. Western blot detection system ECL+plus Kit was used to determine p53 expression according to the instruction manual.

### ELISA of GM-CSF gene expression

Expression of human GM-CSF was detected by enzyme-linked immunosorbent assay. Briefly, the cells were seeded in 6-well plates at a density of  $1 \times 10^6$  cells/well. After 24 h, the cells were infected with BB-102 at a MOI of 50 pfu/cell for 1 h, then BB-102 suspensions were replaced with either culture medium alone, or culture medium containing 100  $\mu\text{mol/L}$  quercetin. After 48 h, the suspension was collected. The GM-CSF present in each suspension was quantified using the ELISA kit according to the protocol.

### FCM of B7-1 gene expression

HCC cells were seeded in 6-well plates at a density of  $5 \times 10^5$  cells/well. After 24 h, the cells were either treated with 100  $\mu\text{mol/L}$  quercetin, infected with BB-102 at a MOI of 50 pfu/cell, or infected with BB-102 at a MOI of 50 pfu/cell then treated with 100  $\mu\text{mol/L}$  quercetin. Culture medium was used for mock infection. After 48 h incubation, the cells were collected. Cells were washed twice in PBS and resuspended in PBS containing 1 % bovine serum albumin (BSA) prior to incubation with anti-human B7-1 monoclonal antibody (MoAb) for 30 min at 4 °C in the dark, followed by two washes in PBS/BSA. The cells were stained with FITC-conjugated goat anti-mouse IgG for 30 min at 4 °C. Nonspecific binding was controlled by incubation with isotypic controls. Fluorescence was measured with FACSCalibur flow cytometer (Becton Dickinson).

### Proliferation of cells treated with both quercetin and BB-102

HCC cells were seeded in 96-well plates at a density of  $5 \times 10^3$  cells/well. After 24 h, cells were infected with Ad-GFP or BB-102 at a MOI of 50 pfu/cell. Culture medium was used for mock infection. After 48 h, cells were treated with various concentrations of quercetin from 3.125 to 50  $\mu\text{mol/L}$ . Culture medium was used for mock treatment. After 72 h, the viable cell numbers were tested by MTT assay.

## RESULTS

### Antitumor effect of quercetin on HCC cells

Quercetin was shown to inhibit HCC proliferation and induce HCC apoptosis *in vitro* in a dose-dependent manner until it reached peak inhibition at 50  $\mu\text{mol} \cdot \text{L}^{-1}$  (Figure 1).

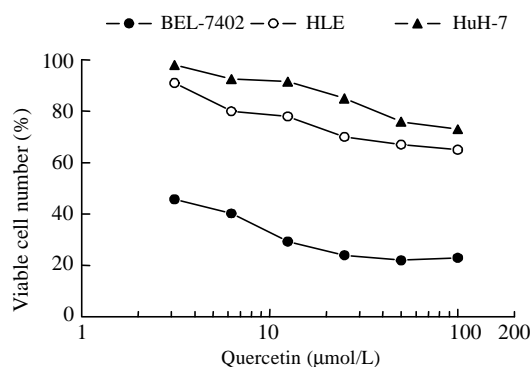


**Figure 1** The suppressive effect of quercetin on the proliferation of BEL-7402, HLE and HuH-7 cell lines *in vitro*.

### BB-102 inhibit the growth of HCC cells

Introduction of p53, GM-CSF and B7-1 through BB-102 infection led to significant suppression of growth proliferation in BEL-7402, HLE and HuH-7 cells compared with those infected with Ad-GFP or mock infected (Figure 2). Among them, there was a lower suppression in BEL-7402 cell line compared with HLE and HuH-7 cell lines ( $P < 0.05$ ), which might be related

to the fact that BEL-7402 expresses an endogenous wild-type p53, while HLE and HuH-7 both express endogenous mutant p53, resulting in BEL-7402 being less sensitive to the effects of the exogenous p53 protein expressed by BB-102.

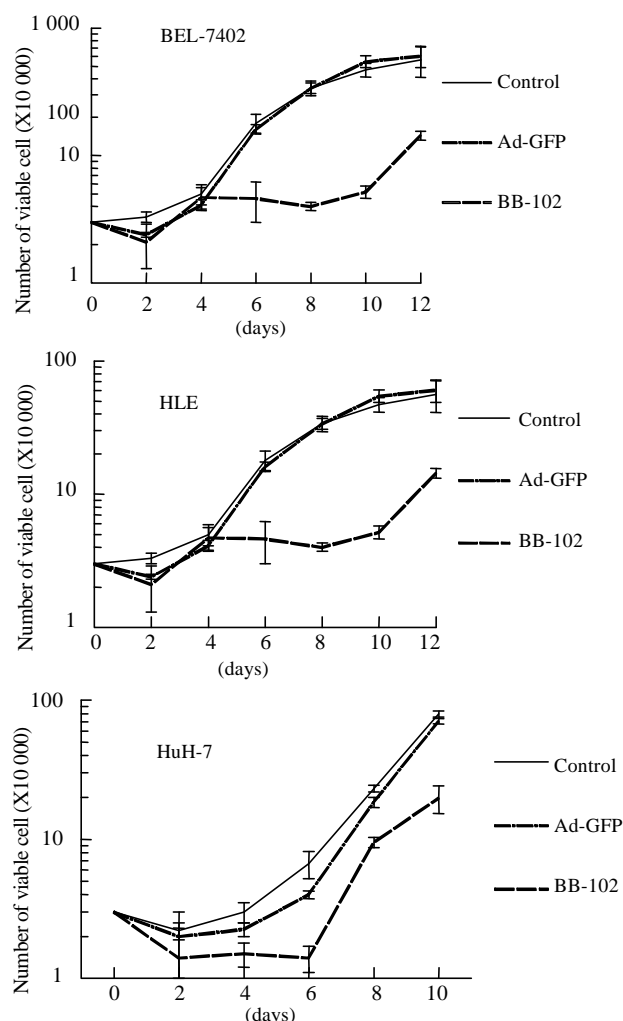


**Figure 2** Proliferation inhibition of HCC cell lines transduced with BB-102.

### BB-102 induces HCC cells apoptosis

As measured by TdT assay, apoptotic rates in BEL-7402, HLE and HuH-7 cells lines were 12.75 %, 57 % and 49.5 %, respectively. This suggests that HLE and HuH-7 cells were more sensitive to BB-102 than BEL-7402 cells.

### Quercetin induces apoptosis of HCC cells

DNA laddering (Figure 3) suggests that quercetin induces HCC cell apoptosis, and that BB-102 further promoted the quercetin-treated cell apoptosis.

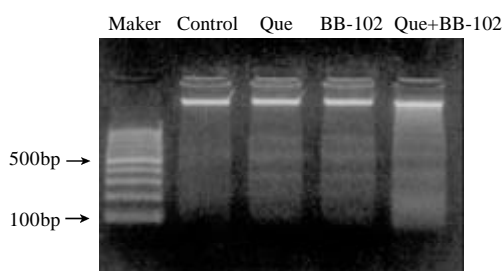


**Figure 3** The promotion of Que on HCC cell apoptosis induced by BB-102.

### Quercetin does not affect exogenous gene expression in BB-102-infected cells

**Expression of exogenous P53 in BB-102-infected cells** By using Western blot analysis, high levels of p53 protein were detected in BB-102-infected HCC cell lines. These levels were not affected by treatment with quercetin (Figure 4).

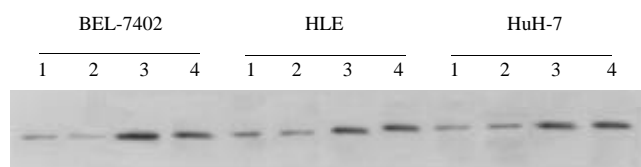


**Figure 4** Effect of Que on the p53 expression in HCC cell lines transferred with BB-102. (lane1: control; lane2: with Que; lane3: with BB-102; lane4: with Que and BB-102).

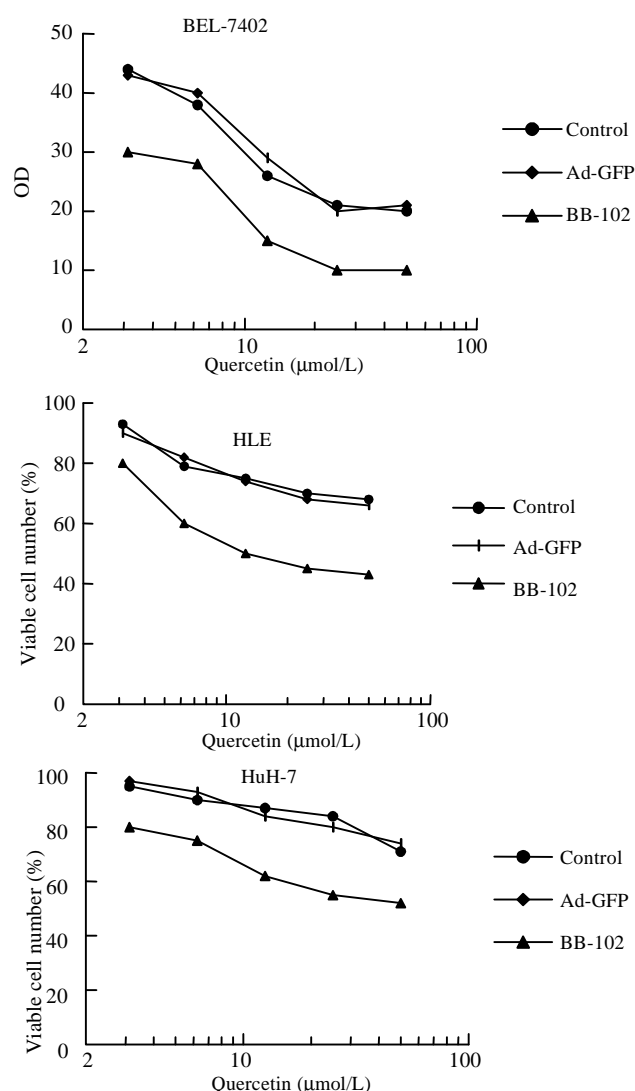


**Figure 5** Synergistic effect of BB-102 on quercetin suppression of growth of HCC cell lines.

### Expression of exogenous GM-CSF protein in BB-102-infected cells

ELISA assay showed that a high-level expression of GM-CSF was detected in the culture suspension of BB-102-infected cells 48 h after infection. There was no statistical difference in GM-CSF level between the cells treated with quercetin and untreated cells (Table 1).

### Expression of exogenous B7-1 protein in BB-102-infected cells

B7-1 gene expression was observed flow cytometric analysis 48 h after BB-102 infection (Table 2). There was no

significant difference in B7-1 expression between cells treated with quercetin and untreated cells.

**Table 1** Effect of Que on the GM-CSF expression in HCC cell lines transferred with BB-102 (pg·L<sup>-1</sup>), ( $\bar{x} \pm s$ ), (n=6)

Cell line	Infected with BB-102	Infected with BB-102+Que
BEL-7402	118.9±29.9	147.7±13.2
HLE	209.6±55.7	248.3±15.9
HuH-7	250.7±21.9	283.7±21.6

**Table 2** Effect of Que on the B7-1 expression in HCC cell lines transferred with BB-102 (%) (n=4)

Cell line	Control	Que	BB-102	Que+BB-102
BEL-7402	10.0±2.5	11.2±1.7	80.0±10.3 <sup>b</sup>	85.0±12.0 <sup>b</sup>
HLE	15.3±2.1	14.0±2.0	31.0±7.8 <sup>a</sup>	35.2±5.6 <sup>b</sup>
HuH-7	20.0±2.6	22.0±3.0	59.8±8.5 <sup>b</sup>	64.0±8.8 <sup>b</sup>

<sup>a</sup>P<0.01, <sup>b</sup>P<0.001, vs their controls

### Quercetin enhances the inhibition of the proliferation in BB-102-infected HCC cell lines

The proliferation suppression pattern of HCC cells treated with quercetin was not significantly different between Ad-GFP-infected cells and Ad-mock infected cells. In contrast, BB-102-infected cells showed a significant increase of suppression when treated with quercetin. This implies that BB-102 transduction and quercetin treatment synergistically suppress HCC proliferation (Figure 5). The control data indicates that it was the exogenous gene expression that induced this effect, not the adenovirus.

## DISCUSSION

Gene therapy, the introduction of functional genes into cells to treat or prevent a disease, is a promising approach for the treatment of human cancer. In an effort to explore potential gene therapy approaches to the treatment of stubborn HCC, we investigated the synergetic effects of dietary component (quercetin) plus gene transfer (BB-102 infection). BB-102 is a recombinant adenoviral vector expressing the genes for human wild-type p53, GM-CSF and B7-1<sup>[23]</sup>. Our study showed that BB-102 infection arrested the growth of HCC cells lines BEL-7402, HLE, HuH-7, and induced their apoptosis by the expression of exogenous wild-type p53 (a transcriptional activator that induces cell cycle arrest and apoptosis<sup>[48-50]</sup>). BB-102 also enhanced immunogenicity of HCC cells and improved host antitumor immune reaction.

We then examined the possible synergy between these exogenous genes and quercetin, which is thought to have a long-term preventive effect on chemical carcinogenesis, especially in people who eat a diet rich in fruits and vegetables<sup>[30,31,36,51,52]</sup>. Previously, we had found that antineoplastic drug concentrations exerting cytotoxic activity were markedly lower when cells were pretreated with quercetin<sup>[28,35]</sup>. In addition, quercetin has been shown to inhibit the growth of human breast cancer cell line MDA-MB468 in a dose-dependent fashion by specifically inhibiting the expression of mutant p53 in cellular transformation<sup>[53]</sup>. Because HCC patients are generally resistant to chemotherapy (possibly due to the loss of a functional p53 gene<sup>[54]</sup>, which is known to occur in 50 % of cancers<sup>[55-58]</sup>), we

questioned whether quercetin could reverse the multi-drug resistance of HCC cells, perhaps through down-regulation of mutated p53 or glycoprotein<sup>[53,59,60]</sup>. In addition to its possible role in adjusting p53 levels, quercetin is also known to inhibit the synthesis of HSP70 (heat shock protein 70) and change its intracellular distribution. HSP70 is involved in apoptosis, and the link between the two suggests that quercetin may be involved in the induction of apoptosis<sup>[35,61]</sup>.

We found enhancement of apoptosis and inhibition of the proliferation of BB-102-infected HCC cell lines treated with quercetin, suggesting that there is a synergetic anticancer effect between quercetin and BB-102. There was no change in p53, GM-CSF and B7-1 gene expressions in BB-102-infected HCC cell lines following quercetin treatment, indicating that quercetin did not affect exogenous gene expression in BB-102-infected HCC cells. We believe it is possible that this synergetic effect might be due to BB-102 transduction promoting the chemosensitivity of HCC cells to quercetin, but this and other mechanisms will need further study.

BEL-7402 cells were more sensitive to quercetin than HLE and HuH-7 cells. At a concentration of 50 μmol/L quercetin (peak proliferation inhibition), proliferation inhibition was 78 %, 33 % and 24 % for BEL-7402, HLE and HuH-7, respectively. Our previous studies have shown that the doubling time of BEL-7402 is the shortest among these cells. This suggests that the cells that proliferate quickly are more sensitive to quercetin in this study. In addition, quercetin induced apoptosis in HCC cells at G1 and S in a dose- and time-dependent manner, and the effect was enhanced by BB-102 infection. This enhancement was less in BEL-7402, possibly due to its wild-type endogenous p53 status<sup>[62]</sup>. Overall, HCC cells treated with both quercetin and BB-102 showed inhibition of proliferation and increased apoptosis, suggesting that quercetin may be useful as an adjuvant in chemotherapy treatment of HCC patients. The combination of quercetin and BB-102 transduction is a promising new strategy for the treatment of typically chemo-resistant hepatomas.

## REFERENCES

- 1 Venook AP. Hepatocellular carcinoma. *Curr Treat Options Oncol* 2000; **1**: 407-415
- 2 Mohr L, Geissler M, Blum HE. Gene therapy for malignant liver disease. *Expert Opin Biol Ther* 2002; **2**: 163-175
- 3 Peller S. Clinical implications of p53: effect on prognosis, tumor progression and chemotherapy response. *Semin Cancer Biol* 1998; **8**: 379-387
- 4 Friess H, Kleeff J, Korc M, Buchler MW. Molecular aspects of pancreatic cancer and future perspectives. *Dig Surg* 1999; **16**: 281-290
- 5 Rocco JW, Sidransky D. p16(MTS-1/CDKN2/INK4a) in cancer progression. *Exp Cell Res* 2001; **264**: 42-55
- 6 Canote R, Du Y, Carling T, Tian F, Peng Z, Huang S. The tumor suppressor gene RIZ in cancer gene therapy (review). *Oncol Rep* 2002; **9**: 57-60
- 7 Farid NR. P53 mutations in thyroid carcinoma: tidings from an old foe. *J Endocrinol Invest* 2001; **24**: 536-545
- 8 Muschen M, Warskulat U, Beckmann MW. Defining CD95 as a tumor suppressor gene. *J Mol Med* 2000; **78**: 312-325
- 9 Behrens J. Cadherins and catenins: role in signal transduction and tumor progression. *Cancer Metastasis Rev* 1999; **18**: 15-30
- 10 Wu Q, Moyana T, Xiang J. Cancer gene therapy by adenovirus-mediated gene transfer. *Curr Gene Ther* 2001; **1**: 101-122
- 11 Xu GW, Sun ZT, Forrester K, Wang XW, Coursen J, Harris CC. Tissue-specific growth suppression and chemosensitivity promotion in human hepatocellular carcinoma cells by retroviral-mediated transfer of the wild-type p53 gene. *Hepatology* 1996; **24**: 1264-1268
- 12 Qin LX, Tang ZY. The prognostic molecular markers in hepatocellular carcinoma. *World J Gastroenterol* 2002; **8**: 385-392
- 13 Buendia MA. Genetics of hepatocellular carcinoma. *Semin Can-*

- cer Biol* 2000; **10**: 185-200
- 14 **Yu JS**, Burwick JA, Dranoff G, Breakefield XO. Gene therapy for metastatic brain tumors by vaccination with granulocyte-macrophage colony-stimulating factor-transduced tumor cells. *Hum Gene Ther* 1997; **8**: 1065-1072
  - 15 **Hogge GS**, Burkholder JK, Culp J, Albertini MR, Dubielzig RR, Keller ET, Yang NS, MacEwen EG. Development of human granulocyte-macrophage colony-stimulating factor-transfected tumor cell vaccines for the treatment of spontaneous canine cancer. *Hum Gene Ther* 1998; **9**: 1851-1861
  - 16 **Lu L**, Hsieh M, Oriss TB, Morel PA, Starzl TE, Rao AS, Thomson AW. Generation of DC from mouse spleen cell culture in response to GM-CSF: Immunophenotypic and functional analyses. *Immunology* 1995; **84**: 127-134
  - 17 **Ogawa T**, Kusumoto M, Mizumoto K, Sato N, Tanaka M. Adenoviral GM-CSF Gene Transduction into Breast Cancer Cells Induced Long-Lasting Antitumor Immunity in Mice. *Breast Cancer* 1999; **6**: 301-304
  - 18 **Felzmann T**, Ramsey WJ, Blaese RM. Anti-tumor immunity generated by tumor cells engineered to express B7-1 via retroviral or adenoviral gene transfer. *Cancer Lett* 1999; **135**: 1-10
  - 19 **Horig H**, Lee DS, Konkright W, Divito J, Hasson H, LaMare M, Rivera A, Park D, Tine J, Guito K, Tsang KW, Schlom J, Kaufman HL. Phase I clinical trial of a recombinant canarypoxvirus (ALVAC) vaccine expressing human carcinoembryonic antigen and the B7.1 co-stimulatory molecule. *Cancer Immunol Immunother* 2000; **49**: 504-514
  - 20 **Takahashi T**, Hirano N, Takahashi T, Chiba S, Yazaki Y, Hirai H. Immunogene therapy against mouse leukemia using B7 molecules. *Cancer Gene Ther* 2000; **7**: 144-150
  - 21 **Nakatsuka K**, Sugiyama H, Nakagawa Y, Takahashi H. Purification of antigenic peptide from murine hepatoma cells recognized by class- I major histocompatibility complex molecule-restricted cytotoxic T-lymphocyte induced with B7-1-gene-transfected hepatoma cells. *J Hepatol* 1999; **30**: 1119-1129
  - 22 **Kim KY**, Kang MA, Nam MJ. Enhancement of natural killer cell-mediated cytotoxicity by coexpression of GM-CSF/B70 in hepatoma. *Cancer Lett* 2001; **166**: 33-40
  - 23 **Qiu ZH**, Lao MF, Wu ZZ. Construction of recombinant adenovirus co-expressing human wild-type p53, GM-CSF and B7-1 genes. *Zhongguo Shengwuxue Yu Fengzishengwu Xuebao* 2001; **17**: 33-38
  - 24 **Qiu ZH**, Lao MF, Wang YF, Wu ZZ. Adenovirus mediate multigenes expressing in lung cancer and inducing apoptosis. *Zhongguo Zhongliu Shengwuzhilia Zazhi* 1999; **6**: 83-86
  - 25 **Qiu ZH**, Lao MF, Wu ZZ. Co-transfer of human wild-type p53 and granulocyte-macrophage colony-stimulating factor genes via recombinant adenovirus induces apoptosis and enhances immunogenicity in laryngeal cancer cells. *Cancer Lett* 2001; **167**: 25-32
  - 26 **Larocca LM**, Teofili L, Sica S, Piantelli M, Maggiano N, Leone G, Ranelletti FO. Quercetin inhibits the growth of leukemic progenitors and induces the expression of transforming growth factor-beta 1 in these cells. *Blood* 1995; **85**: 3654-3661
  - 27 **Scambia G**, Panici PB, Ranelletti FO, Ferrandina G, De Vincenzo R, Piantelli M, Masciullo V, Bonanno G, Isola G, Mancuso S. Quercetin enhances transforming growth factor beta 1 secretion by human ovarian cancer cells. *Int J Cancer* 1994; **57**: 211-215
  - 28 **Ranelletti FO**, Ricci R, Larocca LM, Maggiano N, Capelli A, Scambia G, Benedetti-Panici P, Mancuso S, Rumi C, Piantelli M. Growth-inhibitory effect quercetin and presence of type II estrogen-binding sites in human colon-cancer cell lines and primary colorectal tumors. *Int J Cancer* 1992; **50**: 486-492
  - 29 **Choi JA**, Kim JY, Lee JY, Kang CM, Kwon HJ, Yoo YD, Kim TW, Lee YS, Lee SJ. Induction of cell cycle arrest and apoptosis in human breast cancer cells by quercetin. *Int J Oncol* 2001; **19**: 837-844
  - 30 **Pawlikowska-Pawlega B**, Jakubowicz-Gil J, Rzymowska J, Gawron A. The effect of quercetin on apoptosis and necrosis induction in human colon adenocarcinoma cell line LS180. *Folia Histochem Cytobiol* 2001; **39**: 217-218
  - 31 **Kampa M**, Hatzoglou A, Notas G, Damianaki A, Bakogeorgou E, Gemetzi C, Kouroumalis E, Martin PM, Castanas E. Wine antioxidant polyphenols inhibit the proliferation of human prostate cancer cell lines. *Nutr Cancer* 2000; **37**: 223-233
  - 32 **Iwashita K**, Kobori M, Yamaki K, Tsushida T. Flavonoids inhibit cell growth and induce apoptosis in B16 melanoma 4A5 cells. *Biosci Biotechnol Biochem* 2000; **64**: 1813-1820
  - 33 **Uddin S**, Choudhry MA. Quercetin, a bioflavonoid, inhibits the DNA synthesis of human leukemia cells. *Biochem Mol Biol Int* 1995; **36**: 545-550
  - 34 **Caltagirone S**, Rossi C, Poggi A, Ranelletti FO, Natali PG, Brunetti M, Aiello FB, Piantelli M. Flavonoids apigenin and quercetin inhibit melanoma growth and metastatic potential. *Int J Cancer* 2000; **87**: 595-600
  - 35 **Sliutz G**, Karlseder J, Tempfer C, Orel L, Holzer G, Simon MM. Drug resistance against gemcitabine and topotecan mediated by constitutive hsp70 overexpression in vitro: implication of quercetin as sensitizer in chemotherapy. *Br J Cancer* 1996; **74**: 172-177
  - 36 **Yang CS**, Landau JM, Huang MT, Newmark HL. Inhibition of carcinogenesis by dietary polyphenolic compounds. *Annu Rev Nutr* 2001; **21**: 381-406
  - 37 **Wang HK**. The therapeutic potential of flavonoids. *Expert Opin Investig Drugs* 2000; **9**: 2103-2119
  - 38 **Asaumi J**, Matsuzaki H, Kawasak S, Kuroda M, Takeda Y, Kishi K, Hiraki Y. Effects of quercetin on the cell growth and the intracellular accumulation and retention of adriamycin. *Anticancer Res* 2000; **20**: 2477-2483
  - 39 **Damianaki A**, Bakogeorgou E, Kampa M, Notas G, Hatzoglou A, Panagiotou S, Gemetzi C, Kouroumalis E, Martin PM, Castanas E. Potent inhibitory action of red wine polyphenols on human breast cancer cells. *J Cell Biochem* 2000; **78**: 429-441
  - 40 **Yamashita N**, Kawanishi S. Distinct mechanisms of DNA damage in apoptosis induced by quercetin and luteolin. *Free Radic Res* 2000; **33**: 623-633
  - 41 **Musonda CA**, Helsby N, Chipman JK. Effects of quercetin on drug metabolizing enzymes and oxidation of 2',7-dichlorofluorescein in HepG2 cells. *Hum Exp Toxicol* 1997; **16**: 700-708
  - 42 **Exon JH**, Magnuson BA, South EH, Hendrix K. Dietary quercetin, immune functions and colonic carcinogenesis in rats. *Immunopharmacol Immunotoxicol* 1998; **20**: 173-190
  - 43 **Drewa G**, Wozzak A, Palgan K, Schachtschabel DO, Grzanka A, Sujkowska R. Influence of quercetin on B16 melanotic melanoma growth in C57BL/6 mice and on activity of some acid hydrolases in melanoma tissue. *Neoplasma* 2001; **48**: 12-18
  - 44 **Weber G**, Shen F, Yang H, Prajda N, Li W. Regulation of signal transduction activity in normal and cancer cells. *Anticancer Res* 1999; **19**: 3703-3709
  - 45 **Weber G**, Shen F, Prajda N, Yeh YA, Yang H, Herenyiova M, Look KY. Increased signal transduction activity and down-regulation in human cancer cells. *Anticancer Res* 1996; **16**: 3271-3282
  - 46 **Richter M**, Ebermann R, Marian B. Quercetin-induced apoptosis in colorectal tumor cells: possible role of EGF receptor signaling. *Nutr Cancer* 1999; **34**: 88-99
  - 47 **Shen F**, Herenyiova M, Weber G. Synergistic down-regulation of signal transduction and cytotoxicity by tiazofurin and quercetin in human ovarian carcinoma cells. *Life Sci* 1999; **64**: 1869-1876
  - 48 **Levine AJ**. p53, the cellular gatekeeper for growth and division. *Cell* 1997; **88**: 323-331
  - 49 **Greenblatt MS**, Bennett WP, Hollstein M, Harris CC. Mutation in the P53 tumor suppressor gene: clues to cancer etiology and molecular pathogenesis. *Cancer Res* 1994; **54**: 4855-4878
  - 50 **Hui AM**, Makuuchi M, Li X. Cell cycle regulators and human hepatocarcinogenesis. *Hepatogastroenterology* 1998; **45**: 1635-1642
  - 51 **Yang CS**, Landau JM, Huang MT, Newmark HL. Inhibition of carcinogenesis by dietary polyphenolic compounds. *Annu Rev Nutr* 2001; **21**: 381-406
  - 52 **Hollman PC**, Katan MB. Health effects and bioavailability of dietary flavonols. *Free Radic Res* 1999; **31** (Suppl): S75-80
  - 53 **Avila MA**, Velasco JA, Cansado J, Notario V. Quercetin mediate the down-regulation of mutation p53 in the human breast cancer cell line MDA-MB468. *Cancer Research* 1994; **54**: 2424-2428
  - 54 **Thottassery**, Zambetti GP, Arimori K, Schuetz EG, Schuetz JD.

- p53-dependent regulation of mdr1 gene expression causes selective resistance to chemotherapeutic agents. *Proc Natl Sci USA* 1997; **94**: 11037-11042
- 55 **Wang D**, Shi JQ. Overexpression and mutations of tumor suppressor gene p53 in hepatocellular carcinoma. *China Natl J New Gastroenterol* 1996; **2**: 161-164
- 56 **Wang XJ**, Yuan SL, Li CP, Iida N, Oda H, Aiso S, Ishikawa T. Infrequent p53 gene mutation and expression of the cardia adenocarcinomas from a high incidence area of Southwest China. *Shijie Huaren Xiaohua Zazhi* 2000; **6**: 750-753
- 57 **Li ZX**, Liu PY, Xu WX, Cong B, Ma ZX, Li Y. p53 gene mutations in primary gastric cancer. *China Natl J New Gastroenterol* 1996; **2**: 41-43
- 58 **Peng XM**, Peng WW, Yao JL. Codon 249 mutations of p53 gene in development of hepatocellular carcinoma. *World J Gastroenterol* 1998; **4**: 125-127
- 59 **Scambia G**, Ranelletti FO, Panici PB, De Vincenzo R, Bonanno G, Ferrandina G, Piantelli M, Bussa S, Rumi C, Cianfriglia M. Quercetin potentiates the effect of adriamycin in a multidrug-resistant MCF-7 human breast-cancer cell line: P-glycoprotein as a possible target. *Cancer Chemother Pharmacol* 1994; **34**: 459-464
- 60 **Beniston RG**, Morgan IM, O'Brien V, Campo MS. Quercetin, E7 and p53 in papillomavirus oncogenic cell transformation. *Carcinogenesis* 2001; **22**: 1069-1076
- 61 **Wei YQ**, Zhao X, Kariya Y, Fukata H, Teshigawara K, Uchida A. Induction of apoptosis by quercetin: Involvement of heat shock protein. *Cancer Research* 1994; **54**: 4952-4957
- 62 **Shi M**, Wang FS, Liu MX, Jin L, Shi H, Lei ZY. The examination of p53 gene status in BEL-7402, HLE and HuH-7 cells. *Shijie Huaren Xiaohua Zazhi* 2001; **9**: 1330-1332

**Edited by** Wu XN



# Construction of IL-2 gene-modified human hepatocyte and its cultivation with microcarrier

Nan-Hong Tang, Yian-Ling Chen, Xiao-Qian Wang, Xiu-Jin Li, Feng-Zhi Yin, Xiao-Zhong Wang

**Nan-Hong Tang, Xiao-Qian Wang, Yian-Ling Chen, Xiu-Jin Li, Feng-Zhi Yin**, Hepato-Biliary Surgery Institute of Fujian Province, Union Hospital Affiliated to Fujian Medical University, Fuzhou 350001, Fujian Province, China

**Xiao-Zhong Wang**, Gastroenterology Department, Union Hospital Affiliated to Fujian Medical University, Fuzhou 350001, Fujian Province, China

**Supported by** Science and Technology Development Foundation of Fujian Province, No. 98-Z-214

**Correspondence to:** Nan-Hong Tang, Hepato-Biliary Surgery Institute of Fujian Province, Union Hospital, 29 Xinquan Road, Fuzhou 350001, Fujian Province, China. fztmh@sina.com

**Telephone:** +86-591-3671667

**Received:** 2002-08-24 **Accepted:** 2002-10-12

## Abstract

**AIM:** To construct interleukin-2 gene-modified human hepatocyte line (L-02/IL-2) and investigate the changes of the function of liver cells and IL-2 secretion in culture with microcarrier, laying the foundation for further experimentation on hepatocyte transplantation.

**METHODS:** hIL-2 gene was transduced into L-02 hepatocytes by recombinant retroviral vector pLNCIL-2, and the changes of morphology and clonogenicity rate of the transduced cells were observed, the secretion levels of hIL-2 in cultural supernatant were detected by ELISA and NeoR gene was amplified by PCR. The growth of L-02/IL-2, the special biochemistry items and the levels of IL-2 were detected after cultivation with microcarrier.

**RESULTS:** The clonogenicity rate of the L-02/IL-2 cells was lower than that of L-02/Neo cells and L-02 cells. The levels of hIL-2 could reach 32 000 pg/10<sup>6</sup> cells per day and kept secreting for more than ten weeks. NeoR gene segment was respectively obtained by PCR from both L-02/IL-2 and L-02/Neo cell's genomic DNA. At the 6<sup>th</sup> day in culture with microcarrier, the matrix-induced liver cell aggregates were formed, the number of alive L-02/IL-2 cell were 16.8±0.53 ×10<sup>6</sup>/flask and the levels of ALB and UREA were 52.54±1.28 mg/L and 5.29±0.17 mmol/L, respectively. These data had not significantly changed as compared with those of L-02 cells (*P*>0.05); However, the levels of IL-2 in IL-2/L-02 cells remarkably exceeded that in L-02 cells in the whole culture process (*P*<0.001).

**CONCLUSION:** The IL-2 gene-modified hepatocyte line has been successfully constructed. The L-02/IL-2 cellular aggregates cultured with microcarrier have a high capacity of IL-2 production as well as protein synthesis and amino acid metabolism.

Tang NH, Chen YL, Wang XQ, Li XJ, Yin FZ, Wang XZ. Construction of IL-2 gene-modified human hepatocyte and its cultivation with microcarrier. *World J Gastroenterol* 2003; 9(1): 79-83  
<http://www.wjgnet.com/1007-9327/9/79.htm>

## INTRODUCTION

Gene therapy has become an important therapeutic alternative in recent years, thanks to the growing improvement of gene-transduction techniques in eukaryotic cells. There are a large number of proteins expression in hepatocyte with high levels, and many genes that are involved in metabolism also express in hepatocytes, so hepatocyte is one of the crucial tools for gene therapy<sup>[1]</sup>, for example, the therapeutic implement for patient with hyperbilirubinemia by hepatocyte transplantation after gene modification *in vitro*, which was approved by FDA<sup>[2]</sup>.

As an important approach for inhibiting the growth of tumor, immune therapy of cytokines further broadens the prospect of clinical application of hepatocytes and gene therapy of cytokines. Recent studies have demonstrated the feasibility of cytokine gene transference to enhance the antitumor activities of host immune cell<sup>[3]</sup>. With regards to therapy for hepatocarcinoma, there are many good results obtained from the study of hepatocarcinoma cells modified by cytokine genes<sup>[4-11]</sup>, especially using IL-2 gene modified hepatocarcinoma cells that conquered the substantial toxicity from administration of high doses of IL-2<sup>[9,12]</sup>. However, few studies focus on the antitumor immune function of hepatocyte transduced with cytokine gene in hepatocyte transplantation. In this study, IL-2 gene was transduced into human hepatocyte line L-02 by recombinant retroviral vector. The experiments of its biologic activities and cultivation with microcarriers were performed, laying the foundation for further experimentation on hepatocyte transplantation.

## MATERIALS AND METHODS

### Material

Human hepatocyte line L-02, amphotropic packaging cell PA317 and mouse fibroblast cell line NIH3T3 were purchased from Shanghai Cell Biology Institute, Chinese Academy of Science and grown in DF medium (DMEM: Ham's F12=3:1) containing 100 mL·L<sup>-1</sup> fetal calf serum, penicillin 1×10<sup>5</sup>U·L<sup>-1</sup> and streptomycin 100 mg·L<sup>-1</sup>. The cells were kept at 37 °C in a 50 mL/LCO<sub>2</sub> humidified atmosphere and subcultured from one to three when the cells proliferated into a full monolayer. Recombinant retroviral vector, LNCX and LNCIL-2, were kindly provided by Prof. Joo Hang Kim from Yonsei University in Korea. Plasmid extraction and purification kit, Wizard® Plus SV Minipreps DNA, and transfection kit TransFast™ were from Promega. hIL-2 ELISA kit was purchased from Jingmei Biological Engineering, Shenzhen. Microcarrier Cytodex3 was from Pharmacia. Poly-HEMA, DMEM and Ham's F12 medium were the products of Sigma. Calf serum were purchased from Four Season Green Biological Co., Hangzhou, China.

### Methods

**Construction of recombinant retrovirus producer cell line**  
Transformation of recombinant retroviral vector was performed as previously described<sup>[13]</sup>. The extraction and purification of the product was operated according to the manufacturer's protocol. The purified products were quantitated by spectrophotometer (DU 640), digested with *Hind* III at 37 °C for 2 h and identified by electrophoresis through a 10 g/L

formaldehyde agarose gel. The amphotropic packaging cells PA317 were plated into 12-well plates and cultured till nearly 60-70 % confluence. Then LNCX or LNCIL-2 transduction to PA317 cell line was made with lipo-transfection technique. The PA317/Neo and PA317/IL-2 cell clones which produced pLNCX and pLNCIL-2 were respectively selected by G418 and subcultured for amplification in G418-free DF media for 24 h. Furthermore, the supernatant of above cells containing recombinant retrovirus were collected, and the retrovirus titer was detected by NIH3T3 cells according to that described<sup>[14]</sup>, quantitated highest titer was kept at -70 °C.

**Transduction of IL-2 gene into the hepatocyte cell line** The L-02 hepatocyte line were grown to a confluence of 60-70 % in 24-well plate. The supernatant were discarded and replaced with 1 mL recombinant retroviral supernatant supplemented with 8 µg of Polybrene. Two hours later, 2 mL fresh DF media containing 800 mg/L were added and cultured at 37 °C for 24 h. The whole process of the cell clone against G418 selection lasted 15 days followed by amplified cultivation.

**Growth of transfected cells** The growth of transfected cells were observed and photographed, total of  $3 \times 10^3$  L-02, L-02/Neo and L-02/IL-2 cells were put into the media respectively with a final volume of 200 µL, and then plated on a 96-well plate and incubated at 37 °C in 5 mL/LCO<sub>2</sub> humidified atmosphere for 7 days. Each group had six wells. The assay of cell proliferation was performed by MTT every 24 h. Briefly, 20 µL of 5 g/L MTT were added into each well and cultured for another 4 h. The supernatant was discarded and replaced with 200 µL of dimethyl sulfoxide (DMSO). When the crystals were dissolved, the absorbance (A) value of the slides was read at 490 nm. In addition,  $1 \times 10^3$  cells per well of the three kinds of cell were plated into 24-well plate in 1 mL media and cultured for 7 days, respectively. The colonogenicity rate (CR) of transferred cells were calculated by using the following equation:  $CR = (\text{average clones per well} / 1000) \times 100 \%$ .

**NeoR gene analysis of the transfected cells by PCR** The total genomic DNA were extracted from  $1.0 \times 10^6$  of L-02, L-02/Neo and L-02/IL-2 cells in 200 mL TE buffer respectively, then quantitated by spectrophotometer and digested with *Bam*HI. The NeoR gene was amplified under following conditions: denaturation at 94 °C for 5 min followed by 94 °C 1 min, 62 °C 1 min and 72 °C 1 min 15 s for 30 cycles. The sequence of NeoR gene primers and length of PCR products were as follows: forward-5' -CAAGATGGATTGCACGCAGG-3' and reverse-5' -CCCGCTCAGAAGAACTCGTC-3', size, 790 bp. For analysis, 10 µL of reaction product were checked in 10 g/L agarose gel with ethidium bromide staining and followed by camera photographing.

**Detection of the levels of hIL-2 secreted by the transduced cells** The supernatant of  $1.0 \times 10^6$  of L-02, L-02/Neo and L-02/IL-2 cells that cultured in flask for 24 h were obtained and stored at -70 °C after centrifugation. L-02/IL-2 cells were especially cultured for 10 wk and the supernatants were collected every week. The levels of hIL-2 were measured by ELISA according to the manufacturer's protocol.

**Cultivation with microcarriers** All glassware with which Cytodex3 came into contact, should be siliconized before use. The hydration of Cytodex3 was carried out as the protocol. Briefly, 200 mg Cytodex3 were dipped in Ca<sup>2+</sup> and Mg<sup>2+</sup>-free PBS in a siliconized container overnight and sterilized by autoclaving, then replaced with fresh DF media; The flasks were covered with 0.1 mL/cm<sup>2</sup> 120 g/L Poly-HEMA dissolved in ethanol and then air-dried sterilizedly. The hydrated Cytodex3, 20 mg a flask, along with L-02 and L-02/IL-2 cells,  $3.0 \times 10^6$  a flask in 2 mL media, were seeded into Poly-HEMA covered flasks, respectively. Each group had five bottles. They were all cultured in incubator at 37 °C for 4 h following shakes twice for 1 min every 4 h, the media were replaced every 24 h,

and the supernatants were kept at -70 °C after centrifugation at 1000r/min.

**Morphologic observation and cell proliferation** The culture process was observed and photographed. The cell samples at 6<sup>th</sup> day were fixed by 25 g/L glutaraldehyde and observed by HU-12A electronmicroscope. The proliferation was performed as follows: (1) 100 µL cell suspension were taken out from every flask at day 2, 4, 6, 8 and 10 in culture and added into a new flask without Poly-HEMA; (2) When all microcarriers went down, the supernatants were discarded, 100 µL 2.5 g/L trypsinase were added and cultured at 37 °C for 5 min; (3) After 100 µL DF media were added for termination of trypsinization, the flasks were put up slowly with all microcarriers anchored to the bottom of the flask, and the supernatant were rapidly dipped out for cell calculation with trypan blue dye exclusion method.

**Measurement of biochemical items and IL-2 in the supernatant** With γ calculator (SN-682), the concentration of human ALB was detected by RIA kit from North Biotechnique Institute, Beijing, others as UREA (BUN $\times 2.14$ ), AST and LDH were measured by biochemical autoanalyzer (CX Δ 7, Beckman).

## RESULTS

### Identification of amplified retroviral vector

The amplified products of LNCX and LNCIL-2 were digested with *Hind* III, and then checked with 20 g/L agarose gel electrophoresis (Figure 1). The length of LNCX (6 620 bp) and LNCIL-2 (7 293 bp) were identical with that predicted, showing the success of amplification, extraction and purification.

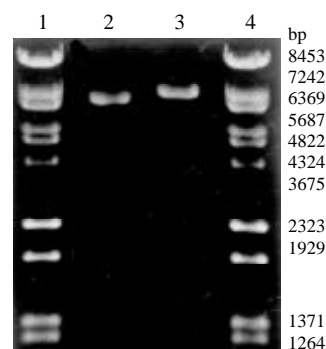


**Figure 1** Restriction enzyme analysis of pLNCX and pLNCIL-2

### Cultivation of virus producer cell and measurement of viral concentration

21 and 25 anti-G418 clones appeared after PA317 cells were transduced by LNCX and LNCIL-2 and cultured in media containing 800 mg/L of G418 for 2 weeks. 10 clones selected were performed amplified culture, respectively. The titer of retrovirus of all collected supernatants was between  $5.4 \times 10^7$  cfu/L and  $1.4 \times 10^9$  cfu/L.

### Morphological changes

Under the light microscope, L-02 cells were seen flake-like growth (Figure 2A), L-02/Neo and L-02/IL-2 cells represented the trend of island-like growth with clear margin (Figure 2B). The growing speed of L-02/IL-2 cells was slightly slower than that of L-02 and L-02/Neo cells (Figure 3). Clonogenicity rate of the L-02 /IL-2 cells were significantly lower than those of L-02/Neo and L-02 cells ( $P < 0.01$ ) (Table 1).

### PCR analysis of NeoR gene

NeoR gene segment (790 bp) was amplified by PCR from genomic DNA of L-02/Neo and L-02/IL-2 cells and tested with 20 g/L agarose gel electrophoresis, but none from L-02 cells

(Figure 4). These suggested that LNCX and LNCIL-2 were successfully integrated into the genome of L-02 cells.

#### IL-2 secretion from IL-2 transduced hepatocyte line

After IL-2 transduction and G418 selection using LNCX and LNCIL-2 retroviral vector, maximal amount of IL-2 production in L-02/IL-2 cells was 32 000 pg/10<sup>6</sup> cells·24 h, remarkably exceeding 56 pg/10<sup>6</sup> cells·24 h in L-02 cells and 48 pg/10<sup>6</sup> cells·24 h in L-02/Neo cells. Moreover, more than ten weeks later the levels of hIL-2 could rise to 27 500 pg/10<sup>6</sup> cells·24 h.

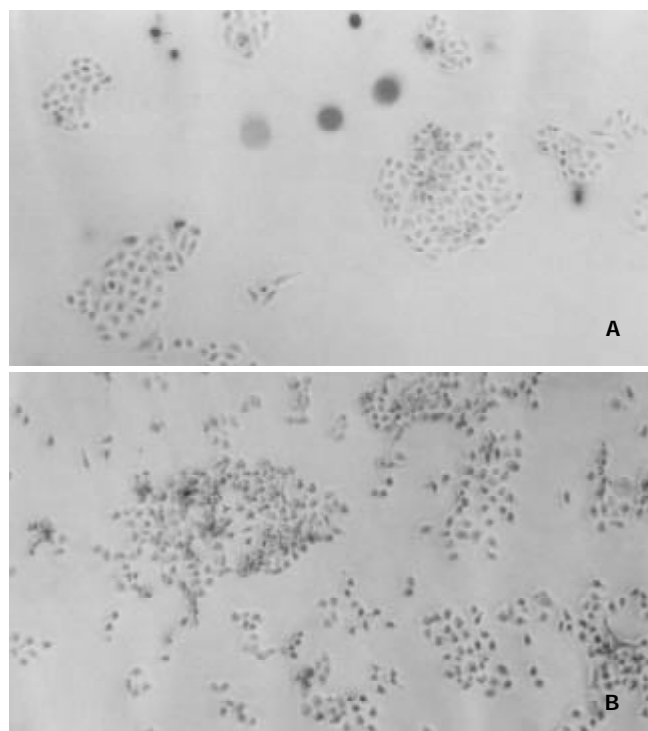


**Figure 2** Morphological changes of cultured L-02/IL-2 and L-02 cells at 24 hours (×100). A: L-02/IL-2 cells; B: L-02 cells

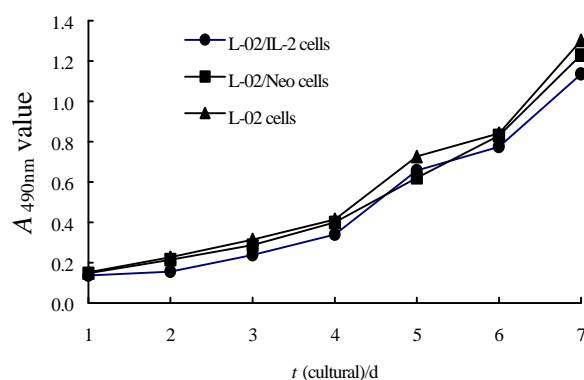


**Figure 3** The growth curves of L-02/IL-2, L-02/Neo and L-02 cells

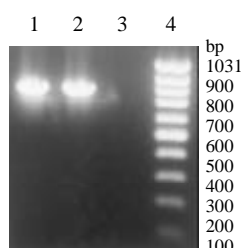


**Figure 4** Integration of NeoR gene cell's genomic DNA by PCR. 1: L-02/IL-2 cells; 2: L-02/Neo cells; 3: L-02 cells; 4: PCR DNA marker

**Table 1** The clonogenicity rate of L-02/IL-2, L-02/Neo and L-02 cells

No. of repeated wells	L-02/IL-2	L-02/Neo	L-02
1	124	148	150
2	135	144	157
3	133	154	144
4	144	141	153
5	128	166	162
6	123	152	156
Mean value	131.2(13.1%) <sup>b</sup>	150.8(15.1%)	153.7(15.4%)

<sup>b</sup>*P*<0.01, vs L-02/Neo and L-02 cells

#### Morphology and proliferation of cells in culture with microcarrier

After cultivation with microcarrier for 4 h, all the cells anchored to microcarriers. At the 4<sup>th</sup> day 70 % of microcarriers were filled with cells, at the 6<sup>th</sup> day all microcarriers' s surface were full of cells or cellular mass (Figure5), at the 8<sup>th</sup> day some dead cells could be seen shedded from microcarriers. Under the electronmicroscope, L-02 and L-02/IL-2 cells had normal super-microstructure, such as integral cell membrane, affluent mitochondria, glycogen and rough endoplasmic reticulum (Figure 6); 3) L-02 and L-02/IL-2 began an exponential growth after two days in culture. At the 6<sup>th</sup> day, the number of alive L-02 was 17.1±0.76×10<sup>6</sup>/flask and L-02/IL-2 was 16.8±0.53×10<sup>6</sup>/flask. At the day of 10, the number of alive cells were 6.1±0.34×10<sup>6</sup>/flask and 5.9±0.52×10<sup>6</sup>/flask, respectively.

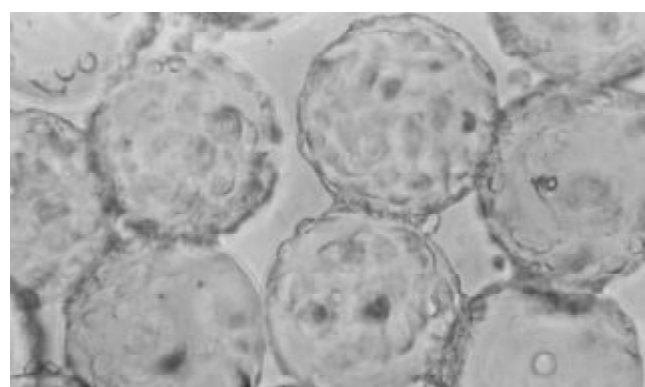


**Figure 5** Hepatocytes-anchored microcarriers linked in mass(×200)

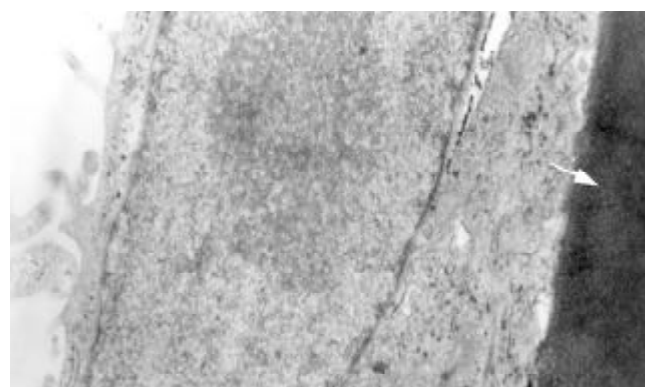


**Figure 6** Hepatocyte with normal super-microstructures tightly anchors microcarrier (↑) (×15 000)

#### Values of biochemical items and IL-2 in the supernatant

The trend levels of ALB and UREA of L-02/IL-2 cells were consistent with the cell proliferation. The values reached the peak at the 6<sup>th</sup> day and decreased with growing cell death. The

**Table 2** Values of biochemical items and IL-2 in supernatant of L-02/IL-2 cells cultured with microcarrier

	Cultivation of day					
	0	2	4	6	8	10
ALB(mg/L)						
L-02	0	8.58±0.30	25.01±0.50	53.81±1.64	39.13±1.22	12.16±0.68
L-02/IL-2	0	8.23±0.39	26.14±0.33	52.54±1.28	40.42±1.15	11.87±0.51
UREA(mmol/L)						
L-02	0.64±0.03	0.90±0.06	2.45±0.14	5.35±0.13	2.92±0.11	1.15±0.07
L-02/IL-2	0.60±0.05	0.85±0.03	2.57±0.23	5.29±0.17	2.93±0.14	1.08±0.09
AST(IU/L)						
L-02	1.0±0.58	3.3±0.75	14.0±0.58	17.6±0.98	46.6±1.62	70.3±1.80
L-02/IL-2	1.0±0.43	3.5±0.93	15.1±0.65	18.6±0.72	47.0±1.69	72.1±2.04
LDH(IU/L)						
L-02	15.9±0.69	25.3±0.95	63.0±1.41	87.4±2.07	522±11.7	687±13.4
L-02/IL-2	14.5±0.62	25.0±1.05	64.6±1.57	88.7±2.35	534±14.6	694±15.7
IL-2 (pg/L)						
L-02	0	<10	33.2±2.6	78.3±3.5	43.6±3.1	21.7±1.8
L-02/IL-2	0	6 456±373 <sup>b</sup>	23 765±688 <sup>b</sup>	52 180±1483 <sup>b</sup>	38 643±1104 <sup>b</sup>	4 360±587 <sup>b</sup>

<sup>b</sup>*P*<0.001, vs L-02 cells.

levels of AST and LDH elevated slowly before the 6<sup>th</sup> day and rapidly increased with the cell death after the peak of growth. These data had not significantly changed as compared with L-02 cells. However, the levels of IL-2 in IL-2/L-02 cells remarkably exceeded that in L-02 cells in the whole cultural process (*P*<0.001) (Table 2).

## DISCUSSION

IL-2, an important regulatory factor in immune network, can induce proliferation of T cell and enhance the immune response function of T cell, B cell, NK cell and monocytes. It plays an important role in antitumor and antiinfection immune function in the body<sup>[15-17]</sup>. As one of the most therapeutically effective genes, IL-2 gene has been transduced into a varieties of cells in research<sup>[8,12,18]</sup>. Recently, there were some reports about direct injection of viral vector that expressed IL-2 gene for therapy of hepatocarcinoma<sup>[7]</sup>. Worldwide, 80 % of gene-therapy projects that were applied clinically with approval were using retroviral vector, for example, LNCX, LXCX, LXSX, etc.<sup>[19,20]</sup>. LNCX, which contained the immediate early promoter of human cytomegalovirus (CMV), was not limited by cell type or animal species and it was more powerful than the other types of enhancer<sup>[21]</sup>. In our study, LNCX, and its derivation LNCIL-2 were transduced into human hepatocyte line L-02. Clonogenicity rate of the L-02 /IL-2 cells were obviously lower than that of L-02/Neo cells and L-02 cells, due to the change of function of IL-2 as an inhibited signal in cell proliferation. The levels of IL-2 in supernatant of L-02/IL-2 cells were remarkably higher than that of L-02/Neo cells and L-02 cells, and the L-02/IL-2 cells could secrete IL-2 for more than ten weeks. These data showed that IL-2 gene was successfully integrated into the genome of L-02 cells.

Highly differentiated liver cell line were easy to proliferate in culture *in vitro*, and had many features of normal hepatocyte, so the construction of hepatocyte line is a very significant subject<sup>[22]</sup>. Japanese scholars had constructed immortalized hepatocyte lines and used them for hepatocyte transplantation and bioartificial liver system with high efficacy<sup>[23-26]</sup>. In this study, the hepatocyte line we used, L-02, was histologically originated from normal human liver tissue and immortalized. High levels of ALB and UREA reflected the cell's good

biological activity in protein synthesis and amino acid metabolism. When IL-2 gene was inserted, these characteristics were not notably changed.

As a alternative for amplifying the number of cells, the technique of cultivation with microcarrier is increasingly playing an important role in bio-engineering. For example, researchers can use it to produce monoclonal antibody<sup>[27]</sup>, hormone<sup>[28]</sup>, vaccine<sup>[29]</sup>, cytokine<sup>[30]</sup> and even viral vector for gene therapy<sup>[31]</sup>, and moreover use it to culture hepatocyte for bioartificial liver system<sup>[32,33]</sup> or hepatocyte transplantation<sup>[34,35]</sup> for clinical use. Regardless of the type of liver cell, two requirements must be considered: First, the number of cell is adequate and easily available. Second, the cells should form congeries, because the work of hepatocytes depends on the contact between the cells or cell and the matrix. With charges-free, Cytodex3, formed by chemically coupling a thin layer of denatured collagen to the cross-linked dextran matrix, has a good adhesive character. So Cytodex3 became the core of hepatocyte aggregation and gradually formed the matrix-induced liver cell aggregates (MILCA)<sup>[36]</sup>.

The significances of construction of L-02/IL-2 cell are as follow. Theoretically, if hepatocytes modified by IL-2 gene can be transplanted into a patient with HCC who is subjected to operation, these cells might provide some functions of hepatocyte as well as antitumor immune function of IL-2 that can induce the regression of cancer cells and inhibit the metastasis, due to the activation of T-cell and other effector cells. Of course, the immune rejection of transplantation should be taken into account, two strategies are available. (1) The fetal hepatocytes, which are poor in immunogenicity and susceptible to retrovirus<sup>[25,37]</sup>, can be selected to be transfected by target-gene and cultured with microcarrier. (2) Microencapsular technique can be used to encapsule transgenetically immortalized hepatocytes, realizing the continuous expression of exogenous gene<sup>[38,39]</sup>, which can be testified by further animal experimentation.

## REFERENCES

- 1 **Strauss M.** Liver-directed gene therapy: prospects and problems. *Gene Ther* 1994; **1**: 156-164
- 2 **Raper SE.** Hepatocyte transplantation and gene therapy. *Clin Transplant* 1995; **9**: 249-254

- 3 **Ojeifo JO**, Su N, Ryan US, Verma UN, Mazumder A, Zwiebel JA. Towards endothelial-cell-directed cancer immunotherapy: in vitro expression of human recombinant cytokine genes by human and mouse primary endothelial cells. *Cytokines Mol Ther* 1996; **2**: 89-101
- 4 **Tang ZY**. Hepatocellular carcinoma-cause, treatment and metastasis. *World J Gastroenterol* 2001; **7**: 445-454
- 5 **Tang YC**, Li Y, Qian GX. Reduction of tumorigenicity of SMMC-7721 hepatoma cells by vascular endothelial growth factor antisense gene therapy. *World J Gastroenterol* 2001; **7**: 22-27
- 6 **Wang Z**, Qiu SJ, Ye SL, Tang ZY, Xiao X. Combined IL-12 and GM-CSF gene therapy for murine hepatocellular carcinoma. *Cancer Gene Ther* 2001; **8**: 751-758
- 7 **Barajas M**, Mazzolini G, Genove G, Bilbao R, Narvaiza I, Schmitz V, Sangro B, Melero I, Qian C, Prieto J. Gene therapy of orthotopic hepatocellular carcinoma in rats using adenovirus coding for interleukin 12. *Hepatology* 2001; **33**: 52-61
- 8 **Hirschowitz EA**, Naama HA, Evoy D, Lieberman MD, Daly J, Crystal RG. Regional treatment of hepatic micrometastasis by adenovirus vector-mediated delivery of interleukin-2 and interleukin-12 cDNAs to the hepatic parenchyma. *Cancer Gene Ther* 1999; **6**: 491-498
- 9 **Kim JH**, Gong SJ, Yoo NC, Lee H, Shin DH, Uhm HD, Jeong SJ, Cho JY, Rha SY, Kim YS, Chung HC, Roh JK, Min JS, Kim BS. Effects of interleukin-2 transduction on the human hepatoma cell lines using retroviral vector. *Oncol Rep* 1999; **6**: 49-54
- 10 **Bui LA**, Butterfield LH, Kim JY, Ribas A, Seu P, Lau R, Glaspy JA, McBride WH, Economou JS. *In vivo* therapy of hepatocellular carcinoma with a tumor-specific adenoviral vector expressing interleukin-2. *Hum Gene Ther* 1997; **8**: 2173-2182
- 11 **Caruso M**, Pham-Nguyen K, Kwong YL, Xu B, Kosai KI, Finegold M, Woo SL, Chen SH. Adenovirus-mediated interleukin-12 gene therapy for metastatic colon carcinoma. *Proc Natl Acad Sci USA* 1996; **93**: 11302-11306
- 12 **Huang H**, Chen SH, Kosai K, Finegold MJ, Woo SL. Gene therapy for hepatocellular carcinoma: long-term remission of primary and metastatic tumors in mice by interleukin-2 gene therapy *in vivo*. *Gene Ther* 1996; **3**: 980-987
- 13 **Sambrook J**, Fritsch EF, Maniatis T. Molecular cloning: A laboratory manual, 2nd edition. *Cold spring harbor* 1996: 55
- 14 **Byun J**, Kim JM, Kim SH, Yim J, Robbins PD, Kim S. A simple and rapid method for the determination of recombinant retrovirus titer by G418 selection. *Gene Ther* 1996; **3**: 1018-1020
- 15 **Correale P**, Campoccia G, Tsang KY, Micheli L, Cusi MG, Sabatino M, Bruni G, Sestini S, Petrioli R, Pozzessere D, Marsili S, Fanetti G, Giorgi G, Francini G. Recruitment of dendritic cells and enhanced antigen-specific immune reactivity in cancer patients treated with hr-GM-CSF (Molgramostim) and hr-IL-2. results from a phase Ib clinical trial. *Eur J Cancer* 2001; **37**: 892-902
- 16 **Zheng N**, Ye SL, Sun RX, Zhao Y, Tang ZY. Effects of cryopreservation and phenylacetate on biological characters of adherent LAK cells from patients with hepatocellular carcinoma. *World J Gastroenterol* 2002; **8**: 233-236
- 17 **Chen B**, Timiryasova TM, Gridley DS, Andres ML, Dutta-Roy R, Fodor I. Evaluation of cytokine toxicity induced by vaccinia virus-mediated IL-2 and IL-12 antitumor immunotherapy. *Cytokine* 2001; **15**: 305-314
- 18 **Cao XT**, Zhang WP, Tao Q. Enhanced immune functions and antitumor activity of fibroblast-mediated interleukin-2 gene therapy. *Zhonghua Yixue Zazhi* 1995; **75**: 521-524
- 19 **Wang X**, Liu FK, Li X, Li JS, Xu GX. Inhibitory effect of endostatin expressed by human liver carcinoma SMMC7721 on endothelial cell proliferation in vitro. *World J Gastroenterol* 2002; **8**: 253-257
- 20 **Fakhrai H**, Shawler DL, Van Beveren C, Lin H, Dorigo O, Solomon MJ, Gjerset RA, Smith L, Bartholomew RM, Boggiano CA, Gold DP, Sobol RE. Construction and characterization of retroviral vectors for interleukin-2 gene therapy. *J Immunother* 1997; **20**: 437-448
- 21 **Boshart M**, Weber F, Jahn G, Dorsch-Hasler K, Fleckenstein B, Schaffner W. A very strong enhancer is located upstream of an immediate early gene of human cytomegalovirus. *Cell* 1985; **41**: 521-530
- 22 **Cascio SM**. Novel strategies for immortalization of human hepatocytes. *Artif Organs* 2001; **25**: 529-538
- 23 **Kobayashi N**, Noguchi H, Fujiwara T, Westerman KA, Leboulch P, Tanaka N. Establishment of a highly differentiated immortalized adult human hepatocyte cell line by retroviral gene transfer. *Transplant Proc* 2000; **32**: 2368-2369
- 24 **Kobayashi N**, Miyazaki M, Fukaya K, Inoue Y, Sakaguchi M, Noguchi H, Matsumura T, Watanabe T, Totsugawa T, Tanaka N, Namba M. Treatment of surgically induced acute liver failure with transplantation of highly differentiated immortalized human hepatocytes. *Cell Transplant* 2000; **9**: 733-735
- 25 **Kobayashi N**, Noguchi H, Watanabe T, Matsumura T, Totsugawa T, Fujiwara T, Tanaka N. Role of immortalized hepatocyte transplantation in acute liver failure. *Transplant Proc* 2001; **33**: 645-646
- 26 **Kobayashi N**, Noguchi H, Watanabe T, Matsumura T, Totsugawa T, Fujiwara T, Tanaka N. A tightly regulated immortalized human fetal hepatocyte cell line to develop a bioartificial liver. *Transplant Proc* 2001; **33**: 1948-1949
- 27 **Voigt A**, Zintl F. Hybridoma cell growth and anti-neuroblastoma monoclonal antibody production in spinner flasks using a protein-free medium with microcarriers. *J Biotechnol* 1999; **68**: 213-226
- 28 **Hamid M**, McCluskey JT, McClenaghan NH, Platt PR. Culture and function of electrofusion-derived clonal insulin-secreting cells immobilized on solid and macroporous microcarrier beads. *Biosci Rep* 2000; **20**: 167-176
- 29 **Junker BH**, Wu F, Wang S, Waterbury J, Hunt G, Hennessey J, Aunins J, Lewis J, Silberklang M, Buckland BC. Evaluation of a microcarrier process for large-scale cultivation of attenuated hepatitis A. *Cytotechnology* 1992; **9**: 173-187
- 30 **Bing RJ**, Dudek R, Kahler J, Narayan KS, Ingram M. Cytokine production from freshly harvested human mononuclear cells attached to plastic beads. *Tissue Cell* 1992; **24**: 203-209
- 31 **Wu SC**, Huang GY, Liu JH. Production of retrovirus and adenovirus vectors for gene therapy: a comparative study using microcarrier and stationary cell culture. *Biotechnol Prog* 2002; **18**: 617-622
- 32 **Gao Y**, Xu XP, Hu HZ, Yang JZ. Cultivation of human liver cell lines with microcarriers acting as biological materials of bioartificial liver. *World J Gastroenterol* 1999; **5**: 221-224
- 33 **Suh KS**, Lilja H, Kamohara Y, Eguchi S, Arkadopoulos N, Neuman T, Demetriou AA, Rozga J. Bioartificial liver treatment in rats with fulminant hepatic failure: effect on DNA-binding activity of liver-enriched and growth-associated transcription factors. *J Surg Res* 1999; **85**: 243-250
- 34 **Demetriou AA**, Levenson SM, Novikoff PM, Novikoff AB, Chowdhury NR, Whiting J, Reisner A, Chowdhury JR. Survival, organization, and function of microcarrier-attached hepatocytes transplanted in rats. *Proc Natl Acad Sci USA* 1986; **83**: 7475-7479
- 35 **Nyberg SL**, Peshwa MV, Payne WD, Hu WS, Cerra FB. Evolution of the bioartificial liver: the need for randomized clinical trials. *Am J Surg* 1993; **166**: 512-521
- 36 **Kong LB**, Chen S, Demetriou AA, Rozga J. Matrix-induced liver cell aggregates (MILCA) for bioartificial liver use. *Int J Artif Organs* 1996; **19**: 72-78
- 37 **Koch KS**, Brownlee GG, Goss SJ, Martinez-Conde A, Leffert HL. Retroviral vector infection and transplantation in rats of primary fetal rat hepatocytes. *J Cell Sci* 1991; **99**: 121-130
- 38 **Aoki K**, Hakamada K, Umehara Y, Seino K, Itabashi Y, Sasaki M. Intraperitoneal transplantation of microencapsulated xenogeneic hepatocytes in totally hepatectomized rats. *Transplant Proc* 2000; **32**: 1118-1120
- 39 **Umehara Y**, Hakamada K, Seino K, Aoki K, Toyoki Y, Sasaki M. Improved survival and ammonia metabolism by intraperitoneal transplantation of microencapsulated hepatocytes in totally hepatectomized rats. *Surgery* 2001; **130**: 513-520

# Effects of p16 gene on biological behaviour in hepatocellular carcinoma cells

Jian-Zhao Huang, Sui-Sheng Xia, Qi-Fa Ye, Han-Ying Jiang, Zhong-Hua Chen

**Jian-Zhao Huang**, Department of Hepatobiliary Surgery, DaPing Hospital, Third Military Medical University, Chongqing 400042, China  
**Sui-Sheng Xia, Qi-Fa Ye, Han-Ying Jiang, Zhong-Hua Chen**, Institute of Organ Transplantation, Tong Ji Hospital, School of Medicine, Hua Zhong University of Science and Technology, Wuhan 430030, Hubei Province, China

**Correspondence to:** Dr. Jian-Zhao Huang, Department of Hepatobiliary Surgery, Daping Hospital, 10 Chang Jiang Road, Chongqing 400042, China. hjz999@mail.tmmu.com.cn

**Telephone:** +86-23-68757247

**Received:** 2002-06-11 **Accepted:** 2002-07-12

## Abstract

**AIM:** To investigate the effects of p16 gene on biological behaviour in hepatocellular carcinoma cells.

**METHODS:** HCC cell lines SNU-449 and HepG2.2.15 were infected respectively by a replication defective, recombinant retrovirus capable of producing a high level of p16 protein expression (pCLXSN-p16). G418 resistant stable P16 protein expression cell lines were selected. And the biological behaviours of the p16 gene transfected HCC cells were observed.

**RESULTS:** Initial *in vitro* experiments in HCC cell line SNU-449 with loss of p16 protein expression demonstrated the pCLXSN-p16 treatment significantly inhibited cell growth. But there was no treatment effect when the pCLXSN-p16 was used in another HCC cell line HepG2.2.15 which has positive p16 protein expression. Subsequent study in a nude mouse model demonstrated that the p16 gene transfected SNU-449 had a lower succeeding rate in the first time establishment of tumors and grew more slowly in the nude mice when compared with non-transfected SNU-449. Moreover, the nude mice inoculated with transfected SNU-449 had a longer surviving time than those inoculated with non-transfected SNU-449.

**CONCLUSION:** Our results show that the p16INK4a gene transfer can inhibit the proliferation and reduce the invasion ability of hepatocellular carcinoma.

Huang JZ, Xia SS, Ye QF, Jiang HY, Chen ZH. Effects of p16 gene on biological behaviour in hepatocellular carcinoma cells. *World J Gastroenterol* 2003; 9(1): 84-88  
<http://www.wjgnet.com/1007-9327/9/84.htm>

## INTRODUCTION

Hepatocellular carcinoma (HCC) is a common malignant tumor with a increasing incidence<sup>[1]</sup>, and the treatment has been extremely difficult. HCCs are generally highly resistant to chemotherapeutic agents and radiotherapy. Despite a variety of treatment options including surgical resection, chemoembolization, percutaneous injection of ethanol or acetic acid, and liver transplantation, the prognosis of HCC patients is poor<sup>[2]</sup>. Thus, new treatment strategies are necessary

to improve the survival rate. It is believed that molecular changes that occur during carcinogenesis, such as overexpression of the multidrug resistant gene and the loss of tumor suppressor genes may allow many kinds of tumor cell populations to become resistant to most therapeutic approaches. Gene therapy may offer certain advantages in the treatment of HCC.

P16 gene encoded for a protein that was initially identified as a specific inhibitor of the CDKs, CDK4 and CDK6. By binding to and inhibiting CDK4 and CDK6, p16 prevents both pRb phosphorylation and subsequent progression into the S phase of the cell cycle. P16 gene alterations were found in many kinds of cancers<sup>[3-13]</sup>. Our previously study has showed that the frequency of P16 gene inactivation was high (36 %)<sup>[14]</sup> in HCC. Other's Reports have also showed frequent P16 gene inactivations<sup>[15-21]</sup>. Thus, P16 gene may be an ideal candidate for the treatment of HCC. In this study, we constructed the retrovirus p16 expression vector and then investigated whether it could control the proliferation of HCC cell lines.

## MATERIALS AND METHODS

### *P16 cDNA subcloning and construction of pCLXSN-p16*

The original P16 cDNA was amplified from the total RNA of normal human lymphocytes by reverse transcription PCR. The PCR product was subcloned into pCLXSN expression vector, a deficient retrovirus vector which derived from pLXSN (IMAGENEX). Then the recombinant p16 expression vector was cotransfected with the pCL-Ampho packaging construct into 293 cells by using a modification of the HEPES-buffered saline calcium phosphate method<sup>[22]</sup>. Two days after infection the 293 cells were placed under G418 selection (800 µg/ml) and grew for 10 days. Then the G418 resistant 293 cells were amplified and the supernatant which contained the pCLXSN-p16 pseudo retrovirus were collected and filtered through a 0.45 µm pore size filter. The pseudo retroviruses were tited through infecting NIH 3T3 cells<sup>[22]</sup>. We also packaged a reporter gene expression vector pCLMFG-LacZ as a control. The viral titer was  $1.6 \times 10^5$  CFU/ml.

### *Cell lines*

Human HCC cell lines SNU-449 (with loss of p16 expression) and HepG2.2.15 (with p16 expression) were kindly provided by Dr. Zhang Mingyi (Tumor Hospital of Sichuan Province, Chengdu, China,) and Dr. Gao Yong (the Union Hospital, Tongji Medical University, Wuhan, China) respectively. They were grown in RPMI 1640 containing 10 % fetal bovine serum.

### *Infection of retroviral vectors and selection of stable expression cell lines*

SNU-449 and HepG2.2.15 cell lines were seeded and cultured in two 6 cm plates at a density of  $2 \times 10^5$  cells for 24hs respectively. Immediately before infection, the culture medium was replaced and 1 ml viral supernatant of pCLXSN-p16 or pCLMFG-LacZ (control) was added. Then the polybrene was added to the medium in 8 µg/ml. The infected cells were grown for 24hs and split into 10 cm plates at 1:10 dilution, then grown in the medium containing G418 in 800 µg/ml. The



medium was replaced every 3-4 days and the G418 resistant cells were selected and named SNU-449/pCLXSN-p16, HepG2.2.15/pCLXSN-p16, SNU-449/pCLMFG-LacZ and HepG2.2.15/pCLMFG-LacZ, respectively.

#### Immunohistochemical analysis and western blotting

SNU-449 cells were collected 24hs after infected by pCLXSN-p16. The stable G418 resistant SNU-449/pCLXSN-p16 cells were also collected. Both of them were examined for p16 expression immunohistochemically by the labeled streptavidin-biotin method. The SNU-449/pCLXSN cells were also screened for p16 expression by Western blotting. The cells for immunochemical analysis were grown on the glass slides.

Immunohistochemical detection procedure was carried out according to the manufacture's recommendations. Western blotting was performed as previously described<sup>[23]</sup>.

#### Growth curves

The effect of p16 expression on cell growth was examined in all six cell lines, including SNU-449, SNU-449/pCLXSN-p16, SNU-449/pCLMFG-LacZ, HepG2.2.15, HepG2.2.15/pCLXSN-p16, and HepG2.2.15/pCLMFG-LacZ. Triplicate samples of log phase cells were seeded at a density of  $1 \times 10^4$  in 6 holes culture plates. Cells were harvested for counting by digestion with trypsin/EDTA for 3 min, followed by the addition of fresh media to inhibit further digestion. Cells were then pelleted by centrifugation at 1000rpm for 5 min, followed by resuspension in fresh media. Triplicate sets of cells were counted at 1, 3 and 5 days after seeded. The mean cell number for each harvesting was calculated, and cell growth curves were determined.

#### Cell cycle and apoptosis analysis

The effect of pCLXSN-p16 expression on cell cycle dynamics and cell apoptosis was examined in both the SNU-449/pCLXSN-p16 and HepG2.2.15/pCLXSN-p16 cell lines using FACS analysis. In the meanwhile, the cell cycle distribution and apoptosis analysis of SNU-449, SNU-449/pCLMFG-LacZ and HepG2.2.15 cells were also examined for controls. Briefly,  $1 \times 10^6$  cells of each cell line were collected by centrifugation at 1000 rpm for 5 min, followed by two washes in ice-cold PBS. Cells were then fixed in 2.0 ml of 70 % ethanol and stored at 4 °C for a minimum of 1 h. Prior to FACS analysis, cells were washed twice with ice-cold PBS, and the cell pellet was resuspended in 10 µg/ml of propidium iodide (Sigma Chemical Co.). Add 100 µg/ml of Rnase (Sigma Chemical Cop.) and incubated at 37 °C for 30 min. Then the FACS analysis was performed.

#### In vivo studies

Nude mice were used at the weight of 23-27 grams. Log phase SNU-449/pCLXSN-p16 and SNU-449 cells were harvested and centrifuged at 1000 rpm for 5 min, then resuspended in 0.9 % salt solution at  $1 \times 10^8$ , respectively. Cells were immediately implanted subcutaneously into the right flank of nude mice ( $1 \times 10^7$  cells for each animal). Tumor formation and subsequent growth were monitored. The tumor volume at 23 days after implantation and the survival rate of the mice at 52 days after implantation were also observed. Statistical significance was assessed by Mann-Whitney statistical analysis (Statmost for windows).

## RESULTS

#### Detection of p16 protein expression

SNU-449 cells exhibited a loss of p16 protein expression (Figure 1), and HepG2.2.15 cells showed positive p16 staining. About 20 % SNU-449 cells showed positive p16 staining 24 hours after infected by pCLXSN-p16 pseudo virus. All the

G418 resistant SNU-449/pCLXSN-p16 cells exhibited p16 protein expression (Figure 2). Western blot analysis also confirmed that SNU-449 cells showed loss of p16 protein expression and SNU-449/pCLXSN-p16 cells could express p16 protein (Figure 3).

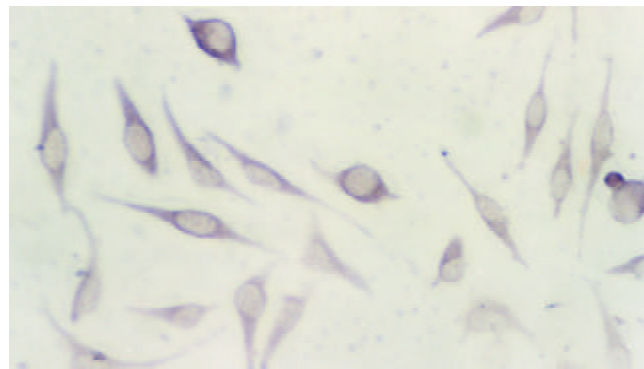


**Figure 1** SNU-449 cells show negative p16 staining (original magnification $\times 400$ ).

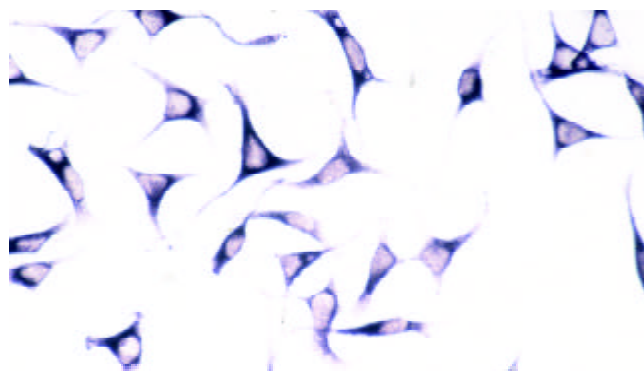


**Figure 2** SNU-449/pCLXSN-p16 cells show positive p16 staining (original magnification $\times 200$ ).

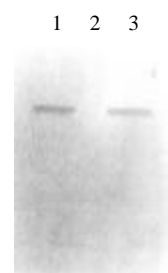


**Figure 3** Western blot analysis. Lanes 1 and 3: SNU-449/pCLXSN-p16 cells; Lane 2: SNU-449 cells.

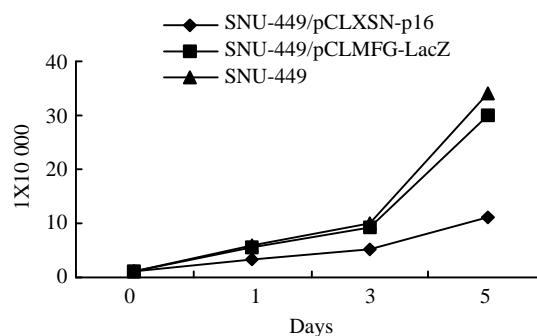


**Figure 4** *In vitro* growth curves of SNU-449/pCLXSN-p16, SNU-449/pCLMFG-LacZ and SNU-449 cell lines.



### Cell growth curves

As shown in Figure 4, *in vitro* growth rates of SNU-449/pCLXSN-p16 cell line, a selected stable p16 protein expression cell line, were significantly inhibited when compared with cell lines SNU-449 and SNU-449/pCLMFG-LacZ in which p16 protein expression was lost. Nearly equal growth rates were observed in both HepG 2.2.15 and HepG 2.2.15/pCLXSN-p16 cell lines.

### Cell cycle distribution and cell apoptosis status

The underlying mechanism of *in vitro* growth inhibition seen in the pCLXSN-p16 treated cell line SNU-449/pCLXSN-p16 was investigated by cell cycle analysis using flow cytometry. As shown in table 1, SNU-449/pCLXSN-p16 cell line exhibited significant increase in the percentage of cells in G<sub>0</sub>-G<sub>1</sub> phase (68 %), consistent with a cell cycle arrest at the G<sub>1</sub> transition when compared with cell lines SNU-449 and SNU-449/pCLMFG-LacZ. However there was no obvious cell cycle difference between cell lines HepG2.2.15/pCLXSN-p16 and HepG2.2.15.

**Table 1** Cell cycle analysis

Cell type	Cell cycle(%)		
	G <sub>0</sub> -G <sub>1</sub>	G <sub>2</sub> -M	S
SNU-449	37	36	27
SNU-449/pCLXSN-p16	68	21	11
SNU-449/pCLMFG-LacZ	39	38	23
HepG2.2.15	29	42	29
HepG2.2.15/pCLXSN-p16	32	43	25

Cell apoptosis analysis was performed in cell lines SNU-449, SNU-449/pCLXSN-p16, HepG2.2.15 and HepG2.2.15/pCLXSN-p16 and showed no difference between these cell lines.

### Effects of pCLXSN-p16 treatment on HCC tumor growth in vivo

The therapeutic potential of pCLXSN-p16 to treat HCC tumors *in vivo* was studied in nude mice. Tumors were created by injecting 1×10<sup>7</sup> SNU-449 or SNU-449/pCLXSN-p16 cells in 100 μl 0.9 % salt solution into the right flank of nude mice as described above. The succeed rate of tumor establishment at the first time injection of tumor cells SNU-449/pCLXSN-p16 in nude mice was 70 % (7/10). At the same time only 40 % (4/10) nude mice succeeded to establish tumors at the first time injection of SNU-449 cells. Animals who were succeeded to establish tumors were observed over a period of 52 days from the day of injecting tumor cells. During the observing period animals injected with SNU-449/pCLXSN-p16 cell line survived significantly longer than those injected with SNU-449 (*P*<0.05). The mean survival time of animals injected with SNU-449/pCLXSN-p16 and SNU-449 were 42.1±9.0 days and 32.7±6.7 days, respectively (Table 2). The survival rate of nude mice injected with SNU-449/pCLXSN-p16 cell line was higher than that of those injected with SNU-449. Figure 5 was the survival curves of nude mice injected with cell lines SNU-449/pCLXSN-p16 and SNU-449, respectively.

Two groups of nude mice with each of 6 animals were established with tumors by injection of cell lines SNU-449/pCLXSN-p16 and SNU-449, respectively and were observed for a period of 23 days. All the animals survived during the observing period. At 23th day after injection of tumor cells they were all sacrificed for measurement of tumor volumes. The tumor volume in nude mice injected with SNU-449/

pCLXSN-p16 was 234±125 mm<sup>3</sup>, significantly smaller than that in those injected with SNU-449 cell line (726±513 mm<sup>3</sup>).

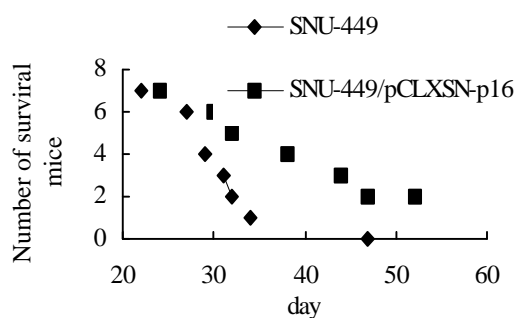


**Figure 5** Survival curves of nude mice.

**Table 2** The survival time and survival rate of nude mice

Group	animal number	survival time(d)	survival rate
Salt solution	5	52.0±0.0	100%
SNU-449	7	32.7±6.7	0%
SNU-449/pCLXSN-p16	7	42.1±9.0 <sup>a</sup>	28.6%

<sup>a</sup>*P*<0.05 Compared with group SNU-449

## DISCUSSION

The hypothesis that the inactivation or loss of certain genes, specially tumor suppressor genes, leads to both tumor growth and progression is now well established and provides a unique opportunity in cancer gene therapy. The decision to use p16 gene as a therapeutic agent against human hepatocellular carcinoma was based on our earlier work where we had found p16 gene was frequently inactivated in HCCs<sup>[14]</sup>. In the fact, P16 gene was widely used in the study of tumor gene therapy and showed obvious tumor suppressing effects in many kinds of tumors<sup>[23-31]</sup>. In the present study we cloned human p16 cDNA and constructed a replication-defective, recombinant retrovirus that express high levels of the tumor suppressor protein p16.

The pCLXSN vector was modified from pLXSN vector. It's more safe and can produce higher titers of retrovirus when cotransfected with the pCL-Ampho packaging construct into 293 cells than its' prototype pLXSN. It permits the expression of a number of cell cycle-regulatory proteins such as p16 that are otherwise difficult to study in retroviruses because of their potent cytostatic or cytotoxic effects<sup>[22]</sup>. In this study we cotransfected a report gene LacZ expression vector pLMFG-LacZ and packaging constructs pCL-Ampho into 293 cells. The transfecting efficiency was determined and only 1 % (data not shown), much lower than reported 30 %<sup>[15]</sup>. Considering the lower transfecting efficiency we selected a stable virus-producing cell lines after the p16 protein expression vector pCLXSN-p16 was cotransfected with pCL-Ampho into 293 cells. The titer of pCLXSN-p16 retrovirus produced by the stable virus-producing cell line was determined to be 1.6×10<sup>5</sup>CFU/ml. It is much lower than reported 5×10<sup>5</sup>-2×10<sup>6</sup><sup>[22]</sup>. Only 20 % SNU-449 cells showed positive p16 protein expression 24hs after infected by the pCLXSN-p16 pseudo retroviruses. We then determined to select a SNU-449 cell line which stably expresses p16 protein after infected by the pCLXSN-p16 and use it to study the treatment effect of p16 gene transfer to the HCC cells.

Initial *in vitro* experiments demonstrated that the reintroduction of p16 gene significantly inhibited cell growth

by inducing G1-S cell cycle arrest in the SNU-449 HCC cell line in which p16 gene was originally inactivated. In contrast, no inhibition of cell growth was found when wild type p16 gene was transfected into another HCC cell line HepG2.2.15 in which p16 protein was normally expressed. This suggested that inactivation of p16 gene and its downstream gene may contributed to the carcinogenesis of HCC. Our results were similar to others' reports about treatment study of some tumors using p16 gene transfer<sup>[32-35]</sup>. No changes of tumor cell apoptosis were found when wild type p16 gene was introduced to cell lines SNU-449 or HepG2.2.15. This suggested that introduction of p16 gene may not cause apoptosis of HCC cells.

Subsequent *in vivo* studies showed that the first time establishment of tumors in nude mice was more difficult using p16 gene treated SNU-449 cells (SNU-449/pCLXSN-p16) than using the cells without treatment. This suggested that reintroduction of p16 gene could reduce the invasion ability of HCC tumor cells. Further observation demonstrated that reintroduction of p16 gene into tumor cells significantly inhibited tumor growth rate in tumor-established animals and extended the survival time and survival rate of these animals during the observing period. The results of *in vitro* and *in vivo* study were consistent.

Our results support the use of retrovirus-mediated p16 gene treatment for HCC and provide an important foundation from which to build future preclinical studies and initiate future human clinical trials. If pCLXSN-p16 is proved to be effective in the clinical setting, it will offer a much useful addition to present therapeutic regimens. PCLXSN-p16 may potentially develop into an important adjuvant therapy, expedient in treating unresectable HCC or microscopic residual disease after surgical resection. However, the titer of pCLXSN-p16 pseudo retrovirus must be boosted in the future studies.

## REFERENCES

- Ince N**, Wands JR. The increasing incidence of hepatocellular carcinoma. *N Engl J Med* 1999; **340**: 798-799
- Bruix J**. Treatment of hepatocellular carcinoma. *Hepatology* 1997; **25**: 259-262
- He XS**, Su Q, Chen ZC, He XT, Long ZF, Ling H, Zhang LR. Expression, deletion [was deletion] and mutation of p16 gene in human gastric cancer. *World J Gastroenterol* 2001; **7**: 515-521
- Yi J**, Wang ZW, Cang H, Chen YY, Zhao R, Yu BM, Tang XM. P16 gene methylation in colorectal cancers associated with Duke's staging. *World J Gastroenterol* 2001; **7**: 722-725
- Liu LH**, Xiao WH, Liu WW. Effect of 5-Aza-2'-deoxycytidine on the P16 tumor suppressor gene in hepatocellular carcinoma cell line HepG2. *World J Gastroenterol* 2001; **7**: 131-135
- Simon M**, Park TW, Koster G, Mahlberg R, Hackenbroch M, Bostrom J, Loning T, Schramm J. Alterations of INK4a(p16-p14ARF)/INK4b(p15) expression and telomerase activation in meningioma progression. *J Neurooncol* 2001; **55**: 149-158
- Hibi K**, Taguchi M, Nakayama H, Takase T, Kasai Y, Ito K, Akiyama S, Nakao A. Molecular detection of p16 promoter methylation in the serum of patients with esophageal squamous cell carcinoma. *Clin Cancer Res* 2001; **7**: 3135-3138
- Sanchez-Beato M**, Saez AI, Navas IC, Algara P, Sol-Mateo M, Villuendas R, Camacho F, Sanchez-Aguilera A, Sanchez E, Piris MA. Overall survival in aggressive B-cell lymphomas is dependent on the accumulation of alterations in p53, p16, and p27. *Am J Pathol* 2001; **159**: 205-213
- Bazan V**, Zanna I, Migliavacca M, Sanz-Casla MT, Maestro ML, Corsale S, Macaluso M, Dardanoni C, Restivo S, Quintela PL, Bernaldez R, Saleno S, Morello V, Tomasino RM, Cebbia N, Russo A. Prognostic significance of p16INK4a alterations and 9p21 loss of heterozygosity in locally advanced laryngeal squamous cell carcinoma. *J Cell Physiol* 2002; **192**: 286-293
- Sato N**, Ueki T, Fukushima N, Iacobuzio-Donahue CA, Yeo CJ, Cameron JL, Hruban RH, Goggins M. Aberrant methylation of CpG islands in intraductal papillary mucinous neoplasms of the pancreas. *Gastroenterology* 2002; **123**: 365-372
- Costentin L**, Pages P, Bouisson M, Berthelemy P, Buscail L, Escourrou J, Pradayrol L, Vaysse N. Frequent deletions of tumor suppressor genes in pure pancreatic juice from patients with tumoral or nontumoral pancreatic diseases. *Pancreatol* 2002; **2**: 17-25
- Child FJ**, Scarisbrick JJ, Calonje E, Orchard G, Russell-Jones R, Whittaker SJ. Inactivation of tumor suppressor genes p15(INK4b) and p16(INK4a) in primary cutaneous B cell lymphoma. *J Invest Dermatol* 2002; **118**: 941-948
- Hasegawa M**, Nelson HH, Peters E, Ringstrom E, Posner M, Kelsey KT. Patterns of gene promoter methylation in squamous cell cancer of the head and neck. *Oncogene* 2002; **21**: 4231-4236
- Huang J**, Shen W, Li B, Luo Y, Liao S, Zhang W, Cheng N. Molecular and immunohistochemical study of the inactivation of the p16 gene in primary hepatocellular carcinoma. *Chin Med J (Engl)* 2000; **113**: 889-893
- Herath NI**, Kew MC, Walsh MD, Young J, Powell LW, Leggett BA, MacDonald GA. Reciprocal relationship between methylation status and loss of heterozygosity at the p14(ARF) locus in Australian and South African hepatocellular carcinomas. *J Gastroenterol Hepatol*, 2002; **17**: 301-307
- Roncagli M**, Bianchi P, Bruni B, Laghi L, Destro A, Di Gioia S, Gennari L, Tommasini M, Malesci A, Coggi G. Methylation framework of cell cycle gene inhibitors in cirrhosis and associated hepatocellular carcinoma. *Hepatology* 2002; **36**: 427-432
- Azechi H**, Nishida N, Fukuda Y, Nishimura T, Minata M, Katsuma H, Kuno M, Ito T, Komeda T, Kita R, Takahashi R, Nakao K. Disruption of the p16/cyclin D1/retinoblastoma protein pathway in the majority of human hepatocellular carcinomas. *Oncology* 2001; **60**: 346-354
- Liew CT**, Li HM, Lo KW, Leow CK, Lau WY, Hin LY, Lim BK, Lai PB, Chan JY, Wang XQ, Wu S, Lee JC. Frequent allelic loss on chromosome 9 in hepatocellular carcinoma. *Int J Cancer* 1999; **81**: 319-324
- Liew CT**, Li HM, Lo KW, Leow CK, Chan JY, Hin LY, Lau WY, Lai PB, Lim BK, Huang J, Leung WT, Wu S, Lee JC. High frequency of p16INK4A gene alterations in hepatocellular carcinoma. *Oncogene* 1999; **18**: 789-795
- Wong IH**, Lo YM, Zhang J, Liew CT, Ng MH, Wong N, Lai PB, Lau WY, Hjelm NM, Johnson PJ. Detection of aberrant p16 methylation in the plasma and serum of liver cancer patients. *Cancer Res* 1999; **59**: 71-73
- Saito Y**, Kanai Y, Sakamoto M, Saito H, Ishii H, Hirohashi S. Expression of mRNA for DNA methyltransferases and methyl-CpG-binding proteins and DNA methylation status on CpG islands and pericentromeric satellite regions during human hepatocarcinogenesis. *Hepatology* 2001; **33**: 561-568
- Naviaux RK**, Costanzi E, Hass M, Verma IM. The pCL vector system: rapid production of helper-free, high-titer, recombinant retroviruses. *J Virol* 1996; **70**: 5701-5705
- Urashima M**, Teoh G, Akiyama M, Yuza Y, Anderson KC, Maekawa K. Restoration of p16INK4A protein induces myogenic differentiation in RD rhabdomyosarcoma cells. *Br J Cancer* 1999; **79**: 1032-1036
- Kim SK**, Wang KC, Cho BK, Chung HT, Kim YY, Lim SY, Lee CT, Kim HJ. Interaction between p53 and p16 expressed by adenoviral vectors in human malignant glioma cell lines. *J Neurosurg* 2002; **97**: 143-150
- Rui HB**, Su JZ. Co-transfection of p16(INK4a) and p53 genes into the K562 cell line inhibits cell proliferation. *Haematologica* 2002; **87**: 136-142
- Calbo J**, Marotta M, Cascallo M, Roig JM, Celpi JL, Fueyo J, Mazo A. Adenovirus-mediated wt-p16 reintroduction induces cell cycle arrest or apoptosis in pancreatic cancer. *Cancer Gene Ther* 2001; **8**: 740-750
- Wang TJ**, Huang MS, Hong CY, Tse V, Silverberg GD, Hsiao M. Comparisons of tumor suppressor p53, p21, and p16 gene therapy effects on glioblastoma tumorigenicity *in situ*. *Biochem Biophys Res Commun* 2001; **287**: 173-180
- Ghaneh P**, Greenhalf W, Humphreys M, Wilson D, Zumstein L, Lemoine NR, Neoptolemos JP. Adenovirus-mediated transfer of p53 and p16(INK4a) results in pancreatic cancer regression *in vitro* and *in vivo*. *Gene Ther* 2001; **8**: 199-208

- 29 **Frizelle SP**, Rubins JB, Zhou JX, Curiel DT, Kratzke RA. Gene therapy of established mesothelioma xenografts with recombinant p16INK4a adenovirus. *Cancer Gene Ther* 2000; **7**: 1421-1425
- 30 **Campbell I**, Magiocco A, Moyana T, Zheng C, Xiang J. Adenovirus-mediated p16INK4 gene transfer significantly suppresses human breast cancer growth. *Cancer Gene Ther* 2000; **7**: 1270-1278
- 31 **Kawabe S**, Roth JA, Wilson DR, Meyn RE. Adenovirus-mediated p16INK4a gene expression radiosensitizes non-small cell lung cancer cells in a p53-dependent manner. *Oncogene* 2000; **19**: 5359-5366
- 32 **Lee SH**, Kim MS, Kwon HC, Park IC, Park MJ, Lee CT, Kim YW, Kim CM, Hong SI. Growth inhibitory effect on glioma cells of adenovirus-mediated p16/INK4a gene transfer *in vitro* and *in vivo*. *Int Mol Med* 2000; **6**: 559-563
- 33 **Todd MC**, Sclafani RA, Langan TA. Ovarian cancer cells that coexpress endogenous Rb and p16 are insensitive to overexpression of functional p16 protein. *Oncogene* 2000; **19**: 258-264
- 34 **Allay JA**, Steiner MS, Zhang Y, Reed CP, Cockcroft J, Lu Y. Adenovirus p16 gene therapy for prostate cancer. *World J Urol* 2000; **18**: 111-120
- 35 **Kobayashi S**, Shirasawa H, Sashiyama H, Kawahira H, Kaneko K, Asano T, Ochiai T. P16INK4a expression adenovirus vector to suppress pancreas cancer cell proliferation. *Clin Cancer Res* 1999; **5**: 4182-4185

**Edited by** Ma JY

# Mutation analysis of novel human liver-related putative tumor suppressor gene in hepatocellular carcinoma

Cheng Liao, Mu-Jun Zhao, Jing Zhao, Hai Song, Pascal Pineau, Agnès Marchio, Anne Dejean, Pierre Tiollais, Hong-Yang Wang, Tsai-Ping Li

**Cheng Liao, Mu-Jun Zhao, Jing Zhao, Hai Song, Tsai-Ping Li,** State Key Laboratory of Molecular Biology, Institute of Biochemistry and Cell Biology, Shanghai Institutes for Biological Sciences, Chinese Academy of Sciences, Shanghai, 200031, China

**Pascal Pineau, Agnès Marchio, Anne Dejean, Pierre Tiollais,** Unité de Recombinaison et Expression Génétique, INSERM U163, Institute Pasteur, Paris, France

**Hong-Yang Wang,** Shanghai Eastern Hepatobiliary Surgery Hospital, Shanghai, 200433, China

**Supported by** a grant from National High Technology “863” Program of China, No. 2001AA221021, a grant from Special Funds for Major State Basic Research “973” of China, No. 001CB510205, a grant from the National Natural Sciences Foundation of China, No. 30170524 and Chine-France PRA dans le domaine de la Biologie 2001, No. PRA B 01-05

**Correspondence to:** Professor Mu-Jun Zhao, State Key Laboratory of Molecular Biology, Institute of Biochemistry and Cell Biology, Shanghai Institutes for Biological Sciences, Chinese Academy of Sciences, 320 Yueyang Road, Shanghai, 200031, China. mjzhao@sunm.shnc.ac.cn  
**Telephone:** +86-21-64315030 Ext.5295 **Fax:** +86-21-64338357

**Received:** 2002-07-26 **Accepted:** 2002-08-23

## Abstract

**AIM:** To find the point mutations meaningful for inactivation of liver-related putative tumor suppressor gene (LPTS) gene, a human novel liver-related putative tumor suppressor gene and telomerase inhibitor in hepatocellular carcinoma.

**METHODS:** The entire coding sequence of LPTS gene was examined for mutations by single strand conformation polymorphism (SSCP) assay and PCR products direct sequencing in 56 liver cancer cell lines, 7 ovarian cancer and 7 head & neck tumor cell lines and 70 pairs of HCC tissues samples. The cDNA fragment coding for the most frequent mutant protein was subcloned into GST fusion expression vector. The product was expressed in *E.coli* and purified by glutathione-agarose column. Telomeric repeat amplification protocol (TRAP) assays were performed to study the effect of point mutation to telomerase inhibitory activity.

**RESULTS:** SSCP gels showed the abnormal shifting bands and DNA sequencing found that there were 5 different mutations and/or polymorphisms in 12 tumor cell lines located at exon2, exon5 and exon7. The main alterations were A(778)A/G and A(880)T in exon7. The change in site of 778 could not be found in HCC tissue samples, while the mutation in position 880 was seen in 7 (10 %) cases. The mutation in the site of 880 had no effect on telomerase inhibitory activity.

**CONCLUSION:** Alterations identified in this study are polymorphisms of LPTS gene. LPTS mutations occur in HCC but are infrequent and of little effect on the telomerase inhibitory function of the protein. Epigenetics, such as methylation, acetylation, may play the key role in inactivation of LPTS.

Liao C, Zhao MJ, Zhao J, Song H, Pineau P, Marchio A, Dejean A, Tiollais P, Wang HY, Li TP. Mutation analysis of novel human liver-related putative tumor suppressor gene in hepatocellular carcinoma. *World J Gastroenterol* 2003; 9(1): 89-93

<http://www.wjgnet.com/1007-9327/9/89.htm>

## INTRODUCTION

Human hepatocellular carcinoma (HCC), the predominant histological subtype of primary liver cancer is one of the most common malignancies of the liver worldwide. The development of human cancer results from the clonal expansion of genetically modified cells that acquired selective growth advantage through accumulated alterations of proto-oncogenes and tumor suppressor genes<sup>[1]</sup>. Chromosomal analysis using polymorphic DNA markers that distinguish different alleles has revealed loss of heterozygosity (LOH) of specific chromosomal regions in various types of cancers and mapping of regions with a high frequency of LOH has been critical for identifying negative regulators of tumor growth, which will be of great help in positional cloning of tumor suppressor genes<sup>[2]</sup>.

We have cloned a novel human liver-related putative tumor suppressor gene, LPTS by means of allelic-loss mapping and positional candidate cloning<sup>[3]</sup>. LPTS gene mapped to chromosome 8p23, a locus with high-frequency LOH and a hot spot of tumor suppressor in HCC<sup>[2, 4]</sup>. The expression of LPTS was ubiquitous in normal human tissues, whereas levels appeared to be significantly reduced, or sometimes undetectable in HCC cells and neoplastic tissues. The gene for LPTS is a growth-arrest gene that acts directly or indirectly to control the proliferation of cells, and might be a tumor suppressor gene<sup>[3]</sup>. LPTS gene has 7 exons totally and encodes two transcripts, one is LPTS-S, lacking exon6 and encoding a 174-a.a. protein; the other is LPTS-L, encoding a 328-a.a. protein with entire 7 exons. The LPTS-L is highly homologous to PinX1 identified recently<sup>[5]</sup>. LPTS-L and PinX1 have quite different 3' -untranslated region and encode a same protein, referred to LPTS-L/PinX1. LPTS-L/PinX1 has strong telomerase inhibitory activity both *in vivo* and *in vitro*.

In this study, we collected 56 HCC cell lines, 7 ovarian cancer cell lines and 7 head & neck tumor cell lines to perform single strand conformation polymorphism (SSCP) assay<sup>[6,7]</sup> to screen the point mutations in LPTS gene. Then we detected those mutations identified from SSCP assay in 70 pairs of HCC tissues to confirm the existence of real mutations in HCC tissue samples. Finally, telomerase activity assay was done to study the effect of the point mutation on the function of protein *in vitro*.

## MATERIALS AND METHODS

### Tumor cells and HCC tissue samples

The cell lines, including 56 liver cancer cell lines, 7 ovarian cell lines and 7 head and neck tumor cell lines, were from mainland of P.R. China, Japan, France, Taiwan, Hongkong and America separately. The cell lines were cultured in Dulbecco's Modified Eagle Medium (DMEM, Life Technologies Inc., Grand Island, NY) or in RPMI medium 1 640 (Life Technologies Inc.),

supplemented with 10 % fetal calf serum (FCS, Life Technologies Inc.) with or without non-essential amino acid (Life Technologies Inc.) according to suppliers. All the samples of primary HCC (Ks), adjacent samples of nontumorous tissues (Ls), were obtained from Shanghai Eastern Hepatobiliary Surgery Hospital (Shanghai, P.R. China), with the agreement of each patient. The serial numbers were those recorded by the hospital. All tissues were placed in liquid nitrogen immediately after surgical resection.

### Point mutation assay

According to the genome sequence of LPTS gene, we synthesized 11 pairs of primers covering 7 exons of the gene, with length of each PCR product around 170 to 250 bp (Table 1). Genomic DNA was separated as described<sup>[8]</sup>. PCR was performed in a 25-μL reaction mixture that contained 2 μL Genomic DNA (around 50 ng) from each cell line as template, 2 μL primers mix (20 μM each), 0.4 μL dNTP mix (12.5 mM each), 4.75 μL H<sub>2</sub>O, 0.25 μL Taq DNA polymerase (Life Technologies Inc.), and 15.6 μL premix (16 mM TrisHCl pH8.4, 80 mM KCl, 2.4mM MgCl<sub>2</sub> and 0.16 % Tween-20). PCR reaction conditions were described in Table 1. In Table 1, SD referred to the step-down PCR, the annealing temperature was declined 3 °C every 3 cycles for 94 °C 45 sec, annealing temperature 1 min and 72 °C 1 min from 68 °C until the indicated temperature and then for another 25 cycles of standard PCR reaction. The products of PCR were separated by electrophoresis on 2 % agarose gel to check the specificity of each PCR reaction. The PCR products were sequenced directly or performed SSCP assay as described below.

**Table 1** Primer sequences for the coding region of the LPTS gene

Exon	Nucleotide sequences	PCR conditions	Product size (bp)
1	Forward: 5' -CGTGCTCGAGGAGCGAGTCG-3' Reverse: 5' -ACCCGGCATCTTCACCAACG-3'	52 °C SD	241
2	Forward: 5' -TCCATTGCTGATGATAATGC-3' Reverse: 5' -CTCCAGTCTCCTAAGAAGG-3'	50 °C SD	230
3	Forward: 5' -TGAGAGGAATGTTCTAACTC-3' Reverse: 5' -AGCCAAYYAYCAAAGACAC-3'	50 °C SD	178
4	Forward: 5' -AACTACAGGCTTACCTCTCG-3' Reverse: 5' -AACATATTTGCATTGAGAAC-3'	55 °C SD	196
5	Forward: 5' -CAAGACTATCCACTGTTAGG-3' Reverse: 5' -GGACAAACACGTAGATTTCATAAC-3'	52°C Standard	220
6	Forward: 5' -GCTGCATAGTTCATGTCTGC-3' Reverse: 5' -CACAGGTGAAAATCAGACAG-3'	50 °C SD	194
7.1	Forward: 5' -CTGCCCTTTAACTCTTCTGC-3' Reverse: 5' -GGCTGGAGGTAACCTTCCAC-3'	50 °C SD	247
7.2	Forward: 5' -GGCCACAGGTAAAGATGTGG-3' Reverse: 5' -CAGGCGGCTGCACATGGTCC-3'	55 °C Standard	200
7.3	Forward: 5' -GCCTCTGCTCAGGATGCAGG-3' Reverse: 5' -GCCCCGGCTGGGAAGGATTC-3'	50 °C SD	191

SD: step-down PCR

For SSCP assay<sup>[9,10]</sup>, 3 μL PCR product, added with 4 μL denaturing buffer (95 % formamide, 10 mM NaOH, 0.25 % bromophenol blue and 0.25 % xylene cyanol), were kept at 95 °C for 5 min and then loaded 5 μL denatured mixture sample

directly into each of sample wells of GeneGel Excel, 0.5 mm thin, pre-cast polyacrylamide ready-to-run gel for DNA electrophoresis (Amersham Pharmacia Biotech Inc.). Electrophoresis was done on GenePhor DNA separation system (Amersham Pharmacia Biotech Inc.) at 150 Voltage for 10 min and then 600 Voltage for 2 hours at 4 °C. At the end of running, silver stained the gel with DNA silver staining kit (Amersham Pharmacia Biotech Inc.) in accordance with the manufacturer's protocol.

### Expression and purification of GST fusion protein

The coding sequence of protein fragment for expression was cloned in frame into the *E.coli* GST fusion expression vector pGEX-4T2 (Amersham Pharmacia Biotech Inc.), then transfected the construct into *E.coli* BL21(DE3). The protein was expressed with IPTG induction for 3 hours and purified by glutathione-agarose (Sigma) column.

### TRAP telomerase activity assay

HCC cells SMMC-7721 were lysed in lysis buffer (10 mM TrisHCl pH7.5, 1 mM MgCl<sub>2</sub>, 1 mM EGTA, 0.1 mM PMSF, 5 mM 2-mercaptoethanol, 0.5 % CHAPS, 10 % glycerol) on ice for 30 min and then centrifuged at high speed for 30 min, the suspension containing telomerase was used for TRAP assay. The GST-fused protein was incubated with cell extract for 10 min at 4 °C before subjecting to telomerase extension according reference<sup>[11]</sup>. Telomerase products were separated on 10 % polyacrylamide gels, which were stained with silver nitrate.

## RESULTS

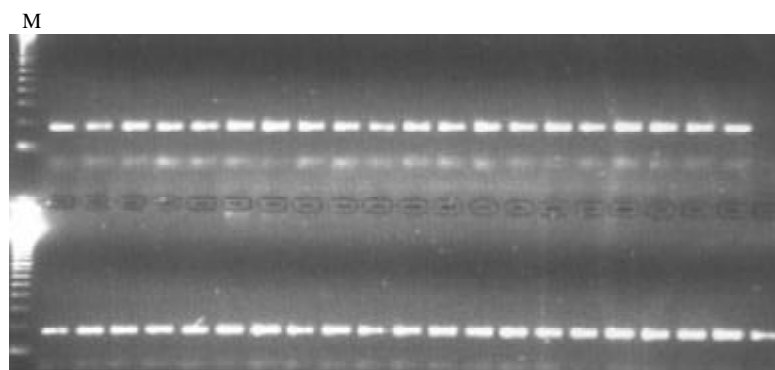
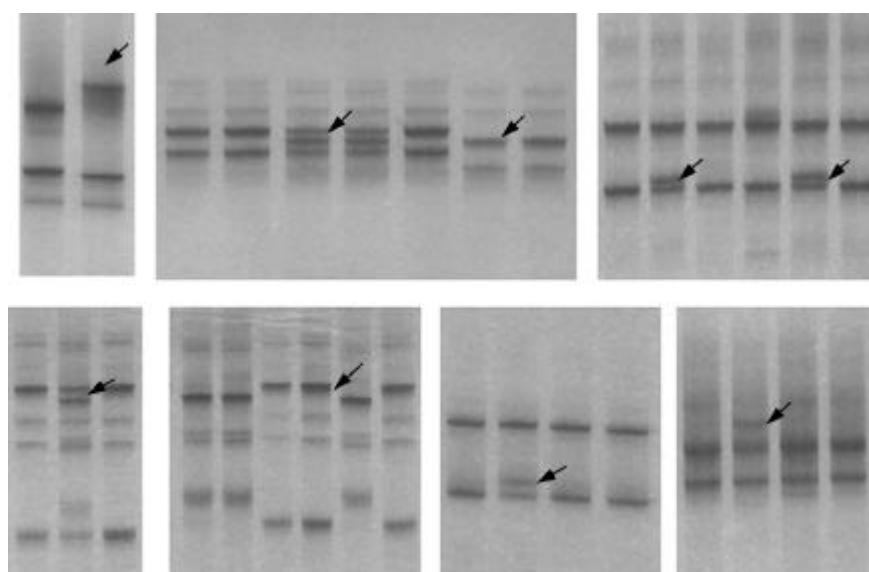
### 5 alterations were found in 12 tumor cell lines

We mainly screened the point mutations of LPTS gene in 56 liver cancer cell lines by means of SSCP. For chromosome 8p23 is a hot spot containing tumor suppressor in many types of tumors except for liver, including ovarian cancer and head and neck tumors, we checked LPTS gene in another 7 ovarian cancer cell lines and 7 head and neck tumor cell lines altogether. Among the cell lines analyzed, about half of those are homozygous in region between D8S550 and D8S518 on chromosome 8p23, covering the LPTS gene, by fine mapping of allele deletion (loss of heterozygosity) in Chromosome 8p.

After PCR amplification the fragment, PCR products were checked for specificity on 2 % agarose gel. Only the good specific amplification could be used in the latter assay (Figure 1). The specific PCR products were separated in PAGE gel and stained with silver nitrate. The abnormal band patterns, such as loss or gain of extra bands, different migration of bands, comparing to the negative and positive controls which had been sequenced in advance, suggested this sample might have point mutations (Figure 2). The products with abnormal migration pattern were sequenced and determined. The point mutations as shown in Table 2, were mainly located in exon 2, exon 5 and exon 7. In exon 2, there were two types of alterations, C (161) changed to T, predicted effect was the change from alanine to valine in cholangiocarcinoma cell CCLP1, and the other was C (183) to T, which was silent at the protein level and might therefore be considered as a polymorphism. In exon 5, only one point mutation of A (497) to G in HCC cell line PLCPRF5 was found, causing the encoded amino acid changing from tyrosine to cysteine. Two frequent mutations clustering at positions 778 and 880 were found in exon 7. The A778G changed the threonine residue to an alanine. All cell lines harboring this polymorphism were heterozygous at position 778 with the second allele retaining the wild type. The second mutation cluster A880T caused a change from serine to cysteine.

**Table 2** The alterations of LPTS-S and LPTS-L in tumor cell lines

Cell line	Cell type	Mutation	Exon	Codon	Predicted effect
CCLP1	Cholangiocarcinoma	C161T	Exon 2	gct→gtt	Ala→Val
HepG2	HCC	A701A, G(LPTS-S)	Exon 7	Outside ORF	/
		A778A, G(LPTS-L)		aca→gca	Thr→Ala
HepT1	HCC	C183T	Exon 2	gcc→gct	Ala
MEK	HCC	A701A, G(LPTS-S)	Exon 7	Outside ORF	/
		A778A, G(LPTS-L)		aca→gca	Thr→Ala
SNU182	HCC	A701A, G(LPTS-S)	Exon 7	Outside ORF	/
		A778A, G(LPTS-L)		aca→gca	Thr→Ala
Li7A	HCC	A803T(LPTS-S)	Exon 7	Outside ORF	/
		A880T(LPTS-L)		agc→tgc	Ser→Cys
Li21	HCC	C183T	Exon 2	gcc→gct	Ala
		A803T(LPTS-S)	Exon 7	Outside ORF	/
		A880T(LPTS-L)		agc→tgc	Ser→Cys
MZCHA1	HCC	A803T(LPTS-S)	Exon 7	Outside ORF	/
		A880T(LPTS-L)		agc→tgc	Ser→Cys
PCI-SG231	HCC	G111C	Exon 1	Before ATG	/
		A803T(LPTS-S)	Exon 7	Outside ORF	/
		A880T(LPTS-L)		agc→tgc	Ser→Cys
PLCPRF5	HCC	A497G	Exon5	tat→tgt	Tyr→Cys
IGR-OV1	Ovarian tumor	A701A, G(LPTS-S)	Exon 7	Outside ORF	/
		A778A, G(LPTS-L)		aca→gca	Thr→Ala
SW579	Head and neck tumor	C183C, T	Exon 2	gcc→gct	Ala

**Figure 1** Agarose gel analysis of PCR products for SSCP assay. Agarose gel separation was used to determine the specificity of PCR reaction. PCR products with only one specific band of right size in the gel can be used to SSCP assay. M: 100 bp ladder.**Figure 2** Some different electrophoresis patterns in SSCP assay of each exon. Arrows showed the differences, including extra bands, differential bands shifting, and so on.

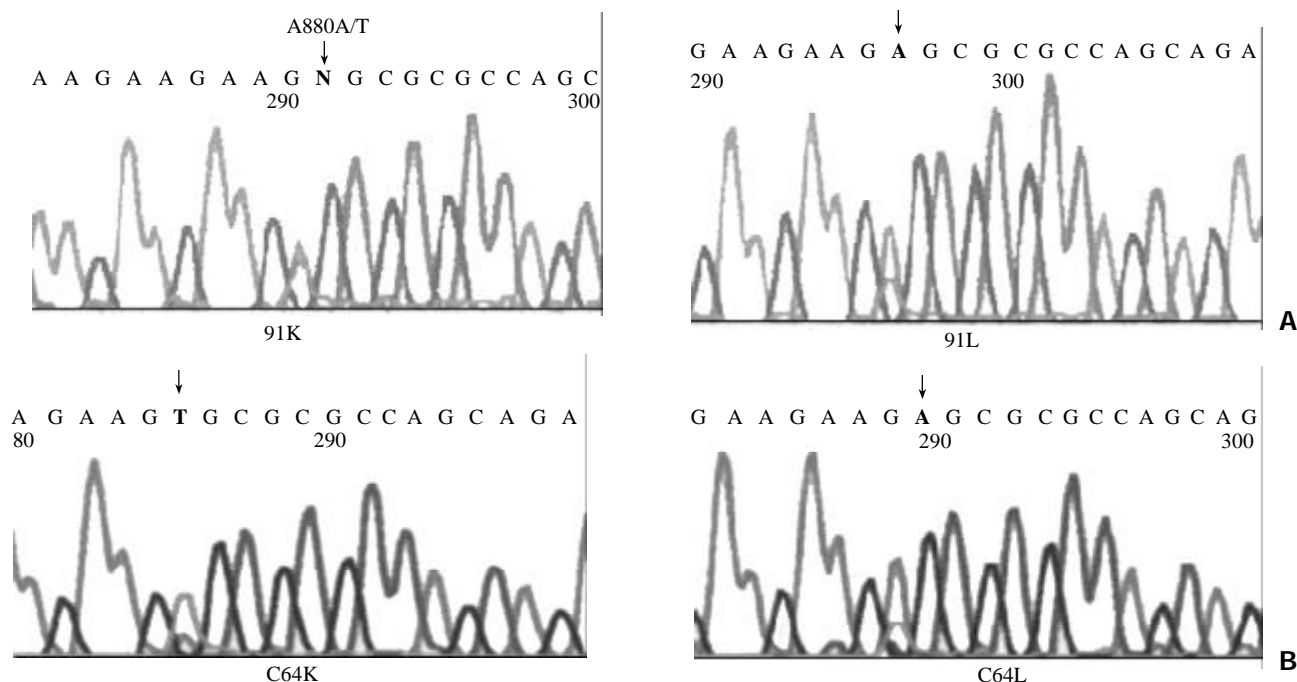


**Figure 3** The sequences of mutation site of 880 in two pairs of HCC tissues. (A) HCC sample 91K, 91L; (B) HCC sample C64K, C64L. 'K' represents HCC tissue and 'L' represents adjacent nontumorous liver tissue. Arrow indicated the site of 880.

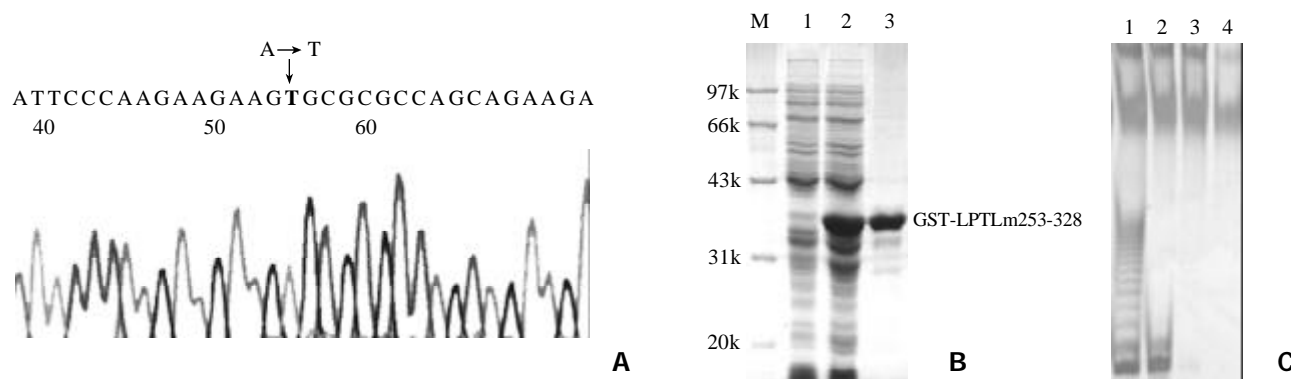


**Figure 4** The point mutation in position 880 has no effect on the telomerase inhibitory activity of LPTS-L. A. The 'A' in position 880 of LPTS-L transcript was mutated to 'T'; B. The expression and purification of GST-LPTLm253-328, 1, without IPTG induction; 2, IPTG induction; 3, purified protein. C. The telomerase inhibiting activity assay in vitro of mutant protein LPTLm253-328 in SMMC-7721 cell extract. 1-4 were 0.1, 0.5, 1, 5 µg protein added in cell extract for 10 min, respectively.

#### Position (880) A to T was identified in 7 patients (10 %)

From the assay in HCC and other tumor cell lines, we can see that the major point mutations are in exon 7. The point mutation in 778 and 880 nt caused threonine and serine which being the candidate sites for phosphorylation changed to alanine and cysteine. The mutation in 880 nt turned to the cysteine, which might form disulfide bond and affect the conformation of the protein. It would be very important to confirm the existence of these two mutations in HCC tissues. Next, we collected 70 pairs of HCC samples, amplified the exon 7 and sequenced directly. In all 70 pairs samples, we could not find the point mutation in position 778, whereas the mutation in site of 880 was detected in 7 HCC samples and the mutation frequency was 10 %. The mutation in the site of 880 was also A/T heterozygous, which was shown double pits in sequence reaction (Figure 3).

#### The significance of A(880) mutation

LPTS-L/PinX1 possessing strong telomerase inhibitory activity had been determined by *in vivo* and *in vitro* experiments. To

study the effect of telomerase inhibitory function of A(880) mutant, we designed PCR primer with point mutation at the site of 880, 5'-GAA TTC CCA AGA AGA AGT GCG CGC CA-3', the mutated site of 'T' was indicated in italic type. We subcloned the mutated cDNA fragment (from amino acid subunit 253 to 328) into GST fusion expression vector pGEX-4T2 and purified the GST-fused mutant protein. After TRAP telomerase activity assay, we found that the mutant protein still had strong telomerase inhibitory activity in HCC cell line SMMC-7721 cell extract (Figure 4). From these results, we concluded that the point mutation in position 880 of LPTS gene had no effect on telomerase inhibition.

#### DISCUSSION

Somatic inactivation of a tumor suppressor gene is usually achieved by intragenic mutation in one allele of the gene, with subsequent by loss of a chromosome region that spans the second allele, showed loss of heterozygosity (LOH). Among the various deleted chromosome regions identified by several laboratories, chromosome 8p has a particularly high frequency



of LOH<sup>[2, 12-14]</sup> and a growing body of evidence suggests that chromosome 8p is active in many types of carcinogenesis and metastasis including liver, breast, colorectal, prostate, lung, head and neck, pancreatic and urinary bladder carcinomas<sup>[14-18]</sup>. However, there have been no reports of the identification of a tumor suppressor gene on 8p.

LPTS gene is a possible candidate tumor suppressor localized in 8p23 region, which is a negative regulator in cell proliferation<sup>[3]</sup>. According to Kundson's tumor suppressor "two-hit" model<sup>[19]</sup>, one tumor suppressor needs to be hit twice to be inactivated. To clarify the relationship between LPTS gene and HCC, we searched for point mutations in all seven exons of LPTS gene in HCC tissue samples and HCC cell lines. In 70 tumor cell lines and 70 pairs of HCC tissues analyzed, there were mainly two point mutations in exon 7, position 778 and 880. The mutation at the site of 778 was found only in several HCC cell lines, but not in clinical HCC tissues. The mutation at the site of 880 has the mutation frequency of 10 % in HCC tissues, but the mutation has no effect of the telomerase inhibitory activity of LPTS-L/PinX1 protein, suggesting that this position is a polymorphism site of LPTS gene.

During our preparation of this manuscript, another research group in Korea reported their research work of genetic analysis of LPTS gene in HCC sample from South Korea. They also found that LPTS gene indeed had very high LOH frequency (34.5 %) in HCC patients, but also no point mutations could be found in HCC patients from South Korea, same with our results in Chinese HCC patients<sup>[20]</sup>. Taken the above data together, LPTS gene has high frequency of LOH in HCC, but has no point mutation in the last allele, suggesting that inactivation of LPTS gene may not be caused by point mutation. However, we cannot rule out completely the epigenetic inactivation, such as methylation, acetylation etc<sup>[21-23]</sup>. Indeed, we found that there were two CpG islands, about 1.2 kb in length, in the upstream of LPTS gene transcription initiating site. Study of the methylation status in the regulation of LPTS gene is being performed now.

## REFERENCES

- 1 **Weinberg RA.** Tumor suppressor genes. *Science* 1991; **254**: 1138-1146
- 2 **Nagai H,** Pineau P, Tiollais P, Buendia MA, Dejean A. Comprehensive allelotype of human hepatocellular carcinoma. *Oncogene* 1997; **14**: 2927-2933
- 3 **Liao C,** Zhao M, Song H, Uchida K, Yokoyama KK, Li T. Identification of the gene for a novel liver-related putative tumor suppressor at a high-frequency loss of heterozygosity region of chromosome 8p23 in human hepatocellular carcinoma. *Hepatology* 2000; **32**: 721-727
- 4 **Pineau P,** Nagai H, Prigent S, Wei Y, Gyapay G, Weissenbach J, Tiollais P, Buendia MA, Dejean A. Identification of three distinct regions of allelic deletions on the short arm of chromosome 8 in hepatocellular carcinoma. *Oncogene* 1999; **18**: 3127-3134
- 5 **Zhou XZ,** Lu KP. The Pin2/TRF1-interacting protein PinX1 is a potent telomerase inhibitor. *Cell* 2001; **107**: 347-359
- 6 **He XS,** Su Q, Chen ZC, He XT, Long ZF, Ling H, Zhang LR. Expression, deletion and mutation of p16 gene in human gastric cancer. *World J Gastroenterol* 2001; **7**: 515-521
- 7 **Peng XM,** Yao CL, Chen XJ, Peng WW, Gao ZL. Codon 249 mutations of p53 gene in non-neoplastic liver tissues. *World J Gastroenterol* 1999; **5**: 324-326
- 8 **Sambrook J,** Fritsch E F, Maniatis T ed, *Molecular cloning*. Cold spring harbor laboratory press, 1989: 463-467
- 9 **Bailey A.** Single-stranded conformational polymorphisms, PCR strategies. *Academic Press, Inc* 1995: 121-129
- 10 **Yap EPH,** McGee JO. Non-isotopic single-strand conformation polymorphism (SSCP) analysis of PCR products, PCR Technology: Current Innovations, Chapter 20. *CRC Press Inc* 1994: 165-177
- 11 **Kim NW,** Piatyszek MA, Prowse KR, Harley CB, West MD, Ho PL, Coviello GM, Wright WE, Weinrich SL, Shay JW. Specific association of human telomerase activity with immortal cells and cancer. *Science* 1994; **266**: 2011-2015
- 12 **Marchio A,** Meddeb M, Pineau P, Danglot G, Tiollais P, Bernheim A, Dejean A. Recurrent chromosomal abnormalities in hepatocellular carcinoma detected by comparative genomic hybridization. *Genes Chromosomes & Cancer* 1997; **18**: 59-65
- 13 **Fujimori M,** Tokino T, Hino O, Kitagawa T, Imamura T, Okamoto E, Mitsunobu M, Ishikawa T, Nakagama H, Harada H. Allelotype study of primary hepatocellular carcinoma. *Cancer Res* 1991; **51**: 89-93
- 14 **Emi M,** Fujiwara Y, Nakajima T, Tsuchiya E, Tsuda H, Hirohashi S, Maeda Y, Tsuruta K, Miyaki M, Nakamura Y. Frequent loss of heterozygosity for loci on chromosome 8p in hepatocellular carcinoma, colorectal cancer, and lung cancer. *Cancer Res* 1992; **52**: 5368-5372
- 15 **Bieche I,** Lidereau R. Genetic alterations in breast cancer. *Genes, Chromosomes Cancer* 1995; **14**: 227-251
- 16 **Macoka JA,** Trybus TM, Benson PD, Sakr WA, Grignon DJ, Wojno KD, Pietruk T, Powell JJ. Evidence for three tumor suppressor gene loci on chromosome 8p in human prostate cancer. *Cancer Res* 1995; **55**: 5390-5395
- 17 **Wistuba II,** Behrens C, Virmani AK, Milchgrub S, Syed S, Lam S, Mackay B, Minna JD, Gazdar AF. Allelic losses at chromosome 8p21-23 are early and frequent events in the pathogenesis of lung cancer. *Cancer Res* 1999; **59**: 1973-1979
- 18 **el-Naggar AK,** Hurr K, Batsakis JG, Luna MA, Goepfert H, Huff V. Sequential loss of heterozygosity at microsatellite motifs in preinvasive and invasive head and neck squamous carcinoma. *Cancer Res* 1995; **55**: 2656-2659
- 19 **Knudson AG.** Mutation and cancer: statistical study of retinoblastoma. *Proc Natl Acad Sci USA* 1971; **68**: 820-823
- 20 **Park WS,** Lee JH, Park JY, Jeong SW, Shin MS, Kim HS, Lee SK, Lee SN, Lee SH, Park CG, Yoo NJ, Lee JY. Genetic analysis of the liver putative tumor suppressor (LPTS) gene in hepatocellular carcinomas. *Cancer Letters* 2002; **178**: 199-207
- 21 **Esteller M,** Herman JG. Cancer as an epigenetic disease: DNA methylation and chromatin alterations in human tumours. *J Pathol* 2002; **196**: 1-7
- 22 **Jones PA,** Takai D. The role of DNA methylation in mammalian epigenetics. *Science* 2001; **293**: 1068-1070
- 23 **Ponder BA.** Cancer genetics. *Nature* 2001; **411**: 336-341

Edited by WuXN

• ESOPHAGEAL CANCER •

# Gene expression profiles at different stages of human esophageal squamous cell carcinoma

Jin Zhou, Li-Qun Zhao, Mo-Miao Xiong, Xiu-Qin Wang, Guan-Rui Yang, Zong-Liang Qiu, Min Wu, Zhi-Hua Liu

**Jin Zhou, Xiu-Qin Wang, Min Wu, Zhi-Hua Liu**, National Laboratory of Molecular Oncology, Cancer Institute, Peking Union Medical College and Chinese Academy of Medical Sciences, Beijing 100021, China

**Li-Qun Zhao, Guan-Rui Yang, Zong-Liang Qiu**, Medical Science Institute of Henan Province, Zhengzhou 450052, China

**Mo-Miao Xiong**, Health Genetics Center, School of Public Health, The University of Texas Houston, Houston, Texas 77225, USA

**Supported by** China Key Program on Basic Research, No. G1998051021; the Chinese Hi-tech R&D program, No.2001AA231310 and National Natural Science Foundation of China, No.30170519

**Correspondence to:** Zhi-Hua Liu, Ph.D. Professor, National Laboratory of Molecular Oncology, Cancer Institute, Peking Union Medical College and Chinese Academy of Medical Sciences, Beijing 100021, China. liuzh@pubem.cicams.ac.cn

**Telephone:** +86-10-67723789 **Fax:** +86-10-67715058

**Received:** 2002-05-06 **Accepted:** 2002-07-26

## Abstract

**AIM:** To characterize the gene expression profiles in different stages of carcinogenesis of esophageal epithelium.

**METHODS:** A microarray containing 588 cancer related genes was employed to study the gene expression profile at different stages of esophageal squamous cell carcinoma including basal cell hyperplasia, high-grade dysplasia, carcinoma *in situ*, early and late cancer. Principle component analysis was performed to search the genes which were important in carcinogenesis.

**RESULTS:** More than 100 genes were up or down regulated in esophageal epithelial cells during the stages of basal cell hyperplasia, high-grade dysplasia, carcinoma *in situ*, early and late cancer. Principle component analysis identified a set of genes which may play important roles in the tumor development. Comparison of expression profiles between these stages showed that some genes, such as P160ROCK, JNK2, were activated and may play an important role in early stages of carcinogenesis.

**CONCLUSION:** These findings provided an esophageal cancer-specific and stage-specific expression profiles, showing that complex alterations of gene expression underlie the development of malignant phenotype of esophageal cancer cells.

Zhou J, Zhao LQ, Xiong MM, Wang XQ, Yang GR, Qiu ZL, Wu M, Liu ZH. Gene expression profiles at different stages of human esophageal squamous cell carcinoma. *World J Gastroenterol* 2003; 9(1): 9-15

<http://www.wjgnet.com/1007-9327/9/9.htm>

## INTRODUCTION

Cancer development is a complex multi-step process, involving various genetic and epigenetic changes. Progress of phenotypes from normal to advanced carcinoma is controlled by a transcriptional hierarchy that coordinates the action of hundreds

of genes. Conventional approaches investigating one or several candidate genes at a time can not show the whole story of carcinogenesis. The generation of vast amounts of DNA sequence information, coupled with advances in technologies developed for the experimental use of such information, allows the description of biological processes from a view of global genetic perspective. One such technology, DNA microarray, permits simultaneous monitoring of thousands of genes<sup>[1,2]</sup>. Fuller *et al*<sup>[3]</sup> and Sgroi *et al*<sup>[4]</sup> have used this new technique in analyzing gene expression profiles in human glioblastoma, human breast cancer and matched normal tissues. However, little is known about the exact expression changes in each stage of tumorigenesis, which will help us identify the exact series of events that leads to the initiation and progression of cancer development.

In this study, esophageal cancer was chosen as a model to analyze the changes of expression profiles in different stages of carcinogenesis. By using microarray membranes, expression of 588 known cellular genes were profiled in normal esophageal tissues, basal cell hyperplasia, high-grade dysplasia, carcinoma *in situ*, early and advanced cancer. Our results revealed some genes differently expressed in a certain stage, and some kept up or down regulated in all stages toward cancer.

## MATERIALS AND METHODS

### *Biopsy specimens and primary esophageal cancer tissues*

Biopsy specimens were collected from the individuals who were more than 35 years old, underwent endoscopy examination in a screening for early cases of esophageal cancer in Henan province in North China, where has the highest incidence rate of this fatal cancer in the world. Agreements have been obtained from all individuals informed consents issued. In each case, 4 pieces of tissues with the size of 0.01 cm<sup>3</sup> were separately removed from the mucosa, two of them were instantly frozen and kept in liquid nitrogen until use, and the other two underwent pathologic diagnosis according to the criteria of Riddell and associates. Specimens of normal esophagus, basal cell hyperplasia, high-grade dysplasia, carcinoma *in situ*, and early carcinoma were obtained in this study. Every tissue specimen was mostly composed of normal or abnormal epithelial cells.

Cancer and adjacent almost normal tissues with size of about 0.5 cm<sup>3</sup> were collected from patients with primary esophageal cancer in Cancer Hospital of the Chinese Academy of Medical Sciences after informed consent was obtained. Fresh samples were dissected manually to remove mixed connective tissue and stored in liquid nitrogen. Pathological diagnosis showed that the cancers were from squamous cell at medium to high grade differentiation, the matched almost normal mucosa did not show any invasion of cancer cells.

### *Human cancer cDNA expression array*

Human cancer cDNA expression array membrane was purchased from Clontech Laboratories Inc. (Palo Alto, CA), each membrane contains of 588 well characterized genes along with 9 housekeeping genes as internal control. During this study, membranes of the same lot were used to ensure the reproducibility.

### RNA extraction

The biopsy specimens of the same histological diagnosis were pooled and the total RNA of different kinds of samples was extracted with Micro RNA isolation kit (Stratagene, La Jolla, CA). Before labeling, 5 µg total RNA of each type was treated with 2 µl DNase I (10 unit/ml, Boehringer Mannheim, Mannheim, Germany), 1 µl RNasin (40 units/µl, Promega) at 37 °C for 15 min to remove contaminated DNA.

### Hybridization and exposure

Following the recommendation of the manufacturer, <sup>32</sup>P-labelled cDNA probes were generated by reverse transcription from 5 µg of RNA sample in the presence of [ $\alpha$ -<sup>32</sup>P]dATP (3 000 ci/mmol, Du Pont). Each cDNA probe was then hybridized to a membrane at 65 °C overnight. The membranes were washed twice in 2×SSC, 0.5 % SDS at 65 °C for 30 minutes, then twice in 0.2×SSC, 0.5 % SDS at 65 °C for 30 minutes, then exposed to X-ray film at -80 °C for 2-3 days.

### Hybridization pattern analysis

Images of individual autoradiography for each stage of carcinogenesis were digitalized by Fluor-S<sup>TM</sup> MultiImager System (Bio-Rad Laboratories, Inc.) The hybridization pattern of arrays was analyzed and compared using AtlasImage<sup>TM</sup> 1.01 software (Clontech). To normalize the relative gene expression, beta-actin and alpha tubulin were used as internal references whose expression level was found stable in different developmental stages in our study. These genes were preferred also because they are conventionally used as internal references for measuring gene expression levels in Northern blot, RNase protection and semi-quantitative RT-PCR.

### Confirmation by semi-quantitative RT-PCR analysis

To validate the expression pattern identified on the expression arrays, 5 genes were randomly picked and semi-quantitative RT-PCR was performed to confirm their differential expression with cDNA template from esophageal cancer and adjacent almost normal tissues. First strand cDNA was synthesized from 5 µg RNase-free DNase treated total RNA using the Superscript<sup>TM</sup> Preamplification system for First Strand cDNA Synthesis (Life Technologies, Inc) as described by the manufacturer. An aliquot of 1/20 of the reverse transcribed product was used as template in the following PCR amplification. Reactions undergone in 25 µl total volume containing 1×PCR buffer, 1.5 mmol/L MgCl<sub>2</sub>, 200 µmol/L dNTPs, 1.5 u Taq Polymerase (Life Technologies, Inc) and 40 µmol/L gene specific primers under the conditions: 94 °C 5 min, followed by 25-28 cycles each of 94 °C 20 sec, 58 °C 30 sec, 72 °C 1 min. Amplification of beta actin with same aliquot of cDNA template was used as internal reference to determine the relative gene expression.

Gene specific primers: Rho8 5' -GGACACTTCGGGTTCTCCTTAC-3', 5' -TGTGGCTCTCTGTGATTTGTTTC-3'; IL-1 beta 5' -GCAGAAAGGGAACAGAAAGGTT-3', 5' -AAGGAGGCACACCAGTCCAAAT-3'; Interleukin 1 receptor antagonist 5' -ACTCTCCTCCTCTTCTGTTC-3', 5' -GCTTGTCTGCTTTCTGTTCTC-3'; Cytokeratin 4 5' -GGGAACAAAGCATCTCCAT-3', 5' -ATCTCAGGGTCAATCTCCAC-3'; Wnt-13 5' -GCCAAAGTTAGATGGGACAAAG-3', 5' -TTGAACAGGCAGCAAGTAAGC-3'.

### Principle component analysis

A principle component analysis was used to explain the variance-covariance structure of the gene expressions in 6 stages of tumor development. The purpose of principle component analysis is data reduction, and interpretation through a few linear combinations of the original variables (gene expressions)<sup>[5]</sup>.

Principle component analysis starts with  $k$  variables which

represent the expression profiles of  $k$  genes. The  $t$  th element of the  $j$  variable corresponds to the expression level of the  $j$  th gene in the  $t$  stage of the tumor development. Principle component analysis intends to replace the  $k$  variables by  $p$  principle components where  $p$  is smaller than  $k$ , while minimizing loss of information. The principle component is a linear combination of the variables  $x_1, x_2, \dots, x_k$  and can be constructed by the eigenvector  $e_i$  ( $i=1,2,\dots,k$ ) of the covariance matrix  $V$  of the variables  $x_1, x_2, \dots, x_k$ , where the eigenvector  $e_i$  of the matrix  $V$  is defined as any vector satisfying the equation  $V e_i = \lambda_i e_i$ , and  $\lambda_i$  is called the corresponding eigenvalue associated with the eigenvector  $e_i$ . The elements of the eigenvector measure the importance (loading score) of the genes to the principle component and the eigenvalue measures the variance of the corresponding principle component explaining variations of expressions of a linear combination of genes represented by the principle component. The first principle component with the largest eigenvalue has the largest variance, the second principle component with the second largest eigenvalue has the second largest variance and so on. It can be shown that  $\lambda_i$  is equal to the variance of the  $i$  th principle component.

Although  $k$  variables are required to reproduce the total system variability, often much of this variability can be accounted for by a small number of principle components with larger eigenvalues (variances) which explain large proportions of variations of gene expressions underlying some biological processes. Principle component analysis was used to identify a set of genes which may contribute to the tumor development.

## RESULTS

### Expression pattern of 588 known genes in progression of carcinoma

High quality total RNA was isolated from biopsy specimens. The RNA was reverse-transcribed into <sup>32</sup>P-labeled cDNA probe and hybridized to Atlas<sup>TM</sup> Human Cancer cDNA expression array to profile the expression of 588 known genes. The hybridization patterns were imaged by the Fluor-S<sup>TM</sup> MultiImage System and analyzed by AtlasImage<sup>TM</sup> 1.01 software. Genes with adjusted intensity difference >20 000 or ratio>2 between two stages were supposed to be regulated differentially. Figure 1 showed the cDNA array images along with color charts indicating up-regulated genes with red, down-regulated ones with blue, and non-changed with green.

There were more than 100 genes up or down regulated substantially in every abnormal stage when compared to human normal mucosa. In stage of basal cell hyperplasia II, there were 122 genes up regulated and 17 down regulated; in stage of high grade dysplasia, there were 134 genes up regulated and 33 down regulated; in stage of squamous cell carcinoma in situ, there were 114 genes up regulated and 10 down regulated; in stage of early cancer, there were 169 genes up regulated and 13 down regulated; In stage of late cancer, there were 77 genes up regulated and 60 down regulated. As shown in the color charts of Figure 1 the types as well as expression level of genes are different among each stage.

### Validation of Array Data with RT-PCR

To further investigate the reliability of our array data, we randomly picked 5 differentially expressed genes and measured the expression of the genes in the paired cancer and adjacent almost normal tissues using RT-PCR. Figure 2 showed that the different expression pattern of each of the five genes as determined by RT-PCR were similar to those observed with cDNA array in more than half of 12 pairs of matched tissues (squamous esophageal cancer and matched adjacent almost normal tissue), confirming the reliability of our array data. Our observed correlation between the cDNA array and RT-PCR are consistent with that observed by others<sup>[6,7]</sup>.

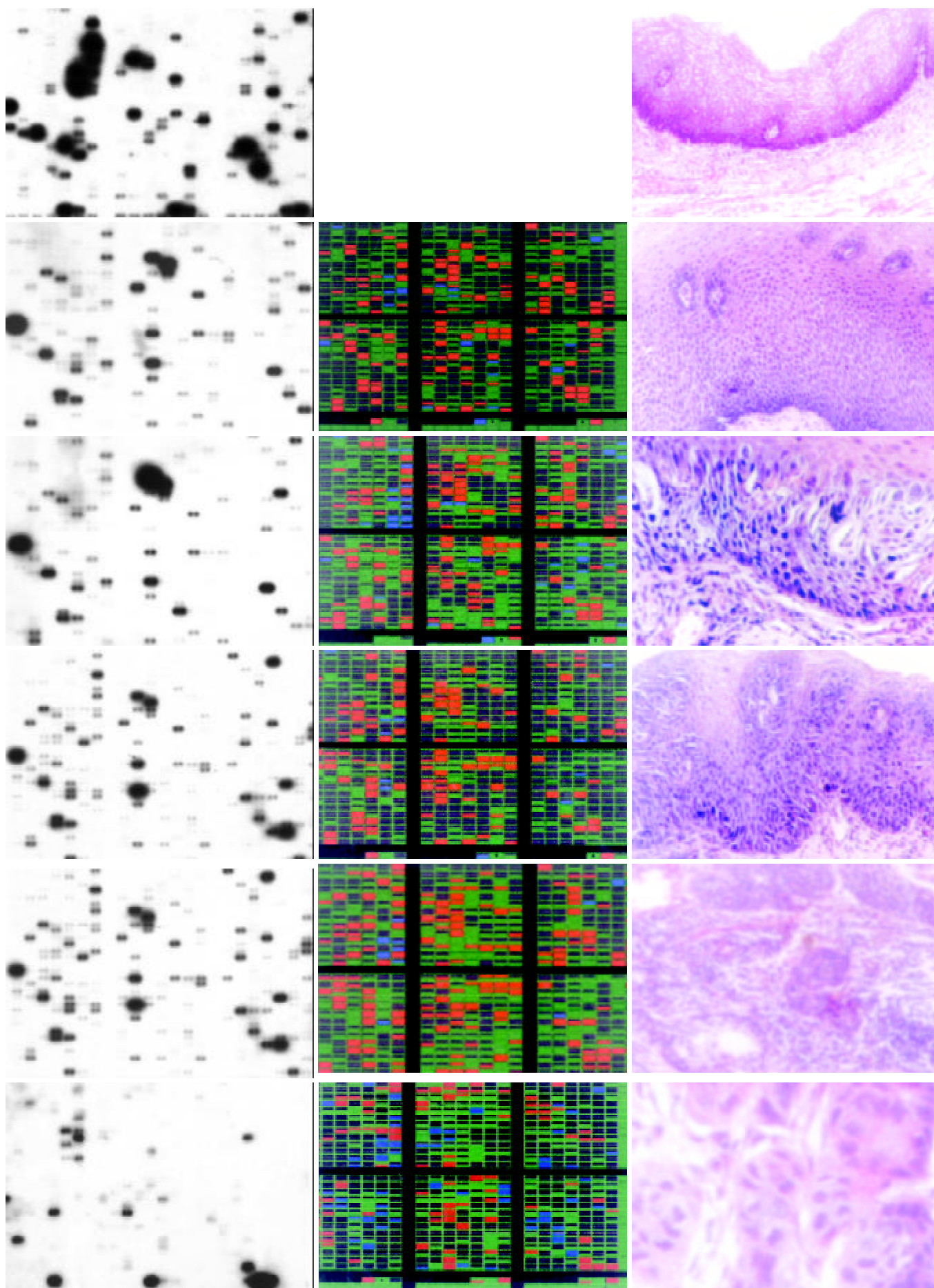


**Figure 1** Expression patterns of genes in esophageal tissue of normal, basal cell hyperplasia, high-grade dysplasia, carcinoma in situ, early and advanced cancer. Total RNAs were isolated from these tissues, reverse-transcribed into  $^{32}\text{P}$ -labeled cDNAs and hybridized to Atlas<sup>TM</sup> Human Cancer cDNA expression arrays. A complete list of names and location of the arrayed gene can be

found in the instruction manual and website from Clontech. Data was analyzed by AtlasImage™ 1.01 software. A,B,C,D,E,F showed hybridization result of normal cells, basal cell hyperplasia, high-grade dysplasia, carcinoma in situ, early and advanced cancer; G, H, I, J, K showed the color charts indicating up-regulated genes with red, down-regulated genes with blue, and non-changed genes with green in the later 5 stages when compared to normal tissue; L, M, N, O, P showed the pathological image of normal, basal cell hyperplasia, high-grade dysplasia, carcinoma in situ, early and advanced cancer respectively.

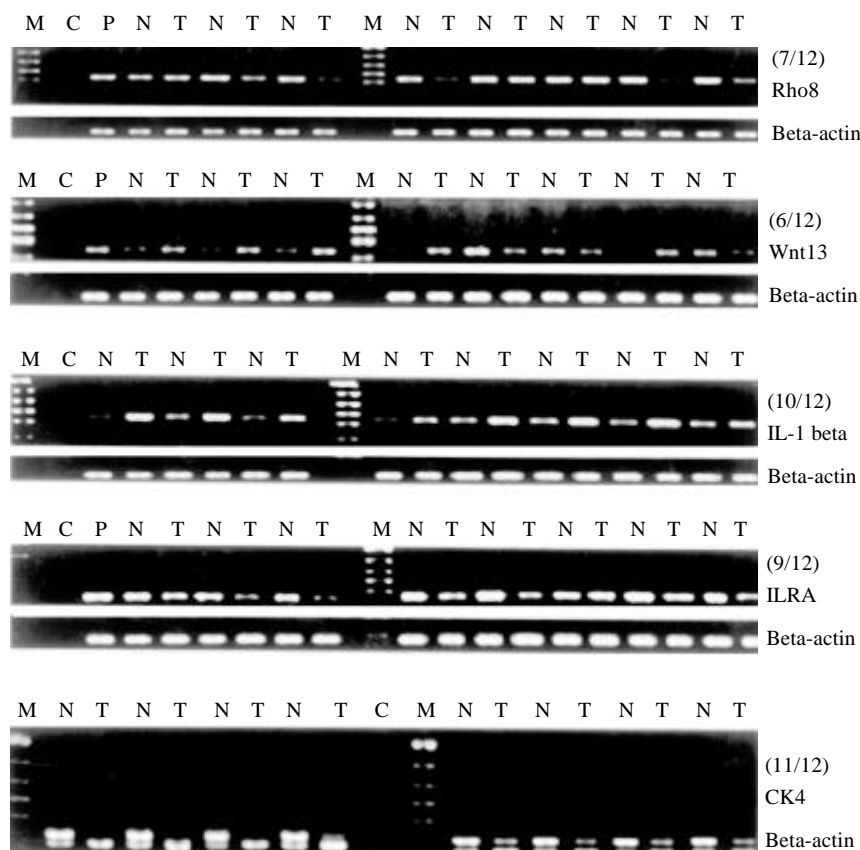


**Figure 2** Validation of array data with RT-PCR: Rho8, Wnt 13, IL-1 beta, IL-1 receptor antagonist and cytokeratin 4 were chosen to further investigate the reliability of the array data using RT-PCR. The figures showed part of the RT-PCR results of five genes in cancer (designated T) and matched almost normal tissues(designated N). P means positive control.

#### **Principle component analysis Identified a set of genes which may play Important roles in cancer development**

Principle component analysis showed that there were 5 principle components in the 6 stages of cancer development. The three principle components with eigenvalues 233.52, 121.59 and 101.34 respectively, accounted 92 % of total variations of gene expressions in 6 stages. Table 1 showed a set of genes with largest loading score (negative or positive) in the first three principle components in the ascending order. The loading scores are highly correlated with the expression level of genes. In Table 1 we also listed the ratio of the gene expressions in the corresponding stages of the tumor development. From Table 1 we can see that the first principle component roughly describes the changes of the gene expression level in the first and last stage of tumor development. Nine genes in the upper of the table were up-regulated in the stages of basal cell hyperplasia and early cancer, meanwhile seven genes in the bottom of the table were down-regulated in these stages. Genes GAF, CAPR, CASP8, BMP5, MIF and MYC may play important roles in the esophagus tumorigenesis. GAF (Glia-activating factor) is a novel heparin-binding growth factor purified from the culture supernatant of a human glioma cell line with growth-stimulating effect on glial cells *in vitro*. GAF domains are ubiquitous motifs present in cyclic GMP (cGMP)-regulated cyclic nucleotide phosphodiesterases and form a new class of cyclic nucleotide receptors distinct from the regulatory domains of cyclic nucleotide-regulated protein

kinases and ion channels<sup>[8]</sup>, the role of GAF in tumor development has not been characterized yet; CAPR is cadherin-associated protein related, also named as alpha 2 catenin, the abnormal expression of adhesion molecules (E-cadherin, alpha-catenin) has been reported as markers of high malignant potential in esophageal cancer<sup>[9]</sup>, and it was suggested that alpha catenin has prognostic significance in colorectal and prostate cancer<sup>[10]</sup>; The human CASP8 gene, whose product is also well known as caspase 8, encodes an interleukin-1beta converting enzyme (ICE)-related cysteine protease that is activated by the engagement of several different death receptors. Caspase 8 is a cysteine protease regulated in both a death-receptor-dependent and -independent manner during apoptosis, it is well characterized in apoptosis and tumor development<sup>[11]</sup>; BMP5 (Bone morphogenetic protein-5) is a signaling molecule which have the ability to induce ectopic bone when placed under the skin of an animal<sup>[12]</sup>; MIF (macrophage migration inhibitory factor) is involved in tumorigenesis via promotion of angiogenesis<sup>[13]</sup>, it is an ubiquitous cytokine whose expression has been investigated in tumors, showing a correlation between tumor aggressiveness and production of this protein by neoplastic cells. MIF is known to function as a cytokine, hormone, and glucocorticoid-induced immunoregulator, it is likely that MIF may function as a novel growth factor that stimulates incessant growth and invasion of melanoma concomitant with neovascularization; Myc is a well known oncogene which was involved in most of tumorigenesis, and

obviously it plays an important role in esophageal cancer development.

The second component involves three stages of the tumor development: basal cell hyperplasia, dysplasia and carcinoma in situ. Table 1 listed nine genes which were up-regulated and eight genes which were down-regulated in the stages of basal cell hyperplasia and dysplasia. The third principle component reflects the changes of the gene expression level in the transition from normal to basal cell hyperplasia and from basal cell hyperplasia to dysplasia. The table listed genes may play an important role in these transitions.

**Table 1A** Ratio of expression level for a set of genes with the largest loading scores in the first two principal components

Component 1			Component 2		
Gene	Ratio ELCA/LaCa	Ratio BCH/N	Gene	Ratio BCH/N	Ratio DYS/CAIN
GAF	131	16	PCTK1	122	8
CAPR	582	25	DAXX	5	95
CASP8	743	37	P70	7	62
MMp16	143	17	CCNH	174	87
DCC Precursor	316	12	CD153 antigen	70	31
Tenascin-R	742	21	TLAA	9	39
ZAP70	157	83	XPG	90	26
IL-13	110	22	Apoptosis Inhibitor Survivin	3	107
TRAIL.receptor	66	82	Bcl-1 oncogene	122	19
	LaCa/ELCA	N/BCH		N/BCH	CAIN/DYS
BMP5	284	170	MERLIN	3	411
MIF	79	72	LERK-8	31	334
N-myc	14	110	DSG2; HDGC	355	395
RPSA	19	68	MMP11	2	271
RBL2	33	18	CDK2	13	51
RAD52	27	9	CLK1	60	798
RBQ1	15	55	MDMX	3	225

N: Normal; BCH: Basal cell hyperplasia; DYS: Dysplasia; CAIN: Carcinoma in situ; ELCA: Early cancer; LaCa: Late cancer.

**Table 1B** Ratio of expression level for a set of genes with the largest loading scores in the third principal components

Gene	Ratio N/BCH	Ratio DYS/BCH
Bcl-2L8	803	227
SRC1	333	141
Muscle cadherin precursor	299	111
Neurogenic locus notch protein	488	104
CASP3	232	92
BCL2A1;GRS protein	133	665
Type 1 cytoskeletal 10 protein	302	370
TRAF5	83	650
Transcription factor E2F5	615	30
MAP kinase p38	147	86
	BCH/N	BCH/DYS
KRT7	2	105
GRB-IR	5	96
GAS1	4	210
BMP8	21	21
DVL	12	187
CAM-PDE1B	18	18
Apoptosis regulator bcl-2	60	59

N: Normal; BCH: Basal cell hyperplasia; DYS: Dysplasia.

**Table 2** Genes up or down regulated in all five stages of grade II basal cell hyperplasia, high-grade dysplasia, carcinoma in situ, early and advanced squamous cell carcinoma. Position indicates the gene position on the microarray membrane

Position	Gene Name
<b>Up Regulated Genes</b>	
A2k	G1/S-specific cyclin C
A4i	ERK5
A4j	ERK6
A5b	ERK activator kinase 1
A5l	transcription factor DP2
B3g	caspase-8 precursor
B3i	caspase-9 precursor
B3j	caspase-10 precursor (CASP10)
C1a	DNA-dependent protein kinase
C2c	DNA-repair protein XRCC1
C2j	RAD1
C4b	Wnt-5A
C4k	DVL1
C6m	CCK4
C7k	retinoic acid receptor epsilon
C7l	retinoic acid receptor gamma 1
C7m	retinoic acid receptor beta
D4b	integrin alpha 8
D4j	integrin beta 7 precursor
D4k	integrin beta 8 precursor
D5g	ezrin; cyto villin 2; villin 2
D5j	CD56 antigen
D7f	placenta growth factor 1
E1f	MMP9
E2a	MMP18
F3j	early growth response protein 1
F4l	IL-6
F5e	IL-13
F5k	interferon gamma precursor
F5l	leukocyte interferon-inducible peptide
<b>Down regulated Genes</b>	
C6c	insulin-like growth factor binding protein 2 (IGFBP2)
F4d	interleukin-1 receptor antagonist protein precursor (IL-1RA; IRAP)

### *Some genes are activated in particular stages*

According to their specificity to stages, differentially expressed genes fall into two main categories. The first category contains genes that are up or down regulated in the same way in all 4 abnormal stages. 77 genes belong to this category, including G1/S-specific cyclin C, proliferating cyclic nuclear antigen (PCNA), E2F dimerization partner 2, Wnt5A, retinoic acid receptors (epsilon, gamma 1, beta), early growth response protein 1 (hEGR1), etc. Part of these genes are listed in Table 2. Most of which are genes related to cell proliferation or differentiation. These expression profiles are accordant with the generality of characteristic phenotype of all of the 4 abnormal stages, i.e. decrease in extent of differentiation and increase in rate of proliferation.

The second category contains genes that were up or down regulated in particular stages, some of them seemed to be activated in early stages of carcinogenesis, p160ROCK is one of such genes. Figure 3 showed the expression level of



p160ROCK in 5 stages. P160 ROCK peaked its expression level in the stage of high grade dysplasia, down-regulated rapidly after this stage, recovered its expression level in early and late cancer, which revealed that this gene was transcriptionally activated at pre-cancerous stage.

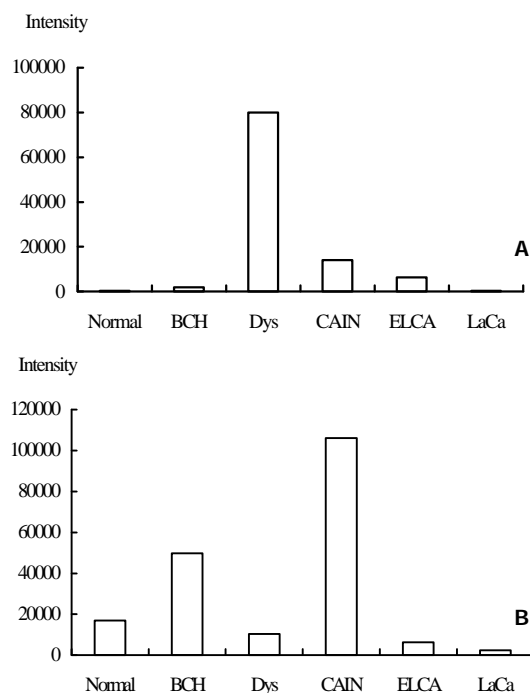


**Figure 3** Expression level of p160ROCK (3A) and JNK2 (3B) in 6 different stages, p160ROCK peaked its expression at stage of high-grade dysplasia and JNK2 peaked its expression at stage of carcinoma in situ. The column chart indicated expression levels of p160ROCK and JNK2 in stages of normal mucosa (designated normal), basal cell hyperplasia II (designated BCH), high grade dysplasia (designated Dys), squamous cell carcinoma in situ (designated CAIN), early cancer (designated ELCA) and late cancer (designated LaCa).

p160ROCK belongs to a family of Rho-associated serine/threonine kinase isozymes and has been identified as a new class of Rho effectors. Its main function is participating the reorganization of the cytoskeletal, and plays an important role in signal transduction from Rho to cytoskeletal<sup>[14]</sup> and also get involved in cell motility and morphological changes<sup>[15]</sup>. In human hepatocellular carcinoma cells, dominant active p160ROCK transfectants showed increased motility, and dominant negative p160ROCK transfectants showed reduced motility under stimulation. Furthermore, implantation of dominant negative p160ROCK transfectants resulted in a reduced metastatic rate *in vivo* compared with the parent cells or a control transfectant<sup>[16]</sup>. In this study, p160ROCK was found transcriptionally activated at the stage of high grade dysplasia, a pre-malignant stage, which imply that activation of the gene may be one of the early events during progress of esophageal carcinogenesis and may be one of the events responsible for morphological changes and increase in cell motility in early stages of carcinogenesis.

JNK2 is another representative gene which peaked its expression level in the stage of carcinoma in situ. Its expression levels in the 5 stages were shown in Figure 3. JNK2, c-Jun N-terminal kinase 2, also named as protein kinase mitogen-activated 9, is a proline-directed serine/threonine kinase activated by dual phosphorylation on threonine and tyrosine residues in response to a wide array of extracellular stimuli. Multiple research showed that JNK2 plays a critical role in coordinating the cellular response to stress and has been

implicated in regulating cell growth and transformation, antisense JNK2 induced growth inhibition which correlated with significant apoptosis<sup>[17]</sup>. It was shown that JNK2 plays an important role in cell transformation and carcinogenesis. In this study, JNK2 was found activated at stage of carcinoma in situ, and down regulated in early and late cancer, which showed that this may also be an early events of carcinogenesis and one of the forces pushing the cell from pre-malignancy to malignancy.

## DISCUSSION

Tumorigenesis is a complex and multistage process with many genes involved in. As a step toward understanding the complicated changes between normal and malignant cells, this report focused on gene expression profile variations among normal and abnormal esophageal epithelium tissues. Analyzing alterations of gene expression profiles in different stages of neoplasia is necessary for establishing the preventive, diagnostic, therapeutic, and prognostic potential of each related gene. To illustrate the mechanisms controlling malignant changes at molecular level may provide a further understanding of tumorigenesis, as well as new approaches in early detection and treatment of esophageal cancer. Furthermore, since it is impossible to get tissue samples of different stages from one patient, we got the biopsy specimens from different patients and pooled the samples with same pathologic diagnosis together to avoid the individual differences, and semi-quantitative RT-PCR was performed to confirm the reliability of the data. Moreover, we observed that many genes expressed abnormally in this complicated process and those changes mainly involved in cell proliferation, apoptosis, DNA repair, growth factors and cytokines. These genes and their expression alteration constitute a molecular atlas that is stage-specific and esophageal cancer-specific, and possibly being an important supplement to the traditional morphological diagnosis.

Principle component analysis identified a set of genes which plays important role in different stages of tumor development. Although many genes were related to tumorigenesis and development of esophageal cancer, further investigation is still needed to elucidate which gene (s) is the most critical one (s) to this complex process.

## REFERENCES

- 1 **DeRisi J**, Penland L, Brown PO, Bittner ML, Meltzer PS, Ray M, Chen M, Su YA, Trent JM. Use of a cDNA microarray to analyze gene expression patterns in human cancer. *Nat Genet* 1996; **14**: 457-460
- 2 **Schena M**, Shalon D, Davis RW, Brown PO. Quantitative monitoring of gene expression patterns with a complementary DNA microarray. *Science* 1995; **270**: 467-470
- 3 **Fuller GN**, Rhee CH, Hess KR, Caskey LS, Wang R, Bruner JM, Yung WK, Zhang W. Reactivation of insulin-like growth factor binding protein 2 expression in glioblastoma multiforme: a revelation by parallel gene expression profiling. *Cancer Res* 1999; **59**: 4228-4232
- 4 **Sgroi DC**, Teng S, Robinson G, LeVangie R, Hudson JR, Elkahoul AG. *In vivo* gene expression profile analysis of human breast cancer progression. *Cancer Res* 1999; **59**: 5656-5661
- 5 **Johanson RA**, Wichern DW. Applied multivariate statistical analysis, Prentice Hall, Inc., New York. 1982
- 6 **Lyer VR**, Eisen MB, Ross DT, Schuler G, Moore T, Lee JC, Trent JM, Staudt LM, Hudson J, Boguski MS, Lashkari D, Shalon D, Botstein D, Brown PO. The transcriptional program in the response of human fibroblasts to serum. *Science* 1999; **283**: 83-87
- 7 **Luo L**, Salunga RC, Guo H, Bittner A, Joy KC, Galindo JE, Xiao H, Rogers KE, Wan JS, Jackson MR, Erlander MG. Gene expression profiles of laser-captured adjacent neuronal subtypes. *Nat Med* 1999; **5**: 117-122
- 8 **Ho YS**, Burden LM, Hurley JH. Structure of the GAF domain, a



- ubiquitous signaling motif and a new class of cyclic GMP receptor. *EMBO J* 2000; **19**: 5288-5299
- 9 **Krishnadath KK**, Tilanus HW, van Blankenstein M, Hop WC, Kremers ED, Dinjens WN, Bosman FT. Reduced expression of the cadherin-catenin complex in oesophageal adenocarcinoma correlates with poor prognosis. *J Pathol* 1997; **182**: 331-338
  - 10 **Aaltomaa S**, Lippinen P, Ala-Opas M, Eskelinen M, Kosma VM. Alpha-catenin expression has prognostic value in local and locally advanced prostate cancer. *Br J Cancer* 1999; **80**: 477-482
  - 11 **Teitz T**, Wei T, Valentine MB, Vanin EF, Grenet J, Valentine VA, Behm FG, Look AT, Lahti JM, Kidd VJ. Caspase 8 is deleted or silenced preferentially in childhood neuroblastomas with amplification of MYCN. *Nat Med* 2000; **6**: 529-535
  - 12 **DiLeone RJ**, Marcus GA, Johnson MD, Kingsley DM. Efficient studies of long-distance Bmp5 gene regulation using bacterial artificial chromosomes. *Proc Natl Acad Sci USA* 2000; **97**: 1612-1617
  - 13 **Shimizu T**, Abe R, Nakamura H, Ohkawara A, Suzuki M, Nishihira J. High expression of macrophage migration inhibitory factor in human melanoma cells and its role in tumor cell growth and angiogenesis. *Biochem Biophys Res Commun* 1999; **264**: 751-758
  - 14 **Maekawa M**, Ishizaki T, Boku S, Watanabe N, Fujita A, Iwamatsu A, Obinata T, Ohashi K, Mizuno K, Narumiya S. Signaling from Rho to the actin cytoskeleton through protein kinases ROCK and LIM-kinase. *Science* 1999; **285**: 895-898
  - 15 **Hirose M**, Ishizaki T, Watanabe N, Uehata M, Kranenburg O, Moolenaar WH, Matsumura F, Maekawa M, Bito H, Narumiya S. Molecular dissection of the Rho-associated protein kinase (p160ROCK)-regulated neurite remodeling in neuroblastoma N1E-115 cells. *J Cell Biol* 1998; **141**: 1625-1636
  - 16 **Genda T**, Sakamoto M, Ichida T, Asakura H, Kojiro M, Narumiya S, Hirohashi S. Cell motility mediated by rho and Rho-associated protein kinase plays a critical role in intrahepatic metastasis of human hepatocellular carcinoma. *Hepatology* 1999; **30**: 1027-1036
  - 17 **Potapova O**, Gorospe M, Dougherty RH, Dean NM, Gaarde WA, Holbrook NJ. Inhibition of c-Jun N-terminal kinase 2 expression suppresses growth and induces apoptosis of human tumor cells in a p53-dependent manner. *Mol Cell Biol* 2000; **20**: 1713-1722

Edited by Xu JY

# Application of poly-lactide-co-glycolide-microspheres in the transarterial chemoembolization in an animal model of hepatocellular carcinoma

Jun Qian, Jochen Truebenbach, Florian Graepler, Philippe Pereira, Peter Huppert, Thomas Eul, Gundula Wiemann, Claus Claussen

**Jun Qian, Jochen Truebenbach, Florian Graepler, Philippe Pereira, Peter Huppert, Thomas Eul, Gundula Wiemann, Claus Claussen**, Department of Diagnostic Radiology, Eberhard-Karls-University Tübingen, Hoppe-Seyler-Strasse-3, Tübingen 72076, Germany

**Supported by** Bundesministerium fuer Bildung, Wissenschaft, Forschung und Technologie (Germany), No. 01KS9602

**Correspondence to:** Dr. Jun Qian, Department of Radiology, Xiehe Hospital, Tongji Medical College, Huazhong University of Science and Technology, Wuhan 430022, China. junqian\_tjmc@yahoo.com.cn  
**Telephone:** +86-27-85726432 **Fax:** +86-27-85727002

**Received:** 2002-01-28 **Accepted:** 2002-02-20

## Abstract

**AIM:** To introduce an animal model of hepatocellular carcinoma (HCC) in ACI-rats, and to evaluate the therapeutic effects of Poly-lactide-co-glycolide(Plcg)-microspheres in the transarterial chemoembolization (TACE) in this model, as well the value of this model in the experiments of interventional therapy.

**METHODS:** Subcapsular implantation of a solid Morris Hepatoma 3 924A (1 mm<sup>3</sup>) in the livers was carried out in 11 male ACI-rats. The tumor volume (V1) was measured by magnetic resonance imaging (MRI) (13 days after implantation). After laparotomy and retrograde placement of catheter into the gastroduodenal artery (14 days after implantation), the following protocols of interventional treatment were performed: (A) mitomycin C+Poly-lactide-co-glycolide(Plcg)-microspheres ( $n=4$ ); (B) 0.9 % NaCl (control group,  $n=7$ ). 13 days after these therapies the change of the tumor volume (V2) was determined by MRI again.

**RESULTS:** The success rate of tumor implantation reached to 100 %. The mean tumor volume before TACE (V1) were 0.082 cm<sup>3</sup> in group A and 0.096 cm<sup>3</sup> in group B respectively. The mean tumor volume after TACE (V2) were 0.230 cm<sup>3</sup> in group A and 1.347 cm<sup>3</sup> in group B respectively. The mean V2/V1 were 2.860 in group A and 27.120 in group B respectively. Compared to the control group (group B), groups A showed a significant reduction of tumor growth ( $P=0.004$ ) in the period of observation.

**CONCLUSION:** The growth of liver tumor could be obviously prevented by utilizing Plcg-mitomycin-microspheres in TACE in animal model. This rat model of HCC is suitable for the experimental studies of interventional therapy.

Qian J, Truebenbach J, Graepler F, Pereira P, Huppert P, Eul T, Wiemann G, Claussen C. Application of poly-lactide-co-glycolide-microspheres in the transarterial chemoembolization in an animal model of hepatocellular carcinoma. *World J Gastroenterol* 2003; 9(1): 94-98

<http://www.wjgnet.com/1007-9327/9/94.htm>

## INTRODUCTION

Hepatocellular carcinoma (HCC) is one of the most common malignancies in the world, responsible for an estimated one million deaths annually<sup>[1,2]</sup>. In China, HCC has been ranked second of cancer mortality since 1990s<sup>[3]</sup>. It has a poor prognosis due to its rapid infiltrating growth and complicating liver cirrhosis<sup>[4]</sup>. Surgical resection is still the only potentially curative treatment for HCC, particularly for small HCC<sup>[3]</sup>. To date, the resection rate for HCC is unfortunately less than 30 %<sup>[5, 6]</sup>. Transarterial chemoembolization (TACE) is currently the first choice of treatment for most unresectable HCC and improve the survival rate in selected patients<sup>[7-13]</sup>. However, the technical variants of TACE have often been chosen on an empirical basis and it is not always safe and effective<sup>[14-16]</sup>. Although TACE advantageously combines arterial embolization of the vascular supply of HCC with controlled intra-arterial infusion of chemotherapeutic drugs, its application is limited by the lack of appropriate and reliable embolization materials<sup>[15,16]</sup>. Recently, poly-lactide-co-glycolide (Plcg)-microspheres has been proved to be a new promising embolic agent<sup>[17,18]</sup>. In order to study the interventional therapeutic strategies for HCC, it is necessary to establish a suitable and reproducible animal model. The aim of the present study was to introduce an animal model of HCC with the technique of tumor implantation in ACI-rats, and to evaluate the therapeutic effect of different methods of TACE, including the efficiency of Plcg-microspheres in this animal model. MRI was performed for measuring the tumor volume before and after the TACE in this study.

## MATERIALS AND METHODS

### Tumor

Morris hepatoma 3 924A, a rapidly growing, poorly differentiated hepatocellular carcinoma, was induced by dietary administration of N-2-fluorenyldiacetamide in an ACI rat. The hepatoma specimens were obtained from the German Cancer Research Center in Heidelberg (DKFZ).

### Animal

Inbred male ACI-rats weighing 200 to 220 g ( $n=15$ ) were obtained from the company of Harlan Winkelmann in Germany. The animals were kept under conventional conditions with a temperature of  $22\pm2$  °C, a relative humidity of  $55\pm10$  %, a dark-light rhythm of 12 hr, and were fed standard laboratory chow and tap water ad libitum.

### Anesthesia

All interventional and imaging procedures were carried out under intraperitoneally applied anesthesia with ketamine hydrochloride (Ketanest, Parke-Davis, Germany; 100 mg·kg<sup>-1</sup>), Xylazinehydrochlorid (Rompun, Bayer, Germany; 15 mg·kg<sup>-1</sup>) and atropine sulfate (Atropinsulfat Braun, Braun, Germany; 0.1 mg·kg<sup>-1</sup>).

### Tumor implantation (At day 1)

The technique for tumor implantation was basically similar to that described by Yang *et al*<sup>[19,20]</sup> with minor modifications<sup>[21]</sup>.

The Morris Hepatoma 3 924A tumor tissue, recovered from the passaged animals 2 weeks after subcutaneous implantation (corresponding to  $5 \times 10^6$  tumor cells), was cut into small cubes about  $1 \text{ mm}^3$ .

The recipient ACI-rats were intraperitoneally anesthetized, and the upper abdomen was shaved. A small subcapsular incision on the left lateral lobe of the liver was made. The tumor fragment was gently placed into the pocket with a small cotton swab on the liver surface as hemostasis and the abdominal wall was then closed.

#### Catheterization and TACE (At day 14)

A PE-10 polyethylene catheter (inner diameter 0.28 mm, outer diameter 0.61 mm; Wenzel/Heidelberg, Germany) was used for experiments of TACE under a second laparotomy. By using a binocular operative microscope (M651, Leica/Wetzler, Germany), the catheter was retrograde inserted into the gastroduodenal artery (Figure 1). After slightly drawing the thin rope around the common hepatic artery, the following different agents were injected through the catheter: Group A ( $n=4$ ): TACE with mitomycin C ( $0.25 \text{ mg} \cdot \text{kg}^{-1}$ ) and Plcg-microspheres ( $200 \text{ mg} \cdot \text{kg}^{-1}$ , diameter:  $40 \mu\text{m}$ ; Institute of Pharmacological Technology, Philipps University, Marburg/Germany).

Group B (control group,  $n=7$ ): injection of 0.9 % NaCl alone.

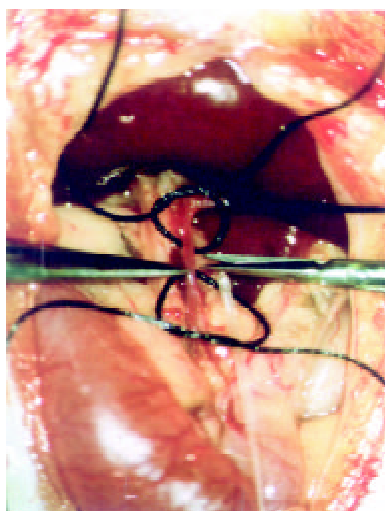


**Figure 1** Catheterization of the gastroduodenal artery *in vivo*

#### MRI

MRI was performed in a 1.0 Tesla Magnetom superconducting system (Siemens, Erlangen, Germany) supplemented by a commercial coil (Small Field of View) before and after the catheterization (At day 13 and 27). T1-weighted (TR/TE, 400/14 ms) and T2-weighted (TR/TE, 3 000/96 ms) axial SE images with spatial presaturation for controlling the flow artifact were acquired. Slice thickness was 2.0 mm, Matrix was  $192 \times 256$ . There was no gap between sections. The findings on T1- and T2-weighted SE images were examined in all 11 rats. Tumor volume was determined and evaluated according to the formula: Tumor volume ( $\text{mm}^3$ ) =  $\text{Length}(\text{mm}) \times \text{Width}^2(\text{mm})^2 / 2^{[22]}$ .

#### RESULTS

In all the rats receiving tumor implantation with Morris Hepatoma 3 924A, the rate of tumor implantation reached 100 %. None of the animals died during implantation or in the postoperative period.

The sensitivity of MRI for detecting HCC reached 100 %. HCC showed a hypointense pattern on T1-weighted images and a hyperintense pattern on T2-weighted images in the left lateral lobe of the liver (Figure 2, Figure 3). Necrosis,

hemorrhage and metastase of the tumor were not observed. The liver tumor was well discernible from the surrounding liver tissue on each image.

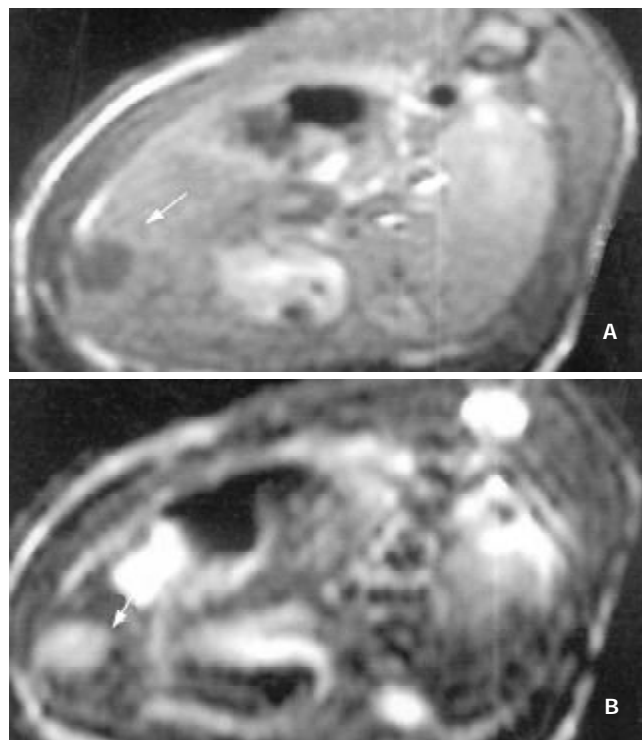


**Figure 2** MR images of HCC before the application of Plcg-Mitomycin-microspheres: (a) T1-weighted image (400/14 ms) showed a hypointense pattern in the left lateral lobe of the liver, (b) T2-weighted image (3 000/96 ms) showed a hyperintense pattern in the liver. Necrosis, hemorrhage and metastase of the tumor were not observed.

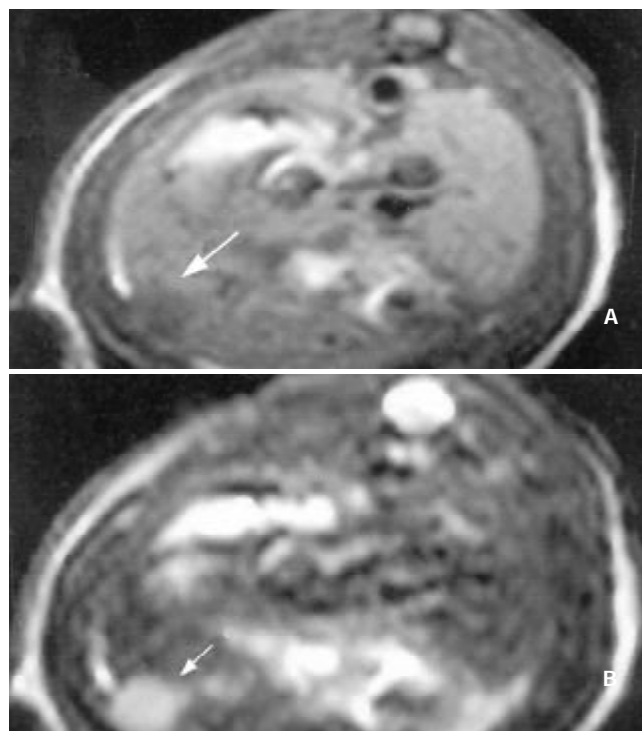


**Figure 3** MR images of HCC after the application of Plcg-Mitomycin-microspheres: (a) MRI T1WI (400/14 ms); (b) MRI T2WI (3 000/96 ms). The tumor volume after the application of Plcg-Mitomycin-microspheres was not changed compared to that before the application.

The efficiencies of Plcg-Mitomycin-microspheres in the interventional therapy of HCC in ACI-rats were shown in Table 1.

**Table 1** The efficiencies of Plcg-Mitomycin-microspheres in the interventional therapy of HCC in ACI-rats

	Group A (Plcg)	Group B (control group)
Mean volume (V1) before TACE (cm <sup>3</sup> )	0.082	0.096
Mean volume (V2) after TACE (cm <sup>3</sup> )	0.230	1.347
Mean V2/V1	2.86	27.12

Compared to the control group (group B), groups A showed a significant reduction of tumor growth ( $P=0.004$ ) in the period of observation by *t*-test.

## DISCUSSION

In order to investigate the efficiency of TACE for HCC, it is necessary to have a suitable and reproducible animal model. Various animal models of liver tumor have been established. The diethylnitrosamine model for hepatic tumor induction was simple, and provided a more representative range of tumors for experimental evaluation. However, the high mortality of the animals and various localization/number/size of the tumor in the liver were the major shortcomings. Therefore, the application of this model was extremely limited. The technique with a needle injection of tumor cells into hepatic parenchyma often caused tumor spill from the puncture channel and might result direct injection of the tumor cells into the circulation<sup>[19]</sup>. Although a relative high tumor take rate could be obtained by using the Walker-256/VX2 model in rats or rabbits with the technique of tumor implantation, these animal models belonged to carcinosarcoma or adenocarcinoma and were usually utilized for the study of liver metastases<sup>[23-27]</sup>. It is well known that the metastasis way and the therapeutic strategies as well the related effects of HCC and sarcoma are quite different from the aspect of histopathology, and a characteristic of HCC which distinguishes it from most metastases to the liver is that it is a highly vascular tumor<sup>[28]</sup>, so that these animal models are unsatisfactory and not suitable for studying the interventional therapy.

In our present study, an animal model of HCC with the technique of tumor implantation previously described by Yang *et al*<sup>[19,20]</sup> was established. The rate of tumor implantation reached 100 %<sup>[17]</sup>. Necrosis, hemorrhage and metastases of the tumor were not observed. Histopathologically, Morris hepatoma 3 924A was a poorly differentiated hepatocellular carcinoma, mimicking the Edmondson grade-III hepatoma in humans<sup>[20]</sup> (Edmonson's classification is based on the degree of differentiation of HCC). The appropriate growth speed of the liver tumor made it easy for MRI examination<sup>[29]</sup>. The blood supply of the tumor mainly came from hepatic arteries which was similar to that in human liver cancers<sup>[19, 29]</sup>. As is known to all, HCC was usually hypervascular except for differentiated HCC and TACE was usually effective only for hypervascular HCC<sup>[30-33]</sup>. Compared to other animal models, our rat model was more suitable for the study of interventional therapy of HCC, and the related conclusion of the study was more convincing.

MRI examination for measuring the tumor volume without utilizing contrast media was carried out in our experiments. There was no single parameter better than tumor growth rate that could give information on the effects of different therapeutic maneuvers on tumor growth<sup>[22]</sup>. In another study of ours, we have demonstrated that MRI as an invasive imaging modality was superior to CT, DSA in the diagnosis of HCC in experiments<sup>[29]</sup>. It was supported by histological examination that MRI was also superior to ultrasonography for judging the tumor dimensions<sup>[29]</sup>. Another advantage of MRI was its

excellent soft-tissue contrast resolution<sup>[34]</sup>. T1-weighted imaging was superior to T2-weighted imaging in depicting early HCC, but the latter could be useful in evaluating the progression of HCC in the histopathologically early stages<sup>[35]</sup>. The signal intensity on T2-weighted images correlated with the histological grade and histopathological change of HCC<sup>[35-37]</sup>. The detectability of MRI was 100 % in the present study. HCC showed a hypointense pattern on T1-weighted images and a hyperintense pattern on T2-weighted images in the left lateral lobe of the liver. Necrosis, hemorrhage and metastase of the tumor were not observed. The contrast between the tumor and surrounding normal liver parenchyma was clear to observe. Based on these results, we concluded that MRI was useful in the assessment of the therapeutic effects of TACE in HCC.

TACE is one choice of the palliative treatment for unresectable HCC, particularly for patients with multifocal HCC and with acceptable liver functions. TACE caused tumor necrosis by occlusion of the feeding artery of HCC, and its clinical efficiencies have been generally recognized<sup>[38-41]</sup>. By using TACE with a combination of cytostatic drugs (mitomycin, doxorubicin, epirubicin, cisplatin, 5-Fu), a reduction of vital tumor tissue could be achieved<sup>[42-44]</sup>, although the prolongation of survival remained questionable<sup>[45, 46]</sup>. As stated before, although TACE advantageously combined arterial embolization of the vascular supply of a neoplasm with controlled intra-arterial infusion of chemotherapeutic drugs, its application was limited by the lack of appropriate and reliable embolic agents. The major problem with embolic agents are twofold<sup>[47]</sup>: first, they could often completely obstruct the hepatic artery, leading to difficulties in administration of subsequent courses of hepatic artery chemotherapy. With a relative short half-life of embolic agents, the effectiveness of TACE was not significantly improved; and second, it was easy to aggravate the liver cirrhosis and lead to hepatic failure after repeated TACE. The optimal treatment modality of TACE was unknown<sup>[14, 48]</sup>.

Recently, Plcg-microspheres have been proved to be a new promising embolic agent in TACE in experiments<sup>[17,18]</sup>. Verrijk and co-workers<sup>[49,50]</sup> reported that TACE with Plcg-microspheres and CDDP significantly improved the delivery of cytotoxic drugs to liver tumor and simultaneously reduced systemic toxicity in animals. Plcg-microspheres are biodegradable polymers with high molecular size and possess a good tissue compatibility. The degradation rate of polylactides is known to depend on the polymer microstructure that may be of the L, D or D, L type. The polyester lifetime could be controlled in a range of a few days or months<sup>[49-51]</sup>. It has been suggested that this drug could slowly release into the tumor tissues principally by a diffusion mechanism. It has also been indicated that the microspheres size of 40  $\mu$ m allows a distal and homogeneous migration of the embolic agent within the targeted organ, without passing through the capillary filter<sup>[18]</sup>, it is this reason that Plcg-microspheres with the size of 40  $\mu$ m were chosen in our experiments. Verrijk *et al*<sup>[49,50]</sup> also demonstrated, that the absence of a burst effect and an adequate CDDP release from Plcg-CDDP-microspheres then significantly prolonged the first-pass effect, with the result that low systemic platinum levels were maintained while a liver platinum concentration was achieved which was high enough for an antitumor effect. The results of our present studies indicated that Plcg-microspheres could effectively retard the growth of HCC. Compared to the control group (group B), groups A (Plcg) showed a significant reduction of tumor growth ( $P=0.004$ ) in the period of observation by *t*-test. The therapeutic efficiencies of Plcg-mitomycin-microspheres was similar to Gelform+Mitomycin+Lipiodol in our another study (Mean V2/V1=2.86,  $P=0.748$ , unpublished results).

To conclude, the growth of liver tumor was markedly

prevented by the use of Plcg-mitomycin-microspheres in the TACE in an animal model. This effective and reliable embolic agent might be useful in clinic in future. However, the mechanism of effect of Plcg-microspheres is not clear so far. Data on a large number of animals and the test of application of various cytotoxic agents in the TACE, as well the repeated TACE will be required.

## REFERENCES

- 1 **Cha C**, DeMatteo RP, Blumgart LH. Surgery and ablative therapy for hepatocellular carcinoma. *J Clin Gastroenterol* 2002; **35**: S130-137
- 2 **Teo EK**, Fock KM. Hepatocellular carcinoma: an Asian perspective. *Dig Dis* 2001; **19**: 263-268
- 3 **Tang ZY**. Hepatocellular carcinoma-cause, treatment and metastasis. *World J Gastroenterol* 2001; **7**: 445-454
- 4 **Yuen MF**, Cheng CC, Lauder IJ, Lam SK, Ooi CG, Lai CL. Early detection of hepatocellular carcinoma increases the chance of treatment: Hong Kong experience. *Hepatology* 2000; **31**: 330-335
- 5 **Sturm JW**, Keese MA, Bonninghoff RG, Wustner M, Post S. Locally ablative therapies of hepatocellular carcinoma. *Onkologie* 2001; **24** (Suppl 5): 35-45
- 6 **Chung JW**. Transcatheter arterial chemoembolization of hepatocellular carcinoma. *Hepatogastroenterology* 1998; **45** (Suppl 3): 1236-1241
- 7 **Acunans B**, Rozanes I. Hepatocellular carcinoma: treatment with transcatheter arterial chemoembolization. *Eur J Radiol* 1999; **32**: 86-89
- 8 **Rose DM**, Chapman WC, Brockenbrough AT, Wright JK, Rose AT, Meranze S, Mazer M, Blair T, Blanke CD, Debelak JP, Pinson CW. Transcatheter arterial chemoembolization as primary treatment for hepatocellular carcinoma. *Am J Surg* 1999; **177**: 405-410
- 9 **Liado L**, Virgill J, Figueras J, Valls C, Dominguez J, Rafecas A, Torras J, Fabregat J, Guardiola J, Jaurrieta E. A prognostic index of the survival of patients with unresectable hepatocellular carcinoma after transcatheter arterial chemoembolization. *Cancer* 2000; **88**: 50-57
- 10 **Zangos S**, Gille T, Eichler K, Engelmann K, Woitaschek D, Balzer JO, Mack MG, Thalhammer A, Vogl TJ. Transarterial chemoembolization in hepatocellular carcinomas: technique, indications, results. *Radiologe* 2001; **41**: 906-914
- 11 **Tang ZY**. Hepatocellular carcinoma. *J Gastroenterol Hepatol* 2000; **15** (Suppl): G1-7
- 12 **Livraghi T**. Treatment of hepatocellular carcinoma by interventional methods. *Eur Radiol* 2001; **11**: 2207-2219
- 13 **Loewe C**, Cejna M, Schoder M, Thurnher MM, Lammer J, Thurnher SA. Arterial embolization of unresectable hepatocellular carcinoma with use of cyanoacrylate and lipiodol. *J Vasc Interv Radiol* 2002; **13**: 61-69
- 14 **Camma C**, Schepis F, Orlando A, Albanese M, Shahied L, Trevisani F, Andreone P, Craxi A, Cottone M. Transarterial chemoembolization for unresectable hepatocellular carcinoma: meta-analysis of randomized controlled trials. *Radiology* 2002; **224**: 47-54
- 15 **Poon RT**, Ngan H, Lo CM, Liu CL, Fan ST, Wong J. Transarterial chemoembolization for inoperable hepatocellular carcinoma and postresection intrahepatic recurrence. *J Surg Oncol* 2000; **73**: 109-114
- 16 **Trinchet JC**, Ganne-Carrie N, Beaugrand M. Intra-arterial chemoembolization in patients with hepatocellular carcinoma. *Hepatogastroenterology* 1998; **45** (Suppl 3): 1242-1247
- 17 **Qian J**, Feng GS, Truebenbach J, Pereira PL, Huppert PE, Graepler F, Eul T, Claussen CD. Experimentelle Untersuchung zur Effektivität der Transarteriellen Chemoembolisation (TACE) im Tiermodell des hepatozellulären Karzinom. *Acta Universitatis Medicinæ Tongji* 2001; **21**: 115-118
- 18 **Bastian P**, Bartkowski R, Kohler H, Kissel T. Chemo-embolization of experimental liver metastases. Part I: distribution of biodegradable microspheres of different sizes in an animal model for the locoregional therapy. *Eur J Pharm Biopharm* 1998; **46**: 243-254
- 19 **Yang R**, Rescorla FJ, Reilly CR, Faught PR, Sanghvi NT, Lumeng L, Franklin TD, Grosfeld JL. A reproducible rat liver cancer model for experimental therapy: Introducing a technique of intrahepatic tumor implantation. *Journal of Surgical Research* 1992; **52**: 193-198
- 20 **Yang R**, Liu Q, Rescorla FJ, Grosfeld JL. Experimental liver cancer: Improved response after hepatic artery ligation and infusion of tumor necrosis factor-alpha and interferon-gamma. *Surgery* 1995; **118**: 768-774
- 21 **Trubenbach J**, Pereira PL, Graepler F, Huppert PE, Eul T, König CW, Duda SH, Claussen CD. Animal experiment studies on the effectiveness of permanent occlusion of the hepatic artery in transarterial chemoembolization. *Fortschr Röntgenstr* 2000; **172**: 274-277
- 22 **Carlsson G**, Gullberg B, Hafstrom L. Estimation of liver tumor volume using different formulas -an experimental study in rats. *J Cancer Res Clin Oncol* 1983; **105**: 20-23
- 23 **Yarmenitis SD**, Kalogeropoulou CP, Hatjikondi O, Ravazoula P, Petsas T, Siambilis D, Kalfarentzos F. An experimental approach of the Doppler perfusion index of the liver in detecting occult hepatic metastases: histological findings related to the hemodynamic measurements in wistar rats. *Eur Radiol* 2000; **10**: 417-424
- 24 **Ishida H**, Murata N, Yamada H, Nomura T, Shimomura K, Fujioka M, Idezuki Y. Effect of CO(2) pneumoperitoneum on growth of liver micrometastases in a rabbit model. *World J Surg* 2000; **24**: 1004-1008
- 25 **Kuszyk BS**, Boitnott JK, Choti MA, Bluemke DA, Sheth S, Magee CA, Horton KM, Eng J, Fishman EK. Local tumor recurrence following hepatic cryoablation: radiologic-histopathologic correlation in a rabbit model. *Radiology* 2000; **217**: 477-486
- 26 **Goldberg SN**, Walovitch RC, Straub JA, Shore MT, Gazelle GS. Radio-frequency-induced coagulation necrosis in rabbits: immediate detection at US with a synthetic microsphere contrast agent. *Radiology* 1999; **213**: 438-444
- 27 **Guo WJ**, Li J, Ling WL, Bai YR, Zhang WZ, Cheng YF, Gu WH, Zhuang JY. Influence of hepatic arterial blockage on blood perfusion and VEGF, MMP-1 expression of implanted liver cancer in rats. *World J Gastroenterol* 2002; **8**: 476-479
- 28 **Carr BI**. Hepatic artery chemoembolization for advanced stage HCC: experience of 650 patients. *Hepatogastroenterology* 2002; **49**: 79-86
- 29 **Trubenbach J**, Graepler F, Pereira PL, Ruck P, Lauer U, Gregor M, Claussen CD, Huppert PE. Growth characteristics and Imaging properties of the Morris Hepatoma 3924A in ACI rats: A suitable model for transarterial chemoembolization. *Cardiovasc Intervent Radiol* 2000; **23**: 211-217
- 30 **Nakashima Y**, Nakashima O, Hsia CC, Kojiro M, Tabor E. Vascularization of small hepatocellular carcinomas: correlation with differentiation. *Liver* 1999; **19**: 12-18
- 31 **Tang ZY**. Treatment of hepatocellular carcinoma. *Digestion* 1998; **59**: 556-562
- 32 **Hayashi M**, Matsui O, Ueda K, Kawamori Y, Gabata T, Kadoya M. Progression to hypervascular hepatocellular carcinoma: correlation with intranodular blood supply evaluated with CT during intraarterial injection of contrast material. *Radiology* 2002; **225**: 143-149
- 33 **Kamura T**, Kimura M, Sakai K, Ichida T, Seki H, Yamamoto S, Ozaki T. Small hypervascular hepatocellular carcinoma versus hypervascular pseudolesions: differential diagnosis on MRI. *Abdom Imaging* 2002; **27**: 15-24
- 34 **Mueller-Lisse UG**, Heuck AF. Control and monitoring of focal radiotherapy with magnetic resonance tomography-An overview. *Radiologe* 1998; **38**: 200-209
- 35 **Honda H**, Kaneko K, Maeda T, Kuroiwa T, Fukuya T, Yoshimitsu K, Irie H, Aibe H, Takenaka K, Masuda K. Small hepatocellular carcinoma on magnetic resonance imaging: Relation of signal intensity to angiographic and clinicopathologic findings. *Invest Radiol* 1997; **32**: 161-168
- 36 **Inoue E**, Kuroda C, Fujita M, Narumi Y, Kadota T, Kuriyama K, Ishiguro S, Kasugai H, Sasaki Y, Imaoka S. MR features of various histological grades of small hepatocellular carcinoma. *J Comput Assist Tomogr* 1993; **17**: 75-79
- 37 **Yan FH**, Zhou KR, Cheng JM, Wang JH, Yan ZP, Da RR, Fan J, Ji Y. Role and limitation of FMSPGR dynamic contrast scanning in the follow-up of patients with hepatocellular carcinoma treated by TACE. *World J Gastroenterol* 2002; **8**: 658-662
- 38 **Vogl TJ**, Schroeder H, Trapp M, Straub R, Schuster A, Schuster

- M, Mack M, Souchon F, Neuhaus P. Multi-sequential arterial chemoembolization of advanced hepatocellular carcinomas: Computerized tomography follow-up parameters for evaluating effectiveness of therapy. *Fortschr Rontgenstr* 2000; **172**: 43-50
- 39 **Li L**, Wu PH, Li JQ, Zhang WZ, Lin HG, Zhang YQ. Segmental transcatheter arterial embolization for primary hepatocellular carcinoma. *World J Gastroenterol* 1998; **4**: 511-512
- 40 **Chen MS**, Li JQ, Zhang YQ, Lu LX, Zhang WZ, Yuan YF, Guo YP, Lin XJ, Li GH. High-dose iodized oil transcatheter arterial chemoembolization for patients with large hepatocellular carcinoma. *World J Gastroenterol* 2002; **8**: 74-78
- 41 **Fan J**, Ten GJ, He SC, Guo JH, Yang DP, Weng GY. Arterial chemoembolization for hepatocellular carcinoma. *World J Gastroenterol* 1998; **4**: 33-37
- 42 **Kamada K**, Nakanishi T, Kitamoto M, Aikata H, Kawakami Y, Ito K, Asahara T, Kajiyama G. Long-term prognosis of patients undergoing transcatheter arterial chemoembolization for unresectable hepatocellular carcinoma: Comparison of cisplatin lipiodol suspension and doxorubicin hydrochloride emulsion. *J Vasc Interv Radiol* 2001; **12**: 847-854
- 43 **Gattoni F**, Dova S, Uslenghi CM. Three-year follow-up of 62 cirrhotic patients with hepatocellular carcinoma treated with chemoembolization. *Minerva Chir* 2000; **55**: 31-37
- 44 **Poyanli A**, Rozanes I, Acunas B, Sencer S. Palliative treatment of hepatocellular carcinoma by chemoembolization. *Acta Radiol* 2001; **42**: 602-607
- 45 **Roche A**. Therapy of HCC-TACE for liver tumor. *Hepatogastroenterology* 2001; **48**: 3-7
- 46 **Yip D**, Findlay M, Boyer M, Tattersall MH. Hepatocellular carcinoma in central Sydney: a 10 year review of patients seen in a medical oncology department. *World J Gastroenterol* 1999; **5**: 483-487
- 47 **Iwai K**, Maeda H, Konno T. Use of oily contrast medium for selective drug targeting to tumor: Enhanced therapeutic effect and x-ray image. *Cancer Research* 1984; **44**: 2115-2121
- 48 **Lorenz M**, Liermann D, Staib-Sebler E, Gog C, Encke A, Kollath J. Noradrenalin guided selective chemoembolization of hepatocellular carcinoma. *Zentralbl Chir* 1994; **119**: 777-786
- 49 **Verrijk R**, Smolders IJ, Bosnie N, Begg AC. Reduction of systemic exposure and toxicity of cisplatin by encapsulation in polylactide-co-glycolide. *Cancer Research* 1992; **52**: 6653-6656
- 50 **Verrijk R**, Smolders IJ, McVie JG, Begg AC. Polymer-coated albumin microspheres as carriers for intravascular tumor targeting of cisplatin. *Cancer Chemother Pharmacol* 1991; **29**: 117-121
- 51 **Hagiwara A**, Sakakura C, Tsujimoto H, Imanishi T, Ohgaki M, Yamasaki J, Sawai K, Takahashi T, Fujita T, Yamamoto A, Muranishi S, Ikada Y. Selective delivery of 5-fluorouracil (5-FU) to i.p. tissues using 5-FU microspheres in rats. *Anticancer Drug* 1997; **8**: 182-188

Edited by Pang LH

• COLORECTAL CANCER •

# Nested case-control study on the risk factors of colorectal cancer

Kun Chen, Jian Cai, Xi-Yong Liu, Xi-Yuan Ma, Kai-Yan Yao, Shu Zheng

**Kun Chen, Jian Cai**, Department of Epidemiology, Zhejiang University School of Public Health, Hangzhou, 310006, Zhejiang Province, China

**Xi-Yong Liu, Shu Zheng**, Cancer Institute of Zhejiang University, Hangzhou, 310009, Zhejiang Province, China

**Xin-Yuan Ma, Kai-Yan Yao**, Institute of Cancer Research and Prevention, Jiashan County, 314000, Zhejiang Province, China

**Supported by** the National Natural Science Foundation of China, No. 30170828

**Correspondence to:** Kun Chen, Department of Epidemiology, Zhejiang University School of Public Health, 353 Yan-an Road, Hangzhou, 310006 Zhejiang Province, China. ck@zjuem.zju.edu.cn

**Telephone:** +86-571-87217190

**Received:** 2002-04-29 **Accepted:** 2002-06-08

## Abstract

**AIM:** To investigate the risk factors of colon cancer and rectal cancer.

**METHODS:** A nested case-control study was conducted in a cohort of 64 693 subjects who participated in a colorectal cancer screening program from 1989 to 1998 in Jiashan county, Zhejiang, China. 196 cases of colorectal cancer were detected from 1990 to 1998 as the case group and 980 non-colorectal cancer subjects, matched with factors of age, gender, resident location, were randomly selected from the 64 693 cohort as controls. By using univariate analysis and multivariate conditional logistic regression analysis, the odds ratio (OR) and its 95 % confidence interval (95 %CI) were calculated between colorectal cancer and personal habits, dietary factors, as well as intestinal related symptoms.

**RESULTS:** The multivariate analysis results showed that after matched with age, sex and resident location, mucous blood stool history and mixed sources of drinking water were closely associated with colon cancer and rectal cancer, OR values for the mucous blood stool history were 3.508 (95 %CI: 1.370-8.985) and 2.139 (95 %CI: 1.040-4.402) respectively; for the mixed drinking water sources, 2.387 (95 %CI: 1.243-4.587) and 1.951 (95 %CI: 1.086-3.506) respectively. All reached the significant level with a *P*-value less than 0.05.

**CONCLUSION:** The study suggested that mucous blood stool history and mixed sources of drinking water were the risk factors of colon cancer and rectal cancer. There was no any significant association between dietary habits and the incidence of colorectal cancer.

Chen K, Cai J, Liu XY, Ma XY, Yao KY, Zheng S. Nested case-control study on the risk factors of colorectal cancer. *World J Gastroenterol* 2003; 9(1): 99-103

<http://www.wjgnet.com/1007-9327/9/99.htm>

## INTRODUCTION

Colorectal cancer is one of the most common malignant tumors<sup>[1-6]</sup>. During the past decades, the incidence of colorectal cancer was increased all around the world, more than 500 000 cases were diagnosed as colorectal cancer per year. In the east

of China, there has been a higher incidence of colorectal cancer. In Jiashan County, the mortality rate of colorectal cancer was the highest among China, which is about 20/100 000 per year<sup>[7]</sup>.

The causes of colorectal cancer are generally regarded as two aspects: heredity and environment<sup>[8-10]</sup>. The former includes family history of cancer, intestinal polyp history, and so on. The later includes particularly dietary habit and physical activity.

Nested Case-Control Study (NCCS), an analytical epidemiological study method, was first presented by Mantel N, an American epidemiologist, in 1973<sup>[11]</sup>, and it was widely used after 1980's<sup>[12-21]</sup>. All the subjects in such study are selected from a whole cohort, which is generally called cohort set. Compared with the cohort study, NCCS has the privilege of time-saving, money-saving, and trouble-saving; while compared to case-control study, since the exposure data are collected before the incident of disease, it is certain of the causes and time consequences relationship, and observational bias could be controlled efficiently. All of these characteristics of NCCS are suitable to the study of chronic disease, such as cancer.

There are many reports on the risk factors of colorectal cancer using classical case-control study method, however, few studies used nested case-control study method<sup>[22-29]</sup>. The purpose of this study is to explore the risk factors of colorectal cancer, providing evidence for the prevention of colorectal cancer.

## MATERIALS AND METHODS

### Selection of cases and controls

A colorectal cancer screening program beginning on 1<sup>st</sup> May 1989 and ending on 30<sup>th</sup> April 1990 was conducted in ten countries which belonged to Jiashan county, Zhejiang province, China, including Weitan town, Yangmiao country, Xiadianmiao country, *et al*. From 75 842 eligible subjects aged 30 years and over, 64 693 subjects were enrolled as the base cohort set, the response rate was 85.3 %. Moreover, Jiashan county has founded cancer registration system and colorectal cancer report system, monitoring new cancer cases, including colorectal cancer. The cases in this study, who had participated in the 1989-1990 screening program, were the new colorectal cancer patients reported by Institute of Cancer Research and Prevention of Jiashan county. Up to 1998, the total number was 196 cases. Of which, 151 cases were pathological diagnosed, account for 77.1 %, 20 cases were diagnosed in the operation, 10.2 %, 23 cases were diagnosed by endoscopy, 11.7 %. Under the principle of same-country or town, same-sex, and no more than 3 years age disparity, 980 non-colorectal cancer subjects in the cohort set were selected as controls, resulting the final study subjects of 196 cases and 980 controls.

### Contents of the study

The study contents composed of three parts as follow: (1). General characteristics: including age, sex, job types, educational levels, address *et al*; (2). Personal habits: including dietary habits, drinking water sources, alcohol consumption and cigarette smoking, *et al*; (3). Symptoms and disease history related with colorectal cancer: including changes of stool status, abdominal operation history, intestinal disease history, asthma history and allergy history, family cancer history, ancylostomiasis history, drug using history, psychic stimulation history, and so on.



### Investigation methods and quality control

In the 1989-1990 screening investigation, a well-built *Investigation Manual* as the uniform criteria for inquiring the subjects and filling up the constructed questionnaire was used. All interviewers were trained focusing on the skills of inquiring. No subjects refused to be interviewed except that they were out of towns. For building the database, the questionnaires were coded and put into computer twice to control bias. The data used in this study were taken from this database.

### Statistical analysis

Classical analysis methods of case-control study can be used to NCCS data, usually calculating OR value. In this study, Chi-square test was used in the univariate analysis of the data; conditional logistic regression was used in the multivariate analysis. The SPSS 10.0 for windows and the SAS system for windows, version 6.12, were used for completing all the statistical analyses.

## RESULTS

### General information

In this study, there were 196 cases (84 colon cancer, 112 rectal cancer) and 980 controls. The distribution of age between cases and controls for male and female was shown in Table 1.

**Table 1** The distribution of subjects by age and sex

age	male		female	
	case	control	case	control
30-	3	15	7	35
35-	9	49	3	15
40-	14	69	3	19
45-	11	52	14	66
50-	21	110	14	78
55-	24	114	22	104
60-	11	57	13	63
65-	11	54	3	15
70-	2	10	5	26
75-	2	10	3	14
80-	0	0	1	5
Total	108	540	88	440

The average age of case group was  $54.5 \pm 10.6$  years, while that of the control group was  $54.3 \pm 10.6$  year, there was no statistically significant difference ( $t=0.127$ ,  $P=0.899$ ). For sex, there was also no difference statistically ( $\chi^2=0.001$ ,  $P=0.979$ ).

### Univariate analysis

In order to control the possible confounding bias the age, sex and resident location were matched in the study design. Given that the risk factors of colon cancer might be different from that of rectal cancer, the analysis of the risk factors were separated into colon cancer and rectal cancer, instead of colorectal cancer. The OR and its 95 % confidence intervals (95 %CI),  $\chi^2$  and  $P$  values in the univariate analysis were showed respectively in Table 2 and Table 3 (the variables showed  $P>0.20$  were excluded).

**Table 2** Results of univariate analysis for colon cancer (cases  $n=84$ , controls  $n=420$ )

factors	OR	95 % CI	$\chi^2$	$P$
pork eating( $y=1, n=0$ )	1.481	0.846 2.593	1.890	0.169
drining mixed water source* ( $y=1, n=0$ )	2.273	1.255 4.117	7.332	0.007
drining gutter water ( $y=1, n=0$ )	1.639	0.777 3.457	1.680	0.195
drining well water ( $y=1, n=0$ )	0.542	0.338 0.870	6.445	0.011
chronic diarrhea history( $y=1, n=0$ )	2.018	1.003 4.060	3.871	0.049
constipaton history( $y=1, n=0$ )	0.483	0.171 1.363	1.888	0.169
appendicitis history( $y=1, n=0$ )	1.697	0.966 2.981	3.386	0.066
appendix operating history( $y=1, n=0$ )	1.707	0.873 3.334	2.446	0.118
intestinal polyps history( $y=1, n=0$ )	6.503	2.009 21.049	9.762	0.002

\*drinking mixed water source refers to the subjects drinking different type of water sources through his/her lifetime, mostly drinking river water and gutter water. So is Table 2,3 and 4

**Table 3** Results of univariate analysis for rectal cancer (cases  $n=112$ , controls  $n=560$ )

factors	OR	95 % CI	$\chi^2$	$P$
drining mixed water source ( $y=1, n=0$ )	2.021	1.170 3.491	6.363	0.011
mucious blood history ( $y=1, n=0$ )	2.138	1.122 4.072	5.335	0.021
defaecation drug using ( $y=1, n=0$ )	2.280	0.711 7.312	1.923	0.166
cholecyst excision history ( $y=1, n=0$ )	2.294	0.715 7.352	1.195	0.163

In Table 2, it was showed that four variables, well water drinking, mixed water source drinking, chronic diarrhea history and intestinal polyp history, were significantly associated with colon cancer ( $P<0.05$ ). The factor of appendicitis history showed an OR value close to significant level ( $P=0.066$ ). For rectal cancer in Table 3, there were two variables reached the significant level of  $P=0.05$ , which were mixed water source drinking (OR=2.02) and mucous blood stool history (OR=2.14).

### Multivariate analysis

The variables showing associations with the risk of colon cancer and rectal cancer at  $P<0.15$  level were further tested in forward stepwise conditional logistic regression models. The final model consisted of those variables showing a significant association with the risk of colorectal cancer at  $P<0.05$  level. Results were showed in Table 4 and Table 5 for colon and rectal cancers, respectively.

**Table 4** Results of multivariate analysis for colon cancer

factors	OR	95 % CI	$P$
drining mixed source water ( $y=1, n=0$ )	2.387	1.243 4.587	0.009
mucous blood history ( $y=1, n=0$ )	3.508	1.370 8.985	0.009

Table 4 and Table 5 illustrated that, at  $P=0.05$  level, both for colon cancer and rectal cancer, the final logistic regression model comprised two factors: mixed water source drinking and mucous blood stool history.

**Table 5** Results of multivariate analysis for rectal cancer

factors	OR	95%CI	$P$
drinking mixed water source ( $y=1, n=0$ )	1.951	1.086 3.506	0.025
mucous blood history ( $y=1, n=0$ )	2.139	1.040 4.402	0.039
factors	2.870	1.117 7.371	0.029

## DISCUSSION

It is generally believed that colorectal cancer is the combined outcome of heredity and environment<sup>[8-10,30]</sup>. Despite uncertainties regarding the underlying association between heredity and colorectal cancer, the genetic factors may affect the individual sensitivity to cancer<sup>[3,30-37]</sup>; many documents had reported that the environmental factors might also influence colorectal cancer<sup>[37-49]</sup>. On the secondary prevention for colorectal cancer, symptoms and/or disorders of pre-cancer, such as intestinal polyps, ulcerative colitis, should be considered<sup>[50,51]</sup>.

Univariate analysis results of this study showed that drinking well water is a protective factor for colon cancer, OR value was 0.542, ( $P < 0.05$ ); drinking mixed water, mostly drinking river water and gutter water, was a risk factor both for colon cancer and rectal cancer, OR values were 2.387 (95 %CI: 1.247-4.587) and 1.951 (95 %CI: 1.086-3.506) in multivariate conditional logistic model, respectively. The association between drinking mixed water and colorectal cancer is consistent with former study. In this study, country subjects account for about 75 %, most of the mixed water drinking aggregated in country. In the local country, people usually were drinking river water and well water. It reflects that uncertainty of drinking water source, especially mixed drinking river water and gutting water would increase the incidence of colon cancer and rectal cancer. The findings in this study resembled other study reports<sup>[47,52]</sup>.

Chronic diarrhea, mucous blood stool and constipation history are the pre-clinical symptoms of colorectal cancer<sup>[53-56]</sup>. This study has found the positive association between mucous blood stool history and colorectal cancer. In final colon cancer logistic model and rectal cancer logistic model, the OR values of mucous blood stool history were 3.508 (95 %CI: 1.370-8.985) and 2.139 (95 %CI: 1.04-4.402) respectively, both reached statistical significant level. Univariate analysis also showed that, for colon cancer, the OR value of chronic diarrhea history was 2.018 (95 %CI: 1.023-4.06),  $P < 0.05$ , but did not enter the final logistic regression model.

Intestinal polyp history commonly regarded as a high risk factor for colorectal cancer<sup>[57-65]</sup>. Although the univariate analysis result showed a positive association between intestinal polyp history and colon cancer, OR=6.503 (95 %CI: 2.009-21.049),  $P < 0.05$ , after being matched with age, sex and location, the factor did not enter the final logistic regression model. However, the association between intestinal polyp history and rectal cancer could not reach the significant level even in the univariate analysis.

Although the association between dietary habits and colorectal cancer has been reported<sup>[35,38,39,41,45,49, 66,67]</sup>, this study was not able to confirm such a positive association. It was reported that increasing fat while reducing fibrous in diet would increase the incidence of colorectal cancer<sup>[68-70]</sup>. In this study, after merging the two variables, pork eating and vegetable eating, into one variable by cross-difference method, we got a negative association. Red meat eating, such as fish cooked with soy souse, was reported to be the risk factor of colorectal cancer<sup>[71]</sup>, but the result of this did not agree with that. Moreover, recent reports were not consistent with each other about the association between cigarette smoking and colorectal cancer, nor does the alcohol consumption<sup>[71-76]</sup>. This study did not find any statistical association between cigarette smoking, nor was alcohol consumption and colorectal cancer.

Nested case control study, namely case control study within cohort, is based on a cohort set. After baseline investigation for the cohort set, including population structure, exposure factors and pertinent factors, the study subjects are divided into two groups: the disease individuals form the case group and the individuals of control group need to be randomly

selected from the non-disease subjects. This kind of study can be analyzed statistically as a case-control study. The risk factors found in nested one are certain in cause and time consequence. In addition, the number of case in this study was abundance after ten years of follow-up; the controls were randomly selected from the whole disease-free cohort set and can represent the normal public population well. All of these endue the results with persuasion.

It should be noted that, after ten years of follow-up, some exposure factors may have changed, factors such as dietary habits, drinking water sources, intestinal disease history may be different from the primate investigation. All the changes may discount the preciseness of the conclusion. That the association between dietary habits and colorectal cancer could not be put forward any positive evidence might be explained by such changes.

## REFERENCES

- 1 **Zhang YL**, Zhang ZS, Wu BP, Zhou DY. Early diagnosis for colorectal cancer in China. *World J Gastroenterol* 2002; **8**: 21-25
- 2 **This Evensen E**, Hoff GS, Sauar J, Majak BM, Vatn MH. Flexible sigmoidoscopy or colonoscopy as a screening modality for colorectal adenomas in older age groups? Findings in a cohort of the normal population aged 63-72 years. *GUT* 1999; **45**: 834-839
- 3 **Colonna M**, Grosclaude P, Faivre J, Revzani A, Arveux P, Chaplain G, Tretarre B, Launoy G, Lesec'h JM, Raverdy N, Schaffer P, Buemi A, Menegoz F, Black RJ. Cancer registry data based estimation of regional cancer incidence: application to breast and colorectal cancer in French administrative regions. *J Epidemiol Community Health* 1999; **53**: 558-564
- 4 **Smalley W**, Ray WA, Daugherty J, Griffin MR. Use of nonsteroidal anti-inflammatory drugs and incidence of colorectal cancer: a population-based study. *Arch Int Med* 1999; **159**: 161-166
- 5 **Soliman AS**, Smith MA, Cooper SP, Ismail K, Khaled H, Ismail S, McPherson RS, Seifeldin IA, Bondy ML. Serum organochlorine pesticide levels in patients with colorectal cancer in Egypt. *Arch Environ Health* 1997; **52**: 409-415
- 6 **Kee F**, Wilson R, Currie S, Sloan J, Houston R, Rowlands B, Moorehead J. Socioeconomic circumstances and the risk of bowel cancer in Northern Ireland. *J Epidemiol Community Health* 1996; **50**: 640-644
- 7 **LiuXY**, Zheng S, Chen K, Ma XY, Zhou L, Yu H, Yao KY, Chen K, Cai SR, Zhang SZ. Randomized controlled trial of sequence mass screening program for colorectal cancer. *Zhonghua Liuxing Bingxue Zazhi* 2000; **21**: 430-433
- 8 **Haile RW**, Siegmund KD, Gauderman WJ, Thomas DC. Studydesign issues in the development of the University of Southern California Consortium's Colorectal Cancer Family Registry. *J Natl Cancer Inst Monogr* 1999; **26**: 89-93
- 9 **Campbell T**. Colorectal cancer. Part 1: Epidemiology, aetiology, screening and diagnosis. *Prof Nurse* 1999; **14**: 869-874
- 10 **Coughlin SS**, Miller DS. Public health perspectives on testing for colorectal cancer susceptibility genes. *Am J Prev Med* 1999; **16**: 99-104
- 11 **Mantel N**. Synthetic retrospective studies and related topics. *Biometrics* 1973; **29**: 479-490
- 12 **Hellard ME**, Sinclair MI, Fairley CK, Andrews RM, Bailey M, Black J, Dharmage SC, Kirk MD. An outbreak of cryptosporidiosis in an urban swimming pool: why are such outbreaks difficult to detect? *Aust N Z J Public Health* 2000; **24**: 272-275
- 13 **McDonald AD**, McDonald JC, Rando RJ, Hughes JM, Weill H. Cohort mortality study of North American industrial sand workers. I. Mortality from lung cancer, silicosis and other causes. *Ann Occup Hyg* 2001; **45**: 193-199
- 14 **Coker AL**, Gerasimova T, King MR, Jackson KL, Pirisi L. High-risk HPV's and risk of cervical neoplasia: a nested case-control study. *Exp Mol Pathol* 2001; **70**: 90-95
- 15 **Josefsson AM**, Magnusson PK, Ylitalo N, Sorensen P, QvarforthTubbin P, Andersen PK, Melbye M, Adami HO, Gyllenstein UB. Viral load of human papilloma virus 16 as a determinant for development of cervical carcinoma in situ: a nested case-control study. *Lancet* 2000; **355**: 2189-2193

- 16 **Akre O**, Lipworth L, Tretli S, Linde A, Engstrand L, Adami HO, Melbye M, Andersen A, Ekbom A. Epstein-Barr virus and cytomegalovirus in relation to testicular-cancer risk: a nested case-control study. *Int J Cancer* 1999; **82**: 1-5
- 17 **DeAmo J**, Petrukevitch A, Phillips AN, De Cock KM, Stephenson J, Desmond N, Hanscheid T, Low N, Newell A, Obasi A, Paine K, Pym A, Theodore C, Johnson AM. Risk factors for tuberculosis in patients with AIDS in London: a case-control study. *Int J Tuberc Lung Dis* 1999; **3**: 12-17
- 18 **Mathews WC**, Caperna J, Toerner JG, Barber RE, Morgenstern H. Neutropenia is a risk factor for gram-negative bacillus bacteremia in human immunodeficiency virus-infected patients: results of a nested case-control study. *Am J Epidemiol* 1998; **148**: 1175-1183
- 19 **Wideroff L**, Potischman N, Glass AG, Greer CE, Manos MM, Scott DR, Burk RD, Sherman ME, Wacholder S, Schiffman M. A nested case-control study of dietary factors and the risk of incident cytological abnormalities of the cervix. *Nutr Cancer* 1998; **30**: 130-136
- 20 **Deacon JM**, Evans CD, Yule R, Desai M, Binns W, Taylor C, Peto J. Sexual behaviour and smoking as determinants of cervical HPV infection and of CIN3 among those infected: a case-control study nested within the Manchester cohort. *Br J Cancer* 2000; **83**: 1565-1572
- 21 **Ylitalo N**, Sorensen P, Josefsson AM, Magnusson PK, Andersen PK, Ponten J, Adami HO, Gyllenstein UB, Melbye M. Consistent high viral load of human papillomavirus 16 and risk of cervical carcinoma *in situ*: a nested case-control study. *Lancet* 2000; **355**: 2194-2198
- 22 **Garcia Rodriguez LA**, Huerta Alvarez C. Reduced incidence of colorectal adenoma among long-term users of nonsteroidal anti-inflammatory drugs: a pooled analysis of published studies and a new population-based study. *Epidemiology* 2000; **11**: 376-381
- 23 **Knekt P**, Hakulinen T, Leino A, Heliovaara M, Reunanen A, Stevens R. Serum albumin and colorectal cancer risk. *Eur J Clin Nutr* 2000; **54**: 460-462
- 24 **Bertario L**, Russo A, Crosignani P, Sala P, Spinelli P, Pizzetti P, Andreola S, Berrino F. Reducing colorectal cancer mortality by repeated faecal occult blood test: a nested case-control study. *Eur J Cancer* 1999; **35**: 973-977
- 25 **Collet JP**, Sharpe C, Belzile E, Boivin JF, Hanley J, Abenham L. Colorectal cancer prevention by non-steroidal anti-inflammatory drugs: effects of dosage and timing. *Br J Cancer* 1999; **81**: 62-68
- 26 **Kato I**, Dnistrian AM, Schwartz M, Toniolo P, Koenig K, Shore RE, Akhmedkhanov A, ZeleniuchJacquotte A, Riboli E. Serum folate, homocysteine and colorectal cancer risk in women: a nested case-control study. *Br J Cancer* 1999; **79**: 1917-1922
- 27 **Kato I**, Dnistrian AM, Schwartz M, Toniolo P, Koenig K, Shore RE, ZeleniuchJacquotte A, Akhmedkhanov A, Riboli E. Iron intake, body iron stores and colorectal cancer risk in women: a nested case-control study. *Int J Cancer* 1999; **80**: 693-698
- 28 **Karlen P**, Kornfeld D, Brostrom O, Lofberg R, Persson PG, Ekbom A. Is colonoscopic surveillance reducing colorectal cancer mortality in ulcerative colitis? A population based case control study. *Gut* 1998; **42**: 711-714
- 29 **Meijer GA**, Baak JP, Talbot IC, Atkin WS, Meuwissen SG. Predicting the risk of metachronous colorectal cancer in patients with rectosigmoid adenoma using quantitative pathological features. A case-control study. *J Pathol* 1998; **184**: 63-70
- 30 **Hemminki K**, Lonnstedt I, Vaittinen P, Lichtenstein P. Estimation of genetic and environmental components in colorectal and lung cancer and melanoma. *Genet Epidemiol* 2001; **20**: 107-116
- 31 **Chapman PD**, Burn J. Genetic predictive testing for bowel cancer predisposition: the impact on the individual. *Cytogenet Cell Genet* 1999; **86**: 118-124
- 32 **Thorson AG**, Knezetic JA, Lynch HT. A century of progress in hereditary nonpolyposis colorectal cancer (Lynch syndrome). *Dis Colon Rectum* 1999; **42**: 1-9
- 33 **Briskey EN**, Pamies RJ. Colorectal cancer: update on recent advances and their impact on screening protocols. *J Natl Med Assoc* 2000; **92**: 222-230
- 34 **Lichtenstein P**, Holm NV, Verkasalo PK, Iliadou A, Kaprio J, Koskenvuo M, Pukkala E, Skytthe A, Hemminki K. Environmental and heritable factors in the causation of cancer-analyses of cohorts of twins from Sweden, Denmark, and Finland. *N Engl J Med* 2000; **343**: 78-85
- 35 **Marchand LL**. Combined influence of genetic and dietary factors on colorectal cancer incidence in Japanese Americans. *J Natl Cancer Inst Monogr* 1999; **26**: 101-105
- 36 **Bonaiti Pellie C**. Genetic risk factors in colorectal cancer. *Eur J Cancer Prev* 1999; **8** (Suppl 1): S27-32
- 37 **Ponz de Leon M**, Pedroni M, Benatti P, Percesepe A, Rossi G, Genuardi M, Roncucci L. Epidemiologic and genetic factor in colorectal cancer: development of cancer in dizygotic twins in a family with Lynch syndrome. *Ital J Gastroenterol Hepatol* 1999; **31**: 218-222
- 38 **Prichard PJ**, Tjandra JJ. Colorectal cancer. *Med J Aust* 1998; **169**: 493-498
- 39 **Rafter J**, Glinghammar B. Interactions between the environment and genes in the colon. *Eur J Cancer Prev* 1998; **7** (Suppl 2): S69-74
- 40 **Gandhi SK**, Reynolds MW, Boyer JG, Goldstein JL. Recurrence and malignancy rates in a benign colorectal neoplasm patient cohort: results of a 5-year analysis in a managed care environment. *Am J Gastroenterol* 2001; **96**: 2761-2767
- 41 **Ritenbaugh C**. Diet and prevention of colorectal cancer. *Curr Oncol Rep* 2000; **2**: 225-233
- 42 **Hemminki K**, Lonnstedt I, Vaittinen P, Lichtenstein P. Estimation of genetic and environmental components in colorectal and lung cancer and melanoma. *Genet Epidemiol* 2001; **20**: 107-116
- 43 **Lichtenstein P**, Holm NV, Verkasalo PK, Iliadou A, Kaprio J, Koskenvuo M, Pukkala E, Skytthe A, Hemminki K. Environmental and heritable factors in the causation of cancer-analyses of cohorts of twins from Sweden, Denmark, and Finland. *N Engl J Med* 2000; **343**: 78-85
- 44 **Park JG**, Park YJ, Wijnen JT, Vasen HF. Gene-environment interaction in hereditary nonpolyposis colorectal cancer with implications for diagnosis and genetic testing. *Int J Cancer* 1999; **82**: 516-519
- 45 **Jansen MC**, Bueno de Mesquita HB, Buzina R, Fidanza F, Menotti A, Blackburn H, Nissinen AM, Kok FJ, Kromhout D. Dietary fiber and plant foods in relation to colorectal cancer mortality: the Seven Countries Study. *Int J Cancer* 1999; **81**: 174-179
- 46 **Gertig DM**, Hunter DJ. Genes and environment in the etiology of colorectal cancer. *Semin Cancer Biol* 1998; **8**: 285-298
- 47 **Gulis G**, Fitz O, Wittgruber J, Suchanova G. Colorectal cancer and environmental pollution. *Cent Eur J Public Health* 1998; **6**: 188-191
- 48 **Van Kranen HJ**, van Iersel PW, Rijnkels JM, Beems DB, Alink GM, van Kreijl CF. Effects of dietary fat and a vegetable-fruit mixture on the development of intestinal neoplasia in the ApcMin mouse. *Carcinogenesis* 1998; **19**: 1597-1601
- 49 **Kenji T**, Hedio O, Yasuharu O, Iwao Y, Tomohiro S, Katsuya Y, Kiichi M, Shigeru T, Hideki A. Dietary factors and prevention of colon cancer. *Nippon Geka Gakkai Zasshi* 1998; **99**: 368-372
- 50 **Charalambopoulos A**, Syrigos KN, Ho JL, Murday VA, Leicesters RJ. Colonoscopy in symptomatic patients with positive family history of colorectal cancer. *Anticancer Res* 2000; **20**: 1991-1994
- 51 **Winawer SJ**. Natural history of colorectal cancer. *Am J Med* 1999; **106**: 3S-6S, 50S-51S
- 52 **Wang ZQ**, He J, Chen Y, Zhou TS, Lin YC. Relationship between different sources of drinking water, water quality improvement and gastric cancer mortality in Changle County-A retrospective-cohort study in high incidence area. *World J Gastroenterol* 1998; **4**: 45-47
- 53 **Martinez Martinez L**, Lopez Santamaria M, Prieto Bozano G, Molina Arias M, Jimenez Alvarez C, Tovar Larrucea JA. Diagnosis and therapeutic options in chronic idiopathic intestinal pseudo-obstruction: review of 16 cases. *Cir Pediatr* 1999; **12**: 71-74
- 54 **Browning SM**. Constipation, diarrhea, and irritable bowel syndrome. *Prim Care* 1999; **26**: 113-139
- 55 **Ho KY**, Kang JY, Seow A. Prevalence of gastrointestinal symptoms in a multiracial Asian population, with particular reference to reflux-type symptoms. *Am J Gastroenterol* 1998; **93**: 1816-1822
- 56 **Iacono G**, Cavataio F, Montalto G, Florena A, Tumminello M, Soresi M, Notarbartolo A, Carroccio A. Intolerance of cow's milk and chronic constipation in children. *N Engl J Med* 1998; **339**: 1100-1104
- 57 **Lal G**, Ash C, Hay K, Redston M, Kwong E, Hancock B, Mak T, Kargman S, Evans JF, Gallinger S. Suppression of intestinal polyps in Msh2-deficient and non-Msh2-deficient multiple intesti-

- nal neoplasia mice by a specific cyclooxygenase-2 inhibitor and by a dual cyclooxygenase-1/2 inhibitor. *Cancer Res* 2001; **61**: 6131-6136
- 58 **Rex DK**. Surveillance colonoscopy following resection of colorectal polyps and cancer. *Can J Gastroenterol* 2001; **15**: 57-59
  - 59 **Anderson J**. Clinical practice guidelines. Review of the recommendations for colorectal screening. *Geriatrics* 2000; **55**: 67-73, quiz 74
  - 60 **Katsumata T**, Igarashi M, Kobayashi K, Sada M, Yokoyama K, Saigenji K. Usefulness of endoscopic polypectomy in early colorectal cancer. *Nippon Geka Gakkai Zasshi* 1999; **100**: 782-786
  - 61 **Tobi M**. Polyps as biomarkers for colorectal neoplasia. *Front Biosci* 1999; **4**: 329-338
  - 62 **Gruber M**, Lance P. Colorectal cancer detection and screening. *Lippincotts Prim Care Pract* 1998; **2**: 369-376, quiz 377-378
  - 63 **Kennedy BP**, Soravia C, Moffat J, Xia L, Hiruki T, Collins S, Gallinger S, Bapat B. Overexpression of the nonpancreatic secretory group II PLA2 messenger RNA and protein in colorectal adenomas from familial adenomatous polyposis patients. *Cancer Res* 1998; **58**: 500-503
  - 64 **Luo YQ**, Ma LS, Zhao YL, Wu KC, Pan BR, Zhang XY. Expression of proliferating cell nuclear antigen in polyps from large intestine. *World J Gastroenterol* 1999; **5**: 160-164
  - 65 **Steindorf K**, Tobiasz Adamczyk B, Popiela T, Jedrychowski W, Penar A, Matyja A, Wahrendorf J. Combined risk assessment of physical activity and dietary habits on the development of colorectal cancer. A hospital-based case-control study in Poland. *Eur J Cancer Prev* 2000; **9**: 309-316
  - 66 **Negri E**, Franceschi S, Parpinel M, La Vecchia C. Fiber intake and risk of colorectal cancer. *Cancer Epidemiol Biomarkers Prev* 1998; **7**: 667-671
  - 67 **Jarvinen R**, Knekt P, Hakulinen T, Rissanen H, Heliovaara M. Dietary fat, cholesterol and colorectal cancer in a prospective study. *Br J Cancer* 2001; **85**: 357-361
  - 68 **Franceschi S**, Favero A. The role of energy and fat in cancers of the breast and colon-rectum in a southern European population. *Ann Oncol* 1999; **10**(Suppl): 661-663
  - 69 **Rieger MA**, Parlesak A, Pool Zobel BL, Rechkemmer G, Bode C. A diet high in fat and meat but low in dietary fibre increases the genotoxic potential of "faecal water". *Carcinogenesis* 1999; **20**: 2311-2316
  - 70 **Giovannucci E**. An updated review of the epidemiological evidence that cigarette smoking increases risk of colorectal cancer. *Cancer Epidemiol Biomarkers Prev* 2001; **10**: 725-731
  - 71 **Gertig DM**, Stampfer M, Haiman C, Hennekens CH, Kelsey K, Hunter DJ. Glutathione S-transferase GSTM1 and GSTT1 polymorphisms and colorectal cancer risk: a prospective study. *Cancer Epidemiol Biomarkers Prev* 1998; **7**: 1001-1005
  - 72 **Terry P**, Ekblom A, Lichtenstein P, Feychting M, Wolk A. Long-term tobacco smoking and colorectal cancer in a prospective cohort study. *Int J Cancer* 2001; **91**: 585-587
  - 73 **Chao A**, Thun MJ, Jacobs EJ, Henley SJ, Rodriguez C, Calle EE. Cigarette smoking and colorectal cancer mortality in the cancer prevention study II. *J Natl Cancer Inst* 2000; **92**: 1888-1896
  - 74 **Yoshioka M**, Katoh T, Nakano M, Takasawa S, Nagata N, Itoh H. Glutathione S-transferase (GST) M1,T1, P1, N-acetyltransferase (NAT) 1 and 2 genetic polymorphisms and susceptibility to colorectal cancer. *J UOEH* 1999; **21**: 133-147
  - 75 **Sinha R**, Chow WH, Kulldorff M, Denobile J, Butler J, Garcia Closas M, Weil R, Hoover RN, Rothman N. Well done, grilled red meat increases the risk of colorectal adenomas. *Cancer Res* 1999; **59**: 4320-4324
  - 76 **Neugut AI**, Rosenberg DJ, Ahsan H, Jacobson JS, Wahid N, Hagan M, Rahman MI, Khan ZR, Chen L, Pablos Mendez A, Shea S. Association between coronary heart disease and cancers of the breast, prostate, and colon. *Cancer Epidemiol Biomarkers Prev* 1998; **7**: 869-873

Edited by Zhao M